PO Box 2345, Beijing 100023, China
www.wjgnet.com
wjg@wjgnet.com

ELSEVIER

World J Gastroenterol 2005;11(28):4291-4299
World Journal of Gastroenterology ISSN 1007-9327

• *REVIEW* •

Treatment of uncomplicated reflux disease

Joachim Labenz, Peter Malfertheiner

Joachim Labenz, Department of Medicine, Jung-Stilling Hospital Siegen, Germany
Peter Malfertheiner, Department of Gastroenterology, Hepatology and Infectious Diseases, University of Magdeburg, Germany
Correspondence to: Joachim Labenz, MD, Jung-Stilling Hospital, Wichern str. 40, D-57074 Siegen, Germany. j.labenz@t-online.de
Telephone: +49-271-333-4569 Fax: +49-271-333-4242
Received: 2004-12-24 Accepted: 2005-01-13

Abstract

Uncomplicated reflux disease comprises the non-erosive reflux disease (NERD) and erosive reflux disease (ERD). The objectives of treatment are the adequate control of symptoms with restoration of quality of life, healing of lesions and prevention of relapse. Treatment of NERD consists in the administration of proton pump inhibitors (PPI) for 2-4 wk, although patients with NERD show an overall poorer response to PPI treatment than patients with ERD owing to the fact that patients with NERD do not form a pathophysiologically homogenous group. For long-term management on-demand treatment with a PPI is probably the best option. In patients with ERD, therapy with a standard dose PPI for 4-8 wk is always recommended. Long-term treatment of ERD is applied either intermittently or as continuous maintenance treatment with an attempt to reduce the daily dosage of the PPI (step-down principle). In selected patients requiring long-term PPI treatment, antireflux surgery is an alternative option. In patients with troublesome reflux symptoms and without alarming features empirical PPI therapy is another option for initial management. Therapy should be withdrawn after initial success. In the case of relapse, the long-term care depends on a careful risk assessment and the response to PPI therapy.

Key words: Erosive reflux disease; Non-erosive reflux disease; Proton pump inhibitor; Uninvestigated reflux disease

Labenz J, Malfertheiner P. Treatment of uncomplicated reflux disease. *World J Gastroenterol* 2005; 11(28): 4291-4299
http://www.wjgnet.com/1007-9327/11/4291.asp

INTRODUCTION

Gastroesophageal reflux disease (GERD) is a common condition affecting approximately 10-20% of the adult population of industrialized countries[1]. In the great majority of patients with GERD, the disease does not lead to complications, instead presents with often severe symptoms. Some 60% of patients in primary care with troublesome reflux symptoms have no endoscopically recognizable lesions of the esophageal mucosa, 35% have erosive esophagitis (75% of which are mild, corresponding to Los Angeles A/B, and 25% severe, corresponding to Los Angeles C/D). In about 5% of the patients, complications, such as stricture, ulcer and in particular Barrett's esophagus or even adenocarcinoma, must be expected (Figure 1)[2]. Epidemiological data support the hypothesis that GERD is not a spectrum disease with occasional reflux symptoms but no lesions at the one end, and severe complications at the other, but can instead be classified into three distinct categories-nonerosive reflux disease (NERD)-erosive reflux disease (ERD), and Barrett's esophagus-in each of which the respective patient remains, that is, progression of the disease over time is, overall, very rare[3]. This category model of GERD is supported by the latest data from a large prospective European study (ProGERD) involving more than 6 000 patients with NERD and ERD: the rate of progression (to severe esophagitis or Barretts') for patients with NERD and mild erosive esophagitis (Los Angeles A/B) was less than 1% per year (Labenz *et al*., unpublished data).

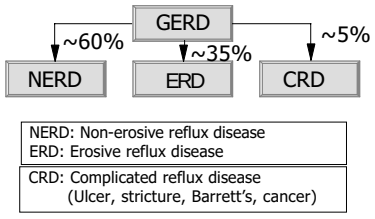

Figure 1 GERD-a categorical disease with three distinct entities[after 2,3].

INITIAL MANAGEMENT OF GERD

Uncomplicated reflux disease comprises the non-erosive form, that is, symptoms that impact negatively on the patient's quality of life, but which are not associated with endoscopic evidence of mucosal breaks in the esophagus, and erosive reflux esophagitis of varying degrees of severity, e.g. grades A-D in the Los Angeles classification[4].

Contrary to commonly held beliefs, symptom evaluation is the most important assessment for the initial phase of GERD management[5], although an evidence-based analysis of symptoms is hardly possible[6]. Characteristic symptoms are heartburn and acid regurgitation[6]. However, these symptoms are predictive of GERD in only 70% of the patients, even in cases with an unequivocal history[7]. It must

be emphasized that there is no diagnostic gold standard for GERD: endoscopy has a sensitivity of only 30-40%, microscopic features such as dilated intracellular spaces and regenerative changes in the absence of endoscopically visible mucosal breaks of the squamous epithelium in the distal esophagus are currently not sufficiently validated, and pH-monitoring is far from being a diagnostic gold standard, since 30-60% of patients with NERD, as well as 10-20% of those with ERD, have normal results of 24-h pH-monitoring, and intra-individual comparisons have also shown that pH-metry is subject to appreciable fluctuations[4,8]. Moreover, there is consistent observation that there is virtually no correlation between the severity of endoscopic findings and symptom severity (Figure 2)[9]. All these aspects have an important impact on the clinical management of GERD which is distinct in the initial phase and long-term care.

Basic goals of treatment are:

- to provide complete, or at least sufficient, control of symptoms,
- to maintain symptomatic remission,
- to heal underlying esophagitis and maintain endoscopic remission, and
- to treat or, ideally, prevent complications.

Adequate control of symptoms is considered to have been achieved when mild reflux symptoms occur at most once a week-more frequent or more pronounced complaints are not accepted as satisfactory by the patient[10]. Initially, a symptom-based diagnosis is established, and an individual risk assessment made (Figure 3). If such alarming symptoms such as dysphagia, unintended weight loss and/or signs of bleeding are present, an endoscopic examination is mandatory, with further management dictated by the endoscopic findings. Other indications for endoscopy at this point in time may include, for example, a family history of upper gastrointestinal tract malignancies, a long prior history of severe complaints, age over 50 years, use of NSAIDs, and a positive *Helicobacter pylori* status[11]. Otherwise, empirical therapy can be offered (Figure 3). Withholding endoscopy in the initial phase is, of course, associated with the theoretical risk that serious complications of GERD or other significant pathologies in the upper gastrointestinal tract mimicking the symptoms of reflux disease may be overlooked or recognized too late. On the other hand, given the facts that GERD is extremely common, and complications are generally rare, endoscopic evaluation of all patients with GERD is hardly justifiable, especially since an endoscopy-based management strategy has not been subjected to appropriate evaluation. In a cross-sectional study from Finland the detection rate of serious complications of GERD did not differ between regions with low and those with high referral to endoscopy[12]. Considering that most patients have mild GERD and that the disease is not progressive over time, restricted use of endoscopy does not appear to put the patients at risk. However, the economic impact of different diagnostic strategies on expense remains to be established, at least in countries with low endoscopy costs[13]. A recent study in 742 patients with uncomplicated GERD showed no correlation between endoscopic findings and subsequent therapeutic decisions[14]. Further arguments for a primarily symptom-driven strategy are that the ultimate benchmark for the clinical efficacy of treatment of GERD is patient satisfaction and that accurate determination of esophagitis requires the withholding of therapy before endoscopy, which in many cases is not possible[15].

For the sake of simplicity, the following sections first discuss the initial and long-term treatment of patients with NERD and ERD (endoscopy-based approach), and then consider the management of uninvestigated GERD, which is doubtless the more common treatment that is applied in the clinical setting.

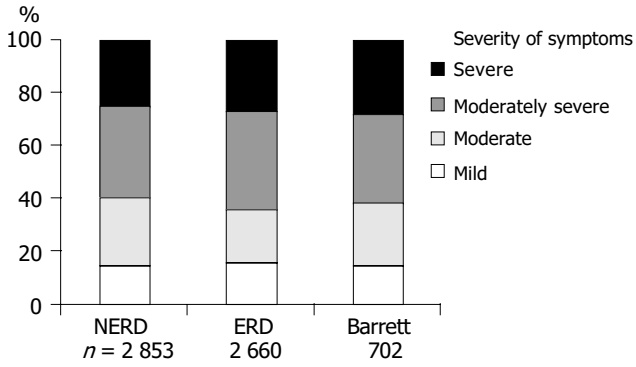

Figure 2 No correlation between endoscopic findings and symptom severity in patients with GERD[9].

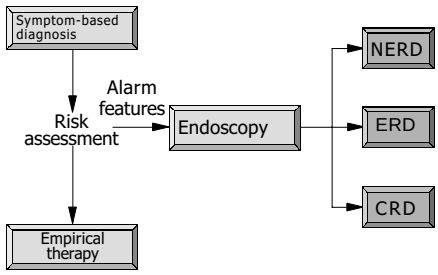

Figure 3 Initial management of patients with symptoms suggestive of GERD.

TREATMENT OF NERD

While NERD is the most common manifestation of reflux disease, patients with this entity do not form a pathophysiologically homogeneous group. A differentiation can be made between patients with unequivocally pathological acid reflux, patients with an acid-sensitive (hypersensitive) esophagus, which means that more than 50% of the symptomatic episodes were associated with acid reflux (positive symptom index), and those with symptoms that are independent of acid-reflux events (functional heartburn)[8,16]. This latter category explains the observation that patients with NERD did not respond as well to acid suppressants as patients with erosive esophagitis do[17,18]. Possible pathophysiological causes of functional heartburn include non-acid reflux (liquid, gas, mixed), minute changes in the esophageal acidity above a pH of 4, motility disorders such as sustained contractions of the longitudinal musculature, visceral hypersensitivity, and emotional and psychological abnormalities[19].

Initial therapy of NERD

Initially, patients should receive a proton pump inhibitor (PPI) for 2-4 wk (Figure 4). The effect of other substances such as H_2 blockers or prokinetic drugs is hardly better than that of placebo[20]. In a large, placebo-controlled study, a dose-response relationship was established for omeprazole: omeprazole 20 mg proved to be more effective than omeprazole 10 mg[21]. In a further controlled study, lansoprazole 30 mg was no more effective than lansoprazole 15 mg[22]. The S-isomer of omeprazole, esomeprazole, was investigated in two large, double-blind, multicenter studies involving patients with NERD[23]. Esomeprazole at a dose of 20 and 40 mg per day proved more effective than placebo, but a dose-response effect could not be shown. Three further randomized, double-blind, multicenter studies involving a total of more than 2 600 patients with NERD treated for 4 wk with omeprazole 20 mg, and esomeprazole 20 or 40 mg revealed comparable success rates (resolution of symptoms in 60-70% of the patients)[24]. Assessment of the response to treatment in studies like these are greatly influenced by the target criterion (e.g. complete elimination of symptoms, satisfactory symptom control), so that the studies can hardly be compared. From the above remarks it may be concluded that appropriately dosed PPI treatment can achieve a satisfactory initial response in some two-thirds of the patients. If initial treatment with 4 wk of PPI fails to elicit adequate symptom control (Figure 4), increasing the PPI dose (e.g. standard dose PPI twice daily) is recommended, since studies have shown that patients with acid-sensitive esophagus respond better to a high PPI dose[25-27]. In non-responders to appropriate PPI treatment, it is recommended that esophageal pH-monitoring be performed during PPI therapy and, if symptomatic acid reflux can be excluded, to discontinue PPI therapy and initiate a trial with a low-dose tricyclic antidepressant at bedtime[28]. Potential therapeutic options for the future might be serotonin reuptake inhibitors, kappa agonists and substances with an impact on transient sphincter relaxation such as baclofen.

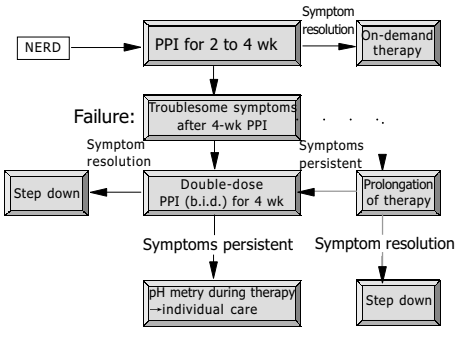

Figure 4 Initial therapy and long-term care of patients with NERD.

Long-term care of patients with NERD

If initial treatment is successful, medication should be discontinued, since 25% (or more) of the patients may remain in remission over prolonged periods of time[29], and this clinical entity does not appear to necessitate measures aimed at preventing complications. In the event of a relapse, indicating the need for long-term management, a number of different options are available: continuous maintenance therapy starting with a PPI and subsequent attempts to step down to lower dosages of the PPI or even less potent drugs (Figure 5)[5], intermittent courses of treatment for 2-4 wk with initially successful PPI[30], and patient-controlled on-demand therapy with a PPI[11]. On-demand therapy means that the patient himself determines both the start and the end of treatment. Medication should be discontinued when the symptoms have been eliminated. This last option in particular, has met with great interest in recent years on account of its potential economic advantages[31,32]. In a first large randomized, controlled study lasting 6 mo, Lind *et al*., were able to show that more than 80% of the patients were satisfactorily treated with an on-demand strategy employing omeprazole 20 mg[33]. In this study, omeprazole 20 mg proved more effective than omeprazole 10 mg. The convincing efficacy of this new treatment option was then confirmed with esomeprazole 20 mg[34,35]. All these studies also showed that roughly one-half of these patients were satisfactorily treatable with placebo medication and the use of antacids as required. In a recently presented randomized, open international multicenter study involving 598 patients, on-demand treatment with esomeprazole 20 mg was compared with continuous treatment with esomeprazole 20 mg o.d. in patients with NERD[36]. The vast majority of patients in both treatment groups were satisfied with the regimen, and medication consumption was considerably lower in the on-demand therapy arm (average consumption: 0.41 *vs* 0.91 tablets per day). However, the final endoscopic examination revealed mild erosive esophagitis (Los Angeles A: $n = 14$; Los Angeles B: $n = 1$) in 5% of the patients receiving on-demand treatment, while none of the patients on continuous treatment had this finding. From the viewpoint of a clinician, this observation

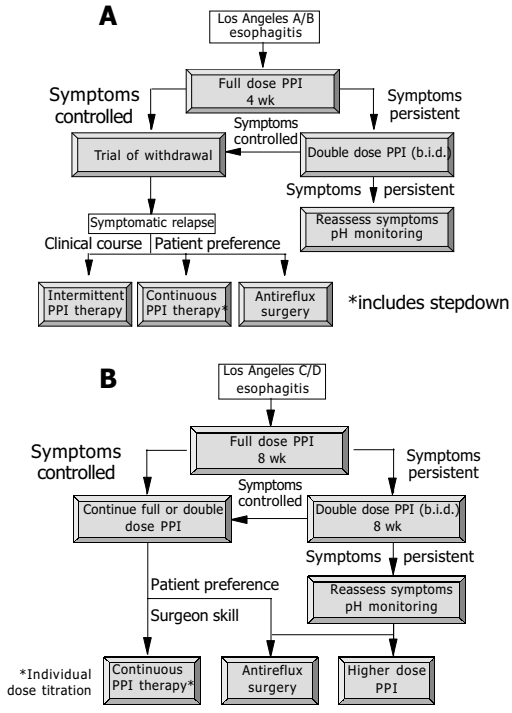

Figure 5 Management of patients with mild to moderate erosive esophagitis (**A**) and moderate to severe esophagitis (**B**)[after 4,5].

occasions no major concern, since alternation between the categories NERD and mild ERD (corresponding to Los Angeles A and B) often occurs during the spontaneous course of the disease. In another large scale study, 622 patients with NERD were randomized to esomeprazole 20 mg on demand or lansoprazole 15 mg o.d. for 6 mo after an initial successful treatment with esomeprazole[37]. Based on the target criterion "willingness to continue" on-demand treatment was superior to continuous treatment (93% *vs* 88%; $P = 0.02$). Patients on continuous treatment complained more often about heartburn and adverse events, the main reasons for "unwillingness to continue". Other PPIs (lansoprazole, pantoprazole, rabeprazole) have also proven their superiority to placebo in on-demand treatment in individual studies[11]. Head-to-head comparisons between various PPIs are, however, lacking, so that a comparative assessment is not possible.

TREATMENT OF ERD

Erosive reflux esophagitis can be found in about 30-40% of GERD patients[2]. Endoscopically, reflux esophagitis is categorized into various degrees of severity. In recent years, and especially in therapeutic studies, the Los Angeles classification in particular has been applied[38,39]. This distinguishes the four degrees of severity A-D (A: mucosal breaks of less than 5 mm on the top of folds; B: mucosal breaks >5 mm in extent on mucosal folds; C: circumferential spreading of mucosal breaks involving less than 75% of the circumference; D: mucosal breaks involving more than 75% of the circumference). The gradings A and B correspond to mild to moderate esophagitis and C and D to moderate to severe esophagitis. One fourth of patients with erosive esophagitis are categorized in grade C or D[40-42].

Numerous controlled studies have investigated the efficacy of a variety of medications in the healing of esophagitis and the elimination of symptoms. In a meta-analysis, Chiba *et al*.[43], showed that PPIs (omeprazole, lansoprazole, pantoprazole) heal the esophagitis within 8 wk in 83.6% of the patients, with a symptom-resolution rate of 77.4%. All other medications (H_2-receptor antagonists, cisapride, sucralfate) were appreciably less effective. A placebo-related healing rate of 28.2% documents the fluctuating nature of the course of reflux disease in some patients, with spontaneous remissions and exacerbations. When using highly potent PPIs, elimination of symptoms after 8 wk is predictive for healing of the esophagitis[41,42].

Initial therapy of ERD

In patients with erosive reflux esophagitis, treatment with a standard dose of a PPI is always recommended (Figure 5)[4]. Mild cases (Los Angeles grade A/B) usually heal within 4 wk, while severe cases (Los Angeles C/D) often require longer treatment-eight or, in some cases, more weeks. Resolution of symptoms in those responding to therapy is achieved appreciably more quickly (median time to sustained symptom resolution 5-10 d). The major predictive factor for the healing rate is the severity of the erosive esophagitis, but also of significance are concomitant Barrett's metaplasia in the lower esophagus, which reduces the healing rate, and infection with *H pylori*, which enhances the efficacy of the PPI[44,45].

Is there any clinically relevant difference between the PPIs available in the market? Racemic PPIs (omeprazole, lansoprazole, pantoprazole, rabeprazole) differ in such pharmacokinetic characteristics as bioavailability and the rapidity with which an effect occurs. This, however, is irrelevant for the healing of esophagitis at 4 and 8 wk[46,47], although the substances do differ in terms of the time required to eliminate symptoms. In a large randomized, controlled study involving more than 3 500 patients with erosive esophagitis, lansoprazole 30 mg o.d. relieved heartburn significantly faster than did omeprazole 20 mg o.d.[48]. There is a linear relationship between the degree of acid suppression measured by the time per day that gastric pH is higher than 4, and the healing kinetics of esophagitis[49]. With regard to the healing rates of reflux esophagitis after 4 and 8 wk, no differences are to be seen between the standard doses of the racemic PPIs (omeprazole 20 mg, lansoprazole 30 mg, pantoprazole 40 mg, rabeprazole 20 mg)[46,47], nor did doubling the individual dose (e.g. lansoprazole 60 mg, pantoprazole 80 mg) increases efficacy. Of significance for the healing rates and symptom elimination, however, is cytochrome 2C19 polymorphism. Thus, it has been recently shown that the response to treatment with lansoprazole 30 mg o.d. is poorer in extensive metabolizers than in intermediate and poor metabolisers[50].

Cross-over pH-monitoring studies in healthy volunteers and patients with GERD have shown that esomeprazole is more effective than corresponding doses of the racemic PPIs omeprazole, lansoprazole, pantoprazole and rabeprazole[51,52]. In large controlled studies, significantly higher healing rates were achieved with esomeprazole at a dose of 40 mg o.d. than with omeprazole 20 mg o.d., lansoprazole 30 mg o.d., and pantoprazole 40 mg o.d.[40-42,53,54]. The therapeutic advantage of esomeprazole over the other PPIs increased with increasing severity of the esophagitis as defined by the Los Angeles classification[55]. These studies also showed a significant superiority of esomeprazole in terms of the time to sustained symptom (heartburn) resolution. Small non-inferiority studies claiming equivalence between different PPIs did not have the statistical power to detect a difference of the magnitude that has been consistently established by the large scale studies mentioned above[56-58].

In the event of inadequate efficacy (insufficient control of symptoms or healing of the esophagitis), doubling the individual dose of PPI does not reliably improve clinical efficacy, but switching to another PPI, or shortening the interval between doses (e.g. twice daily) might increase the response to treatment[59]. In recent years there has been intense discussion on the clinical relevance of nocturnal acid breakthrough (NABT) in difficult-to-treat cases[60,61]. NABT is defined as a decrease in gastric pH to <4 for more than 1 h during the course of the night. The clinical relevance of this phenomenon has not yet been established. H_2-receptor antagonists given at bedtime can prevent this acid breakthrough, but when administered over a longer period of time, they rapidly lose this effect[62]. Treatment with combinations of PPI and prokinetic drugs is of unproven value.

Long-term care of patients with ERD

After responding well to initial treatment, ERD shows a tendency to relapse. Up to 90% of the patients will relapse already within the next 6 mo[29]. Patients with mild esophagitis (Los Angeles A/B) often have a longer relapse-free interval than patients with severe esophagitis (Los Angeles C/D), who frequently suffer a relapse within days of discontinuing successfully the initial treatment[63,64]. In the light of these observations, it is recommended that, in patients with mild esophagitis, therapy should first be discontinued and the further course of the disease kept under surveillance, while in severe esophagitis, initial successful therapy should be followed, *a priori*, by maintenance treatment (Figure 5). Established options for long-term management are intermittent treatment for some weeks and continuous maintenance treatment with an attempt to reduce the daily dosage of the PPI (step-down principle)[4,30]. On-demand therapy has, to date, been investigated in only two studies in patients with erosive esophagitis[65,66]. Satisfactory control of symptoms was achieved in the vast majority of patients, but continuous therapy proved to be superior with respect to maintenance of remission of erosive esophagitis, so that an evidenced-based recommendation is currently not possible. However, since GERD is usually not progressive, attempts to realize on-demand treatment does not appear to harm the patients[3].

For the prevention of relapse in patients with healed esophagitis, PPIs are clearly superior to H_2-receptor antagonists, prokinetic drugs and combinations of these medications[67-69]. The yield between a standard dose of a PPI and one-half of this dose is, in individual studies, often small, although significant, and even probably clinically relevant differences have occasionally been observed[67]. On the basis of a cost effectiveness analysis using a Markov model designed to simulate the economic and clinical outcomes of GERD in relation to the cost per symptom-free patient years gained and the cost per QALY gained treatment with a standard dose of a PPI appears to be superior despite the higher drug costs[69]. Nevertheless, in view of the overall high response rates, an initial attempt with half the standard dose of a PPI is recommended in patients with mild erosive esophagitis, while patients with more severe disease should be kept on the dose of PPI required to induce remission (Figure 5). If this approach proves successful, a dose reduction, or a changeover to a less potent drug can be attempted[70,71]. If the reduced dose proves unsuccessful, the dose must be increased appropriately. Occasionally, a higher-than-standard dose may be necessary to maintain remission[72].

With long-term therapy also, differences are found between the isomeric PPI esomeprazole, and the racemic PPIs lansoprazole or pantoprazole. In large double-blind randomized studies in patients with healed esophagitis, esomeprazole 20 mg o.d. applied over 6 mo was significantly more effective than lansoprazole 15 mg o.d. (therapeutic gain 8-9%), or pantoprazole 20 mg o.d. (therapeutic gain 12%)[73-75]. As in the case of acute treatment, this superiority was more pronounced with increasing disease severity. Apart from the severity of the baseline esophagitis, concomitant Barrett's esophagus (poorer results) and *H pylori* infections (better results) also have a role as predictors of treatment outcome[76].

Eradication of Helicobacter pylori in patients with GERD

Whether a concomitant *H pylori* infection in patients with GERD should be treated or not is still under discussion[77,78]. Since *H pylori* is probably not involved in the pathogenesis of GERD, it cannot be expected that its eradication can heal this condition[79] nor, according to the data of Moayyedi *et al*., is an aggravation of the spontaneous course of GERD to be expected. *H pylori* does, however, have an impact on the pH-elevating effect of PPIs, which leads to higher healing rates and faster elimination of symptoms in patients with reflux esophagitis[45]. PPI treatment in *H pylori*-infected patients leads to an aggravation of corpus gastritis, possibly also accompanied by an accelerated development of atrophy, while at the same time, antral gastritis is improved. The resulting gastritis type (corpus dominant) is found more frequently in patients with gastric cancer, and is therefore termed as "risk gastritis" or "gastritis of the cancer phenotype". Whether long-term PPI treatment in patients with *H pylori* gastritis actually does increase the gastric cancer risk is unclear. It does, however, appear certain that PPI treatment for over more than 10 years is also safe in patients infected with *H pylori*[72]. Whether this also applies to treatment for over 20, 30 or more years is not known at present. On the basis of these considerations, some authors advocate the eradication of *H pylori* before initiating long-term PPI treatment[80].

Antireflux surgery

In selected patients requiring long-term PPI treatment, a possible alternative option is antireflux surgery, which, however, is no more effective than tailored PPI therapy, and also carries a significant complication risk[81-83]. To date, no advantages of surgery in terms of economics have been unequivocally demonstrated[83,84]. The best candidates for fundoplication are probably those with esophagitis documented by endoscopy, a need for continuous PPI therapy, abnormal pH monitoring studies, normal esophageal motility studies, and at least partial symptom relief with PPI therapy[85]. Further arguments for surgery are high-volume reflux and young age. Relevant concomitant diseases, in contrast, tend to militate in favor of sticking with a conservative approach. A "treatment-refractory" GERD patient should certainly not be automatically referred for antireflux surgery.

Endoscopic antireflux procedures

In recent years, a number of different methods for endoscopic endoluminal treatment of GERD have been investigated (endoscopic gastroplication with differing suturing techniques, application of radiofrequency energy to the lower esophageal sphincter, endoscopic submucosal or intramuscular injection of inert materials). To date, the efficacy of endoluminal therapy for GERD is not supported by a high level of evidence[86]. Only a single fully published controlled study (radio-frequency energy delivery *vs* sham procedure) that documented a benefit in terms of symptom relief, but no effect on acid reflux, has been reported[87].

Overall, too few data are currently available on efficacy and safety, so that the use of these methods outside of controlled studies cannot be recommended. In particular, controlled studies comparing endoscopic antireflux procedures with the established options of treatment would be desirable.

UNINVESTIGATED GERD

In patients with troublesome reflux symptoms but no alarm symptoms (e.g. dysphagia, unintended loss of weight, signs of bleeding), empirical PPI therapy is another option for initial management.

The goals of empirical therapy are: (1) to succeed with initial therapy; (2) to determine need for ongoing therapy; (3) to maintain satisfactory symptom control; (4) to minimize risks from esophagitis and other consequences of abnormal reflux.

These aims should be achieved at the lowest possible cost and with minimal risks[88]. Initial therapy should via rapid relief of symptoms confirm the symptom based diagnosis, reassure the patient as to the benign and treatable nature of the reflux disease, and if present cure the esophagitis. For many years, patients with GERD received step-up therapy beginning with weakly effective substances, such as antacids and H_2-receptor antagonists, and increasing the intensity of the treatment if the effect was inadequate. With this strategy, the above-mentioned aims of empirical treatment cannot be achieved. For this reason, initiation of treatment with a PPI at a standard dose applied for 4 wk is favored (step-in approach) (Figure 6). However, few scientific data are available on this approach. In a four-arm controlled double-blind study involving 593 patients and conducted over 20 wk, the patients initially received lansoprazole 30 mg o.d. or ranitidine 150 mg b.i.d. over a period of 8 wk, followed by either continuation of this medication, or a step-down from lansoprazole to ranitidine or a step-up from ranitidine to lansoprazole[89]. The most effective strategy was step-in with a PPI and continuation with this medication. These results were confirmed in another study comparing omeprazole with ranitidine[90].

Therapy should be withdrawn after initial success. In the case of a relapse, the long-term care depends on a careful assessment of the risk and the response to PPI therapy. Potential strategies are on-demand therapy or intermittent treatment. In a controlled three-arm study involving 1 357 patients with uninvestigated GERD, Meineche-Schmidt *et al*.[91], compared on-demand therapy with esomeprazole 20 mg and GP-controlled intermittent strategy with esomeprazole 40 mg o.d. for 2 or 4 wk applied over 6 mo. The direct medical costs were similar in all three arms, but the total costs were substantially higher in patients treated with a GP-controlled intermittent strategy. If continuous maintenance therapy is needed to preserve remission, or if an initial positive response is rapidly followed by relapse, an endoscopic evaluation to exclude/detect severe erosive esophagitis or complicated reflux disease is recommended. If initial treatment is not successful, and if the clinical data militate against a severe form of GERD, the PPI dose can be increased (standard dose twice daily) or a changeover to a more potent substance implemented[59]; otherwise, in this clinical situation, too, endoscopy should be performed[88]. It is not clear whether patients who respond to initial treatment with a PPI and are then well controlled with on-demand therapy need to be submitted to endoscopy at all. Earlier calls for "once in a life-time" endoscopy for every patient with reflux disease are no longer considered mandatory. Moreover, the timing of endoscopy is critical: endoscopy off therapy is required to correctly assess the severity of esophagitis, which is important for the choice of further management, and endoscopy on therapy is needed to assess Barrett's esophagus which is important with regard to cancer risk and the planning of surveillance.

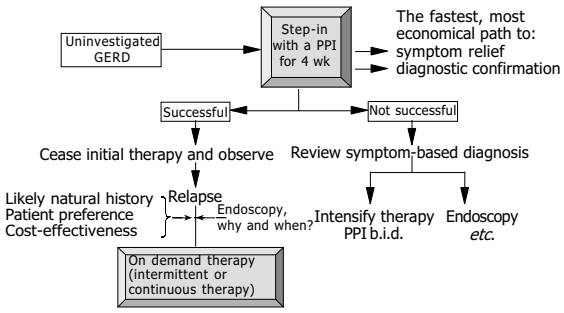

Figure 6 Proposal for the empirical management of patients with uninvestigated GERD[88].

REFERENCES

1 **Locke GR,** Talley J, Fett SL, Zinsmeister AR, Melton LJ. Prevalence and clinical spectrum of gastroesophageal reflux: a population-based study in Olmsted County, Minnesota. *Gastroenterology* 1997; **112**: 1448-1456

2 **Quigley EM.** Non-erosive reflux disease (NERD); part of the spectrum of gastro-oesophageal reflux, a component of functional dyspepsia, or both? *Eur J Gastroenterol Hepatol* 2001; **13** (Suppl 1): S13-18

3 **Fass R,** Ofman JJ. Gastroesophageal reflux disease – should we adopt a new conceptual framework? *Am J Gastroenterol* 2002; **97**: 1901-1907

4 **Dent J,** Brun J, Fendrick AM, Fennerty MB, Janssens J, Kahrilas PJ, Lauritsen K, Reynolds JC, Shaw N, Talley NJ. An evidence-based appraisal of reflux disease management – the Genval Workshop Report. *Gut* 1999; **44**(Suppl 2): S1-S16

5 **Dent J.** Management of reflux disease. *Gut* 2002; **50**(Suppl 4): iv67-71

6 **Dent J,** Armstrong D, Delaney B, Moayyedi P, Talley NJ, Vakil N. Symptom evaluation in reflux disease: workshop background, processes, terminology, recommendations, and discussion outputs. *Gut* 2004; **53**(Suppl 4): iv1-24

7 **Klauser AG,** Schindlbeck NE, Müller-Lissner SA. Symptoms in gastro-oesophageal reflux disease. *Lancet* 1990; **335**: 205-208

8 **Martinez SD,** Malagon IB, Garewal HS, Cui H, Fass R. Non-erosive reflux disease (NERD) – acid reflux and symptom patterns. *Aliment Pharmacol Ther* 2003; **17**: 537-545

9 **Kulig M,** Nocon M, Vieth M, Leodolter A, Jaspersen D, Labenz J, Meyer-Sabellek W, Stolte M, Lind T, Malfertheiner P, Willich SN. Risk factors of gastroesophageal reflux disease: methodology and first epidemiological results of the ProGERD study. *J Clin Epidemiol* 2004; **57**: 580-589

10 **Junghard O,** Carlsson R, Lind T. Sufficient control of heartburn in endoscopy-negative gastro-oesophageal reflux disease trials. *Scand J Gastroenterol* 2003; **38**: 1197-1199

11 **Bytzer P,** Blum AL. Personal view: rationale and proposed algorithms for symptom-based proton pump inhibitor therapy

for gastro-oesophageal reflux disease. *Aliment Pharmacol Ther* 2004; **20**: 389-398
12 **Mäntynen T,** Färkkilä M, Kunnamo I, Mecklin JP, Voutilainen M. The impact of upper GI endoscopy referral volume on the diagnosis of gastroesophageal reflux disease and its complications: 1-year cross sectional study in a referral area with 260 000 inhabitants. *Am J Gastroenterol* 2002; **97**: 2524-2529
13 **Koop H.** Gastroesophageal reflux disease and Barrett´s esophagus. *Endoscopy* 2004; **36**: 103-109
14 **Blustein PK,** Beck PL, Meddings JB, Van Rosendaal GM, Bailey RJ, Lalor E, Thomson AB, Verhoef MJ, Sutheland LR. The utility of endoscopy in the management of patients with gastroesophageal reflux symptoms. *Am J Gastroenterol* 1998; **93**: 2508-2512
15 **Jones MP.** Acid suppression in gastro-oesophageal reflux disease: Why? How? How much and when? *Postgrad Med J* 2002; **78**: 465-468
16 **Fass R,** Tougas G. Functional heartburn: the stimulus, the pain, and the brain. *Gut* 2002; **51**: 885-892
17 **Dean BB,** Gano AD Jr, Knight K, Ofman JJ, Fass R. Effectiveness of proton pump inhibitors in nonerosive reflux disease. *Clin Gastroenterol Hepatol* 2004; **2**: 656-664
18 **Venables TL,** Newland RD, Patel AC, Hole J, Wilcock C, Turbitt ML. Omeprazole 10 milligrams once daily, omeprazole 20 mg once daily, or ranitidine 150 milligrams twice daily, evaluated as initital therapy for the relief of symptoms in general practice. *Scand J Gastroenterol* 1997; **32**: 965-973
19 **Tack J,** Fass R. Review article: approaches to endoscopic-negative reflux disease: part of the GERD spectrum or a unique acid-related disorder? *Aliment Pharmacol Ther* 2004; **19**(Suppl 1): 28-34
20 **Lauritsen K.** Management of endoscopy-negative reflux disease: progress with short-term treatment. *Aliment Pharmacol Ther* 1997; **11**(Suppl 2): 87-92
21 **Lind T,** Havelund T, Carlsson R, Anker-Hansen O, Glise H, Hernqvist H, Junghard O, Lauritsen K, Lundell L, Pedersen SA, Stubberöd A. Heartburn without oesophagitis: efficacy of omeprazole therapy and features determining therapeutic response. *Scand J Gastroenterol* 1997; **32**: 974-979
22 **Richter JE,** Kovacs TOG, Greski-Rose PA, Huang B, Fisher R. Lansoprazole in the treatment of heartburn in patients without erosive oesophagitis. *Aliment Pharmacol Ther* 1999; **13**: 795-804
23 **Katz PO,** Castell DO, Levine D. Esomeprazole resolves chronic heartburn in patients without erosive oesophagitis. *Aliment Pharmacol Ther* 2003; **18**: 875-883
24 **Armstrong D,** Talley NJ, Lauritsen K, Moum B, Lind T, Tunturi-Hihnala H, Venables T, Green J, Bigard MA, Mössner J, Junghard O. The role of acid suppression in patients with endoscopy-negative reflux disease: the effect of treatment with esomeprazole or omeprazole. *Aliment Pharmacol Ther* 2004; **20**: 413-421
25 **Bate CM,** Riley SA, Chapman RW, Durnin AT, Taylor MD. Evaluation of omeprazole as a cost-effective diagnostic test for gastro-oesophageal reflux disease. *Aliment Pharmacol Ther* 1999; **13**: 59-66
26 **Fass R,** Ofman JJ, Grainek IM, Johnson C, Camargo E, Sampliner RE, Fennerty MB. Clinical and economic assessment of the omeprazole test in patients with symptoms suggestive of gastroesophageal reflux disease. *Arch Intern Med* 1999; **159**: 2161-2168
27 **Watson RG,** Tham TC, Johnston BT, McDougall NI. Double blind cross-over study of omeprazole in the treatment of patients with reflux symptoms and physiological levels of acid reflux – the "sensitive oesophagus". *Gut* 1997; **40**: 587-590
28 **Kahrilas PJ.** Refractory heartburn. *Gastroenterology* 2003; **124**: 1941-1945
29 **Carlsson R,** Dent J, Watts R, Riley S, Sheikh R, Hatlebakk J, Haug K, de Groot G, van Oudvorst A, Dalvag A, Junghard O, Wiklund I. Gastro-oesophageal reflux disease (GORD) in primary care – an international study of different treatment strategies with omeprazole. *Eur J Gastroenterol Hepatol* 1998; **10**: 119-124
30 **Bardhan KD,** Müller-Lissner S, Bigard MS, Bianchi Porro G, Ponce J, Hosie J, Scott M, Wein DG, Gillon KRW, Peacock RA, Fulton C. Symptomatic gastro-oesophageal reflux disease: double-blinded controlled study of intermittent treatment with omeprazole or ranitidine. *BMJ* 1999; **318**: 502-507
31 **Gerson LB,** Robbins AS, Garber A, Hornberger J, Triadafilopöulos G. A cost-effectiveness analysis of prescribing strategies in the management of gastroesophageal reflux disease. *Am J Gastroenterol* 2000; **95**: 395-407
32 **Wahlqvist P,** Junghard O, Higgins A, Green J. Cost effectiveness of proton pump inhibitors in gastro-oesophageal reflux disease without oesophagitis: comparison of on-demand esomeprazole with continuous omeprazole strategies. *Pharmacoeconomics* 2002; **20**: 267-277
33 **Lind T,** Havelund T, Lundell L, Glise H, Lauritsen K, Pedersen SA, Anker-Hansen O, Stubberöd A, Eriksson G, Carlsson R, Junghard O. On demand therapy with omeprazole for the long-term management of patients with heartburn without oesophagitis – a placebo-controlled randomized trial. *Aliment Pharmacol Ther* 1999; **13**: 907-914
34 **Talley NJ,** Lauritsen K, Tunturi-Hihnala H, Lind T, Moum B, Bang C, Schulz T, Omland TM, Delle M, Junghard O. Esomeprazole 20 mg maintains symptom control in endoscopy-negative gastro-oseophageal reflux disease: a controlled trial of on-demand therapy for 6 mo. *Aliment Pharmacol Ther* 2001; **15**: 347-354
35 **Talley NJ,** Venables TL, Green JR, Armstrong D, O´Kane KP, Giaffer M, Bardhan KD, Carlsson RG, Chen S, Hasselgren GS. Esomeprazole 40 mg and 20 mg is efficacious in the long-term management of patients with endoscopy-negative gastro-oesophageal reflux disease: a placebo-controlled trial of on-demand therapy for 6 mo. *Eur J Gastroenterol Hepatol* 2002; **14**: 857-863
36 **Bayerdörffer E,** Sipponen P, Bigard M, Weiss W, Mearin F, Rodrigo L, Dominguez-Munoz J, Grundling H, Nauclér E, Svedberg L, Keeling N, Eklund S. Esomeprazole 20 mg continous versus on demand treatment of patients with endoscopy-negative reflux disease (ENRD). *Gut* 2004; **53** (Suppl 4): A106
37 **Tsai HH,** Chapman R, Shepherd A, McKeith D, Anderson M, Vearer D, Duggan S, Rosen JP. Esomeprazole 20 mg on-demand is more acceptable to patients than continuous lansoprazole 15 mg in the long-term maintenance of endoscopy-negative gastro-oesophageal reflux patients: the COMMAND study. *Aliment Pharmacol Ther* 2004; **20**: 657-665
38 **Armstrong D,** Bennett JR, Blum AL, Dent J, De Dombal FT, Galmiche JP, Lundell L, Margulies M, Richter JE, Spechler SJ, Tytgat GN, Wallin L. The endoscopic assessment of esophagitis: a progress report on observer agreement. *Gastroenterology* 1996; **111**: 85-92
39 **Lundell LR,** Dent J, Bennett JR, Blum AL, Armstrong D, Galmiche P, Johnson F, Hongo M, Richter JE, Spechler SJ, Tytgat GN, Wallin L. Endoscopic assessment of oesophagitis: clinical and functional correlates and further validation of the Los Angeles classification. *Gut* 1999; **45**: 172-180
40 **Richter JE,** Kahrilas PJ, Johanson J, Maton P, Breiter JR, Hwang C, Marino V, Hamelin B, Levine JG. Efficacy and safety of esomeprazole compared with omeprazole in GERD patients with erosive esophagitis: a randomized controlled trial. *Am J Gastroenterol* 2001; **96**: 656-665
41 **Castell DO,** Kahrilas PJ, Richter JE, Vakil NB, Johnson DA, Zuckerman S, Skammer W, Levine JG. Esomeprazole (40 mg) compared with lansoprazole (30 mg) in the treatment of erosive esophagitis. *Am J Gastroenterol* 2002; **97**: 575-583
42 **Labenz J,** Armstrong D, Lauritsen K, Katelaris P, Schmidt S, Schütze K, Wallner G, Juergens H, Preiksaitis H, Keeling N, Nauclér E, Eklund S. A randomized comparative study of esomeprazole 40 mg versus pantoprazole 40 mg for healing erosive oesophagitis: the EXPO study. *Aliment Pharmacol Ther* 2005; **21**: 739-746
43 **Chiba N,** De Gara CJ, Wilkinson JM, Hunt RH. Speed of

healing and symptom relief in grade II to IV gastroesophageal reflux disease: a meta-analysis. *Gastroenterology* 1997; **112**: 1798-1810

44 **Malfertheiner P,** Lind T, Willich S, Vieth M, Jaspersen D, Labenz J, Meyer-Sabellek W, Junghard O, Stolte M. Prognostic influence of Barrett´s oesophagus and of *H pylori* infection on healing auf erosive GORD and symptom resolution in non-erosive GORD: Report from the ProGORD study. *Gut* 2005; **54**: 746-751

45 **Holtmann G,** Cain C, Malfertheiner P. Gastric *Helicobacter pylori* infection accelerates healing of reflux esophagitis during treatment with the proton pump inhibitor pantoprazole. *Gastroenterology* 1999; **117**: 11-16

46 **Edwards SJ,** Lind T, Lundell L. Systematic review of proton pump inhibitors for the acute treatment of reflux oesophagitis. *Aliment Pharmacol Ther* 2001; **15**: 1729-1736

47 **Vakil N,** Fennerty MB. Systematic review: direct comparative trials of the efficacy of proton pump inhibitors in the management of gastro-oesophageal reflux disease and peptic ulcer. *Aliment Pharmacol Ther* 2003; **18**: 559-568

48 **Richter JE,** Kahrilas PJ, Sontag SJ, Kovacs TO, Huang B, Pencly JL. Comparing lansoprazole and omeprazole in onset of heartburn relief: results of a randomized, controlled trial in erosive esophagitis patients. *Am J Gastroenterol* 2001; **96**: 3089-3098

49 **Bell NJ,** Burget D, Howden CW, Wilkinson J, Hunt RH. Appropriate acid suppression for the management of gastrooesophageal reflux disease. *Digestion* 1992; **51**(Suppl 1): 59-67

50 **Kawamura M,** Ohara S, Koike T, Iijima K, Suzuki J, Kayaba S, Noguchi K, Hamada S, Noguchi M, Shimosegawa T. The effects of lansoprazole on erosive resflux oesophagitis are influenced by CYP2C19 polymorphism. *Aliment Pharmacol Ther* 2003; **17**: 965-973

51 **Miner P Jr,** Katz PO, Chen Y, Sostek M. Gastric acid control with esomperazole, lansoprazole, omeprazole, pantoprazole, and rabeprazole: a five-way crossover study. *Am J Gastroenterol* 2003; **98**: 2616-2620

52 **Röhss K,** Wilder-Smith C, Nauclér E, Jansson L. Esomeprazole 20 mg provides more effective intragastric acid control than maintenance-dose rabeprazole, lansoprazole or pantoprazole in healthy volunteers. *Clin Drug Invest* 2004; **24**: 1-7

53 **Kahrilas PJ,** Falk GW, Johnson DA, Schmitt C, Collins DW, Whipple J, D´Amico D, Hamelin B, Joelsson B. Esomeprazole improves healing and symptom resolution as compared with omeprazole in reflux oesophagitis patients: a randomized controlled trial. *Aliment Pharmacol Ther* 2000; **14**: 1249-1258

54 **Fennerty MB,** Johanson J, Hwang C, Hoyle P, Sostek M. Esomeprazole 40 mg versus lansoprazole 30 mg in healing and symptom relief in patients with moderate to severe erosive oesophagitis (Los Angeles C & D). *Gut* 2004; **53**(Suppl 4): A111-112

55 **Labenz J,** Armstrong D, Katelaris P, Schmidt S, Nauclér E, Eklund S. Analysis of healing associated with 4 weeks' esomperazole 40 mg treatment relative to lansoprazole 30 mg and pantoprazole 40 mg in patients with all grades of erosive esophagitis. *Gut* 2004; **53**(Suppl 4): A105

56 **Gillessen A,** Beil W, Modlin IM, Gatz G, Hole U. 40 mg pantoprazole and 40 mg esomeprazole are equivalent in the healing of esophageal lesions and relief from gastroesophageal reflux disease-related symptoms. *J Clin Gastroenterol* 2004; **38**: 332-340

57 **Scholten T,** Gatz G, Hole U. Once-daily pantoprazole 40 mg and esomeprazole 40 mg have equivalent overall efficay in relieving GERD-related symptoms. *Aliment Pharmacol Ther* 2003; **18**: 587-594

58 **Tinmouth JM,** Steele LS, Tomlinson G, Glazier RH. Are claims of equivalency in digestive disease trials supported by the evidence? *Gastroenterology* 2004; **126**: 1700-1710

59 **Fass R,** Thomas S, Traxler B, Sostek M. Patient reported outcome of heartburn improvement: doubling the proton pump inhibitor (PPI) dose in patients who failed standard dose PPI versus switching to a different PPI. *Gastroenterology* 2004; **126**: A37

60 **Hatlebakk JG,** Katz PO, Kuo B, Castell DO. Nocturnal gastric acidity and acid breakthrough on different regimens of omeprazole 40 mg daily. *Aliment Pharmacol Ther* 1998; **12**: 1235-1240

61 **Ours TM,** Fackler WK, Richter JE, Vaezi MF. Nocturnal acid breakthrough: clinical significance and correlation with esophageal acid exposure. *Am J Gastroenterol* 2003; **98**: 545-550

62 **Fackler WK,** Ours TM, Vaezi MF, Richter JE. Long-term effect of H2RA therapy on nocturnal gastric acid breakthrough. *Gastroenterology* 2002; **122**: 625-632

63 **Vakil NB,** Shaker R, Johnson DA, Kovacs T, Baerg RD, Hwang C, D'Amico D, Hamelin B. The new proton pump inhibitor esomeprazole is effective as a maintenance therapy in GERD patients with healed erosive oesophagitis: a 6-mo, randomized, double-blind, placebo-controlled study of efficacy and safety. *Aliment Pharmacol Ther* 2001; **15**: 927-935

64 **Johnson DA,** Benjamin SB, Vakil NB, Goldstein JL, Lamet M, Whipple J, D´Amico D, Hamelin B. Esomeprazole once daily for 6 mo is effective therapy for maintaining healed erosive esophagitis and for controlling gastroesophageal reflux disease symptoms: a randomized, double-blind, placebo-controlled study of efficacy and safety. *Am J Gastroenterol* 2001; **96**: 27-34

65 **Johnsson F,** Moum B, Vilien M, Grove O, Simren M, Thoring M. On-demand treatment in patients with oesophagitis and reflux symptoms: comparison of lansoprazole and omeprazole. *Scand J Gastroenterol* 2002; **37**: 642-647

66 **Sjöstedt S,** Befrits R, Sylvan A, Carling L, Harthon C, Modin S, Stubberöd A, Toth E, Lind T. On demand versus continuous treatment with esomeprazole (ESO) 20 mg once daily in subjects with healed erosive esophagitis (EE) after initial healing with ESO 40 mg once daily. An open, randomised, Swedish multicenter study. *Gut* 2004; **53**(Suppl 4): A68

67 **Richter JE,** Fraga P, Mack M, Sabesin SM, Bochenek W. The Pantoprazole US GERD Study Group. Prevention of erosive esophagitis relapse with pantoprazole. *Aliment Pharmacol Ther* 2004; **20**: 1-9

68 **Vigneri S,** Termini R, Leandro G, Badalamenti S, Pantalena M, Savarino V, Di Mario F, Battaglia G, Sandro Mela G, Pilotto A, Blebani M, Davi G. A comparison of five maintenance therapies for reflux esophagitis. *N Engl J Med* 1995; **333**: 1106-1110

69 **You JH,** Lee AC, Wong SC, Chan FK. Low-dose or standard dose proton pump inhibitors for maintenance therapy of gastro-oesophageal reflux disease: a cost-effectiveness analysis. *Aliment Pharmacol Ther* 2003; **17**: 785-792

70 **Inadomi JM,** Jamal R, Murata GH, Hoffman RM, Lavezo LA, Vigil JM, Swanson KM, Sonnenberg A. Step-down management of gastroesophageal reflux disease. *Gastroenterology* 2001; **121**: 1095-1100

71 **Inadomi JM,** McIntyre L, Bernard L, Fendrick AM. Step-down from multiple- to single-dose proton pump inhibitors (PPIs): a prospective study of patients with heartburn or acid regurgitation completely relieved with PPIs. *Am J Gastroenterol* 2003; **98**: 1940-1944

72 **Klinkenberg-Knol EC,** Nelis F, Dent J, Snel P, Mitchell B, Prichard P, Lloyd D, Havu N, Frame MH, Roman J, Walan A. Long-term omeprazole treatment in resistant gastroesophageal reflux disease: efficacy, safety, and influence on gastric mucosa. *Gastroenterology* 2000; **118**: 661-669

73 **Lauritsen K,** Devière J, Bigard MA, Bayerdörffer E, Mózsik G, Murray F, Kristjánsdóttir S, Savarino V, Vetvik K, De Freitas D, Orive V, Rodrigo L, Fried M, Morris J, Schneider H, Eklund S, Larkö A. Esomeprazole 20 mg and lansoprazole 15 mg in maintaining healed reflux oesophagitis: Metropole study results. *Aliment Pharmacol Ther* 2003; **17**: 333-341

74 **DeVault KR,** Liu S, Hoyle P, Sostek M. Esomeprazole 20 mg versus lansoprazole 15 mg for maintenance of healing of erosive esophagitis. *Am J Gastroenterol* 2004; **99**(Suppl): S6-S7

75 **Labenz J,** Armstrong D, Katelaris P, Schmidt S, Adler J,

Eklund S. A comparison of esomeprazole and pantoprazole for maintenance treatment of healed erosive esophagitis. *Gut* 2004; **53**(Suppl 4): A108

76 **Labenz J,** Armstrong D, Katelaris P, Schmidt S, Eklund S. The effect of *Helicobacter pylori* status on maintenance therapy for healed erosive esophagitis with esomeprazole 20 mg or pantoprazole 20 mg. *Helicobacter* 2004; **9**: 544

77 **Labenz J.** Protagonist: Should we eradicate *Helicobacter pylori* before long term antireflux therapy? *Gut* 2001; **49**: 614-616

78 **Freston JW.** Antagonist: Should we eradicate *Helicobacter pylori* before long term antireflux therapy? *Gut* 2001; **49**: 616-617

79 **Moayyedi P,** Bardhan C, Young L, Dixon MF, Brown L, Axon AT. *Helicobacter pylori* eradication does not exacerbate reflux symptoms in gastroesophageal reflux disease. *Gastroenterology* 2001; **121**: 1120-1126

80 **Malfertheiner P,** Megraud F, O´Morain C, Hungin AP, Jones R, Axon A, Graham DY, Tytgat G. Current concepts in the management of *Helicobacter pylori* infection – the Maastricht 2-2000 Consensus Report. *Aliment Pharmacol Ther* 2002; **16**: 167-180

81 **Lundell L,** Miettinen P, Myrvold HE, Pedersen SA, Liedman B, Hatlebakk JG, Julkonen R, Levander K, Carlsson J, Lamm M, Wiklund I. Continued (5-year) lollow-up of a randomized clinical study comparing antireflux surgery and omeprazole in gastroesophageal reflux disease. *J Am Coll Surg* 2001; **192**: 172-179

82 **Lundell L,** Miettinen P, Myrvold HE, Pedersen SA, Thor K, Lamm M, Blomqvist A, Hatlebakk JG, Janatuinen E, Levander K, Nyström P, Wiklund I. Long-term management of gastro-oesophageal reflux disease with omeprazole or open antireflux surgery: results of a prospective, randomized clinical trial. *Eur J Gastroenterol Hepatol* 2000; **12**: 879-887

83 **Arguedas MR,** Heudebert GR, Klapow JC, Centor RM, Eloubeidi MA, Wilcox CM, Spechler SJ. Re-examination of the cost-effectiveness of surgical versus medical therapy in patients with gastroesophagealen reflux disease: the value of long-term data collection. *Am J Gastroenterol* 2004; **99**: 1023-1028

84 **Myrvold HE,** Lundell L, Miettinen P, Pedersen SA, Liedman B, Hatlebakk J, Julkunen R, Levander K, Lamm M, Mattson C, Carlsson J, Stalhammar NO. The cost of long term therapy for gastro-oesophageal reflux disease: a randomised trial comparing omeprazole and open antireflux surgery. *Gut* 2001; **49**: 488-494

85 **Freston JW,** Triadafilopoulos G. Review article: approaches to the long-term management of adults with GERD – proton pump inhibitor therapy, laparoscopic fundoplication or endoscopic therapy? *Aliment Pharmacol Ther* 2004; **19**(Suppl 1): 35-42

86 **Arts J,** Tack J, Galmiche JP. Endoscopic antireflux procedures. *Gut* 2004; **53**: 1207-1214

87 **Corley DA,** Katz P, Wo J, Stefan A, Patti M, Rothstein R, Edmundowicz S, Kline M, Mason R, Wolfe MM. Improvement of gastroesophageal reflux symptoms after radiofrequency energy: a randomized, sham-controlled trial. *Gastroenterology* 2003; **125**: 668-676

88 **Dent J,** Talley NJ. Oveview: initial and long-term management of gastro-oesophageal reflux disease. *Aliment Pharmacol Ther* 2003; **17**(Suppl 1): 53-57

89 **Howden CW,** Henning JM, Huang B, Lukasik N, Freston JW. Management of heartburn in a large, randomized, community-based study: comparison of four therapeutic strategies. *Am J Gastroenterol* 2001; **96**: 1704-1710

90 **Armstrong D,** Barkun AN, Chiba N, Veldhuyzen van Zanten S, Thomson ABR, Smyth S, Chakraborty B, Sinclair P. 'Start high´ - A better acid suppression strategy for heartburn-dominant uninvestigated dyspepsia (DU) in primary care practice (PCP) – the CADET-HR study. *Gastroenterology* 2002; **122**: A472

91 **Meineche-Schmidt V,** Hauschildt Juhl H, Ostergaard JE, Luckow A, Hvenegaard A. Costs and efficacy of three different esomeprazole treatment strategies for long-term management of gastro-oesophageal reflux symptoms in primary care. *Aliment Pharmacol Ther* 2004; **19**: 907-915

Science Editor Guo SY **Language Editor** Elsevier HK

PO Box 2345, Beijing 100023, China
www.wjgnet.com
wjg@wjgnet.com

ELSEVIER

World J Gastroenterol 2005;11(28):4300-4304
World Journal of Gastroenterology ISSN 1007-9327

• *GASTRIC CANCER* •

Oral Xeloda plus bi-platinu two-way combined chemotherapy in treatment of advanced gastrointestinal malignancies

Li Fan, Wen-Chao Liu, Yan-Jun Zhang, Jun Ren, Bo-Rong Pan, Du-Hu Liu, Yan Chen, Zhao-Cai Yu

Li Fan, Wen-Chao Liu, Yan-Jun Zhang, Jun Ren, Bo-Rong Pan, Du-Hu Liu, Yan Chen, Zhao-Cai Yu, Department of Oncology, Xijing Hospital, Fourth Military Medical University, Xi'an 710032, Shaanxi Province, China
Supported by the Funds of Clinical New Technology from Xijing Hospital, Fourth Military Medical University, No. XJGXO4018M13
Correspondence to: Li Fan, Department of Oncology, Xijing Hospital, Fourth Military Medical University, Xi'an 710032, Shaanxi Province, China. fanli@medmail.com.cn
Telephone: +86-29-83375680
Received: 2004-11-20 Accepted: 2005-01-26

Abstract

AIM: To compare the effect, adverse events, cost-effectiveness and dose intensity (DI) of oral Xeloda *vs* calcium folinate (CF)/5-FU combination chemotherapy in patients with advanced gastrointestinal malignancies, both combined with bi-platinu two-way chemotherapy.

METHODS: A total of 131 patients were enrolled and randomly selected to receive either oral Xeloda (X group) or CF/5-FU (control group). Oral Xeloda 1 000 mg/m^2 was administered twice daily from d 1 to 14 in X group, while CF 200 mg/m^2 was taken as a 2-h intravenous infusion followed by 5-FU 600 mg/m^2 intravenously for 4-6 h on d 1-5 in control group. Cisplatin and oxaliplatin were administered in the same way to both the groups: cisplatin 60-80 mg/m^2 by hyperthermic intraperitoneal administration, and oxaliplatin 130 mg/m^2 intravenously for 2 h on d 1. All the drugs were recycled every 21 d, with at least two cycles. Pyridoxine 50 mg was given t.i.d. orally for prophylaxis of the hand-foot syndrome (HFS). Then the effect, adverse events, cost-effectiveness and DI of the two groups were evaluated.

RESULTS: Hundred and fourteen cases (87.0%) finished more than two chemotherapy cycles. The overall response rate of them was 52.5% (X group) and 42.4% (control group) respectively. Tumor progression time (TTP) was 7.35 mo *vs* 5.95 mo, and 1-year survival rate was 53.1% *vs* 44.5%. There was a remarkable statistical significance of TTP and 1-year survival between the two groups. The main Xeloda-related adverse events were myelosuppression, gastrointestinal toxicity, neurotoxicity and HFS, which were mild and well tolerable. Therefore, no patients withdrew from the study due to side effects before two chemotherapy cycles were finished. Both groups finished pre-arranged DI and the relative DI was nearly 1.0. The average cost for 1 patient in one cycle was ￥9 137.35 (X group) and ￥8 961.72 (control group), or US $1 100.89 in X group and $1 079.73 in control group. To add 1% to the response rate costs ￥161.44 *vs* ￥210.37 respectively (US $19.45 *vs* $25.35). One-month prolongation of TTP costs ￥1 243.18 *vs* ￥1 506.17 (US $149.78 *vs* $181.47). Escalation of 1% of 1-year survival costs ￥172.74 *vs* ￥201.64 (US $20.75 *vs* $24.29).

CONCLUSION: Oral Xeloda combined with bi-platinu two-way combination chemotherapy is efficient and tolerable for patients with advanced gastrointestinal malignancies; meanwhile the expenditure is similar to that of CF/5-FU combined with bi-platinu chemotherapy, and will be cheaper if we are concerned about the increase of the response rate, TTP or 1-year-survival rate pharmacoeconomically.

Key words: Pharmacoeconomic; Xeloda; Advanced gastrointestinal malignancy; Hyperthermic intraperitoneal chemotherapy; Dose intensity

Fan L, Liu WC, Zhang YJ, Ren J, Pan BR, Liu DH, Chen Y, Yu ZC. Oral Xeloda plus bi-platinu two-way combined chemotherapy in treatment of advanced gastrointestinal malignancies. *World J Gastroenterol* 2005; 11(28): 4300-4304
http://www.wjgnet.com/1007-9327/11/4300.asp

INTRODUCTION

Pharmacoeconomics is a method to study the various economic costs associated with prescribing a given drug or a treatment regimen. This field of health services research and technology assessment developed in the 1960s, and it is only in the last decade that scholars have been trying to develop strong standards for its use[1]. There are four main kinds of cost analysis involved. First, the analysis of cost minimization is to find the most inexpensive treatment. Second, the cost-effectiveness analysis takes a single outcome into account, such as years of life saved, and attempts to determine the cost for each year of those additional years. The third analysis is cost utility. It is a subtype of cost-effectiveness and incorporates quality-of-life measures that focus on a patient's Quality Adjusted Life Year. The fourth is cost-benefit analysis. This analysis puts a dollar amount on additional years of life. Among the four analyses, the cost-effectiveness analysis is widely and more often used to compare the costs and clinical outcomes of competing treatment options[2]. This analysis provides an estimate of

the costs incurred to achieve a particular outcome. It is measured by dividing a therapy's total cost by its therapeutic effectiveness, which might be cure rate, remission rate, or some other end point depending on the drug and disease involved[3-5]. Oncology pharmacoeconomics differs slightly from pharmacoeconomics for drugs for other diseases. Pharmacoeconomics of anticancer drugs is to offer an effective, safe and economic regimen for patients with end-stage cancer under the precondition of limited medical cost.

Gastrointestinal cancer ranks the top of the morbidity and mortality of the cancer in China. The general chemotherapy usually has little effect on the end-stage patients with little opportunity to resect because of implantation in cavity, local recurrence after operation, or metastasis of lymph node or viscera. From December 2001 to April 2004, 131 end-stage cases of carcinoma of stomach and colorectum in our department were admitted for the new combination chemotherapy. Among them, 51 cases received the regimen of oral Xeloda with bi-platinu (oxaliplatin and cisplatin) in two ways (intravenous and intraperitoneal administration), the other cases received the regimen of calcium folinate (CF)/5-FU with bi-platinu in the same two ways as the former. The cost-effectiveness and quality-of-life index effect of this new chemotherapy regimen were compared with another chemotherapy. The dosage intensity of these two chemotherapy regimens were also compared.

MATERIALS AND METHODS

Patients

A total of 131 cases of advanced gastrointestinal cancer with 80 men and 51 women, mean age being 57.6 years ranging from 33 to 83 years were included. There were 61 cases of gastric carcinoma and 70 cases of colorectal cancer. All the patients were in stage IV by clinical assessment, which was confirmed by biopsy. About 83.7% of patients had received one combination chemotherapy at least, but no chemotherapy was administered to them within a month. Karnofsky performance status of all these patients measured at baseline was $\geqslant$60, and the anticipative survival time was $\geqslant$3 mo with observable objective index of the focus. They were randomly divided into two groups, Xeloda and control group (abbreviated as X group and C group, respectively). The main clinical characteristics of the two groups are listed in Table 1.

Table 1 Clinical characteristics of stage IV gastrointestinal cancer

Clinical characteristics	Gastric cancer		Colorectal cancer	
	X group	C group	X group	C group
Male / female	21 / 11	17 / 12	19 / 16	23 / 12
Age: mean (range / yr)	63.6 (36–83)	61.0 (33–80)	62.9 (45–75)	60.8 (34–74)
Recurrence (%)	14 (43.8)	14 (48.3)	8 (22.9)	9 (25.7)
Metastasis				
Liver (%)	17 (53.1)	16 (55.2)	21 (60.0)	22 (62.9)
Lung (%)	8 (25.0)	7 (24.1)	11 (31.4)	10 (28.6)
Celiac lymph node (%)	21 (65.6)	21 (72.4)	14 (40.0)	15 (42.9)
Others (%)	8 (25.0)	9 (31.0)	12 (34.3)	10 (28.6)
Previous chemotherapy	23 (71.9)	22 (75.9)	17 (48.6)	19 (54.3)

Drugs

Xeloda® was supplied as white film-coated tablets containing 500 mg capecitabine manufactured by Roche Pharmaceutical Ltd. CF and oxaliplatin were purchased from Jiangshu Henrui Pharmaceutical Co. Ltd, packed in 100 or 50 mg per vial and 20 mg of cisplatin in a vial was supplied by Shandong Qilu Pharmaceutical Factory. 5-FU was packed in 250 mg per ampule and manufactured by Shanghai Pharmaceutical Factory.

Treatment regimen

Oral Xeloda 1 000 mg/m^2 was administered twice daily from d 1 to 14 in X group, while CF 200 mg/m^2 was taken as a 2-h intravenous infusion followed by 5-FU 600 mg/m^2 intravenous infusion for 4-6 h on d 1-5 in C group. Cisplatin and oxaliplatin were given in the same way to both the groups: cisplatin 60-80 mg/m^2 hyperthermic intraperitoneal abdominal administration, and oxaliplatin 130 mg/m^2 intravenous infusion for 2 h on d 1. All the drugs were recycled every 21 d, with at least two cycles. Granisetron 40 μg/kg was given by intravenation before intravenous or intraperitoneal chemotherapy. Pyridoxine (vitamin B6) 50 mg was given t.i.d. orally for prophylaxis of the hand-foot syndrome (HFS).

Effectiveness and side effects

The short-term effect is classified into four grades as complete remission (CR), part remission (PR), no-change (NC) and progress of disease (PD) by the evaluation standard of short-term effect introduced by WHO[6]. The responsible effective rate (RR) is prescribed to CR+PR (%). There are two other indexes, TTP (time of tumor progress) and 1-year survival rate, which have been adopted to evaluate the mid-term effect. Side effects were added up by standard grade, also introduced by WHO[7] in both the groups regardless of the kind of disease. The classification HFS was graded according to the criteria of WHO[8]: I-dysesthesia/paresthesia, tingling in the hands and feet; II- discomfort in holding objects and upon walking, painless swelling or erythema; III-painful erythema and swelling of palms and soles, periungual erythema and swelling; IV- desquamation, ulceration, blistering, severe pain.

Dose intensity estimation

Two indexes of dose intensity (DI) were calculated by the following formula: DI = total dosage (mg/m^2)/duration of treatment (weeks), relative DI = actual DI/standard DI[9].

Costs estimation

The costs evaluated consisted of two parts, the direct medical cost and the indirect one[5]. The cost of drugs (chemical drug, GM-CSF or G-CSF, the drug to ameliorate gastrointestinal side effect, and so on), hospital stays, the required medical staff, laboratory and diagnostic tests were included in the direct medical cost. The part indirect cost contained the material loss because of the absence of the patients and their relatives from work. Two periods of treatment were added up, then the average cost per patient in one cycle was obtained. The cost of therapy was expressed in Chinese currency (Ren-Min-Bi, ¥) and in US dollars

Table 2 Different chemotherapeutic effect of gastrointestinal cancers

Therapeutic effect	Gastric cancer		Colorectal cancer		Total	
	X group	C group	X group	C group	X group	C group
n	24	25	31	34	55	59
CR (*n*)	1	1	1	0	2	1
PR (*n*)	13	10	14	14	27	24
NC (*n*)	5	10	12	14	17	24
PD (*n*)	5	4	4	6	9	10
CR+PR (*n*)	14	11	17	14	29	25
(%)	58.3	44.0	54.8	41.2	52.7	42.4
TTP (mo)	7.0±1.3[a]	5.4±0.9	7.8±1.9[a]	6.7±2.0	7.4±1.7[a]	6.0±1.5
1-yr survival (%)	41.7[a]	36.0	64.5[a]	52.9	53.1[a]	44.5

[a]$P<0.05$ *vs* C group.

Table 3 Chemotherapeutic side effects of gastrointestinal cancers (*n*)

Side effects	X group (*n* = 55)				C group (*n* = 59)			
	I	II	III	IV	I	II	III	IV
Leukopenia	21	8	5	0	20	8	4	0
Thrombocytopenia	10	5	1	0	13	4	2	0
Nausea	15	19	10	2	16	20	11	2
Vomiting	11	11	4	1	14	12	3	2
Diarrhea	7	9	3	0	5	6	2	0
HFS	32	2	1	0	8	2	0	0
Neurotoxicity	12	11	0	0	14	12	1	0

(US $). The rate of exchange between them was 1:8.3.

Cost-effectiveness analysis

Based on the total costs, the expenses that add to 1% of the response rate (costs/total efficient rate), one-month prolongation of TTP (costs/TTP) and the escalation of 1% of 1 year (costs/1-year survival rate) were calculated, respectively.

Statistical analysis

All data are expressed as mean±SD, except as otherwise stated. Parameters were compared by using *t* test, or χ^2 test.

RESULTS

Effect

In 131 cases, 17 patients (13.0%) terminated treatment after one cycle because of disease progression, refusal to continue chemotherapy or other reasons. Fifty-eight cases (44.3%) finished two or three cycles of chemotherapy, 33 patients (25.2%) finished four or five cycles of chemotherapy, the other 23 cases (17.6%) finished six or more cycles of chemotherapy. The average number of completed chemotherapy cycles was 2.6. These 114 who finished more than two chemotherapy cycles were analyzed. For both the short-term and mid-term effect, the X group was better than C group. But there was no statistical difference in the short-term effect. Short-term effect of gastric cancer group was superior to that of colorectal cancer group, whereas mid-term effect of the former was inferior to that of the latter (Table 2).

Side effects

To 114 patients who finished more than two chemotherapy cycles, the side effects were observed and summed up when the second cycle ended (Table 3). In X group, the rates of leukopenia, thrombocytopenia, nausea, vomiting, diarrhea and neurotoxicity above grade II were 23.6%, 10.9%, 56.4%, 29.1%, 21.8%, and 20.0%, respectively. In C group, the rates were 20.3%, 10.2%, 55.9%, 28.8%, 13.6%, and 22.0%, respectively. No statistical difference was revealed between the two groups.

The occurrence of HFS that appeared in X group was higher than that of C group (63.6% *vs* 16.9%, $P<0.05$), but 97.1% of HFS episodes were grade 1 or 2. No patient withdrew from the study, and none required dose modification due to side effects before two chemotherapy cycles were finished.

Dose intensity

Relative DI mg/(m^2×week) cannot be achieved due to the delay in the treatment (including side effect and noncompliance), which means that the actual DI is lower than standard DI. There was no statistical difference in relative DI between the two groups (Table 4).

Table 4 Chemotherapeutic DI of gastrointestinal cancers, mg/(m^2·wk)

DI	X group			C group			
	Oxal[1]	DDP[1]	Xeloda	Oxal[1]	DDP[1]	CF	5-FU
Standard	43.3	40.0	9 333.3	43.3	40.0	333.3	1 000.0
Actual	40.7	38.3	8 662.7	41.3	38.7	322.7	966.7
Relative	0.94	0.96	0.93	0.95	0.97	0.97	0.97

[1]Oxal – oxaliplatin; DDP – cisplatin.

Costs and cost-effectiveness

There was a statistical difference in the average hospitalization

Table 5 The average cost per patient of two groups (mean±SD, ￥, US $)

Group	Hospitalization(d)	Cost of drug		Other cost		Total cost	
		￥	US $	￥	US $	￥	US $
X	5.94±3.11[a]	7 887.33±140.92[a]	950.28±16.98[a]	1 250.02±101.43[a]	150.60±12.22[a]	9 137.35±121.18	1 100.89±14.60
C	9.37±2.73	6 108.97±205.44	736.02±24.75	2 852.75±217.73	343.70±26.23	8 961.72±211.59	1 079.73±25.50

[a]P<0.05 *vs* C group.

Table 6 Comparison of cost-effectiveness of two groups

Group	Costs / efficient		Costs / TTP		Costs / 1-year survival	
	￥	US $	￥	US $	￥	US $
X	161.44±2.14[a]	19.45±0.26[a]	1 243.18±16.49[a]	149.78±1.99[a]	172.24±2.28[a]	20.75±0.27[a]
C	210.37±4.97	25.35±0.60	1 506.17±35.56	181.47±4.28	201.61±4.76	24.29±0.57

[a]P<0.05 *vs* C group.

time between the two groups (P<0.05, Table 5). The drug costs of X group was higher than that of C group, but other costs (the costs of hospitalization, cancer clinic care and others) were adverse, so there was no difference in the total costs between the two groups. The cost-effectiveness ratio obtained from X group was more satisfactory than that of C group no matter what the cost of percentage response rate, per TTP and per life-year survival (Table 6).

DISCUSSION

The morbidity caused by gastric and colorectal carcinoma are respectively the first and the fourth in China[10,11]. It is difficult to cure the patients at the end stage without a chance for operation or with recurrence and metastasis. 5-FU is a basic drug for gastrointestinal cancer, but its effective rate is only 10-20%. Increasing the dosage, intravenous injection continually or in combination with intensifier can enhance the effect of 5-FU, whereas its side effects and medical costs will increase too. For example, increasing the dosage can result in higher incidence of stomatitis and extremity syndrome, and intravenous injection continually or in combination with intensifier leads to more severe phlebitis, and all of which raise the cost. The regimen of 5-FU combined with CF and levamisole has stood the dominant status in treating tumor of the digestive system for more than 20 years[12,13]. Recently, oxaliplatin combined with 5-FU and CF has become the most frequent and effective chemical therapy for patients with colorectal cancer, and also has been used to treat gastric cancer[14-17].

Xeloda (capecitabine) is a novel, oral, selectively tumor-activated fluoropyrimidine carbamate and absorbed by small intestine in antetype term. It can be activated and transformed to 5-FU by thymidine phosphorylase that has high competence in tumor. So the concentration of 5-FU in tumor tissue is much higher than that in normal tissue and its systemic side effect is lower[18-21]. Xeloda has already been used to treat advanced gastrointestinal cancer with much better result. If combined with oxaliplatin, there will be good results.

The heat-chemical therapy of abdominal cavity includes heat and chemical drug treatments. This therapy has many advantages. It can increase the concentration, the contact surface and the time of the drug in abdominal cavity by perfusing heat drug into abdominal cavity, which is in favor of prolonging action time and killing of cancer cell. A part of the drug can be absorbed by the peritoneum and come into the liver *via* portal vein, which can prevent and eliminate metastatic focus in liver. Its heat effect (40-45 ℃) can reduce the pH value in and around the tumor, which will result not only in metabolic disturbance of the tumor, but also the amelioration of the function of the cellular immunity. Furthermore, the heat can kill the tumor cell directly by cytotoxic effect[22-24]. Considering those advantages, the oral Xeloda combined with bi-platinu two-way heat-chemical therapeutic regimen was adopted to treat 55 patients with advanced gastrointestinal cancer and this regimen was compared with another regimen, 5-FU/CF combined with bi-platinu two-way heat-chemical therapeutic regimen simultaneously. Our results revealed that the effect, 1 year survival and TTP of the former were much better than the latter, and that there was little difference in primary side effect, such as the reaction of the alimentary system and nervous system, bone marrow depression and extremity syndrome between the two groups.

There is a relationship between the dose and effect for cancer chemotherapy. Following the increasing dosage, the effect will be improved, but the side effect and expenses will be increased. So a balance between effect, side effect and expense is needed. Pharmacoeconomics and the study of DI are the new hot points in cancer chemotherapy. To choose the optimal regimen and distribute the limited medical cost, the cost-effectiveness and quality-of-life index effect of oral Xeloda were investigated and compared with CF/5-FU combination chemotherapy in patients with advanced gastrointestinal malignancies, both combined with bi-platinu two-way chemotherapy. Generally, the expenses of the treatment include the direct medical and non-medical fees and indirect medical fee. The average cost for a patient in one cycle was ￥9 137.35 in X group. This cost was a little higher than that in control group (￥8961.72). But the cost-effectiveness analysis is more important, because the elongation of survival time and increasing the survival rate should be emphasized in addition to the effective rate[25]. The costs of Xeloda group and the cost of unit effect were fewer than C group. Because Xeloda was administered in

lower dosage (1 000 mg/m^2 twice daily) in our study, not 1 250 mg/m^2 twice daily as recommended, the incidence of grade 3 or 4 of HFS was reduced. Pyridoxine being given at a high dose from the beginning may be useful for the prophylaxis of the occurrence of HFS[7,26]. For other minor side effects of the two regimens, all patients having accomplished the treatment on time, would mean the relative DI of two groups is close to one. However, the shorter intermission of Xeloda group (about 7 d) leads to the stronger of the actual DI [8 662.7 mg/(m^2·wk)] which probably is another reason for the better effect of Xeloda group than control group. The DI is an index to evaluate the drug or regimen. The analysis of relation between DI and effect will help to improve the effect of the chemical therapy by increasing the dosage of unit time or decreasing intermission of chemical therapy[27-29].

In summary, oral capecitabine can mimic continuous infusion of 5-FU and avoid the inconvenience, complications, and additional costs associated with intravenous chemotherapy. The regimen of oral Xeloda with bi-platinu in two ways (intravenous and intraperitoneal administration) to treat the advanced gastrointestinal cancer has better short-term and long-term effect. It is an effective, safe and economic regimen for patients, even for the old. For ideal pharmacoeconomics, satisfying DI and good compliance, this regimen has a good prospect in the future.

ACKNOWLEDGMENTS

The authors thank Xiao-Yan Zhang, Ai-Le Zhang and other medical representatives of Xi'an Branch Office of Shanghai Roche Pharmaceuticals Ltd, for their valuable discussion and comments.

REFERENCES

1 **Amber D.** Pharmacoeconomic analyses make way into oncology. *J Natl Cancer Inst* 2000; **92**: 1204-1205
2 **Walt JG,** Lee JT. A cost-effectiveness comparison of bimatoprost versus latanoprost in patients with glaucoma or ocular hypertension. *Surv Ophthalmol* 2004; **49**(Suppl 1): S36-44
3 **Collazo Herrera M,** Cardenas Rodriguez J, Gonzalez Lopez R, Miyar Abreu R, Galvez Gonzalez AM, Cosme Casulo J. Health economics: should it concern the health sector? *Rev Panam Salud Publica* 2002; **12**: 359-365
4 **Cohen BJ.** Discounting in cost-utility analysis of healthcare interventions: reassessing current practice. *Pharmacoeconomics* 2003; **21**: 75-87
5 **Clegg A,** Scott DA, Sidhu M, Hewitson P, Waugh N. A rapid and systematic review of the clinical effectiveness and cost-effectiveness of paclitaxel, docetaxel, gemcitabine and vinorelbine in non-small-cell lung cancer. *Health Technol Assess* 2001; **5**: 1-195
6 **Omori H,** Nio Y, Yano S, Itakura M, Koike M, Toga T, Matsuura S. A fractal dimension analysis: a new method for evaluating the response of anticancer therapy. *Anticancer Res* 2002; **22**: 2347-2354
7 **Cassidy J,** Twelves C, Van Cutsem E, Hoff P, Bajetta E, Boyer M, Bugat R, Burger U, Garin A, Graeven U, McKendric J, Maroun J, Marshall J, Osterwalder B, Perez-Manga G, Rosso R, Rougier P, Schilsky RL. First-line oral capecitabine therapy in metastatic colorectal cancer: a favorable safety profile compared with intravenous 5-fluorouracil/leucovorin. *Ann Oncol* 2002; **13**: 566-575
8 **Abushullaih S,** Saad ED, Munsell M, Hoff PM. Incidence and severity of hand-foot syndrome in colorectal cancer patients treated with capecitabine: a single-institution experience. *Cancer Invest* 2002; **20**: 3-10
9 **Feng FY,** Zhou AP. Dose intensity and high dose chemotherapy used in breast neoplasm cancer. *Chin J Oncol* 2002; **24**: 200-202
10 **Jin ML.** Gastric cancer. In: Sun Yan: *Medical Oncology*. 1sted. *Peoplp's health Press, Beijing* 2001: 549-572
11 **Shao YF,** Zhou ZX, Liu SM, Wang LH, Qian TN, Xu BH. Colorectal cancer. In: Sun Yan: *Medical oncology*. 1sted. *Peoplp's health Press, Beijing* 2001: 593-629
12 **Christopoulou A.** Chemotherapy in metastatic colorectal cancer.*Tech Coloproctol* 2004; **8**(Suppl 1): S43-46
13 **Sobrero A,** Caprioni F, Fornarini G, Mammoliti S, Comandini D, Baldo S, Decian F. Pemetrexed in gastric cancer. *Oncology* 2004; **18**(13 Suppl 8): 51-55
14 **Macdonald JS.** Clinical overview: adjuvant therapy of gastrointestinal cancer. *Cancer Chemother Pharmacol* 2004; **54** (Suppl 1): S4-11
15 **Gowda A,** Goel R, Berdzik J, Leichman CG, Javle M. Hypersensitivity Reactions to oxaliplatin: incidence and management. *Oncology* 2004; **18**: 1671-16755
16 **Grothey A,** Goldberg RM. A review of oxaliplatin and its clinical use in colorectal cancer. *Expert Opinion Pharmacother* 2004; **5**: 2159–2170
17 **Rustum YM.** Thymidylate synthase: a critical target in cancer therapy? *Front Biosci* 2004; **9**: 2467-2473
18 **Diaz-Rubio E.** New chemotherapeutic advances in pancreatic, colorectal, and gastric cancers. *Oncologist* 2004; **9**: 282-294
19 **Hong YS,** Song SY, Lee SI, Chung HC, Choi SH, Noh SH, Park JN, Han JY, Kang JH, Lee KS, Cho JY. A phase II trial of capecitabine in previously untreated patients with advanced and/or metastatic gastric cancer. *Ann Oncol* 2004; **15**: 1344-1347
20 **Diaz-Rubio E,** Evans TR, Tabemero J, Cassidy J, Sastre J, Eatock M, Bisset D, Regueiro P, Baselga J. Capecitabine (Xeloda) in combination with oxaliplatin: a phase I, dose-escalation study in patients with advanced or metastatic solid tumors. *Ann Oncol* 2002; **13**: 558-565
21 **Scheithauer W,** Kornek GV, Raderer M, Schull B, Schmid K, Kovats E, Schneeweiss B, Lang F, Lenauer A, Depisch D. Randomized multicenter phase II trial of two different schedules of capecitabine plus oxaliplatin as first-line treatment in advanced colorectal cancer. *J Clin Oncol* 2003; **21**: 1307-1312
22 **Takahashi I,** Emi Y, Hasuda S, Kakeji Y, Maehara Y, Sugimachi K. Clinical application of hyperthermia combined with anticancer drugs for the treatment of solid tumors. *Surgery* 2002; **131**(1 Suppl): S78-84
23 **Rossi CR,** Mocellin S, Pilati P, Foletto M, Quintieri L, Palatini P, Lise M. Pharmacokinetics of intraperitoneal cisplatin and doxorubicin. *Surg Oncol Clin N Am* 2003; **12**: 781-794
24 **Rossi CR,** Foletto M, Mocellin S, Pilati P, De SM, Deraco M, Cavaliere F, Palatini P, Guasti F, Scalerta R, Lise M. Hyperthermic intraoperative intraperitoneal chemotherapy with cisplatin and doxorubicin in patients who undergo cytoreductive surgery for peritoneal carcinomatosis and sarcomatosis: phase I study. *Cancer* 2002; **94**: 492-499
25 **Wisloff F,** Gulbrandsen N, Nord E. Therapeutic options in the treatment of multiple myeloma: pharmacoeconomic and quality-of-life considerations. *Pharmacoeconomics* 1999; **16**: 329-341
26 **Lassere Y,** Hoff P. Management of hand-foot syndrome in patients treated with capecitabine (Xeloda). *Eur J Oncol Nurs* 2004; **8**(Suppl 1): S31-40
27 **Piccart MJ,** Biganzoli L, Di Leo A. The impact of chemotherapy dose density and dose intensity on breast cancer outcome: what have we learned? *Eur J Cancer* 2000; **36**(Suppl): S4-10
28 **Duthoy W,** De Gersem W, Vergote K, Boterberg T, Derie C, Smeets P, De Wagter C, De Neve W. Clinical implementation of intensity-modulated arc therapy (IMAT) for rectal cancer. *Int J Radiat Oncol Biol Phys* 2004; **60**: 794-806
29 **Sanz Rubiales A,** del Valle Rivero ML, Garavis Vicente M, Rey Castro P, Lopez-Lara Martin F. Dose intensity of chemotherapy in small-cell lung carcinoma. Review of comparative studies. *An Med Interna* 2000; **17**: 378-385

Science Editor Guo SY **Language Editor** Elsevier HK

PO Box 2345, Beijing 100023, China
www.wjgnet.com
wjg@wjgnet.com

ELSEVIER

World J Gastroenterol 2005;11(28):4305-4310
World Journal of Gastroenterology ISSN 1007-9327

• *GASTRIC CANCER* •

Effect of superoxide dismutase and malondialdehyde metabolic changes on carcinogenesis of gastric carcinoma

Shao-Hong Wang, Yi-Zhong Wang, Ke-Yi Zhang, Jin-Hui Shen, Hou-Qiang Zhou, Xiao-Yang Qiu

Shao-Hong Wang, Jin-Hui Shen, Hou-Qiang Zhou, Xiao-Yang Qiu, Department of Pathology, Central Hospital of Shantou City, Shantou 515031, Guangdong Province, China
Yi-Zhong Wang, Department of Laboratory, Central Hospital of Shantou City, Shantou 515031, Guangdong Province, China
Ke-Yi Zhang, Department of Surgical Oncology, Central Hospital of Shantou City, Shantou 515031, Guangdong Province, China
Supported by the Youth Science Fund of Guangdong Province Medicine and Hygiene, No. B19960095
Correspondence to: Dr. Shao-Hong Wang, Department of Pathology, Central Hospital of Shantou City, Shantou 515031, Guangdong Province, China. wsh196303@tom.com
Telephone: +86-754-8550450
Received: 2004-07-05 Accepted: 2005-03-10

Abstract

AIM: To investigate the relationship between the superoxide dismutase (SOD), malondialdehyde (MDA) metabolic changes and the gastric carcinogenesis.

METHODS: The SOD activity and MDA content were measured in the gastric tissues from the focus center, peripheral and far-end areas of gastric carcinoma (n = 52) and gastric ulcer (n = 10). All the tissues were subjected to routine histological examinations and classifications.

RESULTS: The SOD activity was greatly reduced but the MDA content was markedly increased in the center areas of the non-mucous gastric carcinoma (non-MGC); and the poorly differentiated gastric carcinoma varied. The SOD activity was gradually decreased and the MDA content was gradually increased in the tissues from the focus far-end, peripheral to center areas of non-MGC. Both of the SOD activity and the MDA content were significantly declined and were respectively at same low level in the tissues from the focus center, peripheral, and far-end area with the mucous gastric carcinoma (MGC). In contrast to the gastric ulcer and grade I or II of non-MGC, the same level of the SOD activity and the MDA content were found in the focus center areas. Between non-MGC (groups A-D) and gastric ulcer (group F), the differences of SOD activity and MDA content were very noticeable in the gastric tissues from the focus peripheral and far-end areas, in which the SOD activity showed noticeable increase and the MDA content showed noticeable decrease in the gastric ulcer.

CONCLUSION: The active free radical reaction in the gastric tissues can induce the carcinogenesis of non-MGC. The utmost low ability of antioxidation in the gastric tissues can induce the carcinogenesis of MGC. The metabolic change of the free radicals centralized mostly in the center of ulcerated lesions only, which suggested the ability of antioxidation was declined only in these lesions. However, the metabolism of free radicals varied significantly and the ability of antioxidation declined not only in the local focus area but also in the abroad gastric tissues with gastric carcinoma.

Key words: Gastric carcinoma; Free radical; Superoxide dismutase

Wang SH, Wang YZ, Zhang KY, Shen JH, Zhou HQ, Qiu XY. Effect of superoxide dismutase and malondialdehyde metabolic changes on carcinogenesis of gastric carcinoma. *World J Gastroenterol* 2005; 11(28):4305-4310
http://www.wjgnet.com/1007-9327/11/4305.asp

INTRODUCTION

Free radical is the middle product during the phase of the biochemical metabolism in the body[1], and it is the intense toxicant because of being very active in the biochemical nature and oxidizing ability[2-5]. Although recent work has shown that free radical is related to the causing and development of many digestive system diseases[6-8], it did not distinct the relationship between the free radical and the gastric carcinogenesis[9,10]. In the investigation, it was researched that metabolic changes of the free radical play a role in the gastric carcinogenesis, development of gastric carcinoma by investigating the metabolism condition and regularity of the free radicals in the fresh samples of the gastric carcinoma tissues.

MATERIALS AND METHODS

Patients and tissues

From 1998 to 2002, 52 cases of gastric carcinoma and 10 cases of gastric ulcer were obtained from the Central Hospital of Shantou City. All fresh stomach samples were surgically removed from these patients and regular routine histological examination and classification were made. The patients with gastric carcinoma were 11 women and 41 men. The mean age was 59.83 years, ranging from 34 to 76 years. The patients with gastric ulcer were 1 woman and 9 men and the mean age was 53.30 years, ranging from 19 to 69 years.

Measurement of SOD activity and MDA content

Stomach samples were obtained, the tissues at the center,

peripheral (2 cm away from focus lesion) and far-end areas (8-10 cm away from focus lesion) sampled respectively. The fresh tissues were made into 10% tissue homogenate for measurement of the superoxide dismutase (SOD) activity and malondialdehyde (MDA) content. The SOD activity was examined with xanthine oxidase method and the MDA content was examined with sulfur barbituric acid method[11]. SOD and MDA detection kits were purchased from Nanjing Jiancheng Bioengineering Institute.

Statistical analysis

All data were disposed by SPSS9.0 statistical software. Statistical comparisons between interior groups were analyzed with ANOVA followed by Student's *t*-test. Statistical comparisons between different groups were analyzed with one-way ANOVA followed by *q*-test. Experimental results were finally expressed as mean±SD. *P* value less than 0.05 was considered statistically significant.

RESULTS

Histological examination

Fifty-two patients with gastric carcinoma were confirmed by histological examination. Among the 52 cases, 44 were non-mucous gastric carcinoma (non-MGC) including papillary, tubular, poorly differentiated, undifferentiated carcinoma, and were graded into four groups: grade I, 12 cases (group A, Figure 1A); grade II, 15 cases (group B, Figure 1B); grade III, 11 cases (group C, Figure 1C); grade IV, 6 cases (group D, Figure 1D). Eight cases were mucous gastric carcinoma (MGC) including mucinous adenocarcinoma and signet-ring cell carcinoma (group E, Figure 1E). Another 10 patients who were confirmed had gastric ulcer (group F, Figure 1F).

Detection of SOD activity (Table 1 and Figure 2)

The SOD activity was declined gradually in the tissues from the focus far-end, peripheral, to center areas in non-MGC (groups A-D). The SOD activity in the focus center areas was the lowest in the measured gastric tissue. SOD activity reduction was correlated with the grade and differentiation of gastric carcinoma in the focus center areas, in which the level of the SOD activity in groups A and B (grades I and II) was higher than that in groups C and D (grades III and IV). There was no significant difference of the SOD activity in the tissues from the focus far-end areas between groups A-D.

The level of SOD activity was extremely low in the focus center areas in MGC (group E). The level of SOD activity was noticeably low in the focus peripheral and far-end areas. Although reduction tendency was minimized, there were no significant differences of the SOD activity in the tissues from the focus far-end, peripheral to center areas; suggesting that the SOD activity in these areas was at the same low level.

The level of SOD activity was low in the focus center area with gastric ulcer (group F). Notable reduction tendency about SOD activity was shown in the tissues from the focus far-end, peripheral to center areas. The common metabolic characteristics were found in gastric ulcer (group F) and non-MGC (groups A-D). The SOD activity was gradually declined from the focus far-end, peripheral to center areas. The SOD activity was at the same level in the tissues from the focus center areas between gastric ulcer (group F) and non-MGC (grades I and II, groups A and B). Importantly, the SOD activity was noticeably higher in the tissues from the focus peripheral and far-end areas in the gastric ulcer (group F) than non-MGC (groups A-D). To compare the gastric ulcer (group F) and the MGC (group E), the level

Table 1 SOD activity detection in the gastric tissue with gastric carcinoma and gastric ulcer (mean±SD) NU/mg Pr

Group	*n*	Focus center area (1)	Focus peripheral area (2)	Focus far-end area (3)
Non-MGC				
I (A)	12	85.88±8.97	122.79±12.08	135.33±14.74
II (B)	15	81.26±8.68	104.73±11.24	123.13±14.46
III (C)	11	49.01±4.97	93.35±8.32	109.59±11.45
IV (D)	6	52.05±5.13	70.71±6.01	102.25±10.34
MGC (E)	8	23.64±2.31	31.34±3.79	33.47±4.78
Gastric ulcer (F)	10	95.63±8.01	162.88±12.26	186.22±11.74
P: (Statistical comparisons interior group)				
①A_1:A_2<0.05	A_1:A_3<0.01	A_2:A_3>0.05	②B_1:B_2>0.05	B_1:B_3<0.05	B_2:B_3>0.05
③C_1:C_2<0.01	C_1:C_3<0.01	C_2:C_3>0.05	④D_1:D_2<0.05	D_1:D_3<0.01	D_2:D_3<0.05
⑤E_1:E_2>0.05	E_1:E_3>0.05	E_2:E_3>0.05	⑥F_1:F_2<0.01	F_1:F_3<0.01	F_2:F_3>0.05
P: (Statistical comparisons between different groups)				
①A_1:B_1>0.05	A_1:C_1<0.01	A_1:D_1<0.05	A_1:E_1<0.01	A_1:F_1>0.05	B_1:C_1<0.01
B_1:D_1<0.05	B_1:E_1<0.05	B_1:F_1>0.05	C_1:D_1>0.05	C_1:E_1<0.05	C_1:F_1<0.01
D_1:E_1<0.05	D_1:F_1<0.01	E_1:F_1<0.01			
②A_2:B_2>0.05	A_2:C_2<0.05	A_2:D_2<0.01	A_2:E_2<0.01	A_2:F_2<0.05	B_2:C_2<0.05
B_2:D_2:<0.05	B_2:E_2<0.01	B_2:F_2<0.01	C_2:D_2<0.05	C_2:E_2<0.01	C_2:F_2<0.01
D_2:E_2<0.05	D_2:F_2<0.01	E_2:F_2<0.01			
③A_3:B_3>0.05	A_3:C_3>0.05	A_3:D_3>0.05	A_3:E_3<0.01	A_3:F_3<0.01	B_3:C_3>0.05
B_3:D_3>0.05	B_3:E_3<0.01	B_3:F_3<0.01	C_3:D_3>0.05	C_3:E_3<0.01	C_3:F_3<0.01
D_3:E_3<0.01	D_3:F_3<0.01	E_3:F_3<0.01			

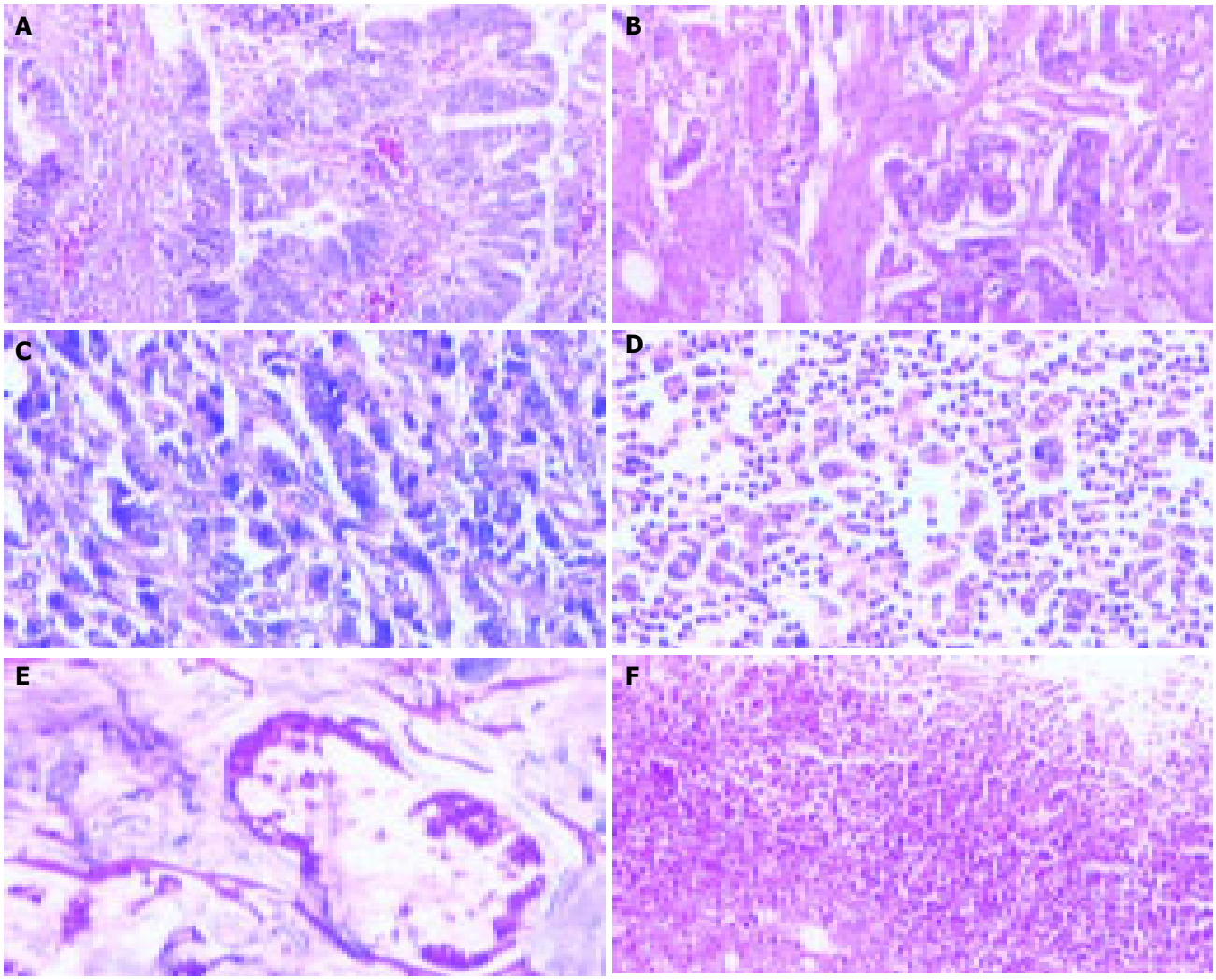

Figure 1 Non-mucous gastric carcinoma. **A**: non-mucous gastric carcinoma, grade I HE ×100; **B**: non-mucous gastric carcinoma, grade II HE ×100; **C**: non-mucous gastric carcinoma, grade III HE ×200; **D**: non-mucous gastric carcinoma, grade IV HE ×200; **E**: mucous gastric carcinoma HE ×100; **F**: gastric ulcer HE ×100.

of SOD activity was noticeably higher in all the tissues in the former than the later, and the SOD activity showed a gradual reduction tendency in the former, same low level in the later from the focus far-end, peripheral to center areas.

Detection of MDA content (Table 2 and Figure 3)

The MDA content increased gradually in the tissues from the focus far-end, peripheral to center areas in non-MGC (groups A-D). The MDA content in the focus center areas was the highest in the measured gastric tissue. The level of MDA content correlated with the grade and differentiation of gastric carcinoma in the tissues from the center areas. The study showed that the level of the MDA content in the groups A and B (grades I and II) was lower than groups C and D (grades III and IV). There were significant differences of the MDA content in the tissues from far-end areas, in which the level of MDA content was noticeably lower in

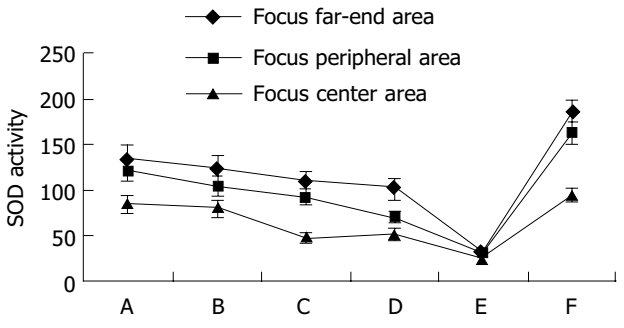

Figure 2 SOD activity detection in the gastric tissue with gastric carcinoma and gastric ulcer.

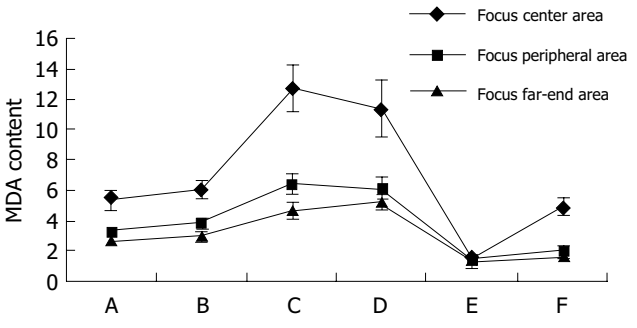

Figure 3 MDA content detection in the gastric tissue with gastric carcinoma and gastric ulcer.

Table 2 MDA content detection in the gastric tissue with gastric carcinoma and gastric ulcer (mean±SD) nmol/mg Pr

Group	*n*	Focus center area (1)	Focus peripheral area (2)	Focus far-end area (3)
Non-MGC				
I (A)	12	5.37±0.61	3.28±0.23	2.56±0.18
II (B)	15	6.07±0.62	3.85±0.31	2.96±0.25
III (C)	11	12.75±1.52	6.46±0.65	4.65±0.52
IV (D)	6	11.41±1.91	6.10±0.71	5.20±0.45
MGC (E)	8	1.55±0.23	1.43±0.18	1.12±0.12
Gastric ulcer (F)	10	4.89±0.56	2.06±0.22	1.68±0.16

P: (Statistical comparisons interior group)					
①A_1:A_2<0.01	A_1:A_3<0.01	A_2:A_3<0.05	②B_1:B_2<0.01	B_1:B_3<0.01	B_2:B_3<0.01
③C_1:C_2<0.01	C_1:C_3<0.01	C_2:C_3<0.05	④D_1:D_2<0.05	D_1:D_3<0.05	D_2:D_3>0.05
⑤E_1:E_2>0.05	E_1:E_3>0.05	E_2:E_3>0.05	⑥F_1:F_2<0.01	F_1:F_3<0.01	F_2:F_3>0.05
P: (Statistical comparisons between different groups)					
①A_1:B_1>0.05	A_1:C_1<0.01	A_1:D_1<0.01	A_1:E_1<0.01	A_1:F_1>0.05	B_1:C_1<0.01
B_1:D_1<0.05	B_1:E_1<0.01	B_1:F_1>0.05	C_1:D_1>0.05	C_1:E_1<0.01	C_1:F_1<0.01
D_1:E_1<0.01	D_1:F_1<0.01	E_1:F_1<0.05			
②A_2:B_2>0.05	A_2:C_2<0.01	A_2:D_2<0.01	A_2:E_2<0.01	A_2:F_2<0.05	B_2:C_2<0.01
B_2:D_2<0.01	B_2:E_2<0.01	B_2:F_2<0.01	C_2:D_2>0.05	C_2:E_2<0.01	C_2:F_2<0.01
D_2:E_2<0.01	D_2:F_2<0.01	E_2:F_2>0.05			
③A_3:B_3>0.05	A_3:C_3<0.01	A_3:D_3<0.01	A_3:E_3<0.01	A_3:F_3<0.05	B_3:C_3<0.01
B_3:D_3>0.01	B_3:E_3<0.01	B_3:F_3<0.01	C_3:D_3>0.05	C_3:E_3<0.01	C_3:F_3<0.01
D_3:E_3<0.01	D_3:F_3<0.01	E_3:F_3>0.05			

the groups A and B than the groups C and D.

The level of MDA content was extremely low in the center, peripheral, and far-end areas in MGC (group E). There was no significant difference of the MDA content; it was at the same low level, although a minimum gradual increase tendency was found in the tissues from the focus far-end, peripheral to center areas.

The level of MDA content was noticeably high in the tissues from the focus center areas in the gastric ulcer (group F). The gradual increase tendency also showed in the tissues from the focus far-end, peripheral to center areas. The common metabolic characteristics were that the MDA content showed a gradual increase tendency in the tissues from the focus far-end, peripheral to center areas between gastric ulcer (group F) and non-MGC (groups A-D). And both in the group F and groups A and B, the MDA content was at the same level in the tissues from the focus center areas. However, when the gastric ulcer (group F) compared to the non-MGC (groups A-D), there was a significant difference: the MDA content declined markedly and varied in the tissues from the focus peripheral and far-end areas. The MDA content was noticeably higher in the tissues from the focus center areas in the gastric ulcer (group F) than the MGC (group E). But, the MDA content was at the same level in the tissues from the peripheral and focus far-end. And in the gastric ulcer (group F) compared to the MGC (group E), it showed a gradual increase tendency in the former, the later was at same low level in the tissues from the focus far-end, peripheral to center areas.

DISCUSSION

SOD is the most important substance that eliminated free radical system in the cell; it makes superoxide anion free radical (O_2^-), dismutates into H_2O_2 and protects the cells from the focus damage by cleaning up O_2^-. The level of SOD activity represents the intracellular antioxidation ability[8,10,12]. MDA is the main metabolite in the lipid peroxidation reaction. The free radicals affect on the membrane structures of the cells, including the membranes of the cell, mitochondrion, lysosome, endoplasmic reticulum, *etc.*, then injury of the cells. The level of MDA content represents the extent of the intracellular lipid peroxidation reaction[13-15]. The SOD activity and the MDA content are the main index of the metabolic condition of the free radicals. We acquired the new knowledge that the free radicals play a key role in the mechanism of the gastric carcinogenesis from our experimental data.

Active free radical reaction in gastric tissue advances the arising of non-MGC

The gastric mucosa from the focus far-end, peripheral to center area in non-MGC showed a pathological change from normal, atypical hyperplasia to carcinoma, by morphological observation. The SOD activity also showed a gradual reduction and the MDA content a gradual increase in gastric tissues from the focus far-end, peripheral to center areas. These results showed that the intracellular antioxidation ability in the gastric tissue was gradually reduced and the free radical reaction was gradually active, resulting in the injury of cells by the lipid peroxidation reaction, which stimulated the pathological changes from normal gastric mucous membrane to carcinoma[16-18].

The results further showed that the lower the differentiation degree of the gastric carcinoma, the more prominent the change of the free radicals metabolism. The SOD activity was lower and the MDA content higher in the groups C and D (gastric carcinoma grades III and IV) than the groups A and B (gastric carcinoma grades I and II). These results suggest two possible mechanisms: the first one was that the active free radical reaction severely damages the gastric mucous membrane cells, resulting in malignant

change in the gastric mucous membrane from the normal cell to poorly differentiated and undifferentiated carcinomas. The second was that the carcinoma cells with poorly differentiated, undifferentiated need to produce an amount of the active free radicals for cells blooming division and breeding for themselves[15,19].

Interestingly, our results showed that there was no significant difference of the SOD activity in the far-end area between groups A, B, C, and D. However, the differences of the MDA content were very noticeable, i.e., the MDA content of the groups C and D (gastric carcinoma grades III and IV) were very much higher than groups A and B (gastric carcinoma grades I and II), indicated that abnormal lipid peroxidation reaction of the gastric tissue in far-end areas in groups C and D was not regulated by the SOD activity, and the reduction of the ability of the antioxidation was correlated with the widespread infiltration of the gastric carcinoma tissue (gastric carcinoma grades III and IV).

The tendency changes of the SOD activity and the MDA content of gastric tissues in non-MGC (groups A-D) were consistent with that in gastric ulcer (group F) from the focus center, peripheral to far-end areas. Between groups A, B and group F, the same level of the SOD activity and the MDA content were found in the gastric tissues from the focus center areas. Importantly, between the non-MGC (groups A-D) and the gastric ulcer (group F), the differences of the SOD activity and the MDA content were highly noticeable in the gastric tissues from the focus peripheral and far-end areas, which the SOD activity showed noticeable increase and the MDA content showed noticeable decrease in the gastric ulcer. It was suggested that there was high ability of the antioxidation for protecting itself against damage by the free radicals and could balance free radical metabolism in the gastric tissue from the focus peripheral and far-end areas in the gastric ulcer (group F). Meantime, it was suggested that the changes of the free radicals metabolism centralized mostly in the center area of gastric ulcer, where the ability of the antioxidation was reduced only in the local focus. Compared to the gastric ulcer (group F), the variation of the SOD activity and the MDA content were very small in the peripheral area and far-end area in the non-MGC (groups A-D), suggested that the ability of the antioxidation was reduced not only in the local focus area but also in the abroad gastric tissues. This imbalance of the free radical metabolism occurs in whole gastric tissue, resulting in the reduction of the protection itself of the gastric tissue and inducing the gastric carcinogenesis, i.e., the arising of non-MGC[20,21].

Extreme reduction of the antioxidation ability in the gastric tissue contributes to the arising of MGC

The mucinous adenocarcinoma and the signet-ring cell carcinoma arising from the gastric mucosa possess large quantity of mucus, inside or/and around the cancer cells. And because of that characteristic nature, the cancer cells have strong ability of infiltration and widespread distribution in the gastric tissue. There were obvious differences of the SOD activity and the MDA content in gastric mucinous adenocarcinoma and signet-ring cell carcinoma, and classified as a special group (group E), compared to other type gastric carcinoma. The obvious reduction and the same low level of the SOD activity and the MDA content were found in the tissues of the focus center, peripheral and far-end areas in the MGC, where the free radical metabolism changed obviously. The data in previous experiments showed an inverse relationship between the SOD activity and the MDA content in the tissues[13,15]. The low SOD activity induced the reduction of the antioxidation ability and the increase of the lipid peroxidation reaction, the metabolic product, MDA, in the tissues. On the contrary, the increase of the SOD activity inhibited the reaction of the lipid peroxidation, resulting in the reduction of the metabolic product, MDA, in the tissues. But in this study, the SOD activity decreased greatly in the gastric tissue in the MGC, and the MDA content as well. Interestingly, the SOD activity and the MDA content decreased markedly to the same low level in the tissues wherever focus center, peripheral and far-end areas in the MGC. This condition of the free radicals metabolism maybe related with the special pathological changes, where there was an abundance of mucus in the tissues. The SOD is the most important substance to eliminate free radical system in cells and tissues and the level of SOD activity represents the intracellular antioxidation ability[12,22]. The utmost low level of the SOD activity represents the utmost low level of the intracellular antioxidation ability in gastric tissue with the MGC. It was considered accordingly that the antioxidation ability was the base and precondition in maintaining the normal physiological function, differentiation, division, multiplication of the cells[20,23]. The loss of the antioxidation ability may contribute to make the normal cells become carcinoma cells[9,24-26] and the gastric tissues cannot resist the infiltration of the cancer cells, resulting in cancer cells spreading extensively in stomach wall.

Compared to gastric ulcer, there was a very low level of the SOD activity in gastric tissues of center, peripheral and far-end areas with the MGC and the low antioxidation ability and the low defense function by themselves. The MDA content, in the tissues from the focus peripheral and far-end areas with the MGC and the ulcer, both were at the same low level. But the SOD activity was increased greatly in the tissues from the focus peripheral and far-end area with gastric ulcer (group F). It suggested that there was still a very strong antioxidation and protecting ability in the gastric tissues from the peripheral and far-end areas with the gastric ulcer (group F). It also confirmed that the extreme low antioxidation ability and the low SOD activity in the gastric tissues in the MGC (group E) were related to the causing and development of the MGC, and can induce the formation of the MGC. On the other hand, the very low level of the MDA suggests the lipid peroxidation reaction was inactive, which indicated that the arising of the MGC was not related with the lipid peroxidation reaction to damage of the tissues.

REFERENCES

1 **Khanzode SS,** Khanzode SD, Dakhale GN. Serum and plasma concentration of oxidant and antioxidants in patients of *Helicobacter pylori* gastritis and its correlation with gastric cancer. *Cancer Lett* 2003; **195**: 27-31

2 **Janssen AM,** Bosman CB, van Duijn W, Oostendorp-van de Ruit MM, Kubben FJ, Griffioen G, Lamers CB, van Krieken JH, van de Velde CJ, Verspaget HW. Superoxide dismutases in gastric and esophageal cancer and the prognostic impact in gastric cancer. *Clin Cancer Res* 2000; **6**: 3183-3192

3 **Fujisawa S,** Atsumi T, Ishihara M, Kadoma Y. Cytotoxicity, ROS-generation activity and radical-scavenging activity of curcumin and related compounds. *Anticancer Res* 2004; **24**: 563-569

4 **Sander CS,** Chang H, Hamm F, Elsner P, Thiele JJ. Role of oxidative stress and the antioxidant network in cutaneous carcinogenesis. *Int J Dermatol* 2004; **43**: 326-335

5 **Sanders PM,** Tisdale MJ. Role of lipid-mobilising factor (LMF) in protecting tumour cells from oxidative damage. *Br J Cancer* 2004; **90**: 1274-1278

6 **Kim JJ,** Chae SW, Hur GC, Cho SJ, Kim MK, Choi J, Nam SY, Kim WH, Yang HK, Lee BL. Manganese superoxide dismutase expression correlates with a poor prognosis in gastric cancer. *Pathobiology* 2002-2003; **70**: 353-360

7 **Korenaga D,** Yasuda M, Honda M, Nozoe T, Inutsuka S. MnSOD expression within tumor cells is closely related to mode of invasion in human gastric cancer. *Oncol Rep* 2003; **10**: 27-30

8 **Yasuda M,** Takesue F, Inutsuka S, Honda M, Nozoe T, Korenaga D. Prognostic significance of serum superoxide dismutase activity in patients with gastric cancer. *Gastric Cancer* 2002; **9**: 148-153

9 **Toh Y,** Kuninaka S, Oshiro T, Ikeda Y, Nakashima H, Baba H, Kohnoe S, Okamura T, Mori M, Sugimachi K. Overexpression of manganese superoxide dismutase mRNA may correlate with aggressiveness in gastric and colorectal adenocarcinomas. *Int J Oncol* 2000; **17**: 107-112

10 **Izutani R,** Asano S, Imano M, Kuroda D, Kato M, Ohyanagi H. Expression of manganese superoxide dismutase in esophageal and gastric cancers. *J Gastroenterol* 1998; **33**: 816-822

11 **Pang ZJ,** Zhou M, Chen Y. The research method of free radicals medical science. 1st. Beijing: *PEOPLE HYGIENE Pub* 2000: 64 –66

12 **Inoue M,** Sato EF, Nishikawa M, Park AM, Kira Y, Imada I, Utsumi K. Mitochondrial generation of reactive oxygen species and its role in aerobic life. *Curr Med Chem* 2003; **10**: 2495-2505

13 **Arivazhagan S,** Kavitha K, Nagini S. Erythrocyte lipid peroxidation and antioxidants in gastric cancer patients. *Cell Biochem Funct* 1997; **15**: 15-18

14 **Lee IS,** Nishikawa A. Polyozellus multiplex, a Korean wild mushroom, as a potent chemopreventive agent against stomach cancer. *Life Sci* 2003; **73**: 3225-3234

15 **Skrzydlewska E,** Kozuszko B, Sulkowska M, Bogdan Z, Kozlowski M, Snarska J, Puchalski Z, Sulkowski S, Skrzydlewski Z. Antioxidant potential in esophageal, stomach and colorectal cancers. *Hepatogastroenterology* 2003; **50**: 126-131

16 **Vukobrat-Bijedic Z.** Carcinoma of the stomach. *Med Arh* 2003; **57**(1 Suppl 2): 81-83

17 **Tahara E.** Genetic pathways of two types of gastric cancer. *IARC Sci Publ* 2004; **157**: 327-349

18 **Correa P.** The biological model of gastric carcinogenesis. *IARC Sci Publ* 2004; **157**: 301-310

19 **Policastro L,** Molinari B, Larcher F, Blanco P, Podhajcer OL, Costa CS, Rojas P, Duran H. Imbalance of antioxidant enzymes in tumor cells and inhibition of proliferation and malignant features by scavenging hydrogen peroxide. *Mol Carcinog* 2004; **39**: 103-113

20 **Eapen CE,** Madesh M, Balasubramanian KA, Pulimood A, Mathan M, Ramakrishna BS. Mucosal mitochondrial function and antioxidant defences in patients with gastric carcinoma. *Scand J Gastroenterol* 1998; **33**: 975-981

21 **Zavros Y,** Kao JY, Merchant JL. Inflammation and cancer III. Somatostatin and the innate immune system. *Am J Physiol Gastrointest Liver Physiol* 2004; **286**: G698-701

22 **Izutani R,** Kato M, Asano S, Imano M, Ohyanagi H. Expression of manganese superoxide disumutase influences chemosensitivity in esophageal and gastric cancers. *Cancer Detect Prev* 2002; **26**: 213-221

23 **Zheng QS,** Sun XL, Wang CH. Redifferentiation of human gastric cancer cells induced by ascorbic acid and sodium selenite. *Biomed Environ Sci* 2002; **15**: 223-232

24 **Magalova T,** Bella V, Brtkova A, Beno I, Kudlackova M, Volkovova K. Copper, zinc and superoxide dismutase in precancerous, benign diseases and gastric, colorectal and breast cancer. *Neoplasma* 1999; **46**: 100-104

25 **Shimoyama S,** Aoki F, Kawahara M, Yahagi N, Motoi T, Kuramoto S, Kaminishi M. Early gastric cancer development in a familial adenomatous polyposis patient. *Dig Dis Sci* 2004; **49**: 260-265

26 **Macarthur M,** Hold GL, El-Omar EM. Inflammation and Cancer II. Role of chronic inflammation and cytokine genepolymorphisms in the pathogenesis of gastrointestinal malignancy. *Am J Physiol Gastrointest Liver Physiol* 2004; **286**: G515-520

Science Editor Guo SY **Language Editor** Elsevier HK

PO Box 2345, Beijing 100023, China
www.wjgnet.com
wjg@wjgnet.com

ELSEVIER

World J Gastroenterol 2005;11(28):4311-4316
World Journal of Gastroenterology ISSN 1007-9327

• *GASTRIC CANCER* •

Nutritional factors and gastric cancer in Zhoushan Islands, China

Jiong-Liang Qiu, Kun Chen, Jian-Ning Zheng, Jian-Yue Wang, Li-Jun Zhang, Li-Ming Sui

Jiong-Liang Qiu, Jian-Ning Zheng, Department of Health and Quarantine, Ningbo Entry-Exit Inspection and Quarantine Bureau, Ningbo 315012, Zhejiang Province, China
Kun Chen, Department of Epidemiology, Zhejiang University School of Public Health, Hangzhou 310006, Zhejiang Province, China
Jian-Yue Wang, Zhoushan Center for Disease Prevention and Control, Zhoushan 316000, Zhejiang Province, China
Li-Jun Zhang, Li-Ming Sui, Jiangdong Center for Disease Prevention and Control, Ningbo 315000, Zhejiang Province, China
Supported by the Foundation of Ministry of Public Health of China, No. WKZ-2001-1-17
Correspondence to: Dr. Jiong-Liang Qiu, Department of Health and Quarantine, Ningbo Entry-Exit Inspection and Quarantine Bureau, 9 Ma-yuan Road, Ningbo 315012, Zhejiang Province, China. qiujunliang@163.com
Telephone: +86-574-87022519 Fax: +86-574-87146206
Received: 2004-10-26 Accepted: 2004-12-21

Abstract

AIM: To investigate the association between nutrient intakes and high incidence rate of gastric cancer among residents in Zhoushan Islands.

METHODS: A frequency-matched design of case-control study was used during the survey on dietary factors and gastric cancer in Zhoushan Islands, China. A total of 103 cases of gastric cancer diagnosed in 2001 were included in the study and 133 controls were randomly selected from the residents in Zhoushan Islands. A food frequency questionnaire was specifically designed for the Chinese dietary pattern to collect information on dietary intake. A computerized database of the dietary and other relative information of each participant was completed. Total calories and 15 nutrients were calculated according to the food composition table and their adjusted odds ratios (ORs) and 95% confidence intervals (CIs) were estimated by gender using unconditional logistic regression models.

RESULTS: High intakes of protein, saturated fat, and cholesterol were observed with the increased risk of gastric cancer particularly among males ($OR_{Q4\ vs\ Q1}$ were 10.3, 3.24, 2.76 respectively). While carbohydrate was a significant high-risk nutrient ($OR_{Q4\ vs\ Q1}$ = 14.8; *P* for linear trend = 0.024) among females. Regardless of their gender, the cases reported significantly higher daily intake of sodium mainly from salts. As to the nutrients of vitamins A and C, an inversed association with the risk of GC was found. Baseline characteristics of participants were briefly described.

CONCLUSION: The findings from this study confirm the role of diet-related exposure in the etiology of gastric cancer from the point of view of epidemiology. An increased risk of gastric cancer is associated with high intakes of protein, saturated fat, cholesterol and sodium, while consumption of polyunsaturated fat, vitamin A and ascorbic acid may have a protective effect against gastric cancer.

Key words: Gastric cancer; Nutrient intake; Case-control; Risk factor; Protective effect; Antioxidants

Qiu JL, Chen K, Zheng JN, Wang JY, Zhang LJ, Sui LM. Nutritional factors and gastric cancer in Zhoushan Islands, China. *World J Gastroenterol* 2005; 11(28): 4311-4316
http://www.wjgnet.com/1007-9327/11/4311.asp

INTRODUCTION

Though a decreasing trend is observed in nearly all countries, gastric cancer is one of the most common cancers in the world and the second leading cause of cancer death[1]. Although many risk factors have been suggested, the causative and protective agents for gastric cancer remain to be clarified. Nutritional factors are thought to be paramount, with *N*-nitroso and other dietary compounds acting as carcinogens, while anti-oxidants and other protective substances in foods inhibit the carcinogenic process[2].

In China, parts of high-risk areas for gastric cancer are located in the eastern coastlands including Zhoushan Islands, the fourth archipelago and also the largest fishing ground in China. As the first leading cancer in Zhoushan, the age-standardized annual incidence rate of gastric cancer varied from 35 to 40 per 100 000 in 1980-1985, which is higher than the national level (about 25.0 per 100 000). To investigate the risk factors for this common cancer in the coastal areas, we conducted a population-based case-control study in Zhoushan to obtain information on the frequency of consumption and portion size of common foods, and found that intake of certain nutrients in these foods influences the risk of gastric cancer.

MATERIALS AND METHODS

The data-collection period for the study spanned through the whole year of 2001 and comprised all the islands in Zhoushan, Zhejiang Province. The study population included 138 newly diagnosed patients with gastric cancer between December 1, 2000 and November 30, 2001 and 140 controls as a representative sample of residents in the same area.

All the cases were identified at the five largest hospitals in Zhoushan Islands. Of the 138 eligible patients, 10 (7.3%) died before interview, 18 (10.2%) could not be contacted as they were from distant islands, 7 (5.1%) refused to participate. Of the 103 (81 men and 22 women) patients included in the analysis, 56.3% were confirmed by histology according to the Lauren classification[3] and 43.7% by other diagnostic methods including surgery, endoscopy, X-ray and ultrasound. Controls were selected from permanent residents in Zhoushan Islands, frequency matched to the expected distribution of cases by gender, age (10-year groups), and residents of the islands. Of the 140 eligible controls randomly selected from the Zhoushan resident files, 133 (95 men and 38 women) were interviewed, yielding a response rate of 95.0%. Each subject was interviewed face-to-face by trained interviewers.

Dietary information

A questionnaire was designed to collect information on demographic and socio-economic conditions, diet, cigarette smoking, alcohol drinking, history of selected diseases, family history of cancer, occupation, and other factors. Frequency of intake and portion size in a 12-mo period 1 year before the interview were assessed for more than 60 food and beverage items, which included information on dairy products, fruits, meat, processed meat, fish, vegetables and candies, *etc*. These items accounted for over 85% of food intake in Zhoushan residents. For each food, amount consumed was estimated according to models of the more frequently consumed foods. Consumption of seasonal vegetables and fruits was assessed on the basis of average intake during the relevant period of the year.

Nutrient intake

Fifteen priority nutrients and total calories were selected beforehand as previously described[4-6]. Quantitative estimate of cumulative nutrient intake per day in each food was based on food tables derived from the Chinese Food Composition Tables. Total intake of each nutrient was summed over all foods consumed. The Matlab5.0 software was used for processing these procedures by the method of multiplication of matrix[7].

Data analysis and control of confounding

Descriptive analysis of nutrient intake for cases and controls was carried out by computing medians and percentages because of biased distributions of the data, which could not be transformed into normal with logarithmic transformations. The medians were compared by the nonparametric median test.

Then continuous variables of nutrient intake were divided into quartiles based on the distribution in controls, with an approximately equal number of controls in each intake stratum. The amount of intake varied substantially between the sexes, hence sex-specific cutpoints were used for amount of nutrient intake. Risk of gastric cancer associated with dietary factors was estimated by odds ratios (ORs) and its 95% confidence intervals (CIs), using unconditional logistic regression models. Each classified nutrient was introduced into the model as a dummy variable. The lowest level of consumption was used as the reference category in the estimation. All ORs were adjusted for age, economic status (based on monthly family *per capita* income), present residence, educational level and total calories. In addition, ORs for men were further adjusted for cigarette smoking and alcohol drinking, confounding factors common in Chinese men but not in Chinese women (only 5% of women smoke, and 6.7% drink alcohol regularly).

For testing of linear trends, the ordinal nutrient intake variables were treated as continuous variables. In this step, $P \leqslant 0.05$ was considered as evidence for a dose-response relationship. All analyses were carried out by the SPSS version 10.0 software.

RESULTS

Selected characteristics of the study population are shown in Table 1. Due to the frequency-matching procedure by age, gender and present residence, the characteristics of these three variables were similar. Compared to controls, only the age of patients was slightly older (median age 63 years for cases and 60 years for controls). Among

Table 1 Distribution of 103 cases of gastric cancer and 133 controls according to age, gender, address and selected variables

Characteristics	Cases (n = 103)	Controls (n = 133)	χ^2	P
Age (yr)				
Average	3 (30–85)	60 (28–82)		
⩽45	6	20		
46–55	27	32		
56–65	32	38		
66–75	30	38		
76–85	8	5	6.40	0.172
Gender				
Males	81	95		
Females	22	38	1.59	0.210
Present residence[1]				
Large islands	70	76		
Medium islands	17	33		
Small islands	16	24	3.20	0.202
Education (yr)				
<7	43	45		
7–12	58	76		
⩾13	2	12	5.89	0.053
Economic status				
Low	46	30		
Medium	32	44		
High	25	51	12.15	0.002
Cigarette smoking				
Ever-smokers	62	70		
Non-smokers	41	63	1.35	0.246
Alcohol drinking				
Ever-drinkers	58	63		
Non-drinkers	45	70	1.86	0.173

[1]Three categories of islands were classified according to the number of permanent residents on islands: Dinghai, Putuo, and Daishan Islands, which are the three main islands in Zhoushan, predefined as the large islands; the islands on which the number of permanent residents is over 25 000, defined as the medium islands; the residual defined as the small islands.

Table 2 Medians of daily intake of nutrients in gastric cancer cases and controls, Zhoushan, China

Nutrient / d	Males		Females		All	
	Cases (n = 81)	Controls (n = 95)	Cases (n = 22)	Controls (n = 38)	Cases (n = 103)	Controls (n = 133)
Total calories (kJ)	2 963.25	3 073.16	3 002.32[b]	2 420.08[b]	2 984.54	2 937.73
Macronutrients						
Protein (g)	94.21	88.33	98.34[a]	76.92[a]	95.17[a]	85.21[a]
Fat (g)	61.04	65.04	56.23[a]	42.65[a]	60.60	57.48
Saturated fat (g)	8.90	9.44	6.33[a]	4.64[a]	8.70	8.44
Mono-unsaturated fat (g)	22.42	24.47	18.29	14.92	22.38	20.82
Polyunsaturated fat (g)	16.74	16.69	14.43	14.46	16.11	16.23
Fiber (g)	10.11	10.40	9.78	9.39	10.10	10.33
Carbohydrates (g)	403.36	404.93	411.34	287.31	404.19	359.27
Cholesterol (mg)	170.75	136.44	144.57[a]	62.56[a]	160.43[a]	115.02[a]
Micronutrients						
Carotene (μg)	443.54[b]	521.48[b]	455.38	827.38	443.62[a]	555.30[a]
Vitamin A (μg)	135.35[a]	181.01[a]	164.59	175.70	142.13[a]	179.96[a]
Vitamin C (mg)	42.49	38.94	49.29	61.36	43.64	41.04
Vitamin E (mg)	26.12	25.64	21.54	21.46	24.82	24.95
Mineral salts						
Na (mg)	6 700.32	5 074.32	7 000.52[a]	4 960.27[a]	6 734.41[a]	4 963.28[a]
Ca (mg)	464.08	448.26	560.28	460.57	478.91	448.26
Se (μg)	57.35	49.78	53.60	56.02	53.96	52.13

[a]P<0.05; [b]P<0.10 *vs* others.

non-dietary variables considered, the major determinants of gastric cancer risk were indicators of socio-economic status. For instance, 41.8% of the cases and 33.8% of the controls reported less than 7 years of education, 58.2% of the cases and 66.2% of the controls reported 7 years or more of education. As for the economic status, patients tended to have lower monthly income (44.7% of cases and 22.6% of controls with an average *per capita* income of 36 Chinese Yuan/month or less). No material difference in smoking/drinking habits was observed between cases and controls.

Table 2 shows the medians of daily nutrient intakes in the gastric-cancer cases and the controls according to gender. Overall, the cases reported significantly higher consumption of protein, cholesterol and Na (sodium) than controls, but these differences were significant only in the females. For controls, consumption of carotene and vitamin E was much higher, and on the contrary, the differences were significant in the males.

The multivariate-adjusted ORs for the quartile distributions of the macronutrients (Table 3) showed a significant positive linear trend for the risk of gastric cancer with increasing consumption of protein and cholesterol in males, whereas total fat and carbohydrates in females. The ORs for the highest quartile compared to the lowest quartile of consumption frequency significantly elevated for protein

Table 3 Odds ratios[1] (ORs) and 95% confidence intervals (CIs) of gastric cancer in relation to quartiles of macronutrients by sex, Zhoushan, China

Nutrient / d[2]	Males				P for trend	Females				P for trend
	Q_1	Q_2	Q_3	Q_4		Q_1	Q_2	Q_3	Q_4	
Total calories	1.0	1.20 (0.50–2.87)	1.02 (0.39–2.64)	1.26 (0.51–3.11)	>0.10	1.0	1.45 (0.27–7.89)	1.41 (0.26–7.74)	2.75 (0.45–16.84)	>0.10
Protein	1.0	3.00 (1.02–8.85)	5.11 (1.26–20.76)	10.30 (1.83–58.12)	0.010	1.0	4.28 (0.50–36.77)	1.71 (0.13–22.37)	6.10 (0.39–94.66)	>0.10
Fat	1.0	1.29 (0.52–3.2)	1.21 (0.46–3.17)	1.01 (0.35–2.92)	>0.10	1.0	1.38 (0.21–8.9)	1.85 (0.23–14.74)	8.26 (1.03–66.51)	0.023
Saturated fat	1.0	2.51 (0.90–6.97)	2.34 (0.81–6.8)	3.24 (1.11–9.49)	0.060	1.0	0.24 (0.02–3.11)	3.34 (0.52–21.44)	3.42 (0.48–24.49)	0.094
Monounsaturated fat	1.0	1.62 (0.67–3.94)	1.24 (0.49–3.17)	1.17 (0.43–3.22)	>0.10	1.0	0.30 (0.03–2.59)	1.83 (0.31–10.76)	1.32 (0.17–10.4)	>0.10
Polyunsaturated fat	1.0	1.21 (0.46–3.17)	1.72 (0.66–4.46)	0.96 (0.33–2.78)	>0.10	1.0	0.21 (0.03–1.37)	0.47 (0.09–2.57)	0.10 (0.01–0.80)	0.068
Fiber	1.0	1.69 (0.58–4.92)	0.69 (0.20–2.37)	2.41 (0.51–11.52)	>0.10	1.0	1.82 (0.30–10.9)	1.9 (0.27–13.44)	0.72 (0.06–8.97)	>0.10
Carbohydrates	1.0	1.39 (0.47–4.11)	1.6 (0.41–6.27)	2.14 (0.35–13.04)	>0.10	1.0	0.94 (0.1–8.57)	3.27 (0.37–28.84)	14.78 (1.11–197.32)	0.024
Cholesterol	1.0	1.08 (0.40–2.87)	2.53 (0.99–6.44)	2.76 (1.01–7.53)	0.050	1.0	6.05 (0.53–69.17)	5.31 (0.44–63.44)	11.9 (0.97–146.53)	0.062

[1]Adjusted for age, present residence, education, economic status, smoking (males only), alcoholics (males only) and total calories intake; [2]Data are ORs, with 95%CIs in parentheses.

Table 4 Odds ratios (ORs)[1] and 95% confidence intervals (CIs) of gastric cancer in relation to quartiles of micronutrients and mineral salts by sex, Zhoushan, China

Nutrient / d[2]	Males				*P* for trend	Females				*P* for trend
	Q_1	Q_2	Q_3	Q_4		Q_1	Q_2	Q_3	Q_4	
Carotene	1.0	1.82 (0.81–4.08)	0.40 (0.12–1.35)	0.81 (0.23–2.85)	>0.10	1.0	0.37 (0.08–1.70)	0.37 (0.08–1.78)	-[3]	0.025
Vitamin A	1.0	0.59 (0.24–1.45)	0.91 (0.39–2.15)	0.43 (0.16–1.21)	>0.10	1.0	0.32 (0.05–2.21)	0.55 (0.10–3.14)	0.10 (0.01–0.89)	0.091
Vitamin C	1.0	1.15 (0.42–3.18)	1.40 (0.53–3.67)	0.88 (0.31–2.53)	>0.10	1.0	0.48 (0.09–2.5)	0.73 (0.15–3.6)	0.07 (0.01–0.95)	>0.10
Vitamin E	1.0	0.79 (0.29–2.11)	0.88 (0.34–2.29)	0.77 (0.26–2.26)	>0.10	1.0	0.93 (0.17–5.03)	1.32 (0.24–7.26)	0.95 (0.15–6.16)	>0.10
Na	1.0	1.36 (0.50–3.7)	0.91 (0.33–2.5)	3.22 (1.25–8.26)	0.070	1.0	3.70 (0.43–31.75)	0.75 (0.09–6.62)	8.40 (1.09–64.77)	>0.10
Ca	1.0	1.65 (0.64–4.20)	1.30 (0.46–3.62)	2.37 (0.81–6.91)	>0.10	1.0	2.30 (0.32–16.54)	3.78 (0.44–32.28)	4.79 (0.58–39.17)	>0.10
Se	1.0	0.48 (0.17–1.37)	0.78 (0.26–2.39)	1.23 (0.37–4.09)	>0.10	1.0	1.18 (0.20–6.87)	0.68 (0.11–4.23)	0.75 (0.12–4.68)	>0.10

[1]Adjusted for age, present residence, education, economic status, smoking (males only), alcoholics (males only) and total calories intake; [2]Data are ORs, with 95%CIs in parentheses; -[3]$OR_{Q4\ vs\ Q1}$ and $95\%CI_{Q4\ vs\ Q1}$ could not be calculated because of the null value of cases in the 4th group among females.

(OR, 10.30; 95%CI, 1.83-58.12), saturated fat (OR, 3.24; 95%CI, 1.11-9.49) and cholesterol (OR, 2.76; 95%CI, 1.01-7.53) in males. In females the risks remained elevated with increasing consumption of total fat ($OR_{Q4\ vs\ Q1}$, 8.26; 95%CI, 1.03-66.51) and carbohydrates ($OR_{Q4\ vs\ Q1}$, 14.78; 95%CI, 1.11-197.32). A marginally significant inverse linear trend was also observed for frequent consumption of polyunsaturated fat ($OR_{Q4\ vs\ Q1}$, 0.10; 95%CI, 0.01-0.80) with the test for trend ($P = 0.068$).

The results of the micronutrient-intake (Table 4) uncovered a protective effect of vitamin A, with a marginally significant linear trend that held only for females ($OR_{Q4\ vs\ Q1}$, 0.10; 95%CI, 0.01-0.89). Similarly, a protective effect was seen for the highest category of vitamin C consumption in female cases of gastric cancer (OR, 0.07; 95%CI, 0.01-0.95), but no linear trend was found ($P>0.10$). In this data set, we found no significant relationship of gastric cancer with intake of vitamin E and carotene, although most OR values suggested a protective effect of them. Results from the analysis of mineral salt intake suggested a significant high-risk effect of sodium, regardless of their gender ($OR_{Q4\ vs\ Q1}$, 3.22; 95%CI, 1.25-8.26 in males; $OR_{Q4\ vs\ Q1}$, 8.4; 95%CI, 1.09-64.77 in females).

Further adjustment for other potential confounding factors, such as green tea drinking, occupation and family history of cancer, did not affect the associations with nutrient intakes. While 44% of the cases were diagnosed by methods other than histological confirmation, exclusion of these cases also did not alter our main findings.

DISCUSSION

The findings of this study confirm that several dietary factors identified elsewhere can also explain the incidence of gastric cancer in Zhoushan, Zhejiang Province, though gastric cancer did not decline in Zhoushan during the last 20 years. We also found that the incidence of gastric cancer in males and females is differently related to the intake of specific nutrients.

The results pertaining to an increased risk of gastric cancer due to the consumption of protein, fat and cholesterol are similar to those reported by Palli *et al*., in Italy[4]. In our study, the relationship between protein, saturated fat and cholesterol intake and gastric cancer was stronger in males after adjustment for other confounding factors. Nitrites and salt in processed and smoked meats, commonly in the Zhoushan diet, are thought to play a role in the etiology of gastric cancer[9]. In this regard, it is possible that saturated fat, cholesterol and protein consumption should be considered as proxy indicators for processed-meat consumption. We also found a protective effect of polyunsaturated fat against gastric cancer particularly in females, which is supported by other studies[10,11].

A positive association with dietary carbohydrates has been reported in several studies of gastric cancer[5,12,13]. In our study, the excess risk associated with carbohydrates contained in rice, noodles, and biscuits in the Chinese diet, could not be explained by education, present residence and economic status, although residual confounding by these or other unmeasured variables remains possible. Furthermore, the risk effect was stronger in females. The mechanism by which high consumption of carbohydrates may increase the risk of gastric cancer is unclear, but several possibilities have been suggested, including physical irritation (especially from rough whole-grain cereals), reduction in gastric mucin, and lowering of gastric pH with promotion of acid-catalyzed nitrosation[14].

The most consistent finding in the relation between diet and gastric cancer is the protective effect of vegetables and fruits[15-17]. A large number of potentially anti-carcinogenic agents are found in these food sources, such as carotenoids, vitamin C, vitamin A, fiber, and vitamin E, *etc.* In our study, we found a strong protective effect of vitamin A and vitamin C consumption against gastric cancer, particularly in females. Although the protective effect of vitamin C against gastric cancer has been mostly ascribed to its ability to inhibit formation of *N*-nitroso compounds from secondary amines and nitrite in the stomach, the role of vitamin C as a free-radical scavenger may be equally important[18,19]. Vitamin A is also a well-known antioxidant, but its protective effect against gastric cancer is only occasionally reported[12,20]. The decrease of gastric cancer risk in association with consumption of dietary fiber has also been observed[21]. However, the mechanism of this protective effect has not yet been identified[6]. Because vegetables and fruits not only are sources of fiber, but are the main contributions of vitamins A and C. Fiber may simply be a good indicator of consumption of plant food. As for the protective effect of vitamin E against gastric cancer, the epidemiologic results

are also inconsistent[6,13,22-24]. In view of the anti-oxidant properties of vitamin E, it has the same mechanism as ascorbic acid. Our results are more inclined to support the hypothesis that vitamin E might reduce the risk of gastric cancer.

The analysis of mineral salts suggested that only sodium mainly from salts had an increased risk for gastric cancer, regardless of the gender. Foods that are high in salt or preserved with salt in some form (dried or pickled food) are associated with an increased risk for gastric cancer[1,23,25]. Although the exact mechanism by which salt predisposes to gastric cancer is not known, salt can irritate the gastric cancer mucosa, making it more susceptible to carcinogenic change. Salt may also lead to atrophic gastritis, which is associated with increased risk for gastric cancer[26-29]. Atrophic gastritis can lead to colonization by bacteria that can catalyze the conversion of nitrites to carcinogenic *N*-nitroso compounds[30,31].

Although our findings are consistent with most previous studies of gastric cancer conducted in other countries, several potential limitations of our study should be noted. While the participation rate of the controls was relatively high (95%), only 75% of the eligible cases participated. Since there was generally a 3-mo delay between diagnosis and interview with cases, a few (10%) could not be connected for living in distant islands. Another main reason for non-participation was the death that occurred among cases (7.3%), thus raising the possibility of survival bias. If the identified risk factors could also affect the survival of gastric cancer patients, then exclusion of deceased cases may underestimate the true risks associated with these factors. On the other hand, selection bias, which tends to shift the risk estimates away from unity, should also be minimal since a small percentage of subjects refused to participate. As for the recall bias commonly existed in the dietary survey, efforts have been made to minimize it in various ways, including extensive training of interviewers, use of a standardized questionnaire and models of the more frequently consumed foods. But there were still many other potential recall biases not considered.

An additional limitation is that many nutrients are contained in the same food, and there is some correlation between the intake of certain nutrients, making it difficult to differentiate individual effects. Associations may also appear merely by chance because of the associations analyzed.

In summary, our results from the coastal areas confirm again that the diet plays an important role in the etiology of gastric cancer, and interventions against bad dietary structures may be important for the prevention of gastric cancer.

ACKNOWLEDGMENTS

The authors thank Dr. Yong-Nian Zhou *et al*., and interns Jing Zhen *et al*., for their participation in the dietary survey, and Zhoushan No. 1 Hospital, Zhoushan No. 3 Hospital, Zhoushan Traditional Chinese Medicine Hospital, People's Hospital of Putuo Islands, People's Hospital of Daishan Islands for their participation in this study.

REFERENCES

1 **Geng GY,** Liu RZ, Wang PS. EPIDEMIOLOGY (Volume Three). *Beijing, People's Medical Publishing House* 1996: 210-238
2 **Palli D.** Epidemiology of gastric cancer: an evaluation of available evidence. *J Gastroenterol* 2000; **35**(Suppl): 1284-1289
3 **Laur'En P**. The two histological main types of gastric carcinoma: diffuse and so called intestinal-type carcinoma. An attempt at a histo-clinical classification. *Acta Pathol Microbiol Scand* 1965; **64**: 31-49
4 **Palli D,** Russo A, Decarli A. Dietary patterns, nutrient intake and gastric cancer in a high-risk area of Italy. *Cancer Causes Control* 2001; **12**: 163-172
5 **Chen H,** Tucker KL, Graubard BI, Heineman EF, Markin RS, Potischman NA, Russell RM, Weisenburger DD, Ward MH. Nutrient intakes and adenocarcinoma of the esophagus and distal stomach. *Nutr Cancer* 2002; **42**: 33-40
6 **Lopez-Carrillo L,** Lopez-Cervantes M, Ward MH, Bravo-Alvarado J, Ramirez-Espitia A. Nutrient intake and gastric cancer in Mexico. *Int J Cancer* 1999; **83**: 601-605
7 **Xiao JS,** Wang MR. Matlab5.X and Scientific Calculation. *Beijing, Tsinghua Publishing House* 2000: 28-36
8 **Ngoan LT,** Mizoue T, Fujino Y, Tokui N, Yoshimura T. Dietary factors and stomach cancer mortality. *Br J Cancer* 2002; **87**: 37-42
9 **van den Brandt PA,** Botterweck AA, Goldbohm RA. Salt intake, cured meat consumption, refrigerator use and stomach cancer incidence: a prospective cohort study (Netherlands). *Cancer Causes Control* 2003; **14**: 427-438
10 **Kim DY,** Cho MH, Yang HK, Hemminki K, Kim JP, Jang JJ, Kumar R. Detection of methylation damage in DNA of gastric cancer tissues using 32P postlabelling assay. *Jpn J Cancer Res* 1999; **90**: 1104-1108
11 **Chung S,** Park S, Yang CH. Unsaturated fatty acids bind Myc-Max transcription factor and inhibit Myc-Max-DNA complex formation. *Cancer Lett* 2002; **188**: 153-162
12 **Azevedo LF,** Salgueiro LF, Claro R, Teixeira-Pinto A, Costa-Pereira A. Diet and gastric cancer in Portugal-a multivariate model. *Eur J Cancer Prev* 1999; **8**: 41-48
13 **Jedrychowski W,** Popiela T, Steindorf K, Tobiasz-Adamczyk B, Kulig J, Penar A, Wahrendorf J. Nutrient intake patterns in gastric and colorectal cancers. *Int J Occup Med Environ Health* 2001; **14**: 391-395
14 **Munoz N,** Plummer M, Vivas J, Moreno V, De Sanjose S, Lopez G, Oliver W. A case-control study of gastric cancer in Venezuela. *Int J Cancer* 2001; **93**: 417-423
15 **De Stefani E,** Correa P, Boffetta P, Ronco A, Brennan P, Deneo-Pellegrini H, Mendilaharsu M. Plant foods and risk of gastric cancer: a case-control study in Uruguay. *Eur J Cancer Prev* 2001; **10**: 357-364
16 **Engel LS,** Chow WH, Vaughan TL, Gammon MD, Risch HA, Stanford JL, Schoenberg JB, Mayne ST, Dubrow R, Rotterdam H, West AB, Blaser M, Blot WJ, Gail MH, Fraumeni JF Jr. Population attributable risks of esophageal and gastric cancers. *J Natl Cancer Inst* 2003; **95**: 1404-1413
17 **Palli D,** Russo A, Ottini L, Masala G, Saieva C, Amorosi A, Cama A, D'Amico C, Falchetti M, Palmirotta R, Decarli A, Costantini RM, Fraumeni JF Jr. Red meat, family history, and increased risk of gastric cancer with microsatellite instability. *Cancer Res* 2001; **61**: 5415-5419
18 **Steinmetz KA,** Potter JD. Vegetables, fruit, and cancer. II. Mechanisms. *Cancer Causes Control* 1991; **2**: 427-442
19 **Bartsch H,** Ohshima H, Pignatelli B. Inhibitors of endogenous nitrosation. Mechanisms and implications in human cancer prevention. *Mutat Res* 1988; **202**: 307-324
20 **Abneth CC,** Qiao YL, Dawsey SM, Buckman DW, Yang CS, Blot WJ, Dong ZW, Taylor PR, Mark SD. Prospective study of serum retinol, beta-carotene, beta-cryptoxanthin, and lutein / zeaxanthin and esophageal and gastric cancers in China. *Cancer Causes Control* 2003; **14**: 645-655
21 **Roth J,** Mobarhan S. Preventive role of dietary fiber in gastric cardia cancers. *Nutr Rev* 2001; **59**: 372-374
22 **Taylor PR,** Qiao YL, Abnet CC, Dawsey SM, Yang CS, Gunter

EW, Wang W, Blot WJ, Dong ZW, Mark SD. Prospective study of serum vitamin E levels and esophageal and gastric cancers. *J Natl Cancer Ins* 2003; **95**: 1414-1416

23 **Ekstrom AM,** Serafini M, Nyren O, Hansson LE, Ye W, Wolk A. Dietary antioxidant intake and the risk of cardia cancer and noncardia cancer of the intestinal and diffuse types: a population-based case-control study in Sweden. *Int J Cancer* 2000; **87**: 133-140

24 **Kono S,** Hirohata T. Nutrition and stomach cancer. *Cancer Causes Control* 1996; **7**: 41-55

25 **Tsugane S,** Sasazuki S, Kobayashi M, Sasaki S. Salt and salted food intake and subsequent risk of gastric cancer among middle-aged Japanese men and women. Salt and salted food intake and subsequent risk of gastric cancer among middle-aged Japanese men and women. *Br J Cancer* 2004; **90**: 128-134

26 **Wang M,** Guo C, Li M. A case-control study on the dietary risk factors of upper digestive tract cancer. *Zhonghua Liuxingbingxue Zazhi* 1999; **20**: 95-97

27 **Fox JG,** Dangler CA, Taylor NS, King A, Koh TJ, Wang TC. High-salt diet induces gastric epithelial hyperplasia and parietal cell loss, and enhances *Helicobacter pylori* colonization in C57BL/6 mice. *Cancer Res* 1999; **59**: 4823-4828

28 **Tuyns AJ.** Salt and gastrointestinal cancer. *Nutr Cancer* 1988; **11**: 229-232

29 **Kuipers EJ.** Review article: Relationship between *Helicobacter pylori*, atrophic gastritis and gastric cancer. *Aliment Pharmacol Ther* 1998; **12**(Suppl 1): 25-36

30 **Hill MJ.** Bacterial N-nitrosation and gastric carcinogenesis in humans. *Ital J Gastroenterol* 1991; **23**: 17-23

31 **Walters CL,** Smith PL, Reed PI, Haines K, House FR. N-nitroso compounds in gastric juice and their relationship to gastroduodenal disease. *IARC Sci Publ* 1982: 345-355

Science Editor Wang XL and Guo SY **Language Editor** Elsevier HK

PO Box 2345, Beijing 100023, China
www.wjgnet.com
wjg@wjgnet.com

ELSEVIER

World J Gastroenterol 2005;11(28):4317-4320
World Journal of Gastroenterology ISSN 1007-9327

Growth inhibition of high-intensity focused ultrasound on hepatic cancer *in vivo*

Xiu-Jie Wang, Shu-Lan Yuan, Yan-Rong Lu, Jie Zhang, Bo-Tao Liu, Wen-Fu Zeng, Yue-Ming He, Yu-Rui Fu

Xiu-Jie Wang, Shu-Lan Yuan, Yan-Rong Lu, Jie Zhang, Division of Experimental Oncology, Key Laboratory of Biotherapy of Human Diseases of Ministry of Education, PR China; West China Hospital, Sichuan University, Chengdu 610041, Sichuan Province, China
Bo-Tao Liu, Wen-Fu Zeng, Yue-Ming He, Yu-Rui Fu, Mianyang Electronic Equipment Factory, Mianyang 621000, Sichuan Province, China
Supported by the Grant from National Economic Trade Committee, No. 2000-312-2
Correspondence to: Xiu-Jie Wang, Division of Experimental Oncology, Key Laboratory of Biotherapy of Human Diseases of Ministry of Education, PR China; West China Hospital, Sichuan University, Chengdu 610041, Sichuan Province, China. xiujiewang@sina.com
Telephone: +86-28-5423039 Fax: +86-28-85171476
Received: 2004-09-25 Accepted: 2004-10-26

Abstract

AIM: To investigate the damaging effect of high-intensity focused ultrasound (HIFU) on cancer cells and the inhibitory effect on tumor growth.

METHODS: Murine H_{22} hepatic cancer cells were treated with HIFU at the same intensity for different lengths of time and at different intensities for the same length of time *in vitro*, the dead cancer cells were determined by trypan blue staining. Two groups of cancer cells treated with HIFU at the lowest and highest intensity were inoculated into mice. Tumor masses were removed and weighed after 2 wk, tumor growth in each group was confirmed pathologically.

RESULTS: The death rate of cancer cells treated with HIFU at 1 000 W/cm^2 for 0.5, 1, 2, 4, 8, and 12 s was 3.11±1.21%, 13.37±2.56%, 38.84±3.68%, 47.22±5.76%, 87.55±7.32%, and 94.33±8.11%, respectively. A positive relationship between the death rates of cancer cells and the length of HIFU treatment time was found (r = 0.96, P<0.01). The death rate of cancer cells treated with HIFU at the intensity of 100, 200, 400, 600, 800, and 1 000 W/cm^2 for 8 s was 26.31±3.26%, 31.00±3.87%, 41.97±5.86%, 72.23±8.12%, 94.90±8.67%, and 99.30±9.18%, respectively. A positive relationship between the death rates of cancer cells and the intensities of HIFU treatment was confirmed (r = 0.98, P<0.01). The cancer cells treated with HIFU at 1 000 W/cm^2 for 8 s were inoculated into mice *ex vivo*. The tumor inhibitory rate was 90.35% compared to the control (P<0.01). In the experimental group inoculated with the cancer cells treated with HIFU at 1 000 W/cm^2 for 0.5 s, the tumor inhibitory rate was 22.9% (P<0.01). By pathological examination, tumor growth was confirmed in 8 out of 14 mice (57.14%, 8/14) inoculated with the cancer cells treated with HIFU at 1 000 W/cm^2 for 8 s, which was significantly lower than that in the control (100%, 15/15, P<0.05).

CONCLUSION: HIFU is effective on killing or damage of H_{22} hepatic cancer cells *in vitro* and on inhibiting tumor growth in mice *ex vivo*.

Key words: HIFU; Liver cancer; Growth inhibition

Wang XJ, Yuan SL, Lu YR, Zhang J, Liu BT, Zeng WF, He YM, Fu YR. Growth inhibition of high-intensity focused ultrasound on hepatic cancer *in vivo*. *World J Gastroenterol* 2005; 11(28): 4317-4320
http://www.wjgnet.com/1007-9327/11/4317.asp

INTRODUCTION

High-intensity focused ultrasound (HIFU) consists of focused ultrasound (ULS) waves emitted from a transducer and is capable of inducing tissue damage. By means of this thermal effect and other mechanisms, HIFU-treated tumor tissues result in direct thermal cytotoxic necrosis and fibrosis, thus leading to inhibition of tumor growth. Therefore, HIFU is a new-sophisticated high-technology based minimally invasive treatment option for some cancers, which allows radiation-free treatment. Until now there are many kinds of tumors, such as tumors of prostate, liver, kidney, bladder, breast, and brain, that were treated with HIFU clinically and experimentally, some cancers were effectively controlled after HIFU treatment. As one of the minimally invasive surgical techniques for cancer treatment, HIFU is of great interest today[1,2].

Malignant cells are sensitive to therapeutic ULS treatment, which leads to a transient decrease in cell proliferation[3] through inducing a complex signaling cascade with upregulation of proapoptotic genes and downregulation of cellular survival genes[4]. In *in vitro* study, it was confirmed that CZ901 HIFU inhibits proliferation and induces apoptosis of cancer cells[5]. This study aimed to investigate the effects of HIFU on cancer cell damage *in vitro* and tumor growth inhibition *ex vivo*.

MATERIALS AND METHODS

Experimental materials

Cancer cell line in mouse Murine hepatoma H_{22} cell line

was kept in liquid nitrogen for regular use in our laboratory[6].

Experimental animals Female Balb/C mice, weighing 18-22 g, were purchased from Beijing Biological Products Research Institute under Ministry of Public Health (approval number: 013072). The procedures involving animals and their care were conducted in accordance with institutional guidelines for Laboratory Animal Care of Experimental Animal Center, Sichuan University.

Experimental device CZ901 HIFU device for cancer treatment was designed and supplied by Mianyang Electronic Equipment Factory.

Experimental methods

Experiment *in vitro* Ascites taken from H_{22} hepatic cancer bearing mouse on d 8 or 9 was diluted with normal saline at 1∶5 (2.5×10^7 cells/mL) and distributed into 14 PVC tubes, 7 tubes in each test, each containing 1.8 mL. Twelve tubes were treated with HIFU, and two were used as controls. H_{22} hepatic cancer cells were treated with HIFU at the frequency of 1.048 MHz and at the intensity of 1 000 W/cm^2 for 0.5, 1, 2, 4, 8, and 12 s, respectively, and for 8 s at intensity of 100, 200, 400, 600, 800, and 1 000 W/cm^2, respectively. After HIFU treatment, the cells were incubated in a humidified atmosphere of 50 μg/mL CO_2 at 37 ℃ for 6 h, and then the viability of cancer cells was determined by exclusion of trypan blue staining. The viable cells were not stained, the dead cells were stained blue. The viable cells and dead cells were counted with an erythrocytometer under microscope, respectively (total cell number counted >1 000). The death rate was determined by dead cell number÷(the dead cell number+the viable cell number)×100%. Each experiment was performed in triplicate.

Inoculation of HIFU-treated cancer cells *ex vivo* Cancer cells including viable and dead cells treated with HIFU at 1 000 W/cm^2 for 8 s were inoculated into 14 mice, 2×10^6 cells/0.2 mL per mouse. The same number of untreated cancer cells was inoculated into 20 mice as control. In addition, cancer cells treated with HIFU at 1 000 W/cm^2 for 0.5 s were inoculated into 18 mice, 2×10^6 cells/0.2 mL per mouse. The same number of untreated cancer cells was inoculated into 20 mice as control.

Examining the tumor growth *ex vivo* The animals inoculated with cancer cells were raised routinely, with free access to food and water and weighed every 2 d. After 2 wk of inoculation, the animals were killed, the tumor masses were removed and weighed, and the tumor inhibitory rate was calculated[6].

Histopathological examination Tumor masses were fixed with 4% paraformaldehyde, embedded with paraffin, sectioned and stained with HE. The tumor growth inhibition was confirmed by microscopy.

Statistical analysis

The experimental data were expressed as mean±SD and analyzed with χ^2 test. $P<0.05$ was considered statistically significant.

RESULTS

Cell damage effect of HIFU in vitro

The death rate of cancer cells in controls was 3-5% (Figure 1A), and increased significantly after HIFU treatment (Figure 1B). The death rate of cancer cells treated with HIFU at 1 000 W/cm^2 for 0.5, 1, 2, 4, 8, and 12 s were 3.11±1.21%, 13.37±2.56%, 38.84±3.68%, 47.22±5.76%, 87.55±7.32%, and 94.33±8.11%, respectively (Figure 1C). A positive

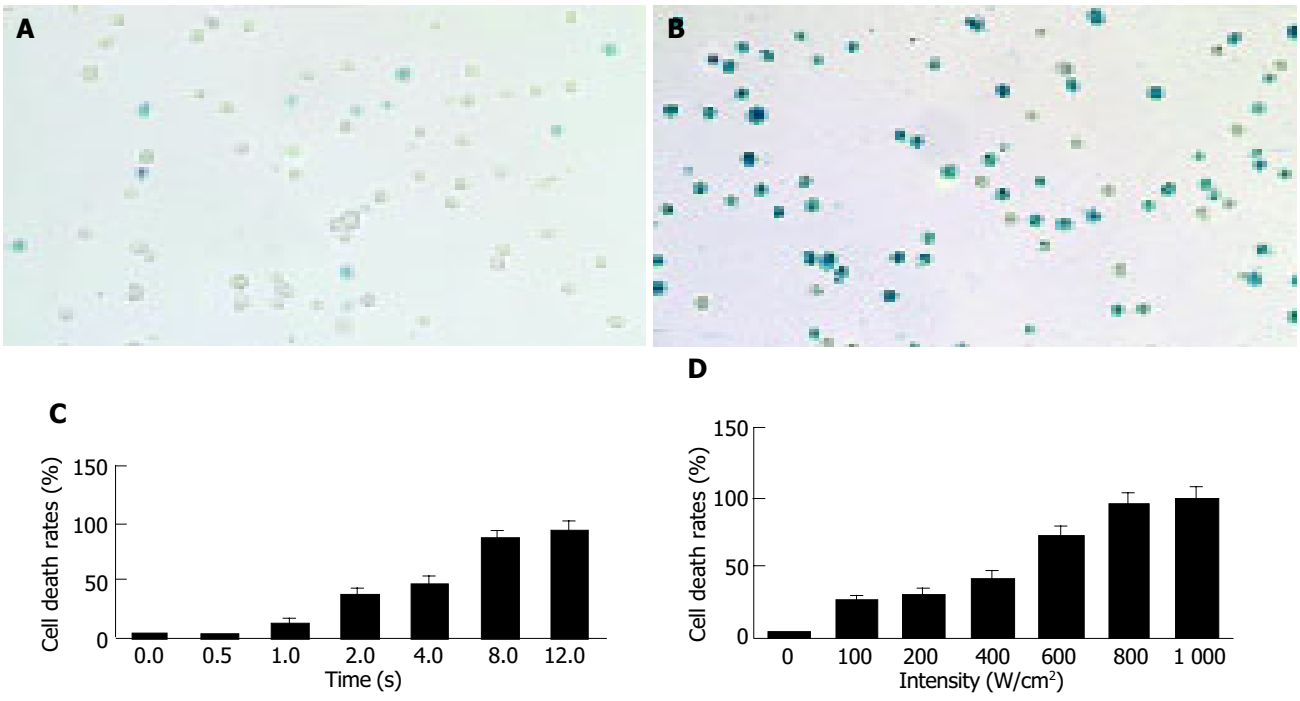

Figure 1 Cell damage effect of HIFI *in vitro*. **A**: Murine hepatic cancer cells before HIFU treatment; **B**: murine hepatic cancer cells treated with HIFU at 1 000 W/cm^2 for 8 s; **C**: significant difference between cell death rate and time of HIFU treatment; **D**: significant difference between the cell death rate and intensity of HIFU treatment.

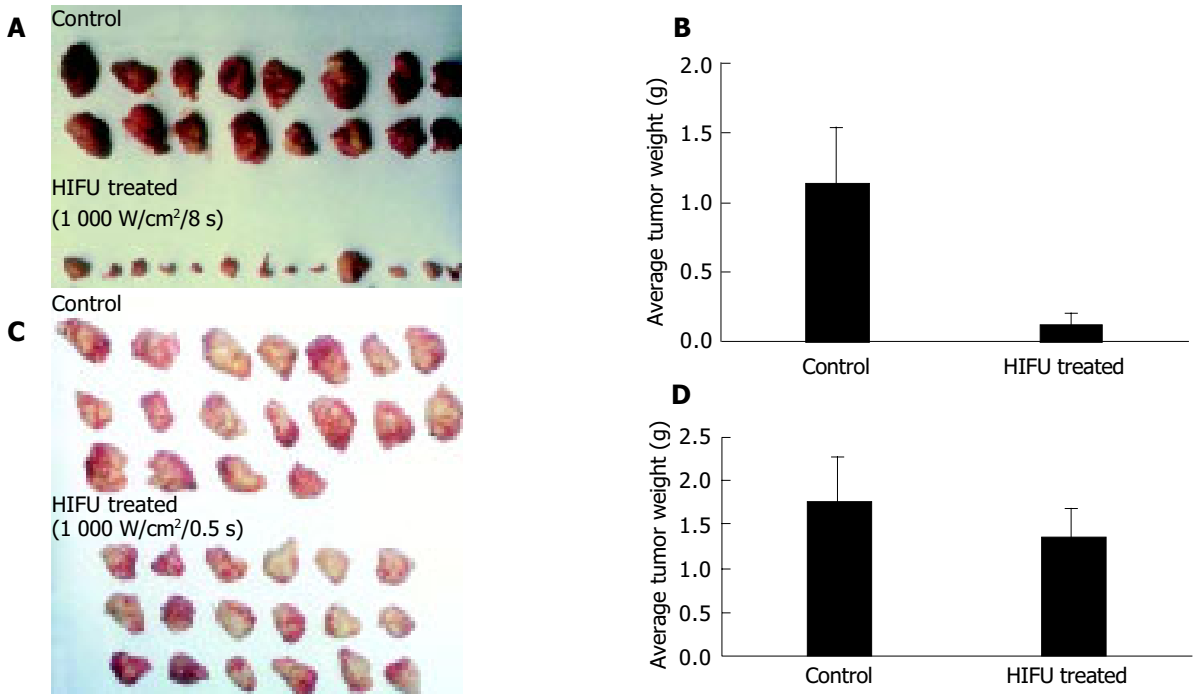

Figure 2 Tumor growth inhibition of HIFU *ex vivo*. **A**: Tumor growth inhibition of HIFU at 1 000 W/cm^2 for 8 s; **B**: significant difference in average tumor weight between the control and HIFU-treated mice; **C**: tumor growth inhibition of HIFU at 1 000 W/cm^2 for 0.5 s; **D**: significant difference in average tumor weight between the control and HIFU-treated mice.

relationship was found between the death rate of cancer cells and the time of HIFU treatment (r = 0.96, P<0.01).

The death rate of cancer cells treated with HIFU at the intensity of 100, 200, 400, 600, 800, and 1 000 W/cm^2 for 8 s was 26.31±3.26%, 31.00±3.87%, 41.97±5.86%, 72.23±8.12%, 94.90±8.67%, and 99.30±9.18%, respectively (Figure 1D). A positive relationship was confirmed between the death rates of cancer cells and the intensities of HIFU treatment (r = 0.98, P<0.01).

Tumor growth inhibition of HIFU ex vivo

Tumor growth inhibition of cancer cells treated with HIFU *ex vivo* is listed in Table 1. In experiment 1, six mice in the control group died of tumor burden spontaneously, none died in the HIFU-treated group. There was no significant difference in body weight increase between two groups of animals. In the group of animals inoculated with cancer cells treated with HIFU at 1 000 W/cm^2 for 8 s, the average tumor weight was 0.11±0.16 g, and the average tumor weight in control group was 1.14±0.4 g (Figures 2A and B), the tumor inhibition rate was 90.35% compared to the control (P<0.01). In experiment 2, cancer cells treated with HIFU at 1 000 W/cm^2 for 0.5 s were inoculated. The average tumor weight in HIFU-treated group and control was 1.36±0.33 and 1.75±0.53 g, respectively (Figures 2C and D), the tumor inhibitory rate was 22.90% (P<0.01).

By pathological examination, tumor growth was confirmed in 8 out of 14 mice (57.14%, 8/14) inoculated with cancer cells treated with HIFU at 1 000 W/cm^2 for 8 s, which was significantly lower than that of the control (100%, 15/15, P<0.05).

DISCUSSION

HIFU consists of focused ULS waves emitted from a transducer and is capable of inducing tissue damage. By means of this thermal effect and other mechanisms, HIFU-treated tumor tissues resulted in direct thermal cytotoxic necrosis and fibrosis, thus leading to inhibition of tumor growth. Therefore, HIFU is a new-sophisticated high-technology based, minimally invasive treatment option for some cancers[1,4,5]. But, there are many factors affecting its therapeutic effect, such as, intensity of the transmitted pulse, the exposure time, the signal frequency, the time interval

Table 1 Inhibitory effect of HIFU on growth of hepatic cancer *ex vivo* (mean±SD)

Experiment group		HIFU treatment (1 000 W/cm^2)	Animals (n)		Average BW (g)		Tumor wt (g)	TIR (%)
			d_1	d_{14}	d_1	d_{14}		
1	Control	0	20	15	19.05±2.03	19.62±2.13	1.14±0.40	
	HIFU	8	14	14	19.69±1.34	21.45±0.99	0.11±0.16^b	90.35
2	Control	0	20	19	21.03±2.14	28.39±3.83	1.75±0.53	
	HIFU	0.5	18	18	22.68±2.73	27.46±4.03	1.36±0.33^b	22.29

BW: Body weight; wt: weight; TIR: tumor inhibitory rate. $^b P$<0.01 *vs* control.

between two firing bursts, and biological medium, *etc.*[1,7-9].

The HIFU device used in this experimental study was designed and manufactured in Mianyang Electronic Equipment Factory. Its signal frequency emitted is 1.048 MHz, the intensity of the transmitted pulse and exposure time can be manipulated[5]. In this experimental study, H_{22} hepatic cancer cells were treated with HIFU at the same intensity for different lengths of time and for the same length of time at different intensities *in vitro*. It showed a intensity and time-dependent damaging effect on cancer cells (Figures 1B-D), suggesting that HIFU has a damaging or killing effect on cancer cells *in vitro*. The effective parameters are: an intensity of 1 000 W/cm^2 and an exposure time of 8 s.

There are many experimental and clinical studies on treatment of tumors with HIFU[1,10-14], especially hepatic cancers[15-19]. The results of these studies *in vitro* and *in vivo* indicate that HIFU has damaging or killing effect on cancer cells *in vitro* and inhibitory effect on tumor growth *in vivo*. However, to our best knowledge, there is no study on the growth potential of cancer cells after HIFU treatment. The findings in this study indicate that most cancer cells treated with HIFU at 1 000 W/cm^2 would die and lose the proliferating potential, but few cells may survive and form tumors.

Although minimally invasive methods for the treatment of cancer, such as HIFU, and high-energy shock waves, have been proposed recently, their feasibility for treatment of human cancers needs to be confirmed[1,20]. This experimental study has confirmed that HIFU has effects on killing or damage of H_{22} hepatic cancer cells *in vitro* and on the inhibiting tumor growth in mice *ex vivo*. Its inhibitory and therapeutic effects on other cancers, and mechanisms of action need to be studied and confirmed further.

REFERENCES

1 **Chaussy CG,** Thuroff S. High-intensive focused ultrasound in localized prostate cancer. *J Endourol* 2000; **14**: 293-299
2 **Beerlage HP,** Thuroff S, Madersbacher S, Zlotta AR, Aus G, de Reijke TM, de la Rosette JJ. Current status of minimally invasive treatment options for localized prostate carcinoma. *Eur Urol* 2000; **37**: 2-13
3 **Ashush H,** Rozenszajn LA, Blass M, Barda-Saad M, Azimov D, Radnay J, Zipori D, Rosenschein U. Apoptosis induction of human myeloid leukemic cells by ultrasound exposure. *Cancer Res* 2000; **60**: 1014-1020
4 **Abdollahi A,** Domhan S, Jenne JW, Hallaj M, Aqua GD, Mueckenthaler M, Richter A, Martin H, Debus J, Ansorge W, Hynynen K, Huber PE. Apoptosis signals in lymphoblasts induced by focused ultrasound. *FASEB J* 2004; **18**: 1413-1414
5 **Wang XJ,** Yuan SL, Zhang J, Lu YR, Wang YP, Chen XH, Ning QZ, Fu YR, Liu BT, Zeng WF, He YM. A study of the proliferation inhibition effect of HIFU and its mechanism of action on human breast cancer cells. *Sichuan Daxue Xuebao Yixueban* 2004; **35**: 60-63
6 **Wang X,** Yuan S, Wang C. A preliminary study of the anticancer effect of tanshinone on hepatic carcinoma and its mechanism of action in mice. *Zhonghua Zhongliu Zazhi* 1996; **18**: 412-414
7 **Beerlage HP,** Thuroff S, Debruyne FM, Chaussy C, de la Rosette JJ. Transrectal high-intensity focused ultrasound using the Ablatherm device in the treatment of localized prostate carcinoma. *Urology* 1999; **54**: 273-277
8 **Chapelon JY,** Ribault M, Vernier F, Souchon R, Gelet A. Treatment of localised prostate cancer with transrectal high intensity focused ultrasound. *Eur J Ultrasound* 1999; **9**: 31-38
9 **Wang Z,** Bai J, Li F, Du Y, Wen S, Hu K, Xu G, Ma P, Yin N, Chen W, Wu F, Feng R. Study of a "biological focal region" of high-intensity focused ultrasound. *Ultrasound Med Biol* 2003; **29**: 749-754
10 **Yang R,** Reilly CR, Rescorla FJ, Faught PR, Sanghvi NT, Fry FJ, Franklin TD Jr, Lumeng L, Grosfeld JL. High-intensity focused ultrasound in the treatment of experimental liver cancer. *Arch Surg* 1991; **126**: 1002-1009
11 **Cheng SQ,** Zhou XD, Tang ZY, Yu Y, Bao SS, Qian DC. Iodized oil enhancesthe thermal effect of high-intensity focused ultrasound on ablating experimental liver cancer. *J Cancer Res Clin Oncol* 1997; **123**: 639-744
12 **Adams JB,** Moore RG, Anderson JH, Strandberg JD, Marshall FF, Davoussi LR. High-intensity focused ultrasound ablation of rabbit kidney tumors. *J Endourol* 1996; **10**: 71-75
13 **Madersbacher S,** Kratzik C, Susani M, Pedevilla M, Marberger M. Transcutaneous high-intensity focused ultrasound and irradiation: an organ-preserving treatment of cancer in a solitary testis. *Eur Urol* 1998; **33**: 195-201
14 **Van Leenders GJ,** Beerlage HP, Ruijter ET, de la Rosette JJ, van de Kaa CA. Histopathological changes associated with high intensity focused ultrasound (HIFU) treatment for localised adenocarcinoma of the prostate. *J Clin Pathol* 2000; **53**: 391-394
15 **Prat F,** Centarti M, Sibille A, Abou el Fadil F, Henry L, Chapelon JY, Cathignol D. Extracorporeal high-intensity focused ultrasound for VX2 liver tumors in the rabbit. *Hepatology* 1995; **221**: 832-836
16 **Sibille A,** Prat F, Chapelon JY, Abou el Fadil F, Henry L, Theillere Y, Ponchon T, Cathignol D. Extracorporeal ablation of liver tissue by high-intensity focused ultrasound. *Oncology* 1993; **50**: 375-379
17 **Yang R,** Sanghvi NT, Rescorla FJ, Kopecky KK, Grosfeld JL. Liver cancer ablation with extracorporeal high-intensity focused ultrasound. *Eur Urol* 1993; **23**(Suppl 1): 17-22
18 **Sibille A,** Prat F, Chapelon JY, Abou el F, Henry L, Theillere Y, Ponchon T, Cathignol D. Characterization of Extracorporeal ablation of normal and tumor-bearing liver tissue by high-intensity focused ultrasound. *Ultrasound Med Biol* 1993; **19**: 803-813
19 **Arefiev A,** Prat F, Chapelon JY, Tavakkoli J, Cathignol D. Ultrasound-induced tissue ablation: studies on isolated perfused porcine liver. *Ultrasound Med Biol* 1998; **24**: 1033-1043
20 **Thuroff S,** Chaussy C. High-intensity focused ultrasound: complications and adverse events. *Mol Urol* 2000; **4**: 183-187

Science Editor Wang XL and Guo SY **Language Editor** Elsevier HK

PO Box 2345, Beijing 100023, China
www.wjgnet.com
wjg@wjgnet.com

ELSEVIER

World J Gastroenterol 2005;11(28):4321-4325
World Journal of Gastroenterology ISSN 1007-9327

Classification of right hepatectomy for special localized malignant tumor in right liver lobe

Ning Fan, Guang-Shun Yang, Jun-Hua Lu, Ning Yang

Ning Fan, Guang-Shun Yang, Jun-Hua Lu, Ning Yang, Department of Laparoscopy, Affiliated Eastern Hospital of Hepatobiliary Surgery, Second Military Medical University, Shanghai 200438, China
Co-first-authors: Guang-Shun Yang and Ning Fan
Correspondence to: Professor Guang-Shun Yang, Department of Laparoscopy, Affiliated Eastern Hospital of Hepatobiliary Surgery, Second Military Medical University, Shanghai 200438, China. guangshun@smmu.edu.cn
Telephone: +86-21-25070803 Fax: +86-21-25070803
Received: 2004-12-06 Accepted: 2005-01-05

Abstract

AIM: To describe a new classification method of right hepatectomy according to the different special positions of tumors.

METHODS: According to positions, 91 patients with malignant hepatic tumor in the right liver lobe were divided into six groups: tumors in the right posterior lobe and (or) the right caudate lobe compressing the right portal hilum (n = 14, 15.4%), tumors in the right liver lobe compressing the inferior vena cava and (or) hepatic veins (n = 11, 12.9%), tumors infiltrating diaphragmatic muscle (n = 7, 7.7%), tumors in the hepatorenal recess (infiltrating the right fatty renal capsule, transverse colon and right adrenal gland, n = 8, 8.8%), tumors deeply located near the vertebral body (n = 3, 3.3%), tumors at other sites in the right liver lobe (the control group, n = 48, 52.75%). The values of intraoperative blood loss (IBL), tumor's maxim cross-section area (TMCSA), and time of hepatic hilum clamping (THHC) and incidence of postoperative complications were compared between five groups of tumor and control group, respectively.

RESULTS: The THHC in groups 1-4 was significantly longer than that in the control group, the IBL in groups 1-4 was significantly higher than that in the control group, the TMCSA in groups 2-4 was significantly larger than that in the control group, and the ratio of IBL/TMCSA in group 1 was significantly higher than that in the control group. There was no significant difference in the indexes between group 5 and the control group.

CONCLUSION: The site of tumor is the key factor that determines IBL.

Key words: Hepatectomy; Tumor; Position; Complication; Blood Loss; Clamping time

Fan N, Yang GS, Lu JH, Yang N. Classification of right hepatectomy for special localized malignant tumor in right liver lobe. *World J Gastroenterol* 2005; 11(28): 4321-4325
http://www.wjgnet.com/1007-9327/11/4321.asp

INTRODUCTION

Clinically, 60% of malignant tumors occur in the right liver which has a great physical volume and complicated anatomic structure, with a large number of vessels inside and important organs around, such as diaphragmatic muscle, right kidney, right adrenal gland, colon, and inferior vena cava. Therefore, tumors in the right liver lobe with different sizes and diversified positions may induce a widely different series of problems in the process of resection of these tumors. Generally, the easily removed tumor has a diameter less than 5 cm and is located on the surface of liver without infiltrating the surrounding important organs, or does not compress the main blood vessels in the liver. The features of tumors which are different to resect are as follows. (1) The diameter of tumor is larger than 5 cm and the tumor is close to or even infiltrates the major vessels of liver; (2) Although the diameter of tumor is less than 5 cm, it protrudes from the liver surface infiltrating surrounding organs. The tumor is deeply located and hard to be exposed during surgery. The tumor which meets one or more of the above standards is defined as the malignant tumor within the right liver with special position (MTRLSP). For the much more intraoperative blood loss (IBL), the longer the time of hepatic hilum clamping (THHC), the more the postoperative complications. MTRLSP has been a difficulty in right hepatectomy. Little information is available on the classification of right hepatectomy for MTRLSP. This paper presents a prospective observation on the surgical features of 91 cases of right hepatectomies, and the classification according to the standards mentioned above.

MATERIALS AND METHODS

Study population

Ninety-one patients with malignant tumor within the right liver underwent right hepatectomy from 2002-05 to 2003-09 at Eastern Hepatobiliary Surgery Hospital of Second Military Medical University. There were 73 male and 18 female patients, ranging 25-78 years of age, including 87 cases of primary liver cancer, 2 cases of colon metastatic cancer, 1 case of rectum metastatic cancer, and 1 case of

liver lymphoma. There were four cases of tumor thrombosis in portal vein and two cases in the bile duct. No death occurred in hospital.

Grouping

Forty-three cases of MTRLSPs were divided into five groups in light of tumor positions, and 48 cases of tumors at other sites within right liver lobe in the corresponding period served as the control (Table 1).

Table 1 Grouping of 91 cases of right hepatectomies

Tumor position			Cases (%)	Total (%)
MTR				
LSP	Group 1	Tumors within right posterior lobe and (or) right caudate lobe compressing right portal hilum	14/91 (15.4)	
	Group 2	Massive tumors within right liver lobe compressing the inferior vena cava and (or) hepatic veins	11/91 (12.09)	43/91 (47.25)
		Hepato-renal infiltrating transverse colon	7/91 (7.7)	
		Recess infiltrating right adrenal gland	4/91 (4.4)	
	Group 3	Tumors infiltrating diaphragmatic muscle	3/91 (3.3)	
	Group 4	Tumors in the infiltrating right fatty renal capsule	1/91 (1.1)	
	Group 5	Tumors deeply located near vertebral body control	3/91 (3.3)	
	Group 6	Tumors in other places	48/91 (52.75)	

Methods

The Pringle's maneuver was routinely adopted in tumor resection to control bleeding. The THHC was recorded during surgery, and the IBL and the TMCSA were measured after surgery. The postoperative complication of each patient was also recorded. The IBL, THHC (used for evaluating tumor size), TMCSA and postoperative complications in each group were compared to those in the control group respectively.

Statistical analysis

The data were expressed as mean±SE. SPSS for Windows, version 11.0 was used with Dunnett-*t* or Wilcoxon signed rank test.

RESULTS

The values of THHC in each group are shown in Table 2. The time in groups 1-4 was much longer than that in group 6 ($P<0.05$), but not in group 5 ($P>0.05$). For F- test = 0.078>0.05, bilateral Dunnett-*t* was used.

The values of IBL in each group are shown in Table 3. The value of IBL in groups 1-4 was much greater than that in group 6 ($P<0.05$), but not in group 5 ($P>0.05$). For F-test = 0.007<0.05, bilateral Wilcoxon signed rank test was used.

The values of TMCSA in each group are shown in Table 4. The value of TMCSA in groups 2-4 was much larger than that in group 6 ($P<0.05$), but not in groups 1 and 5 ($P>0.05$). For F-test = 0.000<0.05, bilateral Wilcoxon signed rank test was used.

The ratios of IBL/TMCSA in each group are shown in Table 5. The value of IBL in groups 2-5 was not significantly higher than that in group 6 ($P>0.05$), but not in group 1 ($P<0.05$). For F-test = 0.114>0.05, bilateral Dunnett-*t* was used.

The rate of blood transfusion during surgery and the

Table 2 THHC in groups 1-6 (mean±SE)

Group	1	2	3	4	5	6
THHC (min)	31.00±3.53	36.72±2.41	31.42±4.56	29.75±2.53	17±2.51	19.148±1.27
P values	0.001[a]	0.000[a]	0.013[a]	0.028[a]	0.998	-

[a]$P<0.05$ *vs* control.

Table 3 IBL in groups 1-6 (mean±SE)

Group	1	2	3	4	5	6
IBL (mL)	642.85±132.89	1 054.54±200.16	1 085.71±310.47	850.00±185.16	483.33±60.09	257.40±29.44
P values	0.033[a]	0.005[a]	0.046[a]	0.011[a]	0.285	-

[a]$P<0.05$ *vs* control.

Table 4 TMCSA in groups 1-6 (mean±SE)

Group	1	2	3	4	5	6
TMCSA (cm^2)	20.61±4.67	84.95±11.76	56.38±12.50	46.87±5.59	51.88±40.2	22.77±3.67
P values	0.683	0.003[a]	0.028[a]	0.012[a]	0.593	

[a]$P<0.05$ *vs* control.

Table 5 IBL/TMCSA in groups 1-6 (mean±SE)

Group	1	2	3	4	5	6
IBL/TMCSA (mL/cm^2)	38.14±9.91	14.81±2.79	22.85±6.76	17.13±2.61	34.33±20.98	13.42±2.24
P values	0.003[a]	1.000	0.788	0.994	0.387	

[a]*P*<0.05 *vs* control.

Table 6 Blood transfusion and incidence of postoperative complications in groups 1-6 (%)

Group	1	2	3	4	5	6
Blood transfusion	35.71	45.45	42.86	37.5	0	0
Incidence of postoperative complications	14.29	36.36	71.43	37.5	0	0

incidence of postoperative complications in each group are shown in Table 6, the above two values were all zero in groups 5 and 6. The main postoperative complication in groups 1, 2, and 4 was right pleural effusion. The main postoperative complications in group 3 were right pleural effusion and rupture of diaphragm.

DISCUSSION

According to the definition of MTRLSP, the proportion of MTRLSP is 47.25% (Table 1), which shows that nearly half of right hepatectomies for malignant tumors are the high-risk resections for MTRLSPs. The IBL, THHC, and postoperative complications are the three risk factors for the resection for MTRLSP; tumor size and site determine these factors. In this study, taking the influence of tumor size as the index of IBL/TMCSA, we divided the MTRLSPs into five groups according to their positions to analyze and identify the main reason for high-risk resections of tumors in each group.

Tumors in the group 1 (n = 14, 15.4%) within the right posterior lobe and (or) right caudate lobe usually compressed or even infiltrated the right posterior portal vein (RPPV, Figure 1), occasionally with the tumor thrombus in vessels. Tumor thrombi almost all occurred in this (in portal branch, n = 3, 3/4 = 75%; in bile duct, n = 2, 2/2 = 100%). The tumor was usually located between the first and third hepatic hilum with some main blood vessels around, such as the RPPV, inferior vena cava (IVC). It was difficult to control bleeding in an extremely dangerous state once these main vessels rupture when the tumor was exposed, and to injure the first hepatic hilum if blind suture was used to stop bleeding. Therefore, the IBL (642.85±132.89 mL) was much greater than that in the control group (257.40±29.44 mL, P = 0.033), and the THHC (31.00±3.53 min) was also significantly longer than that in the control group (19.148±1.27, P = 0.001), though there was no statistical difference (P = 0.683) in TMCSA between this group (20.61±4.67 cm^2) and control group (22.77±3.67 cm^2). The main reason for high-risk resection of tumors of this group is the site but not the size of tumors, which is further proved by the fact that the index of IBL/TMCSA (38.14±9.91) was significantly higher than that in the control group (13.42±2.24, P = 0.003).

For example, an operation of 1 patient with the tumor in the right caudate going down to left caudate ran into trouble. After the tumor was ablated from the wall of the compressed IVC and RPPV, it was impossible to suture the wound because the nude right portal branch was just on the surface of the incision wedge. A drainage tube was placed instead of suture of the wound. A bile leakage was found 3 d after surgery which was closed after drainage.

Generally, to handle the tumor at this site, we should remove it as soon as possible, and suture the liver wound by any possible way, and observe the characteristics of drainage carefully in case the severe bile leakage occurs after surgery[1].

Tumors (n = 11, 12.9%) in group 2 compressing part or completely at the inferior vena cava (n = 6, Figure 2) and (or) hepatic veins (n = 4, Figure 3) had the largest size in groups 1-6, with TMCSA being 84.95±11.76 cm^2, larger than that in the control group 22.77±3.67 cm^2, P = 0.003. They were so large that they almost occupy the whole right

Figure 1 Tumor infiltrating right posterior portal vein (→).

Figure 2 Tumor compressing IVC (→).

liver lobe.

The IBL (1 054.54±200.16 mL) and THHC (36.72± 2.41 min) were much greater and longer than those in the control group (IBL: 257.40±29.44 mL, $P = 0.005$; THHC: 19.148±1.27 min, $P = 0.000$), suggesting a higher risk for surgery in this group. But there was no statistical difference in the index of IBL/TMCSA (14.81±2.79) between this group and control group (13.42±2.24, $P = 1.000$), suggesting that IBL is not much greater than that in the control group when the influence of tumor size is excluded. Apparently, the biggest tumor size is the main reason for the top 36 min THHC and 1 054 mL IBL in this group.

Some troubles caused by the compression of the IVC from tumors are as follows. When the tumor is removed from normal liver, severe bleeding may occur due to lacerated breakage on the IVC wall or crevasse of the hepatic short vein (HSV) with ligation falling off. After the tumor is removed, the remnant liver with full-length IVC uncovered on a wide surface of the incision wedge may be hard to be sutured for the fear of IVC obstruction due to compression from suture of wound. The obstruction can induce liver swelling and severe cirrhosis. The treatment strategies may be summarized as follows. (1) If the image of a tumor shows preoperatively that the tumor compresses or infiltrates the IVC, the blocking string should be preplaced around the superior and inferior IVC to the effect that severe bleeding can be easily controlled. The breakage is better sutured with 3-0 prolene, but not clamped. In addition, the HSV and the right adrenal gland vein should be abscised and ligated carefully; (2) To avoid compression of the IVC, an incision wedge should be shaped 'arc' so that both sides can be sutured with the IVC untouched at the bottom of the wound, and the remnant liver can be suspended to the abdomen wall. If the above measures do not work, the sutures of liver wound should be taken out, and then after careful hemostasis, the epiploon can be sutured to the incision wedge. Recently, some studies reported[2,3] that fibrin sealant can be ejected to the surface of liver wound to hemostasis, and results are quick and good.

The other sort of troubles comes from compression and infiltration of right hepatic veins (RHV) by a tumor under which there is usually a part of normal liver (Figure 3). Whether this part of normal liver should be excised with the tumor depends on the following two situations: (1) If a patient has severe liver cirrhosis and small left liver lobe, the normal liver in right posterior should be retained, and so does the RHV or dilated HSV to ensure blood flowing back[4]; (2) If a patient has mild liver cirrhosis and thick left liver lobe, the remnant liver and RHV can be excised with the tumor.

Tumors in group 3 ($n = 7$, 7.7%) had the highest value of IBL among all groups (1 085.71±310.47 mL *vs* the control 257.40±29.44 mL, $P = 0.046$). One reason is that tumors usually grow out of liver surface and adhere to diaphragm with abundant bypass blood vessels. The other reason is the large TMCSA (56.38±12.50 cm^2 *vs* the control 22.77±3.67 cm^2, $P = 0.028$). The larger the tumor and the wider the interface between tumor and diaphragm, the more the bleeding during surgery. But there was no statistical difference in the index of IBL/TMCSA (22.85±6.76) between this group and control group (13.42±2.24, $P = 0.788$), suggesting that IBL is not much greater than that in the control group when the influence of tumor size is excluded. The higher IBL and bigger TMCSA induce longer THHC (31.42±4.56 min *vs* the control 19.148±1.27 min, $P = 0.013$) and higher incidence of postoperative complications ($n = 5/7 = 71.43\%$, Table 6) such as right pleural effusion ($n = 3$) and diaphragm rupture ($n = 2$).

Tumors which infiltrate the diaphragm growing in an expansible fashion are usually too big to control during surgery, and should be excised integrally without the diaphragm being broken. But because of limited operational space for removal of surrounding ligaments around the liver, it is inevitable that tumors are occasionally oppressed. Once tumor raptures, a large quantity of low osmosis water should be used to wash the peritoneal cavity to prevent tumor planting. In addition, a part of the diaphragm approaching the liver is also flimsy and frangible[5] (Figure 4).

Thoracoabdominal approach for resection of this sort of tumors has been adopted by Xia *et al*.[6]. They found that the IBL is less and better exposured to hemostasia than abdominal approach, without an increasing incidence of postoperative complications, but with increased trauma and more complicated operative procedure. Our study also found a higher volume of the IBL and a higher incidence of postoperative complications. Therefore, along with the development of surgical technique and perioperative intensive care, thoracoabdominal approach may be reasonable for the resection of this sort of tumors.

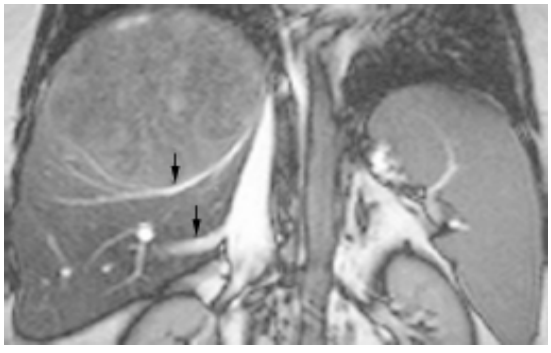

Figure 3 Tumor compressing RHV (→).

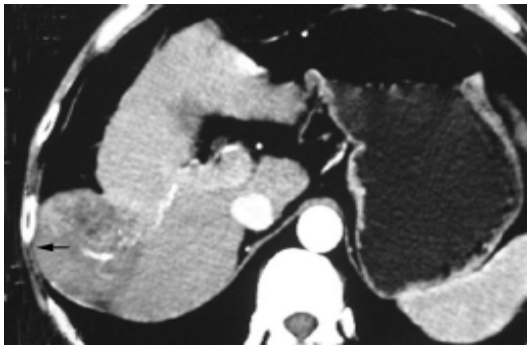

Figure 4 Tumor infiltrating diaphragm muscle (→).

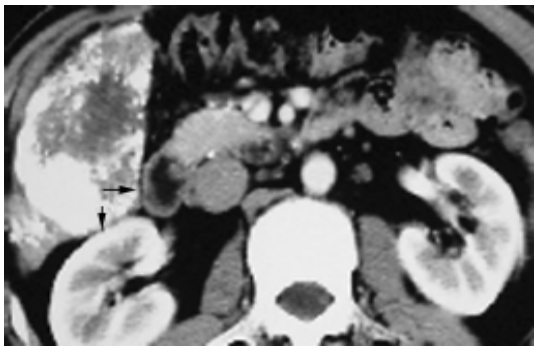

Figure 5 Tumor infiltrating colon (→) and right fatty renal capsule (→).

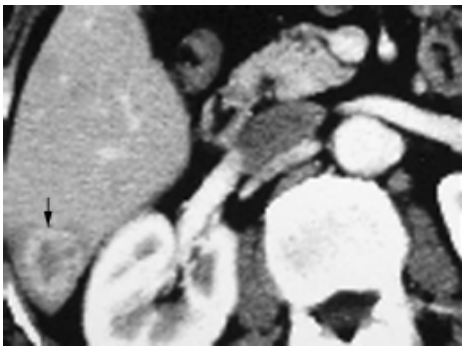

Figure 6 Tumor (→) deeply located at the level of posterior margin of vertebral body.

Tumors in group 4 (n = 8, 8.8%; infiltrating right fatty renal capsule n = 4, transverse colon n = 3, right adrenal gland, n = 1) protruding to hepatorenal recess were prone to infiltrate the right fatty renal capsule, transverse colon (Figure 5) or right adrenal gland and induce wide conglutination which caused the following difficulties. (1) Abundant bypass vessels between tumor and its surroundings were likely to bleed in the course of exploration and liberation. The IBL of this group (850.00±185.16 mL) was significantly greater than that in the control group (257.40±29.44 mL, P = 0.011); (2) Because of larger size (TMCSA 46.87±5.59 cm^2 *vs* the control 22.77±3.67 cm^2, P = 0.012) and severe infiltration and conglutination with surrounding tissues, tumor became a mass which did not leave enough space for hands to move the liver lobe for liberating right ligaments. But there was no statistical difference in the index of IBL/TMCSA (14.81±2.79) between this group and the control group (13.42±2.24, P = 1.000). The retrograde hepatectomy can be used to deal with this situation, and this method has been used for difficult hepatectomy for years[7-9].

Tumors in group 5 were located within the right posterior-inferior segment (Figure 6), and difficult to be exposed during surgery, and had to be padded with absorbent gauze on the surface of post-parietal peritoneum to lift liver and tumors up for a good exposure after liberation of ligaments. As long as there was good exposure, it was not very difficult to remove the tumor in this group.

In conclusion, this study isolated the MTRLSP from malignant tumors in the right liver and classified them into five sorts in terms of their position. The surgical features of each sort are described, which may improve the resection rate of malignant tumors within the right liver lobe and reduce the complications after surgery.

REFERENCES

1 **Tanaka S,** Hirohashi K, Tanaka H, Shuto T, Lee SH, Kubo S, Takemura S, Yamamoto T, Uenishi T, Kinoshita H. Incidence and management of bile leakage after hepatic resection for malignant hepatic tumors. *J Am Coll Surg* 2002; **195**: 484–489

2 **Davidson BR,** Burnett S, Javed MS, Seifalian A, Moore D, Doctor N. Study of a novel fibrin sealant for achieving haemostasis following partial hepatectomy. *Br J Surg* 2000; **87**: 790-795

3 **Liu M,** Lui WY. The use of fibrin adhesive for hemostasis after liver resection. *Zhonghua Yixue Zazhi* 1993; **51**: 19-22

4 **Smyrniotis V,** Arkadopoulos N, Kehagias D, Kostopanagiotou G, Scondras C, Kotsis T, Tsantoulas D. Liver resection with repair of major hepatic veins. *Am J Surg* 2002; **183**: 58–61

5 **Luo YQ,** Wang Y, Chen H, Wu MC. Influence of preoperative transcatheter arterial chemoembolization on liver resection in patients with respectable hepatocelluar carcinoma. *Zhonghua Putong Waike Zazhi* 2002; **17**: 149-151

6 **Xia F,** Poon RT, Fan ST, Wong J. Thoracoabdominal Approach for Right-Sided Hepatic Resection for Hepatocellular Carcinoma. *J Am Coll Surg* 2003; **196**: 418–427

7 **Lin TY,** Sridharan M, Ho ST. Retrograde resection of hepatic lobe for extensive carcinoma of liver. *Med Chir Dig* 1977; **6**: 87

8 **Lai EC,** Fan ST, Lo CM, Chu KM, Liu CL. Anterior approach for difficult major right hepatectomy. *World J Surg* 1996; **20**: 314-317

9 **Wu ZQ,** Fan J, Zhou J, Qiu SJ, Ma CZ, Zhou XD, Tang ZY. Retrograde hepatectomy and research on its procedure. *Zhonghua Gandan Waike Zazhi* 1999; **5**: 301-303

Science Editor Wang XL and Guo SY **Language Editor** Elsevier HK

PO Box 2345, Beijing 100023, China
www.wjgnet.com
wjg@wjgnet.com

ELSEVIER

World J Gastroenterol 2005;11(28):4326-4331
World Journal of Gastroenterology ISSN 1007-9327

Apoptosis and its pathway in X gene-transfected $HepG_2$ cells

Na Lin, Hong-Ying Chen, Dan Li, Sheng-Jun Zhang, Zhi-Xin Cheng, Xiao-Zhong Wang

Na Lin, Hong-Ying Chen, Dan Li, Sheng-Jun Zhang, Zhi-Xin Cheng, Xiao-Zhong Wang, Department of Gastroenterology, Affiliated Union Hospital, Fujian Medical University, Fuzhou 350001, Fujian Province, China
Correspondence to: Dr. Xiao-Zhong Wang, Department of Gastroenterology, Affiliated Union Hospital, Fujian Medical University, Fuzhou 350001, Fujian Province, China. drwangxz@pub6.fz.fj.cn
Telephone: +86-591-83357896-8482
Received: 2004-11-02 Accepted: 2004-11-24

Abstract

AIM: To investigate the effect of hepatitis B virus (HBV) X gene on apoptosis and expressions of apoptosis factors in X gene-transfected $HepG_2$ cells.

METHODS: The HBV X gene eukaryon expression vector *$pcDNA_3$-X* was transiently transfected into $HepG_2$ cells by lipid-media transfection. Untransfected $HepG_2$ and $HepG_2$ transfected with *$pcDNA_3$* were used as controls. Expression of HBx in $HepG_2$ was identified by RT-PCR. MTT and TUNEL were employed to measure proliferation and apoptosis of cells in three groups. Semi-quantified RT-PCR was used to evaluate the expression levels of Fas/FasL, Bax/Bcl-xL, and c-myc in each group.

RESULTS: HBV X gene was transfected into $HepG_2$ cells successfully. RT-PCR showed that HBx was only expressed in $HepG_2$/pcDNA$_3$-X cells, but not expressed in $HepG_2$ and $HepG_2$/pcDNA$_3$ cells. Analyzed by MTT, cell proliferation capacity was obviously lower in $HepG_2$/pcDNA$_3$-X cells (0.08910±0.003164) than in $HepG_2$ (0.14410±0.004927) and $HepG_2$/pcDNA$_3$ cells (0.12150±0.007159) (P<0.05 and P<0.01). Analyzed by TUNEL, cell apoptosis was much more in $HepG_2$/pcDNA$_3$-X cells (980/2 000) than $HepG_2$ (420/2 000), $HepG_2$/pcDNA$_3$ cells (520/2 000) (P<0.05 and P<0.01). Evaluated by semi-quantified RT-PCR, the expression level of Fas/FasL was significantly higher in $HepG_2$ cells transfected with HBx than in $HepG_2$ and $HepG_2$/pcDNA$_3$ cells (P<0.05 and P<0.01). Bax/Bcl-xL expression level was also elevated in $HepG_2$/pcDNA$_3$-X cells (P<0.05 and P<0.01). Expression of c-myc was markedly higher in $HepG_2$/pcDNA$_3$-X cells than in $HepG_2$ and $HepG_2$/pcDNA$_3$ cells (P<0.05 and P<0.01).

CONCLUSION: HBV X gene can impair cell proliferation capacity, improve cell apoptosis, and upregulate expression of apoptosis factors. The intervention of HBV X gene on the expression of apoptosis factors may be a possible mechanism responsible for the change in cell apoptosis and proliferation.

Key words: HBx; Transfect; HepG2; Apoptosis; Fas; FasL; Bax; Bcl-xL; c-myc

Lin N, Chen HY, Li D, Zhang SJ, Cheng ZX, Wang XZ. Apoptosis and its pathway in X gene-transfected $HepG_2$ cells. *World J Gastroenterol* 2005; 11(28): 4326-4331
http://www.wjgnet.com/1007-9327/11/4326.asp

INTRODUCTION

Hepatitis B virus (HBV) is a small DNA virus with partial double-stranded DNA genome. HBV contains four opening reading frames (ORF) namely preS$_1$/preS$_2$/S, preC/C, P, and X. X gene is a unique ORF which is well conserved in different mammalian hepadnaviruses, its product consists of 154 amino acids with a molecular weight of 16.7 ku. Based on epidemical data, HBx is thought to be associated with HBV-related primary hepatocellular carcinoma (HCC), but the molecular basis for the oncogenic activity of HBx remains elusive. HBx is a multiple-functional protein and plays an essential role in viral pathogenesis. HBx can deregulate cell cycle check points, transactivate cells and viral genes, which involve in transcription regulation, single transduction pathway, cell cycle regulation, *etc*.[1]. It has been shown that HBx can co-ordinate balance between proliferation and programmed cell death, and it is able to induce or block apoptosis. The deregulation of apoptosis is involved in a wide range of pathological processes, including development of HCC.

In the present study, we investigated the effect of HBx expression on apoptosis in human hepatoma cell line $HepG_2$, and its effect on the expression level of apoptosis factors.

MATERIALS AND METHODS

Materials

$PcDNA_3$ expression vector and HBV X gene eukaryon expression vector *$pcDNA_3$-X* were previously constructed. Human hepatoma cell line $HepG_2$ was provided by Cell Bank of Chinese Academy of Sciences. Modified Eagle's medium (MEM) was bought from Hyclone Company, USA. Reverse transcription system, DNA purification system, and Transfast™ transfection reagent were obtained from Promega Biotech (USA). Total RNA isolation kit was purchased from Jingmei Biotech Company (Shanghai, China). PCR primers were synthesized by Shanghai Biotechnology Company. In-site cell apoptosis detection kit was provided by Roche Company.

Methods

Cell culture and DNA transfection $HepG_2$ cells were cultured in MEM supplemented with 10% heat-inactivated

fetal bovine serum, 100 IU/mL penicillin and 100 mg/mL streptomycin in a humidified incubator with 50 mL/L CO_2. A total of 1.5×10^6 cells/mL were seeded into a 25 cm^2 cell plate before the experiment. When cells were grown to 80% confluence, *pcDNA3* or *pcDNA3-X* plasmid was transfected into $HepG_2$ cells by lipofection technique, which were named as $HepG_2$/$pcDNA_3$ cells and $HepG_2$/$pcDNA_3$-X cells. A mixture containing 2 mL serum-free MEM (prewarmed to 37 ℃) , 5 μg plasmid DNA, 15 μL transfect reagent was added to a cell plate. After incubation for 24 h, 4 mL complete medium was added into cell plate and then incubated for another 48 h. $HepG_2$ cells, untransfected with any plasmid DNA, were used as controls.

Detection of X gene expression by RT-PCR Total RNA was extracted from $HepG_2$, $HepG_2$/pcDNA3, and $HepG_2$/$pcDNA_3$-X cells respectively, and reverse transcripted into cDNA. One microliter of RT product was used as template, PCR was carried out. The sequences of X gene primers were: 5'-ATGCAAGCTTATGGCTGCTAGGC-TGTACTG-3' and 5'-TGCGAATTCTTAGGCAGAGG-TGAAAAAGTTG-3'. The expected amplification fragment was 467 bp. PCR conditions were as follows: pre-denaturation at 95 ℃ for 5 min, 32 amplification cycles (denaturation at 94 ℃ for 35 s, annealing at 65 ℃ for 35 s, and extension at 72 ℃ for 1 min), and a final extension at 72 ℃ for 7 min. The PCR products were separated by electrophoresis on 1.5% agarose gel, and detected by ultraviolet radiography.

Cell viability assay Cell viability was assayed by MTT. $HepG_2$, $HepG_2$/$pcDNA_3$, and $HepG_2$/$pcDNA_3$-X cells were planted into 96-well plates. Cells in logarithmic growth were used in experiments. One day before the experiment, complete medium was replaced by serum-free medium. During experiment, 75 μL MTT (5 mg/mL, containing in 0.01 mol/L PBS) was added into each well and incubated for 4 h. Then, the medium was replaced by DMSO (75 μL each well) and shaken gently until all crystals were dissolved. A_{492} was detected to measure the proliferative capacity of each group.

Cell apoptosis assay Cell apoptosis was estimated by TUNEL staining. $HepG_2$, $HepG_2$/$pcDNA_3$, and $HepG_2$/$pcDNA_3$-X cells were planted into 96-well plates. Cells at 80% confluence were fixed with 4% paraformaldehyde, and chilled in ice bath for 2 min with permeabilization solution (0.1% Triton X-100 in 0.1% sodium nitrate). Then, 50 μL TUNEL mixture was added, incubated in a humidified chamber at 37 ℃ for 1 h. TUNEL mixture was removed, 50 μL Converter-AP was added and incubated for another 30 min. The cells were rinsed with PBS, counterstained with NBT/BCIP, and detected by optic microscopy.

Effect of HBx transient transfection on apoptosis factor mRNA expression Expressions of Fas/FasL, Bax/Bcl-xL, and c-myc gene were assayed by semi-quantitative RT-PCR. β-Actin was used as internal control. Total RNA was extracted respectively with RNA isolation kit, and reverse transcripted into cDNA. PCR was performed in a 50 μL reaction volume containing 5 μL 10× PCR buffer, 5 μL 2 mmol/L $MgCl_2$, 1 μL 10 mmol/L dNTP, 1 μL 20 pmol/μL target gene sense and anti-sense primers, 0.5 μL 12.5 pmol/μL β-actin primer pair, 2 μL RT product, 1.5 *U* Taq DNA polymerase. The sequences of gene primers and amplification conditions are listed in Table 1. The initial denaturation was at 94 ℃ for 5 min. An additional extension step at 72 ℃ for 10 min was done finally. About 10 μL PCR products was separated by electrophoresis on 1.5% agarose gel, and detected by ultraviolet radiography. The densities of bands were analyzed by Bio imaging system, the ratio of target gene density to β-actin density was representative of the relative expression level of mRNA. The semi-quantitative detection was analyzed five times.

Statistical analysis

All data were expressed as mean±SE. The significance for the difference between groups was assessed with SPSS 10.0 by one-way ANOVA. $P<0.05$ was considered statistically significant.

RESULTS

Expression of HBV X mRNA in $HepG_2$ cells

Expressions of HBx mRNA were detected by RT-PCR. The expected band between 400 and 500 bp was found in $HepG_2$/$pcDNA_3$-X cells, but not in $HepG_2$ and $HepG_2$/$pcDNA_3$ cells (Figure 1).

Table 1 Sequences of gene primers and amplification conditions

Target gene	Primer sequences	Amplification conditions	Product (base)
Fas	5'-TCA GTA CGG AGT TGG GGA AG-3' 5'-CAG GCC TTC CAA GTT CTG AG-3'	Denaturation at 94 ℃ for 45 s, annealing at 64 ℃ for 30 s, extension at 72 °C for 1 min , 35 cycles	207 bp
FasL	5'-GAT GAT GGA GGG GAA GAT GA-3' 5'-TGG AAA GAA TCC CAA AGT GC-3'	Denaturation at 94 ℃ for 45 s, annealing at 58 ℃ for 30 s, extension at 72 ℃ for l min, 38 cycles	203 bp
Bax	5'-TTT GCT TCA GGG TTT CAT CC-3' 5'-CAG TTG AAG TTG CCG TCA GA-3'	Denaturation at 94 ℃ for 45 s, annealing at 58 ℃ for 30 s, extension at 72 ℃ for 1 min, 30 cycles	246 bp
Bcl-xL	5'-GGC TGG GAT ACT TTT GTG GA-3' 5'-ATG TGG TGG AGC AGA GAA GG-3'	Denaturation at 94 ℃ for 45 s, annealing at 64 ℃ for 30 s, extension at 72 ℃ for 45 s, 25 cycles	198 bp
c-myc	5'-TTC GGG TAG TGG AAA ACC AG-3' 5'-CAG CAG CTC GAA TTT CTT CC-3'	Denaturation at 94 ℃ for 45 s, annealing at 58 ℃ for 30 s, extension at 72 ℃ for 1 min, 30 cycles	203 bp
β-actin	5'-GGC ATC GTG ATG GAC TCC G-3' 5'-GCT GGA AGG TGG ACA GCG A-3'	Changed according to different target genes	607 bp

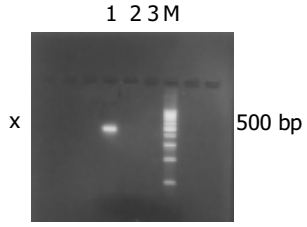

Figure 1 Expression of HBV X mRNA in $HepG_2$ cells. M: 100-bp DNA ladder; lane 1: $HepG_2/pcDNA_3$-X cells; lane 2: $HepG_2/pcDNA_3$ cells; lane 3: $HepG_2$ cells.

Cell viability assay

Cell viability was assessed by MTT. All data are shown in Table 2. A_{492} of $HepG_2/pcDNA_2$-X cells obviously decreased compared to that in other groups ($P<0.05$ and $P<0.01$), indicating that transient expression of HBx impaired the proliferative capacity of $HepG_2$ cells (Figure 2).

Table 2 A_{492} of $HepG_2$, $HepG_2/pcDNA_3$ and $HepG_2/pcDNA_3$-X cells (mean±SE)

Group	*n*	A_{492}
$HepG_2$	10	0.14410±0.004927
$HepG_2/pcDNA_3$	10	0.12150±0.007159
$HepG_2/pcDNA_3$-X	10	0.08910±0.003164

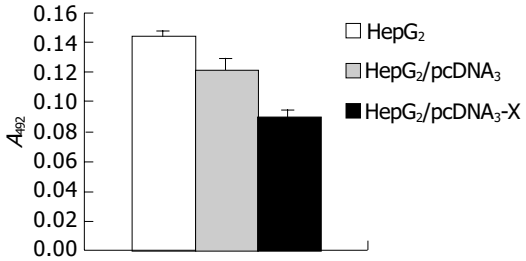

Figure 2 Effect of HBx on cell viability in $HepG_2$ cells.

Cell apoptosis assay

Apoptosis in the three groups was assessed with in-site cell death detecting kit (TUNEL). A total of 2 000 cells of each group were calculated. The number of apoptosis cells was 980 in $HepG_2/pcDNA_3$-X, 520 in $HepG_2/pcDNA_3$ and 420 in $HepG_2$. Cell apoptosis markedly increased in $HepG_2/pcDNA_3$-X (Table 3 and Figure 3), indicating that transient expression of HBx could promote apoptosis of $HepG_2$ cells (Figure 4).

Table 3 Effect of HBx on cell apoptosis of $HepG_2$ cells (mean±SE)

Group	*n*	Apoptosis
$HepG_2$	5	0.2200±0.1000
$HepG_2/pcDNA_3$	5	0.2800±0.1000
$HepG_2/pcDNA_3$-X	5	0.4750±0.015

Effects of HBx transient transfection on apoptosis factors' mRNA expression

Fas/FasL mRNA mRNA level of Fas and FasL was elevated in $HepG_2/pcDNA_3$-X cells (Figures 5A and B, 6A and B), indicating that transient expression of HBx induced expression of Fas and FasL in $HepG_2$ cells.

Bcl-xL/Bax mRNA mRNA level of Bcl-xL and Bax was enhanced in $HepG_2/pcDNA_3$-X cells (Figures 5C and D, 6C and D), indicating that transient expression of HBx induced expression of Bcl-xL or Bax in $HepG_2$ cells.

C-myc mRNA mRNA level of c-myc in $HepG_2/pcDNA_3$-X cells was the highest (Figures 5E and 6E), indicating that transient expression of HBx induced expression of c-myc in $HepG_2$ cells.

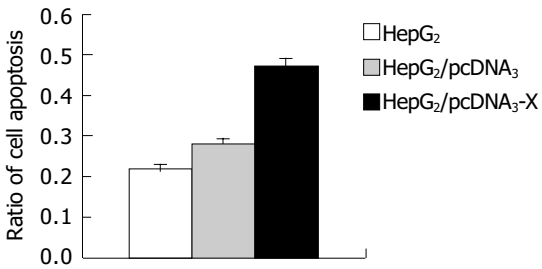

Figure 3 Effect of HBx on apoptosis of $HepG_2$ cells.

DISCUSSION

In previous studies, it was found that HBx inhibits cell apoptosis in different ways. For example, HBx antagonizes TNF-α-induced apoptosis through activating PI3-kinase signaling pathway[2], and inhibits apoptosis in p53-independent manner[3]. There is evidence that HBx activates NF-κB and induce it to translocate into nuclei, NF-κB acts as an inhibitor of cell apoptosis; HBx also downmodulates expression of Bid and blocks Bid-mediated cell apoptosis[4], inactivates caspase-3 through inhibition of CCP32 enzyme, and blocks caspase pathway[5]. It is thought that anti-apoptosis function of HBX is an important mechanism in the development of HCC.

HBx can either inhibit or promote cell apoptosis in a dose-dependent manner. When HBx expresses at high level, it displays pro-apoptosis effect; whereas it inhibits apoptosis when expressing at physiological level. It was reported that moderate expression level of HBx can inhibit liver regeneration in HBx-expressing transgenic mice after partial hepatectomy[6]. HBx stimulates expression of FasL, which plays an important role in cell's escaping from immune surveillance by inducing apoptosis of T cell bearing Fas[7,8]. HBx boosts cell survival by abrogating Bcl-2-mediated cell protection[9,10]. It can also induce expression of myc protein in certain settings, myc sensitizes cells to be killed plus TNF-α[11]. HBx acts through the way that involves DDB2-independent nuclear function of DDB1[12]. Some researchers found that HBx can also localize in mitochondria, bind to voltage-dependent anion channel, which results in alteration of the mitochondrial transmembrane potential, promotes cytochrome *C* and apoptosis-inducing factors to release into cytosol and induces cell apoptosis[13]. In short, HBx has bi-directional function on cell apoptosis regulation. HBx expression levels, availability of survival *vs* apoptogenic factors, and stage of infection may profoundly influence

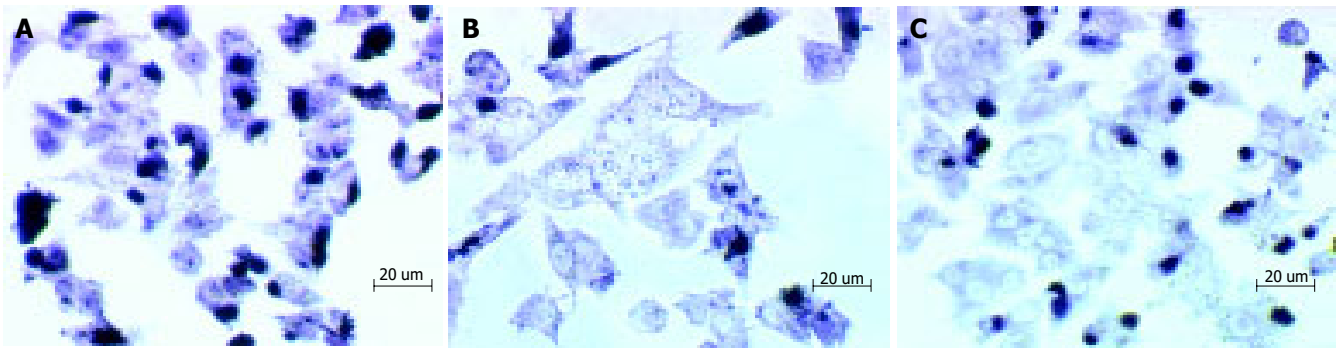

Figure 4 Apoptosis in $HepG_2/pcDNA_3$-X (**A**), $HepG_2/pcDNA_3$ (**B**), and $HepG_2$ (**C**) cells.

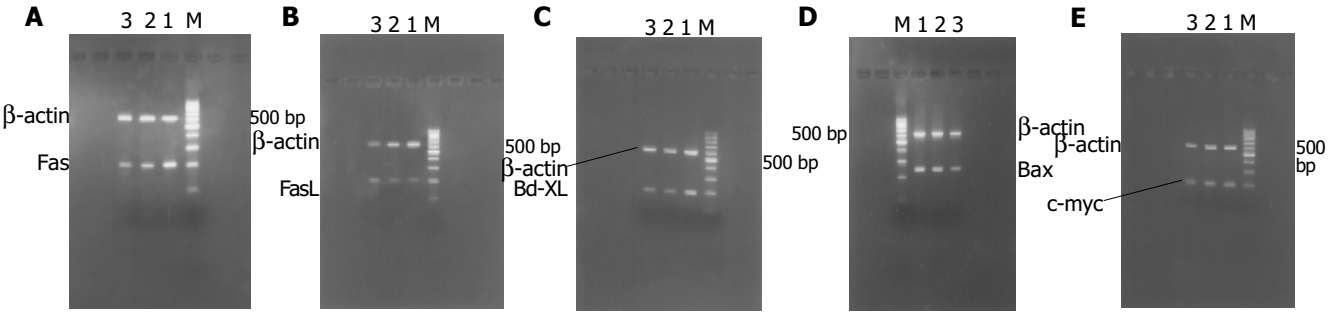

Figure 5 RT-PCR results of mRNA expression of Fas (**A**), FasL (**B**), Bcl-Xl (**C**), Bax (**D**), and c-myc (**E**) in $HepG_2$. M: 100-bp DNA ladder; lane 1: $HepG_2$ cells; lane 2: $HepG_2/pcDNA_3$ cells; lane 3: $HepG_2/pcDNA_3$-X cells.

the fate of cells.

Higher organisms have several mechanisms to eliminate cells by apoptosis. One important role is the signaling pathway mediated by "death factors" including TNFR1, Fas, TNFR2, and their cognate ligand (TNF-α, FasL, and TRAIL) Fas (CD_{95}). The first identified member of "death factors", is a type I glycoprotein which expresses on cell surface. Crosslinking Fas by binding to the ligand FasL leads to conformational changes of Fas, which results in formation of death induced signal complex (DISC) followed by activation of caspase-8. Activated caspase-8 activates itself and other caspases that switch on apoptosis signal cascade[14,15]. It has been found that Fas and FasL express in hepatocytes and hepatoma cells. Since hepatocytes are highly sensitive to Fas/FasL-mediated apoptosis, Fas/FasL pathway plays an essential role in liver lesion and eliminating virus. In our research, HBx elevated expression of Fas and FasL in $HepG_2$ cells. Although the precise mechanism remains unclear, HBx can activate FasL promoter through binding site for Egr and enhance Egr binding to the co-activator cAMP-response element-binding protein, and induce pro-inflammatory cytokines at transcriptional level such as IL-18 which can amplify the expression of FasL[16]. c-FLIP, a key regulator of the DISC, inhibits the Fas/FasL-mediated death pathway in tumors. HBx abrogates the apoptosis-inhibiting function of c-FLIP and renders cells hypersensitive towards the TNF-α apoptotic signal even below the threshold concentration[17,18].

Members of Bcl-2 family are also involved in apoptosis regulation. Members of this family are divided into three subgroups. One group is composed of anti-apoptosis proteins such as Bcl-2, Bcl-xL, with four Bcl-2 homology domains (BH1, BH2, BH3, and BH4). Another group consists of pro-apoptosis proteins such as Bax, Bak, with BH1, BH2, BH3 domains. The last group includes pro-proteins such as Bid, Bik, with only BH3 domain[4,19]. As Bcl-2 family members reside in upstream of irreversible cell damage, they play a pivotal role in deciding whether cells die or live. Indeed, the ratio between pro- and anti-apoptosis molecules determines, in part, the susceptibility of cells to death signal[20]. It was reported recently that the anti-apoptosis members lose their ability to inhibit release of pro-apoptosis factors (such as cytochrome *C*) and trigger apoptosis if they interact with activated pro-apoptosis members[21]. Our data demonstrate that HBx upregulates either pro-apoptosis subset Bax or anti-apoptosis subset Bcl-xL. MTT and TUNEL displayed that apoptosis of $HepG_2$ cells transfected with HBx was enhanced while cell viability was impaired. We postulated that though HBx can upregulate expression of Bax and Bcl-xL, it may promote expression of Bax ever more than Bcl-xL, thus resulting in the predominance of pro-apoptosis protein in the ratio between pro- and anti-apoptosis subsets, then cell apoptosis. On the other hand, interacting with activated Bax, Bcl-xL may lose its anti-apoptosis function and trigger cell death.

C-myc belongs to cell oncogene. HBx accelerates development of primary liver tumors by co-operating with c-myc[22-25]. It was reported that myc can sensitize cells to apoptosis by about two folds in certain conditions such as exposure to TNF-α or other apoptosis factors. In our study, HBx promoted expression of c-myc. Overexpression of c-myc is essential for acute sensitization of cells to be killed

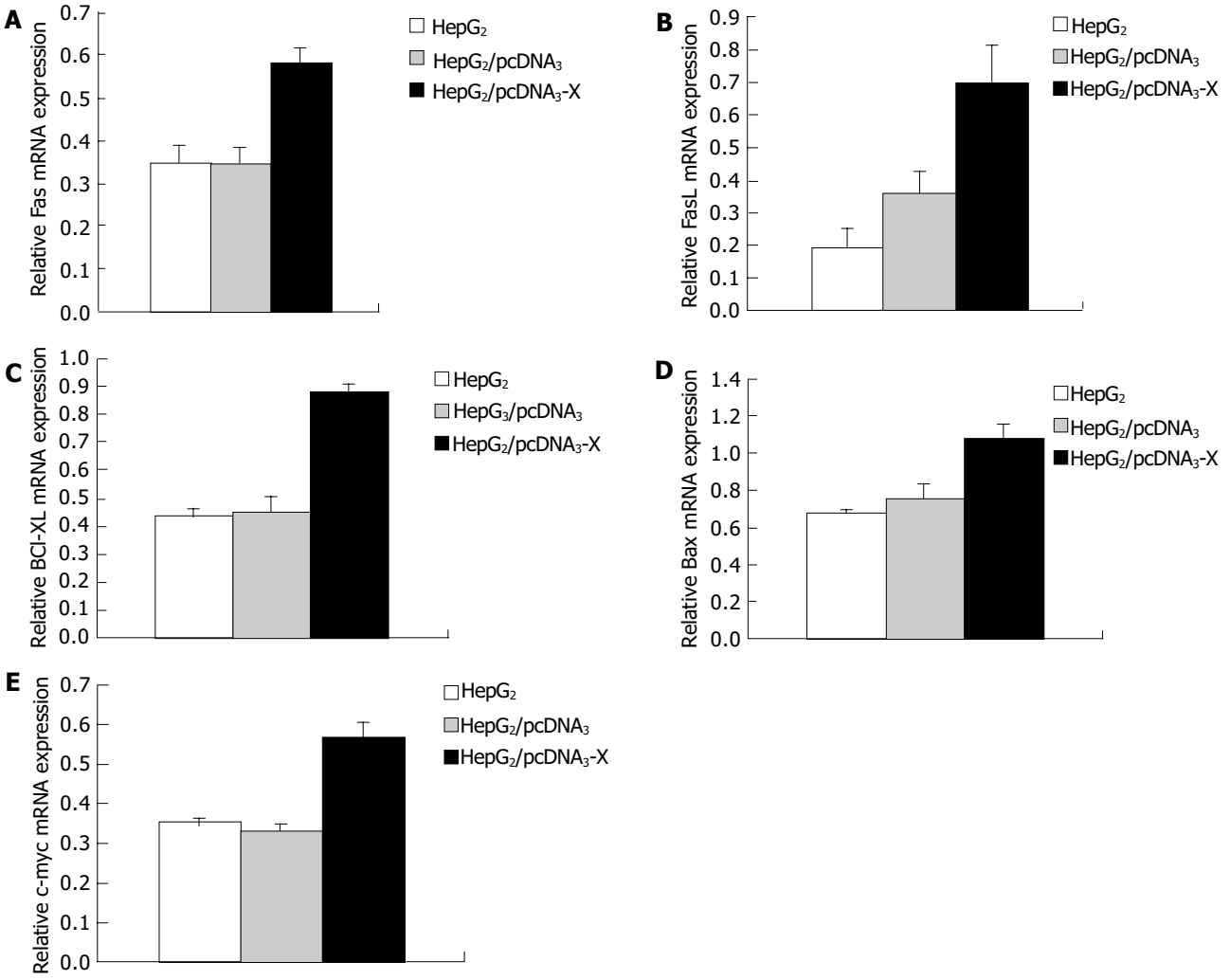

Figure 6 Relative mRNA expression levels of Fas (**A**), FasL (**B**), Bcl-Xl (**C**), Bax (**D**), and c-myc (**E**) in $HepG_2$ cells.

by HBx plus TNF-α[11,26-28], and may enhance cell apoptosis. This result agrees with the data of MTT and TUNEL in our study.

In hepatocarcinogenesis, preneoplastic, and neoplastic cells display an increased ratio of apoptosis as well as enhanced cell proliferation[30]. It is believed that the anti-apoptosis function of HBx is the major determinant factor for development of HCC. The pro-apoptosis function of HBx, however, is also thought to contribute to hepatocarcinogenesis. Firstly, HBx-induced cell apoptosis results in releasing of hepatocyte growth factor that enhances regeneration of liver cells and accumulation of genetic mutation, thus paving the way for cell malignant transformation[29-31]. Secondly, increased apoptosis increase the opportunity of mutation, leading cells to grow out of control and develop to HCC[28,32]. Thirdly, HBx induces expression of FasL in liver cells which can attack T cell bearing Fas and lead to impair of immune defense, which is beneficial for cell bearing HBx to escape from immune detection[33]. Finally, although the accurate mechanism of apoptosis induced by HBx has not been elucidated completely, it may facilitate propagation of viral infection by permitting efficient particle release from cells while minimizing the antiviral inflammation response[14].

Further study should be focused on protein level. Besides, apoptosis mechanic on stably transfected HBx gene in $HepG_2$ cells is another pivot.

REFERENCES

1 **Madden CR,** Slagle BL. Stimulation of cellular proliferation by hepatitis B virus X protein. *Dis Markers* 2001; **17**: 153-157
2 **Shih WL,** Kuo ML, Chuang SE, Cheng AL, Doong SL. Hepatitis B virus X protein inhibits transforming growth factor-beta-induced apoptosis through the activation of phosphatidylinositol 3-Kinase pathway. *J Biol Chem* 2000; **275**: 25858-25864
3 **Shintani Y,** Yotsuyanagi H, Moriya K, Fujie H, Tsutsumi T, Kanegae Y, Kimura S, Saito I, Koike K. Induction of apoptosis after switch-on of the hepatitis B virus X gene mediated by the Cre/*lox*P recombination system. *J Gen Virol* 1999; **80** (Pt 12): 3257-3265
4 **Chen GG,** Lai PB, Chan PK, Chak EC, Yip JH, Ho RL, Leung BC, Lau WY. Decreased expression of Bid in human hepatocellular carcinoma is related to hepatitis B virus X protein. *Eur J Cancer* 2001; **37**: 1695-1702
5 **Gottlob K,** Fuko M, Levrero M, Graessmann A. The hepatitis B virus HBx protein inhibits caspase 3 activity. *J Biol Chem* 1998; **273**: 33347-33353
6 **Guilherme Tralhao J,** Roudier J, Morosan S, Giannini C, Tu H, Goulenok C, Carnot F, Zavala F, Joulin V, Kremsdorf D,

Brechot C. Paracrine *in vivo* inhibitory effects of hepatitis B virus X protein (HBx) on liver cell proliferation: An alternative mechanism of HBx-related pathogenesis. *Proc Natl Acad Sci USA* 2002; **99**: 6991-6996
7 **Yoo YG,** Lee MO. Hepatitis B virus X protein induces expression of fas ligand gene through enhancing transcriptional activity of early growth response factor. *J Biol Chem* 2004; **279**: 36242-36249
8 **Shin EC,** Shin JS, Park JH, Kim H, Kim SJ. Expression of fas ligand in human hepatoma cell lines: role of hepatitis-B virus X (HBX) in induction of Fas ligand. *Int J Cancer* 1999; **82**: 587-591
9 **Schuster R,** Gerlich WH, Schaefer S. Induction of apoptosis by the transactivating domains of the hepatitis B virus X gene leads to suppression of oncogenic transformation of primary rat embryo fibroblasts. *Oncogene* 2000; **19**: 1173-1180
10 **Terradillos O,** de La Coste A, Pollicino T, Neuveut C, Sitterlin D, Lecoeur H, Gougeon ML, Kahn A, Buendia MA. The hepatitis B virus X protein abrogates Bcl-2-mediated protection against Fas apoptosis in the liver. *Oncogene* 2002; **21**: 377-386
11 **Su F,** Theodosis CN, Schneider RJ. Role of NF-kappaB and myc proteins in apoptosis induced by hepatitis B virus HBx protein. *J Virol* 2001; **75**: 215-225
12 **Bontron S,** Lin-Marq N, Strubin M. Hepatitis B virus X protein associated with UV-DDB1 induces cell death in the nucleus and is functionally antagonized by UV-DDB2. *J Biol Chem* 2002; **277**: 38847-38854
13 **Waris G,** Huh KW, Siddiqui A. Mitochondrially associated hepatitis B virus X protein constitutively activates transcription factors STAT-3 and NF-kappa B via oxidative stress. *Mol Cell Biol* 2001; **21**: 7721-7730
14 **Nagata S.** Apoptosis by death factor. *Cell* 1997; **88**: 355-365
15 **Chang YC,** Xu YH. Expression of Bcl-2 inhibited Fas-mediated apoptosis in human hepatocellular carcinoma BEL-7404 cells. *Cell Res* 2000; **10**: 233-242
16 **Lee MO,** Choi YH, Shin EC, Kang HJ, Kim YM, Jeong SY, Seong JK, Yu DY, Cho H, Park JH, Kim SJ. Hepatitis B virus X protein induced expression of interleukin 18 (IL-18): a potential mechanism for liver injury caused by hepatitis B virus (HBV) infection. *J Hepatol* 2002; **37**: 380-386
17 **Korkolopoulou P,** Goudopoulou A, Voutsinas G, Thomas-Tsagli E, Kapralos P, Patsouris E, Saetta AA. c-FLIP expression in bladder urothelial carcinomas: its role in resistance to Fas-mediated apoptosis and clinicopathologic correlations. *Urology* 2004; **63**: 1198-1204
18 **Kim KH,** Seong BL. Pro-apoptotic function of HBV X protein is mediated by interaction with c-FLIP and enhancement of death-inducing signal. *EMBO J* 2003; **22**: 2104-2116
19 **Reed JC.** Bcl-2 family proteins. *Oncogene* 1998; **17**: 3225-3236
20 **Gross A,** McDonnell JM, Korsmeyer SJ. BCL-2 family members and the mitochondria in apoptosis. *Genes Dev* 1999; **13**: 1899-1911
21 **Fu YF,** Fan TJ. Bcl-2 family proteins and apoptosis. *Shengwu Huaxue Yu Shengwu Wuli Xuebao* 2002; **34**: 389-394
22 **Lakhtakia R,** Kumar V, Reddi H, Mathur M, Dattagupta S, Panda SK. Hepatocellular carcinoma in a hepatitis B 'x' transgenic mouse model: A sequential pathological evaluation. *J Gastroenterol Hepatol* 2003; **18**: 80-91
23 **Terradillos O,** Pollicino T, Lecoeur H, Tripodi M, Gougeon ML, Tiollais P, Buendia MA. p53-independent apoptotic effects of the hepatitis B virus HBx protein *in vivo* and *in vitro*. *Oncogene* 1998; **17**: 2115-2123
24 **Hung L,** Kumar V. Specific inhibition of gene expression and transactivation functions of hepatitis B virus X protein and c-myc by small interfering RNAs. *FEBS Lett* 2004; **560**: 210-214
25 **Rabe C,** Cheng B, Caselmann WH. Molecular mechanisms of hepatitis B virus-associated liver cancer. *Dig Dis* 2001; **19**: 279-287
26 **Klefstrom J,** Arighi E, Littlewood T, Jaattela M, Saksela E, Evan GI, Alitalo K. Induction of TNF-sensitive cellular phenotype by c-Myc involves p53 and impaired NF-kappaB activation. *EMBO J* 1997; **16**: 7382-7392
27 **Foo SY,** Nolan GP. NF-kappa B to the rescue: RELs, apoptosis and cellular transformation. *Trends Genet* 1999; **15**: 229-235
28 **Su F,** Schneider RJ. Hepatitis B virus HBx protein sensitizes cells to apoptotic killing by TNF-α. *Proc Natl Acad Sci USA* 1997; **94**: 8744-8749
29 **Kim H,** Lee H, Yun Y. X-gene Product of hepatits B virus induces apoptosis in liver cells. *J Biol Chem* 1998; **273**: 381-385
30 **Jin YM,** Yun C, Park C, Wang HJ, Cho H. Expression of hepatitis B Virus X protein is closely correlated with the high periportal inflammatory activity of liver diseases. *J Viral Hepatitis* 2001; **8**: 322-330
31 **Pollicino T,** Terradillos O, Lecoeur H, Gougeon ML, Buendia MA. Pro-apoptotic effect of the hepatitis B virus X gene. *Biomed Pharmacother* 1998; **52**: 363-368
32 **Sirma H,** Giannini C, Poussin K, Paterlini P, Kremsdorf D, Brechot C. Hepatitis B virus X mutants, present in hepatocellular carcinoma tissue abrogate both the antiproliferative and transactivation effects of HBx. *Oncogene* 1999; **18**: 4848-4859
33 **Milich DR.** Influence of T-helper cell subsets and cross-regulation in hepatitis B virus infection. *J Viral Hepatol* 1997; **4**: 48-59

Science Editor Wang XL and Guo SY **Language Editor** Elsevier HK

PO Box 2345, Beijing 100023, China
www.wjgnet.com
wjg@wjgnet.com

ELSEVIER

World J Gastroenterol 2005;11(28):4332-4336
World Journal of Gastroenterology ISSN 1007-9327

• *COLORECTAL CANCER* •

Treatment of metastatic colorectal carcinomas by systemic inhibition of vascular endothelial growth factor signaling in mice

Volker Schmitz, Miroslaw Kornek, Tobias Hilbert, Christian Dzienisowicz, Esther Raskopf, Christian Rabe, Tilman Sauerbruch, Cheng Qian, Wolfgang H Caselmann

Volker Schmitz, Miroslaw Kornek, Tobias Hilbert, Christian Dzienisowicz, Esther Raskopf, Christian Rabe, Tilman Sauerbruch, Medizinische Klinik und Poliklinik I, Universitätsklinikum Bonn, Germany
Cheng Qian, Universidad de Navarra, Clínica Universitaria, Pamplona, Spain
Wolfgang H Caselmann, Bavarian State Ministry of the Environment, Public Health and Consumer Protection, Munich 81901, Germany
Supported by the Deutsche Krebshilfe, No. 70-3065-SchmI
Correspondence to: Dr. Volker Schmitz, Medizinische Klinik I, Sigmund-Freud-Str. 25, Bonn 53105, Germany. volker.schmitz@ukb.uni-bonn.de
Telephone: +49-228-2876469 Fax: +49-228-2874698
Received: 2004-07-31 Accepted: 2004-11-04

Abstract

AIM: Tumor angiogenesis has been shown to be promoted by vascular endothelial growth factor (VEGF) via stimulating endothelial cell proliferation, migration, and survival. Blockade of VEGF signaling by different means has been demonstrated to result in reduced tumor growth and suppression of tumor angiogenesis in distinct tumor entities. Here, we tested a recombinant adenovirus, AdsFlt1-3, that encodes an antagonistically acting fragment of the VEGF receptor 1 (Flt-1), for systemic antitumor effects in pre-established subcutaneous CRC tumors in mice.

METHODS: Murine colorectal carcinoma cells (CT26) were inoculated subcutaneously into Balb/c mice for *in vivo* studies. Tumor size and survival were determined. 293 cell line was used for propagation of the adenoviral vectors. Human lung cancer line A_{549} and human umbilical vein endothelial cells were transfected for *in vitro* experiments.

RESULTS: Infection of tumor cells with AdsFlt1-3 resulted in protein secretion into cell supernatant, demonstrating correct vector function. As expected, the secreted sFlt1-3 protein had no direct effect on CT26 tumor cell proliferation *in vitro*, but endothelial cell function was inhibited by about 46% as compared to the AdLacZ control in a tube formation assay. When AdsFlt1-3 (5×10^9 PFU/animal) was applied to tumor bearing mice, we found a tumor inhibition by 72% at d 12 after treatment initiation. In spite of these antitumoral effects, the survival time was not improved. According to reduced intratumoral microvessel density in AdsFlt1-3-treated mice, the antitumor mechanism can be attributed to angiostatic vector effects. We did not detect increased systemic VEGF levels after AdsFlt1-3 treatment and liver toxicity was low as judged by serum alanine aminotransferase determination.

CONCLUSION: In this study we confirmed the value of a systemic administration of AdsFlt1-3 to block VEGF signaling as antitumor therapy in an experimental metastatic colorectal carcinoma model in mice.

Key words: Colorectal carcinomas; Vascular endothelial growth factor; Systemic inhibition

Schmitz V, Kornek M, Hilbert T, Dzienisowicz C, Raskopf E, Rabe C, Sauerbruch T, Qian C, Caselmann WH. Treatment of metastatic colorectal carcinomas by systemic inhibition of vascular endothelial growth factor signaling in mice. *World J Gastroenterol* 2005; 11(28): 4332-4336
http://www.wjgnet.com/1007-9327/11/4332.asp

INTRODUCTION

Colorectal carcinoma (CRC) is one of the most common malignant diseases in the Western countries. Even after successful resection of the primary tumor, about one-third of the patients develop tumor recurrence. The most common place of distant CRC metastases are liver and lung[1]. In particular, metastatic CRC disease is associated with limited life expectancy and progressive tumor disease in CRC is associated with increased VEGF levels[2]. Considering clinical studies successfully employing tyrosine kinase inhibitors for systemic tumor therapy[3] and experimental studies showing the antitumor efficacy of VEGF-antagonism in a pancreatic adenocarcinoma animal model[4] and follicular thyroid carcinoma animal model[5], including successful local treatment of subcutaneous CRC[6], we evaluated and confirmed the antitumoral efficacy and mechanism of a systemic gene delivery of a Flt-1 fragment (sFlt1-3) in subcutaneous metastatic CRC in mice.

Vascular endothelial growth factor (VEGF) expression correlates with tumor vascularization in most tumor types, also in CRC[2,7,8]. VEGF binds with different affinity to its cell surface receptors, VEGF receptor 1 (Flt-1), VEGF receptor 2 (Flk-1) and VEGF receptor 3 (Flt-4). All three VEGF receptors are members of the class III receptor-type tyrosine kinase receptor family[9]. Several findings suggest that binding of VEGF to Flt-1 regulates angiogenesis by controlling inter-cellular endothelial interactions[10].

Since angiostatic therapies do not attack the malignant tumor cell itself, but address tumor vascularization, a systemic

treatment is of particular interest. Therefore, we investigated the effect of interruption of the VEGF cascade by systemic gene delivery on pre-established tumors.

MATERIALS AND METHODS

Animals, cell lines and culture conditions

Balb/c mice, 6 wk old, were purchased from Charles River (Sulzfeld, Germany) and kept in the local central animal facility. The mice were housed under standard conditions and had free access to water and food. Animal procedures were performed in accordance to approved protocols and followed recommendations for proper care and use of laboratory animals.

For propagation of adenoviral vectors, 293 cells (embryonic E1 transformed kidney cell line) were obtained from American Type Culture Collection (ATCC, Manassas, VA, USA) Cells were maintained in Dulbecco's modified Eagle medium (DMEM) with 10% heat-inactivated fetal bovine serum (FBS).

To demonstrate vector function and gene expression standard techniques using the human lung cancer cell line A_{549} (ATCC, Manassas, VA, USA) were employed for *in vitro* transfection experiments. Cells were cultured in DMEM supplemented with 10% heat-inactivated FBS. Human umbilical vein endothelial (HUVE) cells were obtained from Cascade Biologics (Portland, OR, USA) and were cultured according to the supplier's instructions.

Murine CRC CT26 cells have originally been described by Brattain[11]. Cells were cultured in DMEM supplemented with 10% heat-inactivated FCS and 1% penicillin/streptomycin.

Construction of recombinant adenoviruses encoding a soluble form of Flt1-3 and vector propagation

The recombinant adenoviruses encoding the LacZ-gene was constructed as described previously[12]. The AdsFlt1-3 construct was generously provided by R. Mulligan, Boston, MA, USA, it consists of the extracellular immunoglobulin-like domains 1-3 of the VEGF-receptor 1 (Flt-1) and has a His-tag; its construction has been described elsewhere[13]. Recombinant adenoviruses were expanded, and purified by double cesium-chloride ultra-centrifugation. Purified viruses were dialyzed against 10 mmol/L Tris/1 mmol/L $MgCl_2$ and stored in glycerol aliquots at -80 ℃. Virus concentrations were determined by measuring virus particles (opu/mL) and by cytotoxic plaque assay (pfu/mL) in 293 cells. Virus productions were tested for wild-type adenovirus contamination by cytotoxic plaque assay in A_{549} cells.

Analysis of protein expression in vitro

A_{549} tumor cells were transfected with 250 multiplicity of infection (MOI) of AdLacZ or AdsFlt1-3. Forty-eight hours later, cells and culture medium (CM) were harvested. RNA was isolated from the using the GenElute Total Mammalian RNA Kit (Sigma, Taufkirchen, Germany) according to the manufacturer's protocol. RNA was then digested with RQ1 DNase (Promega, Mannheim, Germany). RNA concentrations were determined and 1 μg RNA was used in the RT reaction with random primers (Promega, Mannheim, Germany) and MMLV reverse transcriptase (Promega, Mannheim, Germany). PCR for sFlt1-3 was performed with the forward primer 5'-CGTTCCAGTCTTTCAACACC-3' and reverse primer 5'-CCAAGGAAACGTGAAAGC-3'. As positive control, primers for human β-actin were used. The size of the amplified product was about 250 bp. Analysis of the PCR products occurred by electrophoresis on a 1% agarose gel.

For detection of sFlt1-3 100 μL of the harvested CM was dispensed in a 96-well ELISA plate and incubated at 4 ℃ overnight. After washing thrice with PBS, the ELISA plate was incubated for 2 h with anti mouse VEGF-R1 (Flt-1) antibody (1∶200, R&D Systems, Wiesbaden-Nordenstadt, Germany). After antibody incubation, the plate was washed with PBS and incubated with secondary antibody (1∶25 000, monoclonal anti-sheep/goat peroxidase conjugate, Sigma, St. Louis, MO, USA) 2 h. After washing with PBS the plate was incubated for 15 min with TMB substrate (Biozol, Eching, Germany). Color intensity was measured in an ELISA reader (Dynatech Laboratories, Frankfurt, Germany).

BrdU proliferation assay

Five thousand CT26 cells were resuspended in 40 μL of culture medium and dispensed in each well of a 96-culture plate and pre-incubated with 50 μL of CM. After 30 min of pre-incubation time, 150 μL of RPMI 1640 containing 10% FCS was added. Cell culture was continued for 18 h and then cells were labeled with BrdU for further 24 h. The BrdU assay was performed according to the manufacturer's protocol (BrdU proliferation assay, Roche Diagnostics, Mannheim, Germany).

In vitro testing of antiangiogenic effects (tube formation assay)

A 24-well plate was coated with 300 μL Matrigel (BD Biosciences, Bedford, MA, USA). Twenty-four hours later, HUVE cells (passage number <10) in 75 μL Medium200 (2.5×10^4 cells) were seeded on the Matrigel and pre-incubated for 30 min with 75 μL of CM (derived from Huh7 cells). One hundred and fifty microliters of Medium200 was added and the cells were additionally incubated for 4-6 h. Tube-like formations were counted under the light microscope in high power fields.

Tumor induction

In vivo antitumoral efficacies were studied in a subcutaneous CRC mouse model in C3H mice. 10^6 CT26 cells were resuspended in 100 μL FCS-free culture medium and injected subcutaneously via a 28-G syringe.

In vivo antitumor treatment

When reaching a tumor volume of 40 mm^3, tumor treatment was initiated by intravenous injection of 5×10^9 pfu/animal AdLacZ (n = 11) and AdsFlt1-3 (n = 10) in 150 μL NaCl. Tumor volumes were calculated by the formula: v = length $\times$width$^2\times0.52$. From a subgroup of animals treated intravenously with AdLacZ (n = 2), or AdsFlt1-3 (n = 3) serum and tumor samples were taken at different time points (at d 3, 6, 9, 14, 19, and 25) for VEGF-ELISA and histology, respectively.

Immunohistochemistry

Tumor samples were embedded in tissue tech (DAKO), snap

frozen in liquid nitrogen and stored at -80 ℃ for anti-von Willebrand staining. Five millimeters of cryostat sections were gently warmed up at RT. Then fixed in acetone for 10 min and dried on air. Sections were stained with dilution of primary antibody (polyclonal rabbit antihuman von Willebrand factor, 1∶1 600). After washing with PBS, sections were incubated with secondary antibody dilution of biotinylated pig antirabbit immunoglobulin G (1∶300) and streptavidin conjugated to horseradish peroxidase (DAKO). Sections were visualized by using the Dako ChemMate™ detection kit and counterstained with hematoxylin (DAKO).

Statistical analysis

All measured data are given with mean±SE. Differences between values of different experimental groups were analyzed for statistical significance by a non-parametric, two-tailed test (Mann-Whitney test) for unpaired samples and in case of histology by unpaired Student's *t*-test. Survival rates are presented as Kaplan-Maier curves. An error level $P < 0.05$ was supposed to indicate significance.

RESULTS

Propagation of adenoviral vectors

Wild-type contamination of the adenoviral stock solutions was analyzed in A_{549} cells in a cytotoxic plaque assay. Virus concentrations were determined as optical particle units and ranged from 2.13×10^{12} opu/mL for AdLacZ to 7.04×10^{12} opu/mL for AdsFlt1-3, respectively. Virus titration in 293 cell plaque assays showed corresponding concentrations of 8.0×10^{12} pfu/mL for AdLacZ and 1.027×10^{12} pfu/mL for AdsFlt1-3.

Protein expression and secretion of sFlt1-3

CM of infected A_{549} cells was harvested to demonstrate sFlt1-3 gene expression and protein secretion into cell supernatant. The analysis of the RT-PCR showed similar bands for β-actin (500 bp) in all samples and only AdsFlt1-3 infected cells showed an extra band at about 250 bp representing the encoded transgene sFlt1-3 (Figure 1). Protein expression was confirmed by ELISA in AdsFlt1-3 infected cells (106 ng/mL). This data demonstrate correct vector function and protein secretion.

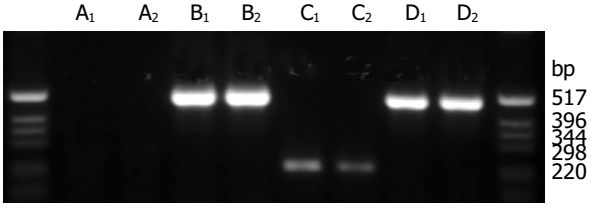

Figure 1 Gene expression of sFlt1-3 *in vitro*. RT-PCR was performed with A_{549} cells infected with AdsFlt1-3 or AdlacZ. Specific primer pairs for sFlt1-3 resulted in bands of about 250 bp (C_1 and C_2), whereas no bands were detectable in the negative control AdLacZ (A_1 and A_2). Expression of the house keeping gene β-actin (514 bp) was similar for AdLacZ (B_1 and B_2) and AdsFlt1-3 (D_1 and D_2).

BrdU proliferation assay

To check for direct effects of sFlt1-3 on CRC tumor cells, conditioned CM was tested for antitumor effects on CT26 tumor cells. As expected, we did not observe any direct anti-proliferative effects (data not shown). We concluded that potential antitumor effects were mediated by indirect (angiostatic) mechanism and not by cytotoxic effects.

In vitro testing of antiangiogenic effects (tube formation assay)

The tube formation assay tests the capability of HUVE cells to form tube-like structures comprising endothelial cell function like migration and tube formation. The results showed that sFlt1-3 inhibited these cell functions by about 46% (Figure 2) compared to the AdlacZ control. This indicates biological activity of sFlt1-3 *in vitro*.

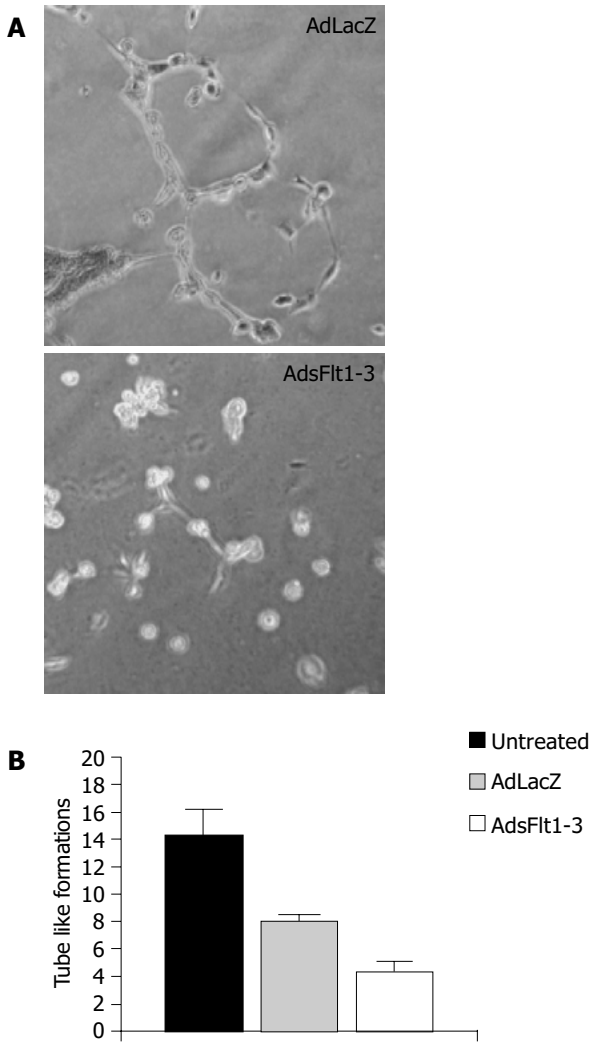

Figure 2 Tube formation assay *in vitro*. HUVE cells were incubated on Matrigel with CM from AdsFlt1-3- or AdLacZ-infected tumor cells. **A:** Exemplary light microscope image (40× magnifications) of HUVE cells incubated with CM of AdLacZ-infected cells and with CM of AdsFlt1-3-infected cells; **B:** So called tube-like formations were quantified per high power field. Data are shown as mean and SE ($P = 0.10$ compared to the control).

Systemic treatment

Since CT26 tumor cells express and secrete VEGF (68 pg/mL) into cell supernatant, the CT26 tumor model is suitable to study antitumor effects of an anti-VEGF therapy. The systemic injection of 5×10^9 pfu/mL AdsFlt1-3 significantly

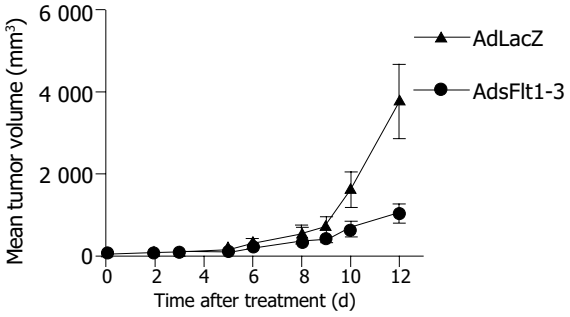

Figure 3 Tumor treatment of pre-established CT-26 CRC. Vectors were administered systemically (5×10^9 pfu, AdsFlt1-3, n = 10; AdLacZ, n = 11). Data are given as mean tumor volume and SE (P = 0.006 compared to the control).

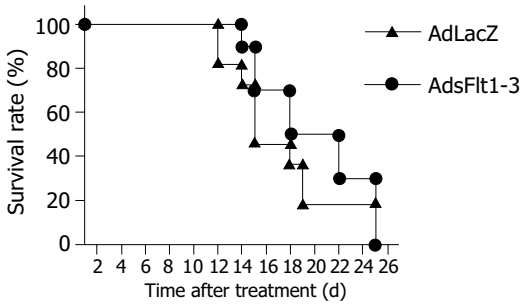

Figure 4 No effect of AdLacZ and AdsFlt1-3 on the survival rate of tumor bearing mice. Tumor treatment of pre-established CT-26 CRC. Vectors were administered systemically (5×10^9 pfu, AdsFlt1-3, n = 10; AdLacZ, n = 11).

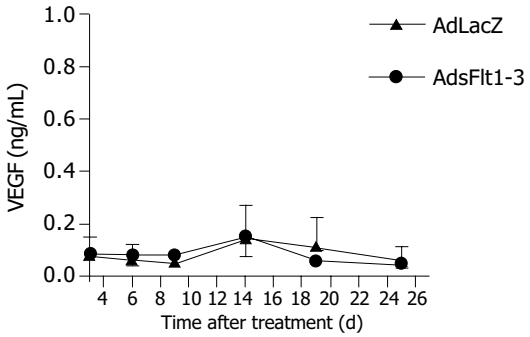

Figure 5 Time course of *in vivo* VEGF serum levels of tumor bearing mice that had been treated with AdLacZ or AdsFlt1-3 (mean±SE).

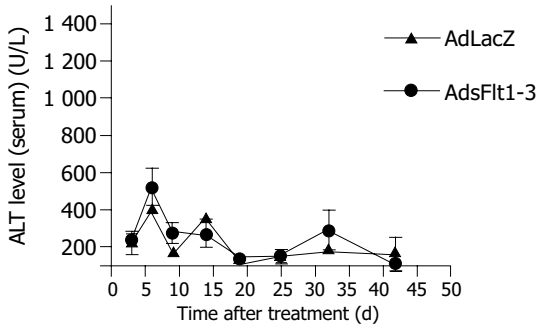

Figure 6 Time course of ALT serum levels as marker of liver toxicity at d 3, 6, 9, 14, 19, 25, 32, and 42 after AdLacZ and AdsFlt1-3 treatment initiation (mean±SE).

reduced tumor growth by 72% compared to the AdLacZ control 12 d after treatment initiation (Figure 3), but did not improve the survival rate (Figure 4). VEGF serum levels were similar in both groups, AdLacZ and AdsFlt1-3, (Figure 5) and we did not observe any compensatory upregulation of VEGF levels in serum. Liver toxicity was tolerable according to alanine aminotransferase levels in serum (Figure 6).

Inhibition of tumor angiogenesis by AdsFlt1-3 in vivo

Intratumoral microvessels density was determined by immunohistochemistry for von Willebrand factor. Tumors were removed 9 d after treatment and as shown in Figure 7, tumors of animals that had received AdLacZ showed intense staining for von Willebrand factor, indicating effective tumor vascularization, and tumor sections of AdsFlt1-3-treated animals showed a marked reduction by 42% in microvessel density (Figure 7).

DISCUSSION

VEGF has been acknowledged as one of the most important pro-angiogenic factors that are known to be involved in

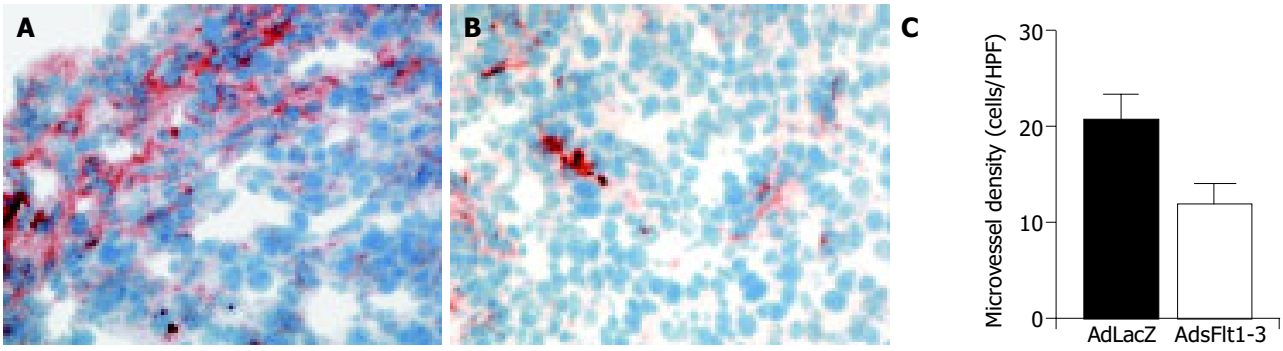

Figure 7 Effective inhibition of tumor angiogenesis *in vivo* by treatment with AdsFlt1-3. Pre-established CRC tumors were treated with AdLacZ or AdsFlt1-3. Animals were killed on d 9 after treatment and tumor tissue was removed. Microvessel density was determined by anti-von Willebrand factor staining. **A** and **B:** Representative photomicrographs show microvessel staining in tumors of AdLacZ- or AdsFlt1-3-treated mice; **C:** quantitative analysis of microvessel density was made by counting the positively stained cells per high-power fields (200× magnification). Data are given as mean of cell number/HPF and SE (P = 0.02 compared to the control).

tumor angiogenesis[7,14-16]. In particular, VEGF expression has been shown to be elevated in metastatic CRC disease[2]. In the case of metastatic CRC, therapeutic options are still limited and innovative approaches are warranted. Therefore, we intended to confirm the antitumor efficacy of blocking VEGF signaling by systemic administration of an adenovirus delivering the VEGF receptor 1 fragment sFlt1-3 in a subcutaneous metastatic murine CRC tumor model. Our data show that the systemic vector application of AdsFlt1-3 induced significant antitumor effects in CRC.

Recently, several angiostatic antitumor approaches have been used to inhibit experimental CRC. In a previous publication, we were able to show that the local gene delivery of angiostatin-like molecule (K1-3) inhibited tumor growth in the same CRC model by 41% at d 8 after treatment initiation. Another group had used a similar approach employing an adenoviral construct encoding a distinct Flt-1 fragment to treat subcutaneous tumors, but then only the local treatment was effective[6]. But principally, angiostatic antitumor strategies do not intend to directly control growth of the malignant tumor cell but rather to curb tumor vascularization. Therefore, systemic gene delivery of angiostatic proteins might even be more effective than local applications. The vector construct we used in this study had been shown to inhibit e.g. tumor growth of fibrosarcoma and lung cancer in experimental studies after systemic vector administration[13]. Here, we were able to confirm the antitumoral efficacy of the AdsFlt1-3 construct in a metastatic subcutaneous CRC model. But, according to other angiostatic gene therapy studies and own findings, the survival rate was not improved.

Since we could not observe any direct antiproliferative effects of sFlt1-3 on CT26 CRC cells, antitumoral effects most probably were mediated by indirect angiostatic effects. This was supported by immune staining for von Willebrand factor revealing decreased microvessel density in the AdsFlt1-3 treatment group. Taken together, these results correspond well to other publications reporting anti-angiogenic effects of similar constructs in corneal or ocular neovascularization assays[13].

Recently, potential side effects of adenoviruses have provoked severe concerns of systemic vector applications regarding particularly liver toxicity. Indeed, we observed some ALT elevations, but at the dosage applied toxicity was well tolerated.

In summary our data demonstrate that the systemic gene transfer of sFlt1-3 induced significant antitumor effects on pre-established subcutaneous metastatic CRC and antitumor mechanism based on angiostatic effects. Thus, these data further confirmed the value of blocking VEGF signaling as an effective approach to treat CRC disease.

ACKNOWLEDGMENTS

AdsFlt1-3 construct was generously provided by R. Mulligan, Boston, MA, USA. We thank I. Höschler for her expert assistance.

REFERENCES

1 **Ohlsson B,** Palsson B. Follow-up after colorectal cancer surgery. *Acta Oncol* 2003; **42**: 816-826
2 **Hanrahan V,** Currie MJ, Gunningham SP, Morrin HR, Scott PA, Robinson BA, Fox SB. The angiogenic switch for vascular endothelial growth factor (VEGF)-A, VEGF-B, VEGF-C, and VEGF-D in the adenoma-carcinoma sequence during colorectal cancer progression. *J Pathol* 2003; **200**: 183-194
3 **Fernando NH,** Hurwitz HI. Inhibition of vascular endothelial growth factor in the treatment of colorectal cancer. *Semin Oncol* 2003; **30** (3 Suppl 6): 39-50
4 **Tseng JF,** Mulligan RC. Gene therapy for pancreatic cancer. *Surg Oncol Clin N Am* 2002; **11**: 537-569
5 **Ye C,** Feng C, Wang S, Wang KZ, Huang N, Liu X, Lin Y, Li M. sFlt-1 gene therapy of follicular thyroid carcinoma. *Endocrinology* 2004; **145**: 817-822
6 **Kong HL,** Hecht D, Song W, Kovesdi I, Hackett NR, Yayon A, Crystal RG. Regional suppression of tumor growth by *in vivo* transfer of a cDNA encoding a secreted form of the extracellular domain of the flt-1 vascular endothelial growth factor receptor. *Hum Gene Ther* 1998; **9**: 823-833
7 **Robinson CJ,** Stringer SE. The splice variants of vascular endothelial growth factor (VEGF) and their receptors. *J Cell Sci* 2001; **114**: 853-865
8 **Fong GH,** Rossant J, Gertsenstein M, Breitman ML. Role of the Flt-1 receptor tyrosine kinase in regulating the assembly of vascular endothelium. *Nature* 1995; **376**: 66-70
9 **Brattain MG,** Strobel-Stevens J, Fine D, Webb M, Sarrif AM. Establishment of mouse colonic carcinoma cell lines with different metastatic properties. *Cancer Res* 1980; **40**: 2142-2146
10 **Qian C,** Bilbao R, Bruna O, Prieto J. Induction of sensitivity to ganciclovir in human hepatocellular carcinoma cells by adenovirus-mediated gene transfer of herpes simplex virus thymidine kinase. *Hepatology* 1995; **22**: 118-123
11 **Kuo CJ,** Farnebo F, Yu EY, Christofferson R, Swearingen RA, Carter R, von Recum HA, Yuan J, Kamihara J, Flynn E, D'Amato R, Folkman J, Mulligan RC. Comparative evaluation of the antitumor activity of antiangiogenic proteins delivered by gene transfer. *Proc Natl Acad Sci USA* 2001; **98**: 4605-4610
12 **Kim KJ,** Li B, Winer J, Armanini M, Gillett N, Phillips HS, Ferrara N. Inhibition of vascular endothelial growth factor-induced angiogenesis suppresses tumour growth *in vivo*. *Nature* 1993; **362**: 841-844
13 **Shibuya M.** Role of VEGF-flt receptor system in normal and tumor angiogenesis. *Adv Cancer Res* 1995; **67**: 281-316
14 **Ferrara N,** Houck K, Jakeman L, Leung DW. Molecular and biological properties of the vascular endothelial growth factor family of proteins. *Endocr Rev* 1992; **13**: 18-32
15 **Schmitz V,** Wang L, Barajas M, Gomar C, Prieto J, Qian C. Treatment of colorectal and hepatocellular carcinomas by adenoviral mediated gene transfer of endostatin and angiostatin-like molecule in mice. *Gut* 2004; **53**: 561-567
16 **Gehlbach P,** Demetriades AM, Yamamoto S, Deering T, Xiao WH, Duh EJ, Yang HS, Lai H, Kovesdi I, Carrion M, Wei L, Campochiaro PA. Periocular gene transfer of sFlt-1 suppresses ocular neovascularization and vascular endothelial growth factor-induced breakdown of the blood-retinal barrier. *Hum Gene Ther* 2003; **14**: 129-141

Science Editor Zhu LH **Language Editor** Elsevier HK

PO Box 2345, Beijing 100023, China
www.wjgnet.com
wjg@wjgnet.com

ELSEVIER

World J Gastroenterol 2005;11(28):4337-4343
World Journal of Gastroenterology ISSN 1007-9327

Effect of NS398 on metastasis-associated gene expression in a human colon cancer cell line

Xue-Qin Gao, Jin-Xiang Han, Hai-Yan Huang, Bao Song, Bo Zhu, Chang-Zheng Song

Xue-Qin Gao, Jin-Xiang Han, Hai-Yan Huang, Bao Song, Bo Zhu, Chang-Zheng Song, Key Laboratory of Ministry of Public Health for Biotech-Drug, Shandong Medicinal and Biotechnology Center, Shandong Academy of Medical Sciences, Jinan 250062, Shandong Province, China
Xue-Qin Gao, Jin-Xiang Han, Shandong University School of Medicine, Jinan 250062, Shandong Province, China
Supported by the Key Technology Research and Development Program of Shandong Province, No. 011100105
Correspondence to: Professor Jin-Xiang Han, Shandong Medicinal and Biological Center, Shandong Academy of Medical Sciences, 89 Jingshi Road, Jinan 250062, Shandong Province, China. han9888@sina.com
Telephone: +86-531-82919888 Fax: +86-531-82951586
Received: 2004-09-08 Accepted: 2004-12-03

Abstract

AIM: To investigate the effect of NS398 on the metastasis-associated gene expression in LoVo colorectal cancer cells.

METHODS: LoVo cells were treated with NS398 at the concentration of 100 μmol/L for 24 and 48 h respectively. Total RNA was extracted with TRIzol reagents and reverse transcribed with Superscript II and hybridized with cDNA microarray (containing oncogenes, tumor suppressor genes, signal transduction molecules, adhesive molecules, growth factors, and ESTs) fabricated in our laboratory. After normalization, the ratio of gene expression of NS398 treated to untreated LoVo cells was either 2-fold up or 0.5-fold down was defined as the differentially expressed genes. Semi-quantitative RT-PCR was used to validate the microarray results.

RESULTS: Among the 447 metastasis-associated genes, 9 genes were upregulated and 8 genes were downregulated in LoVo cells treated with NS398 for 24 h compared to untreated cells. While 31 genes were upregulated and 14 genes were downregulated in LoVo cells treated with NS398 for 48 h. IGFBP-5, PAI-2, JUN, REL, BRCA1, and BRCA2 might be the new targets of NS398 in treatment of colorectal cancer.

CONCLUSION: NS398 might exert its anti-metastasis effect on colorectal cancer by affecting several metastasis-associated gene expression.

Key words: NS398; Colorectal cancer gene expression; Metastasis; cDNA microarray

Gao XQ, Han JX, Huang HY, Song B, Zhu B, Song CZ. Effect of NS398 on metastasis-associated gene expression in a human colon cancer cell line. *World J Gastroenterol* 2005; 11(28): 4337-4343
http://www.wjgnet.com/1007-9327/11/4337.asp

INTRODUCTION

N-[2-(cyclohexyloxy)-4-nitrophenyl] methanesulfonamide (NS398) is a highly selective cyclooxygenase-2 (COX-2) inhibitor. Its mechanism in anticancer effects involves many signal pathways. One is induction of apoptosis of different tumor cells. NS398 inhibits the viability of colon cancer cell lines by apoptosis by the release of cytochrome *C* from mitochondria and by the activation of caspase-9 and caspase-3 and cleavage of poly (ADP-ribose) polymerase. Cytochrome *C* pathway plays an important role in NS398-induced apoptosis in colon cancer cell lines[1]. NS398 may also suppress the growth of tumor cells by inhibiting the cell cycle progression. It can increase the inhibitor of cell cycles p27Kip1 by inhibiting protein degradation to suppress the proliferation of human lung cancer cells, and this in turn is caused by modulating p27Kip1 proteolysis. Non-steroid anti-inflammatory drugs (NSAIDs) suppress the expression of chymotrypsin-like catalytic subunits (LMP5, LMP7, and LMP2), but do not directly block enzymatic activity and inhibit proteasome activity. Reverse transcriptase-competitive PCR and promoter activity assays showed that this inhibition occurred at the transcriptional level[2]. NS398 can exert its anti-angiogenesis and anti-metastasis effects by inhibiting the expression of vascular endothelial growth factor (VEGF)[3]. Its inhibitory effects on the metastasis *in vitro* and *in vivo* are mainly mediated by regulating the matrix metalloproteinase (MMP) family components. NS398 can inhibit the invasiveness of prostate cancer by reducing the release of MMP-2 and MMP-9 and increase of TIMP-2 but not TIMP-1[4]. NS398 inhibits MMP-2 mRNA expression and also decreases the amount of MMP-2 in human lung cancer cells. Additionally, this COX-2 inhibitor attenuates the degrading activity of MMP-2. The synthesis and processing of MMP-2 was significantly suppressed by NS398. NS398 directly inhibits MMP-2 promoter activity. However, the inhibitory effect of NS398 is not fully dependent on inhibition of COX-2 because a high concentration of NS398 is needed to suppress MMP-2 expression and addition of prostaglandin E2 only partially reverses the action of NS398[5].

NS398 and aspirin also upregulate RECK mRNA level in CL-1 human lung cancer cells. Additionally, NSAIDs increase

RECK protein level which was associated with reduction of MMP-2 activity. NSAID-activated RECK expression may not be mediated via inhibition of COXs because addition of prostaglandin E_2 (PGE_2) cannot counteract the effect of NSAIDs and overexpression of COX-2 cannot downregulate RECK[6]. To promote the application of NS398 in the treatment and chemoprevention of colorectal cancer, and observe whether it has other target genes, we detected the effect of NS398 on the expression of metastasis-associated genes in colorectal cancer cell lines by cDNA microarray.

MATERIALS AND METHODS

Microarray fabrication

A total of 447 cDNA clones were obtained from Research Genetics (Invitrogen, Life Technologies, USA). *E.coli* with inserted metastasis-associated genes were cultured with Luria-Bertain culture medium supplemented with ampicillin (50 mg/L in final concentration) or chloromycin (170 mg/L) in Innova™4330 refrigerated incubator shaker (New Brunswick Scientific, USA) at the speed of 250 r/min overnight at 37 ℃. Clone plasmids were extracted with Edge BioSystems (Gaithersburg, MD, Germany). Clone inserts were PCR-amplified from the plasmids with M13 vector-specific universal primer (M13F: 5'-GGT GTA AAA CGA CGG CCA GTG-3'; M13R: 5'CAC ACA GGA AAC AGC TAT G-3') in 96-well PCR microtiters. The PCR products were purified with protocols published[7], and resuspended in Arrayit spot solution. The purified PCR products were printed on silanated slides (CEL Associates, Houston, TX, USA) with Cartisan PixSys 5500 robot (Cartesian Technologies, Irvine, CA, USA) and cDNA microarrays were UV-cross-linked at 3 500 mJ using Cl-1000 ultraviolet cross-linker (Stratagene). Microarrays were post-processed according to protocol online[8].

Cell culture and drug treatment

LoVo cells were grown in the culture incubator at 37 ℃ with 50 mL/L CO_2 in RPMI 1640 (Life Technologies, USA) supplemented with 10% neonatal bovine serum. After the cells were cultured to 60-70% confluence, 12 μL of NS398 dissolved in dimethyl sulfoxide (Me_2SO) was added to make the final concentration 100 μmol/L and further cultured for 24 and 48 h respectively. The same amount of Me_2SO was added to the control.

RNA extraction

LoVo cells treated with NS398 or Me_2SO were lysed with TRIzol (Life Technologies Inc., Rockville, MD, USA) according to the manufacturer's protocol and total RNA was extracted and stored at -80 ℃. The concentration of total RNA were measured with a biophotometer (Eppendorf AG22331, Hamberg, Germany) and the 260/280 ratio of RNA was 1.8-2.0.

Probe preparation

Probes were prepared as described previously[9,10] with some modifications. First strand cDNA was synthesized by priming 10 μg total RNA with 6 μg random hexamers (Life Technologies Inc., Rockville, MD, USA) by heating at 70 ℃ for 10 min, snap-cooling on ice for 30 s and placed at room temperature for additional 5-10 min. Reverse transcription was performed in the presence of 500 μmol/L each of dATP, dCTP and dGTP, 200 μmol/L aminoallyl-dUTP (Sigma Chemical Co., St. Louis, MO, USA), 300 μmol/L dTTP, 1× first strand buffer, 10 mmol/L dithiolthreitol, and 400 U superscript II (Life Technologies) in 30 μL reaction at 42 ℃ overnight. Reactions were quenched with 0.5 mol/L EDTA and RNA template was hydrolyzed by addition of 10 μL NaOH of 1 mol/L followed by heating at 70 ℃ for 10 min. Reactions were neutralized with 10 μL 1 mol/L HCl and cDNA was purified with Amicon Microcon YM100 (Millipore Corporation, Bedford, MA, USA) according to the manufacturer's protocol. cDNA was dried in speed vacuum concentrator 5301 (Eppendorf, Germany) and resuspended in 4.5 μL 0.1 mol/L (pH 9.0) sodium carbonate buffer. Aliquot of Cy3 NHS ester dye (Amersham Pharmacia Biotech, UK) was dissolved in 4.5 μL Me_2SO (1 mg dye from one tube was dissolved in 73 μL of Me_2SO and aliquot in 16 tubes, dried in speed vacuum and stored at 4 ℃) and added to the resuspended cDNA and reactions were incubated at room temperature in the dark for 1 h. Coupling reactions were quenched by addition of 41 μL 0.1 mol/L sodium acetate (pH 5.2), and unincorporated dye was removed using QIAquick PCR purification kit (Qiagen, Germany) following manufacturer's instructions.

Hybridization and image processing

Each slide was printed with duplicate microarrays. Slides were pre-hybridized in 1% BSA, 5× SSC, 0.1% SDS for 45 min, washed twice in de-ionized double distilled H_2O and 2-propanol and air-dried and used in 1 h. Fluorescent cDNA probes were dried in speed vacuum and resuspended in 10 μL hybridization buffer p5 μL formamide, 2.5 μL 20× SSC, 1.0 μL reagent grade double distilled water (RGDD H_2O), 0.5 μL 2% SDS and 1 μL human cot-1DNA]. Probes were denatured at 100 ℃ water bath for 2 min and cooled at room temperature for 5 min. Room temperature probes of NS398 treated and untreated group were applied to the duplicate microarrays on the same pre-hybridized microarrays, covered with hybridized coverslip (Sigma) and placed in the hybridization chamber (Corning). Hybridizations was carried out at 42 ℃ water bath for 20-22 h followed by washing in 2× SSC and 0.1% SDS for 3 min, 1× SSC for 2 min and 0.2× SSC for 1 min and 0.05× SSC for 10 s, and dried by spin at horizontal plate centrifuge at 90 r/min for 4 min. Microarrays were scanned using a ScanArray 4000 (Packard Bioscience, PE, USA) dual color confocal laser scanner. Data were saved as paired TIFF images.

Data analysis

Spots were identified and local background subtracted in the QuantArray 3.0. In the first step, a grid consisting of square cells was drawn around each array element. Spot segmentation was then performed using a fixed segmentation method that uses the distribution of pixel intensity to separate probable signal from background and a binary threshold approach to identify spots, followed by a procedure to exclude disconnected features. Raw intensity for each

element was obtained by first excluding saturated pixels, then summing all remaining pixel intensities inside the spot contours. The area outside the spot contour but inside the cell was used to calculate local background. Background per pixel was estimated as a median of the pixels in this area and multiplied by the spot area to give an estimated spot background value. In the final step, this integrated background value was subtracted from the raw integrated spot intensity to produce the background-subtracted integrated intensities used for further analysis. Furthermore, a quality control filter was used to remove questionable array features. Two criteria for spot rejection were the spot shape deviating greatly from a circle and a low signal to noise ratio. Spots for which the ratio of area to circumference deviated by more than 20% from the value for an ideal circle and spots containing less than 50% of pixels above the median background values were flagged and eliminated from further consideration. The spot intensity above blank plus 2SD was used for the final analysis. Then the data were normalized to total with software supplied by the manufacturer. The two fold up- or down-regulated genes were shown in red or green respectively.

Semi-quantitative RT-PCR validation of microarray results

The upregulated gene IGFBP-5 was measured by RT-PCR to verify the microarray results. RT-PCR was performed on MJ-PTC200 DNA engine using TaKaRa two-step reaction with protocols supplied by the manufacturer. The primers for IGFBP-5 were forward: 5'-TTG CCT CAA CGA AAA GAG C-3', reverse: 5'-AGA ATC CTT TGC GGT CAC A3'[11]. The primers for β-actin were forward: 5'- AAG TAC TCC GTG TGG ATC GG -3', reverse: 5'-TCA AGT TGG GGG ACA AAA AG -3'[12]. PCR was performed at 94 ℃ for 2 min, and 30 cycles at 94 ℃ for 30 s, at 50 ℃ for 30 s and at 72 ℃ for 60 s and a final extension at 72 ℃ for 5 min. PCR products were electrophoresed on 1% agarose gel. Images were captured with Alpha Image™ 2000. The band density was measured with the software supplied by the same system.

RESULTS

Plasmid extraction

The plasmids were extracted by Edge biosystems plasmids extraction kit (Gaithersberg, MD, Germany). The extracted plasmids were run on 1% agarose gel. The results shown in Figure 1 are representative of the 447 clones. PCR amplification of the 447 clones for the inserts is shown in Figure 2. The single band amplification rate was 93%.

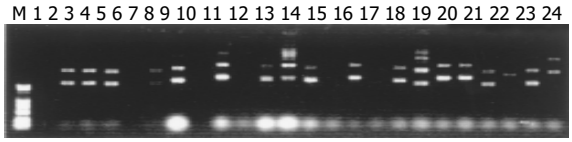

Figure 1 Electrophoresis of clone 73-95 plasmids on 0.7% agarose. M: DL2000, lanes 1-24 represent plasmids of clone 73-95.

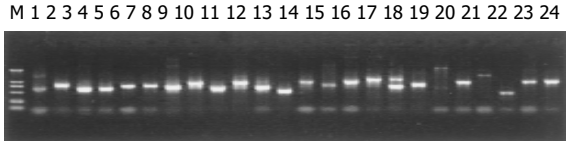

Figure 2 Electrophoresis of PCR products in 1% agarose. M: DL2000, lanes 1-24: the PCR amplification of clone 73-95.

To identify metastasis-associated genes affected by NS398, LoVo cells were treated with 100 μmol/L NS398 for 24 and 48 h respectively. The representative image is shown in Figure 3. Image A represents the hybridized results of untreated cells. Image B represents the hybridization results of the NS398-treated LoVo cells and image C is the overlay image of NS398-treated to control LoVo cells.

After treatment with NS398 for 24 h, 9 genes were upregulated and 8 genes downregulated (Table 1). The

Table 1 Up- and down-regulated genes in NS398-treated LoVo cells for 24 h (mean±SD)

Accession number	Gene descriptions	Ratio
Not found	Hs.23723, "ESTs" (346390)	2.67±1.66
Not found	Hs.106513, "EST" (348242)	2.31±0.67
BC040844	Hs.198253, NS1-associated protein 1 (435598)	1.96±0.25
BC011714	Hs.9605, heterogeneous nuclear ribonucleoprotein D-like (190165)	2.08±0.46
Not found	Hs.277401, ESTs (35363)	2.04±0.13
NT_024524	Hs.277704, PIBF1 gene product (124966)	2.29±0.81
BC007674	Hs.180414, CD24 antigen (small cell lung carcinoma cluster 4 antigen) (115306)	1.98±0.22
NM_003127	Hs.87497, spectrin, alpha, non-erythrocytic 1 (alpha-fodrin, 3021698)	2.27±0.53
Not found	Hs.272073, ESTs (1296662)	1.95±0.24
BT007404	Hs.8037, CD24 antigen (small cell lung carcinoma cluster 4 antigen, 124098)	0.49±0.04
K01500	Hs.18443, alpha-1-antichymotrypsin (117439)	0.51±0.05
Not found	Hs.45209, EST(2118886)	0.49±0.04
NM_005564	LCN2 (oncogene 24p3, 595821)	0.47±0.17
NM_001022	Hs.43913, ribosomal protein S19 (453963)	0.53±0.06
NM_003259	Intercellular adhesion molecule 5, telencephalin (ICAM5, 180864)	0.36±0.14
NM_002228	v-jun avian sarcoma virus 17 oncogene homolog (JUN, 823612)	0.51±0.07
NM_002908	v-rel avian reticuloendotheliosis viral oncogene homolog (REL, 2723459)	0.45±0.06

Table 2 Up- and down-regulated genes in NS398-treated LoVo cells for 48 h (mean±SD)

Accession number	Gene description	Ratio
Not found	Hs.23723, "ESTs" (346390)	3.41±1.76
Not found	Hs.106513, "EST" (348242)	3.05±1.88
BC040844	Hs.198253, NS1-associated protein 1 (435598)	2.51±0.53
AF257505	Hs.23317, butyrophilin, subfamily 3, member A2 (219410)	2.12±0.56
NT_033899	Hs.28043, KIAA0712 gene product (219914)	2.13±0.40
BC011714	Hs.9605, heterogeneous nuclear ribonucleoprotein D-like (190165)	2.34±0.51
M62782	Hs.22907, human insulin-like growth factor binding protein 5 (IGFBP5) mRNA (31397)	2.15±0.43
NM_003127	Hs.87497, spectrin, alpha, non-erythrocytic 1 (alpha-fodrin, 3021698)	2.14±0.13
BC008005	Hs.116459, nucleotide binding protein 2 (*E coli* MinD like, 2498589)	2.01±0.29
Not found	Hs.43913, ESTs (2498857)	2.20±0.28
Not found	Hs.272073, ESTs (1296662)	2.33±0.43
BM508995	Hs.106513, ESTs, highly similar to proteasome (*H sapiens*, 1302647)	2.47±0.76
NM_000624	Hs.150580, alpha-1-antichymotrypsin (1322220)	2.14±0.35
AF248734	Hs.87497, apoptotic protease activating factor (963055)	2.28±0.45
BC002965	Lysosomal-associated membrane protein 2 (LAMP2), transcript variant LAMP2A (134418)	2.34±0.69
NM_006536	Chloride channel, calcium activated, family member 2 (CLCA2, 781187)	2.39±0.42
M90657	Tumor-associated antigen L6 (1964132)	2.85±1.58
Not found	Spliceosome associated protein 145 (1964680)	2.28±0.34
AW674474	Putative insulin-like growth factor ii associated (229316)	2.32±0.50
AF041835	Laminin, gamma 3 (LAMC3, 2497685)	2.16±0.48
AB019987	Chromosome-associated polypeptide-c (2597847)	2.06±0.09
AW277011	Putative vacuolar protein sorting-associated protein c (2744695)	2.20±0.64
BC032547	Homeo box A1 (HOXA1, 3923611)	2.27±1.18
NM_003391	Wingless-type MMTV integration site family member 2 (WNT2, 149373)	2.27±0.28
BC027948	c-fos induced growth factor (VEGF D, FIGF, 160946)	2.15±0.27
NM_001792	Cadherin 2, N-cadherin (neuronal, CDH2, 3617894)	2.03±0.10
NM_001964	Early growth response 1 (EGR1, 182411)	2.61±0.47
AF071400	Plasminogen activator inhibitor, type II (arginine-serpin, PAI2, 323255)	2.41±0.39
NM_002447	Macrophage stimulating 1 receptor (c-met-related tyrosine kinase, MST1R, 586698)	2.45±0.62
NM_003254	Tissue inhibitor of metalloproteinase 1 (erythroid potentiating activity, collagenase inhibitor, TIMP1, 771755)	2.02±0.18
NM_003182	Tachykinin, precursor 1 (substance K, substance P, neurokinin 1, neurokinin 2, neuromedin L, neurokinin alpha, neuropeptide K, neuropeptide gamma, TAC1), transcript variant beta (784179)	2.22±0.30
BC004986	Hs.77202, ribosomal protein S25 (178052)	0.49±0.06
BC035128	Hs.23317, Max-interacting protein (130696)	0.45±0.05
Not found	Hs.23954, ESTs (132543)	0.51±0.06
AJ001810	Hs.106513, pre-mRNA cleavage factor Im (25 ku)	0.48±0.01
BC053521	66834, Hs.76847, spectrin, alpha, non-erythrocytic 1 (alpha-fodrin, 31230)	0.47±0.15
M64716	Hs.234726, ribosomal protein S25 (4932742)	0.46±0.05
BC032589	No, beta-2-microglobulin (1907327)	0.48±0.11
Not found	Hs.45209, EST (2118886)	0.47±0.11
NT_024524	Hs.15058, PIBF1 gene product (1596167)	0.50±0.05
NM_001779	CD58 antigen (lymphocyte function-associated antigen 3, CD58, 490368)	0.50±0.15
NM_002228	v-jun avian sarcoma virus 17 oncogene homolog (JUN, 823612)	0.41±0.11
NM_020979	Adaptor protein with pleckstrin homology and src homology 2 domains (APS, 3056093)	0.49±0.17
NM_000059	Breast cancer 2, early onset (BRCA2, 3850805)	0.30±0.10
NM_001223	Caspase 1, apoptosis-related cysteine protease (interleukin 1, beta, convertase, CASP1, 3858119)	0.48±0.09

The number in parenthesis represents the IMAGE clone number.

downregulated genes included lipocalin 2 (oncogene 24p3) (LCN2), intercellular adhesion molecule 5, telencephalin (ICAM5), v-jun avian sarcoma virus 17 oncogene homolog (JUN), v-rel avian reticuloendotheliosis viral oncogene homolog (REL). Five genes after being treated for 24 h were still highly expressed until 48 h and one gene was still inhibited until 48 h.

After 48 h of treatment more genes were regulated by NS398. Of the 447 genes analyzed, 31 genes were upregulated and 14 genes downregulated (Table 2). IGFBP-5, APAF, LAMP2, CLCA2, laminin gamma3, HOXA1, WNT2, N-cadherin, PAI-2, TIMP could inhibit the metastasis of tumor.

Validation of microarray results by semi-quantitative RT-PCR

IGFBP-5 gene expression was validated with TAKARA version 2.1 RT-PCR kit. The expression level was measured with alpha InnoTech™ 2000 spot density method. The NS398-treated LoVo cells expressed more IGFBP-5 mRNA (Figure 4). The relative expression ratio to β-actin was 0.21,

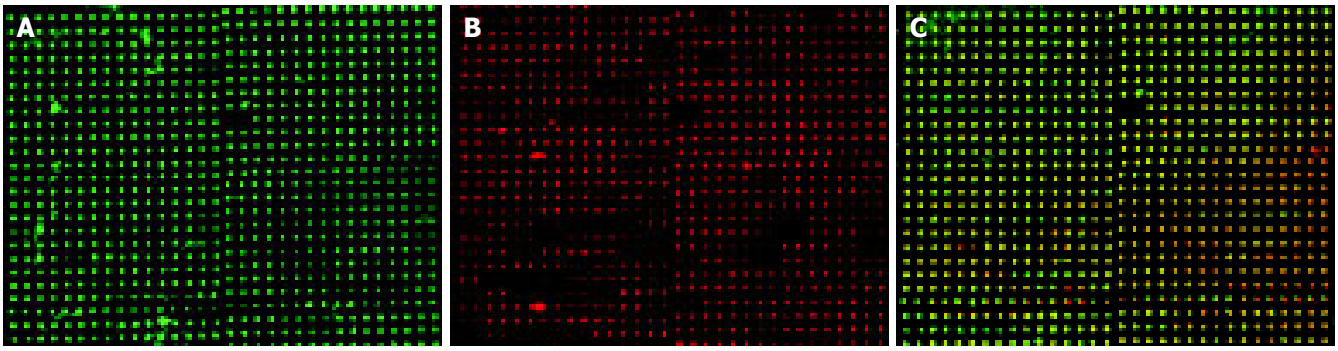

Figure 3 Representative image of cDNA microarray. **A**: Image of the DMSO treated control, **B**: image of NS398-treated LoVo cell, **C**: overlay image of NS398-treated loVo cell to control.

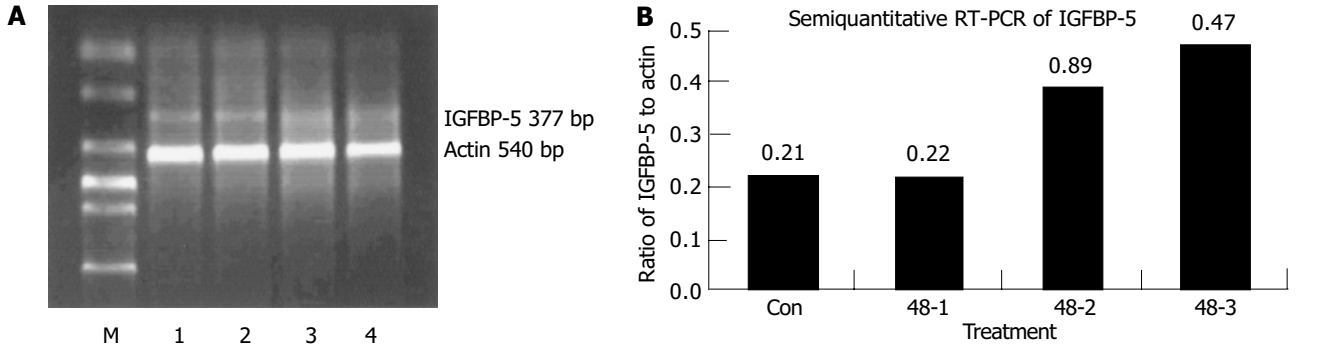

Figure 4 IGFBP-5 mRNA expression in NS398-treated LoVo cell. **A**: mRNA level measured with semi-quantitative RT-PCR. M: DL2000, lanes 1-4 control and 3 replicates of NS398 treated loVo cell; **B**: Relative ratios of the IGFBP-5 to actin.

0.22, 0.39, and 0.47 for the control and the three NS398-treated replicate experiments. The IGFBP-5 mRNA level in NS398-treated LoVo cells to untreated LoVo cells was 1.05, 1.85, and 2.23 respectively for the three replicate experiments. It was in accord with the microarray results.

DISCUSSION

NS398 is a highly selective COX-2 inhibitor. Its anticancer effects have been linked to cell apoptosis and inhibition of MMP and anti-angiogenesis. NS398 also exerts its synergistic effect with radiotherapy for the treatment of head and neck squamous cell cancer (HNSCC) by inhibiting radiation-induced expression of COX-2[12] and increases the sensitivity of chemotherapy by enhancing the expression of cyclin-dependent kinase inhibitors p21 (Waf1) and p27 (Kip1), promoting apoptosis of tumor cells, therefore makes the cells stay in G_1 arrest[13].

cDNA microarray has been widely used in the screening of drug targets. To identify whether NS398 had other target genes in the treatment of colorectal cancer, we treated LoVo cells with NS398 and the expression of metastasis-associated genes were measured with microarray. The results showed that NS398 influenced the expression of some metastasis genes. After being treated for 24 h, NS398 increased the production of NS1-associated protein 1, PIBF1 gene, CD24 antigen, and some ESTS. Simultaneously NS398 can inhibit the expression of some oncogenes such as alpha-1-antichymotrypsin, LCN2 (oncogene 24p3), ICAM5, JUN and REL. It was reported that NS398 downregulates the expression of COX-2, nuclear factor-kappaB, p50 and Rel A p65, and its anti-tumor effect is associated with COX-2 transcription inhibition[14].

After being treated for 48 h with NS398, the metastasis-associated genes expressed by LoVo cells changed more profoundly. Thirty-one genes were upregulated, including NS1-associated protein 1, IGFBP5, spectrin, nucleotide binding protein 2, alpha-1-antichymotrypsin, apoptotic protease activating factor, LAMP2, CLCA2, tumor-associated antigen L6, putative insulin-like growth factor, chromosome-associated polypeptide-c, HOXA1, WNT2, FIGF, N-cadherin, PAI2, macrophage-stimulating 1 receptor (MST1R), TIMP1, tachykinin, and precursor.

E-cadherin and N-cadherin are members of the cadherin family of calcium-dependent cell adhesion molecules that play an important role in the embryogenic development and maintenance of normal tissues. N-cadherin present in the most invasive and dedifferentiated breast cancer cell lines, and its exogenous expression in tumor cells induces a scattered morphology and high motility, invasion, and metastasis. N-cadherin co-operates with the fibroblast growth factor receptor, resulting in signals that lead to the upmodulation of MMP-9 and cellular invasion. N-cadherin probably also supports the systemic dissemination of tumor cells by enabling the circulation of tumor cells to associate with the stroma and the endothelium at distant sites[15]. Ectopically expressed N-cadherin fails to assemble cadherin/catenin adhesion complexes and to inhibit invasion. The

association of N-cadherin with long P120 (ctn) and tyrosine may explain why N-cadherin cannot replace E-cadherin in pancreatic carcinoma cells[16]. But there are conflicting results of the expression of N-cadherin with the invasion of tumor. P-cadherin is detectable in 40%, N-cadherin in 30%, and E-cadherin in 81% invasive carcinomas. P-cadherin but not E/N-cadherin expression in breast carcinomas shows a strong correlation with higher grade (poorer differentiation), lack of ERs, and presence of EGFR, and its expression may aid in the further subdivision of high grade carcinomas[17]. In the upregulated genes, IGFBP-5 is of great importance. Until now the role of IGFBP-5 in the tumor development is different in different tumors. Expression of IGFBP-5, both by stable transfection and adenoviral-mediated infection, can inhibit the growth of MDA-MB-231 and Hs578T human breast cancer cells over a 13-d period. IGFBP-5 is a potent growth inhibitor and proapoptotic agent in human breast cancer cells via modulation of cell cycle and apoptotic mediators[18].

IGFBP5 is also overexpressed in thyroid tumors. IGFBP-5 and gene 44 are significantly overexpressed in papillary carcinoma[19]. IGFBP-5 mRNA levels are the highest in the benign group without edema of meningiomas, whereas IGFBP-6 mRNA levels are the highest in the group with brain invasion[20]. The presence of IGFBP-5 significantly inhibits cell death induced by C2 or RGD. IGFBP-5 promotes the attachment and survival of Hs578T cells by modulating the balance between ceramide and opposing survival signals[21]. IGFBP-5 has no effect on the proliferation, migration and invasiveness of RSVT2/C cells *in vitro*[22].

Insulin-like growth factor (IGF)-I and -II are potent mitogens, and can exert autocrine and paracrine effects on growth regulation in human gastric cancer. Their mitogenic effects are regulated by the IGFBPs. The expression pattern of IGFBPs was heterogeneous in the gastric cancer cell lines. IGFBP-2 is expressed in all gastric cancer cell lines, whereas IGFBP-1 is not detectable in any cell line. IGFBP-4 is expressed in most cell lines. IGFBP-3, IGFBP-5, and IGFBP-6 are expressed in approximately 50% of cell lines. In addition, exogenous IGF-I and -II stimulate the proliferation of gastric cancer cells, suggesting the existence of a functional IGF system in gastric cancer. Our data suggest that the IGF-IGFBP system may play an important role in the initiation, progression, and metastasis of gastric cancer[23].

Osteosarcoma cells transfected with IGFBP-5 reduce proliferation under both anchorage-dependent and -independent manner. The increase of proliferation observed in IGFBP-5-secreting clones after addition of exogenous IGF is significantly less than that observed in mock-transfected cells or parental cells. A similar result has been obtained with long [R3] IGF-I which has a low affinity for all IGFBPs, suggesting that the inhibitory effect of IGFBP-5 is only partially IGF-dependent and this effect may be due to an induction of differentiation in these cells because IGFBP-5 increases the normal component secretion of osteosarcoma cells[24].

Upregulation of PAI-2 in LoVo cells may be another mechanism of NS398 underlying the inhibitory effects of tumor cells. PAI-2 is downregulated in esophageal adenocarcinoma compared to normal esophageal tissues[25].

Plasminogen activator inhibitor-2 (PAI-2), a gene whose expression has been linked to cell invasion, has been identified in head and neck tumor cell line. In addition, immunohistochemical evaluation of biopsy samples reveals a high expression of PAI-2 in both normal and dysplastic epithelia with a marked decrease of expression in areas of the biopsies containing HNSCC[26].

The downregulated genes include Max-interacting protein, spectrin, beta-2-microglobulin, CD58 antigen, JUN, APS, BRCA2, CASP1, and some ESTS. BRCA1 and BRCA2 staining increases in the apical cell pole of epithelial malignant cells and in colorectal tumor specimens. Increased BRCA1 and BRCA2 expression may be explained by the fact that colorectal tissue is subjected to very active proliferation and differentiation[27]. High BRCA2 mRNA level is associated with poor outcome and correlates positively and strongly with cell proliferation in breast cancer[28]. NS398 may inhibit the growth of colorectal cancer by downregulating the expression of BRCA2.

In conclusion, the upregulated and downregulated genes identified by cDNA microarray may be the new target genes of NS398.

REFERENCES

1 **Li M,** Wu X, Xu XC. Induction of apoptosis in colon cancer cells by cyclooxygenase-2 inhibitor NS398 through a cytochrome c-dependent pathway. *Clini Cancer Res* 2001; **7**: 1010-1016

2 **Hung WC,** Chang HC, Pan MR, Lee TH, Chuang LY. Induction of p27(KIP1) as a mechanisms underlying NS398-induced growth inhibition in hung cancer cells. *Mol Pharmacol* 2000; **58**: 1398-1403

3 **Liu XH,** Kirschenbaum A, Yao S, Stearns ME, Holland JF, Claffey K, Levine AC. Upregulation of vascular endothelial growth factor by cobalt chloride-simulated hypoxia is mediated by persistent induction of cyclooxygenase-2 in a metastatic human prostate cancer cell line. *Clin Exp Metastasis* 1999; **17**: 687-694

4 **Attiga FA,** Fernandez PM, Weeraratna AT, Manyak Michael MJ, Patierno SR. Inhibitors of prostaglandin synthesis inhibit human prostate tumor cell invasiveness and reduce the release of matrix metalloproteinases. *Cancer Res* 2000; **60**: 4629-4637

5 **Pan MR,** Chuang LY, Hung WC. Non-steroidal anti-inflammatory drugs inhibit matrix metalloproteinase-2 expression via repression of transcription in lung cancer cells. *FEBS Lett* 2001; **508**: 365-368

6 **Liu LT,** Chang HC, Chiang LC, Hung WC. Induction of RECK by nonsteroidal anti-inflammatory drugs in lung cancer cells. *Oncogene* 2002; **21**: 8347-8350

7 DNA precipitations/Preparation of DNA samples. [Last Update, December1999] [Bioinformatics Manual]. Available from: http://cmgm.stanford.edu/pbrown/protocols/2_DNA.html

8 Post-processing of arrays/Experimental Protocols [updated September 1999] [BioinformaticsManual]http://www.cmgm.stanford.edu/pbrown/protocols/3_post_process.html

9 **Hasseman JP.** Aminoallyl labeling of RNA for microarray. Revision Level:2 (http://pga.tigr.org/sop/Moo4_1a.pdf)

10 **Yang IV,** Chen E, Hasseman JP, Liang W, Frank BC,Wang SB, Sharov V, Saeed AI, White J, Li J, Lee NH, Yeatman TJ, Quackenbush J. Within the fold: assessing differential expression measures and reproductivity in microarray assays. *Genome Biol* 2002; **3**: 1-12

11 **Bushman TL,** Kuemmerle JF. IGFBP-3 and IGFBP-5 production by human intestinal muscle: recipriocal regulation by endogeneous TGF-β1. *Am J Phsiol* 1998; **275**(6 Pt 1): G1282-G1290
12 **Amirghahari N,** Harrison L, Smith M, Rong X, Naumann I, Ampil F, Shi R, Glass J, Nathan CA. NS 398 radiosensitizes an HNSCC cell line by possibly inhibiting radiation-induced expression of COX-2. *Int J Radiat Oncol Biol Phys* 2003; **57**: 1405-1412
13 **Peng JP,** Liu LT, Chang HC, Hung WC. Enhancement of chemotherapeutic drug-induced apoptosis by a cyclooxygenase-2 inhibitor in hypopharyngeal carcinoma cells. *Cancer Lett* 2003; **201**: 157-163
14 **Wen B,** Deutsch E, Eschwege P, De Crevoisier R, Nasr E, Eschwege F, Bourhis J. Cyclooxygenase-2 inhibitor NS398 enhances anti-tumor effect of irradiation on hormone refractory human prostate carcinoma cells. *J Urol* 2003; **170**: 2036-2039
15 **Hazan RB,** Qiao R, Keren R, Badano I, Suyama K. Cadherin switch in tumor progression. *Ann N Y Acad Sci* 2004; **1014**: 155-163
16 **Seidel B,** Braeg S, Adler G , Wedlich D, Menke A. E- and N-cadherin differ with respect to their associated p120(ctn) isoforms and their ability to suppress invasive growth in pancreatic cancer cells. *Oncogene* 2004; **23**: 5532-5542
17 **Kovacs A,** Dhillon J, Walker RA. Expression of P-cadherin, but not E-cadherin or N-cadherin, relates to pathological and functional differentiation of breast carcinomas. *Mol Pathol* 2003; **56**: 318-322
18 **Butt AJ,** Dickson KA, McDougall F, Baxter RC. Insulin-like growth factor-binding protein-5 inhibits the growth of human breast cancer cells *in vitro* and *in vivo*. *J Biol Chem* 2003; **278**: 29676-29685
19 **Stolf BS,** Carvalho AF, Martins WK, Runza FB, Brun M, Hirata R Jr, Jordao Neves E, Soares FA, Postigo-Dias J, Kowalski LP, Reis LF. Differential expression of IGFBP-5 and two human ESTs in thyroid glands with goiter, adenoma and papillary or follicular carcinomas. *Cancer Lett* 2003; **191**: 193-202
20 **Nordqvist AC,** Mathiesen T. Expression of IGF-II, IGFBP-2, -5, and -6 in meningiomas with different brain invasiveness. *J Neurooncol* 2002; **57**: 19-26
21 **McCaig C,** Perks CM, Holly JM. Signaling pathways involved in the direct effects of IGFBP-5 on breast epithelial cell attachment and survival. *J Cell Biochem* 2002; **84**: 784-794
22 **Lee BP,** Rushlow WJ, Chakraborty C, Lala PK. Differential gene expression in premalignant human trophoblast: role of IGFBP-5. *Int J Cancer* 2001; **94**: 674-684
23 **Yi HK,** Hwang PH, Yang DH, Kang CW, Lee DY. Expression of the insulin-like growth factors (IGFs) and the IGF-binding proteins (IGFBPs) in human gastric cancer cells. *Eur J Cancer* 2001; **37**: 2257-2263
24 **Schneider MR,** Zhou R, Hoeflich A, Krebs O, Schmidt J, Mohan S, Wolf E, Lahm H. Insulin-like growth factor-binding protein-5 inhibits growth and induces differentiation of mouse osteosarcoma cells. *Biochem Biophys Res Commun* 2001; **288**: 435-442
25 **Hourihan RN,** O'Sullivan GC, Morgan JG. Transcriptional gene expression profiles of oesophageal adenocarcinoma and normal oesophageal tissues. *Anticancer Res* 2003; **23**: 161-165
26 **Hasina R,** Hulett K, Bicciato S, Di Bello C, Petruzzelli GJ, Lingen MW. Plasminogen activator inhibitor-2: a molecular biomarker for head and neck cancer progression. *Cancer Res* 2003; **63**: 555-559
27 **Bernard-Gallon DJ,** Peffault de Latour M, Hizel C, Vissac C, Cure H, Pezet D, Dechelotte PJ, Chipponi J, Chassagne J, Bignon YJ. Localization of human BRCA1 and BRCA2 in non-inherited colorectal carcinomas and matched normal mucosas. *Anticancer Res* 2001; **21**: 2011-2020
28 **Bieche I,** Tozlu S, Girault I, Lidereau R. Identification of a three-gene expression signature of poor-prognosis breast carcinoma. *Mol Cancer* 2004; **3**: 37

Science Editor Wang XL and Li WZ **Language Editor** Elsevier HK

PO Box 2345, Beijing 100023, China
www.wjgnet.com
wjg@wjgnet.com

ELSEVIER

World J Gastroenterol 2005;11(28):4344-4350
World Journal of Gastroenterology ISSN 1007-9327

Outcome of lamivudine-resistant hepatitis B virus is generally benign except in cirrhotics

Yock-Young Dan, Chun-Tao Wai, Yin-Mei Lee, Dede Selamat Sutedja, Bee-Leng Seet, Seng-Gee Lim

Yock-Young Dan, Chun-Tao Wai, Yin-Mei Lee, Dede Selamat Sutedja, Bee-Leng Seet, Seng-Gee Lim, Division of Gastroenterology, National University Hospital, Singapore
Supported by the National University of Singapore Grant, No. R-182-000-0001-731
Correspondence to: Dr. Seng-Gee Lim, Division of Gastroenterology, Department of Medicine, National University Hospital, 5 Lower Kent Ridge Road, 119074 Singapore. mdclimsg@nus.edu.sg
Telephone: +65-67724353 Fax: +65-67794112
Received: 2004-12-07 Accepted: 2005-01-13

Abstract

AIM: We set to determine factors that determine clinical severity after the development of resistance.

METHODS: Thirty-five Asian patients with genotypic lamivudine resistance were analyzed in three groups: 13/35 (37%) were non-cirrhotics with normal pre-treatment ALT (Group IA), 12/35 (34%) were non-cirrhotics with elevated pre-treatment ALT (Group IB), and 10/35 (29%) were cirrhotics (Group II). Patients were followed for a median of 98 wk (range 26-220) after the emergence of genotypic resistance.

RESULTS: Group IA patients tended to retain normal ALT. Group IB patients showed initial improvement of ALT with lamivudine but 9/12 patients (75%) developed abnormal ALT subsequently. On follow-up however, this persisted in only 33%. Group II patients also showed improvement while on treatment, but they deteriorated with the emergence of resistance with 30% death from decompensated liver disease. Pretreatment ALT levels and CPT score (in the cirrhotic group) were predictive of clinical resistance and correlated with peak ALT levels and CPT score.

CONCLUSION: The phenotype of lamivudine-resistant HBV correlated with the pretreatment phenotype. The clinical course was generally benign in non-cirrhotics. However, cirrhotics had a high risk of progression and death (30%) with the development of lamivudine resistance.

Key words: Lamivudine resistance; YMDD mutants; Hepatitis B treatment; Nucleoside analog

Dan YY, Wai CT, Lee YM, Sutedja DS, Seet BL, Lim SG. Outcome of lamivudine-resistant hepatitis B virus is generally benign except in cirrhotics. *World J Gastroenterol* 2005; 11(28): 4344-4350
http://www.wjgnet.com/1007-9327/11/4344.asp

INTRODUCTION

Treatment of CHB was revolutionized by the introduction of orally administered antiviral agents. Lamivudine, a nucleoside analog and the first orally available antiviral agent for CHB, had demonstrated significant results in clinical trials, with universal suppression of HBV DNA level by 3 logs, 55% improvement in histological necroinflammatory score, normalization of ALT in the majority of patients after 1 year of treatment[1,2]. Even among patients with decompen-sated hepatitis B cirrhosis, there was clinical improvement[3], thus enabling some of them to be taken off liver transplant waiting lists.

However, drug resistance with lamivudine occurs with prolonged usage, rising from 14-24% at the end of first year, to 57% by the end of year 3[4,5]. Resistance occurred primarily as a result of mutations in the YMDD motif of the polymerase gene although subsequently, mutations at other sites have been reported[6]. Initial reports suggested that lamivudine-resistant HBV virus may be less virulent and replication-defective, as the ALT and HBV DNA levels caused by these mutant viruses were lower than the pretreatment values[7]. However, subsequent reports of decompensation, acute exacerbations, and deaths from such mutant viruses suggested otherwise[8,9]. This has given rise to the suggestion of limiting lamivudine therapy to 12 mo duration in order to avoid the development of these mutants[10].

Lamivudine resistance can be divided into genotypic and clinical phenotypic resistance. Genotypic resistance refers to the presence of a lamivudine-resistant strain such as the YMDD mutants, which in itself may not lead to any clinical sequela, since such strains have been detected in patients who have not had prior exposure to lamivudine[11]. Clinical phenotypic resistance refers to the presence of genotypic resistance with the subsequent development of clinical deterioration, defined as elevation of transaminases and/or deterioration of liver histology and liver function. Factors that predict the development of genotypic resistance[5,12] had been evaluated in many studies, which included pretreatment HBV DNA level, ALT level, body mass index, adw serotype, and core promoter mutations[13-15]. However, these studies did not address the more important question of which factor(s) actually lead to clinical resistance.

Hence, we set to examine variables that determined the clinical phenotypes after the development of genotypic lamivudine resistance.

MATERIALS AND METHODS

Patients

From January 1996 to April 2003, we prospectively followed

all patients started on lamivudine 100 or 150 mg daily monotherapy for clinical indications, or who had completed trials of lamivudine monotherapy, at 3 monthly intervals. These included patients who were recruited from the Asian Multicentre Lamivudine Trial and its subsequent rollover follow-up study NUCB3018[1,4,16], which also included patients with normal pre-treatment ALT levels. Patients were also given lamivudine if it was clinically indicated, such as persistently abnormal ALT levels (greater than twice upper limit of normal for at least 3 mo duration), decompensated liver disease (development of variceal hemorrhage, ascites, and hepatic encephalopathy), or were on the liver transplant waiting list. All patients had detectable HBV DNA by a non-PCR based assay prior to initiation of therapy. Lamivudine was prescribed for at least a year and was continued even when genotypic resistance developed. During the duration of the study, none of the patients were given adefovir dipivoxil as a rescue therapy as it was not yet available in Singapore. This study was approved by the Institutional Review Board of the National University Hospital, Singapore.

Exclusion criteria

Patients who tested positive for anti-HCV, anti-HDV, and HIV, had significant history of alcohol intake (defined as more than seven drinks per week), or were non-compliant with lamivudine were excluded from the study. Patients who developed resistance after liver transplants were also excluded.

Measurement of HBV DNA

Prior to March 2000, the Abbott HBV DNA assay (Abbott Laboratories, North Chicago, IL, USA) was used for HBV DNA viral load quantification. After March 2000, this assay was substituted to a branched-chain assay (Chiron Quantiplex™, Chiron Corp). Results of the Abbott HBV DNA assay were converted using the Multimeasurement Method[17].

Phenotypes

Eligible patients were classified into three distinct phenotypes according to their baseline characteristics. The presence of cirrhosis was determined by liver biopsy or by ultrasonographic features in those with clinical decompensated disease.

Group IA	Non-cirrhotic patients with normal baseline ALT level
Group IB	Non-cirrhotic patients with abnormal baseline ALT level
Group II	Cirrhotic patients

Genotypic lamivudine resistance

Genotypic resistance was defined as reappearance of at least two consecutive detectable HBV DNA levels after a period of undetectable level whilst on continuous lamivudine therapy for more than 6 mo.

Characterization of lamivudine resistance by sequencing

Confirmation of genotypic resistance was performed by comparison of results from direct sequencing of the HBV polymerase of the HBV DNA samples before starting lamivudine, and after development of resistance. DNA was extracted and direct sequencing was performed at a 750 bp region between nt 253 and 1 006 of the HBV genome using the two primers:

Forward primer: 5'-GAC TCG TGG TGG ACT TCT CTC AA- 3'.

Reverse primer: 5'-CCC ACA ATT CTT TGA CAT ACT TTC C-3'. The forward and reverse sequences were aligned using the Seqman program (DNAstar). This segment has been known to contain all the mutations known to confer lamivudine resistance. New mutations emerging after treatment of lamivudine were determined for their resistance conferring properties from previously published data and categorized using the new nomenclature[6,18].

Clinical resistance

All patients were followed for a minimum of 6 mo after the emergence of genotypic resistance and for as long as the patients were continued on lamivudine. Serial analysis of ALT, bilirubin, prothrombin time, HBeAg, anti HBe and HBV DNA level by Chiron Quantiplex™, at 3 monthly intervals were done. Serial Child-Pugh Turcot (CPT) scores were also calculated. No serial liver biopsy was performed in our patients.

In the non-cirrhotic group, clinical resistance was defined as abnormal rise in ALT greater than twice upper limit of normal. In the cirrhotic group, clinical resistance was defined as abnormal rise in ALT greater than twice the normal upper limit, or an increase of CPT Score by two points or more.

Clinical severity was assessed at four time points: timepoint 1 (baseline or pretreatment), timepoint 2 (6 mo after the commencement of lamivudine therapy), timepoint 3 (peak ALT or CPT levels after the development of genotypic resistance), and timepoint 4 (last ALT or CPT on follow-up).

HBV genotyping

HBV genotyping was performed using restriction fragment length polymorphism created by Ava2 and Dpn2 action on an amplified segment of the pre-S region as previously described[19].

Statistical analysis

Changes in ALT level and CPT Score were compared at four timepoints within each group of patients. Statistical analysis was performed by Wilcoxon Matched-Pairs Signed Rank Test to avoid the effect of pooling results from different patients. The relationship of two continuous variables was tested by Spearman ρ Correlation test. *P* values of less than 0.05 were considered statistically significant.

The following parameters: age, sex, baseline ALT, ALT at the point of emergence of resistance, baseline HBV DNA level, peak HBV DNA post genotypic resistance, duration of lamivudine treatment, type of mutation, genotype and HBeAg seroconversion were analyzed by univariate analysis to determine factors associated with phenotypic resistance. Categorical variables and continuous variables were compared by Fisher's exact test and Student's *t*-test, as appropriate. Significant factors from univariate analysis were then analyzed by multivariate analysis by forward logistic regression to determine independent factors associated with phenotypic resistance.

All statistical analysis was performed using computer software, SPSS 10.0 for Windows (SPSS Inc., Chicago, IL, USA).

RESULTS

Patients

A total of 78 patients were prescribed lamivudine for hepatitis B related indications or had completed a clinical trial of lamivudine therapy at our institution for a minimum of 1 year during the study period. Of these, 35 patients (45%) developed genotypic resistance to lamivudine while on treatment after a median of 143 wk (range 35-212 wk) and were included in this study. Twenty-one (60%) were part of the Asian Lamivudine Trial (NUCB 3009/NUCB3018) [1], of which 11 received uninterrupted lamivudine treatment while 10 were restarted on open label lamivudine after viral breakthrough when they were on placebo. The remainder of the patients was given lamivudine for clinical indications of chronic hepatitis (n = 4, 11%) and cirrhotic liver disease (n = 10, 29%), respectively. One patient was eligible to enter a trial of adefovir/lamivudine (NUCB 20904) treatment for persistent abnormal transaminases at 56 wk after emergence of resistance. Data up to the point of trial entry was used for analysis but data thereafter was censored. No patient received liver transplant after the emergence of resistance. Thus in total, 35 patients were eligible for analysis. There were no missing patients or dropouts from the cohort.

All 35 patients were stratified into three groups (Table 1): 13 patients (37%) were in Group IA (non-cirrhotic patients with normal baseline ALT), 12 (34%) of patients were in Group IB (non-cirrhotic patients with abnormal baseline ALT), and the remainder of the patients (n = 10, 29%) were in Group II (cirrhotic patients). Group IA and B patients were predominantly from the Asian Lamivudine trial and had a median age of 35 years (range: 21-48 years) and 34 years (range 20-45 years), respectively. Patients in Group II were expectedly older with median age of 52 years (range 42-68). There was a preponderance of male patients (M:F = 30:5). With the exception of one Malay patient, all remaining patients were Chinese (97%). Of these 35 patients, genotypic resistance developed at a median of 143 wk after being on lamivudine (range 35-212). Median patients follow-up after genotypic resistance was 102 wk (range 26-220).

HBV genotypes

Majority of the patients had either genotypes B or C. Eighteen (51%) were of HBV genotype B while 13 patients (37%) had genotype C. Four (12%) had other genotypes: one was Genotype A, one had a mixture of B/C genotypes, and two were untypable (Table 2).

Mutations involved in lamivudine resistance

Sixteen of thirty-five patients (46%) were found to have the rtM204I (YIDD) mutation at the YMDD motif, whilst 12/35 (34%) demonstrated the rtM204V (YVDD) mutation and the remainder had at least one acquired mutation that was not present at the baseline and was known to confer resistance against lamivudine. (Figure 1). These included various combinations of mutations at rtA181T, rtL80V/I and rtL187I.

Table 1 Baseline characteristics of all patients

	Group IA n = 13 (37%)	Group IB n = 12 (34%)	Group II n = 10 (29%)	All patients n = 35 (100%)
Median age (range)	35 (21-48)	34 (20-45)	52 (42-68)	38 (20-68)
Male (%)	9 (69)	11 (92)	10 (100)	30 (86)
Chinese ethnicity (%)	13 (100)	11 (92)	10 (100)	34 (97)
Median (range) baseline ALT, U/L	28 (16-58)	136 (78-1 124)	87 (33-761)	74(16-1 124)
Median (range) baseline HBV DNA, Meg/mL	294 (120–1 680)	253 (38–616)	291 (20–786)	280 (20–1 680)
Median baseline CPT score	NA	NA	7.0 (5-13)	NA
Median (range) duration of lamivudine at emergence of genotypic resistance, wk	160 (35-198)	110 (42-212)	62 (36-120)	143 (35-212)
Follow-up after genotypic resistance, wk	96 (48-220)	124 (26-208)	64 (34-102)	102 (26-220)
Number (%) with phenotypic resistance	3 (23)	9 (75)	6 (60)	18 (51)

Table 2 Comparison between patients with and without phenotypic resistance in univariate analysis

	Patients with phenotypic resistance n = 18	Patients without phenotypic resistance n = 17	P
Median (range) age (yr)	34 (21-60)	37(20-68)	0.95
Male (%)	17 (94)	13 (76)	0.16
Chinese (%)	17/18 (94)	17/17 (100)	0.28
Genotype (B:C:others)	7B/ 7C/ 2 others	11B /6C/ 2 others	0.56
Type of mutation (rtM204I:rtM204V:others)	12:2:4	4:10:3	0.074
Median (range) baseline ALT level, U/L	96 (42-1 124)	40 (16-143)	0.018
ALT level at emergence of genotypic resistance, U/L	48 (22-82)	36 (24-68)	0.36
Successful HBeAg seroconversion (%)	12	17.7	0.43
Median (range) baseline HBV DNA, Meq/mL	249 (20-788)	336 (20-1 680)	0.17
Median (range) peak HBV DNA after emergence of resistance, pg/mL	186 (8.8-1 064)	314 (9-3 920)	0.33
Median (range) duration of lamivudine at onset of resistance, wk	88 (35-212)	124 (36-202)	0.16
Median (range) duration of follow up after resistance, wk	124 (52-204)	102 (26-220)	0.29
Median (range) baseline CPT Score for cirrhotic patients, n = 10	(n = 6) 8 (5-13)	(n = 4) 7 (5-9)	0.038

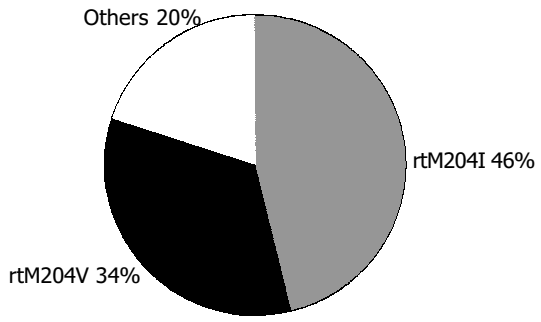

Figure 1 Distribution of the type HBV DNA mutations in the polymerase gene.

Clinical resistance

(1) Group IA (non-cirrhotic with normal baseline ALT), *n* = 13 (Figure 2A).

Only three patients (23%) developed abnormal ALT after the emergence of genotypic resistance at median follow-up of 96 (range: 48-220 wk). The changes in ALT in the group between the four timepoints were non-significant. All three patients normalized their ALT after a median duration of 6 (range: 4-12 wk), one of whom achieved HBeAg seroconversion; (2) Group IB (non-cirrhotic with abnormal baseline ALT), *n* = 12 (Figure 2B).

Normalization of ALT levels 6 mo after starting lamivudine was seen in all patients (Wilcoxon signed Rank *P* = 0.012). However, with the emergence of genotypic resistance, 9 out of 12 patients (75%) developed abnormal ALT (Wilcoxon signed Rank *P* = 0.017) after median follow-up of 124 (range: 26-208) wk. Two patients registered peak ALT elevations of more than 10 times upper limit of normal, one of whom had the highest ALT (>17 X ULN) at the baseline. ALT level at timepoints 3 and 4 were similar to the baseline level at timepoint 1 (*P*>0.05). Five of the nine (56%) patients normalized their ALT after a median duration of 8 (range: 4-14) wk, two of whom achieved HBeAg seroconversion.

(3) Group II (patients with cirrhosis), *n* = 10 (Figure 3).

Six patients (60%) had abnormal ALT at the baseline (Figure 3A). All patients showedALT improvement after treatment with lamivudine (Wilcoxon signed Rank Test, *P* = 0.015). With the emergence of genotypic resistance, abnormal ALT elevations occurred in five patients (50%) after a median follow-up of 64 (range: 34-102) wk. The development of abnormal ALT at timepoint 3 compared to timepoint 2 was statistically significant (*P* = 0.017). When ALT levels among timepoints 1, 3, and 4 were compared, no significant difference was found. All the five patients with flares of ALT normalized their ALT level after a median duration

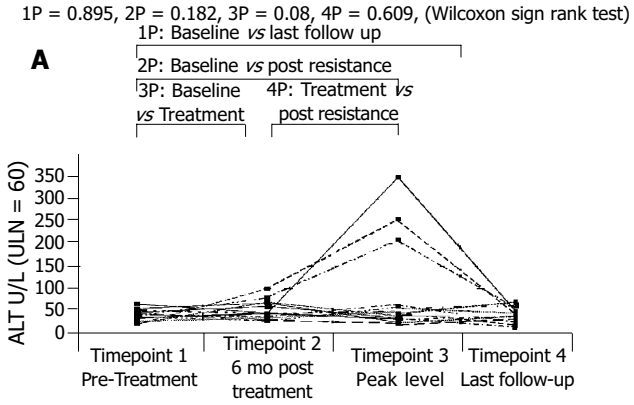

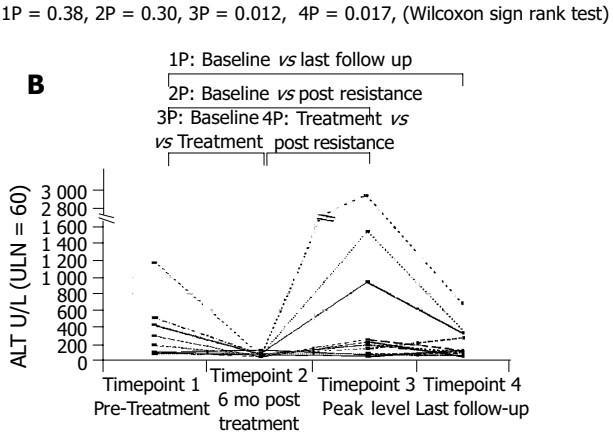

Figure 2 ALT of Group IA and IB. **A**: ALT of Group IA: non cirrhotic patients with normal pre-treatment ALT (*n* = 13); **B:** ALT of Group IB: non-cirrhotic patients with elevated pre-treatment ALT (*n* = 12).

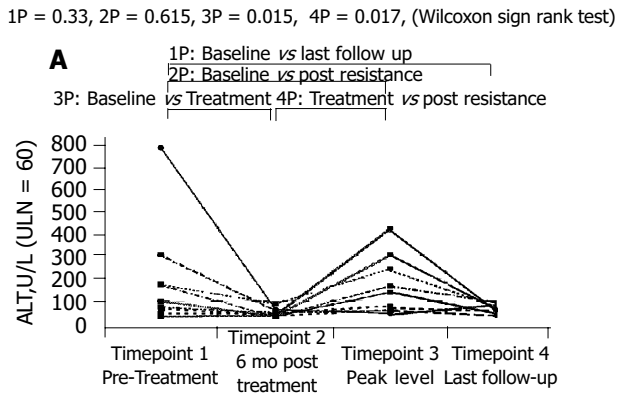

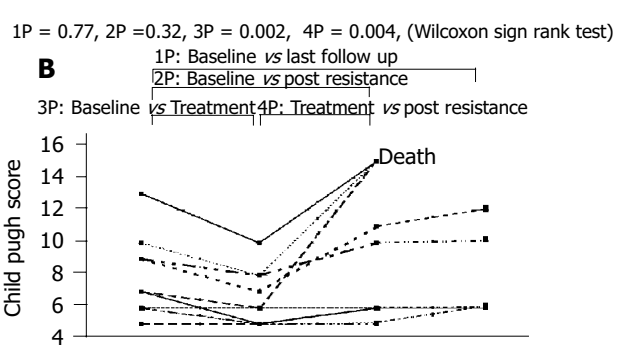

Figure 3 ALT and CPT of Cirrhotic patients. **A:** ALT of Cirrhotic patients; **B:** CPT of Cirrhotic patients.

of 4 (range: 4-8 wk).

CPT score analysis showed a similar trend in this group (Figure 3B). The CPT score at timepoint 2 showed significant improvement compared to timepoint 1 (Wilcoxon Signed Rank, $P = 0.016$) but deteriorated with the emergence of resistance at timepoint 3 (Wilcoxon Signed Rank, $P = 0.041$). No statistical significance was detected between CPT Score at timepoint 1 and timepoint 3 as well as between timepoints 1 and 4, with follow-up median duration of 64 wk after resistance (range 34-102). Three patients died from liver decompensation at 42, 78, and 96 wk, respectively after resistance developed, two of whom had the poorest pretreatment CPT score. None of the patients achieved HBeAg seroconversion although 40% (4 out of 10) were eAg negative Hepatitis B cirrhotics to begin with.

Factors that determine clinical severity of lamivudine-resistant mutants

At univariate analysis, only the baseline ALT in non-cirrhotics and the baseline CPT score in cirrhotics were predictive of phenotypic resistance ($P = 0.018$ and $P = 0.038$, respectively, Table 2).

Multivariate analysis was then performed with these two parameters. Using logistic regression analysis, the baseline ALT was shown to be significantly predictive of phenotypic resistance (OR 9.6, 95%CI 1.2-4.0, $P = 0.03$). The peak ALT level post resistance also correlated with the baseline ALT. (Spearman's $\rho = 0.441$, $P = 0.027$).

Similarly for CPT score, regression analysis showed baseline CPT score to be predictive of phenotypic resistance in terms of deterioration in CPT score after resistance ($P = 0.022$). Every additional CPT score at baseline predicts an additional 1.19 CPT score after resistance ($B = 1.19$, 95% CI: 0.235-2.15). Expectedly, peak CPT score after resistance showed strong correlation with baseline CPT score (Spearman's $\rho = 0.785$, $P = 0.007$).

Interestingly, neither the pretreatment nor the peak HBV DNA post-resistance were shown to be predictive of phenotypic resistance although the peak HBV DNA level post-resistance was noted to correlate with the pretreatment HBV DNA level (Spearman's $\rho = 0.414$, $P = 0.013$).

DISCUSSION

The most important finding of our study was that the course of lamivudine-resistant hepatitis B was generally benign except in cirrhotics. In Group IA (patients with normal baseline ALT), despite the emergence of lamivudine resistance, most (10 of 13, 77%) of the patients maintained normal ALT up to median follow-up of 96 wk. In addition, all three patients in Group IA who developed elevated ALT subsequently normalized their ALT level on follow-up. In Group IB (patients with persistently elevated baseline ALT), lamivudine normalized ALT during therapy, but upon development of resistance, ALT increased in 75% of patients. However, only 4/12 (33%) of patients continued to have persistently elevated ALT on follow-up. Finally, in Group II (patients with decompensated cirrhosis), there was normalization of ALT levels and reduction in CPT scores during lamivudine therapy, but both parameters increased to baseline levels once lamivudine resistance occurred.

Thus the clinical picture of lamivudine-resistant hepatitis B virus demonstrates a spectrum of disease from normal ALT to hepatitis B flares and liver decompensation. Our findings suggest that at the peak of abnormality, the clinical picture correlates most closely with baseline clinical characteristics of the patient. On subsequent follow-up however, the course was relatively benign except for cirrhotics.

The inclusion of patients with normal baseline ALT (Group 1A) provided an invaluable group of patients for studying the pathogenic effects of lamivudine-resistant Hepatitis B virus. This group of patients were treated with lamivudine only because they were part of the Asian Lamivudine Multicenter Trial. Yet on developing lamivudine resistance, most of them retained normal ALT in their follow up. Even in the few who had transient abnormal ALT, these universally resolved in contrast to those with abnormal baseline ALT or liver function. This suggests that lamivudine-resistant virus may not be more pathogenic than the wildtype virus. Although further study with larger number of patients is needed to confirm this, such study would be difficult to perform as clinical guidelines from America, Europe and Asia did not recommend lamivudine treatment for patients with normal baseline ALT levels[20-22].

Our findings also fit the known biology of HBV. Clinical disease in chronic Hepatitis B is a complex interplay between the virus and the immune system. Mutations in the YMDD motif confer resistance to lamivudine and allow high viral replication to resume. On the other hand, it is the mutations in the core region that have been most closely associated with increased immune responses to the virus[23].

Our study complements that of Yuen, who concluded that the majority of patients with lamivudine-resistant hepatitis B flares recovered except some with cirrhosis[24]. In our patients with abnormal baseline ALT, although 75% had elevation of ALT at any time, only 33% had persistently elevated ALT on prolonged follow-up suggesting that the final clinical outcome in those without cirrhosis generally shows a benign course. Similarly, Lok[25] also concluded that lamivudine-resistance led to good outcomes in non-cirrhotics, but this cannot be extrapolated to cirrhotics. Cirrhotic patients, having poorer liver reserve, are less able to tolerate the further necroinflammation that may resume with the return of viral replication in those phenotypically susceptible. Our cohort of cirrhotic patients (Group II) developed decompensation following lamivudine resistance, resulting in death in 30% of patients. These findings concur with the results of NUCB 4006 (CALM study)[26]. In this landmark study, lamivudine therapy in cirrhotic patients proved to provide significant benefit in terms of reduced progression of liver disease and reduction in hepatocellular carcinoma. Patients who developed lamivudine-resistant mutations showed a reduction in this endpoint efficacy, as we have shown, developing progression of their liver disease. Nevertheless, they still had less clinical endpoints than patients on placebo. Unlike the CALM study which enrolled patients with early and non-decompensated cirrhosis, most of the cirrhotic patients in our study had decompensated liver disease and had poor outcomes when lamivudine resistance developed.

We acknowledge the following limitations of our study. Firstly, we did not have histological confirmation of progression of liver disease. However, abnormal ALT has been accepted as a good surrogate marker for necroinflammation of the liver[27]. In addition, an increase in CPT score clearly signifies progressive liver damage and deterioration. Consequently, we feel that the lack of histological data does not detract from the findings of this study. Although our sample size was relatively small, the spectrum of patients included in our study is typical of those seen in a normal hepatology practice or hospital, rather than the pre-selected patients included in clinical trials. In addition, the findings in general are also observed in larger clinical studies. Our study also includes patients with normal ALT and decompensated cirrhosis, which have not been previously described. The duration of follow-up in our series was 102 wk, longer than in most other published studies[8,12,24].

We believe the results of our study could have two therapeutic implications. Firstly, the clinical severity of lamivudine-resistant HBV resembled the baseline phenotype, although on follow-up, the vast majority of the increased ALT normalized. Recent updated American guidelines for Hepatitis B recommends options of continuing or stopping lamivudine or converting to other antiviral drug when lamivudine resistance develops, depending on the patient's clinical state, ALT and HBV DNA levels[20]. Our study suggests that baseline activity can be used as predictive factor in identifying patients who are likely to resume active disease and who thus, should be monitored more closely. Secondly, in patients with poor liver reserve at baseline who developed lamivudine resistance, additional rescue therapy such as adefovir dipivoxil should be instituted early, before clinical deterioration occurred.

In conclusion, the clinical phenotype of patients with genotype resistance to lamivudine resembled the baseline clinical phenotype, suggesting loss of virus suppression and return to the pre-treatment state. Patients with high baseline ALT level or CPT score tended to return to a high ALT level or CPT score once lamivudine resistance occurred. With time, there was normalization of raised ALT levels in those with non-cirrhotic lamivudine resistance. Consequently, in treatment of hepatitis B, lamivudine therapy need not be stopped prematurely for fear of developing more pathogenic lamivudine-resistant strains. However, patients with cirrhosis, particularly decompensated cirrhosis, need to be monitored closely and adefovir dipivoxil started expediently when resistance occurs.

ACKNOWLEDGMENTS

We would like to thank GlaxoSmithkline (Singapore) Private Limited for permission and access to the data for patients in the Asian Multicentre Lamivudine Trial, and Ms. Shen Liang from the Clinical Trials and Epidemiology Research Unit, Singapore Ministry of Health, for statistical support.

REFERENCES

1 **Lai CL,** Chien RN, Leung NW, Chang TT, Guan R, Tai DI, Ng KY, Wu PC, Dent JC, Barber J, Stephenson SL, Gray DF. A one-year trial of lamivudine for chronic hepatitis B. Asia Hepatitis Lamivudine Study Group. *N Engl J Med* 1998; **339**: 61-68

2 **Dienstag JL,** Schiff ER, Wright TL, Perrillo RP, Hann HW, Goodman Z, Crowther L, Condreay LD, Woessner M, Rubin M, Brown NA. Lamivudine as initial treatment for chronic hepatitis B in the United States. *N Engl J Med* 1999; **341**: 1256-1263

3 **Villeneuve JP,** Condreay LD, Willems B, Pomier-Layrargues G, Fenyves D, Bilodeau M, Leduc R, Peltekian K, Wong F, Margulies M, Heathcote EJ. Lamivudine treatment for decompensated cirrhosis resulting from chronic hepatitis B. *Hepatology* 2000; **31**: 207-210

4 **Leung NW,** Lai CL, Chang TT, Guan R, Lee CM, Ng KY, Lim SG, Wu PC, Dent JC, Edmundson S, Condreay LD, Chien RN. Extended lamivudine treatment in patients with chronic hepatitis B enhances hepatitis B e antigen seroconversion rates: results after 3 years of therapy. *Hepatology* 2001; **33**: 1527-1532

5 **Lai CL,** Dienstag J, Schiff E, Leung NW, Atkins M, Hunt C, Brown N, Woessner M, Boehme R, Condreay L. Prevalence and clinical correlates of YMDD variants during lamivudine therapy for patients with chronic hepatitis B. *Clin Infect Dis* 2003; **36**: 687-696

6 **Fu L,** Cheng YC. Role of additional mutations outside the YMDD motif of hepatitis B virus polymerase in L(-)SddC (3TC) resistance. *Biochem Pharmacol* 1998; **55**: 1567-1572

7 **Melegari M,** Scaglioni PP, Wands JR. Hepatitis B virus mutants associated with 3TC and famciclovir administration are replication defective. *Hepatology* 1998; **27**: 628-633

8 **Liaw YF,** Chien RN, Yeh CT, Tsai SL, Chu CM. Acute exacerbation and hepatitis B virus clearance after emergence of YMDD motif mutation during lamivudine therapy. *Hepatology* 1999; **30**: 567-572

9 **Kim JW,** Lee HS, Woo GH, Yoon JH, Jang JJ, Chi JG, Kim CY. Fatal submassive hepatic necrosis associated with tyrosine-methionine-aspartate-aspartate-motif mutation of hepatitis B virus after long-term lamivudine therapy. *Clin Infect Dis* 2001; **33**: 403-405

10 **Leung NW,** Chan HL, Sung JJ. How good is 1 year lamivudine treatment in HBeAg positive chronic hepatitis B patients with elevated ALT levels? Experience from a regional hospital.[ABSTRACT]. *J Gastroenterol Hepatol* 2001; **16** (Suppl): 212

11 **Kobayashi S,** Ide T, Sata M. Detection of YMDD motif mutations in some lamivudine-untreated asymptomatic hepatitis B virus carriers. *J Hepatol* 2001; **34**: 584-586

12 **Yuen MF,** Sablon E, Hui CK, Yuan HJ, Decraemer H, Lai CL. Factors associated with hepatitis B virus DNA breakthrough in patients receiving prolonged lamivudine therapy. *Hepatology* 2001; **34** (4 Pt 1): 785-791

13 **Mutimer D,** Pillay D, Dragon E, Tang H, Ahmed M, O'Donnell K, Shaw J, Burroughs N, Rand D, Cane P, Martin B, Buchan S, Boxall E, Barmat S, Gutekunst K, McMaster P, Elias E. High pre-treatment serum hepatitis B virus titre predicts failure of lamivudine prophylaxis and graft re-infection after liver transplantation. *J Hepatol* 1999; **30**: 715-721

14 **Zollner B,** Petersen J, Schroter M, Laufs R, Schoder V, Feucht HH. 20-fold increase in risk of lamivudine resistance in hepatitis B virus subtype adw. *Lancet* 2001; **357**: 934-935

15 **Lok AS,** Hussain M, Cursano C, Margotti M, Gramenzi A, Grazi GL, Jovine E, Benardi M, Andreone P. Evolution of hepatitis B virus polymerase gene mutations in hepatitis B e antigen-negative patients receiving lamivudine therapy. *Hepatology* 2000; **32**: 1145-1153

16 **Liaw YF,** Leung NW, Chang TT, Guan R, Tai DI, Ng KY, Chien RN, Dent J, Roman L, Edmundson S, Lai CL. Effects of extended lamivudine therapy in Asian patients with chronic hepatitis B. Asia Hepatitis Lamivudine Study Group. *Gastroenterology* 2000; **119**: 172-180

17 **Krajden M,** Minor J, Cork L, Comanor L. Multi-measurement method comparison of three commercial hepatitis B virus DNA quantification assays. *J Viral Hepat* 1998; **5**: 415-422

18 **Stuyver LJ,** Locarnini SA, Lok A, Richman DD, Carman WF,

Dienstag JL, Schinazi RF. Nomenclature for antiviral-resistant human hepatitis B virus mutations in the polymerase region. *Hepatology* 2001; **33**: 751-757

19 **Lindh M,** Gonzalez JE, Norkrans G, Horal P. Genotyping of hepatitis B virus by restriction pattern analysis of a pre-S amplicon. *J Virol Methods* 1998; **72**: 163-174

20 **Lok AS**, McMahon BJ. Chronic hepatitis B: update of recommendations. *Hepatology* 2004; **39**: 857-861

21 **de Franchis R,** Hadengue A, Lau G, Lavanchy D, Lok A, McIntyre N, Mele A, Paumgartner G, Pietrangelo A, Rodes J, Rosenberg W, Valla D. EASL International Consensus Conference on Hepatitis B. 13-14 September, 2002 Geneva, Switzerland. Consensus statement (long version). *J Hepatol* 2003; **39** (Suppl 1): S3-25

22 **Liaw YF,** Leung N, Guan R, Lau GK, Merican I. Asian-Pacific consensus statement on the management of chronic hepatitis B: an update. *J Gastroenterol Hepatol* 2003; **18**: 239-245

23 **Koziel MJ.** The immunopathogenesis of HBV infection. *Antivir Ther* 1998; **3** (Suppl 3): 13-24

24 **Yuen MF,** Kato T, Mizokami M, Chan AO, Yuen JC, Yuan HJ, Wong DK, Sum SM, Ng IO, Fan ST, Lai CL. Clinical outcome and virologic profiles of severe hepatitis B exacerbation due to YMDD mutations. *J Hepatol* 2003; **39**: 850-855

25 **Lok AS,** Lai CL, Leung N, Yao GB, Cui ZY, Schiff ER, Dienstag JL, Heathcote EJ, Little NR, Griffiths DA, Gardner SD, Castiglia M. Long-term safety of lamivudine treatment in patients with chronic hepatitis B. *Gastroenterology* 2003; **125**: 1714-1722

26 **Liaw YF,** Sung JJ, Chow WC, Farrell G, Lee CZ, Yuen H, Tanwandee T, Tao QM, Shue K, Keene ON, Dixon JS, Gray DF, Sabbat J. Lamivudine for patients with chronic hepatitis B and advanced liver disease. *N Engl J Med* 2004; **351**: 1521-1531

27 **Cahen DL,** van Leeuwen DJ, ten Kate FJ, Blok AP, Oosting J, Chamuleau RA. Do serum ALAT values reflect the inflammatory activity in the liver of patients with chronic viral hepatitis? *Liver* 1996; **16**: 105-109

Science Editor Guo SY **Language Editor** Elsevier HK

PO Box 2345, Beijing 100023, China
www.wjgnet.com
wjg@wjgnet.com

ELSEVIER

World J Gastroenterol 2005;11(28):4351-4356
World Journal of Gastroenterology ISSN 1007-9327

Possible mechanism for hepatitis B virus X gene to induce apoptosis of hepatocytes

Sheng-Jun Zhang, Hong-Ying Chen, Zhi-Xin Chen, Xiao-Zhong Wang

Sheng-Jun Zhang, Hong-Ying Chen, Zhi-Xin Chen, Xiao-Zhong Wang, Department of Gastroenterology, Union Hospital of Fujian Medical University, Fuzhou 350001, Fujian Province, China
Supported by the Science and Technology Fund of Fujian Province, No. 99-Z-162
Correspondence to: Xiao-Zhong Wang, Department of Gastroenterology, Union Hospital of Fujian Medical University, Fuzhou 350001, Fujian Province, China. drwangxz@pub6.fz.fj.cn
Telephone: +86-591-83357896-8482
Received: 2004-11-23 Accepted: 2004-11-26

Abstract

AIM: To investigate the possible mechanism for HBV X gene to induce apoptosis of hepatocyte HL-7702 cells.

METHODS: HBV X gene eukaryon expression vector pcDNA3-X was established and transfected into HL-7702 cells by lipid-mediated transfection, including transient and stable transfection. Positive clones were screened by incubating in the selective medium with 600 μg/mL G418 and named HL-7702/HBV-encoded X protein (HBx) cells. The expressions of Fas/FasL, Bax/Bcl-2, and c-myc mRNA were measured by semi-quantitative RT-PCR in HL-7702/HBx and control group, respectively.

RESULTS: RT-PCR analysis confirmed that HBV X gene was transfected into HL-7702 cells successfully. By semi-quantitative RT-PCR analysis, Bax and c-myc mRNA levels in HL-7702/HBx cells of transient transfection were significantly higher than those in control, FasL and c-myc mRNA levels in HL-7702/HBx cells of stable transfection were significantly higher than those in control, whereas the Bcl-2 mRNA levels in HL-7702/HBx cells of transient and stable transfection were significantly lower than those in control.

CONCLUSION: HBV X gene may promote the apoptosis of hepatocytes by regulating the expressions of Fas/FasL, Bax/Bcl-2, and c-myc gene in a dose-dependent manner.

Key words: Hepatitis B virus; X gene; Apoptosis; Gene expression

Zhang SJ, Chen HY, Chen ZX, Wang XZ. Possible mechanism for hepatitis B virus X gene to induce apoptosis of hepatocytes. *World J Gastroenterol* 2005; 11(28): 4351-4356
http://www.wjgnet.com/1007-9327/11/4351.asp

INTRODUCTION

HBV X gene is the smallest open reading frame of HBV, codes for a 16.5-ku protein (X protein, HBx) consisted of 154 amino acids. Previous studies showed that HBV X gene and HBx modulate apoptosis of hepatocytes and play an important role in HBV-associated liver disease[1]. HBV X gene could inhibit apoptosis of hepatocytes in several ways and contribute to the generation of hepatocellular carcinoma (HCC). It was reported that HBx displays a pro-apoptotic function and induces apoptosis of liver cells[2-5]. But the relationship between this function of HBx and HBV-associated liver disease remains obscure. So far no molecular mechanism or target for HBx-mediated apoptosis has been clearly elucidated. In this study, we transfected X gene into hepatocyte line HL-7702 by transient and stable transfection. Thus, cell lines that expressed different levels of HBx were established. To explore the possible mechanism for HBx to modulate apoptosis, we investigated the effect of HBx on expressions of apoptosis-associated genes in hepatocytes. The expressions of Fas/FasL, Bax/Bcl-2, and c-myc mRNA were measured by semi-quantitative RT-PCR in HL-7702/HBx and control group, respectively.

MATERIALS AND METHODS

Materials

PcDNA3 expression vector and HBV X gene eukaryon expression vector pcDNA3-X were previously constructed and stored[6]. The normal hepatic cell line HL-7702 was provided by Cell Bank of Chinese Academy of Sciences. Reverse transcription system, DNA purification system, G418, and TransFast™ transfection reagent were obtained from Promega Biotech. Total RNA isolation kit was purchased from Jingmei Biotech Company. PCR primers were synthesized by Shanghai Biotechnology Company. RPMI-1640 was bought from Gibco BRL Company.

Transfection and expression of HBV X gene in HL-7702

Cell culture and DNA transfection HL-7702 cells were cultured in RPMI-1640 supplemented with 20% FBS. The cells in logarithmic growth were separately transfected with pcDNA3-X and pcDNA3 plasmids using lipid-mediated transfection technique according to the protocol for transient or stable transfection of adherent cells. About 2 mL transfection mixture containing 5 μg plasmid DNA, 15 μL TransFast™ reagent and RPMI-1640 was added to a 25-mm^2 culture plate. At 48 h post-transfection, all cells were trypsinized. Cells for transient transfection were

transferred to a 25-mm^2 culture plate and cultured in RPMI-1640 supplemented with 20% FBS for 72 h. Cells used for stable transfection were cultured in the selective medium with 600 μg/mL G418 for 2 wk. Then, drug-resistant individual clones were isolated and transferred to a 96-well plate for further amplification in the presence of selective medium. Cells that transiently transfected with pcDNA3-X and pcDNA3 were named as HL-7702/HBx^T and HL-7702/pcDNA3^T, respectively. Cells that stably transfected with pcDNA3-X and pcDNA3 were named as HL-7702/HBx^S and HL-7702/pcDNA3^S, respectively. HL-7702 was used as control.

Determination of X gene expression by RT-PCR analysis Total RNA was extracted separately from the cells of each group with a RNA isolation kit, and RT-PCR was carried out. β-Actin served as an internal control, 2 μL of RT product was used as template, X gene and β-actin were amplified together. The sequence of β-actin primers was 5-'GGCATCGTGATGGACTCCG-3' and 5'-GCTGGAAGGTGGACAGCGA-3'. The sequence of X gene primers was: 5'-ATGCAAGCTTATGGCTGCT-AGGCTGTACTG-3' and 5'-TGCGAATTCTTAGGCA-GAGGTGAAAAAGTTG-3'. The expected amplification fragment length of β-actin and X gene was 607 and 467 bp, respectively. PCR was carried out as follows: pre-denaturation at 95 ℃ for 5 min, 32 amplification cycles (denaturation at 94 ℃ for 35 s, annealing at 65 ℃ for 35 s, and extension at 72 ℃ for 1 min), and a final extension at 72 ℃ for 7 min.

Effect of HBV X gene on apoptosis-associated gene mRNA expression in hepatocytes by transient and stable transfection

RT-PCR for Fas/FasL, Bax/Bcl-2, and c-myc Total RNA was extracted from HL-7702/HBx, HL-7702/PcDNA3, and HL-7702 according to the RNA isolation kit instructions. The content and purity of total RNA were determined by spectrophotography. RNA (260/280 was between 1.8 and 2.0) was further used for reverse transcription reaction, which was carried out according to the reverse transcription kit instructions. Two microgrammes of total RNA was used in each reverse transcription reaction and the final volume was 20 μL. Glyceraldehyde-3-phosphate dehydrogenase (GAPDH) was used as an internal control and amplified together with target genes. PCR was performed in 50 μL reaction volume containing 5 μL 10×PCR buffer, 5 μL 2 mmol/L $MgCl_2$, 1 μL 10 mmol/L dNTP, 1 μL 20 pmol/μL target gene sense and anti-sense primers, 0.4 μL 12.5 pmol/μL GAPDH primer pair, 2 μL RT product, 1.5 U *Taq* DNA polymerase. The specific sets of primers and the target gene amplification conditions are shown in Table 1. All initial denaturations were at 94 ℃ for 5 min. Finally an additional extension step at 72 ℃ for 7 min was done.

Result determination The PCR products were electrophoresed on 2% agarose gel and visualized by ethidium bromide staining. Bioimaging system was used to detect the densities of bands of the PCR products. The ratio of target gene density to GAPDH density was respectively used to represent the relative expression level of Fas/FasL, Bax/Bcl-2, and c-myc mRNA. The semi-quantitative detection was analyzed five times.

Statistical analysis

All data were expressed as mean±SE. The significance for the difference between the groups was assessed with SPSS 10.0 by one-way ANOVA. $P<0.05$ was considered statistically significant.

RESULTS

Expression of HBV X gene mRNA in HL-7702 cells

HBV X gene mRNA was detected in HL-7702/HBx^T and HL-7702/HBx^S cells by RT-PCR. The expected band was found between 400 and 500 bp in both kinds of transfected cells (Figure 1). The relative level of HBV X gene mRNA in HL-7702/HBx^T was higher than that in HL-7702/HBx^S by about 2.5-folds (0.815±0.013 *vs* 0.308±0.021), indicating that HBV X gene mRNA could be expressed in HL-7702 after transient or stable transfection, and cell lines that expressed different levels of HBx were established.

Table 1 Primer sequences for PCR and amplification conditions for each target gene

Primer	Sequence	Amplification conditions	Product (base)
Fas	5'-TCAGTACGGAGTTGGGGAAG-3' 5'-CAGGCCTTCCAAGTTCTGAG-3'	Denaturation at 94 ℃ for 45 s, annealing at 63 ℃ for 30 s and synthesizing at 72 ℃ for 1 min for 35 cycles	207
FasL	5'-GATGATGGAGGGGAAGATGA-3 5'-TGGAAAGAATCCCAAAGTGC-3'	Denaturation at 94 ℃ for 45 s, annealing at 58 ℃ for 30 s and synthesizing at 72 ℃ for 1 min for 30 cycles	203
Bax	5'-TTTGCTTCAGGGTTTCATCC-3' 5'-CAGTTGAAGTTGCCGTCAGA-3'	Denaturation at 94 ℃ for 45 s, annealing at 58 ℃ for 30 s and synthesizing at 72 ℃ for 1 min for 30 cycles	246
Bcl-2	5'-CGACGACTTCTCCCGCCGCTACCGC-3' 5'-CCGCATGCTGGGGCCGTACAGTTCC-3'	Denaturation at 94 ℃ for 45 s, annealing at 67 ℃ for 30 s and synthesizing at 72 ℃ for 1 min for 30 cycles	318
c-myc	5'-TTCGGGTAGTGGAAAACCAG-3' 5'-CAGCAGCTCGAATTTCTTCC-3'	Denaturation at 94 ℃ for 45 s, annealing at 58 ℃ for 30 s and synthesizing at 72 ℃ for 1 min for 28 cycles	203
GAPDH	5'-ACCACAGTCCATGCCATCAC-3' 5'-TCCACCACCCTGTTGCTGTA-3'	Changed according to different target genes	452

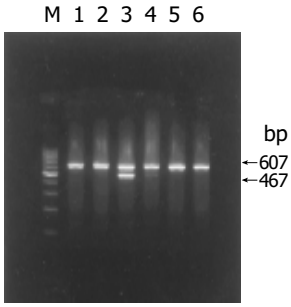

Figure 1 RT-PCR analysis of HBV X gene mRNA expression in HL-7702. M: 100-bp DNA ladder; lane 1: HL-7702^{T}; lane 2: HL-7702/pcDNA3^{T}; lane 3: HL-7702/HBx^{T}; lane 4: HL-7702/HBx^{S}; lane 5: HL-7702/pcDNA3^{S}; lane 6: HL-7702^{S}.

Effects of HBV X gene on apoptosis-associated genes mRNA expression in HL-7702 by transient transfection

Fas/FasL mRNA As shown in Figures 2A, B, and 3A, both Fas mRNA and FasL mRNA were expressed in HL-7702 of each group. Both of their expression levels had no significant differences among the three groups, indicating that HBx had no effect on Fas and FasL expression in normal hepatocytes though it was expressed at a relatively high level after transient transfection.

Bcl-2/Bax mRNA Both Bax and Bcl-2 mRNA were expressed in HL-7702 after transient transfection (Figures 2C, D, and 3B). As it could be seen from Figures 2C, 3B, and C, the expression level of Bax mRNA in HL-7702/HBx^{T} was higher than that in HL-7702 or in HL-7702/pcDNA3^{T} (0.614±0.014 *vs* 0.536±0.009 or 0.494±0.015, $P<0.01$). The expression level of Bcl-2 mRNA in HL-7702/HBx^{T} was lower than that in HL-7702 or in HL-7702/pcDNA3^{T} (0.811±0.010 *vs* 1.243±0.033, $P<0.01$) (0.811±0.010 *vs* 0.901±0.014, $P<0.05$). There was also a significant difference in Bcl-2 mRNA expression level between the two control groups (0.901±0.014 *vs* 1.243±0.033, $P<0.01$; Figures 2D, 3B, and D). The data indicated that HBx could induce the pro-apoptotic factor Bax expression in normal hepatocytes and inhibit the anti-apoptotic factor Bcl-2 expression.

c-myc mRNA c-myc mRNA was expressed in both HL-7702 and HL-7702/pcDNA3, and there was no significant difference between them. The expression level of c-myc mRNA was significantly higher in HL-7702/HBx^{T}, suggesting that HBx was able to promote the c-myc expression in normal hepatocytes (0.719±0.020 *vs* 0.569±0.026, $P<0.01$, 0.719±0.020 *vs* 0.630±0.012, $P<0.05$; Figures 2E and 3C).

Effects of HBV X gene on apoptosis-associated gene mRNA expression in HL-7702 by stable transfection

Fas/FasL mRNA The expression levels of Fas mRNA had no significant difference among the three groups (Figures 4A and 5A). There was no significant difference in FasL mRNA expression between HL-7702 and HBV X gene expressing stable cell line HL-7702/HBx^{S}. The expression of FasL in HL-7702/HBx^{S} was significantly higher than that in HL-7702/pcDNA3^{S} (0.261±0.043 *vs* 0.217±0.012, $P<0.01$), suggesting that HBx at a low level could improve the FasL expression, which was different from the effect of HBx at a relatively higher level as shown in the former part (Figures 4B, 5A, and B).

Bax/Bcl-2 mRNA HBV X gene stably expressed in HL-7702/HBx^{S} seemed to have no effect on Bax mRNA expression (Figures 4C, 5B, and C). The expression level of Bcl-2 mRNA had no significant difference between the

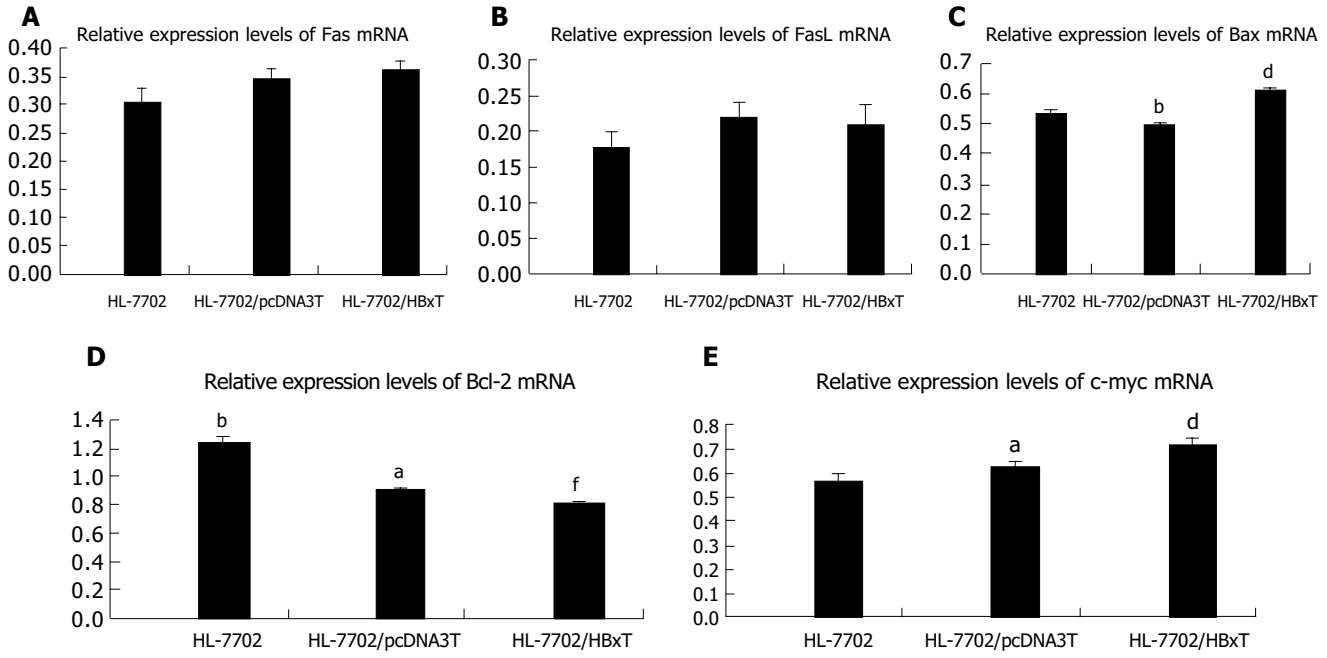

Figure 2 Relative expression levels of apoptosis-associated gene mRNA in HL-7702 of different transiently transfected groups assessed by RT-PCR. **A**: Relative Fas mRNA expression levels; **B**: relative FasL mRNA expression levels; **C**: relative Bax mRNA expression levels; **D**: relative Bcl-2 mRNA expression levels; **E**: relative c-myc mRNA expression levels. $^{a}P<0.05$ *vs* HL-7702/HBx^{T}, $^{b}P<0.01$ *vs* HL-7702/HBx^{T}, $^{d}P<0.01$ *vs* HL-7702, $^{f}P<0.01$ *vs* HL-7702/pcDNA3T, $P>0.05$ between random two groups.

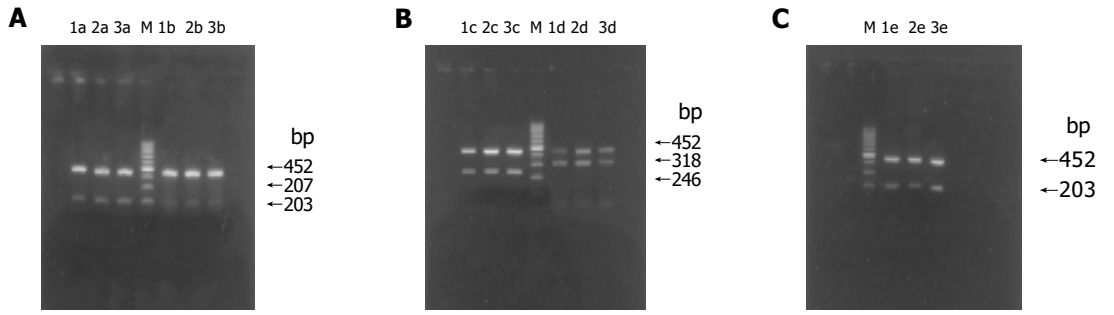

Figure 3 RT-PCR results of apoptosis-associated gene mRNA expression in HL-7702 of different transiently transfected groups. **A**: RT-PCR results of Fas/FasL mRNA expression; **B**: RT-PCR results of Bax/Bcl-2 mRNA expression; **C**: RT-PCR results of c-myc mRNA expression; M: 100-bp DNA ladder; lane 1: HL-7702; lane 2: HL-7702/pcDNA3^{T}; lane 3: HL-7702/HBx^{T}; a: Fas; b: FasL; c: Bax; d: Bcl-2; e: c-myc.

two control groups, HL-7702 and HL-7702/pcDNA3^{S}, but it was lower in HL-7702/HBx^{S} (0.300±0.028 *vs* 0.498±0.035, $P<0.01$; 0.300±0.028 *vs* 0.420±0.032, $P<0.05$; Figures 4D, 5B, and D), suggesting that HBx could downregulate Bcl-2 expression in normal hepatocytes.

c-myc mRNA Similar to the effect of HBV X gene transient transfection, c-myc was expressed in both HL-7702 and HL-7702/pcDNA3^{S}, and there was no significant difference between them. The expression level of c-myc mRNA was significantly higher in HL-7702/HBx^{S}, suggesting that even a low level of HBx was able to upregulate the c-myc expression in normal hepatocytes (0.603±0.035 *vs* 0.449±0.023 or 0.461±0.022, $P<0.01$; Figures 4E and 5C).

DISCUSSION

HBV infection is a major cause of chronic hepatitis, cirrhosis, and hepatocellular carcinoma and accounts for one million deaths annually. HBx is a multifunctional protein that is implicated in the pathogenesis of HBV-associated liver disease by regulating gene transcription, causing cell proliferation, suppressing DNA repair and inducing cell death[7]. The role of HBx in carcinogenesis and its transactivation function have been well documented[8]. The role of HBx in liver cell proliferation and apoptosis is still controversial. A number of studies have revealed that HBx exert dual activity on cell apoptosis[9,10].

On the one hand, HBx has an anti-apoptosis function in different ways and plays an important role in the development of HCC. HBx can activate and upregulate transcription factor NF-κB[11]. It induces Fas-ligand in human hepatoma cells, which contributed to the apoptosis of T cells, thus the hepatoma cells might escape from immune surveillance[12]. There is evidence that HBx blocks apoptosis via downregulating expression of Bid in human hepatocellular carcinoma[13]. The distal C-terminal domain of HBx, independent of its

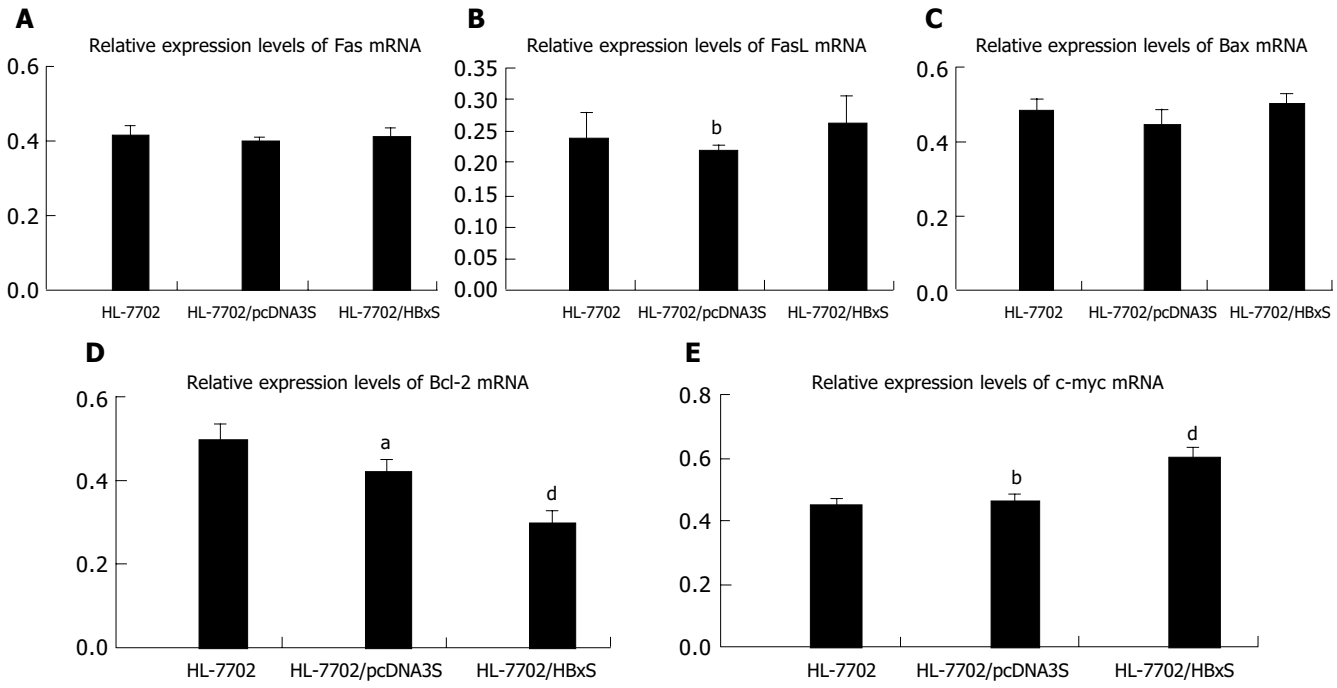

Figure 4 Relative expression levels of apoptosis-associated gene mRNA in HL-7702 of different stably transfected groups assessed by RT-PCR. **A**: Relative Fas mRNA expression levels; **B**: relative FasL mRNA expression levels; **C**: relative Bax mRNA expression levels; **D**: relative Bcl-2 mRNA expression levels; **E**: relative c-myc mRNA expression levels. $^{a}P<0.05$ *vs* HL-7702/HBx^{S}; $^{b}P<0.01$ *vs* HL-7702/HBx^{S}, $^{d}P<0.01$ *vs* HL-7702, $P>0.05$ between random two groups.

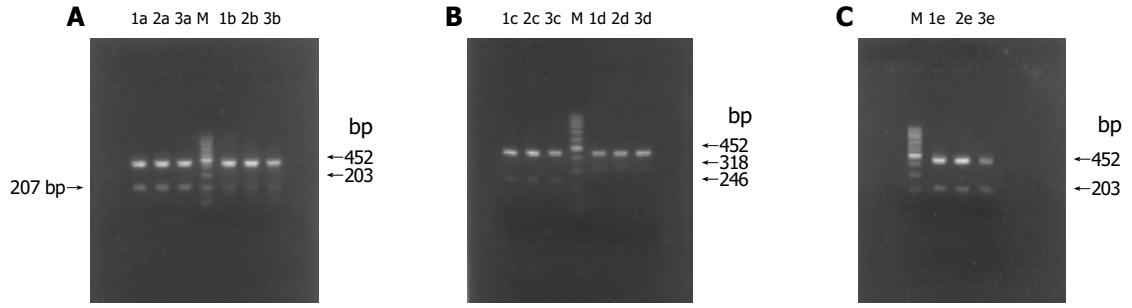

Figure 5 RT-PCR results of apoptosis-associated gene mRNA expression in HL-7702 of different stably transfected groups. **A**: RT-PCR results of Fas/FasL mRNA expression; **B**: RT-PCR results of Bax/Bcl-2 mRNA expression; **C**: RT-PCR results of c-myc mRNA expression; M: 100-bp DNA ladder; lane 1: HL-7702; lane 2: HL-7702/pcDNA3^S; lane 3: HL-7702/HBx^S; a: Fas; b: FasL; c: Bax; d: Bcl-2; e: c-myc.

transactivation activity, is complexed with p53 in the cytoplasm and partially prevents its nuclear entry and ability to induce apoptosis[14]. On the other hand, HBx induces or sensitizes cells to apoptotic killing by pro-apoptotic stimuli[2-5]. The possible mechanisms may include upregulating the expression of Fas and Fas-ligand in hepatocytes[15,16], inducing cell death by causing loss of mitochondrial membrane potential and mitochondrial aggregation at the nuclear periphery[17,18], antagonizing the anti-apoptosis function of the normal level of p53[19], abrogating the apoptosis-inhibitory function of c-FLIP and enhancing the death-inducing signal[20], inducing TNF-α expression and sensitizing liver cells to TNF-α-mediated apoptosis even below the threshold concentration[20-22], affecting the apoptosis control function of Bcl-2 family members by interaction with mitochondria[23]. The above data suggest that the possible mechanism for HBx to regulate cell apoptosis is a "network" implicated with multiple factors and various pathways, and the exact mechanism remains obscure.

Fas and FasL are regarded as the most important factors that switch on the Fas/FasL-mediated apoptosis. The Bcl-2 family proteins play an important role in modulating cell survival and apoptosis. Bcl-2 and Bax act as an anti-apoptotic factor and a pro-apoptotic factor respectively. The proportion of apoptosis-inducing forces and apoptosis-inhibiting forces determines the cells' response to death-inducing signals and their final fate[24-26]. C-myc, usually acting as a proto-oncogene and exerting a dual activity on cell proliferation and apoptosis, is also involved in apoptosis regulation. We have previously demonstrated that the apoptosis rate in HBx-expressing cells by transient or stable transfection is much higher than that in control groups, suggesting that there is a quantity-effect relationship between HBx expression and apoptosis rate, and that HBx can induce apoptosis in normal hepatocytes, during which the expression level of HBV X gene may play a vital role. This study aimed to investigate the possible mechanism for HBV X gene to induce apoptosis of hepatocytes. Thereby, we established cell models that expressed different levels of HBV X gene by transfecting HBV X gene into HL-7702 through transient and stable transfection, and studied the effect of HBx on the mRNA expression of apoptosis-associated genes.

We found that HBx at a relatively higher level could induce the pro-apoptotic factor Bax expression in normal hepatocytes and inhibit the anti-apoptotic factor Bcl-2 expression, though it had no effect on Fas and FasL expression. However, HBx at a low level could improve FasL expression, while it had no effect on Bax. The data show that HBx may induce the apoptosis of HL-7702 by reinforcing the death signal of Fas-FasL pathway and increasing the proportion of pro-apoptotic forces and anti-apoptotic forces in Bcl-2 family members. The dose of HBx may decide which is the chief pathway. The c-myc expression in HL-7702 significantly increased after transient or stable transfection with X gene expression vector, which is consistent with previous reports[9,27]. C-myc protein could sensitize cells to apoptotic killing in certain conditions, such as during exposure to TNF-α or other factors[28-30]. Thus, c-myc may also act as an important medium in HBx-mediated apoptosis. Su *et al*.[30], found that the combination of HBx and c-myc increases the sensitivity of WT 3T3 cells to TNF-α killing by about 10-fold. They also demonstrated that cell killing by HBx plus TNF-α is suppressed by activation of NF-κB, but can be overridden by a high level of c-myc protein.

Our results show that different levels of HBV X gene expression have different effects on apoptosis-associated gene expression. Wang *et al*.[31], studied the effects of regulatory endoplasmic HBx expression on hepatic cell apoptosis and found that low HBx expression cannot induce apoptosis. Thereby, the effect of HBx on apoptosis may be dose dependent. We hypothesize that there may be a threshold concentration for HBx to induce apoptosis, only that beyond the threshold can exert a pro-apoptosis function. Further studies are needed to confirm it.

In conclusion, HBx may induce apoptosis in part via regulating the expression of apoptosis-associated genes. HBV X gene expression may play a vital role, although the underlying mechanism may be complicated and crisscrossing.

REFERENCES

1 **Birrer RB,** Birrer D, Klavins JV. Hepatocellular carcinoma and hepatitis virus. *Ann Clin Lab Sci* 2003; **33**: 39-54
2 **Terradillos O,** Pollicino T, Lecoeur H, Tripodi M, Gougeon ML, Tiollais P, Buendia MA. p53-independent apoptotic effects of the hepatitis B virus HBx protein *in vivo* and *in vitro*. *Oncogene* 1998; **17**: 2115-2123
3 **Pollicino T,** Terradillos O, Lecoeur H, Gougeon ML, Buendia MA. Pro-apoptotic effect of the hepatitis B virus X gene. *Biomed Pharmacother* 1998; **52**: 363-368

4 **Chirillo P,** Pagano S, Natoli G, Puri PL, Burgio VL, Balsano C, Levrero M. The hepatitis B virus X gene induces p53-mediated programmed cell death. *Proc Natl Acad Sci USA* 1997; **94**: 8162-8167

5 **Shintani Y,** Yotsuyanagi H, Moriya K, Fujie H, Tsutsumi T, Kanegae Y, Kimura S, Saito I, Koike K. Induction of apoptosis after switch-on of the hepatitis B virus X gene mediated by the Cre/loxP recombination system. *J Gen Virol* 1999; **80**(Pt 12): 3257-3265

6 **Chen HY,** Tang NH, Zhang SJ, Chen ZX, Wang XZ. Construction of hepatitis B virus X gene expression vector in eucaryotic cells and its transfection in HL-7702 cells. *Shijie Huaren Xiaohua Zazhi* 2004; **12**: 614-617

7 **Murakami S**. Hepatitis B virus X protein: a multifunctional viral regulator. *J Gastroenterol* 2001; **36**: 651-660

8 **Yoo YG,** Oh SH, Park ES, Cho H, Lee N, Park H, Kim DK, Yu DY, Seong JK, Lee MO. Hepatitis B virus X protein enhances transcriptional activity of hypoxia-inducible factor-1alpha through activation of mitogen-activated protein kinase pathway. *J Biol Chem* 2003; **278**: 39076-39084

9 **Su F,** Schneider RJ. Hepatitis B virus HBx protein sensitizes cells to apoptotic killing by tumor necrosis factor. *Proc Natl Acad Sci USA* 1997; **94**: 8744-8749

10 **Lee S,** Tarn C, Wang WH, Chen S, Hullinger RL, Andrisani OM. Hepatitis B virus X protein differentially regulates cell cycle progression in X-transforming versus nontransforming hepatocyte (AML12) cell lines. *J Biol Chem* 2002; **277**: 8730-8740

11 **Su F,** Schneider RJ. Hepatitis B virus HBx protein activates transcription factor NF-kappaB by acting on multiple cytoplasmic inhibitors of rek-related proteins. *Virol* 1996; **70**: 4558-4566

12 **Shin EC,** Shin JS, Park JH, Kim H, Kim SJ. Express of fas ligand in human hepatoma cell lines: role of hepatitis-B virus X (HBX) in induction of Fas ligand. *Cancer* 1999; **82**: 587-591

13 **Chen GG,** Lai PB, Chan PK, Chak EC, Yip JH, Ho RL, Leung BC, Lau WY. Decreased expression of Bid in human hepatocellular carcinoma is related to hepatitis B virus X protein. *Eur J Cancer* 2001; **37**: 1695-1702

14 **Elmore LW,** Hancock AR, Chang SF, Wang XW, Chang S, Callahan CP, Geller DA, Will H, Harris CC. Hepatitis B virus X protein and p53 tumor suppressor interactions in the modulation of apoptosis. *Proc Natl Acad Sci USA* 1997; **94**: 14707-14712

15 **Yoo YG,** Lee MO. Hepatitis B virus X protein induces expression of Fas ligand gene through enhancing transcriptional activity of early growth response factor. *J Biol Chem* 2004; **279**: 36242-36249

16 **Sejima T,** Miyagawa I. The evaluation of Fas/Fas ligand system in renal cell carcinoma-the effect of preoperative interferon-alpha therapy. *Nippon Hinyokika Gakkai Zasshi* 1999; **90**: 826-832

17 **Shirakata Y,** Koike K. Hepatitis B virus X protein induces cell death by causing loss of mitochondrial membrane potential. *J Biol Chem* 2003; **278**: 22071-22078

18 **Takada S,** Shirakata Y, Kaneniwa N, Koike K. Association of hepatitis B virus X protein with mitochondria causes mitochondrial aggregation at the nuclear periphery, leading to cell death. *Oncogene* 1999; **18**: 6965-6973

19 **Kim H,** Lee H, Yun Y. X-gene product of hepatitis B virus induces apoptosis in liver cells. *J Biol Chem* 1998; **273**: 381-385

20 **Kim KH,** Seong BL. Pro-apoptotic function of HBV X protein is mediated by interaction with c-FLIP and enhancement of death-inducing signal. *EMBO J* 2003; **22**: 2104-2116

21 **Lara-Pezzi E,** Majano PL, Gomez-Gonzalo M, Garcia-Monzon C, Moreno-Otero R, Levrero M, Lopez-Cabrera M. The hepatitis B virus X protein up-regulates tumor necrosis factor alpha gene expression in hepatocyte. *Hepatology* 1998; **28**: 1013-1021

22 **Yi YS,** Park SG, Byeon SM, Kwon YG, Jung G. Hepatitis B virus X protein induces TNF-alpha expression via down-regulation of selenoprotein P in human hepatoma cell line, HepG2. *Biochim Biophys Acta* 2003; **1638**: 249-256

23 **Terradillos O,** de La Coste A, Pollicino T, Neuveut C, Sitterlin D, Lecoeur H, Gougeon ML, Kahn A, Buendia MA. The hepatitis B virus X protein abrogates Bcl-2-mediated protection against Fas apoptosis in the liver. *Oncogene* 2002; **21**: 377-386

24 **Cory S,** Adams JM. The Bcl2 family: regulators of the cellular life-or-death switch. *Nat Rev Cancer* 2002; **2**: 647-656

25 **Gross A,** McDonnell JM, Korsmeyer SJ. BCL-2 family members and the mitochondria in apoptosis. *Genes Dev* 1999; **13**: 1899-1911

26 **Bouillet P,** Strasser A. BH3-only proteins-evolutionarily conserved proapoptotic Bcl-2 family members essential for initiating programmed cell death. *J Cell Sci* 2002; **115**: 1567-1574

27 **Balsano C,** Avantaggiati ML, Natoli G, De Marzio E, Will H, Perricaudet M, Levrero M. Full-length and truncated versions of the hepatitis B virus (HBV) X protein (pX) transactivate the cmyc protooncogene at the transcriptional level. *Biochem Biophys Res Commun* 1991; **176**: 985-992

28 **Juin P,** Hueber AO, Littlewood T, Evan G. c-Myc-induced sensitization to apoptosis is mediated through cytochrome c apoptosis release. *Genes Dev* 1999; **13**: 1367-1381

29 **Juin P,** Hunt A, Littlewood T, Griffiths B, Swigart LB, Korsmeyer S, Evan G. c-Myc functionally cooperates with Bax to induce apoptosis. *Mol Cell Biol* 2002; **22**: 6158-6169

30 **Su F,** Theodosis CN, Schneider RJ. Role of NF-kappaB and myc proteins in apoptosis induced by hepatitis B virus HBx protein. *J Virol* 2001; **75**: 215-225

31 **Wang HP,** Chen XP, He SQ, Ding L. Effects of regulatory endoplasmic HBX expression on hepatic cell apoptosis. *Zhonghua Ganzangbing Zazhi* 2003; **11**: 440

Science Editor Wang XL and Guo SY **Language Editor** Elsevier HK

PO Box 2345, Beijing 100023, China
www.wjgnet.com
wjg@wjgnet.com

ELSEVIER

World J Gastroenterol 2005;11(28):4357-4362
World Journal of Gastroenterology ISSN 1007-9327

Expression of CD86 and increased infiltration of NK cells are associated with *Helicobacter pylori*-dependent state of early stage high-grade gastric MALT lymphoma

Sung-Hsin Kuo, Li-Tzong Chen, Chi-Long Chen, Shin-Lian Doong, Kun-Huei Yeh, Ming-Shiang Wu, Tsui-Lien Mao, Hui-Chen Hsu, Hsiu-Po Wang, Jaw-Town Lin, Ann-Lii Cheng

Sung-Hsin Kuo, Departments of Oncology, National Taiwan University Hospital, Taipei; Cancer Research Center, and Graduate Institute of Clinical Medicine, National Taiwan University College of Medicine, Taipei, Taiwan, China
Li-Tzong Chen, Division of Cancer Research, National Health Research Institutes, Taipei; Department of Internal Medicine, Kaohsiung Medical University Hospital, Kaohsiung, Taipei, Taiwan, China
Chi-Long Chen, Department of Pathology, Taipei Medical University, Taipei, Taiwan, China
Shin-Lian Doong, Graduate Institute of Microbiology, National Taiwan University College of Medicine, Taipei, Taiwan, China
Kun-Huei Yeh, Hui-Chen Hsu, Departments of Oncology, National Taiwan University Hospital, Taipei; Cancer Research Center, National Taiwan University College of Medicine, Taipei, Taiwan, China
Ming-Shiang Wu, Jaw-Town Lin, Department of Internal Medicine, National Taiwan University Hospital, Taipei, Taiwan, China
Tsui-Lien Mao, Department of Pathology, National Taiwan University Hospital, Taipei, Taiwan, China
Hsiu-Po Wang, Department of Emergency Medicine, National Taiwan University Hospital, Taipei, Taiwan, China
Ann-Lii Cheng, Department of Internal Medicine and Department of Oncology, National Taiwan University Hospital, Taipei; Cancer Research Center, National Taiwan University College of Medicine, Taipei; Division of Cancer Research, National Health Research Institutes, Taipei, Taiwan, China
Supported by the Research Grants, No. NSC91-3112-B-002-009, No. NSC92-3112-B-002-027, and No. NSC93-3112-B-002-007 from the National Science Council, No. NHRI-CN-CA9201S (92A084, and 93A059) from the National Health Research Institutes, and No. NTUH 93-N012, No. NTUH 94S155 from National Taiwan University Hospital, Taiwan, China
Correspondence to: Ann-Lii Cheng, MD, PhD, Department of Internal Medicine and Department of Oncology, National Taiwan University Hospital, No. 7, Chung-Shan South Road, Taipei, Taiwan, China. andrew@ha.mc.ntu.edu.tw
Telephone: +886-2-2312-3456-7251 Fax: +886-2-2371-1174
Received: 2004-11-04 Accepted: 2004-12-08

Abstract

AIM: A high percentage of early-stage high-grade gastric mucosa-associated lymphoid tissue (MALT) lymphomas remain *Helicobacter pylori* (*H pylori*)-dependent. However, unlike their low-grade counterparts, high-grade gastric MALT lymphomas may progress rapidly if unresponsive to *H pylori* eradication. It is mandatory to identify markers that may predict the *H pylori*-dependent status of these tumors. Proliferation of MALT lymphoma cells depends on cognate help and cell-to-cell contact of *H pylori*-specific intratumoral T-cells. To examine whether the expression of co-stimulatory marker CD86 (B7.2) and the infiltration of CD56 (+) natural killer (NK) cells can be useful markers to predict *H pylori*-dependent status of high-grade gastric MALT lymphoma.

METHODS: Lymphoma biopsies from 26 patients who had participated in a prospective study of *H pylori*-eradication for stage I_E high-grade gastric MALT lymphomas were evaluated. Tumors that resolved to Wotherspoon grade II or less after *H pylori* eradication were classified as *H pylori*-dependent; others were classified as *H pylori*-independent. The infiltration of NK cells and the expression of CD86 in pre-treatment paraffin-embedded lymphoma tissues were determined by immunohistochemistry.

RESULTS: There were 16 *H pylori*-dependent and 10 *H pylori*-independent cases. CD86 expression was detected in 11 (68.8%) of 16 *H pylori*-dependent cases but in none of 10 *H pylori*-independent cases ($P = 0.001$). *H pylori*-dependent high-grade gastric MALT lymphomas contained significantly higher numbers of CD56 (+) NK cells than *H pylori*-independent cases (2.8±1.4% *vs* 1.1±0.8%; $P = 0.003$). CD86 positive MALT lymphomas also showed significantly increased infiltration of CD56 (+) NK cells compared to CD86-negative cases (2.9±1.1% *vs* 1.4±1.3%; $P = 0.005$).

CONCLUSION: These results suggest that the expression of co-stimulatory marker CD86 and the increased infiltration of NK cells are associated with *H pylori*-dependent state of early-stage high-grade gastric MALT lymphomas.

Key words: MALT lymphoma; *H pylori;* CD86; CD56

Kuo SH, Chen LT, Chen CL, Doong SL, Yeh KH, Wu MS, Mao TL, Hsu HC, Wang HP, Lin JT, Cheng AL. Expression of CD86 and increased infiltration of NK cells are associated with *Helicobacter pylori*-dependent state of early stage high-grade gastric MALT lymphoma. *World J Gastroenterol* 2005; 11(28): 4357-4362
http://www.wjgnet.com/1007-9327/11/4357.asp

INTRODUCTION

Extranodal marginal zone B-cell lymphoma of mucosa-

associated lymphoid tissue (MALT) of the stomach is the most common extranodal lymphoma of humans. Although not completely acknowledged by all experts, gastric MALT lymphoma is often classified into high-grade and low-grade subtypes by histological criteria[1-3]. Low-grade gastric MALT lymphoma is characterized by its close association with *Helicobacter pylori* (*H pylori*) infection; and eradication of *H pylori* by antibiotics, cures 70% of these tumors[4-6]. However, high-grade gastric MALT lymphomas, in contrast to their low-grade counterparts, are believed to consist of highly-transformed cells, the growth of which is independent of *H pylori*[7-9].

Recently, several groups of investigators have demonstrated that a substantial portion of early-stage high-grade gastric MALT lymphomas remains *H pylori*-dependent, and can be cured by *H pylori* eradication[10-12]. However, high-grade gastric MALT lymphoma, unlike its low-grade counterpart, may progress rapidly if unresponsive to *H pylori* eradication therapy. Molecular markers such as chromosomal aberration *t*(11;18), which is highly predictive of *H pylori*-independent status of low-grade gastric MALT lymphoma, are rarely found in the high-grade counterpart[13]. It is mandatory to identify cellular or molecular markers which can help predict the *H pylori*-dependent status of newly diagnosed patients.

In the early process of MALT lymphomagenesis, the proliferation response depends at least partly on the stimulation of *H pylori*-specific intratumoral T-cells[14]. *In vitro* experiments have demonstrated that the growth and differentiation of MALT lymphoma cells requires CD40-mediated signaling and T helper-2 (Th-2)-type cytokines[15,16]. The dependence on T-cells for the growth of malignant B-cell clones may explain the tendency of early-stage low-grade MALT lymphomas to remain localized and to regress after *H pylori* eradication. Expression of co-stimulatory molecules, including CD80 (B7.1), CD86 (B7.2), and their ligands, has been demonstrated in gastric MALT lymphoma cells[17]. The presence of the co-stimulatory marker CD86 (B7.2) on lymphoma cells may promote T-cell-mediated neoplastic B cell proliferation. We hypothesized that a loss of co-stimulatory markers might preclude tumor cell/reactive T-cell interaction and thereby contribute to the transition from a *H pylori*-dependent to a *H pylori*-independent state in high-grade gastric MALT lymphoma.

CD56 (+) natural killer (NK) cells are important components of the innate immune system, and have the ability to modulate both humoral- and cell-mediated immune responses[18,19]. *H pylori* can stimulate T-cells and thereby enhance the production of Th-2 cytokines, which can promote the proliferation of CD56 (+) NK cells in gastric MALT lymphomas[20,21]. Although low-grade gastric MALT lymphomas contain significantly higher numbers of CD56 (+) NK cells than high-grade gastric MALT lymphomas[21], the presence of CD56 (+) NK cells in high-grade gastric MALT lymphomas indicate that the promotion of these lymphoma cells triggered by *H pylori*-specific intratumoral T-cells and Th-2 type cytokines may still be present *in vivo*. Therefore, these CD56 (+) NK cells may limit the autonomous growth of MALT lymphoma cells, and may contribute to the remission of high-grade MALT lymphomas after the eradication of *H pylori*.

This study, was conducted to examine the expression of CD86 and the infiltration of CD56 (+) NK cells in 16 *H pylori*-dependent and 10 *H pylori*-independent high-grade gastric MALT lymphomas.

MATERIALS AND METHODS

Patients, treatment, and evaluation of the tumors

Twenty-six patients who had participated in a prospective study of *H pylori* eradication for stage I_E high-grade gastric MALT lymphomas at our institutions from June 1995 to June 2003 were included in this study. The clinicopathologic features of the 22 patients have been previously reported[13]. Although high-grade MALT lymphomas are classified as diffuse large B-cell lymphomas (with areas of marginal zone/MALT-type lymphoma) in the REAL/WHO classification[2], and a consensus on the use of the term " high-grade MALT lymphoma" has not been achieved, many experts consider it as a useful and reasonable clinicopathologic entity[1,3,10,21]. In this study, the diagnosis of high-grade gastric MALT lymphoma was made using the histologic criteria as described by Chan *et al*.[1], and de Jong *et al*.[3], based on the presence of a diffuse increase of large cells resembling centroblasts or lymphoblasts to between 1% and 10% of the total tumor cells within predominantly low-grade centrocyte-like cell infiltrate, or the predominance of a high-grade lymphoma with only a small residue, low-grade foci and/or the presence of lymphoepithelial lesions. Specimens with occasional clusters of transformed blast cells or sheets of transformed blast cells (upto 20 cells not forming larger sheets) confined within the colonized follicles were found within a low-grade lymphoma, they were considered as an immune response to *H pylori* stimulation rather than high-grade MALT lymphoma. Patients with primary pure large cell lymphoma, without evidence of a low-grade component of the stomach were excluded from this study. All specimens were immuohistochemically stained by CD20, CD79a, CD3, and CD45RO for routine diagnostic purposes and to highlight lymphoepithelial lesions. Moreover, to exclude misinterpretation of reactive, benign germinal centers as transformed foci, CD21 (follicular dendritic cells markers) and BCL-2 (highly suggestive of a neoplastic origin of the blast cells) were included in all cases. The histopathologic characteristics of all tumor specimens were independently reviewed by two expert hematopathologists. Staging was based on Musshoff's modification of the Ann Arbor staging system[22]. Staging procedures included physical examination, routine laboratory tests, inspection of Waldeyer's ring, chest radiography, chest and abdominal CT scan, bone marrow aspiration, and trephine biopsy. Diagnosis of *H pylori* infection was based on histologic examination, biopsy urease test, or bacterial culture. When at least one test was positive, the cases were considered as *H pylori infected*. All patients consented to a brief trial of *H pylori* eradication therapy.

At the beginning of the study period in June 1995, the eradication regimen consisted of amoxicillin 500 mg and metronidazole 250 mg q.i.d., with either bismuth subcitrate 120 mg q.i.d. or omeprazole 20 mg b.i.d., for 4 wk. The regimen was changed to amoxicillin 500 mg q.i.d., clarithromycin 500 mg b.i.d., plus omeprazole 20 mg b.i.d. for 2 wk beginning in March 1996. Patients were scheduled to undergo a first follow-up upper gastrointestinal endoscopic examination 4-6 wk after completion of antimicrobial

therapy, and follow-up was then repeated every 6-12 wk until histologic evidence of remission was found. At each follow-up examination, four to six biopsy specimens were taken from the antrum and body of the stomach for a *H pylori* infection evaluation, and a minimum of six biopsy specimens were taken from each of the tumors and suspicious areas for histologic evaluation. Tumors that resolved to Wotherspoon grade II or less were considered as histological complete remission[4]. Tumors showing both histological and endoscopic complete remission were considered *H pylori*-dependent. Tumors showing stable or progressive disease on follow-up endoscopic examination and persistent or increasing proportion of large cells on microscopic examination were considered *H pylori*-independent.

Immunohistochemistry

Formalin-fixed paraffin embedded sections cut at a thickness of 4 μm were deparaffinized and rehydrated through xylene and a graded descending series of alcohol. After antigen retrieval by heat treatment in 0.1 mol/L citrate buffer at pH 6.0, endogenous peroxidase activity was blocked by 3% H_2O_2. Briefly, slides were incubated for 30 min in 2.5% normal donkey serum or goat serum. The slides were then incubated overnight at 4 ℃ either with goat polyclonal anti-CD86 antibody (1:50; AF-141-NA; R&D Systems, Abingdon, UK) or mouse monoclonal anti-CD56 antibody (1:100; NCL-CD56-1B6, Novacastra), and incubated with secondary antibodies (CD86, donkey antigoat immunoglobulin; CD56, goat antimouse immunoglobulin; Santa Cruz Biotechnology, Santa Cruz, CA, USA), following the manufacturer's instructions. Finally, antibody binding was detected with the avidin–biotin–peroxidase method. Reaction products were developed using 3', 5'-diaminobenzidine (Dako) as a substrate for peroxidase. Sections were counterstained with Mayer's hematoxylin. All the washes were performed in PBS (pH 7.4). Staining was considered as positive for CD86 when the protein was detected in more than 10% of tumor cells. A minimum of 1 000 cells (normal and neoplastic) were counted for each single determination and reported as the percentage of CD56 (+) NK cells in total mononuclear cells.

Statistical analysis

The primary aims of this study were to investigate the correlation between the *H pylori*-dependent status of MALT lymphomas, the expression of CD86 and the infiltration of CD56 (+) NK cells. Fisher's exact test and χ^2 test were used to analyze the correlation between the *H pylori*-dependent status of MALT lymphomas with CD86 expression patterns. The results for the CD56 (+) NK cells are expressed as mean±SD of percentages of positive cells in the total cell count for a given marker. Nonparametric Mann-Whitney *U* test was used to evaluate the difference in the distribution of positive CD56 (+) NK cell count between *H pylori*-dependent and *H pylori*-independent high-grade MALT lymphomas and the difference in the distribution of positive CD56 (+) NK cell count between CD86 positive and CD86 negative high-grade MALT lymphomas.

RESULTS

Patients and tumor response

There were 16 patients with *H pylori*-dependent and 10 patients with *H pylori*-independent tumors. The clinicopathologic features of these patients are summarized in Table 1. The

Table 1 Clinicopathologic features of the patients and tumor expression of CD86

Patient number	Sex	Age (yr)	Depth of tumor invasion	Tumor response to *H pylori* eradication	Current status	Immunohistochemistry CD86
1	F	48	Muscularis propria	CR		-
2	M	21	Muscularis propria	PD	Chemotherapy	-
3	F	63		SD	Chemotherapy	-
4	F	68		CR		+
5	F	52	Submucosa	PD	Chemotherapy	-
6	F	42	Serosa	CR		+
7	F	66	Serosa	CR		-
8	F	71	Muscularis propria	CR		+
9	F	54		CR		+
10	M	83	Muscularis propria	PD	Chemotherapy	-
11	F	52	Submucosa	CR		+
12	F	73	Muscularis propria	CR		+
13	M	46	Submucosa	CR		-
14	F	38		CR		-
15	M	73	Serosa	PD	Chemotherapy	-
16	F	45	Muscularis propria	PD	Chemotherapy	-
17	F	56	Submucosa	CR		+
18	F	59	Serosa	PD	C/T+gastrectomy	-
19	F	65		CR		+
20	M	35	Submucosa	CR		+
21	F	73		CR		-
22	M	45	Serosa	SD	Chemotherapy	-
23	F	53	Submucosa	SD	Chemotherapy	-
24	F	80	Muscularis propria	PD	Chemotherapy	-
25	M	70	Submucosa	CR		+
26	F	84	Submucosa	CR		+

Evaluated by EUS (19 cases) and histologic examination of surgical specimens (1 case). +: Positive; -: negative; CR, complete remission; SD, stable disease; PD, progressive disease.

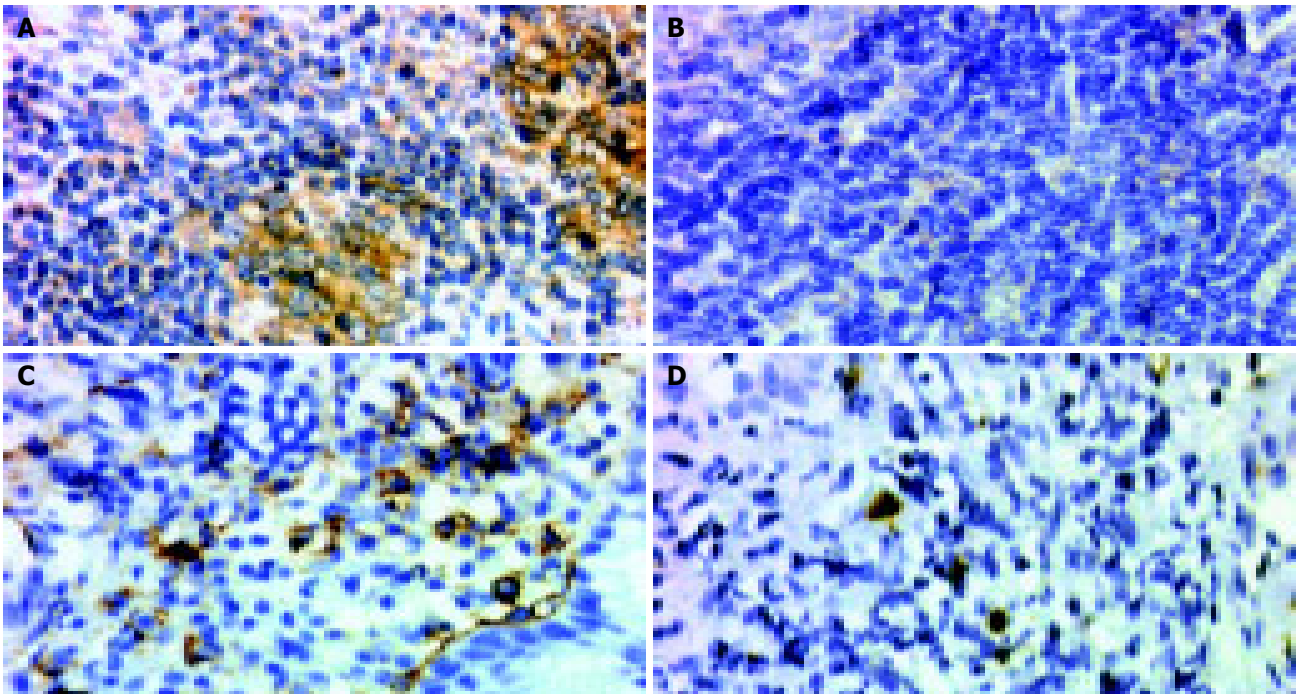

Figure 1 Examples of immunohistochemical analysis of CD86 and CD56 (+) NK on B-cells of high-grade gastric MALT lymphoma. **A:** *H pylori*-dependent case (case 4) shows positive staining for CD86; **B:** *H pylori*-independent case (case 18) shows negative staining for CD86; **C:** *H pylori*-dependent case (case 8) carries a larger proportion of CD56 (+) NK cells; **D:** *H pylori*-independent case (case 5) contains a lower proportion of CD56 (+) NK cells. Original magnification, ×400.

median duration between *H pylori* eradication and complete histologic remission was 5.0 mo (range, 1.5-17.7 mo). At a median follow-up of 56 mo (range, 8.0-90 mo), all 16 patients who had achieved complete histologic remission after eradication of *H pylori* were alive and free of lymphoma. Seven patients whose tumors grossly increased in size or had microscopic findings of an increased large-cell fraction and three patients whose tumor remained grossly stable at the first follow-up endoscopic examination, were immediately referred for systemic chemotherapy.

Correlation of expression of CD86 and infiltration of CD56 (+) NK cells with tumor response to H pylori eradication

The expression of CD86 was detected in 11 (68.8%) of 16 *H pylori*-dependent high-grade gastric MALT lymphomas, but in none of 10 *H pylori*-independent MALT lymphomas ($P = 0.001$, Figure 1 and Table 1). Therefore, the expression of CD86 had a sensitivity of 68.8% and a specificity of 100% in predicting the *H pylori*-dependence of high-grade gastric MALT lymphomas.

As shown in Figure 2, the infiltration of CD56 (+) NK cells differed between *H pylori*-dependent and *H pylori*-independent high-grade gastric MALT lymphomas. *H pylori*-dependent high-grade gastric MALT lymphomas contained significantly higher numbers of CD56 (+) NK cells than *H pylori*-independent MALT lymphomas (2.8±1.4% *vs* 1.1±0.8%; $P = 0.003$). Meanwhile, CD86 positive MALT lymphomas also showed significantly increased infiltration of CD56 (+) NK cells compared to CD86-negative cases (2.9±1.1% *vs* 1.4±1.3%; $P = 0.005$).

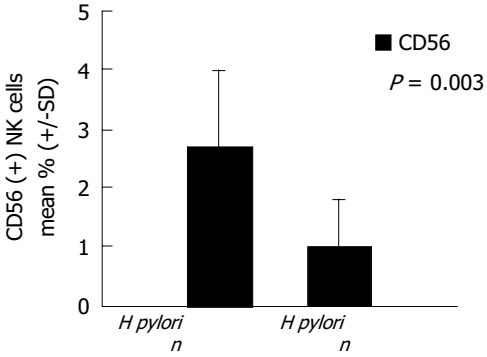

Figure 2 Histograms showing the mean percentage (±SD) of cells staining CD56 (+) NK in *H pylori*-dependent and *H pylori*-independent high-grade gastric MALT lymphomas (2.8±1.4% *vs* 1.1±0.8%; $P = 0.003$).

DISCUSSION

In this study, we found that expression of CD86 on tumor cells and increased infiltration of NK cells in tumor tissues were associated with the *H pylori*-dependent status of early-stage high-grade gastric MALT lymphomas. These findings suggest that the interaction of B- and T-cells may play a pivotal role in the determination of antigen-dependence, as well as in the subsequent response to *H pylori* eradication therapy in a substantial portion of early-stage high-grade gastric MALT lymphomas. Since high-grade gastric MALT lymphomas may progress rapidly if unresponsive to *H pylori* eradication therapy, this information is invaluable for the physician who must select a first-line treatment.

It has been demonstrated that the growth of MALT lymphomas requires the help of *H pylori*-reactive tumor-infiltrating T-cells. For effective communication between T-cells and neoplastic B-cells, two subsets of co-stimulatory molecules, CD80 (B7.1) and CD86 (B7.2), of the neoplastic B-cells should interact with CD28 or CTLA-4 of the

T-cells[23]. However, the precise role of CD80 and CD86 molecules in the signaling of B-cells remains unclear. In earlier studies, the CD28-CTLA4/B7-signaling pathway was found to be involved in the proliferation and differentiation of B-cells[24,25]. There is also evidence that CD86 may promote proliferation and immunoglobulin synthesis of normal B-cells and malignant B cells[26]. Compared with CD86, CD80 delivered a down-regulator signal for B-cell response[26]. In a recent study of low-grade gastric MALT lymphomas, the expression of CD86 was significantly associated with *H pylori*-dependence, while CD80 and CD40 and their ligands were not[27]. These results are in line with our observation that the co-stimulatory molecule CD86 is present in high-grade gastric MALT lymphomas, and is also significantly associated with *H pylori*-dependence. Our findings support the notion that the growth of a substantial portion of early-stage high-grade gastric MALT lymphomas, as well as their low-grade counterparts, remains dependent on functional B-cell/T-cell interaction.

In addition to promoting the proliferation and differentiation of malignant B-cell clones, tumor-infiltrating T-cells in low-grade gastric MALT lymphomas are found to be defective in both perforin-mediated cytotoxicity and Fas-Fas ligand mediated apoptosis[28]. On the other hand, the tumor tissues of high-grade MALT lymphomas appear to contain a much higher number of apoptotic lymphoma cells and CD8+ cytotoxic T lymphocytes (CTLs)[21]. Study using a murine model demonstrated that Th-1 response and CD8+ CTLs activity were strongly inhibited in the presence of persistent gastric *H pylori* infection[29]. Moreover, activated CD8+ CTLs may compete with CD56 (+) NK cells and downregulate the function of the latter[17]. Besides regulating the differentiation of CD8+ CTLs, CD56 (+) NK cells may have an equally important role in immune regulation, where they limit the host response to foreign antigens and prevent autoimmunity[18]. Recently, it has been demonstrated that CD56 (+) NK cells can be functionally activated by co-stimulatory molecules through the interaction of their activation receptor and CD86 on target cells, and thereby limit the extent of *H pylori*-related auto-reactive and neoplastic B lymphoid cells in the stomach[30]. In the current study, we found that *H pylori*-dependent high-grade MALT lymphomas showed significantly increased infiltration of CD56 (+) NK cells compared to *H pylori*-independent lymphomas. Interestingly, we also found that CD86 positive MALT lymphomas showed significantly increased infiltration of CD56 (+) NK cells compared to CD86-negative cases. These findings suggest that the loss of *H pylori*-dependence may be associated with a change in the immunological microenvironment, including a shift towards a Th-1 response that enhances the activity of CD8+ CTLs, and decreases the activity of CD56 (+) NK cells.

In conclusion, the expression of co-stimulatory marker CD86 on lymphoma cells and the increased infiltration of CD56 (+) NK cells in tumor tissues are useful markers in the identification of *H pylori*-dependent tumors and in the selection of patients for first-line *H pylori* eradication therapy.

REFERENCES

1 **Chan JK,** Ng CS, Isaacson PG. Relationship between high-grade lymphoma and low-grade B-cell lymphoma of mucosa-associated lymphoid tissue (MALToma) of the stomach. *Am J Pathol* 1990; **136**: 1153-1164

2 **Harris NL,** Jaffe ES, Stein H, Banks PM, Chan JK, Cleary ML, Delsol G, De Wolf-Peeters C, Falini B, Gatter KC. A revised European-American classification of lymphoid neoplasms: A proposal from the International Lymphoma Study Group. *Blood* 1994; **84**: 1361-1392

3 **de Jong D,** Boot H, van Heerde P, Hart GA, Taal BG. Histological grading in gastric lymphoma: Pretreatment criteria and clinical relevance. *Gastroenterology* 1997; **112**: 1466-1474

4 **Wotherspoon AC,** Doglioni C, Diss TC, Pan L, Moschini A, de Boni M, Isaacson PG. Regression of primary low-grade B-cell gastric lymphoma of mucosa-associated lymphoid tissue type after eradication of *Helicobacter pylori*. *Lancet* 1993; **342**: 575-577

5 **Du MQ,** Isaacson PG. Gastric MALT lymphoma: from aetiology to treatment. *Lancet Oncol* 2002; **3**: 97-104

6 **Boot H,** De Jone D. Gastric lymphoma: the revolution of the past decade. *Scand J Gastroenterol* 2002; **236** (Suppl): 27-36

7 **Bayerdorffer E,** Neubauer A, Rudolph B, Thiede C, Lehn N, Eidt S, Stolte M. Regression of primary low-grade B-cell gastric lymphoma of mucosa-associated lymphoid tissue type after cure of *Helicobacter pylori* infection. *Lancet* 1995; **345**: 1591-1594

8 **Neubauer A,** Thiede C, Morgner A, Alpen B, Ritter M, Neubauer B, Wundisch T, Ehninger G, Stolte M, Bayerdorffer E. Cure of *Helicobacter pylori* infection and duration of remission of low-grade gastric mucosa associated lymphoid tissue lymphoma. *J Natl Cancer Inst* 1997; **89**: 1350-1355

9 **Zucca E,** Roggero E, Pileri S. B-cell lymphoma of MALT type: A review with special emphasis on diagnostic and management problems of low-grade gastric tumors. *Br J Haematol* 1998; **100**: 3-14

10 **Morgner A,** Miehlke S, Fischbach W, Schmitt W, Muller-Hermelink H, Greiner A, Thiede C, Schetelig J, Neubauer A, Stolte M, Ehninger G, Bayerdorffer E. Complete remission of primary high-grade B cell gastric lymphoma after cure of *Helicobacter pylori* infection. *J Clin Oncol* 2001; **19**: 2041–2048

11 **Nakamura S,** Matsumoto T, Suekane H, Takeshita M, Hizawa K, Kawasaki M, Yao T, Tsuneyoshi M, Iida M, Fujishima M. Predictive value of endoscopic ultrasonography for regression of gastric low grade and high-grade MALT lymphomas after eradication of *Helicobacter pylori*. *Gut* 2001; **48**: 454-460

12 **Chen LT,** Lin JT, Shyu RY, Jan CM, Chen CL, Chiang IP, Liu SM, Su IJ, Cheng AL. Prospective study of *Helicobacter pylori* eradication therapy in stage I_E high-grade mucosa-associated lymphoid tissue lymphoma of the stomach. *J Clin Oncol* 2001; **19**: 4245-4251

13 **Kuo SH,** Chen LT, Yeh KH, Wu MS, Hsu HC, Yeh PY, Mao TL, Chen CL, Doong SL, Lin JT, Cheng AL. Nuclear expression of BCL10 or nuclear factor kappa B predicts *Helicobacter pylori*-independent status of early-stage, high-grade gastric mucosa-associated lymphoid tissue lymphomas. *J Clin Oncol* 2004; **22**: 3491-3497

14 **Hussell T,** Isaacson PG, Crabtree JE, Spencer J. *Helicobacter pylori* specific tumor infiltrating T-cells provide contact dependent help for the growth of malignant B-cells in low-grade gastric lymphoma of mucosa-assocaited lymphoid tissue. *J Pathol* 1996; **178**: 122-127

15 **Hauer AC,** Finn TM, MacDonald TT, Spencer J, Isaacson PG. Analysis of TH1 and TH2 cytokine production in low-grade B-cell gastric MALT-type lymphomas stimulated in vitro with *Helicobacter pylori*. *J Clin Pathol* 1997; **50**: 957-959

16 **Greiner A,** Knorr C, Qin Y, Sebald W, Schimpl A, Banchereau J, Muller-Hermelink HK. Low-grade B-cell lymphomas of mucosa-associated lymphoid tissue (MALT-type) require CD40-mediated signalling and Th2-type cytokines for *in vitro* growth and differentiation. *Am J Pathol* 1997; **150**: 1583-1593

17 **Vyth-Dreese FA,** Boot H, Dellemijn TA, Majoor DM, Oomen LC, Laman JD, Van Meurs M, De Weger RA, De Jong D. Localization *in situ* of costimulatory molecules and cytokines in B-cell non-Hodgkin's lymphoma. *Immunology* 1998; **94**:

580-586
18 **Kos FJ,** Engleman EG. Immune regulation: a critical link between NK cells and CTLS. *Immunol Today* 1996; **17**: 174-176
19 **Horwitz DA,** Gray JD, Ohtsuka K, Hirokawa M, Takahashi T. The immunoregulatory effects of NK cells: the role of TGF-beta and implication for autoimmunity. *Immunol Today* 1997; **18**: 538-542
20 **Biron CA,** Nguyen KB, Pien GC, Cousens LP, Salazar-Mather TP. Natural killer cells in antiviral defense function and regulation by innate cytokines. *Annu Rev Immunol* 1999; **17**: 189-220
21 **Guidoboni M,** Doglioni C, Laurino L, Boiocchi M, Dolcetti R. Activation of infiltrating cytotoxic T lymphocytes and lymphoma cell apoptotic rates in gastric MALT lymphomas: Differences between high-grade and low-grade cases. *Am J Pathol* 1999; **155**: 823-829
22 **Musshoff K.** Klinische Stadieneinteilung der nicht-Lymphome. *Strahlenthreapie Onkol* 1977; **153**: 218-221
23 **Guindi M.** Role of activated host T cells in the promotion of MALT lymphoma growth. *Seminar Cancer Biol* 2000; **10**: 341-344
24 **Boussiotis VA,** Freeman GJ, Gribben JG, Nadler LM. The role of B7-1/B7-2: CD28/CTLA4 pathways in the prevention of anergy, induction of productive immunity and down-regulation of the immune response. *Immunol Rev* 1996; **153**: 5-26
25 **Ikemizu S,** Gilbert RJ, Fennelly JA, Collins AV, Harlos K, Jones EY, Stuart DI, Davis SJ. Structure and dimerization of a soluble form of B7-1. *Immunity* 2000; **12**: 51-60
26 **Suvas S,** Singh V, Sahdev S, Vohra H, Agrewala JN. Distinct Role of CD80 and CD86 in the Regulation of the Activation of B Cell and B Cell Lymphoma. *J Biol Chem* 2002; **277**: 7766-7775
27 **de Jong D,** Vyth-Dresse F, Dellemijn T, Verra N, Ruskone-Fourmestraux A, Lavergne-Slove A, Hart G, Boot H. Histological and immunological parameters to predict treatment outcome of *Helicobacter pylori* eradication in low-grade gastric MALT lymphoma. *J Pathol* 2001; **193**: 318–324
28 **D'Elios MM,** Amedei A, Manghetti M, Costa F, Baldari CT, Quazi AS, Telford JL, Romagnani S, Del Prete G. Impaired T-cell regulation of B-cell growth in *Helicobacter pylori*related gastric low-grade MALT lymphoma. *Gastroenterology* 1999; **117**: 1105–1112
29 **Shirai M,** Arichi T, Nakazawa T, Berzofsky JA. Persistent infection by *Helicobacter pylori* down-modulates virus-specific CD8+ cytotoxic T cells response and prolongs viral infection. *J Infect Dis* 1998; **177**: 72–80
30 **Wilson JL,** Charo J, Martin-Fontecha A, Dellabona P, Casorati G, Chambers BJ, Kiessling R, Bejarano MT, Ljunggren HG. NK cells triggering by the human costimulatory molecules CD80 and CD86. *J Immunol* 1999; **163**: 4207-4212

Science Editor Guo SY **Language Editor** Elsevier HK

PO Box 2345, Beijing 100023, China
www.wjgnet.com
wjg@wjgnet.com

ELSEVIER

World J Gastroenterol 2005;11(28):4363-4366
World Journal of Gastroenterology ISSN 1007-9327

Effect of *Helicobacter pylori* infection on *p53* expression of gastric mucosa and adenocarcinoma with microsatellite instability

Jian-Hua Li, Xian-Zhe Shi, Shen Lv, Min Liu, Guo-Wang Xu

Jian-Hua Li, Shen Lv, Min Liu, Laboratory of Molecular Biology, the Second Hospital of Dalian Medical University, Dalian 116027, Liaoning Province, China
Xian-Zhe Shi, Guo-Wang Xu, National Chromatographic Research and Application Center, Dalian Institute of Chemical Physics, The Chinese Academy of Sciences, Dalian 116011, Liaoning Province, China
Correspondence to: Professor Shen Lv, PhD, Laboratory Center of Molecular Biology, the Second Hospital of Dalian Medical University, Dalian 116027, Liaoning Province, China. lijianhua_ljh@126.com
Telephone: +86-411-84687554
Received: 2004-10-26 Accepted: 2004-12-03

Abstract

AIM: To investigate the relationship between *Helicobacter pylori* (*H pylori*) infection, microsatellite instability and the expressions of the *p53* in gastritis, intestinal metaplasia and gastric adenocarcinoma and to elucidate the mechanism of gastric carcinogenesis relating to *H pylori* infection.

METHODS: One hundred and eight endoscopic biopsies and gastric adenocarcinoma were available for the study including 33 cases of normal, 45 cases of gastritis, 30 cases of intestinal metaplasia, and 46 cases of gastric adenocarcinoma. Peripheral blood samples of these patients were also collected. *H pylori* infection and *p53* expressions were detected by means of streptavidin-peroxidase (SP) immunohistochemical method. Microsatellite loci were studied by PCR-SSCP-CE using the markers BAT-26, D17S261, D3S1283, D2S123, and D3S1611. MSI was defined as the peak shift in the DNA of the gastric tissue compared with that of the peripheral blood samples. Based on the number of mutated MSI markers, specimens were charac-terized as high MSI (MSI-H) if they manifested instability at two or more markers, low MSI (MSI-L) if unstable at only one marker, and microsatellite stable (MSS) if they showed no instability at any marker.

RESULTS: *H pylori* infection was detected in the samples of gastritis, intestinal metaplasia, and gastric adenocarcinoma and the infection frequencies were 84.4%, 76.7%, and 65.2%, respectively, whereas no *H pylori* infection was detected in the samples of normal control. There was a significant difference in the infection rates between gastritis and carcinoma samples ($P = 0.035$). No MSI was detected in gastritis samples, one MSI-H and two MSI-L were detected among the 30 intestinal metaplasia samples, and 12 MSI-H and 3 MSI-L were detected in the 46 gastric carcinomas. In those gastric carcinomas, the MSI-H frequency in *H pylori*-positive group was significantly higher than that in *H pylori*-negative group. No *p53* expression was detected in the normal and gastritis samples from dyspeptic patients. *P53*-positive immunohistochemical staining was detected in 13.3% of intestinal metaplasia samples and in 43.5% of gastric carcinoma samples. The levels of *p53* in *H pylori*-positive samples were higher than those in the negative group when the carcinoma samples were subdivided into *H pylori*-positive and -negative groups ($P = 0.013$). Eight samples were detected with positive *p53* expression out of the 11 MSI-H carcinomas with *H pylori* infection and no *p53* expression could be seen in the *H pylori*-negative samples.

CONCLUSION: *H pylori* affect the *p53* pattern in gastric mucosa when MMR system fails to work. Mutations of the *p53* gene seem to be an early event in gastric carcinogenesis.

Key words: Dyspepsia; *H pylori*; Gastric cancer; MSI; *p53*

Li JH, Shi XZ, Lv S, Liu M, Xu GW. Effect of *Helicobacter pylori* infection on *p53* expression of gastric mucosa and adenocarcinoma with microsatellite instability. *World J Gastroenterol* 2005; 11(28): 4363-4366
http://www.wjgnet.com/1007-9327/11/4363.asp

INTRODUCTION

Gastric cancer is one of the most common forms of malignant tumors in adults and is the leading cause of death from carcinomas in China. A close association between *Helicobacter pylori* (*H pylori*) and gastric cancer has been found[1,2], mainly on the basis of epidemiological data. Although *H pylori* has been classified as a type I carcinogen for gastric cancer by the International Agency for Research on Cancer (IARC), the exact pathway has remained indistinct[3,4]. It has been known that some gastric carcinomas are characterized by microsatellite instability resulting from defect of mismatch repair. Mismatch repair genes, as house keeping genes, have a central role in maintaining genomic stability by repairing DNA replication errors and inhibiting recombination between non-identical sequences. Loss of MMR genes causes destabilization of the genome and results in high mutation rates, which predisposes human to diverse cancers including gastric carcinoma[5-7]. The *p53* protein is a transcriptional factor that arrests the cell cycle in the G1 phase when DNA is damaged by inducing the expression of the p21 protein, an inhibitor of Cdk kinase and PCNA[8,9]. Thus, damaged

DNA cannot replicate, allowing time for the repair system to act[8]. If this system fails, *p53* induces apoptosis by transactivation of the *bax* gene[10]. Both mismatch repair and suppressor are two main pathways involved in the tumorigenesis of gastric carcinoma. In this study, we examine microsatellite instability and *p53* protein accumulation in patients with *H pylori*-infected gastric mucosa and in patients with gastric adenocarcinoma to elucidate whether any relationship exists between these genetic alterations and *H pylori* infection.

MATERIALS AND METHODS

Patients

One hundred and eight dyspeptic patients (65 men and 43 women; median age, 46 years; range, 20-73 years) undergoing upper endoscopy, and 46 consecutive patients (29 men and 17 women; median age, 56 years; range, 32-69 years) who underwent surgical excision for gastric adenocarcinoma at the hospitals of Dalian area entered the study. Peripheral blood samples of these patients were also collected. The ethical approval for this study was granted by the Local Research Ethics Committee. Endoscopic biopsies were removed with standard gastric biopsy forceps and then cut in half with sterile scalpel blades. Half the biopsy sample was fixed in 10% buffered neutral formalin and embedded in paraffin and serial sections (4-μm thick), while the other half was stored at -80 ℃. Hematoxylin-eosin (HE) staining was used for the histopathological diagnosis. Among the 108 endoscopic biopsies, 33 samples were normal, 45 samples were gastritis and 30 samples were intestinal metaplasia.

DNA extraction

DNA was extracted from the frozen gastric tissues and peripheral leukocytes using a regular phenol-chloroform method and stored at -20 ℃ until use.

Microsatellite analysis

Microsatellite instability was studied using five markers (Table 1), PCR was performed in 12.5 μL of reaction mixture containing 1.5 mmol/L $MgCl_2$, 200 μmol/L each dNTP, 0.5 Unit ampli Taq polymerase (TaKaRa Biotech., Dalian, China), 0.5 μmol/L of each primer, and 50 ng genomic DNA. The reaction was carried out in a thermal cycler (Perkin-Elmer Model 2700, CA, USA) at 94 ℃ for 30 s, 58-60 ℃ for 30 s, and 72 ℃ for 30 s, for 35 cycles with an initial denaturation step of 94 ℃ for 5 min and a final extension step of 72 ℃ for 5 min. 0.5 μL each PCR product was mixed with 1 μL GeneScan 500 size standard and 12 μL water, and heated at 95 ℃ for 10 min, then immediately put into ice water and kept for 5 min. Microsatellite was analyzed by an ABI PRISM 310 (Perkin-Elmer, ABI Prism) with 6% SLPA and 8 mol/L urea as sieving medium under constant voltage 15 kV at 60 ℃. Single-stranded microsatellite fragments were detected by LIF and the data were collected and analyzed by GeneScan. MSI was defined as the peak shift in the DNA of the gastric tissue compared with that of the peripheral blood samples. Based on the number of mutated MSI markers, specimens were characterized as high MSI (MSI-H) if they manifested instability at two or more markers, low MSI (MSI-L) if unstable at only one marker, and microsatellite stable (MSS) if they showed no instability at any marker.

Table 1 Primers of microsatellite markers

Markers	Primers	T_m (℃)
BAT-26	5'-FAM-TGACTACTTTTGACTTCAGCC	58
	5'-AACCATTCAACATTTTTAACCC	
D17S261	5'-HEX-AGGGATACTATTCAGCCCGAGGTG	60
	5'-ACTGCCACTCCTTGCCCCATTC	
D3S1283	5'-TET-GGCAGTACCACCTGTAGAAATG	60
	5'-GAGTAACAGAGGCATCGTGTATTC	
D2S123	5'-FAM-AAACAGGATGCCTGCCTTTA	60
	5'-GGACTTTCCACCTATGGGAC	
D3S1611	5'-HEX-CCCCAAGGCTGCACTT	60
	5'-AGCTGAGACTACAGGCATTTG	

Immunohistochemical staining

Immunostaining was performed using the streptavidin-peroxidase (SP) method as previously described by Lan *et al*. Negative control sections were processed in the same manner, replacing the primary antibody with buffered saline. A total of 300 cells were counted in random fields from representative areas and the immunoreactive cells were assessed and expressed as percentages. Samples with *p53* staining in more than 10% were considered positive (the nuclei, staining brown-yellow). However, the *H pylori* immunostaining was assessed positive as long as the brown-black dotish were stained on the surface of mucosa.

Statistical analysis

The χ^2 test and the Fisher's exact probability test were used to compute the frequencies by SPSS 12.0 for Windows. $P<0.05$ was considered to be statistically significant.

RESULTS

H pylori status

Sixty-one of the 108 (56.5%) dyspeptic patients and 30 of the 46 (65.2%) gastric cancer patients showed *H pylori* infection. None of the normal gastric mucosa was infected with *H pylori*. The infection rates of gastritis, intestinal metaplasia and tumor samples were largely more than the normal. χ^2 tests also revealed a significant difference in the infection rates between gastritis and carcinoma samples ($P = 0.035$, Table 2).

Table 2 *H pylori* infection in the normal, gastritis, intestinal metaplasia, and tumor samples

Tissue type	Number of samples	Infection number of *H pylori*	Infection rates (%)
Normal	33	0	0
Gastritis	45	38	84.4
Intestinal metaplasia	30	23	76.7
Carcinoma	46	30	65.2

Microsatellite analysis

In the 33 normal and 45 gastritis samples, no microsatellite status shift was detected. One MSI-H and two MSI-L were

Table 3 MSI frequency according to *H pylori* status

MSI frequency	*H pylori* positive (30)	*H pylori* negative (16)	P^1
MSI-H (12)	36.7% (11/30)	6.3% (1/16)	0.035
MSI-L (3)	6.7% (2/30)	6.25 % (1/16)	1.000

[1]*H pylori* positive *vs H pylori* negative.

Table 4 *P53* expression with regard to *H pylori* status in carcinomas

H pylori status	*P53* positive (20)	*P*
H pylori positive (30)	17	0.013[1]
H pylori negative (16)	3	

[1]*H pylori* positive *vs H pylori* negative.

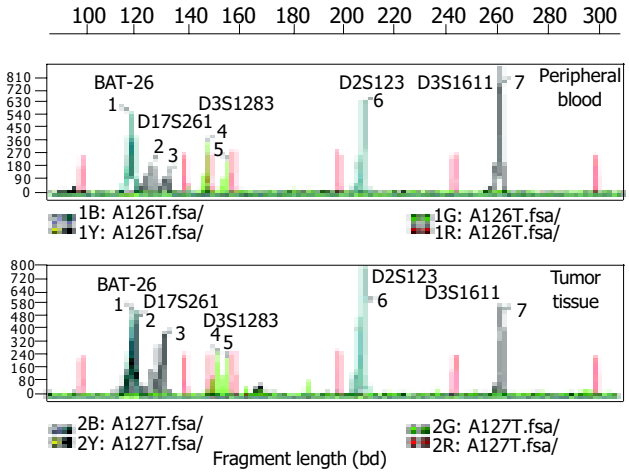

Figure 1 Electropherograms of five microsatellite loci in the peripheral blood sample and tumor tissue of one gastric cancer patient. Red peaks: interval standard peaks.

detected among the 30 samples of intestinal metaplasia, whereas in the 46 gastric carcinomas, 12 MSI-H and 3 MSI-L were detected. The MSI status was significantly higher in *H pylori* positive samples of carcinomas than that in *H pylori* negative samples of carcinomas (Table 3 and Figure 1).

p53 overexpression

No *p53* expression was detected in the normal and gastritis samples from dyspeptic patients. Four of the 30 intestinal metaplasia samples showed *p53*-positive immunohistochemical staining, and in the 46 patients with gastric cancer, 20 (43%) *p53*-positive samples were identified. Eight manifested *p53* positivity out of the 11 MSI-H carcinomas with *H pylori* infection and no *p53* expression could be seen in the *H pylori*-negative group. When the carcinoma samples were subdivided into *H pylori*-positive and -negative groups, immunohistochemical staining revealed that the levels of *p53* in *H pylori*-positive samples were higher than those in the negative samples ($P = 0.013$, Tables 4 and 5, Figures 2A and B).

DISCUSSION

Both genetic and environmental factors are crucial in gastric cancer development and progression. *H pylori* infection has been documented as an important risk factor for gastric cancer[12]. It is fully agreed that the bacterium is effectively able to induce chronic mucosal injury with increased mucosal proliferation that could facilitate malignant transformation[13-15]. In this study, we detected a high infection rate of *H pylori* in both dyspeptic samples and gastric adenocarcinoma samples, which is consistent with the documents[16,17]. The reason why infection rate was significantly higher in gastritis samples than that in carcinoma samples is probable that *H pylori* density is lower in atrophic gastritis mucosa and very low in the intestinal metaplasia and in patients with gastric cancer, the degree of atrophic gastritis and intestinal metaplasia is

Table 5 Length of representative fragments of five microsatellite loci in the normal tissue and peripheral blood sample of the gastric cancer patient

Peak no.	BAT-26 1# (bp)	D17S261 2# (bp)	D17S261 3# (bp)	D3S1283 4# (bp)	D3S1283 5# (bp)	D2S123 6# (bp)	D3S1611 7# (bp)
Normal	119.15	127.52	133.78	149.12	147.25	209.42	262.76
Tumor	120.30	121.63	131.45	143.23	147.36	209.30	262.85

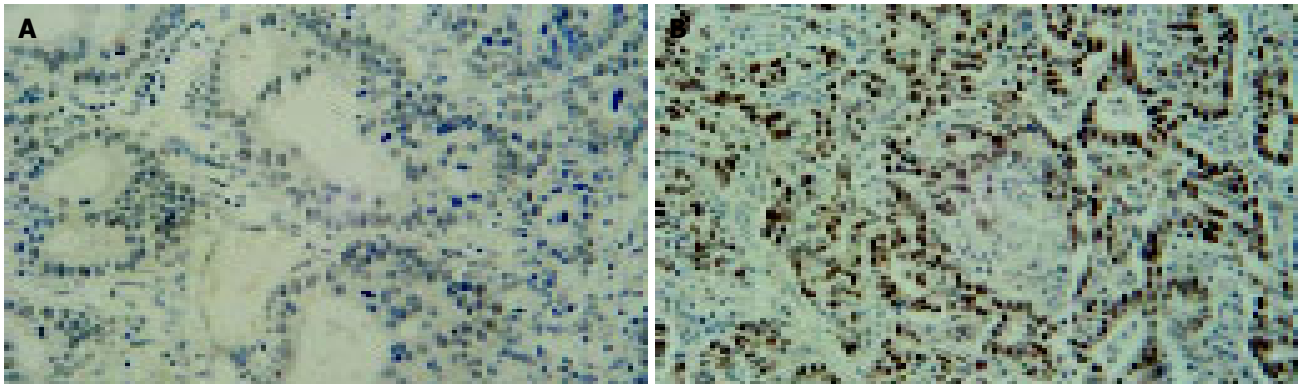

Figure 2 p53 in the normal and gastric carcinoma samples. **A:** p53-Negative staining in normal gastric glands from a dyspeptic patient, **B:** gastric carcinoma showing nuclear p53 immunoreactivity.

higher than in patients without cancer. Another reason may be that different strains contribute differently to the occurrence of gastritis or gastric carcinoma, and it is not adequate to compare *H pylori* infection only by histology.

Epithelial cell proliferation is not carcinogenic in itself. It is likely that *H pylori* promote neoplastic transformation in combination with additional factors. In this study, we detected microsatellite instability and p53 protein expression in accordance with the development from gastric gastritis, intestinal metaplasia to gastric cancer with regard to *H pylori* infection status.

Microsatellites are short sequences of tandem repeats dispersed throughout the mammalian genome. Repeat units range from 1 to 4 bp in length, and the entire sequence of a typical repeat tract is less than 100 bp long[18,19]. Microsatellite instability is characterized by the insertion or deletion of one or more repeat units, which is caused by a failure of the DNA-MMR system to repair errors that occur during the replication of DNA[20]. MSI has been regarded as one of the most important indication of MMR defect. In this study, we detected five microsatellite loci sensitive to gastric cancer and found MSI-H in 26% carcinoma samples. The frequency of MSI-H in *H pylori*-positive group was significantly higher than that in *H pylori*-negative group. Among gastritis and intestinal metaplasia samples, the MSI-H frequency was 0% and 3% respectively although with higher *H pylori* infection. MSI existed in intestinal metaplasia samples although the frequency was much lower than that in carcinoma samples. That is to say, MMR defect happened before the malignant transformation of gastric mucous membrane cells. These results together indicated that *H pylori* infection induce tumorigenesis of gastric carcinoma when MMR system of gastric mucosa fails to work functionally.

It has been proved that wild type p53 protein can induce cell apoptosis but the intracellular accumulation of mutant p53 protein can inhibit cell apoptosis and promote cell transformation and proliferation, resulting in carcinogenesis. The overexpression of *p53* protein is generally mutant forms, for the half-life of wild-type *p53* is very short and *p53* protein expression is usually negative in normal tissues. In our present study, *p53* expressions were found in 0% of the control, 0% of gastritis samples, 13.3% of intestinal metaplasia samples and 43% gastric carcinomas samples. The detection of *p53* expression in intestinal metaplasia indicates that *p53* mutation can be an early event in the pathogenesis of gastric cancer. When the carcinomas samples were subdivided into *H pylori*-positive and -negative, and the positive rates of their *p53* expression compared, we found a higher expression rate in *H pylori*-positive group than that in *H pylori*-negative group. The carcinoma samples from MSI study were also analyzed to determine whether there was any relationship with *p53* protein accumulation. No significant difference was shown to exist between samples in terms of their MSI status and *p53* expression. Nevertheless, MSI was found in 11 with *H pylori* infection, 8 manifested *p53* positive, this suggests that *H pylori* infection may play a role by inducing *p53* gene mutations in those MSI or MMR defect gastric mucosa, but only in certain individuals.

In conclusion, the association between *H pylori* infection, MSI and *p53* mutations observed in intestinal metaplasia and gastric carcinoma samples leads us to hypothesize that *H pylori* affect *p53* pattern in gastric mucosa when MMR system fails to work. Mutations of the *p53* gene seem to be an early event in gastric carcinogenesis.

REFERENCES

1 **Xia HH,** Talley NJ. Apoptosis in gastric epithelium induced by *Helicobacter pylori* infection: implications in gastric carcinogenesis. *Am J Gastroenterol* 2001; **96**: 16-26
2 **Meining A,** Bayerdorffer E, Stolte M. Extent, topography and symptoms of *Helicobacter pylori* gastrititis. Phenotyping for accurate diagnosis and therapy? *Pathologe* 2001; **22**: 13-18
3 **Fujioka T,** Honda S, Tokieda M. *Helicobacter pylori* infection and gastric carcinoma in animal models. *J Gastroenterol Hepatol* 2000; **15**(Suppl): D55-59
4 International Agency for research on Cancer. Schistosomes, Liver flukes and *Helicobacter pylori*. Evaluation of carcinogenic risks to humans. *IARC Monograph Evaluating Carcinogenic Risks to Humans* 1994; **61**: 1-241
5 **Jacob S,** Praz F. DNA mismatch repair defects: role in colorectal carcinogenesis. *J Biochimie* 2002; **84**: 27-47
6 **Coleman WB,** Tsongalis GJ. The role of genomic instability in human carcinogenesis. *Anticancer Res* 1999; **19**: 4645-4664
7 **Duval A,** Hamelin R. Genetic instability in human mismatch repair deficient cancers. *Ann Genet* 2002; **45**: 71-75
8 **Kastan MB,** Onyekwere O, Sidransky D, Vogelstein B, Craig RW. Participation of p53 protein in the cellular response to DNA damage. *Cancer Res* 1991; **51**: 6304-6311
9 **Chen J,** Jackson PK, Kirschner MW, Dutta A. Separate domains of p21 involved in the inhibition of Cdk kinase and PCNA. *Nature* 1995; **374**: 386-388
10 **Waga S,** Hannon GJ, Beach D, Stillman B. The p21 inhibitor of cyclin-dependent kinases controls DNA replication by interaction with PCNA. *Nature* 1994; **369**: 574-578
11 **Miyashita T,** Reed JC. Tumor suppressor p53 is a direct transcriptional activator of the human bax gene. *Cell* 1995; **80**: 293-299
12 **Fuchs CS**, Mayer RJ. Gastric carcinoma. *N Engl J Med* 1995; **333**: 32-41
13 **Parente F,** Caselli M, Bianchi Porro G. Gastric apoptosis and *Helicobacter pylori* infection: an intricate matter. *Scand J Gastroenterol* 2001; **2**: 113-115
14 **Parsonnet J,** Friedman GD, Vandersteen DP, Chang Y, Vogelman JH, Orentreich N, Sibley RK. *Helicobacter pylori* infection and the risk of gastric carcinoma. *N Engl J Med* 1991; **325**: 1127-1131
15 **Blaser MJ,** Chyou PH, Nomura A. Age at establishment of *Helicobacter pylori* infection and gastric carcinoma, gastric ulcer, and duodenal ulcer risk. *Cancer Res* 1995; **55**: 562-565
16 **Berloco P,** Russo F, Cariola F, Gentile M, Giorgio P, Caruso ML, Valentini AM, Di Matteo G, Di Leo A. Low presence of *p53* abnormalities in *H pylori*-infected gastric mucosa and in gastric adenocarcinoma. *J Gastroenterol* 2003; **38**: 28-36
17 **Wang XW,** Tseng A, Ellis NA, Spillare EA, Linke SP, Robles AI, Seker H, Yang Q, Hu P, Beresten S, Bemmels NA, Garfield S, Harris CC. Functional interaction of p53 and BLM DNA helicase in apoptosis. *J Biol Chem* 2001; **276**: 32948-32955
18 **Aaltonen LA,** Peltomaki P, Leach FS, Sistonen P, Pylkkanen L, Mecklin JP, Jarvinen H, Powell SM, Jen J, Hamilton SR, Leach FS. Clues to the pathogenesis of familial colorectal cancer. *Science* 1993; **260**: 812-816
19 **Bowcock A,** Osborne-Lawrence S, Barnes R, Chakravarti A, Washington S, Dunn C. Microsatellite polymorphism linkage map of human chromosome 13q. *Genomics* 1993; **15**: 376-386
20 **Harfe BD,** Robintson SJ. DNA mismatch repair and genetic instability. *Annu Rev Genet* 2000; **34**: 359-399

Science Editor Li WZ **Language Editor** Elsevier HK

PO Box 2345, Beijing 100023, China
www.wjgnet.com
wjg@wjgnet.com

ELSEVIER

World J Gastroenterol 2005;11(28):4367-4374
World Journal of Gastroenterology ISSN 1007-9327

• *CLINICAL RESEARCH* •

Sensory-motor responses to mechanical stimulation of the esophagus after sensitization with acid

Asbjørn Mohr Drewes, Hariprasad Reddy, Camilla Staahl, Jan Pedersen, Peter Funch-Jensen, Lars Arendt-Nielsen, Hans Gregersen

Asbjørn Mohr Drewes, Hariprasad Reddy, Camilla Staahl, Jan Pedersen, Hans Gregersen, Center for Biomechanics and Pain, Department of Gastroenterology, Aalborg Hospital, Aarhus University Hospital, Aalborg, Denmark
Lars Arendt-Nielsen, Center for Sensory-Motor Interactions (SMI), Department of Health Science and Technology, Aalborg University, Aalborg, Denmark
Peter Funch-Jensen, Department of Surgical Gastroenterology L, Aarhus University Hospital, Aarhus, Denmark
Supported by the "Det Obelske Familiefond", "Spar Nord Fonden" and the Danish Technical Research Council
Correspondence to: Professor Asbjørn Mohr Drewes, MD, PhD, DMSc, Center for Biomechanics and Pain, Department of Medical Gastroenterology, Aalborg Hospital, DK-9000 Aalborg, Denmark. drewes@smi.auc.dk
Telephone: +45-99322505 Fax: +45-99322503
Received: 2004-11-09 Accepted: 2004-12-23

Abstract

AIM: Sensitization most likely plays an important role in chronic pain disorders, and such sensitization can be mimicked by experimental acid perfusion of the esophagus. The current study systematically investigated the sensory and motor responses of the esophagus to controlled mechanical stimuli before and after sensitization.

METHODS: Thirty healthy subjects were included. Distension of the distal esophagus with a balloon was performed before and after perfusion with 0.1 mol/L hydrochloric acid for 30 min. An impedance planimetry system was used to measure cross-sectional area, volume, pressure, and tension during the distensions. A new model allowed evaluation of the phasic contractions by the tension during contractions as a function of the initial muscle length before the contraction (comparable to the Frank-Starling law for the heart). Length-tension diagrams were used to evaluate the muscle tone before and after relaxation of the smooth muscle with butylscopolamine.

RESULTS: The sensitization resulted in allodynia and hyperalgesia to the distension volumes, and the degree of sensitization was related to the infused volume of acid. Furthermore, a nearly 50% increase in the evoked referred pain was seen after sensitization. The mechanical analysis demonstrated hyper-reactivity of the esophagus following acid perfusion, with an increased number and force of the phasic contractions, but the muscle tone did not change.

CONCLUSION: Acid perfusion of the esophagus sensitizes the sensory pathways and facilitates secondary contractions. The new model can be used to study abnormal sensory-motor mechanisms in visceral organs.

Key words: Esophagus; Mechanical; Sensitization; Motility; Reflux; Pain

Drewes AM, Reddy H, Staahl C, Pedersen J, Funch-Jensen P, Arendt-Nielsen L, Gregersen H. Sensory-motor responses to mechanical stimulation of the esophagus after sensitization with acid. *World J Gastroenterol* 2005; 11(28): 4367-4374
http://www.wjgnet.com/1007-9327/11/4367.asp

INTRODUCTION

Pain arising from the esophagus is very common clinically and in the normal population, but the mechanisms involved are poorly understood[1]. Due to the difficulties in characterizing clinical pain, human experimental models have been developed to investigate the pain pathways in a standardized way in volunteers and patients. These models provide the possibility to control the stimulus parameters and to assess the response quantitatively[2,3]. Furthermore, the nociceptive system can be sensitized in the laboratory, resulting in allodynia (painful sensations to stimuli that are not normally painful), hyperalgesia (increased sensation to stimuli that are normally painful) and increase in the evoked referred pain area[4]. The sensitization most likely plays an important role in chronic visceral pain disorders[3,5]. Experimental chemical stimulation with acid has been used to sensitize the esophagus[6-8]. However, the literature has not been consistent with respect to the evoked mechanical hyperalgesia, probably due to methodological problems related to the stimulus modalities used[9].

Distension of the gut is a physiologic stimulus, and consequently most researchers have used experimental balloon distension models to investigate basic pain mechanisms in the gastrointestinal (GI) tract[10]. Most previous studies have used volume and pressure as proxies of the mechanical deformation and force applied to the gut wall[10]. However, the mechanical parameters tension, stress and strain are of more value than pressure and volume when studying the esophagus, as these parameters provide more valid information about the mechanical forces and deformation (elastic properties) during distension[11-15]. Furthermore, the muscle function is better evaluated when

the forces and tensions can be quantitated, rather than measuring the luminal pressure[16-18]. However, the sensory-motor responses of the organ during a mechanical stimulus cannot be evaluated independently of the mechanical forces and deformation. Thus, phasic contractions and changes in muscle tone can influence the sensory response themselves[18], and in diseases of the esophagus hyper-reactivity may give major contribution to the symptoms[19,20]. Methods to estimate and control the mechanical response will thus allow better explanations of the effects on the sensory-motor response during the mechanical stimulations with and without sensitization of the pain system.

Systematic investigation of both the sensory and motor responses to controlled mechanical stimuli following experimental sensitization of the esophagus has to the best of our knowledge never been investigated. The aims of the current study were to (1) investigate the effect on sensitization of the esophagus with acid on the sensory response to controlled mechanical stimulation; (2) calculate the evoked referred pain areas to the mechanical stimulation before and after sensitization as a proxy for the central neuronal changes; and (3) evaluate the motor response to the sensitization by a new *in vivo* method evaluating the change in tension during contraction (the afterload tension) as function of the initial muscle length before the contraction (the preload radius).

MATERIALS AND METHODS

Thirty healthy subjects, 14 males and 16 females, mean age 36.5±12.9 years, were included. The subjects did not suffer from any kind of chronic pain, GI symptoms or disturbances in personality. All subjects gave informed written and verbal consent prior to the study. The protocol was approved by the local ethics committee and performed in accordance with the Helsinki Declaration.

Mechanical stimulations

The impedance planimetry system including the principle for measurement of the cross-sectional area (CSA) has been described in detail previously[18,21,22]. The 70-cm long probe with a diameter of 4.5 mm had a cylindrical large-sized bag near the tip. The bag was 40 mm in length and was made of 35-μm thick, non-conducting polyester urethane. A side-hole for acid perfusion was placed 2 cm above the bag. The probe had a four-electrode impedance planimetry system with four sets of ring electrodes inside the bag (GMC Aps, Hornslet, Denmark). The bag could be inflated with electrically conducting fluid (0.09% saline) through a pair of infusion channels. The change in impedance of the fluid during distension of the bag reflects the change in the CSA[18]. The infusion channels were connected to an infusion pump (Type 111, Ole Dich Instrument Makers, Hvidovre, Denmark) that was able to fill or empty the bag continuously. The bag could be inflated to a CSA of approximately 2 000 mm^2 (diameter equal to 50 mm) without stretching the wall of the bag. The fluid in the connecting tube between the pump and the probe was heated to 37 ℃. A safety valve was connected with the pump allowing the subjects to stop the infusion at any time. The system was calibrated before the probe was inserted into the esophagus. Non-linearity of the CSA was corrected for in the whole measurement range by means of a software feature. The pressure was measured by means of a low-compliance perfusion system connected to external transducers.

Sensory ratings

The sensory intensity was assessed continuously during the experiment using an electronic visual analog scale (VAS, GMC, Hornslet, Denmark). The volunteers were trained in assessment of sensation to deep pressure at the muscles on the right forearm several times before the visceral stimuli were given. A scale for both non-painful and painful sensations was used[3]. The intensities of the *non-painful* sensations were scored with the following descriptors added to facilitate the scoring: 1 = vague perception of mild sensation; 2 = definite perception of mild sensation; 3 = vague perception of moderate sensation; 4 = definite perception of moderate perception; 5 = the pain threshold. For the *painful* sensations the patients used the scale from 5 to 10 anchored at 5 = pain threshold to 10 = unbearable pain, with the following anchor words: 6 = slight pain; 7 = moderate pain; 8 = medium pain intensity; 9 = intense pain; and 10 = unbearable pain. This part of the scale was red to clearly separate the non-painful and painful range of sensations. The first three distensions were used to practice the sensory ratings[3]. The subjects were carefully instructed to score the evoked chest pain and to differentiate this from the unpleasantness in the throat caused by traction due to the distension-evoked esophageal contractions. The scale has previously been shown to be robust, and to discriminate sensations in the esophagus[8,11,12], and the small and large intestine[13,14,23,24].

After the last distension before butylscopolamine injection (see below) the volunteers were asked about referred pain to the chest or other remote areas evoked by the distensions at moderate pain (VAS = 7). If present the referred pain area was marked with a pen and transferred to a transparent paper. Later the area was digitized (ACECAD D900+ Digitizer, Taiwan) and the size calculated (Sigma-Scan, Jandel Scientific, Canada).

Protocol

The subjects fasted for at least 4 h prior to the experiment. Intubation was performed through the mouth. The bag was inserted into the stomach and then retracted to identify the location of the lower esophageal sphincter as a zone of high resting pressure that decreased with swallowing. Then the bag was placed 7 cm proximal to the sphincter and the probe was taped to the cheek. The subjects were asked to lie down with the head tilted by 30° after the placement of the bag. The experiment was performed in that position after 30 min of rest.

Three bag distension stimuli with a constant infusion rate of 25 mL/min were done to precondition the tissue and to obtain repeatable sensory data[3,13,15,23,24]. The inter-stimulus interval was 60 s for all experiments. When the subjects reported slight pain (6 on the VAS), the bag was deflated using the same flow rate as during the inflation until it was empty. After these stimuli, two more distensions

were done at the same infusion rate. When moderate pain intensity (7 on the VAS) was reached, the pump was reversed and the bag deflated. Then 20 mg butylscopolamine was given intravenously and after abolishment of the contractile activity the two last distensions were repeated.

After the first series of mechanical stimuli, the participants underwent a modified acid perfusion test[25]. Hence, during a perfusion channel in the catheter 0.1 mol/L hydrochloric acid was infused at a rate of 7 mL/min for 30 min. If the evoked sensations due to the acid stimulation were reported unpleasant (rated $\geqslant$5 on the VAS), the perfusion was stopped for 30 s and the subjects were allowed to swallow 10 mL water. In case the perfusion was too unpleasant for the subjects, it was stopped and the amount of infused acid was measured.

After the acid perfusion, bag distensions before and after butylscopolamine were given using the same protocol as described above, before acid perfusion.

During all stimuli autonomic reactions were monitored and displayed on-screen using a Biopac MP100 system (Biopac Systems Inc., Santa Barbara, CA, USA) including sensors and recording system for electrocardiogram, pulse rate and respiration.

Data analysis

The circumferential wall tension was calculated according to the law of Laplace for cylindrical structures as

$$T = \triangle Pr$$

where T is the circumferential wall tension, r is the balloon radius, and $\triangle P$ is the transmural pressure. The geometry of the esophagus during distension can be considered circular except at very low pressure levels[18]. Therefore, the radius was determined as

$$r = \sqrt{\frac{CSA}{\pi}}$$

All subjects stated that they more reliably rated the sensory intensity at the second distension compared to the first. Therefore, only data from the second distension were used in the analysis. After butylscopolamine the first distension was used as the maximal decrease in contractile activity was seen at the first few minutes after the injection.

As criteria for valid contractions before and after acid perfusion a pressure amplitude above 2.5 kPa was used.

In a representative sample of 10 subjects (5 males and 5 females, mean age 36.1±14.3 years) the change in tension during individual distension-induced contractions (afterload tension) was computed and expressed as function of the radius immediately before the contractions (preload radius). The diagrams were made before and after perfusion of the distal esophagus with a mean of 123 mL hydrochloric acid. An example from an individual subject is shown in Figure 1. The data were fitted with a third order polynomial. These diagrams correspond to the well-known heart ventricular function curves in terms of the ventricular stroke working as function of the mean atrial length. Such curves demonstrate the Frank-Starling mechanism of the heart now adapted to the esophagus-see appendix.

The pressure and CSA data obtained between the evoked contractions (without infusion of butylscopolamine) were used to compute the total tonic tension, whereas the tracings during butylscopolamine infusion were used for calculation of the passive tension. The active tonic tension was obtained by subtracting the passive tension from the total tonic tension[14,18].

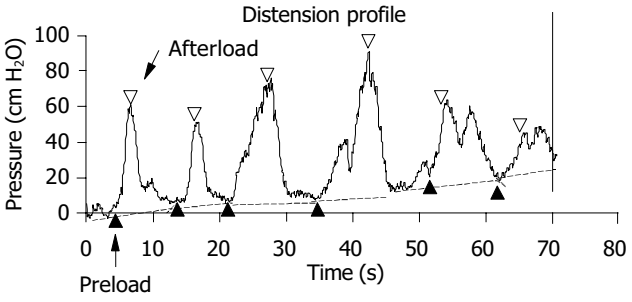

Figure 1 Raw data in a typical subject showing the change in pressure during bag-distension-induced contractions. The change in tension during maximal distension-induced contractions (afterload tension) was computed at the open triangles and expressed as function of the radius immediately before the contractions marked with solid triangles (preload radius). The radius was calculated on the basis of the CSA measured simultaneously. For details regarding the calculations see Methods section.

Statistical analysis

The results are expressed as mean±SD unless otherwise indicated. Continuous data were analyzed using *t*-tests. For multiple comparisons, two-way analysis of variance (ANOVA) was used with the factors: (1) before and after acid and (2) the different VAS levels. $P<0.05$ was considered significant. The software package SPSS v. 10.0 was used for the statistical analysis.

RESULTS

Mechanical stimuli before and after acid

All subjects completed the experiment. After the preconditioning stimuli, the curve characteristics and sensory ratings were reproducible in all subjects. The stimulus-response curves after preconditioning the tissue are shown in Figure 2 for the infused volume, CSA, pressure, and tension. The sensation intensity was approximately linear as functions of all four stimulation variables. The sensory rating increased after acid, when expressed as a function of the volume ($F = 4.75$, $P = 0.03$), whereas no differences were found for the CSA ($F = 1.0$, $P = 0.3$), pressure ($F = 0.7$, $P = 0.4$) and tension ($F = 1.2$, $P = 0.3$). The curves during butylscopolamine infusion showed the same pattern as described above, before and after acid perfusion (data not shown).

The acid infusion resulted in a more hyper-reactive esophagus as the number of contractions with pressure amplitudes above 2.5 kPa during the distensions increased from 2.9±1.5 to 3.5±1.5 after acid perfusion ($P = 0.03$).

The change in tension during bag-distension-induced contractions (the afterload tension) was plotted as a function of the preload radius for 10 representative subjects (Figure 3). No contractions were observed at radii below 5 mm. Before acid infusion the afterload tension increased until a plateau was reached. This corresponds to the "Frank-Starling mechanism" relating to the less interdigitation of

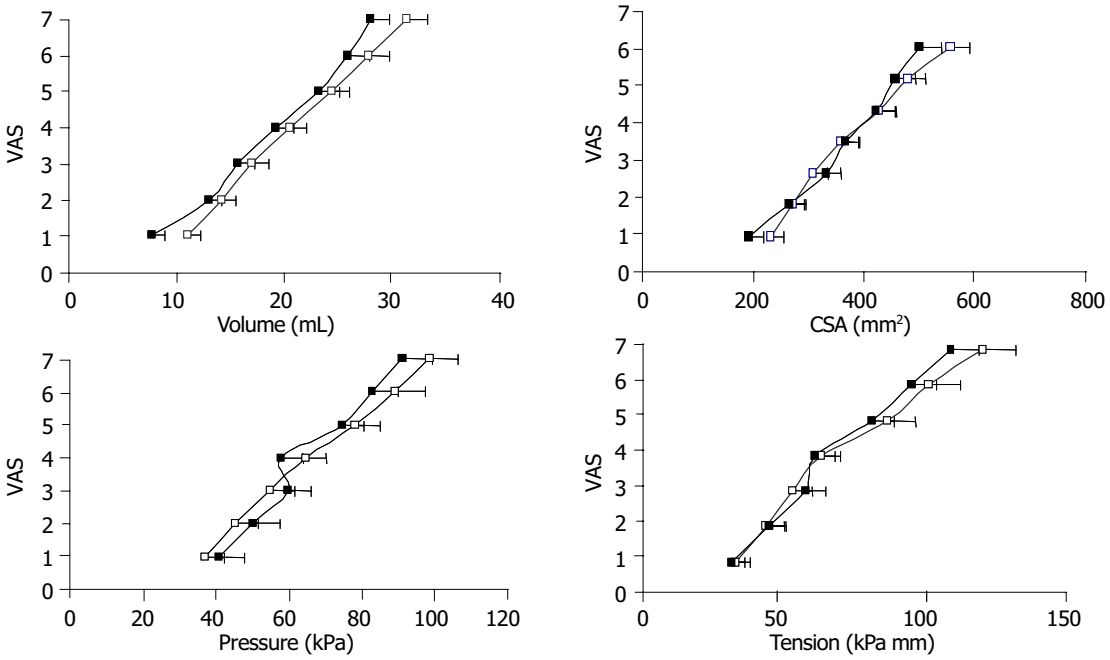

Figure 2 Sensory response to bag distension of the distal esophagus expressed as functions of the volume, CSA, pressure and tension. The curves were drawn before (□) and after (■) perfusion of the distal esophagus with acid. The sensory response increased after acid perfusion when expressed as a function of the volume.

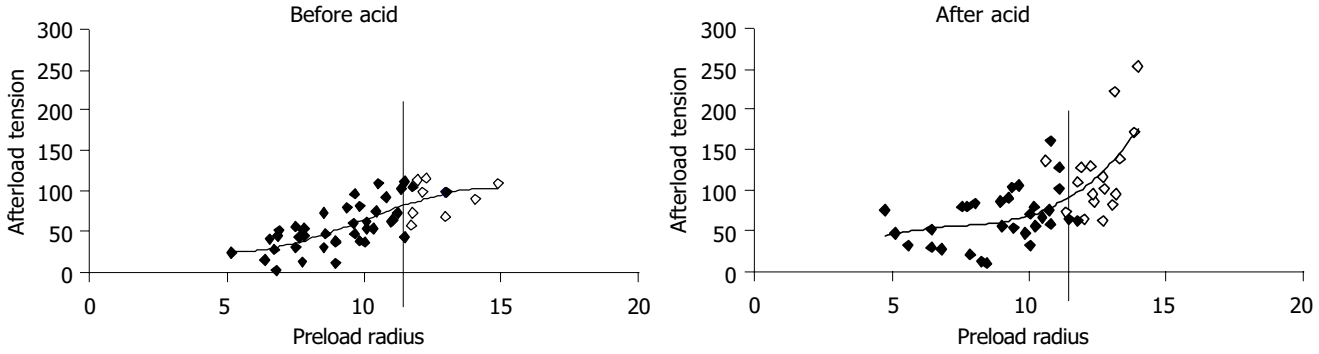

Figure 3 Tension during bag-distension-induced contractions (the afterload tension) plotted as functions of the radius immediately before the contractions (the preload radius) as shown in Figure 1. Five to eight datasets were computed during the distension for 10 representative subjects. Data calculated at painful sensations were all above preload radii of 11.5 mm and are shown as open markings.

muscle filaments when the muscles are overstretched. Painful sensations (VAS ⩾5) were experienced at preload radii higher than 11.5 mm. After the acid infusion higher afterload tensions were observed at both low and high radii as compared to baseline, and there was a tendency to more spreading of the data as some individuals obtained very high afterload tensions. The painful sensations were also only evoked at radii higher than 11.5 mm.

The total, passive and active tonic tensions before and after acid infusion are shown in Figure 4. There was no difference in curve shape between before and after acid, indicating that acid infusion does not change esophageal muscle tone.

High and low acid responders

The subjects tolerated a mean of 101±53 mL of acid. To see if the sensory response was related to the amount of acid infused, the subjects were divided into two groups. One group could accept 100-200 mL of acid (n = 17) and the other group, less than 100 mL of acid (n = 13). There was a relation between the evoked sensitization and the acid load as those who accepted more than 100 mL were sensitized to volume (F = 5.3, P = 0.02), pressure (F = 5.5, P = 0.02) and tension (F = 6.0, P = 0.01), but not to CSA (F = 0.9, P = 0.3). The group tolerating less than 100 mL were not sensitized to neither volume (F = 0.3, P = 0.6), pressure (F = 0.6, P = 0.4), tension (F = 0.8, P = 0.4) nor CSA (F<0.01, P = 0.99).

Referred pain areas

All subjects reported referred pain to the stimulations. The referred pain areas to mechanical stimuli at moderate pain are shown in Figure 5. Additionally one male and two females had referred pain in the back. The referred pain areas increased from 27.9±29.3 cm^2 before acid to 41.4±39.0 cm^2 after acid (P = 0.047), although the volume was smaller at the distensions after acid.

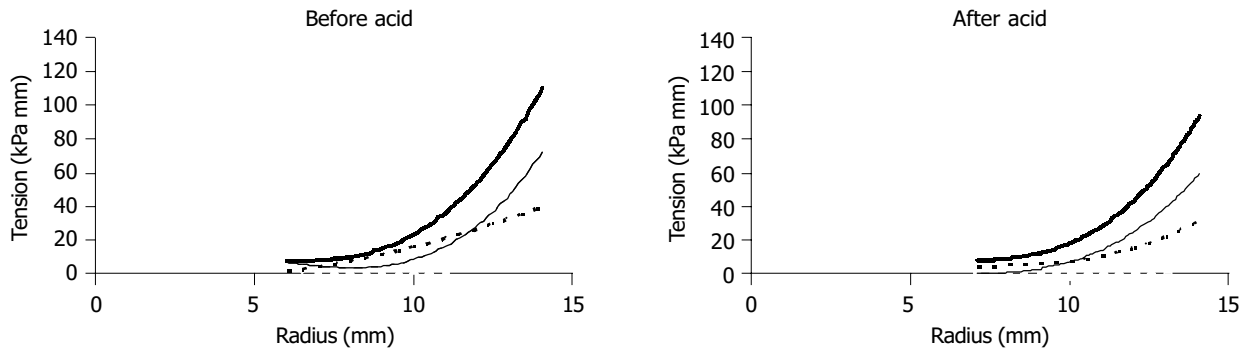

Figure 4 Plots of the total tonic (top), the passive (dotted) and the active (thin) tonic tensions as functions of radius before and after acid infusion. For explanations see text. Acid did not change the curve shapes. Hence, esophageal muscle tone was not affected by the acid infusion.

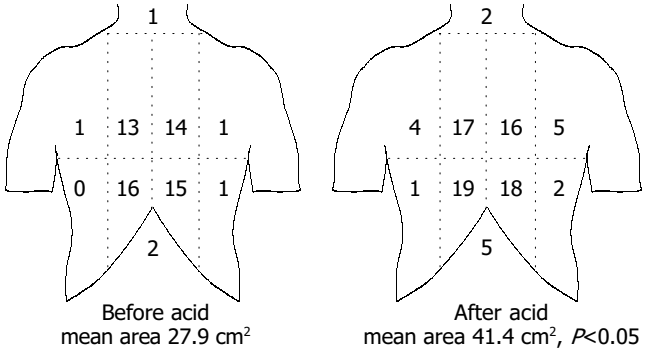

Figure 5 A schematic illustration of the referred pain areas drawn by the subjects following mechanical stimuli of the esophagus before and after perfusion with acid. The stimuli were given with an intensity corresponding to moderate pain. The chest was divided into eight areas by a horizontal line 5 cm above the xiphoid process, a vertical midline and two vertical lines 5 cm lateral to the midline. The numbers on the figure refer to the number of subjects reporting referred pain to that particular region of the chest. The referred pain area increased following the sensitization with acid.

DISCUSSION

The current experiment used controlled ramp distensions and preconditioning to evoke experimental pain in the esophagus in 30 subjects. The sensory response was assessed before and after sensitization of the lower esophagus by acid perfusion. The sensory rating increased after acid when expressed as a function of the volume, and the degree of sensitization was related to the infused volume of acid. Furthermore, an increase in referred pain to a standardized distension was seen reflecting activation of central facilitatory pain mechanisms. The mechanical analysis demonstrated hyper-reactivity of the esophagus following acid perfusion, with an increased number and force of the phasic contractions, but the muscle tone did not change. This illustrates that acid perfusion not only sensitizes the sensory pathways, but also facilitates motor reflexes.

Sensory response to sensitization with acid

Chronic pain is associated with modifications of the central nervous system such as central sensitization[4]. Animal experiments have demonstrated neuronal changes such as increased spontaneous activity, decreased firing threshold, and expansion of the receptive fields of spinal neurons subjected to activation and/or experimental sensitization of their peripheral afferents[5,26,27]. Sensitization of the human esophagus with acid is a valuable experimental pain model, as the evoked allodynia, hyperalgesia and referred pain patterns reflect sensitization of the nervous system and can be studied systematically[3]. Hence, decreased thresholds to physiologic stimuli seem to contribute to many of the symptoms reported by patients with inflammatory and functional diseases in the gut[28,29]. Thus, a combination of mechanical stimulation and sensitization of the esophagus may mimic the widespread pain and other sensations reported by patients with reflux disease and unexplained chest pain[16,30,31].

Acid-sensitive fibers have been demonstrated in animal studies, and mucosal afferents are often sensitive to different chemical stimuli[32,33]. Increased responses to mechanical, electrical and thermal stimuli after acid perfusion of the esophagus have also been demonstrated in human beings[6-9,34], although previous studies using latex balloons were not consistent. This can be due to methodological problems using latex balloons, where the distension data must be corrected for the intrinsic mechanical properties of the balloons and for the uncontrollable deformation in longitudinal direction[9,16]. Non-compliant polyester urethane bags overcome these problems. The effect of preconditioning the tissue by several distensions until the stress-strain relationship becomes reproducible has also not been considered in most previous studies[3,18]. Different modifications of the acid perfusion test have been used as a chemogenic stimulus by several authors[6,7,9,35,36]. When the current material was divided into those who tolerated below and above 100 mL of acid, significant increased sensation to the mechanical stimulus was only seen in the high acid group. Hence, it is recommended to use volumes higher than 100 mL in future studies.

The present study demonstrated increased sensation to the infused bag volume, but not to pressure and tension. The intraluminal pressure and tension are highly dependent of the contractile force state of the esophageal muscles, and hence not as reliable parameters as the deformation[18]. Despite the decrease in volume after acid infusion, the CSA did not decrease significantly. Thus it seems that the bag conforms to a shape where it is shorter after acid infusion. Such a shape change is likely caused by changes in the contractile activity in the acid exposed area and even in regions affected by nerve-mediated reflex responses.

Secondary contractions and muscle hyper-responsiveness can be evoked by acid in the distal esophagus due to reflex loops between mucosal afferents and the motor system[37-40]. After acid perfusion increased force of the secondary contractions was evoked by the distension in the non-painful and painful range. Animal studies have shown that-in contrast to the somatic system-afferents encoding both non-painful and painful sensations can sensitize in the viscera[41]. The current observations in the human esophagus are in line with these studies, as the sensitization of afferents encoding conscious sensations to distension seems to change the contractile activity in the muscle via local and/or central reflexes[42,43]. However, the curve form changed mostly in the pain range (to the right of the vertical line in Figure 3) and hence there seems to be a higher effect of sensitization on the painful sensations. The Frank-Starling mechanism predicts a decrease in contractile activity when the muscle is overstretched corresponding to less optimal interdigitation of actin and myosin filaments. In the current experiment the baseline curve form showed no decrease in afterload tension at maximal distension. The fact that the afterload tensions were higher after acid infusion indicates that bag distension itself does not activate the muscle maximally.

Another manifestation of the acid perfusion was the increased referred pain area to the mechanical stimulation, although the bag volume was lower after the perfusion. Enlarged referred pain areas is also a characteristic in clinical gut disorders[44-46], and are very similar to what is observed in patients suffering from chronic musculoskeletal pain[47]. Previously, we have shown that sensitization of the esophagus results in increased referred pain areas[8], a finding which was confirmed in the current study. The mechanism is of central origin[4], which was also shown in previous papers using neurophysiological assessment of the spinal and supraspinal pain response after acid perfusion of the esophagus[8,48].

Mechanical and motor responses to sensitization with acid

The sensitization resulted not only in allodynia and hyperalgesia to the distension volumes, but the esophagus also exhibited hyper-reactivity as illustrated by the increased number of contractions after the acid perfusion. Such hyper-reactivity has also been seen in animal studies[37,38]. The contractions were also stronger to a given preload radius. However, the acid infusion did not change the total tonic tension, the passive tension and the active tonic tensions (Figure 4). Hence, the hyper-reactivity only accounts for phasic contractions, not for tone in the esophageal body. Previously, Sifrim *et al*.[49], showed that acid reflux into the esophagus stimulated tone in the esophageal body. However, simultaneous distension seemed to inhibit the acid induced tone. These issues obviously need further investigations.

The preload radius where contractions were evoked by the painful stimuli (VAS = 5 and higher) did not change after acid (vertical line in Figure 2). This corresponds with the "strain theory", *i.e.*, that the mechanoreceptors are activated by circumferential stretch independent of the contractile state of the muscles[12,13,15,50]. The receptors encoding distension of the gut are mainly believed to be localized in the muscle and nerve layers, where they are not exposed to acid[33,43]. Hence, the contractions are probably initiated by reflex loops between strain-sensitive mechanosensitive afferents localized in the muscle layers and the smooth muscle cells. Whether such reflexes are local or mediated via central (vagal and/or spinal) afferents cannot be concluded from the current data[40,42,43]. We believe, however, that a central component is important as the contractions were more powerful after perfusion with acid. The acid perfusion may thus result in sensitization of mucosal afferents as well as central hyperexcitability[8,43,48]. As the enteric nervous system is partly under inhibitory central control[51], the sensitization may result in dampening of the central control. This mechanism is expedient as such reflexes will tend to move acid from reflux towards the stomach where it is harmless.

Modeling diseases of the esophagus

Sensation and pain detection thresholds to distension, electrical and acid stimuli of the esophagus were found to be lower in patients with non-cardiac chest pain compared to healthy subjects[6,7,52,53]. Such hypersensitivity can be mimicked in the current model. Furthermore, the muscles of the esophagus are hyper-reactive in patients with unexplained chest pain[19,54-56]. In the present model the acid perfusion evoked an increased number of contractions, which were characterized by a higher force. Thus diseases characterized by primary and secondary motor disorders can also be mimicked experimentally, and in patients the preload-afterload plots will be valuable for description of the aberrant motor function. The model can therefore be used to study abnormal sensory-motor mechanisms in visceral organs, and may also prove useful in pharmacological studies with drugs targeted to treat patients with unexplained chest pain and motor disorders of the esophagus.

Appendix

The preload is considered in this study to be initial muscle length (radius) preceding the contraction during the distension, whereas the afterload is evaluated as the active tension during the contraction. In cardiac physiology the preload is usually considered to be the end-diastolic pressure or radius and the afterload is considered to be the arterial pressure during the systole. The explanation of the Frank-Starling mechanism is that when an extra amount of blood flows into the ventricles, the cardiac muscle itself is stretched to greater length. This in turn causes the muscle to contract with increased force because the actin and myosin filaments then are brought to a more nearly optimal degree of interdigitation for force generation. In cardiac physiology the importance of the concept of preload and afterload is that in many abnormal functional states of the heart and circulation, the pressure during filling of the ventricle or the arterial pressure against which the ventricle must contract, or both, are severely altered from the normal. The Frank-Starling mechanism has been important in the understanding of drugs with effect on the myocardial function, and transferring this concept to esophageal physiology, the development in the current model will have interest for evaluation of normal esophageal physiology and in the pathophysiology of esophageal disorders.

REFERENCES

1 **Bochus HL.** Abdominal Pain. In: Berk JE, ed. Gastroenterology. *Philidelphia: WB Saunders* 1985: 22-47
2 **Arendt-Nielsen L.** Induction and assessment of experimental pain from human skin, muscle, and viscera. In: Jensen TS, Turner JA, and Wiesenfeld-Hallin Z, eds. Proceedings of the 8th World Congress of Pain, Progress in Pain Research and Management. *Seattle: ISAP Press* 1997: 393-425
3 **Drewes AM,** Gregersen H, Arendt-Nielsen L. Experimental pain in gastroenterology: A reappraisal of human studies. *Scand J Gastroenterol* 2003; **38**: 1115-1130
4 **Arendt-Nielsen L,** Laursen RJ, Drewes AM. Referred pain as an indicator for neural plasticity. *Prog Brain Res* 2000; **129**: 343-356
5 **Garrison DW,** Chandler MJ, Foreman RD. Viscerosomatic Convergence Onto Feline Spinal Neurons from Esophagus, Heart and Somatic Fields - Effects of Inflammation. *Pain* 1992; **49**: 373-382
6 **Mehta AJ,** De Caestecker JS, Camm AJ, Northfield TC. Sensitization to painful distention and abnormal sensory perception in the esophagus. *Gastroenterology* 1995; **108**: 311-319
7 **Sarkar S,** Aziz Q, Woolf CJ, Hobson AR, Thompson DG. Contribution of central sensitisation to the development of non-cardiac chest pain. *Lancet* 2000; **356**: 1154-1159
8 **Drewes AM,** Schipper KP, Dimcevski G, Petersen P, Andersen OK, Gregersen H, Arendt-Nielsen L. Multi-modal induction and assessment of allodynia and hyperalgesia in the human oesophagus. *Eur J Pain* 2003; **7**: 539-549
9 **Hu WH,** Martin CJ, Talley NJ. Intraesophageal acid perfusion sensitizes the esophagus to mechanical distension: a Barostat study. *Am J Gastroenterol* 2000; **95**: 2189-2194
10 **Whitehead WE,** Delvaux M. Standardization of barostat procedures for testing smooth muscle tone and sensory thresholds in the gastrointestinal tract. *Dig Dis Sci* 1997; **42**: 223-224
11 **Drewes AM,** Schipper KP, Dimcevski G, Petersen P, Andersen OK, Gregersen H, Arendt-Nielsen L. Multimodal assessment of pain in the esophagus: a new experimental model. *Am J Physiol Gastrointest Liver Physiol* 2002; **283**: G95-103
12 **Drewes AM,** Pedersen J, Liu W, Arendt-Nielsen L, Gregersen H. Controlled mechanical distension of the human oesophagus: Sensory and biomechanical findings. *Scand J Gastroenterol* 2003; **38**: 27-35
13 **Gao C,** Arendt-Nielsen L, Liu W, Petersen P, Drewes AM, Gregersen G. Sensory and biomechanical responses to ramp-controlled distension of the human duodenum. *Am J Physiol Gastrointest Liver Physiol* 2003; **284**: G461-471
14 **Pedersen J,** Gao C, Egekvist H, Bjerring P, Arendt-Nielsen L, Gregersen H, Drewes AM. Pain and biomechanical responses to distension of the duodenum in patients with systemic sclerosis. *Gastroenterol* 2003; **124**: 1230-1239
15 **Petersen P,** Gao C, Arendt-Nielsen L, Gregersen H, Drewes AM. Pain intensity and biomechanical responses during ramp-controlled distension of the human rectum. *Dig Dis Sci* 2003; **48**: 1310-1316
16 **Gregersen H,** Kassab G. Biomechanics of the gastrointestinal tract. *Neurogastroenterol Motil* 1996; **8**: 277-297
17 **Gregersen H,** Christensen J. Gastrointestinal tone. *Neurogastroenterol Mot* 2000; **12**: 501-508
18 **Gregersen H.** Biomechanics of the Gastrointestinal Tract. *London: Springer Verlag* 2002
19 **Rao SS,** Gregersen H, Hayek B, Summers RW, Christensen J. Unexplained chest pain: the hypersensitive, hyperreactive, and poorly compliant esophagus. *Ann Intern Med* 1996; **124**: 950-958
20 **Richter JE.** Oesophageal motility disorders. *Lancet* 2001; **358**: 823-828
21 **Gregersen H,** Andersen MB. Impedance measuring system for cross-sectional area in the gastrointestinal tract. *Med Biol Eng Comput* 1991; **29**: 108-110
22 **Gregersen H,** Giversen IM, Rasmussen LM, Tottrup A. Biomechanical wall properties and collagen content in the partially obstructed opossum esophagus. *Gastroenterology* 1992; **103**: 1547-1551
23 **Drewes AM,** Schipper KP, Dimcevski G, Petersen P, Gregersen H, Funch-Jensen P, Arendt-Nielsen L. Gut pain and hyperalgesia induced by capsaicin: A human experimental model. *Pain* 2003; **104**: 333-341
24 **Drewes AM,** Babenko L, Birket-Smith L, Funch-Jensen P, Arendt-Nielsen L. Induction of non-painful and painful intestinal sensations by hypertonic saline: A new human experimental model. *Eur J Pain* 2003; **7**: 81-91
25 **Bernstein LM,** Baker LA. A clinical test for esophagitis. *Gastroenterology* 1958; **34**: 760-781
26 **Coderre TJ,** Katz J, Vaccarino AL, Melzack R. Contribution of central neuroplasticity to pathological pain: review of clinical and experimental evidence. *Pain* 1993; **52**: 259-285
27 **Laird JMA,** de la Rubia PG, Cervero F. Excitability changes of somatic and viscero-somatic nociceptive reflexes in the decerebrate-spinal rabbit: role of NMDA receptors. *J Physiol* 1995; **489**: 545-555
28 **Mayer EA,** Munakata J, Mertz H, Lembo T, Bernstein CN. Visceral hyperalgesia and irritable bowel syndrome. In: Gebhart GF, ed. Visceral pain, Progress in Pain Research and Management. *Volume 5. Seattle: IASP Press* 1995: 429-468
29 **Yaksh TL.** Spinal systems and pain processing: development of novel analgesic drugs with mechanistically defined methods. *Trends Pharmacol Sci* 1999; **20**: 329-337
30 **Eslick GD,** Fass R. Noncardiac chest pain: evaluation and treatment. *Gastroenterol Clin N Am* 2003; **32**: 531-552
31 **Clouse RE,** Richter JE, Heading RC, Janssens J, Wilson JA. Functional esophageal disorders. *Gut* 1999; **45**: 31-36
32 **Ness TJ,** Gebhart GF. Visceral pain: a review of experimental studies. *Pain* 1990; **41**: 167-234
33 **Sengupta JN,** Gebhart GF. Gastrointestinal afferent fibers and sensation. In: Johnson L, ed. Physiology of the Gastrointestinal Tract. Third ed. *New York: Raven Press* 1994: 484-519
34 **Sarkar S,** Hobson AR, Hughes A, Growcott J, Woolf CJ, Thompson DG, Aziz Q. The prostaglandin E2 receptor-1 (EP-1) mediates acid-induced visceral pain hypersensitivity in humans. *Gastroenterology* 2003; **124**: 18-25
35 **DeVault KR.** Acid infusion does not affect intraesophageal balloon distention- induced sensory and pain thresholds. *Am J Gastroenterol* 1997; **92**: 947-949
36 **Fass R,** Naliboff B, Higa L, Johnson C, Kodner A, Munakata J, Ngo J, Mayer EA. Differential effect of long-term esophageal acid exposure on mechanosensitivity and chemosensitivity in humans. *Gastroenterology* 1998; **115**: 1363-1373
37 **Shirazi S,** Schulzedelrieu K, Custerhagen T, Brown CK, Ren J. Motility changes in opossum esophagus from experimental esophagitis. *Dig Dis Sci* 1989; **34**: 1668-1676
38 **White RJ,** Zhang Y, Morris GP, Paterson WG. Esophagitis-related esophageal shortening in opossum is associated with longitudinal muscle hyperresponsiveness. *Am J Physiol Gastrointest Liver Physiol* 2001; **280**: G463-469
39 **Schoeman MN,** Holloway RH. Integrity and Characteristics of Secondary Esophageal Peristalsis in Patients with Gastroesophageal Reflux Disease. *Gut* 1995; **36**: 499-504
40 **Lang IM,** Medda BK, Shaker R. Mechanisms of reflexes induced by esophageal distension. *Am J Physiol Gastrointest Liver Physiol* 2001; **281**: G1246-1263
41 **Gebhart GF.** Pathobiology of visceral pain: molecular mechanisms and therapeutic implications IV. Visceral afferent contributions to the pathobiology of visceral pain. *Am J Physiol Gastrointest Liver Physiol* 2000; **278**: G834-838
42 **Grundy D.** Neuroanatomy of visceral nociception: vagal and splanchnic afferent. *Gut* 2002; **51**: I2-I5
43 **Szurszewski JH,** Ermilov LG, Miller SM. Prevertebral ganglia and intestinofugal afferent neurones. *Gut* 2002; **51**: I6-I10
44 **Mayer EA,** Gebhart GF. Basic and clinical aspects of visceral hyperalgesia. *Gastroenterology* 1994; **107**: 271-293
45 **Sanger GJ.** Hypersensitivity and hyperreactivity in the irritable bowel syndrome: An opportunity for drug discovery. *Dig Dis* 1999; **17**: 90-99

46 **Mertz H,** Fullerton S, Naliboff B, Mayer EA. Symptoms and visceral perception in severe functional and organic dyspepsia. *Gut* 1998; **42**: 814-822
47 **Johansen MK,** Graven-Nielsen T, Olesen AS, Arendt-Nielsen L. Generalised muscular hyperalgesia in chronic whiplash syndrome. *Pain* 2001; **89**: 293-295
48 **Sarkar S,** Hobson AR, Furlong PL, Woolf CJ, Thompson DG, Aziz Q. Central neural mechanisms mediating human visceral hypersensitivity. *Am J Physiol Gastrointest Liver Physiol* 2001; **281**: G1196-1202
49 **Sifrim D,** Tack J, Lerut T, Janssens J. Transient lower esophageal sphincter relaxations and esophageal body muscular contractile response in reflux esophagitis. *Dig Dis Sci* 2000; **45**: 1293-1300
50 **Barlow JD,** Gregersen H, Thompson DG. Identification of biomechanical factors associated with the perception of distension in the human esophagus. *Am J Physiol Gastrointest Liver Physiol* 2002; **282**: G683-689
51 **Christensen J.** Motor functions of the pharynx and esophagus. In: Johnson LR, Christensen J, Jackson MJ, Jacobsen ED, Walsh JH, eds. Physiology of the gastrointestinal tract. Second ed. *New York: Raven press* 1987: 595-612
52 **Frobert O,** Arendt-Nielsen L, Bak P, Funch-Jensen P, Peder BJ. Pain perception and brain evoked potentials in patients with angina despite normal coronary angiograms. *Heart* 1996; **75**: 436-441
53 **Smout AJ,** Devore MS, Dalton CB, Castell DO. Cerebral Potentials-evoked by esophageal distension in patients with noncardiac chest pain. *Gut* 1992; **33**: 298-302
54 **Rao SS.** Visceral hyperalgesia: the key for unrevealing functional gastrointestinal disorders. *Dig Dis* 1996; **14**: 271-275
55 **Balaban DH,** Yamamoto Y, Liu JM, Pehlivanov N, Wisniewski R, DeSilvey D, Mittal RK. Sustained esophageal contraction: A marker of esophageal chest pain identified by intraluminal ultrasonography. *Gastroenterology* 1999; **116**: 29-37
56 **Pehlivanov N,** Liu JM, Mittal RK. Sustained esophageal correlate of heartburn contraction: a motor symptom. *Am J Physiol Gastrointest Liver Physiol* 2001; **281**: G743-751

Science Editor Guo SY **Language Editor** Elsevier HK

PO Box 2345, Beijing 100023, China
www.wjgnet.com
wjg@wjgnet.com

ELSEVIER

World J Gastroenterol 2005;11(28):4375-4381
World Journal of Gastroenterology ISSN 1007-9327

• *CLINICAL RESEARCH* •

Relationship between gastrointestinal and extra-gastrointestinal symptoms and delayed gastric emptying in functional dyspeptic patients

N Pallotta, P Pezzotti, E Calabrese, F Baccini, E Corazziari

N Pallotta, P Pezzotti, E Calabrese, F Baccini, E Corazziari, Dpt Scienze Cliniche, Università degli Studi di Roma "La Sapienza"; Reparto AIDS e Malattie Sessualmente Trasmesse, Istituto Superiore di Sanità; Rome, Italy
Correspondence to: Professor E Corazziari, Dpt di Scienze Cliniche, Università "La Sapienza", Policlinico "Umberto I", V.le del Policlinico, Rome 00161, Italy. enrico.corazziari@uniroma1.it
Telephone: +39-6-49978384 Fax: +39-6-49978385
Received: 2004-07-17 Accepted: 2005-01-05

Abstract

AIM: Delayed gastric emptying and an enlarged fasting gastric antrum are common findings in functional dyspepsia but their relationship with gastrointestinal (GI), and the frequently associated extra-GI symptoms remains unclear. This study evaluated the relationship between GI and extra-GI symptoms, fasting antral volume and delayed gastric emptying in functional dyspepsia.

METHODS: In 108 functional dyspeptic patients antral volume and gastric emptying were assessed with ultrasonography (US). Symptoms were assessed with standardized questionnaire. The association of symptoms and fasting antral volume with delayed gastric emptying was estimated with logistic regression analysis.

RESULTS: Delayed gastric emptying was detected in 39.8% of the patients. Postprandial drowsiness (AOR 11.25; 95%CI 2.75-45.93), nausea (AOR 3.51; 95%CI 1.19-10.32), fasting antral volume (AOR 1.93; 95%CI 1.22-3.05), were significantly associated with delayed gastric emptying. Symptoms, mainly the extra-GI ones as postprandial drowsiness and nausea, combined with fasting antral volume predicted the modality of gastric emptying with a sensitivity and specificity of 78%.

CONCLUSION: In functional dyspeptic patients, (1) an analysis of fasting antral volume and of symptoms can offer valuable indication on the modality of gastric emptying, and (2) it seems appropriate to inquire on postprandial drowsiness that showed the best correlation with delayed gastric emptying.

Key words: Functional dyspepsia; Gastric emptying; Ultrasonography

Pallotta N, Pezzotti P, Calabrese E, Baccini F, Corazziari E. Relationship between gastrointestinal and extra-gastrointestinal symptoms and delayed gastric emptying in functional dyspeptic patients. *World J Gastroenterol* 2005; 11(28): 4375-4381
http://www.wjgnet.com/1007-9327/11/4375.asp

INTRODUCTION

The term dyspepsia is widely used in clinical practice to describe symptoms arising from the upper abdomen and, depending on the definition, its prevalence has been reported to vary from 20% to 40%[1-3] in the adult population. Although dyspeptic symptoms may arise from several pathological conditions, more than 70%[4-8] of patients, do not have definite structural or biochemical alterations[9-11] and, based on the Rome Diagnostic Criteria functional dyspepsia (FD) is made[12,13]. In the assumption that symptoms may predict specific underlying pathophysiology of FD it has been suggested that patients be subdivided in accordance with symptom clusters[12] such as ulcer-like and dysmotility-like dyspepsia or, more recently, with the predominant symptom[13]. Several studies have looked for possible correlation between symptoms and pathophysiological abnormalities such as *Helicobacter pylori* infection, visceral hypersensitivity and abnormal motor function of the stomach. Up to 40% of patients with FD evaluated in referral centers have delayed gastric emptying[14] and 40% impaired postprandial relaxation of the proximal stomach[15]. So far however, there is little evidence[16] that gastric motor abnormalities correlate unequivocally with different symptom clusters[17-19] and not even in those patients with dysmotility-like dyspepsia, referring symptoms suggestive of an abnormal motor function of the stomach such as postprandial fullness, nausea, early satiety and vomiting. Female gender, and, severe and predominant, postprandial fullness and vomiting have been reported to be associated with delayed gastric emptying[20], a finding not confirmed in a subsequent study[21] performed in a large cohort of patients with dysmotility-functional and organic (i.e., diabetic) dyspepsia. Drowsiness is a subjective experience often reported after food ingestion and it has been shown that solid meal results in a decreased sleep onset latency in healthy volunteers[22].

Patients with functional dyspepsia complain of several gastrointestinal (GI) and extra-GI symptoms[23], some of the latter like drowsiness[24,25] and headache[24] are related to meal ingestion. It is not known, however, whether postprandial drowsiness and other extra-GI symptoms have any relationship with gastric functions.

An enlarged fasting antral volume assessed by ultrasonography (US)[26,27] is an additional finding in patients with FD but its relationship, if any, with delayed gastric emptying is not known.

We, therefore aimed to evaluate in functional dyspeptic patients whether and which symptoms either GI or extra-GI are related to, and might predict, delayed gastric emptying of a regular meal. Additional aim was to assess whether the US measurement of basal antral volume may predict the modality of gastric emptying.

MATERIALS AND METHODS

Two hundred and ten consecutive patients referring symptoms of dyspepsia (140 F; age 42.8±12.5 years, mean±SD) referred to the gastroenterology outpatient clinic were assessed. Functional dyspepsia was defined as persistent or recurrent pain or discomfort centered in the upper abdomen for at least 3 mo in the preceding 12 mo, in the absence of any known organic disease that is likely to explain the symptoms[12,13] and no evidence that dyspeptic symptoms were exclusively relieved by defecation or associated with the onset of a change in stool frequency or stool form[13].

Organic abnormalities, psychiatric illnesses, history of alcohol abuse, use of NSAIDs, steroids or drugs affecting gastric functions, previous surgery of the GI tract (except appendectomy and cholecystectomy) and systemic disorders were ruled out by history, clinical examination, biochemical investigations, upper GI endoscopy, and transabdominal US. Dyspeptic patients with Rome diagnostic criteria of irritable bowel syndrome (IBS) and/or referring heartburn and/or regurgitation as predominant or frequent symptoms, were excluded from the study.

Epigastric pain and upper abdominal discomfort were graded 0-4 according to its influence on patient's daily activities: 0, absent; 1, mild (present but easily bearable if distracted by usual activities); 2, moderate (bearable but not influencing usual activities); 3, relevant (influencing usual activities); 4, severe (interruption of usual activities).

Patients were enrolled into the study if symptomatic at the time of evaluation with a symptom score value of $\geqslant$2 for epigastric pain or discomfort.

Overall 102 patients (67 F, age 46±13.2 years, mean±SD) were excluded from the study because of the following diagnosis: gastroesophageal reflux disease, 52; IBS, 15; peptic ulcer, 14; migraine, 16; psychiatric disorders, 3; celiac disease, 2.

One hundred and eight patients with functional dyspepsia entered the study (73 F, age 42±12.5 years, mean±SD). Twenty-eight healthy asymptomatic volunteers (10 F, mean age 31±5.5 years, mean±SD) were also investigated. None of them had GI disorders or symptoms or were taking medications of any kind. None had been previously submitted to surgery of the GI tract.

Informed consent was obtained from each subject and the study protocol was approved by the local ethics committee.

Analysis of symptoms

Consecutive patients were interviewed with a standardized questionnaire[28] made of 50 items, inquiring on demography (5 items), daily habits (10 items) that included meal timing and composition, alcohol consumption, smoking and sleep, past medical history (3 items), GI symptoms (15 items), gastroesophageal symptoms (4 items), bowel pattern (7 items), and somatic extra-GI symptoms that included 5 items as indicated in a previously published study[23]. Postprandial drowsiness, defined as a state of impaired awareness associated with a desire or inclination to sleep[29] was also included in the questionnaire since this meal-related symptom has been reported[2] and confirmed by personal observations, to be bothersome in dyspeptic patients. Dyspeptic symptoms were defined according to Rome criteria[12,13].

Frequency and time relationship with meal assumption was assessed for each investigated symptom and, relationship of drowsiness with sleep disturbances was specifically looked for.

In addition patients were requested to refer any other symptom they considered to be bothersome and relating to meal ingestion.

Assessment of gastric emptying

Gastric emptying was evaluated with US according to previously validated and standardized methods[30-34]. Gastric antral volume was evaluated by US according to previously published methods[33,34] with a 4 MHz linear probe and 3.5 MHz convex probe (Toshiba SAL 38B, Tosbee, Toshiba, Japan).

All drugs affecting the GI tract were discontinued at least 3 d before the gastric emptying studies. Subjects refrained from smoking for a 12-h period preceding, and during, the examination. After an overnight fast the subjects ate an ordinary standard solid 1 050 kcal meal containing 140 g bread, 70 g cheese, 80 g ham, (50% carbohydrates, 25% lipids, 25% proteins), 3.5 g alimentary fibers, 250 mL of water. The time of meal ingestion did not exceed 30 min (range 15-30 min). Gastric antral US measurements were performed by the same operator with the subjects standing in the upright position, in fasting condition, immediately, and at 30 and 60 min after the end of the meal ingestion, and at 60-min intervals thereafter over a total period of 300 min. In the intervals between measurements subjects could move freely.

Delayed gastric emptying was defined as the final antral volume (i.e., gastric antral volume at 300 min after meal ingestion) exceeding the mean value plus 2SDs of the 28 healthy volunteers (31 mL).

Statistical analysis

Descriptive statistics as median values and interquartile ranges were calculated. Box-plots[35] were used for inter-group comparison of antral volume distributions. The Mann-Whitney test[35] was used to compare the median values of antral volume between healthy controls, FD patients with delayed and those with normal gastric emptying.

Sensitivity and specificity of each symptom for three different threshold levels of fasting antral volume were calculated. Odds ratios (OR) were also calculated as a synthetic measure of both sensitivity and specificity[35].

Logistic regression analysis[36] was then applied to estimate crude and adjusted odds-ratios (AOR) and 95% confidence intervals (95%CI) of having delayed gastric emptying for

each symptom, fasting antral volume, gender, age, and body mass index (BMI). In addition, we reported results from two multivariate logistic regression analyses, respectively, without and with fasting antral volume, obtained through a backward selection strategy having excluded factors with a log-likelihood *P*-value >0.20[35]. Two-sided *P* values were defined statistically significant when $P<0.05$, and marginally significant when $0.05<P<0.2$.

Estimated coefficients from multivariate logistic regression were used to calculate the probability of having (or not having) delayed gastric emptying. Through these probabilities, it is possible to calculate sensitivity, specificity, and the percentage of patients correctly classified[36]. All the analyses were performed using STATA release 5.0[37].

RESULTS

Figure 1 shows antral volume values before, immediately, and in the 300 min after meal ingestion in normal controls and in functional dyspeptic patients with normal and delayed gastric emptying.

In healthy volunteers, the mean gastric antral volume was 13±5 mL in the fasting state and reached its maximal value at the end of meal ingestion (67±24 mL), then decreased almost linearly to reach 18±6.5 mL at the end of the study. In FD patients, the mean fasting antral volume was 14±8 mL (ns *vs* controls) and reached its maximal value at the end of the meal (53±21 mL) (ns *vs* controls), then decreased to reach the final value of 30±16 mL ($P<0.0001$ *vs* controls).

Gastric emptying was delayed in 43 (39.8%) patients (28 F; mean age 41.4 years; range 23-64 years) and their final AV was 46±11 mL (Figure 1). The mean fasting AV (17±10 mL) was larger in patients with delayed gastric emptying than in those with normal gastric emptying (12±5 mL, $P = 0.005$, Figure 1). The mean delta variation between fasting and final antral volume was 29±14 mL in dyspeptic patients with delayed gastric emptying and 7±8 mL in those with normal gastric emptying ($P<0.0001$).

Frequency, as well as sensitivity, specificity, and crude OR in predicting delayed gastric emptying of each of the GI and extra-GI symptoms reported by at least eight patients as well as fasting antral volume are reported in Table 1. Delayed gastric emptying was not related to age (OR = 1.03; $P = 0.84$), gender (OR = 0.7; $P = 0.4$), while there was a marginally significant inverse association, with BMI (OR = 0.89 per 1 kg/m^2 increase; $P = 0.06$, data not shown in Table 1).

None of the patients with post-prandial drowsiness complained of sleeplessness.

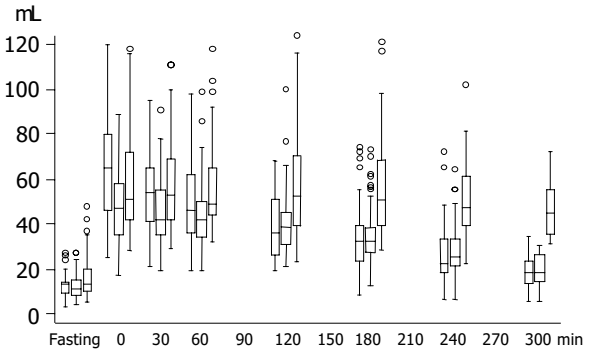

Figure 1 Box-and-whiskers plots of gastric antral volume before (fasting), immediately (0) at 30- and 60-min intervals, after the end of the ingestion of a standard meal, in controls (left) and in dyspeptic patients with normal (middle) and delayed (right) gastric emptying. The boxes at each time unit extend from the 25th percentile ($x_{[25]}$) to the 75th percentile [$x_{[75]}$, i.e., the interquartile range (IQ)]; the lines inside the boxes represent the median values. The line emerging from the boxes (i.e., the "whiskers") extend to the upper and lower adjacent values. The upper adjacent value is defined as the largest data point $\leqslant x_{[75]}$+1.5 X IQ, and the lower adjacent value is defined as the smallest data point $\geqslant x_{[25]}$-1.5 X IQ. Observed values more extreme than the adjacent values, if any, are individually plotted (circles). The widths of the boxes are proportional to the number of observations available at each time unit.

Table 1 Prevalence, sensitivity and specificity and crude OR for delayed gastric emptying of symptoms and of fasting antral volume at three cut-off levels

	Prevalence %	Sensitivity %	Specificity %	OR
Pain centered in the upper abdomen	45.4	58.1	63.1	2.37
Discomfort centered in the upper abdomen	79.6	81.4	21.5	1.20
Upper abdominal bloating	84.3	88.4	18.5	1.72
Fullness	68.5	62.8	27.7	0.64
Early satiety	45.4	48.8	56.9	1.26
Nausea	42.6	53.5	64.6	2.10
Heartburn	26.9	34.9	78.5	1.95
Epigastric burning	11.1	9.3	87.7	0.73
Belching	74	74.4	26.1	1.03
Vomiting	27.8	20.9	67.7	0.55
Acid regurgitation	19.4	23.3	83	1.48
Drowsiness	16.7	32.6	93.9	7.36
Headache	41.7	46.5	61.5	1.39
Palpitation	7.4	6.9	92.3	0.90
Fasting antral volume (mL)				
<10 mL (reference group)	33.3	18.6	43	1.09
10–14 mL	34.3	39.5	30.8	2.97
>15 mL	32.4	41.9	26.2	3.71

Table 2 AOR with 95%CI of having delayed gastric emptying on the basis of symptoms and fasting antral volume (FAV)

	Without FAV and BMI		With FAV and BMI	
	AOR	95%CI	AOR	95%CI
Pain centered in the upper abdomen	3.74	1.34-10.41	2.78	0.92-8.41
Nausea	2.92	1.15-7.44	3.51	1.19-10.32
Postprandial fullness	0.41	0.14-1.14	0.27	0.08-0.84
Discomfort centered in the upper abdomen	3.42	0.88-13.25	4.59	0.99-21.20
Vomiting	0.44	0.15-1.31	0.32	0.09-1.11
Heartburn	-	-	2.31	0.80-6.71
Drowsiness	9.37	2.47-35.45	11.25	2.75-45.93
BMI	-	-	0.89	0.77-1.02
Fasting antral volume[1]	-	-	1.93	1.22-3.05

FAV: Fasting antral volume; AOR: adjusted odds-ratio. [1]AOR estimated per 5 mL increase (e.g., a FAV of 20 mL *vs* 15 mL).

The AOR for symptoms with or without fasting antral volume and BMI included in the multivariate analyses are shown in Table 2. Not taking into consideration fasting antral volume and BMI in the multivariate analyses, upper abdominal pain, nausea, and drowsiness showed a statistically significant association, whereas upper discomfort showed only a marginally significant association with delayed gastric emptying. Post-prandial fullness or vomiting showed a marginally significant association with normal gastric emptying. Including fasting antral volume and BMI in the multivariate analyses, nausea and drowsiness were highly significantly associated with delayed gastric emptying, while upper abdominal pain, upper abdominal discomfort, and heartburn were only marginally significantly associated with delayed gastric emptying. Post-prandial fullness showed a highly significant, and vomiting a marginally significantly, association with normal gastric emptying. Fasting antral volume was significantly associated with delayed gastric emptying increasing the OR of 93% for any additional volume increase of 5 mL. BMI showed a marginally significant inverse association with delayed gastric emptying with an OR decrease of 11% for any 1 kg/m^2 increase.

Using other two different cut-points (29 and 33 mL), instead of 31 mL, as discriminant final antral volume for normal and delayed gastric emptying, all the results of univariate and multivariate analyses did not vary.

Furthermore probabilities of having delayed gastric emptying were assessed with the selected symptoms, fasting antral volume, and BMI as reported from the second model (Table 2 and Figure 2). Sensitivity and specificity of the applied model are plotted for different values of estimated prevalence of delayed gastric emptying ranging from 0 to 1. At the cut-off value of 0.398, i.e., the estimated prevalence of delayed gastric emptying in this sample, sensitivity and specificity were about 78% with a correct classification of 73.3% of the patients. Applying a model based on selected symptoms only, the estimated sensitivity and specificity were negligibly lower, than those obtained with the model including fasting antral volume and BMI, with a correct classification of 68.1% of the patients at the cut-off value of 0.398 (data not shown).

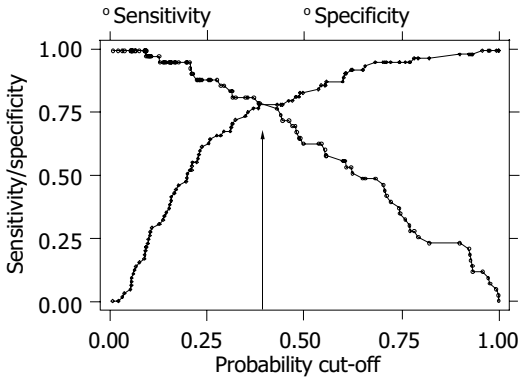

Figure 2 Proportion of patients with delayed and normal gastric emptying who where correctly classified on the basis of their predicted probabilities obtained from the estimated coefficients of the second model reported in Table 2 (i.e., sensitivity and specificity, respectively). These proportions are plotted with cut-off levels varying between 0 and 1 (see "lsens" function in Ref. [37]). As expected, when the cut-off value is close to zero all individuals with an actual delayed gastric emptying will be correctly classified and thus having a very high sensitivity. In contrast, with very low cut-off values also those having a normal gastric emptying will be classified as "delayed" by the model and thus having a very low specificity. As the cut-off value used for classification increases, the model will provide the worst performances for the sensitivity and the best performances for the specificity. Circles identify sensitivity and squares specificity. Arrow indicates the probability cut-off value of 0.398, i.e., the estimated prevalence of delayed gastric emptying in this sample.

DISCUSSION

In the attempt to clarify the pathophysiology of symptoms in functional dyspepsia it has been proposed to classify patients with functional dyspepsia into clinically distinct subgroups on the basis of symptom clusters[12]. Thus the presence of the variable combination of upper abdominal bloating, upper abdominal fullness, early satiety, nausea, belching, retching, and vomiting have been regarded as suggestive of impaired gastric motor activity[38-40]. However several studies[16-19] have so far failed to demonstrate in this subgroup of patients a close correlation between symptoms and disturbances of motor function. More recently[13] it has been proposed to classify dyspeptic subgroup on the basis of the predominant symptom. Nevertheless two studies[15,20] in the attempt to assess the relationship between predominant symptoms and gastric dysfunction reported non-univocal results in populations that did not exclude patients with IBS and gastroesophageal reflux disease (GERD). Delayed gastric emptying was independently associated with severe post-prandial fullness and severe vomiting in the first study[20] and with severe nausea in the second one[15] that also reported early satiety as specifically

associated with impaired gastric accommodation to a meal. In both studies, however, the association between the mentioned symptoms and the altered gastric function was not a universal finding but limited to a subgroup of patients. The uncertainty of the matter is further illustrated by a third study[21] that failed to find an association between any of the dyspeptic symptoms, as well as their severity, and delayed gastric emptying.

Although reported in previous studies[23-25] and frequently referred by dyspeptic patients little attention has been paid to other symptoms not referable to the GI tract. The present study aimed to assess whether single GI or extra-GI symptoms and the simple non-invasive US measure of the gastric antral volume in fasting condition could predict the presence of delayed gastric emptying, in a group of dyspeptic patients in whom symptoms of IBS and GERD were excluded.

The present study differs from the previous ones also for other aspects. A meal having the same composition of a normal everyday lunch was used in the present study whereas unusual experimental and/or low caloric meals ($\leqslant$700 kcal)[17-19] used previously might have not sufficiently challenged the upper GI function. Most of the previously published studies evaluated gastric emptying with the scintigraphic technique that, differently from the US technique, assesses the emptying of the radiolabeled component of the meal rather than of the entire postcibal gastric contents. In addition previous scintigraphic studies have assessed the gastric emptying rate or $t^{1/2}$ gastric emptying time extrapolated from a limited observation period after meal ingestion, two variables that had been shown to be unable to express final gastric emptying time in functional dyspeptic patients[41]. The serial US measurements of the antral volume enables to assess two relevant aspects of the gastric function, i.e., the antral volume, which is the expression of antral distension and the final gastric emptying time. The former cannot be assessed with scintigraphy and the latter has been shown to be the variable that best correlates with the scintigraphic method and to discriminate patients with delayed gastric emptying from controls[30-32,42]. In the present study extra-GI symptoms were reported by 53.7% of the patients. Of relevance is that of all investigated symptoms, including GI symptoms usually regarded characteristic of dyspepsia, post-prandial drowsiness is the one that most correlates with, and is the best predictor of, delayed gastric emptying. Also nausea and pain centered in the upper abdomen, albeit to a lesser degree than post-prandial drowsiness, showed a statistical correlation with delayed gastric emptying. Differently from typical abdominal dyspeptic symptoms, drowsiness showed a high specificity in predicting delayed gastric emptying. The other most frequently referred extra-GI symptoms such as headache and palpitation were not statistically related with delayed gastric emptying. Drowsiness can occur in several neurological conditions, including autonomic failure and truncal vagotomy. In none of the investigated patients drowsiness could be explained with any detectable disorders. In healthy subjects it has been shown that in comparison with an equal volume of water and equicaloric liquid meal, solid meal results in a decreased sleep onset latencies[22]. Furthermore it has been reported a transient decrease in sleep latency after consuming a meal compared to sham feeding[43]. These results together with the observation of a increased feeling of drowsiness after intravenous injection of CCK administration[44], support the hypothesis of a GI effect on postprandial sleepiness. It is conceivable that meal ingestion may release CCK and other neuroendocrine substances, such as serotonin, or activate nervous afferences, that affect the state of consciousness and delay gastric emptying. Alternatively prolonged postprandial antral distension may participate via vagal afferences in the activation of central nervous network regulating the state of consciousness. The sensation of drowsiness may vary from slight to severe and be related to sleep disturbances. Postprandial drowsiness reported in the present investigation refers to a sensation regarded to be bothersome enough to interfere with the daily activities and it was not related to sleeplessness.

In addition this study shows that the fasting antral volume of 15 mL is the cut-off value that may be used to predict delayed gastric emptying. Adjusting data for fasting antral volume and BMI, the following symptoms: nausea and drowsiness appear to be significant independent predictors of delayed gastric emptying.

None of the symptoms conventionally considered to be manifestation of dyspepsia was of value to discriminate between patients with normal and delayed gastric emptying.

The different results of the present study from previously mentioned scintigraphy-based studies, may be due to the use of a different technique and/or the different selection of the patients and/or the different assessment of patient's symptoms[20].

Alternatively, the different results may express a different underlying dysfunction for some of the dyspeptic symptoms. So it may be hypothesized that in patients with functional dyspepsia early satiety[15] is mainly related to impaired relaxation of the proximal stomach; postprandial fullness and vomiting to a reduced rate of gastric emptying[20]; post-prandial drowsiness, nausea, to a delayed final gastric emptying.

This study confirms[26,27] the frequent occurrence in patients with FD of an abnormally distended antral volume during fasting. Whether increased antral volumes may reflect hypotonia of the antral muscular wall or intraluminal distension secondary to gastric retention could not be addressed in the present study.

An increased final antral volume does not necessarily indicate delayed gastric emptying as it may coexist with a normal gastric emptying rate if the fasting antral volume is increased. In the present study, however, the mean final antral volume of dyspeptic patients with delayed gastric emptying exceeded the fasting antral volume of 28 mL indicating the presence of a genuine slowing of the gastric emptying rate.

To identify the cut-off level of 31 mL to discriminate normal and delayed gastric emptying we used data from a control group of healthy people. Similar results were obtained with additional assessments based on other cut-off levels chosen below and above 31 mL. Compared to our patients the control group had a lower percentage of women

and a younger age. However, these differences did not affect the results because these two factors (age and gender) did not have, in the multivariate analysis, any relationship with the gastric emptying. This study confirms previous observations of a statistical correlation between BMI and delayed gastric emptying[20]. This relationship may be interpreted as an effect of gastric dysfunction often associated with symptoms, such as nausea or pain that limit food ingestion. Patients with eating disorders may be underweight and show abnormal gastric function. In the present study patients with such disorders were excluded and the finding of equally delayed gastric emptying in both genders would support that eating disorders were not present. We did not routinely test for *H pylori* in this study, but there is no evidence that Hp infection has any relationship with symptoms and delayed gastric emptying in functional dyspepsia[45-49]. Thus, it seems unlikely that knowledge of the Hp status would have altered the conclusions of the present study.

In conclusion, the presence or, alternatively, the absence of nausea and post-prandial drowsiness, appear to be indicative of delayed or, respectively, normal gastric emptying in functional dyspeptic patients.

Interestingly, despite that the symptom of post-prandial drowsiness is often reported by dyspeptic patients and in some of them it may be the predominant disturbance, it has not been considered part of the definition of dyspepsia. This study shows that post-prandial drowsiness is the symptom that most correlates with delayed gastric emptying and would suggest including it in the clinical definition of functional dyspepsia.

Although it would appear that in FD patients an analysis of dyspeptic symptoms and fasting antral volume can offer valuable indication on the modality of gastric emptying, their ability, either alone or in combination, of correctly classifying individuals with or without delayed gastric emptying was not greater than 73%.

REFERENCES

1 **Johnsen R,** Straume B, Forde OH. Peptic ulcer and non-ulcer dyspepsia a disease and a disorder. *Scand J Prim Health Care* 1988; **6**: 239-243
2 **Jones RH,** Lydeard SE, Hobbs FD, Kenkre JE, Williams EI, Jones SJ, Repper JA, Caldow JL, Dunwoodie WM, BottomLey JM. Dyspepsia in england and scotland. *Gut* 1990; **31**: 401-405
3 **Talley NJ,** Zinsmeister AR, Schleck CD, Melton LI 3rd. Dyspepsia and dyspepsia subgroups: a population-based study. *Gastroenterology* 1992; **102**: 1259-1268
4 **Barnes RJ,** Gear MW, Nicol A. Dew AB . Study of dyspepsia in a general practice as assessed by endoscopy and radiology. *Br Med J* 1974; **26**: 214-216
5 **Mollmann KM,** Bonnevie O, Gudbrand-Hoyer E, Wulff HR. A diagnostic study of patients with upper abdominal pain. *Scand J Gastroenterol* 1975; **10**: 805-809
6 **Horrocks JC,** De Dombal FT. Clinical presentation of patients with "dyspepsia". Detailed systematic study of 360 patients. *Gut* 1978; **19**: 19-26
7 **Holdstock G,** Harman M, Machin D, Patel C, Lloyd RS. Prospective testing of a scoring system designed to improve case selection for upper gastrointestinal investigation. *Gastroenterology* 1986; **90**: 1164-1169
8 **Capurso L,** Koch M, Dezi A. Towards a quantitative diagnosis of dyspepsia: the value of clinical symptoms. The dyspepsia project report. *Ital J Gastroenterol* 1988; **20**: 191-202
9 **Richter JE.** Dyspepsia: organic causes and differential characteristics from functional dyspepsia. *Scand J Gastroenterol Suppl* 1991; **182**: 11-16
10 **Heikkinen M,** Pikkarainen P, Takala J, Rasanen H, Julkunen R. Etiology of dyspepsia: four hundred unselected consecutive patients in general practice. *Scand J Gastroenterol* 1995; **30**: 519-523
11 **Klauser AG,** Voderholzer WA, Knesewitsch PA, Schindlbeck NE, Muller-Lissner SA. What is behind dyspepsia? *Dig Dis Sci* 1993; **38**: 147-154
12 **Talley NJ,** Colin-Jones D, Koch KL. Functional dyspepsia: a classification with guidelines for diagnosis and management. *Gastroenterol Int* 1991; **4**: 145-160
13 **Talley NJ,** Stanghellini V, Heading RC, Koch KL, Malagelada JR, Tytgat GN. Functional gastroduodenal disorder. *Gut* 1999; **45**(Suppl 2): II37-42
14 **Bytzer P,** Talley NJ. Dyspepsia. *Ann Int Med* 2001; **134**: 815-822
15 **Tack J,** Piessevaux H, Coulie B, Caenepeel P, Janssens J. Role of impaired gastric accommodation to a meal in functional dyspepsia. *Gastroenterology* 1998; **115**: 1346-1352
16 **Barbara L,** Camilleri M, Corinaldesi R, Crean GP, Heading RC, Johnson AG, Malagelada JR, Stanghellini V, Wienbeck M. Definition and investigation of dyspepsia. Consensus of an International ad hoc working party. *Dig Dis Sci* 1989; **34**: 1272-1276
17 **Wegener M,** Borsch G, Schaffstein J, Reuter C, Leverkus F. Frequency of idiopathic gastric stasis and intestinal transit disorders in essential dyspepsia. *J Clin Gastroenterol* 1989; **11**: 163-168
18 **Waldron B,** Cullen PT, Kumar R, Smith D, Jankowski J, Hopwood D, Sutton D, Kennedy N, Campbell FC. Evidence for hypomotility in non-ulcer dyspepsia: a prospective multifactorial study. *Gut* 1991; **32**: 246-251
19 **Talley NJ,** Shuter B, McCrudden G, Jones M, Hoschl R, Piper DW. Lack of association between gastric emptying of solids and symptoms in non-ulcer dyspepsia. *J Clin Gastroenterol* 1989; **11**: 625-630
20 **Stanghellini V,** Tosetti C, Paternicò A, Barbara G, Morselli-Labate AM, Monetti N, Marengo M, Corinaldesi R. Risk indicators of delayed gastric emptying of solids in patients with functional dyspepsia. *Gastroenterology* 1996; **110**: 1036-1042
21 **Talley NJ,** Verlinden M, Jones M. Can symptoms discriminate among those with delayed or normal gastric emptying in dysmotility-like dyspepsia? *Am J Gastroenterol* 2001; **96**: 1422-1428
22 **Orr WC,** Shadid G, Harnish MJ, Elsenbruch S. Meal composition and its effect on postprandial sleepiness. *Physiol Behav* 1997; **62**: 709-712
23 **Talley NJ,** Phillips SF, Bruce B, Zinsmeister AR, Wiltgen C, Melton LJ. Multisystem complaints in patients with irritable bowel syndrome and functional dyspepsia. *Eur J Gastroenterol Hepatol* 1991; **3**: 71-77
24 **Corinaldesi R,** Stanghellini V, Raiti C, Rea E, Salgemini R, Barbara L. Effect of chronic administration of cisapride on gastric emptying of solid meal and on dyspeptic symptoms in patients with idiopathic gastroparesis. *Gut* 1987; **28**: 300-305
25 **Distrutti E,** Fiorucci S, Hauer SK, Pensi MO, Vanasia M, Morelli A. Effect of acute and chronic levosulpiride administration on gastric tone and perception in functional dyspepsia. *Aliment Pharmacol Ther* 2002; **16**: 613-622
26 **Ricci R,** Bontempo I, La Bella A, De Tschudy A, Corazzieri E. Dyspeptic symptoms and gastric antrum distribution. An ultrasonographic study. *Ital J Gastroenterol* 1987; **19**: 215-217
27 **Hausken T,** Berstad A. Wide gastric antrum in patients with non-ulcer dyspepsia. Effect of cisapride. *Scand J Gastroenterol* 1992; **27**: 427-432
28 **Talley NJ.** Optimal design of treatment trials. In DA Drossman, JE Richter, NJ Talley, WG Thompson, E Corazziari, WE Whitehead (eds). *Functional Gastrointestinal Disorders:*

Diagnosis, Pathophysiology and Treatment. Boston, Little Brown and Company 1994: 265-310
29 **Aldrich MS.** Narcolepsy. *Neurology* 1992; **42**(Suppl 6): 34-43
30 **Hveem K,** Jones KL, Chatterton BE, Horowitz M. Scintigraphic measurements of gastric emptying and ultrasonographic assessment of antral area: relation to appetite. *Gut* 1996; **38**: 816-821
31 **Benini L,** Sembenini C, Heading RC, Giorgetti PG, Montemezzi S, Zamboni M, Di Benedetto P, Brighenti F, Vantini I. Simultaneous measurement of gastric emptying of a solid meal by ultrasound and by scintigraphy. *Am J Gastroenterol* 1999; **94**: 2861-2865
32 **Benini L,** Sembenini C, Castellani G, Caliari S, Fioretta A, Vantini I. Gastric emptying and dyspeptic symptoms in patients with gastroesophageal reflux. *Am J Gastroenterol* 1996; **91**: 1351-1354
33 **Bolondi L,** Bortolotti M, Santi V, Calletti T, Gaiani S, Labò G. Measurement of gastric emptying time by real-time ultrasonography. *Gastroenterology* 1985; **89**: 752-759
34 **Ricci R,** Bontempo I, Corazziari E, La Bella A, Torsoli A. Real-time ultrasonography of the gastric antrum. *Gut* 1993; **34**: 173-176
35 **Altman DG.** Practical statistics for medical research. Chapman and Hall; 1991
36 **Hosmer DW,** Lemeshow S. Applied logistic regression. New York John Wiley and sons, Inc.; 1989
37 StataCorp. Stata Statistical Software: Release 5.0. Stata Corporation, College Station, TX, USA, 1997
38 **Malagelada JR,** Stanghellini V. Manometric evaluation of functional upper gut symptoms. *Gastroenterology* 1985; **88**: 1223-1231
39 **Rees WD,** Miller LJ, Malagelada JR. Dyspepsia, antral motor dysfunction, and gastric stasis of solids. *Gastroenterology* 1980; **78**: 360-365
40 **Metcalf R,** Youngs GR. Prevalence of symptoms of dyspepsia. *BMJ* 1989; **298**: 526-527
41 **Guo JP,** Maurer AH, Fisher RS, Parkman HP. Extending gastric emptying scintigraphy from two to four hours detects more patients with gastroparesis. *Dig Dis Sci* 2001; **46**: 24-29
42 **Bortolotti M,** Bolondi L, Santi V, Sarti P, Brunelli F, Barbara L. Patterns of gastric emtpying in dysmotility-like dyspepsia. *Scand J Gastroenterol* 1995; **30**: 408-410
43 **Harnish MJ,** Greenleaf SR, Orr WC. A comparison of feeding to cephalic stimulation on postprandial sleepiness. *Physiol Behav* 1998; **64**: 93-96
44 **Stacher G,** Bauer H, Steinringer H. Cholecystokinin decreases appetite and activation evoked by stimuli arising from the preparation of a meal in man. *Physiol Behav* 1979; **23**: 325-331
45 **McColl K,** Murray L, El-Omar E, Dickson A, El-Nujumi A, Wirz A, Kelman A, Penny C, Knill-Jones R, Hilditch T. Symptomatic benefit from eradicating *Helicobacter pylori* infection in patients with nonlcer dyspepsia. *N Engl J Med* 1998; **339**: 1869-1874
46 **Blum AL,** Talley NJ, O'Morain C, Veldhuyzen van Zanted S, Labenz J, Stolte M, Louw JA, Stubberod A, Theodors A, Sundin M, Bolling-Sternevald E, Junghard O. OCAY study Group. Lack of effect of treating *Helicobacter pylori* infection in patients with non-ulcer dyspepsia. *N Engl J Med* 1998; **339**: 1875-1881
47 **Talley NJ,** Vakil N, Ballard ED, Fennerty MB. Absence of benefit of eradicating *Helicobacter pylori* in patients with nonulcer dyspepsia. *N Engl J Med* 1999; **341**: 1106-1111
48 **Tucci A,** Corinaldesi R, Stanghellini V, Tosetti C, Di Febo G, Paparo GF, Varoli O, Paganelli GM, Morselli AM, Masci C, Zoccoli G, Monetti N, Barbara L. *Helicobacter pylori* infection and gastric function in patients with chronic idiopathic dyspepsia. *Gastroenterology* 1992; **103**: 768-774
49 **Rhee PL,** Kim YH, Son HJ, Kim JJ, Koh KC, Paik SW, Rhee JC, Choi KW. Lack of association of *Helicobacter pylori* infection with gastric hypersensitivity. *Am J Gastroenterol* 1999; **94**: 3165-3169

Science Editor Guo SY **Language Editor** Elsevier HK

PO Box 2345, Beijing 100023, China
www.wjgnet.com
wjg@wjgnet.com

ELSEVIER

World J Gastroenterol 2005;11(28):4382-4389
World Journal of Gastroenterology ISSN 1007-9327

• *CLINICAL RESEARCH* •

Expression of adhesion molecules on mature cholangiocytes in canal of Hering and bile ductules in wedge biopsy samples of primary biliary cirrhosis

Hiroaki Yokomori, Masaya Oda, Mariko Ogi, Go Wakabayashi, Shigeyuki Kawachi, Kazunori Yoshimura, Toshihiro Nagai, Masaki Kitajima, Masahiko Nomura, Toshifumi Hibi

Hiroaki Yokomori, Department of Internal Medicine, Kitasato Institute Medical Center Hospital, Saitama 364-8501, Japan
Masaya Oda, Organized Center of Clinical Medicine, International University of Health and Welfare, Tokyo 107-0052, Japan
Mariko Ogi, Laboratory of Pathology, Kitasato Institute Medical Center Hospital, Saitama 364-8501, Japan
Go Wakabayashi, Shigeyuki Kawachi, Masaki Kitajima, Department of Surgery, School of Medicine, Keio University, Tokyo 160-0016, Japan
Kazunori Yoshimura, Masahiko Nomura, Physiology, Saitama Medical School, Saitama 350-0495, Japan
Toshihiro Nagai, Electron Microscopy Laboratory, School of Medicine, Keio University, Tokyo 160-0016, Japan
Toshifumi Hibi, Department of Internal Medicine, School of Medicine, Keio University, Tokyo 160-0016, Japan
Correspondence to: Hiroaki Yokomori, MD, Kitasato Institute Medical Center Hospital, 121-1 Arai, Kitamotoshi, Saitama 364-8501, Japan. yokomori-hr@kitasato.or.jp
Telephone: +81-485-93-1212 Fax: +81-485-93-1239
Received: 2004-07-28 Accepted: 2004-08-31

Abstract

AIM: To examine the expression of intercellular adhesion molecule-1 (ICAM-1) and lymphocyte function-associated antigen-1 (LFA-1) expression on canals of Hering (CoH) and bile ductules associated with the autoimmune process of bile duct destruction in primary biliary cirrhosis (PBC).

METHODS: Ten wedged liver biopsies of PBC (five cases each of stages 2 and 3) were studied. The liver specimens were processed for transmission electron microscopy. Immunohistochemistry was performed using anti-ICAM-1 and anti-LFA-1 mouse mAbs. *In situ* hybridization was done to examine the messenger RNA expression of ICAM-1 in formalin-fixed, paraffin-embedded sections using peptide nucleic acid probes and the catalyzed signal amplification (CSA) technique. Immunogold-silver staining for electron microscopy was performed using anti-ICAM and anti-LFA-1 mouse mAbs. The immunogold particles on epithelial cells of bile ductules and cholangiocytes of CoH cells were counted and analyzed semi-quantitatively. Western blotting was performed to confirm ICAM-1 protein expression.

RESULTS: In liver tissues of PBC patients, immunohistochemistry showed aberrant ICAM-1 expression on the plasma membrane of epithelial cells lining bile ductules, and also on mature cholangiocytes but not on hepatocytes in CoH. LFA-1-positive lymphocytes were closely associated with epithelial cells in bile ductules. ICAM-1 expression at protein level was confirmed by Western blot. *In situ* hybridization demonstrated ICAM-1 mRNA expression in bile ductules and LFA-1 mRNA in lymphocytes infiltrating the bile ductules. By immunoelectron microscopy, ICAM-1 was demonstrated on the basal surface of epithelial cells in bile ductules and on the luminal surfaces of cholangiocytes in damaged CoH. Cells with intermediate morphology resembling progenitor cells in CoH were not labeled with ICAM-1 and LFA-1.

CONCLUSION: *De novo* expression of ICAM-1 both on mature cholangiocytes in CoH and epithelial cells in bile ductules in PBC implies that lymphocyte-induced destruction through adhesion by ICAM-1 and binding of LFA-1-expressing activated lymphocytes takes place not only in bile ductules but also in the CoH.

Key words: Primary biliary cirrhosis; Canal of Hering; Small bile ductile; ICAM-1; LFA-1; Immunohistochemistry; Western blot; Immunogold electron microscopy

Yokomori H, Oda M, Ogi M, Wakabayashi G, Kawachi S, Yoshimura K, Nagai T, Kitajima M, Nomura M, Hibi T. Expression of adhesion molecules on mature cholangiocytes in canal of Hering and bile ductules in wedge biopsy samples of primary biliary cirrhosis. *World J Gastroenterol* 2005; 11(28): 4382-4389
http://www.wjgnet.com/1007-9327/11/4382.asp

INTRODUCTION

The canal of Hering (CoH) is named after Hering who in 1855 described the structure as a link between the hepatocyte canalicular system and biliary tree[1]. Under the electron microscope, the small cells of CoH have a basement membrane like the more distal portions of the biliary tree but an apical surface that appears similar to hepatic canalicular membrane[2]. Functionally, bile canalicular contraction is involved in the canalicular bile flow as demonstrated by an inverted microscope linked to a SIT camera, and disturbance of canalicular contraction would lead to intrahepatic cholestasis[3]. Moreover, contraction of the CoH has been demonstrated, and the interval between contractions was approximately five times longer than that seen in canaliculi[4]. Hepatic cholestasis and hepatic injury are accompanied with

striking morphologic changes. Examination of periportal changes in the liver of graft-*vs*-host disease mice shows that hepatocytes in close contact with lymphocytes had minor degenerative changes, whereas periportal bile ductules and CoH are constantly injured by inflammatory cells[5]. Study of the three-dimensional structure of ductular reactions in massive necrosis suggests that cytokeratin 19-positive reactions are in fact proliferations of the cells lining the CoH[6].

Primary biliary cirrhosis (PBC) is a chronic, progressive cholestatic liver disease characterized by inflammatory obliteration of the intrahepatic bile ducts, leading to fibrosis and ultimately to cirrhosis complicated by liver failure or hypertention[7,8]. Although the pathogenesis of bile duct destruction in PBC remains unknown, increasing evidence has suggested that it is related to autoimmune abnormalities[8-10]. Immunohistochemical analysis of the lymphocytes infiltrating the portal tracts including the bile duct lesions indicates that activated T lymphocyte subsets may play an important role in bile duct destruction[11]. Therefore bile ducts (centrally located, accompanied by a hepatic arterial branch) are the prime targets for immune-mediated damages in PBC and are reduced in number as the disease progresses. Bile ductules (peripherally located, usually without a conspicuous lumen) increase in number in response to bile duct damage (ductular reaction). Bile ductules are frequently associated with a mixed population of inflammatory cells. However, there is no clear evidence that these inflammatory cells are associated with bile ductular destruction[12]. Recent studies have demonstrated increased expression of intercellular adhesion molecule (ICAM)-1 on the bile duct epithelium in PBC[13,14], suggesting that the activated T lymphocytes may specifically react with the bile duct epithelial cells through these adhesion molecules. Expression of intracellular adhesion molecules and their specific ligands are essential for cell-to-cell interactions in autoimmune mechanism[15]. In PBC, ICAM-1 is expressed on plasma membrane of epithelial cell in bile ducts characterized by chronic non-suppurative destructive cholangitis (CNSDC) and on the sinusoidal endothelial cells[16,17]. While immunohistochemical findings of ICAM-1 and lymphocyte function-associated antigen (LFA)-1 expression in PBC tissue have been reported[17], no studies have correlated protein expression of the antigens on CoH by examining serial sections using immunoelectron microscopy. The aim of the present study was to clarify the roles of ICAM-1 and LFA-1 expression on the bile ductule and CoH in PBC. The aim of the present study was to clarify ICAM-1 and LFA-1 expression on the bile ductule and CoH in PBC. We conducted immunohistochemistry, *in situ* hybridization and immunoelectron microscopy on liver biopsy specimens from PBC patients.

MATERIALS AND METHODS

Materials

Surgical liver biopsy specimens were obtained from 10 patients (all female, mean age 55.9 years, range 48-65 years) with PBC (five cases each of Scheuer's stages 2 and 3). PBC was diagnosed clinically and histologically according to the criteria proposed by the Japanese Joint Research Group for Autoi-mmune Hepatitis[18]. As controls, wedge biopsy specimens from normal portions of the liver were obtained from five patients (four male and one female; aged from 54 to 71 years with a mean of 62.6 years) who underwent surgical resection for metastatic liver carcinoma (four colonic carcinomas).

Electron microscopy

The liver specimens were cut into small blocks (approximately 1 mm×1 mm×1 mm). The blocks were fixed in fresh 2.5% glutaraldehyde solution for 1 h at 4 ℃, followed by post-fixation in 2% osmium tetroxide with 0.1 mol/L cacodylate buffer (pH 7.4), and then dehydrated in a graded series of ethanol solutions. For transmission electron microscopy, the liver tissue blocks were embedded in Epon after dehydration. Ultrathin sections were cut with a diamond knife on a LKB ultramicrotome (Bromma), stained with uranyl acetate and lead citrate and observed under a transmission electron microscope (JEM-1200 EX, JEOL, Tokyo, Japan) with a 80-kV acceleration voltage.

Immunohistochemical staining

Liver tissues (approximately 5 mm×5 mm×5 mm) were fixed in periodate-lysine-parafomaldehyde[19], rinsed in 0.01 mol/L phosphate buffer (pH 7.4) containing 15-30% sucrose, embedded in Tissue-Tek OCT-compound (Miles Inc., Elkhart. Inc., Germany) and frozen at -80 ℃ until use. The tissue was incubated overnight at 4 ℃ with anti-ICAM-1 mouse mAb (CD54; DAKO, Glostrup, Denmark) diluted at 1∶50 or anti-LFA-1 mouse mAb (CD11a; DAKO, Glostrup, Denmark) diluted at 1∶20, and then incubated with horseradish peroxidase-conjugated anti-mouse IgG goat antibody (Cosmo Bio Inc., Tokyo, Japan) diluted 1∶100. After repeated washes with PBS, the sections were reacted with diaminobenzidine solution containing 0.01% H_2O_2, and counterstained with hematoxylin for light-microscopic study.

In situ hybridization technique

Messenger RNA of ICAM-1 was detected in formalin-fixed, paraffin-embedded sections by *in situ* hybridization using peptide nucleic acid (PNA) probes[20] and the catalyzed signal amplification (CSA) technique. Liver tissues were cut into 4 μm-thick sections and adhered to silanated RNAse-free glass slides (prepared by heating in an oven at 60 ℃ for 30 min). The sections were dewaxed in xylene (for 15 min, each twice), treated with a graded ethanol series, rehydrated in RNAse-free distilled water, and incubated for 30 min in target retrieval buffer (DAKO Japan, Kyoto, Japan) preheated and maintained at 95 ℃. The slides were allowed to cool at room temperature for 20 min and then digested with 20 μg/mL proteinase K (DAKO) at room temperature for 30 min. The slides were rinsed in distilled water and rapidly air dried. The air-dried sections were covered with approximately 15 mL of hybridization solution containing 100 g/L dextran sulfate, 10 mmol/L NaCl, 300 mL/L formamide, 1 g/L sodium pyrophosphate, 2 g/L polyvinylpyrrolidone, 2 g/L Ficoll, 5 mmol/L Na_2EDTA, 50 mmol/L Tris-HCl, pH 7.5, and 1 μg/mL PNA probe. Probes were constructed according to the sequence information of ICAM-1 and LFA-1[21,22]. The following probes were used: ICAM-1 antisense (FITC-ATTATGACTGCGGCTGC), ICAM-1 sense (FITC-GCAGCCGCAGTCATAAT),

LFA-1 antisense (FITC-CATCCAGCTGCAGAGTGT), and LFA-1 sense (FITC-ACACTCTGCAGCTGGATG). The slides were evenly covered with the hybridization solution and incubated in a moist chamber at 43 ℃ for 90 min. Following hybridization, the cover slips were removed, and the slides were transferred to pre-warmed TBS in a water bath at 49 ℃ and washed for 30 min with gentle shaking (PNA Hybridization Kit; DAKO, Tokyo, Japan). A non-isotopic, colorimetric signal amplification system (GenPoint kit, DAKO Japan) was used to visualize specific hybridization signals. Briefly, tissue sections were incubated with a FITC–horseradish peroxidase reagent for 15 min, washed thrice with TBST (150 mmol/L NaCl, 10 mmol/L Tris; pH 7.5, 11 mL/L Tween 20), incubated with a solution containing H_2O_2 and biotinyl tyramide for 15 min, and washed thrice with TBST[23]. This step resulted in CSA by additional deposition of biotin at the site of probe hybridization. The sections were then incubated in streptavidin-horseradish peroxidase for 15 min, and washed thrice in TBST. Colorimetric signals were developed by incubation in diaminobenzidine solution containing 0.01% H_2O_2, and counterstained with hematoxylin for light microscopic examination.

Immunogold-silver staining method for electron microscopy

For light microscopy, the sections were immersed in three changes of 0.01% PBS (pH 7.4) for 15 min, and then incubated overnight in a moist chamber at 4 ℃ with anti-ICAM-1 mouse mAb at 1:50 dilution and anti-LFA-1 mouse mAb at 1:20 dilution. After washing thrice with PBS for 15 min, the sections were incubated for 40 min with 10-nm colloidal gold-conjugated anti-mouse IgG antibody (Cosmo Bio Co., Tokyo, Japan) diluted at 1:100. The slides were developed with a developing solution described below for 50 min at 20 ℃ in a dark room. After having washed in running water, the sections were briefly counterstained with 0.1% nuclear fast red in 5% aluminum sulfate aqueous solution, dehydrated, cleared and mounted on Biolet. The developing solution had two components. Solution A contained 45 mL of 20% gum arabic aqueous solution (Kanto Chemical Co., Tokyo, Japan) and 1 mL of 10% silver nitrate solution. The gum arabic solution was prepared by centrifuging a 20% suspension at 18 000 *g* for 30 min at 0 ℃ and separating the supernatant for use. Solution B contained 200 mg of hydroquinone (Kanto Chemical Co., Tokyo, Japan) and 300 mg of citric acid monohydrate (Kanto Chemical Co., Tokyo, Japan) in 10 mL of distilled water. The working developing solution was prepared by mixing solutions A and B in a dark room under illumination of a photographic safety lamp[24].

For electron microscopy, the tissue specimens processed for light microscopy as above were treated thrice, with PBS for 15 min, and fixed for 1 h at 4 ℃ in 1.2% glutaraldehyde buffered with 0.01% phosphate buffer (pH 7.4), followed by a graded series of ethanol solutions. After postfixation with 1% osmium tetroxide in 0.01% phosphate buffer (pH 7.4), the liver tissues were embedded in Epon. Ultrathin sections cut with a diamond knife on a LKB ultramicrotome were stained with uranyl acetate and observed under a transmission electron microscope (JEM-1200 EX, Tokyo, Japan) operated at an acceleration voltage of 80 kV.

Western blotting

Western blotting was conducted using fresh control and PBC liver tissues. Briefly, liver tissues were homogenized in 10 volumes of homogenization buffer (20 mmol/L Tris-HCl; pH 7.5, 5 mmol/L $MgCl_2$, 0.1 mmol/L PMSF, 20 μmol/L pepstatin A, and 20 μmol/L leupeptin) using a polytron homogenizer at setting 7 for 90 s. The homogenates were centrifuged at 100 000 *g* for 45 min. The membranes were washed thrice, resuspended in 10 volumes of homogenization buffer, homogenized using a Teflon/glass homogenizer, and centrifuged. The membrane proteins thus obtained were used for immunoblotting. Proteins were separated on SDS/PAGE (4-20% gel, Daiichi-Ikagaku, Tokyo, Japan) and transferred onto polyvinylidene difluoride (PVDF) membranes (Millipore, Bedford, MA). The blots were blocked with 50 g/L dried milk in PBS for 30 min, incubated with 20 μg/mL anti-ICAM-1 (G-5; Santa Cruz Bio., Santa Cruz, CA, USA), washed in 0.1% Tween 20 in PBS, and transferred onto PVDF membranes (NTN Life Science Products). The blots were blocked with 50 g/L dried milk in PBS for 30 min, incubated with anti-mouse goat IgG conjugated with horseradish peroxidase (Amershampharmacia) in 0.1% Tween 20 in PBS, and then processed by the Vectastain ABC system (Vector laboratories, Inc., Burlingame, CA, USA). The immunoreactive bands were visualized with diaminobenzidine solution containing 0.01% H_2O_2.

Semi-quantitative analysis

The immunogold particles on epithelial cells of bile ductules and cholangiocytes of CoH cells were counted. Photographs from 10 fields between the bile ductules and canal of Hering were investigated. The magnification was ×2 000.

RESULTS

Electron microscopic finding

Electron microscopic observation of the PBC liver specimens revealed lymphocytes associated with the bile ductular membrane in bile ductules (Figure 1A). Lymphocytes frequently migrated into the epithelial layer of CoH through their basement membrane (Figure 1B).

Immunohistochemical finding

We examined the immunohistochemical reactions of both ICAM-1 and LFA-1 in serial sections. In control liver specimens, ICAM-1 protein was expressed on sinusoidal lining cells but no specific immunoreactivity was observed on bile duct epithelial cells (Figure 2A). Immunostaining for LFA-1 appears to be present in portal lymphoid cells. Interlobular bile ducts appear to be negative for LFA-1, although there was sparse expression in bile duct epithelial cells (Figure 2B). In PBC liver tissue, *de novo* expression of ICAM-1 was found on the plasma membrane on the luminal side of epithelial cells in bile ductules and on some lymphocytes infiltrating small bile ductules or possibly small blood vessels. ICAM-1 immunoreactivity was also seen on the sinusoidal endothelial cells (Figure 2C). LFA-1 protein was expressed mainly in lymphocytes around and among the proliferated bile ductules (Figure 2D). Immunostaining of ICAM-1 and LFA-1 in CoH was less clearly depicted by immunostaining examined under a light microscope.

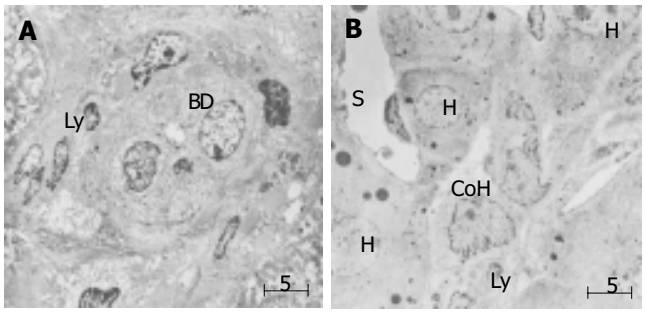

Figure 1 Electron microscopic finding in small bile ductule and CoH in liver specimen of PHC. **A:** Interaction of lymphocytes appear to interact with the bile ductule. Lymphocytes frequently migrate into the epithelial layer of small bile duct through the basement membrane. BD: bile ductule, ly: lymphocyte; **B:** Association of lymphocytes with the cholangiocytes of the CoH. CoH: canal of Hering. S: sinusoid, H: hepatocytes, Ly: lymphocytes, Bar: 5 μm.

Western blot

To confirm the immunohistochemical results, we investigated ICAM-1 protein expression by Western blotting. Samples containing 20 μg of protein were subjected to SDS/PAGE (4-20% gel) and analyzed by blotting with anti-ICAM-1 antibody. A band around 110 ku indicating ICAM-1 was found in abundance in PBC liver tissue (Figure 3).

In situ hybridization

Next, we investigated the expression of ICAM-1 and LFA-1 at mRNA level in PBC liver samples using *in situ* hybridization with PNA probes (Figure 4). Signals showing ICAM-1 mRNA were typically localized in bile ductular epithelial cells surrounding the CNSDC lesions (Figures 4A and B). Interestingly, signals showing LFA-1 were localized in lymphocytes inside the bile ductules of CNSDC lesions (Figures 4C and D).

Immuoelectron microscopy

Light microscopic examination of PBC liver samples depicted the localization of ICAM-1 and LFA-1 in bile ductules, but the localization in the CoH was less clear. We therefore conducted immunoelectron microscopic examin-ation. By immunogold electron microscopy, gold-labeled ICAM-1 particles were observed on cholangiocytes, distributing on the luminal surfaces of small bile ductules. ICAM-1 immunoreactivity was also observed on small portal or peripheral blood vessels and sinusoidal endothelial cells (Figure 5A). In the canal of Hering, gold-labeled ICAM-1 particles were observed on the luminal surfaces of cholangiocytes and hepatocytes (Figure 5C). LFA-1 labeling was concentrated on lymphocytes that were found around bile ductules (Figure 5B) and also around cholangiocytes of CoH (Figure 5D). Immature cells resembling progenitor cells were observed in CoH, and these cells did not show ICAM-1 immunoreactivity (Figure 5E). Around these cells, infiltration of lymphocytes was also absent (Figure 5F).

In the semi-quantitative analysis, immunogold–silver complex particles on epithelial cells of bile ductules and cholangiocytes of CoH were enumerated on immunoelectron micrographs (Figure 6). ICAM-1 immunoreactivity was found in CoH in 4 of the 10 PBC cases and in bile ductules

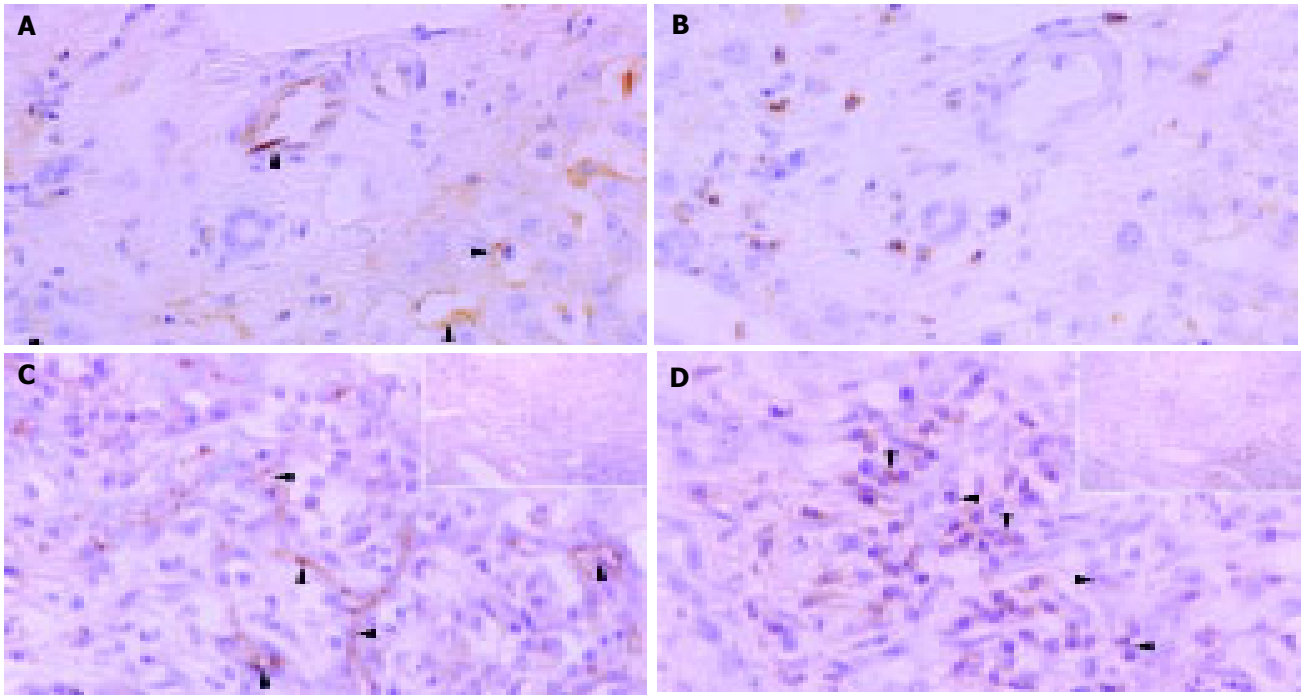

Figure 2 Immunohistochemical distributions of ICAM-1 (**A** and **C**) and LFA-1 (**B** and **D**) in control liver tissue (**A** and **D**) and liver tissue of PHC (**C** and **D**). **A:** ICAM-1 protein expression on sinusoidal lining cells but no specific immunoreactivity on bile duct epithelial cells in control liver specimens; **B:** LFA-1 immunoreactivity in portal lymphoid cells, negative in interlobular bile ducts and sparse expression in bile duct epithelial cells; **C:** Marked ICAM-1 immunoreactivity on the plasma membrane on the luminal side of bile ductules or possibly small blood vessels. Some lymphocytes around the bile ducts were also positive for ICAM-1. Arrowheads denote localization of ICAM-1 (arrows); **D:** LFA-1 immunoreactivity in lymphocytes around and among damaged bile ducts (arrowheads). Original magnification; ×400, hematoxylin counterstained.

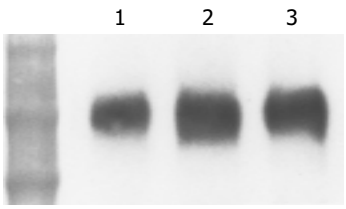

Figure 3 Western blot analysis of expression of ICAM-1 protein in human control and PBC liver tissue. Samples containing 20 μg protein were subjected to SDS/PAGE (4-20% gel) and analyzed by blotting. ICAM-1 was found in abundance in PBC liver tissues. Lanes 2 and 3: PBC liver tissue, lane 1: control liver tissue. Positions of molecular mass markers are shown (ku).

in 8 of the 10 cases. LFA-1 immunoreactivity was found in CoH in 4 of the 10 PBC cases and in bile ductules in 7 of the 10 cases. The extent of immunoreactivity (number of immunogold particles per unit CoH or bile ductule) was also stronger in bile ductules than in CoH. No immunogold–silver complex particles for ICAM-1 and LFA-1 were found in bile ductules and CoH of control liver tissues.

DISCUSSION

Bile duct inflammation and destruction are the fundamental lesions of PBC[25]. Interlobular bile ducts with external diameters of 30-100 μm are selectively affected, displaying variable necrotic and proliferative changes of biliary epithelial cells, as well as periductal lymphoplasmacytic infiltration. These findings are also frequently noted around damaged bile ducts, especially in the early histologic stages of the disease[25]. In our immunohistochemical study, ICAM-1 was strongly expressed on damaged bile ducts and infiltrating inflammatory cells, while LFA-1 was expressed on infiltrating lymphocytes. The presence of ICAM-1/LFA-1 linkage has been reported in CNSDC in PBC[16,17].

In our previous study, we correlated protein and mRNA expression of ICAM-1 and LFA-1 by conducting immunohistochemical and *in situ* hybridization studies on serial sections of CNSDC lesions[26]. We demonstrated abundant protein and mRNA expression of ICAM-1 on damaged biliary epithelial cells and LFA-1 on lymphocytes in CNSDC lesions, strongly suggesting the ICAM-1/LFA-1 linkage[26].

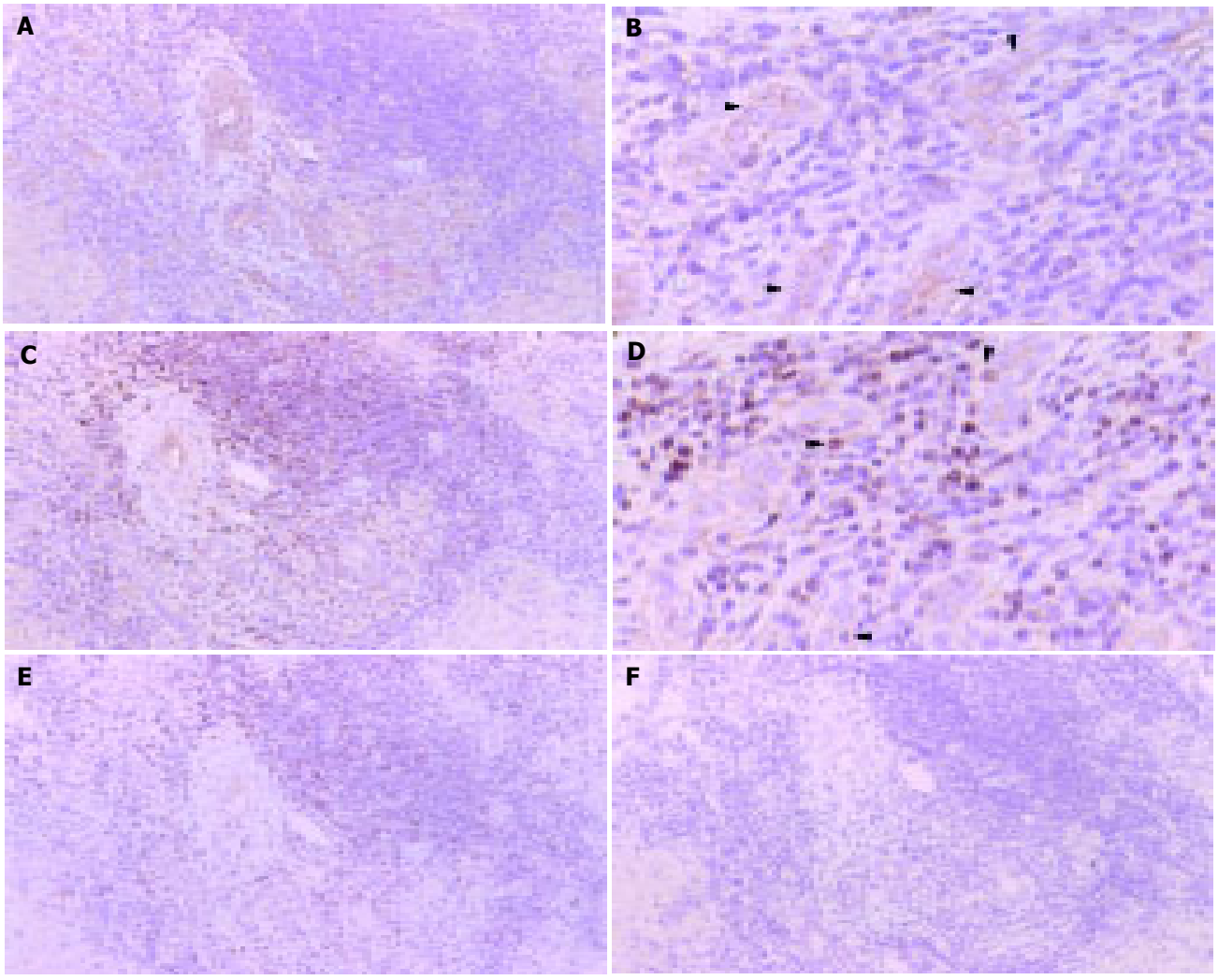

Figure 4 Localization of ICAM-1 (**A** and **B**) and LFA-1 (**C** and **D**) mRNA at bile ductules in PBC liver tissue by *in situ* hybridization with CSA. **A:** ICAM-1 mRNA was expressed in a cytoplasmic pattern on epithelial cells of bile ductile. (**A:** ×100 and **B:** ×300) Arrowhead denotes reaction product; **C:** LFA-1 mRNA is expressed in a cytoplasmic pattern in lymphocytes around bile ductile. (**C:** ×100 and **D:** ×300). Negative controls: **E:** ICAM-1 sense probe, **F:** LFA-1 sense probe. All panels: color was developed by DAB chromogen and hematoxylin counterstained. Arrowhead denotes reaction product.

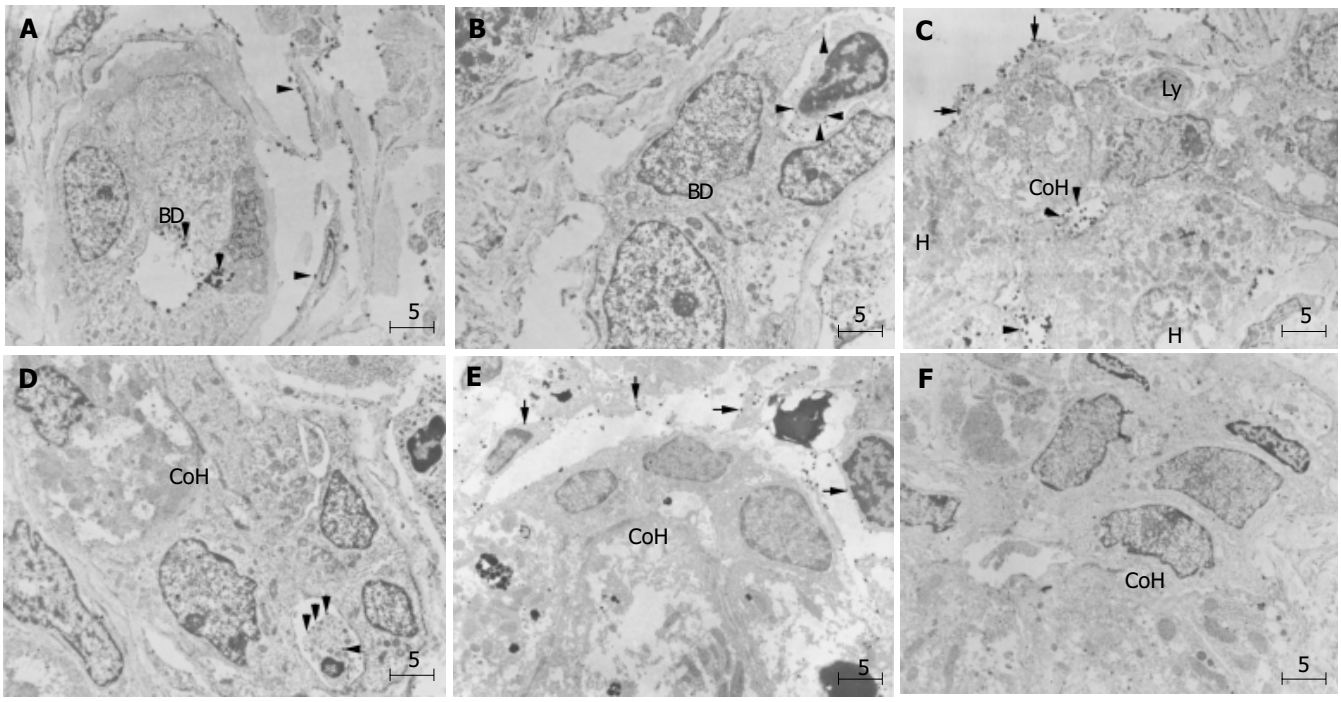

Figure 5 Immunoelectron microscopic findings of ICAM-1 (**A, C,** and **E**) and LFA-1 (**B, D,** and **F**) in periportal small bile ductule and canal of Hering in PBC liver. **A:** Gold-labeled ICAM-1 particles on the surface of cholangiocytes (arrowhead) facing the lumen of small bile ductule, a small portal or peripheral blood vessel, and also on sinusoidal endothelial cells (arrowheads). BD denotes bile ductule; **B:** Lymphocytes with dense labeling of LFA-1 (arrowhead) around small ductule; **C:** Gold-labeled ICAM-1 particles on the luminal surfaces of hepatocytes and cholangiocytes of CoH, on bile canaliculus and also on sinusoidal endothelial cells (arrows); **D:** Lymphocytes densely labeled with LFA-1 (arrows) on the basolateral membrane of cholangiocytes of the CoH; **E:** No ICAM-1 immunoreactivity show immature cells resembling progenitor cells (asterisk) in CoH, and these cells; **F:** No infiltration of lymphocytes is observed around the progenitor-like cells (asterisk). Bar, 5 μm; BD, bile ductile; Ly, lymphocyte; CoH, canal of Hering; H. hepatocyte. Uranyl acetate stain.

Frequent and variable infiltration of lymphocytes, mainly T cells, and other inflammatory cells of the biliary epithelium has been reported in PBC[27]. Some lymphocytes infiltrate by crossing the basement membrane of bile ducts. These changes appear as necro-inflammatory lesions inside the basement membrane of bile ducts and ductules.

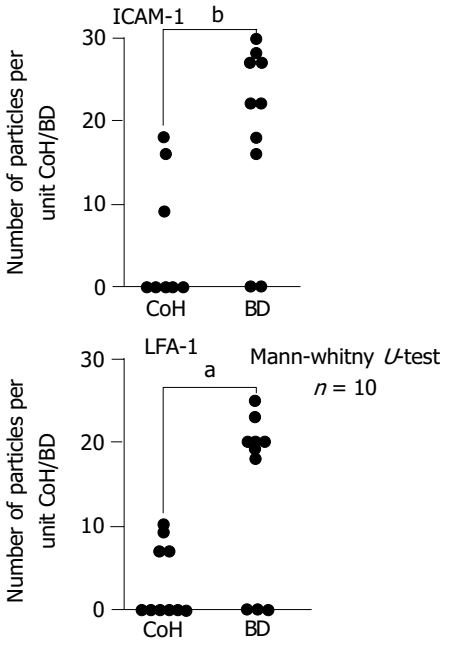

Figure 6 Semi-quantitative analysis of immunogold-silver complex particles on epithelial cells of bile ductules and cholangiocytes of CoH enumerated on immunoelectron micrographs (expressed in number of particles per unit CoH or small bile ductule). Immunoreactivity was significantly greater on bile ductules (Mann-Whitney test). BD, bile ductile; CoH, canal of Hering. [a]$P<0.05$, [b]$P<0.01$ *vs* CoH.

Our immunoelectron microscopic study has confirmed for the first time the ultrastructural localization of ICAM-1 on cholangiocytes and LFA-1 on infiltrating inflammatory cell in damaged CoH. The lymphocytes and other inflammatory cells then penetrated the peribiliary vascular plexus and portal venules, and migrated into perivenular tissue toward the bile ducts[12]. When early stage PBC specimens were immunostained for cytokeratin 19 and HLA-DR, the CoH were found mostly around portal tracts in stages 2 and 3 PBC, but they were destroyed in concert with the destruction of bile ductules[28]. Therefore, CoH in PBC specimens are difficult to be depicted by immunohistochemistry using light microscopy. Our immunoelectron microscopic study successfully demonstrated the ultrastructural localization of ICAM-1 and LFA-1 on CoH.

Previous studies of cell adhesion molecules, especially ICAM, in PBC have reported conflicting results. Adams *et al*.[14], reported a series of 13 patients with PBC studied at liver transplantation and found that ICAM was expressed on interlobular bile ducts and proliferating bile ductules. In contrast, Broome *et al*.[29], found ICAM in 3 of 10 patients with PBC while almost all patients expressed HLA-DR on biliary epithelium. Bloom *et al*.[30] found ICAM-1 expression on bile ducts in two of seven cases of early disease and in only one of five patients with stage three or four disease. According to these reports, ICAM-1 expression in PBC is not very common and not clearly associated with a particular

disorder. Using immunoelectron microscopy, we found that 8 of 10 PBC patients expressed ICAM-1 and 7 of 10 patients expressed IFA-1 on bile ductules. The higher rate probably reflects the higher sensitivity of our method.

In this study, we observed membranous staining of hepatocytes and bile ductules with different intensity with ICAM-1 antibodies (Figure 1C) in PBC. However, ICAM-1 expression on hepatocytes is indefinite or only faint in normal livers. These findings may suggest the involvement of immune-mediated hepatocytolysis related to expression and presentation of target antigens[12].

Bile duct loss can be evaluated semi-quantitatively by calculating the ratio of portal tracts devoid of interlobular bile ducts and also the proportion of hepatic arterial branches without parallel running interlobular bile ducts[12]. Regrowth of bile ducts has been reported, and a ductular reaction precedes the reappearance of neo-bile ducts. In this process, hepatic stem cells or progenitor cells migrate from the periportal area into the biliary tree[31]. On the other hand, in rat liver injury, the role of ICAM-1 is to adhere to neutrophils, and excessive parenchymal apoptosis may be a signal for this neutrophil-induced inflammatory and necrotic reaction[32]. Apoptosis of bile ductules could be one of the processes that explain the reduced proliferation of bile ductules[33]. Therefore, strong expression of ICAM-1 on bile ductules may be a cause of the reduction in proliferation of bile ductules[25,33].

Our semi-quantitative study of immunogold-silver complex in bile ductile epithelium and cholangiocytes in CoH of PBC liver revealed that the rate and intensity of ICAM-1 and IFA-1 expression were higher in the bile ductules than in the upstream CoH. The reason is that there are less mature cholangiocytes in the CoH. We observed cells with intermediate morphology in CoH, which may be progenitor cells labeled with ICAM-1 and LFA-1. Since the adhesion molecules appear to be expressed only on the mature cholangiocytes, this implies that the mature cholangiocytes are targeted for autoimmune destruction in PBC. Destruction in the CoH upstream of bile ductules also occurs because of the presence of mature cholangiocytes. Recently, a human bipotent liver progenitor cell line has been established, which shows comparable immunophenotype restricted to bile neoductules[34]. The mechanisms of how progenitor cells are protected from destruction by the host immune system should be studied.

REFERENCES

1 **Hering E.** Uber den bau der Wirbeltiereber, Sitzber. *Akad wiss Wien Math Naturic KL* 1865; **54**: 496-515
2 **Steiner JW,** Carruthers JS. Studies on the fine structure of the terminal branches of the biliary tree. *Am J Pathol* 1961; **38**; 639-661
3 **Watanabe N,** Tsukada N, Smith CR, Phillips MJ. Motility of bile canaliculi in the living animal- implications for bile flow. *J Cell Biol* 1991; **113**: 1069-10802
4 **Ishii K,** Phillips MJ. *In vivo* contractions of the duct of Hering. *Hepatology* 1995; **22** (4 Pt 2): 159
5 **Nonomura A,** Kono N, Mizukami Y, Nakanuma Y, Matsubara F. Histological changes in the liver in experimental graft-versus-host disease across minor histocompatibility barriers. IV. A light and electron microscopic study of the periportal changes. *Liver* 1991; **11**: 278-286
6 **Theise ND,** Saxena R, Portmann B, Thung SN, Yee H, Chiriboga L, Kumar A, Crawford JM. The canals of Hering and hepatic stem cells in humans. *Hepatology* 1999; **30**: 1425-1433
7 **Kaplan MM.** Primary biliary cirrhosis. *N Engl J Med* 1987; **316**: 512-528
8 **James SP,** Hoofnagle JH, Strober W. Primary biliary cirrhosis: a model autoimmune disease. *Ann Intern Med* 1983; **99**: 500-512
9 **Thomas HC,** Potter BJ, Sherlock S. Is primary biliary cirrhosis an immunocemplex disease? *Lancet* 1977; **2:** 1216-1263
10 **Wands JR,** Dienstag JL, Bhan AK, Feller ER, Isselbacher KJ. Circulating immune complexes and complement activation in primary biliary cirrhosis. *N Engl J Med* 1978; **298**: 233-237
11 **Cancellieri V,** Scaroni C, Vernace SJ, Schaffner F, Paronetto F. Subpopulation of T lymphocyte in primary biliary cirrhosis. *Clin Immunol Immunopathol* 1981; **20**: 255-260
12 **Nakanuma Y,** Yasoshimura M, Tsuneyama K, Harada K. Histopathology of primary biliary cirrhosis with emphasis on expression of adhesion molecules. *Semi Liver Dis* 1997; **17**: 35-47
13 **Volpes R,** Van Den Oord JJ, Desmet VJ. Immunohistochemical study of adhesion molecules in liver inflammation. *Hepatology* 1990; **12**: 59-65
14 **Adams DH,** Hubscher SG, Shaw J, Johnson GD, Babbs C, Rothlein R, Neuberger JM. Increased expression of ICAM-1 on bile ducts in primary biliary cirrhosis and primary sclerosing cholangitis. *Hepatology* 1991; **14**: 426-443
15 **Altmann DM,** Hogg N, Trowsdale J, Wilkinson D. Co-transfection of ICAM-1 and HLA-DR reconstitutes human antigen presenting cell function in mouse L lines. *Nature* 1990; **338**: 512-514
16 **Kaneko H,** Oda M, Yokomori H, Kazemoto S, Kamegaya Y, Komatsu H, Tsuchiya M. Immunohistochemical microscopic analysis of bile duct destruction in primary biliary cirrhosis: Involvement of intercellular adhesion molecules. *Int Hepatol Commun* 1994; **2**: 271-276
17 **Yasoshima M,** Nakanuma Y, Tsuneyama K, van de Water J, Gershwin ME. Immunohistochemical analysis of adhesion molecules in the micro-environment of portal tracts in relation to aberrant expression of PDC-E2 and HLA-DR on the bile ducts in primary biliary cirrhosis. *J Pathol* 1995; **175**: 319-325
18 **Ohta Y.** Diagnostic criteria for primary biliary cirrhosis. *Acta Hepatol Jpn* 1992; **33**: 657
19 **Mclean IW,** Nakane PK. Periodate-lysine-paraforaldehyde fixative: a new fixative for immunoelectron microscopy. *J Histochem Cytochem* 1974; **22**: 1077-1083
20 **Thisted M,** Just T, Pluzek KJ, Petersen KH, Hyldig-Nielsen JJ, Godtfredsen SE. Detection of immunoglobulin kappa light chain mRNA in paraffin sections by *in situ* hybridization using peptide nucleic acid probes. *Cell Vision* 1996; **3**: 358-363
21 **Simmons D,** Makgoba MW, Seed B. ICAM, an adhesion ligand of LFA-1, is homologous to the neural cell adhesion molecule NCAM. *Nature* 1988; **331**: 624-627
22 **Larson RS,** Corbi AL, Berman L, Springer T. Primary structure of the leukocyte function-associated molecule-1 alpha subunit: an integrin with an embedded domain defining a protein superfamily. *J Cell Biol* 1989; **108**: 703-712
23 **Kerstens HM,** Poddighe PJ, Hanselaar AG. A novel in situ hybridization signal amplification method based on the deposition of biotinylated tyramine. *J Histochem Cytochem* 1995; **43**: 347-352
24 **Fujimori O,** Nakamura M. Protein A gold-silver staining methods for light microscopic immunohistochemistry. *Arch Histol Jap* 1985; **48**: 449-452
25 **Nakanuma Y,** Ohta G. Quantitation of hepatic granulomas and epitheloid cells in primary biliary cirrhosis. *Hepatology* 1983; **3**: 423-427
26 **Yokomori H,** Oda M, Yoshimura K, Nomura M, Ogi M, Wakabayashi G, Kitajima M, Ishii H. Expression of intercel-

lular adhesion molecule-1 and lymphocyte function-associated antigen protein and messenger RNA in primary biliary cirrhosis. *Internal Med* 2003; **42**: 947-954

27 **Yamada G,** Hyodo I, Tobe K, Mizuno M, Nishihara T, Kobayashi T, Nagashima H. Ultrastructural immunocytochemical analysis of lymphocytes infiltrating bile duct epithelium in primary biliary cirrhosis. *Hepatology* 1986; **6**: 385-391

28 **Saxena R,** Hytiroglou P, Thung SN, Theise ND. Destruction of canals of Hering in primary biliary cirrhosis. *Hum Pathol* 2002; **33**: 983-988

29 **Broome U,** Hultcrantz R, Forsum U. Lack of concomitant expression of ICAM-1 and HLA-DR on bile duct cells from patients with primary sclerosing cholangitis and primary biliary cirrhosis. *Scand J Gastroentel* 1993; **28**: 126-130

30 **Bloom S,** Fleming K, Chapman R. Adhesion molecule expression in primary sclerosing cholangitis and primary biliary cirrhosis. *Gut* 1995; **36**: 604-609

31 **Gerber MA,** Thung SN. Liver stem cells and development. *Lab Invest* 1993; **68**: 261-263

32 **Kobayashi A,** Imamura H, Isobe M, Matsuyama Y, Sorda J, Matsunaga K, Kawasaki S. Mac-1(CD11b/CD18) and intercellular adhesion molecule-1 in ischemia-reperfusion injury of rat liver. *Am J Physiol* 2001; **281**: G577-585

33 **Bhathal PS,** Gall JA. Deletion of hyperplastic biliary epithelial cells by apoptosis following removal of the proliferative stimuli. *Liver* 1985; **5**: 311-325

34 **Parent R,** Marion MJ, Furio L, Trépo C, Petit MA. Origin and characterization of a human bipotent liver progenitor cell line. *Gastroenterology* 2004; **126**: 1147-1156

Science Editor Wang XL **Language Editor** Elsevier HK

PO Box 2345, Beijing 100023, China
www.wjgnet.com
wjg@wjgnet.com

ELSEVIER

World J Gastroenterol 2005;11(28):4390-4395
World Journal of Gastroenterology ISSN 1007-9327

• *CLINICAL RESEARCH* •

Excretion and detection of SARS coronavirus and its nucleic acid from digestive system

Xin-Wei Wang, Jin-Song Li, Ting-Kai Guo, Bei Zhen, Qing-Xin Kong, Bin Yi, Zhong Li, Nong Song, Min Jin, Xiao-Ming Wu, Wen-Jun Xiao, Xiu-Mei Zhu, Chang-Qing Gu, Jing Yin, Wei Wei, Wei Yao, Chao Liu, Jian-Feng Li, Guo-Rong Ou, Min-Nian Wang, Tong-Yu Fang, Gui-Jie Wang, Yao-Hui Qiu, Huai-Huan Wu, Fu-Huan Chao, Jun-Wen Li

Xin-Wei Wang, Qing-Xin Kong, Zhong Li, Nong Song, Min Jin, Chang-Qing Gu, Jing Yin, Guo-Rong Ou, Fu-Huan Chao, Jun-Wen Li, Tianjin Institute of Environment and Health, Tianjin 300050, China
Jin-Song Li, Bei Zhen, Xiao-Ming Wu, Wen-Jun Xiao, Wei Wei, Min-Nian Wang, Gui-Jie Wang, Institute of Microbiology and Epidemiology, Beijing 100072, China
Ting-Kai Guo, Xiu-Mei Zhu, Wei Yao, Jian-Feng Li, Yao-Hui Qiu, Huai-Huan Wu, Xiao Tang Shan Hospital, Beijing 102211, China
Bin Yi, 309 Hospital of PLA, Beijing 100091, China
Chao Liu, Beijing Institute of Pharmacology and Toxicology, Beijing 100850, China
Tong-Yu Fang, Beijing Institute of Basic Medicine, Beijing 100850, China
Supported by the National High Technology Research and Development Program of China, 863 Program, No. 2004AA649100, and the National Natural Science Foundation of China, No. 30471436
Correspondence to: Dr. Jun-Wen Li, Tianjin Institute of Environment and Health, Tianjin 300050, China. junwenli@eyou.com
Telephone: +86-22-84655345 Fax: +86-22-23328809
Received: 2004-04-22 Accepted: 2004-05-24

Abstract

AIM: To study whether severe acute respiratory syndrome coronavirus (SARS-CoV) could be excreted from digestive system.

METHODS: Cell culture and semi-nested RT-PCR were used to detect SARS-CoV and its RNA from 21 stool and urine samples, and a kind of electropositive filter media particles was used to concentrate the virus in 10 sewage samples from two hospitals receiving SARS patients in Beijing in China.

RESULTS: It was demonstrated that there was no live SARS-CoV in all samples collected, but the RNA of SARS-CoV could be detected in seven stool samples from SARS patients with any one of the symptoms of fever, malaise, cough, or dyspnea, in 10 sewage samples before disinfection and 3 samples after disinfection from the two hospitals. The RNA could not be detected in urine and stool samples from patients recovered from SARS.

CONCLUSION: Nucleic acid of SARS-CoV can be excreted through the stool of patients into sewage system, and the possibility of SARS-CoV transmitting through digestive system cannot be excluded.

Key words: Severe acute respiratory syndrome; Nucleic acid; Digestive system

Wang XW, Li JS, Guo TK, Zhen B, Kong QX, Yi B, Li Z, Song N, Jin M, Wu XM, Xiao WJ, Zhu XM, Gu CQ, Yin J, Wei W, Yao W, Liu C, Li JF, Ou GR, Wang MN, Fang TY, Wang GJ, Qiu YH, Wu HH, Chao FH, Li JW. Excretion and detection of SARS coronavirus and its nucleic acid from digestive system. *World J Gastroenterol* 2005; 11(28): 4390-4395
http://www.wjgnet.com/1007-9327/11/4390.asp

INTRODUCTION

By the end of 2002, there were reports from Guangdong Province in southern China of cases of severe acute respiratory syndrome (SARS). Over 8 439 SARS cases and 812 SARS-related deaths were reported to WHO from 32 countries around the world till 5th July, 2003[1,2]. In response to this outbreak, WHO coordinated an international collaboration that included clinical, epidemiological, laboratory investigations, and initiated efforts to control the spread of SARS. Attempts to identify the etiology of SARS outbreak were successful during the 3rd wk of March 2003, when laboratories in the USA, Canada, Germany, Hong Kong, and China isolated a novel coronavirus from SARS patients[3-6]. Unlike other human coronaviruses, it was possible to isolate the novel coronavirus in Vero cells. Evidence of the coronavirus infection was documented in SARS patients throughout the world. The coronavirus RNA was frequently detected in respiratory specimens, and convalescent-phase serum specimens from SARS patients containing antibodies that reacted with the coronavirus. There was a strong evidence that this new virus was etiologically linked to the outbreak of SARS[5-8].

Investigations of the global outbreak of SARS have shown that the major mode of transmission of SARS virus was through close personal contact, in particular exposure to droplets of respiratory secretions from an infected person[1,9-14]. While in a cluster of SARS cases in an apartment block in Hong Kong, sewage was believed to have played a role through droplets containing coronavirus from the sewage system[11,12]. However, there is no direct evidence to prove that the coronavirus exists in sewage system and is contagious.

In order to confirm whether the digestive system was a possible major transmission way of SARS-CoV, cell culture and the semi-nested RT-PCR were used to directly detect SARS-CoV and its RNA. A kind of electropositive filter media particle[15] was used to concentrate the SARS-CoV from the sewage of hospitals receiving SARS patients in Beijing of China, and then the virus and its RNA were detected.

MATERIALS AND METHODS

Viruses and culture methods

To identify viruses that existed in stools, urine samples, and sewage system, we inoculated a variety of specimens onto Vero E6. Because of the toxicity of sewage concentrates, all cell cultures were inoculated in the presence of growth medium for 1 h at 37 ℃. This procedure virtually eliminated problems with the toxicity of sewage concentrates. Medium was replaced after 1-2 d of incubation. Culture was terminated 7 d after inoculation, and the culture was observed daily for cytopathic effects. Cultures exhibiting identifiable cytopathic effects were subjected to several procedures to identify the cause of the effect[16-18]. If there was no cytopathic effect on the cell culture, the supernate was harvested and added into additional flasks to isolate viruses. The cultures were then used until three generations without cytopathic effects.

Stools and urine samples of SARS patients

Twenty-one stool and urine samples were collected from the Xiao Tang Shan Hospital and 309 Hospital of PLA, which were specially assigned to receive SARS patients in Beijing in 2003, among which 11 samples were collected from the SARS patients with any one of the symptoms of fever, malaise, cough, or dyspnea, and 10 samples were from recovered patients.

Sewage and disinfection

Ten sewage samples were collected at 7 o'clock in the morning from Xiao Tang Shan Hospital and 309 Hospital of PLA for 7 d. Two thousand and five hundred milliliters of sewage before disinfection or 25 000-50 000 mL after disinfection by chlorine was collected.

Electropositive filter media particle

The positively charged filter media particles, which were used to concentrate SARS-CoV from sewage, were prepared as previously described[15].

Detection of residual chlorine

The residual chlorine in sewage was determined by the *N*, *N*, diethyl-*p*-phenyldiamine colorimetric method[19].

Concentration of SARS-CoV from sewage

Two thousand and five hundred milliliters and 25 000 mL `sewage from the hospitals before or after disinfection by chlorine were placed in a 25-L capacity plastic bucket, and 10 mL $Na_2S_2O_3$ (100 g/L) was added to neutralize the residual chlorine. Five hundred or 820 g filter media was packed in a polymethyl methacrylate column (89 or 130 mm i.d.). The filter media bed height was 14 cm. The flow rate was kept at 10 mL/min per cm^2 of the filter surface area. The adsorbed viruses were eluted from filter media with 700 or 900 mL 6× nutrient broth (pH 7.2). The collected eluates were reconc-entrated by PEG precipitation and centrifugation. The pellets were resuspended in 40 mL PBS and assayed.

RNA extraction

Virus RNA extracting kit (TRIzol Reagent) made by Invitrogen™ Life Technologies for extraction of exceedingly pure viral RNA was utilized in our experiment to extract virus RNA, and all procedures were strictly implemented in accordance with the reagent instruction manual.

Primer design for assay of SARS-CoV nucleic acid

Three sets of primers from WHO Network Laboratories[20] were used to detect the SARS-CoV RNA: Cor-p-F2 (+) 5'-CTAACATGCTTAGGATAATGG-3', Cor-p-F3 (+) 5'-GCCTCTCTTGTTCTTGCTCGC-3', and Cor-p-R1 (-) 5'-CAGGTAAGCGTAAAACTCATC-3'. Cor-p-F2/Cor-p-R1 gave a 368-bp product, and Cor-p-F3/Cor-p-R1 yielded a 348-bp segment.

Primer design for assay of enterovirus nucleic acid

A pair of consensus primers of enteroviruses was from the 5' non-coding region because of their presence in many enterovirus serotypes. The sequences of primers were as follows: E1 5'-ATTGTCACCATAAGCAGCCA-3', E2 5'-CCAGCACTTCTGTTTCCCCGG-3', and the product size was 440 bp[21].

Detection of SARS-CoV by semi-nested RT-PCR

Two microliters of RNA solution was analyzed with RT-PCR assay. The KaTaRa one step RNA PCR kit (KaTaRa Biotechnology, Dalian) was used for the reaction (20 μL total volume). Positive and negative RT-PCR controls were included in each run. Reactions contained 10 μL of buffer concentrate, 2 mmol/L of magnesium sulfate, 0.8 μL of enzyme mixture, and 1.9 μmol/L of each of Cor-p-F2 and Cor-p-R1 primers. Thermal cycling comprised 42 ℃ for 30 min, 95 ℃ for 3 min; 10 cycles of 95 ℃ for 10 s, 55 ℃ for 15 s (decreasing by 1 ℃ per cycle), 72 ℃ for 40 s; 40 cycles of 95 ℃ for 10 s, 56 ℃ for 10 s, and 72 ℃ for 40 s. To confirm the PCR products, a semi-nested PCR was developed. The template was the first PCR product, and the primers were Cor-p-F3 and Cor-p-R1, and yielded a 348-bp product. The amplification efficiency of the primers was confirmed by SARS-CoV of BJ-01 isolated from a SARS patient in Guangzhou city, China (Figure 2).

Detection of enteroviruses by RT-PCR

As most of enteroviruses can also grow on the Vero cells, and yield cytopathic effects, enteroviruses should be detected by the specific primers[21]. The RT-PCR method was similar to that for SARS-CoV.

Detection of PCR products

PCR products were analyzed by electrophoresis with 15 g/L agarose gels containing 0.5 μg of ethidium bromide per mL, and visualized with UV illumination and photographed. DNA molecular size standards (100-bp ladder, Gibco/BRL) were included in each run of agarose gel electrophoresis.

In view of the serious nature of SARS and the person-to-person transmission, all clinical specimens were treated in a biosafety level 3 environment. All divisions into aliquots, pipetting, concentration for small sewage and culture attempts were performed in laminar-flow safety cabinets. A similar environment was used when specimens from which nucleic acid was to be extracted and placed in a buffer solution.

Nucleotide sequence analysis

The PCR products from four different samples were purified

with the QIAquick PCR purification kit (QIANEN, Inc.) and sequenced with the ABI PRISM dye terminator cycle sequencing ready reaction kit with Ampli*Taq* DNA polymerase FS (Perkin-Elmer, Applied Biosystem) following the manufacturer's instructions. The sequences were compared with the genome of SARS-CoV in the GenBank and EMBL databases by using the FASTA program of the GCG.

RESULTS

Detection of SARS-CoV by the semi-nested RT-PCR

The detection specificity and sensitivity of semi-nested RT-PCR were confirmed by the isolated SARS-CoV (BJ-01) from Institute of Microbiology and Epidemiology, Academy of Military Medical Sciences, Beijing, China. It was shown that two amplicons were yielded, which were in agreement with the information on the designed primers (Figure 1). The minimum amount of SARS-CoV RNA detected by semi-nested PCR was equivalent to 10 $TCID_{50}$ (Figure 2).

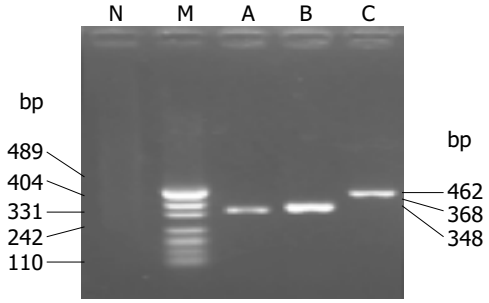

Figure 1 Amplification of SARS-CoV RNA BJ-01 by semi-nested RT-PCR. M: DNA marker (pUC19 DNA/MSP I marker); lane A: 348 bp; lane B: 368 bp; lane C: positive RT-PCR control, 462 bp; lane N: negative RT-PCR control.

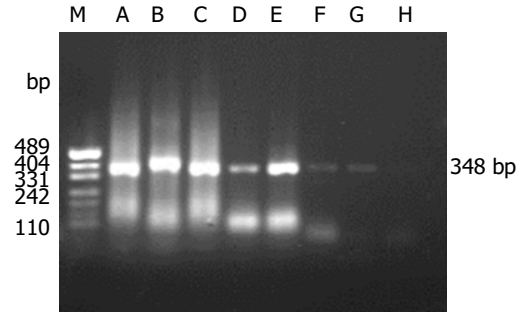

Figure 2 Sensitivity of semi-nested RT-PCR for SARS-CoV. M: DNA marker (pUC19 DNA/MSP I marker); lane A-G: virus concentration was 10^6-10^{10} $TCID_{50}$, lane H: negative control.

Isolation of SARS-CoV and detection of SARS-CoV RNA from stool samples of patients

All the 21 stool samples tested for the presence of infectious SARS-CoV in cell culture were negative. SARS-CoV RNA could be detected in 7 of 11 stool samples from patients with symptoms by semi-nested RT-PCR (Figure 3). However, SARS-CoV RNA could not be detected from the samples of patients who recovered.

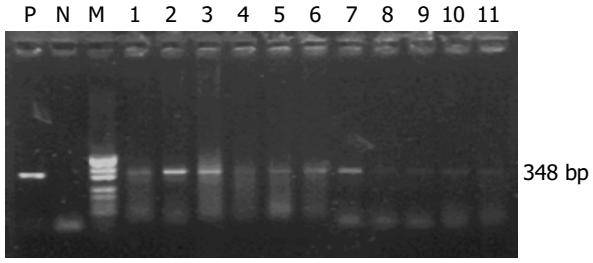

Figure 3 Amplification of SARS-CoV RNA from stool samples. M: DNA marker (pUC19 DNA/MSP I marker); lanes 1-11: samples from different SARS patients; N: negative control; P was the positive RT-PCR control from the RNA of SARS-CoV BJ-01.

Isolation of SARS-CoV and detection of SARS-CoV RNA from urine samples of patients

All the 21 urine samples tested for the presence of infectious SARS-CoV in cell culture were also negative. SARS-CoV RNA could not be detected from the samples or the supernate of cell cultures by semi-nested RT-PCR.

Concentration and detection of SARS-CoV from sewage before disinfection

All sewage samples tested for the presence of infectious SARS-CoV in cell culture were negative. SARS-CoV RNA could be found in the concentrates of sewage from the two hospitals by semi-nested PCR, and in the inoculated cells of the sewage concentrates from 309 Hospital but not from Xiao Tang Shan Hospital. However, SARS-CoV RNA copies in the samples were too low to be detected by the first amplification reaction, the semi-nested RT-PCR in which the products of first amplification reaction were the template of the second PCR, gave the positive amplification results (Tables 1 and 2).

Table 1 Concentration and detection of SARS-CoV in 2 500-mL sewage before disinfection in Xiao Tang Shan Hospital[1]

Date	Cell cult[2]	Concentrate +PCR[3]	Inoculated cells+PCR[4]	Entero.[5] PCR
10 June	-	+	-	-
11 June	-	+	-	-
12 June	-	+	-	-
13 June	-	+	-	-
14 June	-	+	-	-
15 June	-	+	-	-

[1]Glass column diameter: 19 mm, bed height: 14 cm, eluate volume: 500 mL; [2]Cell culture was maintained for 14 d to observe the cytopathic effect; [3]PCR template was from the concentrates; [4]PCR template was from the cultured cells; [5]Enteroviruses were detected by general primer RT-PCR for enteroviruses.

Table 2 Concentration and detection of SARS-CoV in 2 500-mL sewage before disinfection in 309 Hospital of PLA[1]

Date	Cell cult	Concentrate +PCR	Inoculated cells+PCR	Entero. PCR
11 June	-	+	-	-
12 June	-	+	-	-
13 June	-	+	-	-
14 June	-	+	-	-
15 June	-	+	-	-
16 June	-	+	-	-

[1]All explanatory notes are same as in Table 1.

Concentration and detection of SARS-CoV from sewage after disinfection

The samples (25 000 or 50 000 mL) from the two hospitals were all negative by the infectivity methods. SARS-CoV RNA was detected from the concentrates and inoculated cells in three samples (June 11, 13, and 15) from 309 Hospital by semi-nested RT-PCR, while the other samples were negative (Tables 3 and 4).

Table 3 Concentration and detection of SARS-CoV in 25 000- or 50 000-mL sewage after disinfection in Xiao Tang Shan Hospital[1]

Date	Cell culture	Concentrate +PCR	Inoculated cells+PCR	Enterovirus PCR
11 June	-	-	-	-
12 June	-	-	-	-
13 June	-	-	-	-
14 June	-	-	-	-
15 June	-	-	-	-

[1]All explanatory notes are same as in Table 1.

Table 4 Concentration and detection of SARS-CoV in 25 000-mL sewage after disinfection in 309 Hospital of PLA[1]

Date	Cell culture	Concentrate +PCR	Inoculated cells+PCR	Enterovirus PCR
11 June	-	+	+	-
12 June	-	-	-	-
13 June	-	+	+	-
14 June	-	-	-	-
15 June	-	+-	+	-

[1]All explanatory notes are same as in Table 1.

Result of nucleotide sequence analysis

The PCR products from the sewage samples of the two hospitals were sequenced, and submitted to GenBank. The accession numbers are bankit579728 and bankit579738, respectively. Comparison of the nucleotide sequences of PCR products with data from GenBank revealed that the sequences of the PCR products were close to those of SARS-COV genomes, showing about 99% nucleotide homolog.

DISCUSSION

Most SARS cases to date have occurred in young adults. The health care workers in hospitals, patient family members and international travelers were the commonly infected people[22,23].

The isolation of a novel coronavirus was obtained from the respiratory secretions of patients with SARS, and points to the etiologic association with SARS[3-6,8,24-26].

The mechanism of transmission of SARS-CoV is not yet understood completely. However, the fact that transmission has been limited to close contacts with patients, such as household members, health care workers, or other patients who were not protected with contact or respiratory precautions, suggests that either droplet secretions or direct or indirect contact probably has a role[1,10-14,27].

On 15th April, 2003, health authorities reported a total of 321 individuals infected with SARS virus who were residents in Amoy Gardens. A large proportion of cases were concentrated in vertically linked flats in a single building, Block E. On April 17, the Hong Kong Government announced that not one single factor could account for the outbreak in Block E of Amoy Gardens, and attention was focused on possible transmission via the sewage system because laboratory studies showed that patients with the disease excreted coronaviruses in their stools and these viruses were able to survive much longer in feces than on ordinary surfaces, and noted a swab sample taken from the toilet of an infected resident showed a positive test for the coronavirus' genetic material, and about 60% of patients in Amoy Gardens had diarrhea during their illness, and probably would have discharged a large amount of viruses into the soil stacks. Finally, the virus would spread with water droplets through the U-traps of the floor drains, which were dried up in many cases[11,24,28,29].

The elevated levels of aspartate aminotransferase and lactate dehydrogenase indeed suggest that SARS-CoV was also replicating outside the respiratory tract[1]. Electron microscopic examination showed that virus-like particles with 100-150 nm in diameter were found in cytoplasm and dilated reticular endoplasm of the infected alveolar epithelial cells and endothelial cells[6,26,30,31]. Shedding of the virus in feces might be an additional source of spreading, provided the virus was stable in this environment[8].

Tsang *et al*., reported that there were three nurses who worked at Hospital B, where a patient was admitted and remained for 6 d for treatment of pneumonia before he was transferred to Hospital C. During this period, the nurses spent five 8-h shifts stationed on the general ward where the patient was hospitalized. The three nurses recalled close encounter with the patient during which they cleaned him when he had fecal incontinence after an episode of diarrhea on March 3, 2003. The nurses did not wear masks or gowns during their routine nursing care of any patients on the ward and finally were all infected[1].

The detection of SARS-CoV in fecal and serum samples from patients, as well as in respiratory specimens, suggested that this virus, like many animal coronaviruses, might spread both by fecal contamination and by respiratory droplets[4].

Zhang reviewed the data of SARS transmission and believed that, as previously described, most coronaviruses could cause either a respiratory or an enteric disease, which is also transmitted by the fecal-oral route. During this outbreak of SARS, symptoms of the gastrointestinal tract in patients were noticed. Many investigators[1,10,32] found that gastrointestinal symptoms, including diarrhea (19-50%), nausea and vomiting (19.6%), and abdominal pain (13%) were common in SARS patients.

All the above reports suggested that stools of SARS patients or sewage containing stools of SARS patients would transmit the coronavirus. However, except that the positive PCR results were obtained in some patient stools, there were no reports that live viruses were present in patient stool or sewage.

In this study, we isolated and detected the SARS-CoV in stools, urine samples, and sewage from hospitals which were assigned specially to receive SARS patients in Beijing of China. Just as expected, SARS-CoV RNA was detected from

stools of patients, but no live viruses were isolated from stool samples, and no SARS-CoV RNA was found in all stools from patients who recovered. It is suggested that the nucleic acid of SARS-CoV could be really excreted from stools of patients, but infectious SARS-CoV could not be confirmed to excrete through the digestive system. No live virus and its RNA were isolated from the urine samples of patients. It is suggested that SARS-CoV and its RNA could not be excreted from the urinary system.

In order to explore the growth and decline of SARS-CoV and its RNA in environment, SARS-CoV and its RNA were isolated from sewage of hospitals. Although the concen-tration method of SARS-CoV from sewage has not been reported yet, the concentration of enteroviruses from water using different methods was reported, and the electropositive filters have been considered as the most promising method[34,35].

We developed a simple method for concentration of entero-viruses from water with electropositive particles, the adsorption of bacteriophage f_2 was reliable and efficient, not affected by the pH value, temperature, turbidity, and organic materials in water, and gave a recovery of 88.7% for poliovirus I and a comparable recovery of HAV, $CoxB_3$, and Echo 7 from 100 L of tap water[15].

We attempted to concentrate SARS-CoV in sewage from Xiao Tang Shan Hospital and 309 Hospital in Beijing by the electropositive particle adsorption method. The sewage systems in these two hospitals were similar, i.e. the sewage was collected from each isolation ward and converged into the reaction sedimentation basin, and disinfectant (chlorine) was added to inactivate SARS-CoV and other pathogenic microorganisms; finally, the sewage was discharged from the reaction sedimentation basin after a 60-min reaction.

Results of testing for the presence of SARS-CoV in the sewage indicated that no infectious SARS-CoV or live virus could be recovered in these two hospitals. The nucleic acid of SARS-CoV was found in the sewage before disinfection from both hospitals by semi-nested RT-PCR, while after disinfection of sewage by chlorine, SARS-CoV RNA could only be detected in the samples taken on 11th, 13th, and 15th June, 2003 from 309 Hospital.

Cell culture is a very demanding test. However, negative cell culture results or RT-PCR results could not exclude the presence of SARS-CoV. The detection of SARS-CoV from SARS patients could be negative for the following reasons [17]. Patients were not infected with SARS coronavirus, the illness was due to another infectious agent (virus, bacterium, fungus) or a non-infectious cause. The test results were incorrect. Current tests need to be further developed to improve their sensitivity. SARS-CoV was so susceptible to environments that it was inactivated quickly out of the body. SARS-CoV might have been inactivated or eliminated by immunoglobulins (antibody) from the recovered patients before excretion, or in the sewage. Palmer *et al*.[35], reported that human imm-unoglobulins were used to eliminate the enteroviruses in concentrated sewage when they evaluated the immunodeficiency virus (HIV) in sewage effluent by infectivity assay and RT-PCR.

Hong Kong Government explained the reasons of a cluster of SARS cases in Amoy Gardens and believed that there was a combination of factors, including the presence of an index patient who caused the first batch of infections, person-to-person spread, transmission via the sewage system, and environmental contamination[11,29]. This study demonstrated that SARS-CoV RNA could be excreted through the feces or/and urine samples of patients into sewage system.

In conclusion, this study demonstrated that there was SARS-CoV RNA in stool samples of patients with symptoms and in sewage of hospitals though there was no live SARS-CoV isolated from all samples. It provides evidence that the nucleic acid of SARS-CoV can be excreted through the stools of patients into sewage system, but cannot exclude the possibility of SARS-CoV transmitting through the digestive system. Much attention should be paid to the treatment of stools of patients and the sewage of hospitals receiving SARS patients.

ACKNOWLEDGEMENTS

The authors thank Dr. Da-Sheng Zhao, De-Xue Li, Jian-Zhong Sun, Zhong-Hou Huo and Yun-Bo Li from the P3 Laboratory Center for Microorganism Detection, China for supporting of this project; Dr. Fu-Yu Wang, Ying-Kai Li, Meng-Fu Zhu, Jian-Yong Su, Cheng-Yuan Gong, Wu-Chun Chao, Tai-Thi Gong, Bing-Yin Si and Bao-Zhong Guo for providing many reagents, helpful guidance and discussion; Drs. Hong-Wei Zhao, Xin-An Du, Zong-Ze Wang, Ling-Jia Qian, Qing-Yu Zhu, Xiao-Jun Zhang, Tao-Xing Shi, Fei Yu, Jian-Zhong Man, Fan-Rong Zeng, Bang-Rong Han, Yue Jiang, Zhu-Ge Xi, Zhi-Peng Ju and Hua-Shan Zhang for advice and organizing the experiments; the Center for Logistics, Xiao-Tang Shan Hospital for technical support and cooperation. We are also indebted to Professor Su-Qi Cheng for English revision.

REFERENCES

1 **Tsang KW**, Ho PL, Ooi GC, Yee WK, Wang T, Chan-Yeung M, Lam WK, Seto WH, Yam LY, Cheung TM, Wong PC, Lam B, Ip MS, Chan J, Yuen KY, Lai KN. A cluster of cases of Severe acute respiratory syndrome in Hong Kong. *N Engl J Med* 2003; **348**: 1977-1985

2 World Health Organization. SARS: breaking the chains of transmission. Available from:URL: http://www.who.int/features/2003/07/en

3 **Rota PA**, Oberste MS, Monroe SS, Nix WA, Campagnoli R, Icenogle JP, Penaranda S, Bankamp B, Maher K, Chen MH, Tong S, Tamin A, Lowe L, Frace M, DeRisi JL, Chen Q, Wang D, Erdman DD, Peret TC, Burns C, Ksiazek TG, Rollin PE, Sanchez A, Liffick S, Holloway B, Limor J, McCaustland K, Olsen-Rasmussen M, Fouchier R, Gunther S, Osterhaus AD, Drosten C, Pallansch MA, Anderson LJ, Bellini WJ. Characterization of a novel coronavirus associated with severe acute respiratory syndrome. *Science* 2003; **300**: 1394-1399

4 **Holmes KV**. SARS-associated coronavirus. *N Engl J Med* 2003; **348**: 1948-1951

5 **Fouchier RA**, Kuiken T, Schutten M, Van Amerongren G, Van Doorrum GJ, Van Den Hoogen BG, Peiris M, Lim W, Stohr K, Osterhaus AD. Aetiology: Koch's postulates fulfilled for SARS virus. *Nature* 2003; **423**: 240

6 **Ksiazek TG**, Erdman D, Goldsmith CS, Zaki SR, Peret T, Emery S, Tong S, Urbani C, Comer JA, Lim W, Rollin PE, Dowell SF, Ling AE, Humphrey CD, Shieh WJ, Guarner J, Paddock CD, Rota P, Fields B, DeRisi J, Yang JY, Cox N, Hughes JM, LeDuc JW, Bellini WJ, Anderson LJ. A Novel coronavirus associated with severe acute respiratory syndrome. *N Engl J Med* 2003; **348**: 1953-1966

7 **Marra MA**, Jones SJ, Astell CR, Holt RA, Brooks-Wilson A, Butterfield YS, Khattra J, Asano JK, Barber SA, Chan SY, Cloutier A, Coughlin SM, Freeman D, Girn N, Griffith OL, Leach SR, Mayo M, McDonald H, Montgomery SB, Pandoh PK, Petrescu AS, Robertson AG, Schein JE, Siddiqui A, Smailus DE, Stott JM, Yang GS, Plummer F, Andonov A, Artsob H, Bastien N, Bernard K, Booth TF, Bowness D, Czub M, Drebot M, Fernando L, Flick R, Garbutt M, Gray M, Grolla A, Jones S, Feldmann H, Meyers A, Kabani A, Li Y, Normand S, Stroher U, Tipples GA, Tyler S, Vogrig R, Ward D, Watson B, Brunham RC, Krajden M, Petric M, Skowronski DM, Upton C, Roper RL. The Genome sequence of the SARS-associated coronavirus. *Science* 2003; **300**: 1399-1404

8 **Qin ED**, Zhu QY, Peng WM, Jiang T, Fan BC, Chang GH, Yu M, Si BY, Liu BH, Deng YQ, Liu H, Zhang Y. Determination of the partial polymerase gene sequence of novel coronavirus isolated from lung tissue of SARS patients. *Junshi Yixue Kexueyuan Yuankan* 2003; **27**: 81-83

9 **Enserink M**, Vogel G. Infectious diseases. Hungry for details, scientists zoom in on SARS genomes. *Science* 2003; **300**: 715-716

10 **Lee N**, Hui D, Wu A, Chan P, Cameron P, Joynt GM, Ahuja A, Yung MY, Leung CB, To KF, Lui SF, Szeto CC, Chung S, Sung JJ. A major outbreak of severe acute respiratory syndrome in Hong Kong. *N Engl J Med* 2003; **348**: 1986-1994

11 World Health Organization. Amoy Gardens investigation findings make public. Available from:URL: http://www.who.int/csr/sars/en (17 April,2003)

12 **Cyranoski D**, Abbott A. Apartment complex holds clues to pandemic potential of SARS. *Nature* 2003; **423**: 3-4

13 **Poutanen SM**, Low DE, Henry B, Finkelstein S, Rose D, Gree K, Tellier R, Draker R, Adachi D, Ayers M, Chan AK, Skowronski DM, Salit I, Simor AE, Slutsky AS, Doyle PW, Krajden M, Petric M, Brunham RC, McGeer AJ. Identification of severe acute respiratory syndrome in canada. *N Engl J Med* 2003; **348**: 1995-2005

14 **Donnelly CA**, Ghani AC, Leung GM, Hedley AJ, Fraser C, Rileya S, Abu-Raddad LJ, Hob LM, Thach TQ, Chau P, Chan KP, Lam TH, Tsec LY, Tsang T, Liu SH, Kong JH, Lau EM, Ferguson NM, Anderson RM. Epidemiological determinants of spread of causal agent of severe acute respiratory syndrome in Hong Kong. *Lancet* 2003; **361**: 1761-1766

15 **Li JW**, Wang XW, Rui QY, Song N, Zhang FG, Ou YC, Chao FH. A new and simple method for concentration of enteric viruses from water. *J Virol Methods* 1998; **74**: 99-108

16 World Health Organization. Recommendations for laboratories testing by PCR for presence of SARS coronavirus–RNA. Available from: URL: http://www.who.int/csr/sars/coronarecommendation/en

17 World Health Organization. Severe Acute Respiratory Syndrome (SARS): Laboratory diagnostic tests. Available from: URL: http://www.who.int/csr/sars/diagnostictests/en

18 World Health Organization. Use of laboratory methods for SARS diagnosis. Available from: URL: http://www.who.int/csr/sars/labmethods/en

19 **Olivieri VP,** Snead MC, Kruse CW, Kawata K. Stability and effectiveness of chlorine disinfectants in water distribution systems. *Environ Health Perspect* 1986; **69**: 15-29

20 World Health Organization. PCR primers for SARS developed by WHO Network Laboratories. Available from: URL: http://www.who.int/csr/sars/primers/en

21 **Zoll GJ**, Melchers WJ, Kopecka H, Jambroes G, van der Poel HJ, Galama JM. General primer-mediated polymerase chain reaction for detection of enteroviruses: application for diagnostic routine and persistent infections. *J Clin Microbiol* 1992; **30**: 160-165

22 World Health Organization. Update 58 - First global consultation on SARS epidemiology, travel recommendations for Hebei Province (China), situation in Singapore. Available from: URL: http://www.who.int/csr/sars/archive/2003_05_17/en/

23 World Health Organization. SARS epidemiology to date. Available from: URL: http://www.who.int/csr/sars/epi2003_04_11/en/

24 **Peiris JS**, Lai ST, Poon LL, Guan Y, Yam LY, Lim W, Nichollsa J, Yee WK, Yan WW, Cheung MT, Cheng VC, Chan KH, Tsang DN, Yungd RW, Ng TK, Yuen KY. Coronavirus as a possible cause of severe acute respiratory syndrome. *Lancet* 2003; **361**: 1319-1325

25 World Health Organization. Update 31 - Coronavirus never before seen in humans is the cause of SARS. Available from: URL: http://www.who.int/csr/sars/archive/2003_04_16/en

26 **Drosten C**, Gunther S, Preiser W, van der Werf S, Brodt HR, Becker S, Rabenau H, Panning M, Kolesnikova L, Fouchier RAM, Berger A, Burguiere AM, Cinatl J, Eickmann M, Escriou N, Grywna K, Kramme S, Manuguerra JC, Müller S, Rickerts V, Sturmer M, Vieth S, Klenk HD, Osterhaus AD, Schmitz H, Doerr HW. Identification of a novel coronavirus in patients with severe acute respiratory syndrome. *N Engl J Med* 2003; **348**: 1967-1976

27 **Seto WH**, Tsang D, Yung RW, Ching TY, Ng TK, Ho M, Ho LM, Peiris JS. Effectiveness of precautions against droplets and contact in prevention of nosocomial transmission of severe acute respiratory syndrome (SARS). *Lancet* 2003; **361**: 1519-1520

28 World Health Organization. Update 32-Situation in China and Hong Kong, status of diagnostic tests. Available from: URL: http://www.who.int/csr/sarsarchive/2003_04_17/en

29 Amoy Gardens investigation findings make public. Available from: URL: http://www.info.gov/csr/sars/labmethods/en

30 **Wang CE**, Qin ED, Gan YH, Li YC, Wu XH, Cao JT, Yu M, Si BY, Yan G, Li JF, Zhu QY. Pathological observation on sucking mice and Vero E6 cells inoculated with SARS samples. *Jiefangjun Yixue Zazhi* 2003; **28**: 383-384

31 **Hong T**, Wang JW, Sun YL, Duan SM, Chen LB, Qu JG, Ni AP, Liang GD, Ren LL, Yang RQ, Guo L, Zhou WM, Chen J, Li DX, Wen XB, Xu H, Guo YJ, Dai SL, Bi SL, Dong XP, Ruan L. Chlamydia-like and coronavirus-like agents found in dead cases of atypical pneumonia by electron microscopy. *Zhonghua Yixue Zazhi* 2003; **83**: 632-636

32 **Riley S**, Fraser C, Donnelly CA, Ghani AC, Abu-Raddad LJ, Hedley AJ, Leung GM, Ho LM, Lam TH, Thach TQ, Chau P, Chan KP, Lo SV, Leung PY, Tsang T, Ho W, Lee KH, Lau EM, Ferguson NM, Anderson RM. Transmission dynamics of the etiological agent of SARS in Hong Kong: impact of public health interventions. *Science* 2003; **300**: 1961-1966

33 **Sobsey MD**, Jones BL. Concentration of Poliovirus from tap water using positively charged microporous filters. *Appl Environ Microbiol* 1979; **37**: 588-595

34 **Sobsey MD**, Glass JS. Poliovirus concentration from tap water with electropositive adsorbent filters. *Appl Environ Microbiol* 1980; **40**: 201-210

35 **Palmer CJ**, Lee MH, Bonilla GF, Javier BJ, Siwak EB, Tsai YL. Analysis of sewage effluent for human immunodeficiency virus (HIV) using infectivity assay and reverse transcriptase polymerase chain reaction. *Can J Microbiol* 1995; **41**: 809-815

Science Editor Zhang JZ and Wang XL **Language Editor** Elsevier HK

PO Box 2345, Beijing 100023, China
www.wjgnet.com
wjg@wjgnet.com

ELSEVIER

World J Gastroenterol 2005;11(28):4396-4399
World Journal of Gastroenterology ISSN 1007-9327

• *BRIEF REPORTS* •

Effects of iron manipulation on trace elements level in a model of colitis in rats

M Barollo, R D'Incà, M Scarpa, V Medici, R Cardin, M Bortolami, C Ruffolo, I Angriman, GC Sturniolo

M Barollo, R D'Incà, M Scarpa, V Medici, R Cardin, M Bortolami, C Ruffolo, I Angriman, GC Sturniolo, Department of Surgical and Gastroenterological Sciences, University of Padua, Italy
Supported by the MIUR 60% 2000
Correspondence to: GC Sturniolo, Divisione di Gastroenterologia, Via Giustiniani 2, Padova 35128, Italy. gc.sturniolo@unipd.it
Telephone: +39-49-821-8726 Fax: +39-49-876-0820
Received: 2004-05-25 Accepted: 2004-08-22

Abstract

AIM: Trace elements (TE) metabolism is altered in inflammatory bowel diseases. TE (zinc and copper) are constituents of antioxidant enzymes. Iron is involved in the pathogenesis of chronic inflammation. The aim was to evaluate zinc and copper status and the effects of iron manipulation in experimental colitis.

METHODS: Twenty-four male Sprague-Dawley rats were divided into four groups: standard diet, iron-deprived diet, iron-supplemented diet, and sham-treated controls. Macroscopic damage was scored. DNA adducts were measured in the colon. Liver and colonic concentration of TE were measured.

RESULTS: Macroscopic damage was reduced in iron-deprived groups and increased in iron-supplemented rats. Damage to the DNA was reduced in iron-deprived groups and increased in iron-supplemented groups. Liver and colonic iron concentrations were reduced in iron-deprived and increased in iron-supplemented rats. Liver zinc concentration was reduced after supplementation whereas colonic levels were similar in controls and treated rats. Liver copper concentration was reduced in all the colitic groups except in the iron-supplemented group whereas colonic concentration was increased in iron-deprived rats.

CONCLUSION: Iron deprivation diminishes the severity of DNBS colitis while supplementation worsens colitis. Zinc and copper status are modified by iron manipulation.

Key words: Trace elements; Colitis

Barollo M, D'Incà R, Scarpa M, Medici V, Cardin R, Bortolami M, Ruffolo C, Angriman I, Sturniolo GC. Effects of iron manipulation on trace elements level in a model of colitis in rats. *World J Gastroenterol* 2005; 11(28): 4396-4399
http://www.wjgnet.com/1007-9327/11/4396.asp

INTRODUCTION

Trace elements such as zinc and copper are essential for human health[1]. Zinc is required for cell membrane integrity, cell proliferation, and immune function. Several zinc-dependent antioxidant enzyme such as superoxide dismutase and metallothionein can neutralize free radicals production. Copper is necessary for the function of many enzymes involved in cell respiration and in cellular iron metabolism. Copper and zinc are both components of antioxidant enzymes such as superoxide dismutase. On the other hand, copper excess increases free radical levels thus enhancing the biological damage free radicals mediated[2].

In inflammatory conditions large amounts of reactive oxygen species are produced and this contributes with different mechanisms to damage tissue proteins, DNA chains and lipids[3]. Iron is a major peroxidative agent and animal studies demonstrated increased oxidative stress and intestinal inflammation after iron supplementation[4]. As previously reported by Kato *et al*., in Long Evans Cinammon rats, a model of copper liver toxicity, increased iron level is associated to copper excess and iron-deprived diet reduced mortality and fulminant hepatitis[5]. Trace elements homeostasis is altered both in human and animal models of inflammatory bowel diseases with possible implication for disease activity and carcinogenesis[6-8].

We previously demonstrated that dietary iron deprivation is effective in reducing DNA damage and improves the outcome of colitis. The aim of this study was to evaluate the effects of iron supplementation compared to deprivation on disease activity, on trace elements status and on colonic DNA oxidative damage in a model of experimental colitis.

MATERIALS AND METHODS

Experimental protocol

Twenty-four male Sprague-Dawley rats weighing 200 g were divided into four groups; one group was fed with standard diet containing 200 mg/kg of iron and given drinking water ad libitum. The second group was fed with an iron-controlled diet (50 mg/kg) and allowed to drink iron-free water for 5 wk and the third with an iron-supplemented diet (1 700 mg/kg) for 5 wk. The fourth group was fed with a standard diet (200 mg/kg of iron) and at the time of colitis induction was sham treated with saline.

Colitis was induced by the intrarectal instillation of 58 mg dinitro-benzene-sulfonic acid (DNBS) dissolved in 50% ethanol. The rats were anesthetized with ether and a silicone catheter was introduced intrarectally to 5 cm. Animals were kept in the Trendelemburg position for 10 min

to avoid the rapid evacuation of the enema. On d 8, 1 wk after colitis induction, the animals were weighed and anesthetized with intraperitoneal chloral hydrate (400 mg/kg) after which the abdomen was opened with a midline incision and exsanguination was performed. The colon was removed, opened along the antimesenteric border, rinsed with iron-free water and weighed.

The damage was assessed by scoring the number and extension of ulcers, adhesions, and thickness of the colonic wall according to Morris *et al*.[9].

Operators were unaware of the treatment of each group. Colonic tissue samples were obtained and processed for myeloperoxidase and 8-hydroxydeoxyguanosine (8-OHdG) determination and for measuring iron, zinc, and copper concentrations. Similarly liver samples were obtained for the determination of iron, zinc, and copper concentrations.

Iron, zinc, and copper determination

Trace elements concentrations were measured using atomic absorption spectrophotometry. Intestinal and liver tissues, obtained from rats, were dried at 42 ℃ for 24 h. The dried samples were weighed on an analytical balance, transferred into element-free tubes and then dissolved using 4.5 mL of 300 mL/L nitric acid solution. The tubes were incubated at 42 ℃ for 24 h. Iron, copper, and zinc standard solutions (0.05, 0.10, 0.20, 0.50, and 1 μg/mL) were prepared by dilution of concentrated stock solution (Titrisol, Merck Darmstadt, Germany) in deionized water. A Perkin Elmer 3100 atomic absorption spectrophotometer operated with an acetylene air mixture. A lean blue (oxidizing) flame was used with a cathode lamp current of 15 mA, a monochromator wavelength of 248.3 nm, and a slit width of 0.2 nm for Fe; lamp current of 25 mA, a wavelength of 213.9, and a slit width of 0.7 nm for Zn; lamp current of 15 mA, a wavelength of 324.8 nm, and a slit width of 0.7 mm for Cu.

Samples were aspirated directly and the concentration of the element of interest was determined from appropriate standard curves. Standard controls (Bovine liver, Trimital, Magenta, Milan, Italy) were prepared using the same extraction procedure used for sample preparation.

Results were expressed taking into account the dry weight and the dilution factor of the samples.

Myeloperoxidase

MPO activity was assessed following previously described methods[10]. Briefly colonic tissue samples were minced in 1 mL of 50 mmol/L potassium phosphate buffer (pH 6.0) containing 14 mmol/L hexadecyltrimethylammonium bromide (Fluka), homogenized and sonicated. The lysates have tol be frozen and thawed thrice, then centrifuged for 2 min in cold at 15 000 *g*. Aliquots of the supernatants were mixed with potassium phosphate buffer containing o-dianisidine-HCl (Sigma-Aldrich, St. Louis, MO, USA) and 0.0005% H_2O_2. MPO activity was expressed as units/*g* of wet tissue. The enzyme unit was defined as the conversion of 1 moL of H_2O_2 per minute at 25 ℃.

8-OHdG

Oxidative DNA damage was assessed following previously described methods[11]. Briefly colonic biopsy specimens were thawed, homogenized in a separation buffer and approximately 20 μg of purified DNA per sample was injected in the HPLC (Shimadzu, Kyoto, Japan). The 8-OHdG was detected using an electrochemical detector (ESA Coulochem II 5200A, Bedford, MA, USA). The levels of 8-OHdG were expressed as the number of 8-OHdG adducts per 10^5 dG bases. The coefficient of variation was <10%; 100 μg of DNA were required for the determination.

Statistical analysis

Data are expressed as mean +/- standard error. Statistical data were analyzed with Mann-Whitney *U* test for comparison of the four groups and Spearman's rank correlation test to evidence any relation between the evaluated parameters. *P* values less than 0.05 were considered significant.

RESULTS

Before colitis was induced body weight was similar in all groups of animals. The colon weight, a rough measure of edema and inflammation, was significantly increased in colitic animals with respect to controls ($P<0.05$), while iron-deprived rats had colonic weights similar to controls. The macroscopic damage score was significantly lower in the group receiving iron-deprived diet than in the colitis groups. MPO activity was significantly increased in iron-supplemented rats. Iron deprivation was associated with significantly higher MPO levels than controls.

Clinical and biochemical aspects of colitis in all rat groups are summarized in Table 1.

Dietary iron deprivation significantly decreased hepatic and colonic iron concentrations. Iron supplementation increases the iron concentration in liver and colon compared to healthy controls. Iron concentration was increased in the liver and colon of rats with colitis (Fe, 200 mg/kg) whereas supplementation did not affect hepatic iron concentration (Figure 1). There was a significant correlation between hepatic and colonic iron concentrations ($R = 0.567$, $P<0.002$).

Inflammation significantly increased hepatic zinc concentration but neither iron deprivation or supplementation modified zinc concentration in the liver. Although no

Table 1 Clinical and biochemical aspects of colitis

	Controls	Standard diet (Fe, 200 mg/kg)	Iron-supplemented diet (1 700 mg/kg)	Iron-deprived diet (45 mg/kg)
Colon wet weight (g)	2.2±0.2	4.0±0.9[a]	3.8±0.8	2.1±0.4[c]
Macroscopic damage score	0±0	8.75±2.5	7.4±1.4	3.6±1.1[c]
Myeloperoxidase U/mg	3.5±0.6	19.4±5.2	61.4±7.9[b]	24.5±7.1

[a]$P<0.05$ *vs* controls; [b]$P<0.01$ *vs* standard diet; [c]$P<0.05$ *vs* standard diet.

significant change was revealed in any of the treatments the more the colon was damaged the lower was the colonic zinc concentration (R = -0.460, P = 0.02).

Hepatic copper concentration was reduced in all colitic groups with respect to controls except in the iron-supplemented group. On the other hand, copper colonic concentration was increased in the iron-deprived diet group irrespective of treatment and inflammatory status (Table 2). Hepatic copper concentration correlated with colonic copper (R = 0.39, P<0.04).

Colonic DNA adducts were significantly reduced in rats fed with an iron-deprived diet for 5 wk (Figure 2). Colonic DNA adducts significantly correlated with iron colonic concentration (R = 0.44, P<0.02).

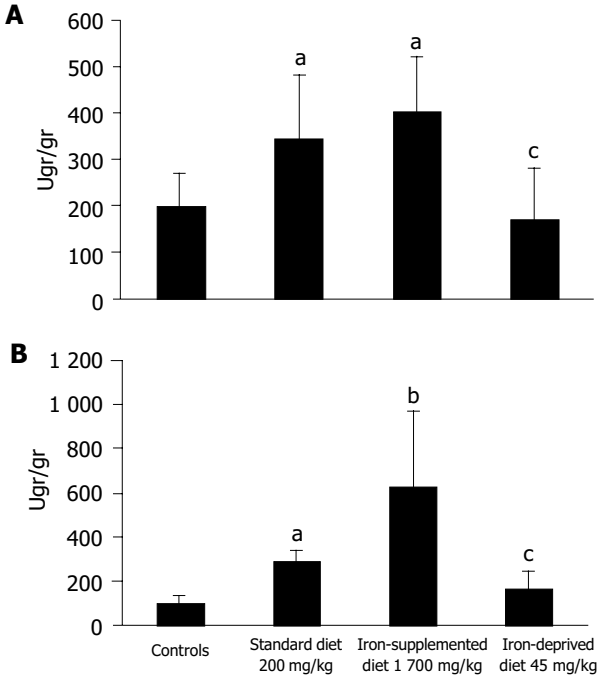

Figure 1 Liver (**A**) and colonic (**B**) iron concentrations. [a]P<0.05, [b]P<0.01 *vs* controls; [c]P<0.05 *vs* standard diet.

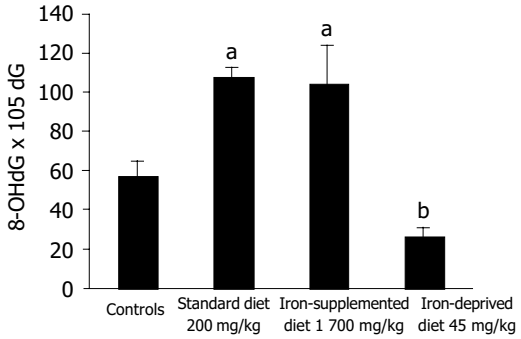

Figure 2 Colonic DNA adducts. [a]P<0.05 *vs* controls; [b]P<0.01 *vs* standard diet.

DISCUSSION

Iron has a major role in chronic inflammatory diseases. Lin *et al*., demonstrated *in vitro* that iron chelation effectively blocks NF-kappa B activation and upregulates TNF-α and IL-6 genes in a model of cholestatic liver injury, suggesting a basic role for iron in the activation of the inflammatory process[12]. In patients with Crohn's disease and anemia, treatment with oral ferrous fumarate decreased cysteine and glutathione peroxidase with consequent altered plasma antioxidant status[13]. Moreover, oxidative stress is increased *in vitro* cell lines from patients with ulcerative colitis treated with iron[14].

Table 2 Hepatic and colonic zinc and copper concentrations in controls and colitis

	Zinc μg/g		Copper μg/g	
	Hepatic	Colonic	Hepatic	Colonic
Controls	99.8±2.1	133.4±6.1	54.4±1.6	18.6±0.9
Standard diet	140.2±6.2[a]	113.9±5.8	20.8±0.7[d]	18.6±0.9
Iron-supplemented diet	92.6±5[b]	132.2±10.2	44.2±3.9	21±2.1
Iron-deprived diet	117.2±4.4	101.6±5.1	19.7±0.8[d]	36.2±5.9[c]

[a]P<0.05 *vs* controls; [b]P<0.01 *vs* standard diet; [c]P<0.05 *vs* controls and standard diet; [d]P<0.001 *vs* controls.

Recent evidence showed that iron dietary deprivation is a reasonable approach to many diseases with a free radical component[15]. It is known that Deferoxamine, an iron chelating agent, effectively reduces mucosal oxidant activity by decreasing the luminol-amplified chemiluminescence *in vitro* by 44% in active ulcerative colitis biopsies[16]. This effect was attributed more to iron chelation than to a direct antioxidant activity.

We observed that iron deprivation was associated with less macroscopic colonic mucosal damage while iron supplementation worsened colitis. Iron and inflammation seem to have a synergic action since MPO levels were greatly increased in the iron-supplemented group. Our observations suggest that iron manipulation may modulate inflammatory damage.

The results of this study confirm that dietary iron deprivation reduces inflammation and oxidative DNA damage in the rat model of DNBS-induced colitis while iron supplementation worsens colitis as we previously reported (in press)[17]. These results further reinforce our previous findings on the role of iron deprivation in DNBS colitis. Carrier *et al*., recently reported that oral iron supplementation may aggravate inflammation and oxidative stress in dextran sulfate sodium-induced colitis[18]. Oxidative damage, expressed by DNA adducts level, was decreased in iron-deprived rats. According to Seril *et al*., reactive oxygen species, produced in abundance in the presence of iron during inflammation, can directly mediate DNA damage thus leading to alterations, which cause loss of suppressor genes and gain of oncogenes function[19].

Trace elements are altered during inflammation and their status is critical for normal cell and enzymes function. Many enzymes, involved in DNA repair mechanisms, are zinc-dependent thus trace elements alteration could contribute to DNA damage[20]. Several human and animal studies have demonstrated altered trace elements status during inflammation. Al Awadi *et al*., reported a significant reduction of colonic zinc level in experimental colitis while copper and manganese remained unaltered[8]. Zinc and copper serum levels were altered in well-nourished patients

with ulcerative colitis and correlated with hematological parameters of disease activity suggesting their role in inflammation[21]. We previously demonstrated that zinc supplementation regulates tight junction permeability in experimental colitis with possible implication on mucosal healing[22]. Several studies have pointed out that zinc, copper, and iron may affect the progression of colonic tumors in experimental model of preneoplastic lesions[23]. Moreover, Ames has recently reported that zinc and other micronutrient deficiencies mimic the effect of radiation on DNA chain with strong implication for carcinogenesis[24].

Hepatic zinc concentration is significantly reduced during iron dietary deprivation. Colonic zinc concentration is similar to controls in all treated groups and it is independent from iron metabolism. The inverse correlation with macroscopic score and colonic weight may suggest the relevant effect of zinc on mucosa healing. In fact as recently reported by Kruidenier superoxide dismutase Zn/Cu dependent is decreased in colonic mucosa of IBD patients with active inflammation[25].

Colonic copper is increased during iron dietary deprivation. Iron supplementation does not seem to affect copper absorption as recently demonstrated in ileostomy subjects[26]. Colonic copper alterations seem therefore a consequence of local inflammation. On the other hand our data showed that inflammation decreased copper concentration in the liver except in the presence of iron supplementation. This is in agreement with the results reported in Long Evans Cinammon rats, in which an iron deprived diet reduced mortality and fulminant hepatitis[5].

In conclusion, we pointed out that iron manipulation affects the severity of experimental colitis. Iron manipulation results in changes of zinc and copper status which may, after a chemical insult, alter the natural course of intestinal inflammation and may have important implications for the development of antioxidant treatment of IBD patients.

REFERENCES

1 **Bogden JD,** Klevay LM. Clinical nutrition of the essential trace elements and minerals. The guide for health professionals. 2000 Humana Press Inc.
2 **Olivares M,** Uauy R. Copper as an essential nutrient. *Am J Clin Nutr* 1996; **63**: 791S-796S
3 **Emerit J,** Beaumont C, Trivin F. Iron metabolism, free radicals, and oxidative injury. *Biomed Pharmacother* 2001; **55**: 333-339
4 **Reifen R,** Matas Z, Zeidel L, Berkovitch Z, Bujanover Y. Iron supplementation may aggravate inflammatory status of colitis in a rat model. *Dig Dis Sci* 2000; **45**: 394-397
5 **Kato J,** Kobune M, Kohgo Y, Sugawara N, Hisai H, Nakamura T, Sakamaki S, Sawada N, Niitsu Y. Hepatic iron deprivation prevents spontaneous development of fulminant hepatitis and liver cancer in Long-Evans Cinnamon rats. *J Clin Invest* 1996; **98**: 923-929
6 **Ringstad J,** Kildebo S, Thomassen Y. Serum selenium, copper, and zinc concentrations in Crohn's disease and ulcerative colitis. *Scand J Gastoenterol* 1993; **28**: 605-608
7 **Brignola C,** Belloli C, De Simone G, Evangelisti A, Parente R, Mancini R, Iannone P, Mocheggiani E, Fabris N, Morini MC. Zinc supplementation restores plasma concentrations and thymulin in patients with Crohn's disease. *Aliment Pharmacol Ther* 1993; **7**: 275-280
8 **Al-Awadi FM,** Khan I, Dashti HM, Srikumar TS. Colitis-induced changes in the level of trace elements in rat colon and other tissues. *Ann Nutr Metab* 1998; **42**: 304-310
9 **Morris GP,** Beck PL, Herridge MS, Depew WT, Szewczuk MR, Wallace JL. Hapten-induced model of chronic inflammation and ulceration in the rat colon. *Gastroenterology* 1989; **98**: 795-803
10 **Krawisz JE**, Sharon P, Stenson WF. Quantitative assay for acute intestinal inflammation based on myeloperoxidase activity. Assessment of inflammation in rat and hamster models. *Gastroenterology* 1984; **87**: 1344-1350
11 **Helbock HJ,** Beckman KB, Shigenaga MK, Walter PB, Woodall AA, Yeo HC, Ames BN. DNA oxidation matters: the HPLC-electrochemical detection assay of 8-oxo-deoxyguanosine and 8-oxo-guanosine. *Proc Natl Acad Sci USA* 1998; **95**: 288-293
12 **Lin M,** Rippe RA, Niemela O, Brittenham G, Tsukamoto H. Role of iron in NF-kappa B activation and cytokine gene expression by rat hepatic macrophages. *Am J Physiol* 1997; **272**: G1355-1364
13 **Erichsen K,** Hausken T, Ulvik RJ, Svardal A, Berstad A, Berge RK. Ferrous fumarate deterioreted plasma antioxidant status in patients with Crohn disease. *Scand J Gastroenterol* 2003; **38**: 543-548
14 **Millar AD,** Rampton DS, Blake DR. Effects of iron and iron chelation *in vitro* on mucosal oxidant activity in ulcerative colitis. *Aliment Pharmacol Ther* 2000; **14**: 1163-1168
15 **Polla BS.** Therapy by taking away: the case of iron. *Biochem Pharmacol* 1999; **57**: 1345-1349
16 **Carotenuto P,** Pontesilli O, Cambier JC, Hayward AR. Desferoxamine blocks IL 2 receptor expression on human T lymphocytes. *J Immunol* 1986; **136**: 2342-2347
17 **Barollo M,** D'Incà R, Scarpa M, Medici V, Cardin R, Fries W, Angriman I, Sturniolo GC. Effects of iron deprivation or chelation on DNA damage in experimental colitis. *Int J Colorectal Dis* 2004; **19**: 461-466
18 **Carrier J,** Aghdassi E, Platt I, Mullen J, Allard JP. Effect of oral iron supplementation on oxidative stress and colonic inflammation in rats with induced colitis. *Aliment Pharmacol Ther* 2001; **15**: 1989-1999
19 **Seril DN,** Liao J, Yang GY, Yang CS. Oxidative stress and ulcerative colitis –associated carcinogenesis: studies in humans and animal models. *Carcinogenesis* 2003; **24**: 353-362
20 **Leon O,** Roth M. Zinc fingers: DNA binding and protein-protein interactions. *Biol Res* 2000; **33**: 21-30
21 **Dalekos GN,** Ringstad J, Savaidis I, Seferiadis KI, Tsianos EV. Zinc, copper and immunological markers in the circulation of well nourished patients with ulcerative colitis. *Eur j Gastroenterol Hepatol* 1998; **10**: 331-337
22 **Sturniolo GC,** Fries W, Mazzon E, Di Leo V, Barollo M, D'Incà R. Effect of zinc supplementation on intestinal permeabilility in experimental colitis. *J Lab Clin Med* 2002; **39**: 311-315
23 **Davis CD,** Feng Y. Dietary copper, manganese and iron affect the formation of aberrant crypts in colon of rats administered 3,2-dimethyl-4-aminobiphenyl. *J Nutr* 1999; **129**: 1060-1067
24 **Ames BN.** DNA damage from micronutrient deficiencies is likely to be a major cause of cancer. *Mutation Research* 2001; **475**: 7-20
25 **Kruidenier L,** Kuiper I, van Duijn W, Marklund SL, van Hogezand RA, Lamers CB, Verspaget HW. Differential mucosal expression of three superoxide dismutase isoforms in inflammatory bowel disease. *J Pathol* 2003; **201**: 7-16
26 **Troost FJ,** Brummer RJ, Dainty JR, Hoogewerff JA, Bull VJ, Saris WH. Iron supplements inhibit zinc but not copper absorption *in vivo* in ileostomy subjects. *Am J Clin Nutr* 2003; **78**: 1018-1023

Science Editor Zhu LH **Language Editor** Elsevier HK

PO Box 2345, Beijing 100023, China
www.wjgnet.com
wjg@wjgnet.com

ELSEVIER

World J Gastroenterol 2005;11(28):4400-4403
World Journal of Gastroenterology ISSN 1007-9327

• *BRIEF REPORTS* •

Relationship between β-catenin expression and epithelial cell proliferation in gastric mucosa with intestinal metaplasia

Adriana Romiti, Angelo Zullo, Francesco Borrini, Ida Sarcina, Cesare Hassan, Simon Winn, Silverio Tomao, Aldo Vecchione, Sergio Morini, Pietro Mingazzini

Adriana Romiti, Ida Sarcina, Aldo Vecchione, Medical Oncology, "Sant'Andrea" Hospital, Rome, Italy
Angelo Zullo, Cesare Hassan, Simon Winn, Sergio Morini, Gastroenterology and Digestive Endoscopy, "Nuovo Regina Margherita" Hospital, Rome, Italy
Francesco Borrini, Pietro Mingazzini, Department of Experimental Medicine and Pathology, "La Sapienza" University, Rome, Italy
Silverio Tomao, Oncology, IRCCS "Regina Elena", Rome, Italy
Co-first-authors: Adriana Romiti and Angelo Zullo
Co-correspondence: Aldo Vecchione
Correspondence to: Dr. Adriana Romiti, Ospedale "S. Andrea", Oncologia Medica, Via di Grottarossa 1035, Rome 00189, Italy. sanoncol@libero.it
Telephone: +39-6-80345338 Fax: +39-6-80345001
Received: 2004-03-23 Accepted: 2005-01-05

Abstract

AIM: To investigate β-catenin expression in patients with intestinal metaplasia, and to look for a possible relationship between β-catenin expression and either epithelial proliferation values or *Helicobacter pylori* (*H pylori*) infection.

METHODS: Twenty patients with complete type intestinal metaplasia were studied. β-Catenin expression and epithelial cell proliferation in antral mucosa were assessed using an immunohistochemical analysis. *H pylori* infection was detected by histology and a rapid urease test.

RESULTS: Reduced β-catenin expression on the surface of metaplastic cells was detected in 13 (65%) out of 20 patients. Moreover, in eight (40%) patients intranuclear expression of β-catenin was found. When patients were analyzed according to *H pylori* infection, the prevalence of both β-catenin reduction at the cell surface and its intranuclear localization did not significantly differ between infected and uninfected patients. Cell proliferation was higher in patients with intranuclear β-catenin expression as compared to the remaining patients, although the difference failed to reach the statistical significance (36±8.9 *vs* 27.2±11.4, $P = 0.06$). On the contrary, a similar cell proliferation value was observed between patients with reduced expression of β-catenin on cell surface and those with a normal expression (28.1±11.8 *vs* 26.1±8.8, $P = 0.7$). *H pylori* infection significantly increased cell proliferation (33.3±10.2% *vs* 24.6±7.4%, respectively, $P = 0.04$).

CONCLUSION: Both cell surface reduction and intranuclear accumulation of β-catenin were detected in intestinal metaplasia. The intranuclear localization of β-catenin increases cell proliferation. *H pylori* infection does not seem to play a direct role in β-catenin alterations, whilst it significantly increases cell proliferation.

Key words: β-Catenin; Intestinal metaplasia; Proliferation; *Helicobacter pylori*

Romiti A, Zullo A, Borrini F, Sarcina I, Hassan C, Winn S, Tomao S, Vecchione A, Morini S, Mingazzini P. Relationship between β-catenin expression and epithelial cell proliferation in gastric mucosa with intestinal metaplasia. *World J Gastroenterol* 2005; 11(28): 4400-4403
http://www.wjgnet.com/1007-9327/11/4400.asp

INTRODUCTION

Catenins are a family of transmembrane proteins, which play a pivotal role in epithelial intercellular adhesion[1]. Moreover, β-catenin participates in the regulation of cell proliferation, being a critical component of the surface-to-nucleus WNT signal transduction pathways[2,3]. Alterations of β-catenin expression have been shown to be involved in cancer development[4]. Indeed, such alterations have been detected in gastric cancer, showing a correlation with tumor type, degree of differentiation, and poor survival of patients[5-9]. On the other hand, scanty data are available regarding β-catenin expression in precancerous conditions. Although alterations of some adhesion molecules have been detected in patients with intestinal metaplasia[10], no significant remarks emerged from the studies regarding β-catenin expression in these patients[10,11]. However, such studies were based on gastrectomy specimens of patients with gastric cancer and, therefore, only an advanced step of the carcinogenic process was evaluated.

Gastric carcinogenesis is a multistep process consisting of a cascade of alterations starting with chronic active gastritis and progressing to atrophy, metaplasia, and dysplasia[12]. In particular, intestinal metaplasia is widely recognized as being the most prevalent precursor of intestinal type gastric carcinoma[13]. Among environmental factors involved in carcinogenesis of the stomach, *Helicobacter pylori* (*H pylori*) infection appears to play an important role. Indeed, epidemiological studies have clearly demonstrated a significant association between this infection and gastric cancer development. Moreover, several changes involved in gastric carcinogenesis such as epithelial cell hyperproliferation,

free oxygen radical formation, ascorbic acid reduction, genetic alterations have been described in the gastric mucosa of infected patients[14-16].

The present study was designed in order to assess β-catenin expression in patients with intestinal metaplasia but with neither dysplasia nor gastric cancer, and to look for a possible relationship between β-catenin expression and either epithelial proliferation index of gastric mucosa or *H pylori* infection status.

MATERIALS AND METHODS

Patients

Patients with dyspeptic symptoms consecutively referred for upper endoscopy with presence of histology of intestinal metaplasia in the antrum and without concomitant evidence of either dysplasia in the stomach or neoplastic lesions in the upper gastrointestinal tract were selected. Patients were enrolled irrespectively of *H pylori* status. Patients who received proton pump inhibitors, H_2-receptor antagonists, antibiotics or NSAIDs in the 4 wk preceding the study as well as those previously treated for *H pylori* infection were excluded from the study. Patients with either liver impairment or kidney failure were also excluded.

Endoscopic procedure

After overnight fasting, all patients underwent upper endoscopy and three biopsies were taken from the antrum and three from the gastric body. Two biopsies from the antrum and two from the gastric body were used for histological assessment. Biopsy specimens of the antrum were also used for immunohistochemical analysis. The remaining two biopsies (one each from the antrum and gastric body) were used to carry out a rapid urease test (CP-test, Yamanouchi, Milan, Italy). *H pylori* infection was considered to be present when both the histological assessment on Giemsa staining revealed the presence of bacteria and rapid urease test was positive, as suggested in current guidelines[17].

Immunohistochemical analysis

For β-catenin and proliferation assessment, immunohistochemistry was carried out by the avidin-biotin-peroxidase method. Briefly the sections were deparaffinized in xylene and rehydrated through a graded alcohol series to distillated water. Antigen retrieval was performed by immersing the slides in 10 mol/L citrate buffer (pH 6.0) and heating them in a microwave for 3 cycles, 5 min each, at 750 W. Endogenous peroxidase activity and non-specific bindings were blocked by incubation with 3% hydrogen peroxide and nonimmune serum, respectively. Sections were then incubated with mAbs against β-catenin (Clone 14, 1:500 dilution; Transduction Laboratories, Lexington, KY, USA) and mAbs against Ki-67 (Clone MIB-1, 1:100 dilution YLEM, Italy) for 1 h at room temperature. Immunoreactivity was revealed with the chromogen DAB test and the sections were counterstained with Mayer hematoxylin solution for 7 min. Negative control sections were prepared by substituting primary antibody with buffered saline.

A semiquantitative approach was used for scoring the β-catenin expression according to the method previously described by Mingchao[10]. Briefly, the staining pattern of the intestinal metaplastic areas was compared with that of the adjacent normal gastric mucosa. Expression of β-catenin in metaplastic areas was considered 'normal' when both the intensity and the frequency of the cell membrane stains were equivalent to those found on the bordering nonmetaplastic gastric mucosa, 'reduced' when the staining was less than the adjacent mucosa, and 'negative' in the absence of staining. In addition, when β-catenin stained clearly in the nuclei of more than 10% of gastric epithelial cells, expression was judged to be positive for nuclear staining.

A quantitative approach was used instead for scoring the Ki67 expression. The number of cells was determined by counting the positively-stained nuclei on 10-20 randomly selected fields at 400×.

All immunostaining evaluations were performed blindly and by two independent observers. All sections for which the two observers disagreed were re-evaluated and, after opportune discussion, a final agreement was achieved.

Statistical analysis

Data between patient subgroups were compared using the Student's *t*-test for unpaired data, and the Fisher's exact test with Yate's correction for small numbers. A P value less than 0.05 was considered statistically significant.

RESULTS

Overall, 20 consecutive patients (9 male and 11 female; mean age: 60.8±8.4 years) were enrolled. At endoscopy, no macroscopic alterations of the gastric mucosa were detected, whilst two patients showed erosions in the duodenal bulb. *H pylori* infection was present in 13 (65%) patients and absent at both rapid urease test and histology in the seven remaining patients. Intestinal metaplasia was graded as complete type in all cases.

β-catenin expression in gastric mucosa

No case of completely negative β-catenin immunostaining was observed. A reduced expression of β-catenin on the surface of metaplastic cells as compared to adjacent normal glands was detected in 13 (65%) out of 20 patients. Moreover, in eight (40%) patients an intranuclear expression of β-catenin was detected. Among this group, six (75%) patients also showed reduced β-catenin expression. When patients were analyzed according to *H pylori* infection, β-catenin expression was decreased in 8 out of 13 infected patients as well as in 5 out of 7 uninfected cases ($P = 0.5$). Similarly, the prevalence of intranuclear localization of β-catenin expression did not significantly differ between infected and uninfected patients (4/13 *vs* 4/7, respectively; $P = 0.2$).

Cell proliferation in gastric mucosa

The mean value of Ki67 labeling index proved to be distinctly higher in eight patients with intranuclear β-catenin expression as compared to the remaining 13 patients, although the difference failed to reach statistical significance (36±8.9 *vs* 27.2±11.4, $P = 0.06$). On the contrary, by

excluding those patients with intranuclear localization of β-catenin, a similar cell proliferation value was observed between the seven patients with reduced membranous expression of β-catenin and the five patients with normal expression (28.1±11.8 *vs* 26.1±8.8, $P = 0.7$). As far the role of *H pylori* infection is concerned, data found that patients with infection had a significantly increased cell proliferation value than that of uninfected patients (33.3±10.2% *vs* 24.6±7.4%, respectively, $P = 0.04$).

DISCUSSION

The integrity of the function of adhesion molecules, such as E-cadherin and α, β, γ-catenins, allows the maintenance of normal interactions between cells necessary during embryogenesis, cell growth, and differentiation[1-3,18]. Loss of intercellular adhesiveness plays a role in the early steps of neoplastic transformation, and it is implicated in invasive growth and metastasization[5-9,19]. β-catenin participates in the adhesion process by binding the cytoplasmic domain of E-cadherin and it has been involved in the surface-to-nucleus WNT signal transduction pathways. Its translocation into the nucleus may contribute to accelerated cell proliferation[3]. β-catenin mutations in exon 3, interfering with the GSK-3β phosphorylation domain and leading to intranuclear accumulation of the protein, have been reported in intestinal gastric carcinoma as well as in colorectal cancer[20-23]. Moreover reduced β-catenin expression was recorded both in intestinal type of gastric cancer[5,6,24] and in intestinal metaplasia surrounding cancer lesions[25], although data are controversial[10,11,24]. In order to determine whether β-catenin alterations could be detected early in gastric carcinogenesis, the present study focused on β-catenin expression in intestinal metaplasia not associated with gastric cancer. Unlike previous study[26], in our series a reduction of β-catenin on the epithelial surface was observed in more than half of the patients. Intriguingly, a nuclear accumulation of β-catenin expression in 40% of patients with intestinal metaplasia was also found, and it was associated with reduced immunostaining at the intercellular boundaries in 75% of these cases. A previous study reported a nuclear accumulation of β-catenin in about 10% of 401 gastric carcinomas, all but one exhibiting reduced membranous staining[24]. Similarly, an inverse correlation between decreased membranous and increased nuclear staining of β-catenin was also observed in colorectal cancer[27,28]. Interestingly, we observed that patients with intranuclear β-catenin expression showed higher values of cell proliferation in the gastric mucosa as compared to those without it. This is a noteworthy remark in keeping with previously reported studies focused on the role of nuclear localization of β-catenin[3]. Indeed, in an experimental model, colonocyte hyperproliferation was associated with immunohistochemical alterations in subcellular distribution of β-catenin and with accumulation of the protein in the nuclear compartment[29]. This finding, however, has been not observed in gastric cancer[23,24]. Therefore, it could be hypothesized that the nuclear β-catenin expression may be linked to the early stage of carcinogenesis, as seen in colorectal polyps[30]. Conversely, loss of membranous expression could allow regenerating cells to dedifferentiate and lose cell-cell cohesiveness, properties that would facilitate the process of epithelial regeneration, as reported for E-cadherin expression during the reparative process of peptic ulcer[31]. Similarly, in endometrial glandular cells in the mid-to-late proliferative phase, nuclear accumulation of β-catenin was described, suggesting that it could play a physiological role in the rapid turnover of the cell cycle without gene mutation[32].

As far the role of *H pylori* infection is concerned, we failed to observe a significant difference in β-catenin expression between infected and uninfected patients, suggesting that this infection is not directly implicated in this phenomenon. On the contrary, in agreement with the results of several studies[14,16], a significant increase in the epithelial cell proliferation index was detected in *H pylori*-positive patients as compared to uninfected patients.

In conclusion, in the present immunohistochemical study, we described alterations in β-catenin expression in the gastric mucosa with intestinal metaplasia not associated to other more advanced histological lesions. β-catenin alterations consisted of both a weakness of membrane staining and in an intranuclear accumulation of the protein. Moreover, we observed a distinct increase in cell proliferation in those patients with intranuclear localization of β-catenin expression. *H pylori* infection does not seem to play a role in β-catenin alterations, whilst it significantly increases cell proliferation in gastric mucosa with intestinal metaplasia.

REFERENCES

1 **Gumbiner BM.** Cell adhesion: the molecular basis of tissue architecture and morphogenesis. *Cell* 1996; **84**: 345-357
2 **Behrens J,** von Kries JP, Kuhl M, Bruhn L, Wedlich D, Grosschedl R, Birchmejer W. Functional interaction of beta-catenin with the trascription factor. *Nature* 1996; **382**: 638-642
3 **Barker N,** Clevers H. Beta-catenins WNT signaling and cancer. *Bioessays* 2000; **22**: 961-965
4 **Hugh TJ,** Dillon SA, O'Dowd G, Getty B, Pignatelli M, Poston GJ, Kinsella AR. Beta-catenin expression in primary and metastatic colorectal carcinoma. *Int J Cancer* 1999; **82**: 504-511
5 **Shun CT,** Wu MS, Lin MT, Chang MC, Lin JT, Chuang SM. Immunohistochemical evaluation of cadherin and catenin expression in early gastric carcinomas: correlation with clinicopathologic characteristics and *Helicobacter pylori* infection. *Oncology* 2001; **60**: 339-345
6 **Joo YE,** Rew JS, Choi SK, Bom HS, Park CS, Kim SJ. Expression of E-cadherin and catenins in early gastric cancer. *J Clin Gastroenterol* 2002; **35**: 35-42
7 **Ougolkov A,** Yamashita K, Bilim V, Takahashi Y, Mai M, Minamoto T. Abnormal expression of E-cadherin, β-catenin, and c-erbB-2 in advanced gastric cancer: its association with liver metastasis. *Int J Colorectal Dis* 2003; **18**: 160-166
8 **Utsunomiya T,** Doki Y, Takemoto H, Shiozaki H, Yano M, Inoue M, Yasuda T, Fuhwara Y, Monden M. Clinical significance of disordered beta-catenin expression pattern in human gastric cancers. *Gastric Cancer* 2000; **3**: 193-201
9 **Karatzas G,** Karayiannakis AJ, Syrigos KN, Chatzigianni E, Papanikolaou S, Simatos G, Papanikolaou D, Bogris S. Expression pattern of the E-cadherin-catenin cell-cell adhesion complex in gastric cancer. *Hepatogastroenterology* 2000; **47**: 1465-1469
10 **Ma MC,** Devereux TR, Stockton P, Sun K, Sills RC, Clayton N, Portier M, Flake G. Loss of E-cadherin expression in gastric intestinal metaplasia and later stage p53 altered expression in gastric carcinogenesis. *Exp Toxic Pathol* 2001; **53**: 237-246
11 **Jawhari A,** Jordan S, Poole S, Browne P, Pignatelli M, Far-

thing JG. Abnormal immunoreactivity of the E-cadherin-catenin complex in gastric carinoma: relationship with patient survival. *Gastroenterology* 1997; **112**: 48-54

12 **Correa P.** Human gastric carcinogenesis: a multistep and multifactorial process - First American cancer society award lecture on cancer epidemiology and prevention. *Cancer Res* 1992; **52**: 6735-6740

13 **Leung WK,** Sung JJ. Review article: intestinal metaplasia and gastric carcinogenesis. *Aliment Pharmacol Ther* 2002; **16**: 1209-1216

14 **Ierardi E,** Francavilla A, Balzano T, Traversa A, Principi M, Monno RA, Amoruso A, Ingrosso M, Pisani A, Panella C. Effect of *Helicobacter pylori* eradication on gastric epithelial proliferation. Relationship with ras oncogene p21 expression. *Ital J Gastroenterol Hepatol* 1997; **29**: 214-219

15 **Zullo A,** Rinaldi V, Hassan C, Diana F, Winn S, Castagna G, Attili AF. Ascorbic acid and intestinal metaplasia in the stomach: a prospective, randomised study. *Aliment Pharmacol Ther* 2000; **14**: 1303-1309

16 **Zullo A,** Romiti A, Rinaldi V, Vecchione A, Hassan C, Winn S, Tomao S, Attili AF. Gastric epithelial cell proliferation in patients with liver cirrhosis. *Dig Dis Sci* 2001; **46**: 550-554

17 **Caselli M,** Parente F, Palli D, Covacci A, Alvisi V, Gasbarrini G, Bianchi Porro G. Cervia Working Group Report: guidelines on the diagnosis and treatment of *Helicobacter pylori* infection. *Digest Liver Dis* 2001; **33**: 7-80

18 **Frenette PS,** Wagner DD. Adhesion molecules. *N Engl J Med* 1996; **334**: 1526-1529

19 **Guilford P.** E-cadherin downregulation in cancer: fuel on the fire? *Mol Med Today* 1999; **5**: 172-177

20 **Park WS,** Oh RR, Park JY, Lee SH, Shin MS, Kim YS, Kim SY, Lee HK, Kim PJ, Oh ST, Yoo NJ, Lee JY. Frequent somatic mutations of the beta-catenin gene in intestinal-type gastric cancer. *Cancer Res* 1999; **59**: 4257-4260

21 **Iwao K,** Nakamori S, Kameyama M, Imoaka S, Kinoshita M, Fukui T, Ishiguro S, Nakamura Y, Miyoshi Y. Activation of the β-catenin gene by interstitial deletions involving exon 3 in primary colorectal carcinomas without adenomatous polyposis coli mutations. *Cancer Res* 1998; **58**: 1021-1026

22 **Miyaki M,** Iijima T, Kimura J, Yasuno M, Mori T, Hayashi Y, Koike M, Shitara N, Iwama T, Kuroki T. Frequent mutation of beta-catenin and APC genes in primary colorectal tumors from patients with hereditary nonpolyposis colorectal cancer. *Cancer Res* 1999; **59**: 4506-4509

23 **Miyazawa K,** Iwaya K, Kuroda M, Harada M, Serizawa H, Koyanagi Y, Sato Y, Mizokami Y, Matsuoka T, Mukai K. Nuclear accumulation of beta-catenin in intestinal-type gastric carcinoma: correlation with early tumor invasion. *Virchows Arch* 2000; **437**: 508-513

24 **Grabsch H,** Takeno S, Nogushi T, Hommel G, Gabbert HE, Mueller W. Different patterns of β-catenin expression in gastric carcinomas: relationship with clinicopathological parameters and prognostic outcome. *Histopathology* 2001; **39**: 141-149

25 **Chan AO,** Wong BC, Lan HY, Loke SL, Chan WK, Hui WM, Yuen Ng I, Hou l, Wong WM, Yuen MF, Luk JM, Lam SK. Deregulation of E-cadherin-catenin complex in precancerous lesions of gastric adenocarcinoma. *J Gastroenterol Hepatol* 2003; **18**: 534-539

26 **Gulmann C,** Grace A, Leader M, Butler D, Patchett S, Kay E. Adenomatous polyposis coli gene, beta-catenin, and E-cadherin expression in proximal and distal gastric cancers precursor lesions: an immunohistochemical study using tissue microarray. *Appl Immunohistochem Mol Morphol* 2003; **11**: 230-237

27 **Inomata M,** Ochiai A, Akimoto S, Hirobashi S. Alteration of β-catenin expression in colonic epithelial cells of familial adenomatous polyposis patients. *Cancer Res* 1996; **56**: 2213-2217

28 **Hao X,** Tomlinson I, Ilyas M, Palazzo JP, Talbot IC. Reciprocity between membranous and nuclear expression of β-catenin in colorectal tumors. *Virchows Arch* 1997; **431**: 167-172

29 **Sellin JH,** Umar S, Xiao J, Morris AP. Increased b-catenin expression and nuclear translocation accompany cellular hyperproliferation *in vitro*. *Cancer Res* 2001; **61**: 2899-2906

30 **Barker N,** Huls G, Korinek V, Clevers H. Restricted high level expression of Tcf-4 protein in intestinal and mammary gland epithelium. *Am J Pathol* 1999; **154**: 29-35

31 **Hanby AM,** Chinery R, Poulsom R, Playford RJ, Pignatelli M. Downregulation of E-cadherin in the reparative ephithelium of the human gastrointestinal tract. *Am J Pathol* 1996; **148**: 723-729

32 **Nei H,** Saito T, Yamasaki H, Mizumoto H, Ito E, Kudo R. Nuclear localization of beta-catenin in normal and carcinogenic endometrium. *Mol Carcinog* 1999; **25**: 207-218

Science Editor Guo SY **Language Editor** Elsevier HK

PO Box 2345, Beijing 100023, China
www.wjgnet.com
wjg@wjgnet.com

ELSEVIER

World J Gastroenterol 2005;11(28):4404-4408
World Journal of Gastroenterology ISSN 1007-9327

• *BRIEF REPORTS* •

Expression of c-erbB-2 and glutathione S-transferase-pi in hepatocellular carcinoma and its adjacent tissue

Zhao-Shan Niu, Mei Wang

Zhao-Shan Niu, Department of Pathology, Medical College of Qingdao University, Qingdao 266021, Shandong Province, China
Mei Wang, Institute of Education, the University of Reading, Britain RG6 1HY, Reading, United Kingdorn
Supported by the Scientific Research Foundation of Shandong Provincial Education Committee (J94, K26)
Correspondence to: Zhao-Shan Niu, Department of Pathology, Medical College of Qingdao University, 38 Dengzhou Road, Qingdao 266021, Shandong Province, China. niumiao1993@hotmail.com
Telephone: +86-532-3812410
Received: 2004-09-22 Accepted: 2004-11-19

Abstract

AIM: To investigate the possible role of c-erbB-2 and glutathione S-transferase (GST-Pi) in primary hepatocellular carcinogenesis and the relationship between liver hyperplastic nodule (LHN), liver cirrhosis (LC), and hepatocellular carcinoma (HCC).

METHODS: The expression of c-erbB-2 and GST-Pi was detected immunohistochemically in 41 tissue specimens of HCC and 77 specimens of its adjacent tissue.

RESULTS: The positive expression of c-erbB-2 in LHN (28.6%) was significantly higher than that in LC (0%) ($P = 0.032<0.05$), but no significant difference was seen between HCC and LHN or LC ($P>0.05$, $\chi^2 = 0.002, 3.447$). The positive expression of GST-Pi in HCC (89.6%) or LHN (71.1%) was significantly higher than that in LC (22.9%, $P<0.001$, $\chi^2 = 49.91, 16.96$). There was a significant difference between HCC and LHN ($P<0.05$, $\chi^2 = 6.353$).

CONCLUSION: The c-erbB-2 expression is an early event in the pathogenesis of HCC. GST-Pi may be a marker enzyme for immunohistochemical detection of human HCC and its preneoplastic lesions. LHN seems to be a preneoplastic lesion related to hepatocarcinogenesis.

Key words: Liver neoplasm; Hyperplastic nodule; C-erbB-2 gene; GST-pi gene; Immunohistochemistry

Niu ZS, Wang M. Expression of c-erbB-2 and glutathione S-transferase-pi in hepatocellular carcinoma and its adjacent tissue. *World J Gastroenterol* 2005; 11(28): 4404-4408
http://www.wjgnet.com/1007-9327/11/4404.asp

INTRODUCTION

Primary hepatocellular carcinoma (HCC) is one of the most common malignant tumors in Asia, and the incidence and mortality of HCC show a tendency to rise year by year. Therefore, the detection of preneoplastic lesions of HCC is crucial for the analysis of carcinogenic processes and developing strategies for prevention and treatment. For many years, liver hyperplastic nodule (LHN) has been considered as a preneoplastic lesion. Our previous studies have also confirmed that LHN is closely related to human HCC.

In the present study, the immunohistochemical LSAB method was used to detect the expression of c-erbB-2 oncogene and glutathione S-transferase-pi (GST-pi) in HCC and pericarcinomatous tissues, in order to investigate the possible roles of these genes in the HCC carcinogenesis, and to find out the relationship between LHN, liver cirrhosis (LC), and HCC.

MATERIALS AND METHODS

Materials

HCC specimens from 100 patients were selected during surgical resections or biopsies performed at the Affiliated Hospital of Medical College of Qingdao University, China. Of these patients, 76 were males and 24 females with an average age of 50.4 years. None of the patients received chemo- or radiotherapy before resection. We randomly selected 41 and 77 cases of HCC to detect the expression of c-erbB-2 and GST-pi, respectively. The same specimens from 16 cases were detected for both c-erbB-2 and GST-pi, which were too few to be analyzed in terms of the correlation between them in the present study. Forty-one specimens for detecting c-erbB-2 oncogene contained 18 pericarcinomatous tissues, including 14 LHN, 17 LC. Seventy-seven specimens for detecting GST-pi contained 40 pericarcinomatous tissues, including 38 LHN, and 35 LC.

Methods

All specimens were routinely processed, alcohol-fixed and paraffin-embedded. Serial paraffin sections of 4 μm thickness were cut and used for hematoxylin and eosin and immunohistochemical staining. Immunohistochemical LSAB method was used to detect c-erbB-2 and GST-pi. Anti-c-erbB-2 multiple clonal antibody, anti-GST-pi multiple clonal antibody and LSAB kits were purchased from Dako Co. Before staining, the sections were microwave heated in 0.05 mol citric acid solution for antigen retrieval. In each staining run, a known c-erbB-2 or GST-pi positive section was added as positive control, PBS was used as substitutes

of the first antibodies for negative control.

Analysis of immunohistochemical staining

When brown granules were found on cell membrane of liver cells and cancer cells, c-erbB-2 was identified positive. When only cytoplasm was stained brown, c-erbB-2 was identified negative. The c-erbB-2 expression was graded semi-quantitatively according to the intensity and the percentage of positivity into negative (-): no positive cells or a weak staining of c-erbB-2 with positive cells<5%; positive (+): c-erbB-2 expression was relatively stronger with the positive cells>5%. For GST-pi, cells with brown granules in cytoplasm were regarded as positive. The criteria of the evaluation of GST-pi expression in this study were as follows. The positive number was semiquantitatively evaluated by counting that in 5-10 randomly chosen medium power (×100 magnification), and the three grades for GST-pi were considered as negative (-): no positive cells; positive (+): the positive reaction being brown and the positive cells <30%; strong positive (++): the positive reaction being brown and the positive cells>30% according to the intensity and extent of GST-pi staining.

Statistical analysis

Results were analyzed by χ^2-test and direct probability calculation. $P<0.05$ was considered statistically significant.

RESULTS

Expression of c-erbB-2 oncogene in HCC and its adjacent tissue

The positive staining for c-erbB-2 in cancer cells was exclusively located in cell membrane stained brown, the expression of c-erbB-2 was observed in both cell membrane and cytoplasm in one of four cases of LHN expressing c-erbB-2 (Figure 1A). The c-erbB-2 positive rate was significantly higher in LHN (28.6%) than that in LC (0%, *P* value 0.032, direct probability calculation, $P<0.05$), but no significant difference was seen between HCC (Figure 1B) and LHN or LC (χ^2 values 0.002, 3.447, $P>0.05$, Table 1).

Table 1 Expression of c-erbB-2 oncogene in HCC and its adjacent tissue

Histological type	Case	Expression of c-erbB-2 oncogene		Positive rate (%)
		-	+	
HCC	41	31	10	24.4[a]
LHN	14	10	4	28.6[a]
LC	17	17	0	0

[a]$P<0.05$ *vs* LC.

Expression of GST-pi in HCC and its adjacent tissue

The positive staining for GST-pi appeared as brown granules, which was predominantly located in the cytoplasm, and the staining of the nuclei was seen in part of the cancer cells. There was strong staining of GST-pi in bile duct epithelial cells. A weak staining of GST-pi was observed in LC with a positive rate of 22.9% (8/35). GST-pi expression was markedly stronger in HCC or LHN (Figure 1C). The rates of positivity were 89.6% (69/77) and 71.1% (27/38), respectively, and significantly higher than that in LC (χ^2 values 49.91, 16.96, $P<0.001$). There was also a significant difference between HCC (Figure 1D) and LHN (χ^2 value 6.353, $P<0.05$, Table 2).

DISCUSSION

The c-erbB-2/neu is a transforming proto-oncogene encoding

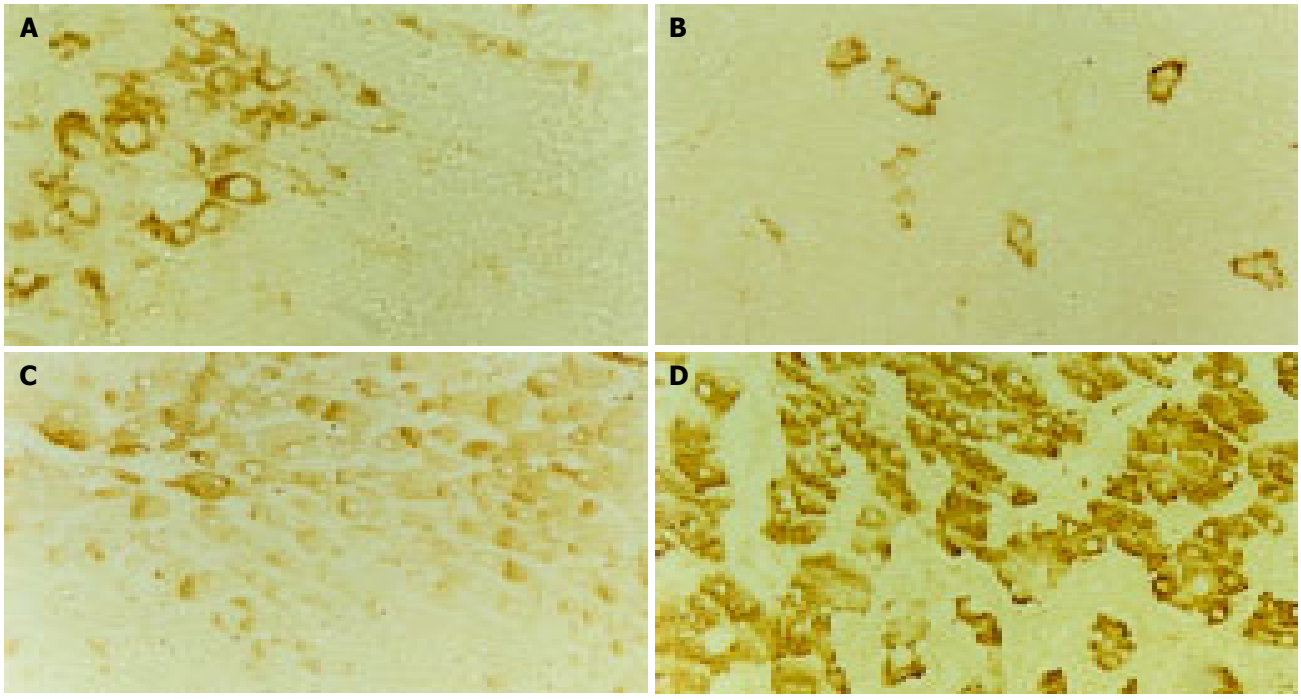

Figure 1 Positive expression of c-erbB-2 and GST-pi in LHN (**A,C**) and HCC (**B,D**), LSAB ×200.

Table 2 Expression of GST-pi in HCC and its adjacent tissue

Histological type	Case	Expression of GST-pi			Positive rate (%)
		- (%)	+ (%)	++ (%)	
HCC	77	8 (10.4)	55 (71.4)	14 (18.2)	89.6
LHN	38	11 (28.9)	25 (65.8)	2 (5.3)	71.1[a]
LC	35	27 (77.1)	8 (22.9)	0	22.9[b]

[a]$P<0.05$, $\chi^2 = 6.353$ *vs* HCC; [b]$P<0.001$, $\chi^2 = 16.96, 49.91$ *vs* LHN and HCC.

a transmembrane glycoprotein of 185 ku (P185) with tyrosine kinase activity and extensive sequence homology to epidermal growth factor receptor. The c-erbB-2 is in a state of inactivation under normal condition, and is involved in regulating cell growth and proliferation[1]. Having been affected by some endogenous or extraneous carcinogens, its structure or expression is dysregulated, thus being activated, and c-erbB-2 becomes oncogene with tumor transformation activity. In human malignancies, the activation of c-erbB-2 is most frequently caused by gene amplification, there is extremely high concordance between copy number of gene amplification and protein overexpression[2,3]. The c-erbB-2 is frequently overexpressed in different tumors in humans, and the activation of c-erbB-2 appears to be an early event in tumorigenesis for some cancers[4-7]. However, there seems to be conflicting reports concerning the role of c-erbB-2 oncogene in carcinogenesis of HCC. Some studies reported that c-erbB-2 does not play a role in tumorigenesis of HCC[7], whereas others reported that the overexpression of c-erbB-2 is found in the middle stage of hepatocarcinogenesis, and might only have promoting effects during the development of this lesion[8]. In the present study, c-erbB-2 overexpression was observed in 24.4% ($n = 41$) of HCC tissue specimens and 22.2% ($n = 18$) of its adjacent tissue specimens, suggesting that the overexpression of c-erbB-2 oncogene plays an initial role in hepatocarcinogeneis, and is an early molecule change in the carcinogenesis of HCC. In addition, the expression of c-erbB-2 did not decrease in the transition from pericarcinomatous tissues into HCC in the present study, indicating that c-erbB-2 expression also occurs later in the process of hepatocarcinogeneis and maintains the transformed hepatocyte phenotype. Apparently, c-erbB-2 expression can contribute to the initiation and progression of HCC.

Many studies have demonstrated that c-erbB-2 gene product not only contributes to the development and maintenance of malignant phenotype, but also plays a pivotal role in transformation and tumorigenesis[4,5,9], because 3T3 cells or immortalized cells transfected with c-erbB-2 oncogene show a highly transformed and tumorigenic phenotype[10,11]. It can be inferred from these studies that those cells overexpressing c-erbB-2 oncogene are either cancerous or have malignant phenotype. In the present study, all four cases overexpressing c-erbB-2 oncogene in pericarcinomatous tissues were LHN, thus, the positive expression rate of c-erbB-2 in LHN was 28.6% ($n = 14$), and similar to that of HCC, suggesting that those cells overexpressing c-erbB-2 oncogene in LHN have at least acquired the malignant phenotype, which may reflect the alterations in different biologic state of LHN. Some studies reported that the increased oncogene expression brings cells into a state of active proliferation that results in an increased frequency of mutation[12]. Therefore, it is reasonable to postulate that the overexpression of c-erbB-2 oncogene may make LHN transform malignantly, and parts of LHN are actually in the preneoplastic state or might be cancerous. In contrast to LHN, the expression of c-erbB-2 oncogene is negative in LC, implying that there is no activation of c-erbB-2 in LC, i.e., it is impossible in this situation for malignant transformation. There is also no mutation of p53 in LC, consequently, LC does not necessarily link with hepatocarcinogenesis. Our findings further confirm the notion that it is not LC but LHN, is a preneoplastic lesion for the occurrence of HCC in humans.

GSTs play an important role in protecting cells against cytotoxic and carcinogenic agents. GST-pi is an acid GST, isolated and purified from human term placenta, which possesses catalytic and ligand-binding properties, and is regarded as a new marker enzyme for tumors. Some studies reported that GST-pi or GST-pi mRNA is hardly detectable in normal liver, but markedly increases in preneoplastic hepatic lesions such as hyperplastic nodules and in HCC by immunohistochemical staining or *in situ* hybridization[13-16], suggesting that GST-pi is a sensitive marker enzyme for preneoplastic lesions and neoplastic cells, not only at the protein level but also at the mRNA level, throughout the hepatocarcinogenesis in rat liver. In addition, other studies reported that single cells immunohistochemically positive for GST-pi induced in the rat liver carcinogenesis by chemical carcinogens are precursor-initiated cells of preneoplastic foci, GST-pi content in the single cells is higher than that in preneoplastic foci, and GST-pi is a more sensitive marker for detection of HCC than γ-GT or AFP[17-20]. Therefore, it has been generally considered that GST-pi is the most accurate marker enzyme for detection of the very early "initiated cells" in chemically induced hepatocarcinogenesis in rats. It is known that human GST-pi has highly immunological cross-reaction with rat GST-pi, and the alteration of GST-pi precedes that of cell morphology. Studies in human HCC are not as advanced as in rats but have revealed close similarities. To investigate the relationship between GST-pi and HCC and its preneoplastic lesions, accordingly, may offer an important enzyme for the early diagnosis of HCC.

The expression of GST-pi might increase abnormally in the course of the carcinogenesis of many tumors, and it has been associated with preneoplastic and neoplastic changes[21,22]. Recently, many researches demonstrated that loss of transcription activity of GST-pi gene promoter in human malignancies appears to be the result of CpG island DNA methylation, and this phenomenon is most frequent in breast and renal carcinomas, and might contribute to the carcinogenetic process in these two carcinomas, while other tumor types show GST-pi promoter methylation only rarely or not at all[21-23]. However, some studies reported that GST-pi promoter hypermethylation changes occur frequently in human HCC, suggesting that somatic GST-pi inactivation via CpG island hypermethylation might contribute to the pathogenesis of HCC[24-27]. When cells display complete GST-pi hypermethylation in the CpG island, and they fail to express GST-pi mRNA and the corresponding protein

product, which is different from our findings. GST-pi expression was present in 89.6% of HCC and in 71.1% of LHN in the present study. There are several possibilities for this (1) There is rare or no GST-pi promoter hypermethylation in pathogenesis of HCC. (2) There is GST-pi promoter hypermethylation, but loss of GST-pi promoter hypermethylation in HCC may be due to the emergence of tumor subclones unmethylated at the GST-pi promoter during HCC transformation. Such subclones may gain additional genetic lesions that rendered GST-pi inactivation no longer necessary for neoplastic cell survival. (3) There is GST-pi promoter hypermethylation, but it is not responsible for GST-pi expression, it is the p53 gene mutation existing in LHN and HCC that activates GST-pi. p53 mutation is frequently observed in Asian HCC, but it is not a common event in Western HCC, thus, it is not difficult to interpret the reason why GST-pi is overexpressed in some studies whereas GST-pi is absent in other studies though GST-pi promoter hypermethylation may exist in pathogenesis of HCC. (4) GST-pi promoter hypermethylation is not a frequent event in pathogenesis of HCC, it may relate to the different etiologies of HCC in different geographical areas.

Markedly increased GST-pi content has been found in HCC investigated, indicating that HCC cells have characteristics of some fetal cells, as GST-pi content in fetal cells is noticeably higher than that in adult cells. It can be preliminarily inferred that GST-pi has relevance to detoxification of liver in pathogenesis of HCC. Meanwhile, the high expression of GST-pi in HCC might be associated with the resistance to anticancer drugs and might protect the tumor cells themselves against the cytotoxic effects of free radicals, as described in other tumors[28-31]. It is well-known that GST-pi can detoxify not only electrophiles derived from xenobiotics, but also endogenous electrophiles usually with the consequence of free radical damage. These data indicate that the overexpression of GST-pi may impart a proliferative advantage in HCC cells due to induction of resistance to several different cytotoxic mechanisms. In the present study, the positive rate of GST-pi in HCC was higher than that in pericarcinomatous tissues, and was significantly higher in LHN than in LC, showing that GST-pi is activated during initiation stage or much earlier stage of cell transformation induced by chemical carcinogens, and may be acquired in increased amounts during malignant progression. Therefore, the data obtained in the present study suggest that GST-pi may be an effective marker enzyme for HCC and its preneoplastic lesions.

As an important enzyme of detoxification, GST-pi protects cells against the influence of carcinogenic materials. However, GST-pi is taken as a double-edged sword in tumorigenesis, namely, GST-pi protects all cells expressing it, including normal cells, cells with malignant phenotype, and tumor cells as well. Many cells in LHN are in a state of active proliferation, and have acquired the malignant phenotype, thus GST-pi evolves specifically to protect these proliferating cells, and these cells inevitably proliferate rapidly, presenting a clonal expansion. Our findings suggest that cells overexpressing GST-pi in LHN may relate to the carcinogenesis of LHN, and some cells in LHN are altered hepatocytes, which should be treated as preneoplastic cells of HCC. In contrast to LHN, the cells in LC appear to represent quiescent phenotypes unlikely to progress into HCC.

REFERENCES

1 **Zhou BP,** Hung MC. Dysregulation of cellular signaling by HER2/neu in breast cancer. *Semin Oncol* 2003; **30** (5 Suppl 16): 38-48
2 **Bankfalvi A.** HER-2 diagnostics. *Magy Onkol* 2002; **46**: 11-15
3 **Nathanson DR,** Culliford AT 4th, Shia J, Chen B, D' Alessio M, Zeng ZS, Nash GM, Gerald W, Barany F, Paty PB. HER 2/neu expression and gene amplification in colon cancer. *Int J Cancer* 2003; **105**: 796-802
4 **Lazar H**, Baltzer A, Gimmi C, Marti A, Jaggi R. Over-expression of erbB-2/neu is paralleled by inhibition of mouse-mammary-epithelial-cell differentiation and developmental apoptosis. *Int J Cancer* 2000; **85**: 578-583
5 **Kumar R**, Yarmand-Baagheri R. The role of HER2 in angiogenesis. *Semin Oncol* 2001; **28** (5 Suppl 16): 27-32
6 **Zhang L,** bewick M, Lafrenie RM. EGFR and ErbB2 differentially regulate Raf-1 translocation and activation. *Lab Invest* 2002; **82**: 71-78
7 **Vlasoff DM,** Baschinsky DY, De Young BR, Morrison CD, Nuovo GJ, Frankel WL. C-erbB2 (Her2/neu) is neither overexpressed nor amplified in hepatic neoplasms. *Appl Immunohistochem Mol Morphol* 2002; **10**: 237-241
8 **Shi G,** Sun C, Han X, Meng X, Wang M, Gu M. Expression of rasp21, C-myc, C-erbB-2, and AFP in 2-FAA induced experimental hepatocarcinogenesis. *Zhonghua Ganzangbing Zazhi* 2001; **9**: 98-99
9 **Neve RM,** Lane HA, Hynes NE. The role of overexpressed HER2 in transformation. *Ann Oncol* 2001; **12**(Suppl 1): S9-13
10 **Yu D,** Hamada J, Zhang H, Nicolson GL, Hung MC. Mechanisms of c-erbB-2/neu oncogene-induced metastasis and repression of metastatic properties by adenovirus 5 E1A gene products. *Oncogene* 1992; **7**: 2263-2270
11 **Kusakari T,** Kariya M, Mandai M, Tsuruta Y, Hamid AA, Fukuhara K, Nanbu K, Takakura K, Fujii S. C-erbB-2 or mutant Ha-ras induced malignant transformation of immortalized human ovarian surface epithelial cells *in vitro*. *Br J Cancer* 2003; **89**: 2293-2298
12 **Lian ZR.** HBV status and expression of ets-2, IGF-II, C-myc and N-ras in human hepatocellular carcinoma and adjacent nontumorous tissues-a comparative study. *Zhonghua Zhongliu Zazhi* 1991; **13**: 5-8
13 **Sawaki M,** Hattori A, Tsuzuki N, Sugawara N, Enomoto K, Sawada N, Mori M. Chronic liver injury promotes hepatocarcinogenesis of the LEC rat. *Carcinogenesis* 1998; **19**: 331-335
14 **Nishikawa T,** Wanibuchi H, Ogawa M, Kinoshita A, Morimura A, Hiroi T, Funae Y, Kishida H, Nakae D, Fukushima S. Promoting effectsof monomethylarsonic acid, dimethylarsinic acid and trimethylarsine oxide on induction of rat liver preneoplastic glutathione S-transferase placental form positive foci: a possible reactive oxygen species mechanism. *Int J Cancer* 2002; **100**: 136-139
15 **Shukla Y,** Arora A. Enhancing effects of mustard oil on preneoplastic hepatic foci development in Wistar rats. *Hum Exp Toxicol* 2003; **22**: 51-55
16 **Imai T,** Masui T, Ichinose M, Nakanishi H, Yanai T, Masegi T, Muramatsu M, Tatematsu M. Reduction of glutathione S-transferase P-form mRNA expression in remodeling nodules in rat liver revealed by in situ hybridization. *Carcinogenesis* 1997; **18**: 545-551
17 **Satoh K,** Itoh K, Yamamoto M, Tanaka M, Hayakari M, Ookawa K, Yamazaki T, Sato T, Tsuchida S, Hatayama I. Nrf2 transactivator-independent GSTP1-1 expression in "GSTP1-1 positive"single cells inducible in female mouse liver by DEN: a preneoplastic character of possible initiated cells. *Carcinogenesis* 2002; **23**: 457-462
18 **Satoh K,** Hatayama I. Anomalous elevation of glutathione

S-transferase P-form (GST-P) in the elementary process of epigenetic initiation of chemical hepatocarcinogenesis in rats. *Carcinogenesis* 2002; **23**: 1193-1198

19 **Tatematsu M,** Mera Y, Inoue T, Satoh K, Sato K, Ito N. Stable phenotypic expression of glutathione S-transferase placental type and unstable phenotypic expression of gamma-glutamyltransferase in rat liver preneoplastic and neoplastic lesions. *Carcinogenesis* 1988; **9**: 215-220

20 **Yusof YA,** Yan KL, Hussain SN. Immunohistochemical expression of pi class glutathione S-transferase and alpha-fetoprotein in hepatocellular carcinoma and chronic liver disease. *Anal Quant Cytol Histol* 2003; **25**: 332-328

21 **Esteller M,** Corn PG, Urena JM, Gabrielson E, Baylin SB, Herman JG. Inactivation of glutathione S-transferase P1 gene by promoter hypermethylation in human neoplasia. *Cancer Res* 1998; **58**: 4515-4518

22 **Miyanishi K,** Takayama T, Ohi M, Hayashi T, Nobuoka A, Nakajima T, Takimoto R, Kogawa K, Kato J, Sakamaki S, Niitsu Y. Glutathione S-transferase-pi overexpression is closely associated with K-ras mutation during human colon carcinogenesis. *Gastroenterology* 2001; **121**: 865-874

23 **Esteller M.** CpG island hypermethylation and tumor suppressor gene: a booming present, a brighter future. *Oncogene* 2002; **21**: 5427-5440

24 **Zhong S,** Tang MW, Yeo W, Liu C, Lo YM, Johnson PJ. Silencing of GSTP1 gene by CpG island DNA hypermethylation in HBV-associated hepatocellular carcinomas. *Clin Cancer Res* 2002; **8**: 1087-1092

25 **Bakker J,** Lin X, Nelson WG. Methyl-CpG binding domain protein 2 represses transcription from hypermethylated pi-class glutathione S-transferase gene promoters in hepatocellular carcinoma cells. *J Biol Chem* 2002; **277**: 22573-22580

26 **Yang B,** Guo M, Herman JG, Clark DP. Aberrant promoter methylation profiles of suppressor genes in hepatocellular carcinoma. *Am J Pathol* 2003; **163**: 1101-1107

27 **Lee S,** Lee HJ, Kim JH, Lee HS, Jang JJ, Kang GH. Aberrant CpG island hypermethylation along multistep hepatocarcinogenesis. *Am J Pathol* 2003; **163**: 1371-1378

28 **Ruscoe JE,** Rosario LA, Wang T, Gate L, Arifoglu P, Wolf CR, Henderson CJ, Ronai Z, Tew KD. Pharmacologic or genetic manipulation of glutathione S-transferase P1-1(GSTpi) influences cell proliferation pathways. *J Pharmacol Exp Ther* 2001; **298**: 339-345

29 **Goto S,** Kamada K, Soh Y, Ihara Y, Kondo T. Significance of nuclear glutathione S-transferase pi in resistance to anti-cancer drugs. *Jpn J Cancer Res* 2002; **93**: 1047-1056

30 **Hara T,** Ishii T, Fujishiro M, Masuda M, Ito T, Nakajima J, Inoue T, Matsuse T. Glutathione S-transferase P1 has protective effects on cell viability against camptothecin. *Cancer Lett* 2004; **203**: 199-207

31 **Chandra RK,** Bentz BG, Haines GK 3rd, Robinson AM, Radosevich JA. Expression of glutathione S-transferase pi in benign mucosa, Barrett's metaplasia, and adenocarcinoma of the esophagus. *Head Neck* 2002; **24**: 575-581

Science Editor Wang XL and Guo SY **Language Editor** Elsevier HK

PO Box 2345, Beijing 100023, China
www.wjgnet.com
wjg@wjgnet.com

ELSEVIER

World J Gastroenterol 2005;11(28):4409-4413
World Journal of Gastroenterology ISSN 1007-9327

• *BRIEF REPORTS* •

Association of polymorphisms of IL and CD14 genes with acute severe pancreatitis and septic shock

Dian-Liang Zhang, Hong-Mei Zheng, Bao-Jun Yu, Zhi-Wei Jiang, Jie-Shou Li

Dian-Liang Zhang, Hong-Mei Zheng, Department of General Surgery, Affiliated Hospital, Qingdao University Medial College, Qingdao 266003, Shandong Province, China
Bao-Jun Yu, Zhi-Wei Jiang, Jie-Shou Li, Research Institute of General Surgery, Jinling Hospital, Nanjing 210093, Jiangsu Province, China
Supported by the Affiliated Hospital of Qindao University Medial College Doctoral Foundation, No. 2003-6
Correspondence to: Dian-Liang Zhang, Department of General Surgery, Affiliated Hospital, Qingdao University Medial College, Qingdao 266003, Shandong Province, China. phdzdl@yahoo.com
Telephone: +86-532-2911324 Fax: +86-532-2911111
Received: 2004-08-26 Accepted: 2005-01-05

Abstract

AIM: To investigate IL-1β+3 594 in the 5th intron, IL-10-1 082 and CD14-159 polymorphisms in patients with acute pancreatitis (AP) and septic shock.

METHODS: The study included 215 patients (109 with acute severe pancreatitis (SAP), 106 with acute mild pancreatitis (MAP)) and 116 healthy volunteers. Genomic DNA was prepared from peripheral blood leukocytes. Genotypes and allele frequencies were determined in patients and healthy controls using restriction fragment length polymorphism analysis of PCR products.

RESULTS: The frequencies of IL-1β+3 594T, IL-10-1082G and CD14-159T allele were similar in patients with mild or severe pancreatitis and in controls. Within SAP patients, no significant differences were found in the allele distribution examined when etiology was studied again. Patients with septic shock showed a significantly higher prevalence of IL-10-1082G allele than those without shock ($\chi^2 = 5.921$, $P = 0.015$).

CONCLUSION: IL-10-1082G plays an important role in the susceptibility of SAP patients to septic shock. Genetic factors are not important in determination of disease severity or susceptibility to AP.

Key words: Gene polymorphism; Septic shock; Pancreatitis; Genes

Zhang DL, Zheng HM, Yu BJ, Jiang ZW, Li JS. Association of polymorphisms of IL and CD14 genes with acute severe pancreatitis and septic shock. *World J Gastroenterol* 2005; 11(28): 4409-4413
http://www.wjgnet.com/1007-9327/11/4409.asp

INTRODUCTION

Acute pancreatitis (AP) is a common disease that normally runs a benign course in the majority of patients. However, in up to 20% of individuals the disease is severe and may have a mortality close to 20%[1]. Two weeks after the onset of acute severe pancreatitis (SAP), sepsis-related complications resulting from systemic inflammatory response syndrome (SIRS) or infection of pancreatic necrosis or bacteria translocation often occur. There is evidence that the production of tumor necrosis factor-α, interleukin (IL)-1β, IL-6, and IL-8 may play a vital role in AP. In addition, anti-inflammatory response, especially IL-10, plays an important role in determining prognosis of AP[2]. Several methods for estimating the complications are widely used in clinic, such as Atlanta classification, Acute Physiology and Chronic Health Evaluation II, Imrie and Ranson scores, Balthazar computed tomographic scoring system, and C-reactive protein. However, these methods have little value in predicting which patients will develop pancreatic infection and SAP-associated septic shock.

It has been hypothesized that there is a correlation between polymorphisms in TNF-α, IL-1β, and IL-10 genes and differential production of respective cytokines[3]. Some of these polymorphisms affect clinical outcome in inflammatory diseases including AP[3-5]. IL-10 is an anti-inflammatory cytokine and plays an important role in downregulating cell-mediated inflammatory responses. Human IL-10 gene is located on chromosome 1 and has been mapped to the junction between 1q31 and 1q32. Three single base pair (bp) substitutions in IL-10 gene promoter at positions -1 082G-A, -819T-C, and -592A-C from the transcriptional start site have been identified. At position -1 082 bp from the transcriptional start site, the presence of G is associated with higher and A with lower production of IL-10 by PBMC cultures[6]. In contrast, IL-1β is a potent proinflammatory cytokine released by macrophages in systemic inflammatory responses. It not only has important biologic effect but also regulates inflammatory reaction and immune response by promoting expression of other cytokines, such as IL-6 and IL-12. IL-1β gene located on chromosome 2 is 7 kb, and has seven exons and six introns. A polymorphism is found at position +3 954 located in the 5th intron of IL-1β gene with a T substitution of C. *In vitro* study demonstrated that IL-1β+3 594 at the 5th exon significantly influences the production of IL-1β[7]. Their polymorphisms may have some association with the development of severe AP and septic shock.

CD14, a 55 ku membrane-anchored protein, is a pattern-recognition receptor for several microbial products,

such as lipopolysaccharide (LPS). It can be expressed on neutrophils, monocytes/macrophages, and fibroblasts, all of which can produce cytokines such as IL-1 and TNF-α in response to LPS stimulation[9]. Recently, a-159 G/A polymorphism in the promoter region of CD14 gene involves a C>T substitution at bp -159 of the 5' flanking region of CD14 gene. Genotypes include CC, CT, and TT alleles. Subjects carrying the T allele have been shown to have significantly higher sCD14 levels than those carrying the C allele[8,9]. Therefore, CD14 polymorphism could be a genetic factor responsible for interindividual differences in the susceptibility to bacterial infection. However, to the best of our knowledge, there were no reports on the linkage of CD14 and pancreatitis.

Our previous studies have shown that some polymorphisms in TNF gene correlate with severe sepsis or SAP-associated septic shock, although no association has been found between TNF gene polymorphisms and SAP[4,5,10]. The purpose of this study was to test the hypothesis that IL and CD14 gene polymorphisms have some correlation with the development of SAP and septic shock.

MATERIALS AND METHODS

Subjects

Patients with a first attack of unequivocal AP from July 2001 to December 2003 were prospectively considered. The diagnosis of AP was based on an increased-amylase activity (enzymatic colorimetric test) in serum and CT verification of pancreatitis. Etiology of AP was gallstones found in radiological and endoscopic retrograde cholangiopancreatography findings, alcoholic if patients were heavy consumers of alcohol (more than 80 g of alcohol per day for over 6 mo)[11], and idiopathic if no other identifiable cause could be discovered. Pancreatitis was classified as severe when APACHE II score ≥ 8[12] and CT severity index ≥ 4[13]. Septic shock was defined according to ACCP/SCCM consensus conference criteria[14]. The control group consisted of 116 healthy volunteers. All subjects gave written informed consent, and the protocol was approved by the local ethics committee.

In order to be eligible for the enrollment, all the subjects from the two groups were yellow Chinese Han. The exclusion criteria were defined as follows: age>75 years, cardiac failure (class>III), liver insufficiency (Child C), patients with evidence suggestive of a diagnosis of chronic pancreatitis and consanguineous mating.

DNA extraction

Genomic DNA was purified from 5 mL of peripheral blood samples using Wizard genomic DNA purification kit (Promega) according to the manufacturer's instructions.

IL-10-1082 G to A substitution

PCR was used to amplify a 377-bp fragment of the IL-10 genomic sequence using primers: upstream, 5'-CCAAGACAACACTACTAAGGCTCCTTT-3; downstream, 5'-GCTTCTTATATGCTAGTCAGGTA-3'[15] (Nanjing Bio Eng Co.). The PCR conditions were at 95 ℃ for 2 min, 35 cycles of 95 ℃ for 40 s, 56 ℃ for 40 s, 72 ℃ for 40 s, 72 ℃ for 7 min using reagents purchased from Promega on a gene cycler (BIO-RAD, Japan). The PCR products were digested directly with 2 U *Xag*I restriction enzyme (Promega) at 37 ℃ for 6 h. Digested DNA was analyzed on 5% polyacrylamide gels. Ethidium bromide staining of the gel demonstrated three fragments of 253, 97, and 27 bp for G/G, four fragments of 280, 253, 97, and 27 bp for G/A, two fragments of 280 and 97 bp for A/A.

IL-1β polymorphism

A 249-bp fragment of the IL-1β genomic sequence including the polymorphic *Taq*I site was amplified using PCR. The following nucleotide sequences were used for PCR amplification: 5'-GTTGTCATCAGACTTTGACC-3', 5'-TTCAGTTCATATGGACCAGA-3'[16] (Nanjing Bio Eng Co.). The PCR conditions were at 97 ℃ for 2 min, 35 cycles of 95 ℃ for 40 s, 55 ℃ for 40 s, 74 ℃ for 30 s, 72 ℃ for 7 min using reagents purchased from Promega on a gene cycler (BIO-RAD, Japan). The PCR products were digested directly with 2 U *Taq*I restriction enzyme (Promega) at 37 ℃ for 4 h. Digested DNA was analyzed on 5% polyacrylamide gels. Ethidium bromide staining of the gel demonstrated the original 249 bp fragment for T/T, two fragments of 135 and 114 bp for C/C, three fragments of 249, 135, and 114 bp for C/T.

CD14-159 C/T polymorphism

PCR was used to amplify a 166-bp fragment of the CD14 genomic sequence using primers: upstream, 5'-TGCCAGGAGACACAGAACCC-3'; downstream, 5'-TGTCATTCAGTTCCCTCCTG-3'[9] (Nanjing Bio Eng Co.). The PCR conditions were at 96 ℃ for 2 min, 35 cycles of 96 ℃ for 40 s, 54 ℃ for 40 s, 72 ℃ for 30 s, and 72 ℃ for 7 min using reagents purchased from Promega on a gene cycler (BIO-RAD, Japan). The PCR products were digested directly with 2 U *Hae*III restriction enzyme (Promega) at 37 ℃ for 4 h. Digested DNA was analyzed on 5% polyacrylamide gels. Ethidium bromide staining of the gel demonstrated the original 166-bp fragment for T/T, two fragments of 86 and 80 bp for C/C, three fragments of 86, 80, and 166 bp for C/T.

In addition, 30% of samples were randomly selected to be genotyped a second time to ensure reproducibility. Genotyping for all subjects was performed with no knowledge of clinical status.

Statistical analysis

Allelic frequencies were determined for statistical significance by χ^2 test. Analysis was made by SPSS 11.0, and $P<0.05$ was considered statistically significant.

RESULTS

Characteristics of the patients

On the basis of the selection criteria, 109 patients (59 females and 50 males) with SAP were studied. Thirty-three developed septic shock (septic shock group), and 76 did not develop septic shock (nonseptic shock group). The APACHE II and CT scores at the time of admission were similar in both septic shock group and nonseptic group.

This study was undertaken in selected patients with acute mild pancreatitis (MAP) (n = 106) as defined by CT severity index and APACHE II score, and matched with SAP for age, sex, and cause of pancreatitis. Patients with MAP had an uneventful recovery. The control group included 116 healthy volunteers (65 females and 51 males).

Polymorphisms of two IL genes

The distribution of IL-10-1 082 and IL-1β polymorphisms in different groups is shown in Tables 1 and 2. The overall IL-10-1 082G and IL-1β+3 594T allele frequencies were similar in patients with mild or severe pancreatitis. Further, no significant difference in allele frequencies studied was noted between patients with AP and control subjects.

Table 1 Comparison of allele frequency between MAP group and SAP group

		MAP (n = 106)	SAP (n = 109)	P
	CC	94	95	
IL-1β	CT	12	14	
+3 594	TT	0	0	
	T allele	12 (5.7)	14 (6.4)	0.740
	GG	0	0	
IL-10	AA	75	81	
-1 082	GA	31	28	
	G allele	31 (14.6)	28 (12.8)	0.592
	CC	62	66	
CD-14	TT	14	14	
-159	CT	30	29	
	T allele	58 (27.4)	57 (26.1)	0.777

Table 2 Comparison of allele frequency between AP and controls

		AP (n = 215)	Controls (n = 116)	P
	CC	189	98	
IL-1β	CT	26	18	
+3 594	TT	0	0	
	T allele	26 (6.0)	18 (7.8)	0.399
	GG	0	0	
IL-10	AA	156	79	
-1 082	GA	59	37	
	G allele	59 (13.7)	37 (15.9)	0.437
	CC	128	71	
CD-14	TT	28	13	
-159	CT	59	32	
	T allele	115 (26.7)	58 (25.0)	0.626

The distribution of IL-10-1082G and IL-1β allele frequencies between septic shock group and nonseptic shock group is shown in Table 3. Patients with septic shock showed a significantly higher prevalence of the IL-10-1082G than those without septic shock (χ^2 = 5.921, P = 0.015). No significant difference in IL-1β+3594T allele frequency was found between septic shock patients and nonseptic shock patients.

CD14-159 C/T polymorphism

The distribution of CD14-159 polymorphism in different groups is shown in Tables 1 and 2. The CD14-159T allele frequency was similar in patients with mild or severe pancreatitis. No significant difference in CD14-159T allele frequency was noted between patients with AP and control subjects.

Comparison of CD14-159 allele frequency between septic shock group and nonseptic shock group is shown in Table 3. No significant difference was found in the allele frequency between septic shock patients and nonseptic shock patients.

Comparisons of polymorphisms in different etiologies of SAP

No significant differences were found in the distribution of allele frequency between any two groups (Table 4).

Table 3 Comparison of allele frequency between septic shock and nonseptic shock groups

		Septic shock (n = 33)	Nonseptic shock (n = 76)	P
	CC	27	68	
IL-1β	CT	6	8	
+3 594	TT	0	0	
	T allele	6 (9.1)	8 (5.3)	0.289
	GG	0	0	
IL-10	AA	19	62	
-1 082	GA	14	14	
	G allele	14 (21.2)	14 (9.2)	0.015
	CC	19	47	
CD-14	TT	5	9	
-159	CT	9	20	
	T allele	19 (28.8)	38 (25.0)	0.559

Table 4 Comparison of allele frequency based on different etiologies of SAP (n)%

Allele	Alcoholic SAP (n = 23)	Gallstone SAP (n = 49)	Idiopathic SAP (n = 34)	P
IL-1β+3 594 T	3 (6.5)	6 (6.1)	5 (7.4)	0.952
IL-10-1 082 G	7 (15.2)	12 (12.2)	9 (13.2)	0.886
CD-14-159 T	11 (23.9)	25 (25.5)	21 (30.9)	0.653

DISCUSSION

In humans, there is increasing evidence that the host's cytokine response is genetically determined[17]. Polymorphic gene sequences of certain cytokines may be potential markers of susceptibility and clinical outcome in different human infectious diseases. In our study, the frequency of well-described variants in IL-1β+3 594 at the 5th exon, IL-10-1 082, and CD14-159 was examined. Our results demonstrated that IL-1β+3594T, IL-10-1082G, and CD14-159T had no correlation with the occurrence or severity of AP. However, the distribution of IL-10-1082G in SAP patients varied, and IL-10-1082G allele was found to be more frequent in septic sock patients than in nonseptic shock patients (P<0.05). The association between septic shock patients and IL-10 polymorphism was restricted to the IL-10-1082G, no such a correlation was seen to either IL-1β+3 594 at the 5th exon or CD14-159 variant.

Before evaluating the role of a cytokine polymorphism played in any disease, three questions need to be answered[18,19]. First, are the subjects homogeneous? To avoid artifact in

population admixture, we selected only Chinese Han people in China. In addition, the consanguineous mating subjects were precluded from our study. Second, does the product of the studied gene play an important role in the pathogenesis of the disease? The central role of IL-1β, IL-10, and CD14 in the occurrence or severity of AP and septic shock has been clearly demonstrated by many studies[20-23]. Third, does the gene polymorphism produce a relevant alteration in the level or function of the gene product? *In vitro*, the *Taq*I polymorphism in human IL-β gene correlates with IL-β secretion[10]. *In vitro* and *in vivo* studies showed that IL-10-1 082 variant significantly influences the secretion of IL-10[24-27]. With regard to CD14-159 polymorphism, there is mounting evidence that the SNP in CD14 genome significantly influences the production of CD14[9].

IL-1 and TNF-α are the most prominent inflammatory mediators and regarded as the "first-line" cytokines. Administration of IL-1β to human beings results in inflammation, tissue injury, and septic shock-like syndrome. Different polymorphisms of the IL-1β gene have been described[7,10], and at least two of them could influence the protein production. One is located within the promoter region, and the other is located in exon 5. In our present study, we examined the frequency of IL-1βA *Taq*I RFLP at the 5th exon and found that it was comparable in patients with mild or severe pancreatitis. Similarly, no significant difference in the allele distribution was noted between patients and controls. In addition, no significant difference in the allele frequency was seen between septic shock patients and nonseptic shock subjects. The results suggest that IL-1βA may not play a principle role in the onset of SAP or SAP-associated septic shock. Our results are in line with the report by Powell *et al*.[28].

In the clinical setting, levels of IL-10 showed a steep increase within the first 24 h from disease onset, and the level of IL-10 on the first day was found to be higher in patients with mild AP than in those with severe AP, suggesting that at position-1082 bp from the transcriptional start site, the presence of G is associated with higher and A with lower production of IL-10[6]. Based on the observation, we postulate that IL-10-1082 polymorphism may have some association with the occurrence or the severity of AP. In our study, no significant difference was found in the frequency of IL-10-1082G between any two groups, but significant difference was found in the distribution of IL-10-1082G between septic shock patients and nonseptic shock patients. The pathophysiology of septic shock is a complex and multifactorial process, involving an imbalance between proinflammatory and anti-inflammatory cytokine release. Our results suggest that in the late stage of SAP, anti-inflammatory cytokine polymorphism likely plays a more important role in the pathopoiesis of septic shock than proinflammatory cytokine polymorphism. The ability to identify patients at high risk for developing septic shock may be a critically important factor that will lead to improvements in the management of septic shock.

CD14, a receptor of LPS, plays a vital role in the mechanism of SIRS and sepsis. Because of the important role of CD14 with respect to LPS binding and signaling, we postulate that the polymorphism in the promoter of CD14 gene might be an important factor in determining the susceptibility to or the severity of AP. In our study, we failed to find an association in CD14-159T frequency between controls and AP or between AP and SAP, indicating that CD14-159T plays no part in disease severity or susceptibility to AP. To the best of our knowledge, there is no report on the association between CD14-159 polymorphism and pancreatitis so far. Our result did not show any difference between patients and controls or between mild pancreatitis and severe pancreatitis. Furthermore, no significant difference was found between CD14-159T frequency and septic shock secondary to severe pancreatitis, indicating that in the late stage of the disease, CD14-159 polymorphism plays little role in the onset of SAP-associated septic shock. This is in line with previous studies[29,30].

Although SAP has many distinct etiologies, the immune system response appears to be almost identical regardless of the cause[1]. In our study, we divided SAP patients into three groups: gallstone pancreatitis, alcohol pancreatitis, and idiopathic pancreatitis according to the etiology of the disease. The observed allele frequency of IL-1β+3594T, IL-10-1082G and CD14-159T was comparable between groups of different etiologies, suggesting that environmental factors may play an important role in the occurrence of SAP.

In conclusion, gene polymorphisms have no association with the occurrence or severity of AP. However, the IL-10-1082G may play an important role in the susceptibility of SAP patients to septic shock.

REFERENCES

1 **Frossard JL,** Morel P, Pastor CM. Why clinical trials might succeed in acute pancreatitis when they failed in septic shock. *JOP* 2003; **4**: 11-16

2 **Chen CC,** Wang SS, Lu RH, Chang FY, Lee SD. Serum interleukin-10 and interleukin-11 in patients with acute pancreatitis. *Gut* 1999; **45**: 895-899

3 **Poli F,** Nocco A, Berra S, Scalamogna M, Taioli E, Longhi E, Sirchia G. Allele frequencies of polymorphisms of TNFA, IL-6, IL-10 and IFNG in an Italian Caucasian population. *Eur J Immunogenet* 2002; **29**: 237-240

4 **Zhang D,** Li J, Jiang ZW, Yu B, Tang X. Association of two polymorphisms of tumor necrosis factor gene and with acute severe pancreatitis. *J Surg Res* 2003; **112**: 138-143

5 **Dianliang Z,** Jieshou L, Zhiwei J, Baojun Y. Association of plasma levels of tumor necrosis factor (TNF)-alpha and its soluble receptors, two polymorphisms of the TNF gene, with acute severe pancreatitis and early septic shock due to ist. *Pancreas* 2003; **26**: 339-344

6 **Schaaf BM,** Boehmke F, Esnaashari H, Seitzer U, Kothe H, Maass M, Zabel P, Dalhoff K. Pneumococcal septic shock is associated with the interleukin-10-1082 gene promoter polymorphism. *Am J Respir Crit Care Med* 2003; **168**: 476-480

7 **Pociot F,** Molvig J, Wogensen L, Worsaae H, Nerup J. A TaqI polymorphism in the human interleukin-1 beta (IL-1 beta) gene correlates with IL-1 beta secretion *in vitro*. *Enr J Clin Invest* 1992; **22**: 396-402

8 **Yamazaki K,** Ueki-Maruyama K, Oda T, Tabeta K, Shimada Y, Tai H, Nakajima T, Yoshie H, Herawati D, Seymour GJ. Single-nucleotide polymorphism in the CD14 promoter and periodontal disease expression in a Japanese population. *J Dent Res* 2003; **82**: 612-616

9 **Baldini M,** Lohman IC, Halonen M, Erichson RP, Holt PG, Martinez FD. A polymorphism in the 5'flanking region of the CD14 gene is associated with circulating soluble CD14 levels and with total serum immunoglobulin E. *Am J Respir Cell Mol*

Biol 1999; **20**: 976-983
10 **Zhang D,** Li J, Jiang Z, Yu B, Tang X, Li W. The relationship between tumor necrosis factor-α gene polymorphism to acute severe pancreatitis. *Chin Medl J* 2003; **116**: 1779-1781
11 **Sargen K,** Demaine AG, Kingsnorth AN. Cytokine gene polymorphisms in acute pancreatitis . *JOP* 2000; **1**: 24-35
12 **Dominguez-Munoz JE,** Carballo F, Garcia MJ, de Diego JM, Campos R, Yanguela J, de la Morena J. Evaluation of the clinical usefulness of APACHE? and SAPS systems in initial prognostic classification of acute pancreatitis: a multiple study. *Pancreas* 1993; **8**: 682-686
13 **Balthazar EJ,** Robinson DL, Megibow AJ, Ranson JH. Acute pancreatttis: value of CT in establishing prognosis. *Radiology* 1990; **174**: 331-336
14 **Muckart DJ,** Bhagwanjee S. American College of Chest Physicians / Society of Critical Care Medicine Consensus Conference definitions of the systemic inflammatory response syndrome and allied disorders in relation to critically injured patients. *Crit Care Med* 1997; **25**: 1789-1795
15 **Koch W,** Kastrati A, Bottiger C, Mehilli J, von Beckerath N, Schomig A. Interleukin-10 and tumor necrosis factor gene polymorphisms and risk of coronary artery disease and myocardial infarction. *Atherosclerosis* 2001; **159**: 137-144
16 **Huang D,** Pirskanen R, Hjelmstrom P, Lefvert AK. Polymorphisms in IL-1β and IL-1 receptor antagonist genes are associated with myasthenia gravis. *J Neuroimmuno* 1998; **81**: 76-81
17 **Walley AJ,** Aucan C, Kwiatkowski D, Hill AV. Interleukin-1 gene cluster polymorphisms and susceptibility to clinical malaria in a Gambian case-control study. *Eur J Hum Genet* 2004; **12**: 132-138
18 **Mira JP,** Cariou A, Grall F, Delclaux C, Losser MR, Heshmati F, Cheval C, Monchi M, Teboul JL, Riche F, Leleu G, Arbibe L, Mignon A, Delpech M, Dhainaut JF. Association of TNF2, a TNF-alpha promoter polymorphism, with septic shock susceptibility and mortality: a multicenter study. *JAMA* 1999; **282**: 561-568
19 **Lander ES,** Schork NJ. Genetic dissection of complex traits. *Science* 1994; **265**: 2037-2048
20 **Norman JG,** Fink G, Franz M, Guffey J, Carter G, Davison B, Sexton C, Glaccum M. Active interleukin-1 receptor required for maximal progression of acute pancreatitis. *Ann Surg* 1996; **223**: 163-169
21 **Rongione AJ,** Kusske AM, Reber HA, Ashley SW, McFadden DW. Interleukin-10 reduces circulating levels of serum cytokines in experimental pancreatitis. *J Gastrointest Surg* 1997; **1**: 159-166
22 **Rongione AJ,** Kusske AM, Kwan K, Ashley SW, Reber HA, McFadden DW. Interleukin 10 reduces the severity of acute pancreatitis in rats. *Gastroenterology* 1997; **112**: 960-967
23 **Landmann R,** Muller B, Zimmerli W. CD14, new aspects of ligand and signal diversity. *Microbes Infect* 2000; **2**: 295-304
24 **Westendorp RG,** Langermans JA, Huizinga TW, Elouali AH, Verweij CL, Boomsma DI, Vandenbroucke JP, Vandenbrouke JP. Genetic influence on cytokine production and fatal meningococcal disease. *Lancet* 1997; **349**: 170-173
25 **van Dissel JT,** van Langevelde P, Westendorp RG, Kwappenberg K, Frolich M. Antiinflammatory cytokine profile and mortality in febrile patients. *Lancet* 1998; **351**: 950-953
26 **Turner DM,** Williams DM, Sankaran D, Lazarus M, Sinnott PJ, Hutchinson IV. An investigation of polymorphism in the interleukin 10gene promoter. *Eur J Immunogenet* 1997; **24**: 1-8
27 **Eskdale J,** Gallagher G, Verweij CL, Keijsers V, Westendorp RG, Huizinga TW. Interleukin10 secretion in relation to human IL 10locus haplotypes. *Proc Natl Acad Sci USA* 1998; **95**: 9465-9470
28 **Powell JJ,** Fearon KC, Siriwardena AK, Ross JA. Evidence against a role for polymorphisms at tumor necrosis factor interleukin-1 and interleukin-1 receptor antagonist gene loci in the regulation of disease severity in acute pancreatitis. *Surgery* 2001; **129**: 633-640
29 **Agnese DM,** Calvano JE, Hahm SJ, Coyle SM, Corbett SA, Calvano SE, Lowry SF. Human toll-like receptor 4 mutations but not CD14 polymorphisms are associated. with an increased risk of gram-negative infections. *J Infect Dis* 2002; **186**: 1522-1525
30 **Hubacek JA,** Stuber F, Frohlich D, Book M, Wetegrove S, Rothe G, Schmitz G. The common functional C(-159)T polymorphism within the promoter region of the lipoplysaccharide receptor CD14 is not associated with sepsis development or mortality. *Genes Immun* 2000; **1**: 405-407

Science Editor Wang XL **Language Editor** Elsevier HK

PO Box 2345, Beijing 100023, China
www.wjgnet.com
wjg@wjgnet.com

ELSEVIER

World J Gastroenterol 2005;11(28):4414-4418
World Journal of Gastroenterology ISSN 1007-9327

• *BRIEF REPORTS* •

Effects of magnolol and honokiol derived from traditional Chinese herbal remedies on gastrointestinal movement

Wei-Wei Zhang, Yan Li, Xue-Qing Wang, Feng Tian, Hong Cao, Min-Wei Wang, Qi-Shi Sun

Wei-Wei Zhang, Yan Li, Xue-Qing Wang, Feng Tian, Department of Gastroenterology, the Second Affiliated Hospital of China Medical University, Shenyang 110004, Liaoning Province, China
Hong Cao, Min-Wei Wang, Department of Pharmacology, School of Pharmacy, Shenyang Pharmaceutical University, Shenyang 110016, Liaoning Province, China
Qi-Shi Sun, Department of Chinese Herbs, School of Pharmacy, Shenyang Pharmaceutical University, Shenyang 110016, Liaoning Province, China
Supported by the Natural Science Foundation of Liaoning Province, No. 20032074
Correspondence to: Yan Li, Department of Gastroenterology, the Second Affiliated Clinical Hospital of China Medical University, 36 Sanhao Street, Heping District, Shenyang 110004, Liaoning Province, China. liyan1@medmail.com.cn
Fax:+86-24-83956416
Received: 2004-06-02 Accepted: 2004-06-28

Abstract

AIM: To study the effects of magnolol and honokiol on isolated smooth muscle of gastrointestinal tract and their relationship with Ca^{2+}, and on the gastric emptying and the intestinal propulsive activity in mice.

METHODS: Routine experimental methods using isolated gastric fundus strips of rats and isolated ileum segments of guinea pigs were adopted to measure the smooth muscle tension. The effects of magnolol 10^{-3}, 10^{-4}, 10^{-5} mol/L, and honokiol 10^{-4}, 10^{-5}, 10^{-6} mol/L on the contractility of gastric fundus strips of rats and ileum of guinea pigs induced by acetylcholine (Ach) and 5-hydroxytryptamine (5-HT) was assessed respectively. The method using nuclein and pigment methylene blue was adopted to measure the gastric retention rate of nuclein and the intestinal propulsive ratio of a nutritional semi-solid meal for assessing the effect of magnolol and honokiol (0.5, 2, 20 mg/kg) on gastric emptying and intestinal propulsion.

RESULTS: Magnolol and honokiol significantly inhibited the contractility of isolated gastric fundus strips of rats treated with Ach or 5-HT and isolated ileum guinea pigs treated with Ach or $CaCl_2$, and both of them behaved as non-competitive muscarinic antagonists. Magnolol and honokiol inhibited the contraction induced by Ach in Ca^{2+}-free medium and extracellular Ca^{2+}-dependent contraction induced by Ach. Each group of magnolol and honokiol experiments significantly decreased the residual rate of nuclein in the stomach and increased the intestinal propulsive ratio in mice.

CONCLUSION: The inhibitory effect of magnolol and honokiol on contractility of the smooth muscles of isolated gastric fundus strips of rats and isolated ileum of guinea pigs is associated with a calcium-antagonistic effect. Magnolol and honokiol can improve the gastric emptying of a semi-solid meal and intestinal propulsive activity in mice.

Key words: Magnolol and honokiol; Gastrointestinal movement

Zhang WW, Li Y, Wang XQ, Tian F, Cao H, Wang MW, Sun QS. Effects of magnolol and honokiol derived from traditional Chinese herbal remedies on gastrointestinal movement. *World J Gastroenterol* 2005; 11(28): 4414-4418
http://www.wjgnet.com/1007-9327/11/4414.asp

INTRODUCTION

Cortex *Magnoliae officinalis* is a traditional Chinese herb, belonging to "prokinetic agent" of Chinese herbs. It can improve the symptoms of abdominal distention, dyspepsia, nausea, and vomiting, *etc*., in gastrointestinal diseases. Magnolol and honokiol are the main components of magnoliae bark. Both can relieve spasm of smooth muscle and stop vomiting, *etc.* Magnolol also has an anti-allergic, anti-asthma and anti-inflammatory effect[1], and honokiol has an anxiolytic effect[2-4] and a cardiac muscle protective effect[5]. We used the isolated gastric fundus strips of rats and isolated ileum segments of guinea pigs to measure the smooth muscle tension for assessing the effects of magnolol and honokiol on the contractility of gastric fundus strips of rats induced by acetylcholine (Ach) and 5-hydroxytryptamine (5-HT), and ileum of guinea pigs induced by Ach and $CaCl_2$. Nuclein and pigment methylene blue were used to measure the gastric retention rate of nuclein and the intestinal propulsive ratio of a nutritional semi-solid meal for assessing the effect of magnolol and honokiol on gastric emptying and intestinal propulsion.

MATERIALS AND METHODS

Preparation of magnolol and honokiol: Magnolia bark (*Magnolia officinalis* Rehd. et Wils.) was purchased from Shenyang Medicinal Material Company. The voucher specimens of *Magnolia officinalis* Rehd. et Wils. was identified by Professor Sun of Shenyang Pharmacy University. Magnolol and honokiol were extracted in Shenyang Pharmacy University.

Magnolol and honokiol were dissolved in a very small amount of ethanol. In isolated and *in vivo* experiments the resultant solution was diluted with a 10% aqueous solution of Tween-80. Subsequently, the solution was diluted with distilled water, so that the final concentration of both ethanol and Tween-80 in the vehicle was 0.5%.

Propulsid (cisapride tablet, 5 mg/tablet) was produced by Xi'an Pharmaceutical Company Ltd (batch number: 030815020). Cisapride was crushed and dissolved in distilled water to make a 0.15 mg/mL cisapride solution.

Methylthioninium chloride injection (20 mg/2 mL) was produced by Beijing Yongkang Pharmaceutical Company Ltd.

Preparation of a semi-solid nutritious meal[6]: Ten grams of carboxymethylcellulose was added to 250 mL of distilled water. After the mixture was agitated, 16 g of milk powder, 8 g of cane sugar and 8 g of cornstarch were added to the mixture. The resulting mixture was a white semisolid paste.

Animals

Rats (200-300 g) and guinea pigs (200-300 g) of either sex were raised in cages in groups of five male mice (18-22 g) at a constant temperature (22±2 ℃) with free access to food and water.

Method

Effects of magnolol and honokiol on contractility of gastric fundus strips of rats induced by Ach and 5-HT Isolated gastric fundus strips of rats were prepared and mounted on an organ bath (Magnus' bath) containing 30 mL of Kreb's solution bubbled with 95% O_2+50 mL/L CO_2 (pH 7.3-7.4 at 37 ℃) under a resting tension of 1 g. The muscular tension, measured with a force transducer, was displayed on a MS-302 biosignal recording and analyzing system. The preparations were allowed to equilibrate for 50 min. After equilibration, 3×10^{-3} mol/L Ach 0.1 mL or 3×10-^{6} mol/L 5-HT 0.2 mL was added in the bath to activate the gastric fundus strips. When it reached its maximum contraction, it was washed with Kreb's solution to regain spontaneous contraction. Then Ach or 5-HT was added to the bath from low to high logarithmic doses to make the final respective concentrations of 10^{-8}, 3×10^{-8}, 10^{-7}, 3×10^{-7}, 10^{-6}, 3×10^{-6}, 10^{-5}, 3×10^{-5}, 10^{-4}, 3×10^{-4} mol/L, or 10^{-10}, 3×10^{-10}, 10^{-9}, 3×10^{-9}, 10^{-8}, 3×10^{-8}, 10^{-7}, 3×10^{-7}, 10^{-6}, 3×10^{-6} mol/L. The accumulated concentration-efficacy curve was made. When the curve reached its peak, the gastric fundus strips were washed thrice at 5-min intervals with Kreb's solution to wash the Ach out. After 15-min equilibration the drugs were added to the organ bath in respective doses (final concentrations of magnolol were 10^{-5}, 10^{-4} or 10^{-3} mol/L, honokiol were 10^{-6}, 10^{-5} or 10^{-4} mol/L). The accumulated concentration-efficacy curve was made after 1 min.

We made the maximum efficacy (E_{max}) of Ach or 5-HT as 100%, and calculated the effect percentage (E/E_{max}) of each concentration of Ach or 5-HT. Then the cumulative concentration-efficacy curves were drawn with E/E_{max} as the ordinates and the negative logarithm of final concentration of Ach or 5-HT (-log[A]) as the abscissae.

Effects of magnolol and honokiol on the contractility of the ileum of guinea pigs induced by Ach Terminal ileum segments from guinea pigs were prepared and suspended vertically in organ baths containing 30 mL of Tyrode's solution bubbled with 95% O_2+50 mL/L CO_2 (pH 7.3-7.4 at 37 ℃) under a resting tension of 1 g. The spontaneous contractions were measured after equilibration for 50 min, 3×10^{-3} mol/L. Ach 0.1 mL was added in the bath to activate the ileum. When it reached its maximum contraction, it was washed in Tyrode's solution to regain spontaneous contractions. The cumulative concentration-efficacy curves of Ach were made, then the curve was remade after magnolol and honokiol were added in the organ bath respectively (the final concentrations were the same in method 1).

Effects of magnolol and honokiol on the contractility of the ileum of guinea pigs induced by $CaCl_2$ After equilibration of guinea pig ileum segments in Ca^{2+}-free Tyrode's solution ($CaCl_2$ was omitted from normal Tyrode's solution) for 40 min they were changed with Ca^{2+}-free high K^+-depolarized Tyrode's solution. Ca^{2+}-free Tyrode's solution was (the equal mole NaCl was replaced with 80 mmol/L KCl in the Ca^{2+}-free Tyrode's solution) to make the smooth muscle depolarization after 30 min, $CaCl_2$ was added to the bath from low to high logarithmic doses (final concentrations were 10^{-5}, 3×10^{-5}, 10^{-4}, 3×10^{-4}, 10^{-3}, 3×10^{-3}, 10^{-3}, and 3×10^{-3} mol/L respectively) and the cumulative concentration-efficacy curves were drawn. The ileum segments were washed with the Ca^{2+}-free Tyrode's solution till the muscular tension regained the normal contraction. After 30 min, Ca^{2+}-free Tyrode's solution was changed with Ca^{2+}-free high K^+ Tyrode's solution and magnolol and honokiol were added respectively. After 30 min, the cumulative concentration-efficacy curves were drawn.

Effects of magnolol and honokiol on the two contractile components of Ach After equilibration for 1 h in Tyrode's solution, guinea pigs ileum segments were washed with Ca^{2+}-free Tyrode's solution thrice and incubated for 30 min, then 3×10^{-3} mol/L Ach 0.2 mL (2×10^{-5} mol/L) was added to the solution and it produced a brief contraction (the first or initial phasic contraction) that was induced by the release of intracellular calcium. When the ileum segments reached maximal contraction, $CaCl_2$ 0.2 mL (2×10^{-2} mol/L) was added and caused an advanced contraction (the second phasic contraction or sustained tonic component) induced by the extracellular calcium influx evoked by Ach. The ileum segments were washed with Ca^{2+}-free Tyrode's solution and incubated in Ca^{2+}-free Tyrode's solution for 30 min; meanwhile magnolol (final concentrations were 10^{-5}, 10^{-4} or 10^{-3} mol/L) or honokiol (final concentrations were 10^{-6}, 10^{-5} or 10^{-4} mol/L) was added respectively, then Ach and $CaCl_2$ were added successively. The guinea pig ileum segments produced the first and second contractions respectively.

Effects of magnolol and honokiol on gastrointestinal movement in mice Magnolol and honokiol were dispensed as before to the concentrations of 0.5, 2.0, and 20 mg/L. Mice were allocated randomly to a control group (administrated orally with distilled water), a cisapride group, and experimental groups. They were given orally either magnolol 0.5, 2.0, and 20 mg/L, or honokiol 0.5, 2.0, and 20 mg/L, respectively. Nuclide and pigment methylene blue were used to measure the gastric retention rate of nuclide and intestinal propulsive ratio of nutritious semi-solid meal. After having fasted for

12 h, the mice were given orally either 0.2 mL/10 g of each of the above substances or 0.2 mL/10 g of distilled water. After 30 min, each mouse was given orally a semi-solid nutritious meal containing ^{99m}Tc-DTPA 0.05 mCi/10 g and a small quantity of methylthioninium chloride. The mice were killed after 20 min, and dissected. Residual nuclide in the gastrointestinal tract was measured by a radioactivity monitor. The gastric residual nuclide rate (%) = (gastric retention nuclide/total nuclide in gastrointestinal tract) ×100%. Intestinal propulsive ratio (%) = (distance from sphincter of pylorus to the distal pigment methylene/ distance from sphincter of pylorus to the ileocecum)×100%.

Statistical analysis

Results were expressed as mean±SD. Comparisons between groups of data were made by the Student's *t*-test or *t*-test of paired comparison.

RESULTS

Effects of magnolol and honokiol on the contractility of gastric fundus strips of rats induced by Ach and 5-HT (Figure 1)

The data showed that magnolol and honokiol inhibited incompetitively the contraction of gastric fundus strips of rats induced by cumulative concentrations of Ach and 5-HT, and the effect increased with the increase of dosage. The antagonistic parameters (PD_2') of magnolol and honokiol were 3.66 and 4.31 for Ach, and 5.08 and 4.91 for 5-HT respectively.

Effects of magnolol and honokiol on the contractility of guinea pig ileum induced by Ach (Figures 2A and B)

The data showed that magnolol and honokiol antagonized incompetitively the contraction of gastric fundus strips of rats induced by cumulative concentration of Ach, and the effect increased with the increase of dosage. The PD_2' values of magnolol and honokiol were 5.09 and 4.99 respectively.

Effects of magnolol and honokiol on the contractility of ileum segments of guinea pigs induced by $CaCl_2$ (Figures 2C and D)

The data showed that magnolol and honokiol antagonized incompetitively the contraction of gastric fundus strips of rats induced by cumulative concentration of $CaCl_2$, and the effect increased with the increase of dosage. The PD_2' values of magnolol and honokiol were 4.34 and 4.84 respectively.

Effects of magnolol and honokiol on the two contractile components of Ach (Table 1)

Magnolol and honokiol inhibited the contraction of ileal segments induced by Ach in Ca^{2+}-free medium and the extracellular Ca^{2+}-dependent contraction induced by Ach.

Magnolol 10^{-5}, 10^{-4} or 10^{-3} mol/L and honokiol 10^{-6}, 10^{-5} or 10^{-4} mol/L inhibited significantly the two contractile components induced by Ach.

Table 1 Effects of magnolol and honokiol on the two contractile components of Ach (%, mean±SD, n = 6)

Group (mol/L)	First phase	Second phase
Magnolol 10^{-3}	89.08±7.32[b]	86.89±8.04[b]
Magnolol 10^{-4}	83.80±11.18[b]	92.97±4.70[b]
Magnolol 10^{-5}	66.48±12.95[b]	75.39±10.53[b]
Honokiol 10^{-4}	74.54±6.75[b]	91.11±3.89[b]
Honokiol 10^{-5}	68.93±10.90[b]	82.11±5.51[b]
Honokiol 10^{-6}	45.68±4.92[b]	78.95±5.83[b]

[b]P<0.01 *vs* others.

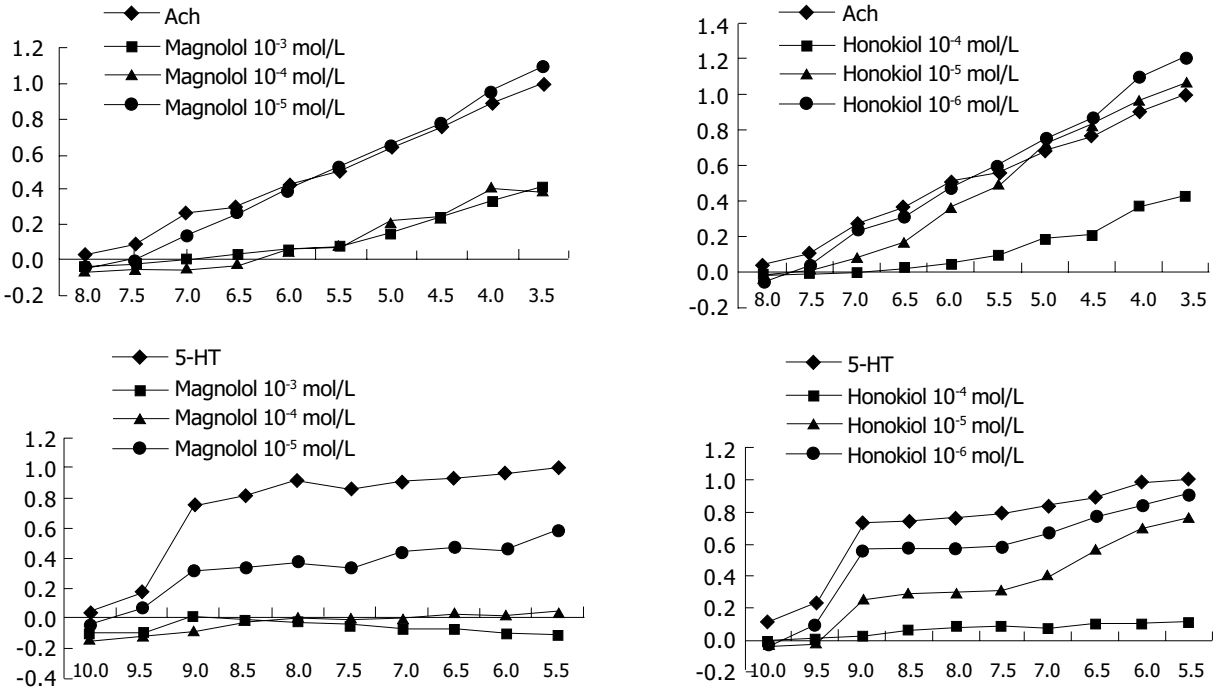

Figure 1 Effect of magnolol and honokiol on the contractility of rat gastric fundus strips induced by Ach and 5-HT. Magnolol effects on contractility of rat gastric fundus strips induced by Ach (A) and 5-HT (C); Honokiol effects on contractility of rat gastric fundus strips induced by Ach (B) 5-HT (D) (n = 6).

Effects of magnolol and honokiol on gastrointestinal movement in mice (Table 2)

In the experimental groups of magnolol 0.5, 2.0, and 20 mg/L, or honokiol 0.5, 2.0, and 20 mg/L, the gastric nuclide retention rate was significantly lower and the intestinal propulsive ratios were significantly higher than those in the control group, indicating that magnolol and honokiol could improve the gastric emptying of a semi-solid meal and intestinal propulsion in mice.

Table 2 Effects of magnolol and honokiol on gastrointestinal movement in mice (mean±SD, n = 20)

Group (mg/kg)	Rate of gastric residual nuclide (%)	Intestinal propulsive ratio (%)
Control	50.05±12.74	47.92±8.49
Cisapride	22.26±9.17[b]	61.92±11.77[b]
Magnolol 0.5	24.61±10.90[b]	57.14±13.12[b]
Magnolol 2	26.40±12.14[b]	55.46±11.26[b]
Magnolol 20	25.96±8.44[b]	60.30±10.52[b]
Honokiol 0.5	24.91±11.30[b]	53.57±9.54[a]
Honokiol 2	34.11±12.25[b]	54.54±8.29[b]
Honokiol 20	33.22±13.64[b]	53.53±9.90[a]

[a]P<0.05, [b]P<0.01 *vs* control.

DISCUSSION

Magnolol and honokiol are neolignan-derivatives present in Magnolia bark, which is used in the treatment of abdominal distention and vomiting. The experimental results indicated that magnolol and honokiol significantly inhibited the contractility of isolated gastric fundus strips of rats treated with Ach or 5-HT and isolated ileum of guinea pigs treated with Ach or $CaCl_2$, and both of them behaved as non-competitive muscarinic antagonists. Magnolol and honokiol inhibited the ileal contraction induced by Ach in Ca^{2+}-free medium and extracellular Ca^{2+}-dependent contraction induced by Ach.

The contraction of gastrointestinal smooth muscle depends on the mediation of intracellular Ca^{2+}, and is accomplished by the process of excitation–contraction coupling (E-C coupling). The free Ca^{2+} originated from the release of intracellular calcium and the restoration of extracellular calcium[7]. A high-K^+ medium could depolarize the cellular membrane of ileum longitudinal smooth muscle, activate the potential-dependent calcium channel (PDC), and result in the inflow of calcium and the contraction of smooth muscles. Our experimental results indicated that magnolol and honokiol could block the transmembrane inflow of calcium through PDC, inhibit the contraction of smooth muscle, and relieve the spasm of smooth muscles.

Physical active substances Ach and 5-HT can increase the tension of gastrointestinal smooth muscle, and the agonist Ca^{2+} is derived from various resources. The two components of intracellular and extracellular calcium were involved in the contraction of smooth muscles induced by Ach. The first phasic contraction induced by Ach in Ca^{2+}-free medium depended on the release of intracellular calcium. The second phasic contraction based on the first phase after the addition of calcium was caused by Ach facilitating the inflow of extracellular calcium through the receptor-operated calcium channel (ROC). In this study, magnolol and honokiol significantly inhibited the first and the second phasic contractions of smooth muscles induced by Ach, indicating that the two components of magnolia bark not only have an intracellular point of action but also inhibit the contraction of smooth muscles by blocking the inflow of calcium through ROC.

Normal gastric motility involves gastric fundus, corpus,

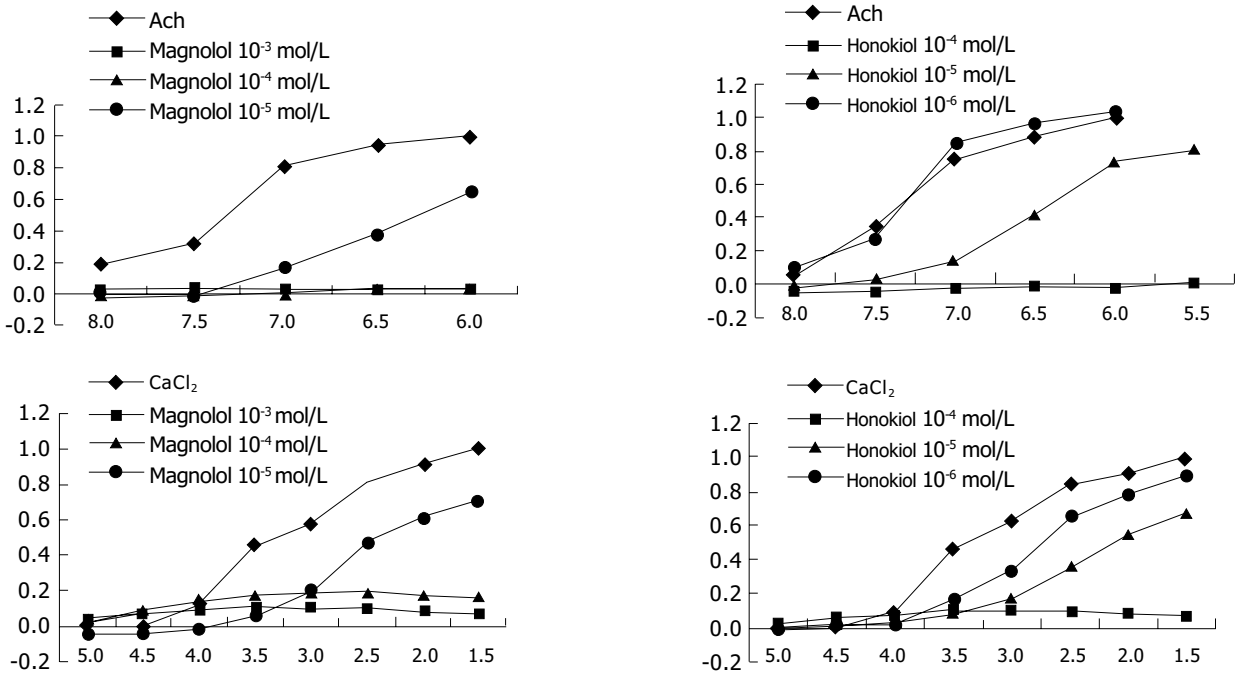

Figure 2 Effect of magnolol and honokiol on the contractility of guinea pig ileum segments induced by Ach and $CaCl_2$. Magnolol effects on the contractility of guinea pig ileum induced by Ach (A) and $CaCl_2$ (C); Honokiol effects on contractility of guinea pig ileum segments induced by Ach (B) and $CaCl_2$ (D) (n = 6).

antrum, pylorus, and antroduodenal coordination. As food is swallowed, the gastric fundus relaxes to accommodate the incoming nutrients. This is termed receptive as relaxation, which is coordinated by vagal efferent activity via nonadrenergic, noncholinergic mechanisms. As swallowing during the meal continues, the fundic filling and relaxation continue with little increase in intraluminal pressure. Gastric distention and activation of mechanoreceptor and stretch receptors stimulate vagal afferent nerve activity, which in turn modifies vagal efferent traffic.

The emptying of solid foods is accomplished by complex interplays among intra-gastric pressure, gastric peristalses, pyloroduodenal resistance, and neuroendocrine responses elicited by the specific components of the particular meal. In this study, magnolol and honokiol could significantly decrease the residual rate of nuclein in stomach and increase the intestinal propulsive ratio of semi-solid nutritious meal in mice, and there was no significant difference between them and cisapride. Combined with the study above, the functions in improving the gastric emptying and intestinal propulsive action may relate to their functions of relaxation of gastrointestinal smooth muscles.

Disorders of stomach motility and intestinal propulsion are involved in functional gastroenterological diseases such as gastroesophageal reflux disease, functional dyspepsia, irritable bowel syndrome, chronic constipation, *etc*.[8], gastroparesis[9], postoperative gastrointestinal atony[10], chronic intestinal pseudo-obstruction[11], and many other diseases. Prokinetic agents such as domperidone and cisapride are important therapeutic drugs[12,13]. But domperidone and cisapride have some severe side-effects, such as prolongation of the QT interval and cardiac arrhythmias[14,15]. There are rich resources of natural herbs in China, which may provide a valuable source of effective prokinetic agents.

REFERENCES

1 **Wang JP,** Ho TF, Chang LC, Chen CC. Anti-inflammatory effect of magnolol, isolated from Magnolia officinalis, on A23187-induced pleurisy in mice. *J Pharm Pharmacol* 1995; **47**: 857-860

2 **Kuribara H,** Kishi E, Hattori N, Yuzurihara M, Mjaruyama Y. Application of the elevated plus-maze test in mice for evaluation of the content of honokiol in water extracts of magnolia. *Phytother Res* 1999; **13**: 593-596

3 **Kuribara H,** Stavinoha WB, Maruyama Y. Behavioural pharmacological characteristics of honokiol, an anxiolytic agent present in extracts of magnolia bark, evaluated by an elevated plus-maze test in mice. *J Pharm Pharmacol* 1998; **50**: 819-826

4 **Kuribara H,** Kishi E, Hattori N, Okada M, Maruyama Y. The anxiolytic effect of two oriental herbal drugs in Japan attributed to honokiol from magnolia bark. *J Pharm Pharmacol* 2000; **52**: 1425-1429

5 **Tsai SK,** Huang SS, Hong CY. Myocardial protective effect of honokiol: an active component in Magnolia officinalis. *Planta Med* 1996; **62**: 503-506

6 **Francis J,** Critchley D, Dourish CT, Cooper SJ. Comparisons between the effects of 5-HT and DL-fenfluramine on food intake and gastric emptying in the rat. *Pharmacol Biochem Behav* 1995; **50**: 581-585

7 **Bauer V,** Holzer P, Ito Y. Role of extra- and intracellular calcium in the contractile action of agonists in the guinea-pig ileum. *Naunyn Schmiedebergs Arch Pharmacol* 1991; **343**: 58-64

8 **Hunt RH.** Evolving concepts in the pathophysiology of functional gastrointestinal disorder. *J Clin Gastroenterol* 2002; **35** (1 Suppl): S2-6

9 **Tomi S,** Plazinska M, Zagorowicz E, Ziolkowski B, Muszynski J. Gastric emptying disorders in diabetes mellitus. *Pol Arch Med Wewn* 2002; **108**: 879-886

10 **Hep A,** Prasek J, Filipinsky J, Navratil P, David L, Dolina J, Dite P. Cisapride (Prepulsid) in the prevention of postoperative gastrointestinal atony. *Rozhl Chir* 1998; **77**: 101-104

11 **Quigley EM.** Chronic Intestinal Pseudo-obstruction. *Curr Treat Options Gastroenterol* 1999; **2**: 239-250

12 **Veldhuyzen van Zanten SJ,** Jones MJ, Verlinden M, Talley NJ. Efficacy of cisapride and domperidone in functional (nonulcer) dyspepsia: a meta-analysis. *Am J Gastroenterol* 2001; **96**: 689-696

13 **Barone JA.** Domperidone: a peripherally acting dopamine2-receptor antagonist. *Ann Pharmacother* 1999; **33**: 429-440

14 **Drolet B,** Rousseau G, Daleau P, Cardinal R, Turgeon J. Domperidone should not be considered a no-risk alternative to cisapride in the treatment of gastrointestinal motility disorders. *Circulation* 2000; **102**: 1883-1885

15 **Layton D,** Key C, Shakir SA. Prolongation of the QT interval and cardiac arrhythmias associated with cisapride: limitations of the pharmacoepidemiological studies conducted and proposals for the future. *Pharmacoepidemiol Drug Saf* 2003; **12**: 31-40

Science Editor Wang XL **Language Editor** Elsevier HK

PO Box 2345, Beijing 100023, China
www.wjgnet.com
wjg@wjgnet.com

ELSEVIER

World J Gastroenterol 2005;11(28):4419-4422
World Journal of Gastroenterology ISSN 1007-9327

• *BRIEF REPORTS* •

Effect of early nutrition on intestine development of intrauterine growth retardation in rats and its correlation to leptin

Xiao-Shan Qiu, Ting-Ting Huang, Zhen-Yu Shen, Hui-Ying Deng, Zhi-Yong Ke

Xiao-Shan Qiu, Ting-Ting Huang, Zhen-Yu Shen, Zhi-Yong Ke, Pediatric Department, the First Affiliated Hospital of Sun Yat-Sen University, Guangzhou 510080, Guangdong Province, China
Hui-Ying Deng, Guangzhou Children's Hospital, Guangzhou 510120, Guangdong Province, China
Supported by the Science and Technology Bureau Foundation of Guangdong Province, No. 99M04815G
Correspondence to: Dr. Ting-Ting Huang, Department of Pediatrics, the First Affiliated Hospital of Sun Yat-Sen University, Guangzhou 510080, Guangdong Province, China. huangtt cn@yahoo.com
Telephone: +86-20-88551570
Received: 2004-09-22 Accepted: 2004-11-19

Abstract

AIM: To investigate the intestine and body development of intrauterine growth retardation (IUGR) rats under early different protein diet and to analyze the correlation between leptin and intestine and body development.

METHODS: An IUGR rat model was established by food restriction of pregnant female rats. Fifty-six neonatal IUGR rats and 24 neonatal normal rats were randomly divided into normal control group (C group), IUGR model group (SC group), low protein diet IUGR group (SL group), and high protein diet IUGR group (SH group). Eight rats were killed per group at wk 0, 4, and 12. Serum leptin, body weight (BW), body length (BL), intestinal weight (IW), intestinal length (IL), and intestinal disaccharidase (including lactase, maltase, and saccharase) were detected.

RESULTS: BW (4.50±0.41 g), BL (5.96±0.40 cm), IW (0.05±0.01 g), and IL (15.9±2.8 cm) in neonatal IUGR rats were much lower than those in C group (6.01±0.55 g, 6.26±0.44 cm, 0.10±0.02 g, 21.8±2.7 cm, $P<0.05$), while intestinal lactase and maltase activities were higher than those in C group. SH group showed the fastest catch up growth and their BW, BL, IW, and IL reached the C group level at wk 4. SC group showed relatively slower catch up growth than SH group, and their BW, BL, IW did not reach the C group level at wk 4. SL group did not show intestine and body catch up growth. Intestinal maltase [344±33 μmol/(min·g)] and saccharase activities [138±32 μmol/(min·g)] in SL group were both markedly lower than those in C group [751±102, 258±27 μmol/(min·g), $P<0.05$]. There were no significant differences in lactase activities at wk 4 and disaccharidase activities at wk 12 among all groups ($P>0.05$). The leptin level in SL group (0.58±0.12 ng/mL) was the highest in all groups, and much lower in SH group (0.21±0.03 ng/mL) than that in any other IUGR groups at wk 4 ($P<0.05$). Leptin was negatively related to BW ($r = -0.556$, $P = 0.001$), IW ($r = -0.692$, $P = 0.001$) and IL ($r = -0.738$, $P = 0.000$) at wk 4, while no correlation was found at wk 12.

CONCLUSION: High protein diet is a reasonable early nutritional mode to IUGR rats in promoting intestine and body catch up growth.

Key words: Intrauterine growth retardation; Rat; Intestine development; Disaccharidase; Leptin; Nutritional intervention

Qiu XS, Huang TT, Shen ZY, Deng HY, Ke ZY. Effect of early nutrition on intestine development of intrauterine growth retardation in rats and its correlation to leptin. *World J Gastroenterol* 2005; 11(28): 4419-4422
http://www.wjgnet.com/1007-9327/11/4419.asp

INTRODUCTION

The incidence rate of intrauterine growth retardation (IUGR) is about 7.5-8.7% in our country. Development of the stomach and intestine is closely related to the body growth, it affects and is also reversely affected by nutrition. As a protein coded by ob gene (obesity gene), leptin is a neuroendocrine regulatory factor secreted from mature adipocytes into blood. Leptin can pass through blood-brain barrier and has a central effect on feeding behavior. It was reported[1] that IUGR rats have temporarily high leptin level to regulate growth hormone secretion and growth during catch up growth. Since the infant growth is mainly regulated by nutrition, and nutritional intake is controlled by the development of stomach and intestine and leptin level, our study aimed to investigate the intestine, intestinal disaccharidase and body development and their relation to serum leptin at wk 4 (childhood) and 12 (adulthood) in order to offer some animal research data for early nutritional intervention of IUGR.

MATERIALS AND METHODS

Materials and animals

Leptin kit was purchased from Diagnostic Systems Laboratories (USA). Glucose and disaccharidase enzyme kits were purchased from Great Wall Company (Baoding, Hebei Province, China).

The second class SD female rats were bought from Animal Center of Sun Yat-Sen University and mated with

male rats. IUGR model was established by food restriction of pregnant female rats[2]. The standard of IUGR was that the birth weight -2SD lower than control normal group (5.1 g). Fifty-six newborn IUGR rats and 24 newborn normal rats were randomly divided into normal control group (C group), IUGR model group (SC group), low protein diet IUGR group (SL group), and high protein diet IUGR group (SH group). The former two groups were fed with 22.5% normal protein diet, while the latter two groups with 11.3% low-protein diet and 28.6% high-protein diet respectively. All the rats were weaned when they were 3 wk old and fed with original diet till the 4th wk and then with normal protein diet till the end of the experiment. Components of the diets are shown in Table 1.

Table 1 Content ratio of different components (g) in 100 g food

Components	Protein	Fat	Carbohydrate	Total energy (kJ/100 g)
Normal diet	22.5	3.9	57.8	1 583.4
High protein diet	28.6	3.9	56.8	1 625.4
Low protein diet	11.3	8.5	58.7	1 558.2
χ^2	10.09	3.04	0.09	–
P	0.006[a]	0.22	0.96	–

[a]*P*<0.05 *vs* other.

Methods

Body weight (BW) and body length (BL, from nose to tail) of each rat were measured at wk 0, 4, and 12. Eight newborn female rats of IUGR group and C group were killed right after birth. Another eight female rats were killed per group after being fasted for 10-12 h at wk 4 and 12 respectively. Blood sample was taken from the eyeballs and kept at -30 ℃. Serum leptin was monitored by ELISA.

Abdomen was opened right after the rats were killed. Intestinal weight (IW) and intestinal length (IL) were measured from the beginning of jejunum to the end of ileum, and then 10 cm proximal end of the jejunum (about 3 cm from the beginning of jejunum) was cut, weighed, and homogenized. The disaccharidase activities (including lactase, saccharase, and maltase) were measured.

Statistical analysis

Results were expressed as mean±SD. All data were analyzed by the SPSS 10.0 statistical package. ANOVA test was used to compare these four groups. Least significant difference was used to compare every two groups when variance was regular, while Dunnett T3 test was used when variance was irregular. Pearson's test was used in correlation analysis.

RESULTS

Development of body and intestine and disaccharide activity in newborn IUGR rats and normal rats

The BW, BL, IW, and IL of newborn IUGR rats were significantly lower than those of C group ($P<0.05$), while lactase and maltase activities were higher than those in C group. There was no significant difference in saccharase activity between the two groups (Table 2).

Development of intestine and body of rats

SH group showed the fastest catch up growth, and BW, BL, IW, and IL reached the C group level at wk 4 ($P>0.05$). BW, BL, IW, and IL in SL group at wk 4 and 12 were all markedly lower than those in normal control group ($P<0.05$). BW, BL, and IW in SC group at wk 4 were all significantly lower than those in C group ($P<0.05$). IL in SC group was lower than that in C group at wk 12. There were no significant differences in BW, BL, and IW between the two groups ($P>0.05$).

Intestinal maltase and saccharase activities in SL group were markedly lower than those in C group ($P<0.05$). There was no significant difference in lactase activity between the two groups at wk 4 ($P>0.05$). Maltase activity in SH group was lower than that in C group ($P<0.05$). There were no significant differences in disaccharidase activity between groups at wk 12 ($P>0.05$).

Leptin in SL group was significantly higher than that in SC and C groups, and lower in SH group than that in SC group at wk 4 ($P<0.05$). Leptin in SC group was higher than that in C group and lower in SH and SL group than that in SC group ($P<0.05$). There were no significant differences between these two groups and C group at wk 12 ($P>0.05$). Results are shown in Table 2.

Correlation analysis

The following results were found in correlation analysis of leptin and BW, BL, IW, and IL. Leptin and BW had a negative correlation at wk 4 ($r = -0.556$, $P = 0.001$), while

Table 2 Leptin, BW, BL, IW, IL, and disaccharidase activities in all groups (mean±SD) *n* = 8/group

Age (yr)	Group	Leptin (ng/mL)	BW (g)	BL (cm)	IW (g)	IL (cm)	Lactase	Saccharase	Maltase
0 wk	C	ND	6.01±0.55	6.26±0.44	0.10±0.02	21.8±2.7	315±19	13±6	58±20
	SC	ND	4.50±0.41[a]	5.96±0.40[a]	0.05±0.01[a]	15.9±2.8[a]	383±39[a]	15±8	269±17[a]
4th wk	C	0.26±0.08	60.8±9.5	23.1±1.4	2.2±0.2	74.8±9.1	54±15	258±27	751±102
	SC	0.36±0.20	52.0±10.9[a]	21.0±2.5[a]	1.4±0.3[a]	70.3±3.4	39±14	254±23	797±95
	SH	0.21±0.03[c]	70.0±4.5[c]	23.6±0.5[c]	1.9±0.2	80.7±9.5	62±8	230±21	368±26[a,c]
	SL	0.58±0.12[a,c]	21.4±3.5[a,c]	16.0±1.3[a,c]	0.8±0.4[a,c]	53.9±3.1[a,c]	66±22	138±32[a,c]	344±33[a,c]
12th wk	C	0.40±0.23	235.5±43.4	38.5±0.8	4.3±0.7	122.7±12.6	48±3	230±32	713±158
	SC	0.79±0.41[a]	208.6±21.6	36.9±1.7	3.9±0.9	101.2±5.8[a]	50±21	262±43	670±157
	SH	0.42±0.15[c]	254.8±23.5[a,c]	37.1±0.4	4.1±0.4	122.3±13.0	48±12	242±27	682±144
	SL	0.38±0.25[c]	169.3±6.7[a,c]	33.2±0.8[a,c]	3.3±0.6[a]	99.6±6.9[a]	53±12	239±35	568±52

Disaccharidase activity unit: μmol/(min·g) protein. [a]*P*<0.05, IUGR group *vs* C group; [c]*P*<0.05, SL, and SH groups *vs* SC group. ND: not determined.

had no correlation at wk 12; leptin and BL had no correlation at wk 4 and 12; leptin and IW had a negative correlation at wk 4 (r = -0.692, P = 0.001), while had no correlation at wk 12; leptin and IL had a negative correlation at wk 4 (r = -0.738, P = 0.001), while had no correlation at wk 12.

DISCUSSION

Multiple lines of evidence show that about 20-50% IUGR cannot catch up the growth after birth, and remains small till they become adults. Growth is mainly regulated by heredity, nutrition, and endocrine system. The early postnatal growth (the first year after birth) is mainly regulated by nutrition. Mother malnutrition during pregnancy not only delays the fetal growth, but also impairs many organ and tissue structures and functions of the fetus[3]. Zhang *et al*.[2], showed that the weight, length and many morphologic structures of intestine in newborn IUGR rats are significantly lower than those of normal newborn rats. Only few reports about the development of stomach and intestine and disaccharidase activity of IUGR are available at present.

Due to the effect of early nutrition on growth, Lucas[4] have raised the "nutritional programming" hypothesis: nutritional conditions during the critical or sensitive stage of growth have long-term or life-long effects on organic structure or function. The mechanism is that early nutrition stimulates clone selection and differentiation of blast cells and causes irreversible changes in cell number of organism. Based on the hypothesis, we carried out the early nutritional intervention during the first 4 wk after birth -a sensitive and critical stage of growth. We investigated its effects on the development of intestine and jejunum mucosa disaccharidase activity and their correlations with serum leptin.

Our research showed that the impaired development of intestine recovered quickly in SH group after high protein diet was given after birth. Ziegler *et al*.[5], found that the development of intestine mainly depends on the proliferation of cells before weaning. Enough nutrition can not only promote intestinal neuron's activity and increase blood supply of viscera but also stimulate the secretion of growth factor. Intestinal epithelium can absorb more nutrition for catch up growth. Although SC group was fed with normal diet after birth, it failed to catch up the normal control group at wk 4. SL group even failed to catch up normal growth at wk 12 and remained small till they became adults, suggesting that early postnatal protein diet has great effects on the development of intestine. Intestine and body catch up growth of IUGR rats depends on sufficient nutrition after birth, especially enough protein.

Intestine is the main organ to absorb sugar and protein. Disaccharidase, gastrin, and intestinal hormones play an important role in this process. Lactase and maltase are often produced at the late stage of gestation, while saccharase activity increases quickly only after intake of solid food. Stomach and intestine develops very fast in neonatal stage. As the stomach and intestine of neonates become mature, their lactase activity decreases, while maltase and saccharase activities increase[6]. Therefore, it is beneficial to the understanding of the development of stomach and intestine by detecting disaccharidase activities. Our research suggested that the premature of lactase and maltase activity in newborn IUGR rats was an adaptive compensation to intrauterine malnutrition. Saccharase activity in newborn IUGR rats was not affected, suggesting that saccharase is not regulated by intrauterine nutrition. Our research also demonstrated that maltase and saccharase activities in SL groups were markedly lower than those in C and SC groups at wk 4, which is consistent with the study by Nichol *et al*.[7]. The relatively higher lactase activity in SL group may be an accommodation response to lack of nutritional supply. The nutrition of neonatal rats is mainly from milk and lactose is the main component of carbohydrate in milk. The high lactase activity is an advantage for neonatal rats to absorb more lactose to compensate for the shortage of protein. But the reason why maltase activity in SH group was markedly lower than that in C and SC groups at wk 4 is still unknown. Gomez *et al*.[8], gave high protein diet to the rats suffering from abdominal wound and found that its lactase activity is markedly higher than in other rats given normal level protein diet. Further research is needed to test whether the decrease of maltase activity in SH group is related to the increase of lactase activity. There was no significant difference in disaccharidase activity between groups at wk 12, suggesting that disaccharidase activity might change with different kinds of food after birth, such as milk, solid food, and different protein diet.

It was reported that IUGR rats are insensitive to leptin during catch up growth[9]. Jaquet *et al*.[10], found that IUGR children are relatively resistant to leptin in order to catch up growth and leptin is closely related to catch up growth and fat tissue development. We know that blood and umbilical leptin level of newborn baby is positively related to birth weight. Leptin reflects not only the body fat level but also nutritional status. Leptin is a medium between neuroendocrine system and fat tissue. It builds a negative loop between fat tissue and neuropeptide Y (NPY). When weight decreases to some extent, the inhibitory effect of leptin on the secretion of NPY from hypothalamus is also weakened[11]. NPY is a strong stimulator of appetite, high level of NPY is advantageous for IUGR children to take in more nutrition and energy to accumulate body fat.

Correlation analysis showed that leptin was negatively related to BW, IW, and length at wk 4. The BW in SL group was the lowest but leptin level was the highest in all groups at wk 4. We found that IUGR rats were relatively resistant to leptin during catch up growth, but this phenomenon disappeared at wk 12, suggesting that leptin resistance is only related to catch up growth in IUGR children.

In conclusion, high protein diet is a reasonable early nutritional mode for IUGR rats. High leptin level in IUGR rats is related to catch up growth and nutritional status.

REFERENCES

1 **Hileman SM,** Pierroz DD, Flier JS. Leptin, nutrition, and reproduction: timing is everything. *J Clin Endocrinol Metab* 2000; **85**: 804-807

2 **Zhang Q,** Li HS, Zheng HL. The effects of timing and causes

of IUGR on gastro in testinal tract in newborn rats. *Zhonghua Erke Zazhi* 1997; **35**: 567-570

3 **Chui YP,** Wang XL, Ye HM. Low birth weight and insulin resistance. *Guowai Yixue Erkexue Fence* 2003; **30**: 10-13

4 **Lucas A.** Programming by early nutrition: an experimental approach. *J Nutr* 1998; **128**(2 Suppl): s401-s406

5 **Ziegler TR,** Estivariz CF, Jonas CR, Gu LH, Jones DP, Leader LM. Interactions between nutrients and peptide growth factors in intestinal growth, repair, and function. *J Parenter Enteral Nutr* 1999; **23**(6 Suppl): s174-s183

6 **Li ZB,** Wu SW, Qian LH. Regulatory effects of bombesin on the activities of disaccharidase in the intestinal mucosal cells in neonatal rabbits. *Shanghai Yixue Zazhi* 2001; **25**: 656-658

7 **Nichols BL,** Nichols VN, Putman M, Avery SE, Fraley JK, Quaroni A, Shiner M, Sterchi EE, Carrazza FR. Contribution of villous atrophy to reduced intestinal maltase in infants with malnutrition. *J Pediatr Gastroenterol Nutr* 2000; **30**: 494-502

8 **Gomez de Segura IA,** Vazquez P, Garcia P, Garcia P, Candela CG, Cos A, Gancedo PG, Lopez JM, De Miguel E. Effect of four enteral foods on the small bowel of undernourished rats after midgut resection. *Eur J Surg* 1999; **165**: 491-499

9 **Gura T.** Obesity research. Tracing leptin's partners in regulating body weight. *Science* 2000; **287**: 1738-1741

10 **Jaquet D,** Leger J, Tabone MD, Czernichow P, Levy-Marchal C. High Serum leptin concentrations during catch-up growth of children born with intrauterine growth retardation. *J Clin Endocri Metab* 1999; **84**: 1949-1952

11 **Kalra SP,** Kalra PS. Neuropeptide Y: a physiological orexigen modulated by the feedback action of ghrelin and leptin. *Endocrine* 2003; **22**: 49-56

Science Editor Wang XL and Guo SY **Language Editor** Elsevier HK

PO Box 2345, Beijing 100023, China
www.wjgnet.com
wjg@wjgnet.com

ELSEVIER

World J Gastroenterol 2005;11(28):4423-4426
World Journal of Gastroenterology ISSN 1007-9327

• *BRIEF REPORTS* •

Protection against hepatic ischemia/reperfusion injury via downregulation of toll-like receptor 2 expression by inhibition of Kupffer cell function

Jin-Xiang Zhang, He-Shui Wu, Hui Wang, Jin-Hui Zhang, Yang Wang, Qi-Chang Zheng

Jin-Xiang Zhang, He-Shui Wu, Yang Wang, Department of Emergency Surgery, Union Hospital, Tongji Medical College, Huazhong University of Science and Technology, Wuhan 430030, Hubei Province, China
Hui Wang, Hereditary Department, Tongji Medical College, Huazhong University of Science and Technology, Wuhan 430030, Hubei Province, China
Jin-Hui Zhang, Qi-Chang Zheng, Department of General Surgery, Union Hospital, Tongji Medical College, Huazhong University of Science and Technology, Wuhan 430030, Hubei Province, China
Supported by the National Natural Science Foundation of China, No. 30200272
Co-first-authors: Jin-Xiang Zhang, He-Shui Wu and Hui Wang
Co-correspondence: He-Shui Wu
Correspondence to: Dr. Jin-Xiang Zhang, Department of Emergency Surgery, Union Hospital, Tongji Medical College, Huazhong University of Science and Technology, Wuhan 430030, Hubei Province, China. camelzjx@yahoo.com.cn
Telephone: +86-27-62707120
Received: 2004-08-18 Accepted: 2004-12-14

Abstract

AIM: To elucidate the mechanism of liver protection by inhibition of Kupffer cells (KCs) function.

METHODS: All the animals were randomly divided into three groups. Blockade group (gadolinium chloride solution ($GdCl_3$) injection plus ischemia/reperfusion (I/R) injury): $GdCl_3$ solution was injected once every 24 h for 2 d via the tail vein before I/R injury. Non-blockade group (saline solution injection plus I/R injury): saline instead of $GdCl_3$ as a control was injected as in the blockade group. Sham group: saline was injected without I/R injury. Liver samples were collected 4 h after blood inflow restoration. The blockade of the function of KCs was verified by immunostaining with an anti-CD68 mAb. Toll-like receptor 2 (TLR2) was immunostained with a goat antimouse polyclonal anti-TLR2 antibody. Membrane proteins were extracted from the liver samples and TLR2 protein was analyzed by Western blot. Portal vein serum and plasma were taken respectively at the same time point for further detection of the levels of tumor necrosis factor-α (TNF-α) and alanine aminotransferase (ALT), an indicator of liver function.

RESULTS: Compared to non-blockade group, $CD68^+$ cells significantly reduced in blockade group (OPTDI, optical density integral): 32.97±10.55 *vs* 185.65±21.88, $P<0.01$) and the liver function impairment was relieved partially (level of ALT: 435.89±178.37 U/L *vs* 890.21±272.91 U/L, $P<0.01$). The expression of TLR2 protein in blockade group significantly decreased compared to that in non-blockade group (method of immunohistochemistry, OPDTI: 75.74±17.44 *vs* 170.58±25.14, $P<0.01$; method of Western blot, *A* value: 125.89±15.49 *vs* 433.91±35.53, $P<0.01$). The latter correlated with the variation of CD68 staining ($r = 0.745$, $P<0.05$). Also the level of portal vein TNF-α decreased in blockade group compared to that in non-blockade group (84.45±14.73 ng/L *vs* 112.32±17.56 ng/L, $P<0.05$), but was still higher than that in sham group (84.45±14.73 ng/L *vs* 6.07±5.33 ng/L, $P<0.01$).

CONCLUSION: Inhibition of the function of KCs may protect liver against I/R injury via downregulation of the expression of TLR2.

Key words: Toll-like receptor 2; Reperfusion injury; Kupffer cell; Liver

Zhang JX, Wu HS, Wang H, Zhang JH, Wang Y, Zheng QC. Protection against hepatic ischemia/reperfusion injury via downregulation of toll-like receptor 2 expression by inhibition of Kupffer cell function. *World J Gastroenterol* 2005; 11 (28): 4423-4426
http://www.wjgnet.com/1007-9327/11/4423.asp

INTRODUCTION

Hepatic ischemia/reperfusion (I/R) injury is one of the major complications of liver resection surgery, transplantation, and hypovolemic shock[1,2]. Although the detailed biochemical mechanisms are unclear, activation of Kupffer cells (KCs) may play an important role. During the very early phase of I/R injury, the secretion of proinflammatory cytokines by activated KCs, such as TNF-α, interleukin-1, participates in liver I/R injury, which precedes the activation of adhesion factors, chemotactic agents, and the sequestration of neutrophils in liver. Neutrophil accumulation in the liver causes direct hepatocellular damage through exhaustion of hepatic microcirculation by blocking the capillary perfusion and releasing proteases. So that we can see that KCs are among the first and key cells that mediate hepatic I/R injury [3]. Inhibition of the function of KCs elicits the protection against liver I/R injury. The mechanism of KCs in such an insult remains unclear. Endotoxin or lipopolysaccharide is a strong stimulator inducing KCs to secret proinflammatory

mediators and ultimately leading to endotoxin-induced liver injury[4,5]. In order to clarify the mechanism of I/R injury without the effect of endotoxin and the corresponding cytokines evoked by endotoxin[5,6], we reproduced a lobar rather than total hepatic I/R injury in a mouse model to produce a severe hepatic ischemic insult without mesenteric venous congestion. So that the development of intestinal congestion and leakage of bacteria or bacterial products into the circulation can be avoided[6,7].

TLR family members, a kind of newly found transmembrane peptides, recognize pathogen-associated molecular patterns derived from both Gram-negative and Gram-positive bacteria such as endotoxin and are capable of sensitizing danger signals in *in vivo* environment[1,7,8]. TLRs participate in the initiation of the downstream inflammatory cascades[8,9]. In previous studies, we have proved that TLR2 and TLR4 are involved in the hepatic I/R pathologic process and the activation of them is not related to endotoxin[10,11]. Whether TLR2 expression is affected by the function of KCs is still unknown. $GdCl_3$ is a kind of experimental drug, which is capable of blocking KC function specifically, while it has no effect on other macrophages, such as those residing in lung or intestinal canals[12,13]. CD68 is a pan-macrophage endosomal glycoprotein, which belongs to a family of acidic, highly glycosylated lysosomal glycoproteins and is found in cytoplasmic granules. It is considered as a specific indicator of KC activation[14]. That is why we used CD68 immunohistological staining to assess the inhibition of KC function.

This experiment aimed to observe the variation of TLR2 expression after the inhibition of the function of KCs and to further clarify the protective mechanism against hepatic I/R injury induced by inhibition of the function of KCs.

MATERIALS AND METHODS

Animal model and grouping

Male BALB/c mice weighing 20-25 g were supplied by Experimental Animal Center in Tongji Medical College. Their age ranged 6-8 wk. The animals were fasted for 12 h with free access to water and randomly divided into $GdCl_3$ injection plus I/R injury group (blockade group), saline solution injection plus I/R injury group (non-blockade group), and sham operation group (sham group). The animals in blockade group received injections of $GdCl_3$ solution (0.1 mmol/kg body weight, Sigma, USA) via tail vein once every 24 h for two times. The operation was performed 24 h after the last injection. The animals in non-blockade group were injected saline solution as control. Mice were anesthetized with pentobarbital (60 mg/kg). Laparotomy was performed through a midline incision and an atraumatic clip was placed across the hepatic hilar to interrupt blood supply to the left and median lobes of the liver. After 60 min of partial hepatic ischemia, the clip was removed to initiate hepatic reperfusion. Sham group mice underwent the same protocol as the control group without vascular occlusion. After the tissue was removed, animals were euthanized by injection of an overdose of pentobarbital. All studies were approved by the Institutional Animal Care and Use Committee of Tongji Medical College.

Detection of KC function variation after injection of $GdCl_3$ by CD68 stain

Liver samples from ischemic lobes were taken after 4 h of blood supply restoration and immediately fixed with 40 g/L formaldehyde, dehydrated, and embedded in paraffin for immu-nohistopathologic examination. Four micrometers of thick sections were stained with anti-CD68 Ab (Boster Bio. Co., Wuhan, China). The results were analyzed with a HPIAS pathological image analyzer and expressed as optical density integral (OPTDI).

Detection of TLR2 protein in ischemic hepatic lobes

Membrane proteins of ischemic liver tissues (100 mg) were extracted (1× PBS, 10 mL/L NP40, 5 g/L sodium desoxycholate, 1 g/L sodium dodecyl sulfate, 10 g/L phenylmethylsulfonyl fluoride, 30 mL/L aprotinin, 1 mol/L sodium orthovanadate). After quantification and aliquot, the samples were degenerated by boiling, separated on 85 g/L SDS-PAGE and transferred to nitrocellulose membranes. Filters were blocked 50 g/L nonfat milk in blocking buffer (TBS-T, 50 mmol/L Tris-Cl, pH 7.5, 150 mmol/L NaCl, 0.2 g/L Tween 20), and incubated with anti-TLR2 antibody (Santa Cruz, CA, USA) for 2 h and with peroxidase-conjugated secondary antibody for 1 h at 37 ℃. Specific bands were revealed with DAB solution and analyzed by Gel-Pro-Analyzer 4 as the value of *A*.

Other 4-μm-thick sections were stained with a goat antimouse TLR2 polyclonal antibody (Santa Cruz, CA, USA). The results were expressed as OPTDI and analyzed with a HPIAS pathological image analyzer.

The relationship between the expressions of CD68 and TLR2 was analyzed with Spearman, bivariate assay.

Examination of ALT and TNF-α in portal vein after injection of $GdCl_3$

Blood samples from portal vein were taken for assay of plasma alanine aminotransferase (ALT) and TNF-α level. The ALT activity was determined by an automatic biochemistry analyzer (HITACHI 2000, Japan) in Laboratory of Union Hospital. TNF-α level was assayed by an ELISA kit (JINGMEI Bio. Co., China).

Statistical analysis

All numeric data were expressed as mean±SD. Differences between blockade and non-blockade groups were analyzed by *t*-test with SPSS 10.0 software. The correlation between CD68 staining and TLR2 expression was analyzed with Spearman assay. $P<0.05$ was considered statistically significant.

RESULTS

Variation of KC function after injection of $GdCl_3$

When KCs were blocked with $GdCl_3$, the $CD68^+$ reaction was weaker in blockade group than in non-blockade group (Figure 1A). CD68 content was shown as absolute value OPTDI (Area×OPTDM), which was 32.97±10.55 *vs* 185.65 ±21.88. The difference between them was significant ($P<0.01$), suggesting that the function of KCs was inhibited in blockade group.

Detection of TLR2 in ischemic hepatic lobes by immunological stain

The positive immunoreaction of TLR2 in slices was weaker

in blockade group than in non-blockade group (Figure 1B), which was shown as OPDTI (75.74±17.44 *vs* 170.58±25.14). The difference between them was significant (P<0.01).

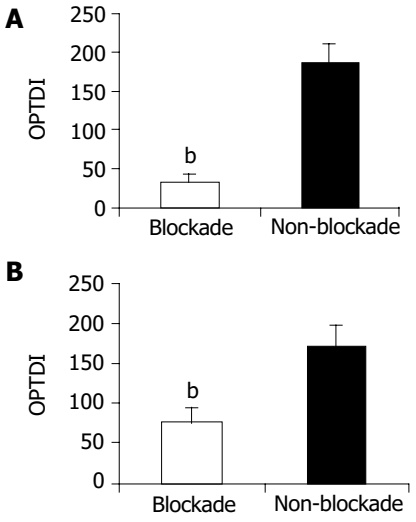

Figure 1 Effect of $GdCl_3$ injection on CD68 (**A**) and TLR2 (**B**) expression in blockade and non-blockade groups. ^bP<0.01 *vs* non-blockade group.

Variation of TLR2 protein expression in ischemic hepatic lobes

After 4 h restoration of blood supply, the expression of TLR2 protein, which was detected by Western blot increased in the non-blockade group compared to sham group (*A*: 433.91±35.53 *vs* 52.86±13.58, P<0.01). The injection of $GdCl_3$ significantly down regulated the expression of TLR2 in ischemic lobes compared to the non-blockade group (125.89±15.49 *vs* 433.91±35.53, P<0.01, Figure 2). Correlation analysis indicated that the downregulation of TLR2 expression between blockade and non-blockade groups was correlated with that of CD68 (r = 0.745, P<0.05).

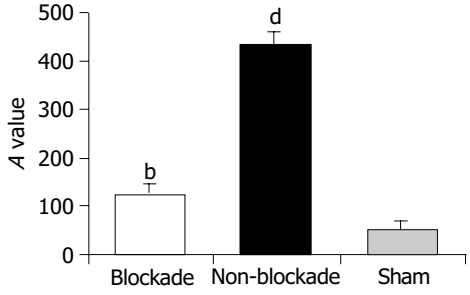

Figure 2 Detection of TLR2 expression by Western blot. ^bP<0.01 *vs* non-blockade group, ^dP<0.01 *vs* sham group.

Effect of $GdCl_3$ injection on portal vein plasma ALT and serum TNF-α

After 4 h restoration of blood supply, the level of ALT in portal vein, an indicator of liver function, was higher in non-blockade group than in sham group (890.21±272.91 U/L *vs* 40.66±15.42 U/L, P<0.01).The value in blockade group decreased to 435.89±178.37 U/L. The difference between blockade and non-blockade groups was significant (P<0.01, Figure 3A).

The serum TNF-α level in portal vein was higher in non-blockade group than in sham group (112.32±17.56 ng/L *vs* 6.07±5.33 ng/L, P<0.01) after 4 h blood supply restoration. When the function of KCs was blocked by injection of $GdCl_3$, the level of portal vein TNF-α was decreased remarkably (84.45±14.73 ng/L *vs* 112.32±17.56 ng/L, P<0.01), which might be an indirect indicator of KC inhibition (Figure 3B).

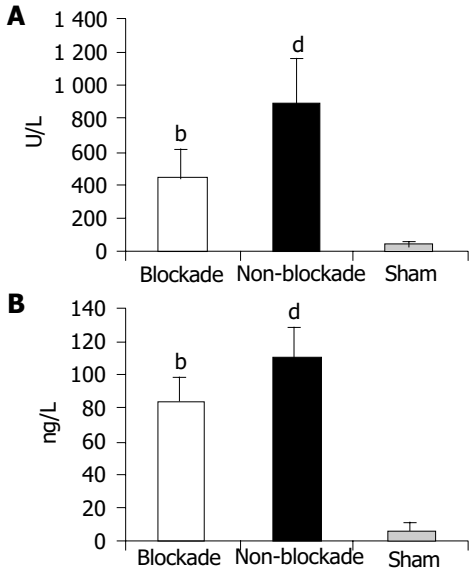

Figure 3 Portal vein ALT (**A**) and TNF-α (**B**) levels. ^bP<0.01 *vs* non-blockade group, ^dP<0.01 *vs* sham group.

DISCUSSION

KCs play an important part in mediating ischemia and reperfusion injury[15]. When activated during ischemia and subsequent reperfusion, they generate excessive inflammatory cytokines and oxygen-derived free radicals, which play a particularly important role in the pathogenesis of hepatic ischemia and reperfusion injury with an increased release of TNF-α and histological impairment. $GdCl_3$, a specific inhibitor of KCs, is often used as a tool for studying the role of KCs[16]. $GdCl_3$ is capable of protecting liver from injury mediated by the activation of KCs through depletion of lipid peroxidation. In the present study, injection of $GdCl_3$ selectively inhibited the activation of KCs, but did not induce hepatotoxicity. On the contrary, the impairment of liver function was relieved.

TLR2 can be activated during the process of hepatic I/R injury[10]. When TLR2 is activated, its cytoplasmic portion would conduct signals to two distinct signaling pathways, JNK and NF-κB, resulting in the proinflammatory cascade and excessive production of TNF-α[17]. TLRs recognize two kinds of signals. One is related to pathogen-associated molecular pattern molecules, which claims the existence of pathogens[9]; the other is linked with some danger signals inside or outside the body, which does not need the existence of pathogens[18]. Hypothesis infers that TLRs may be the

candidate of a key "gate" through which the down stream inflammatory cascade is initiated[17]. TLR2 and TLR4 are activated in liver I/R injury[10,11], but the factors regulating the expression of TLRs have not been revealed.

Previous study has proved that NF-κB activation may be important in "switching off" the cytokine cascade during I/R injury. TNF-α plays a central role in mediating such an insult[7]. Nevertheless, what happens preceding the NF-κB activation and TNF-α release? Where is the switch point that starts a crucial inflammatory cascade involving the activation of NF-κB during the I/R pathological process? Activation of TLR2 results in the activation of NF-κB[17], and NF-κB activation in the liver could be downregulated by KC blockade. In this paper, we confirmed that blocking the function of KCs downregulated the expression of TLR2 in ischemic lobes in mice partial hepatic I/R model, and the levels of TNF-α and ALT in portal vein decreased at the same time, suggesting that inhibition of KC function may protect liver from I/R injury by suppressing the release of TNF-α through downregulation of TLR2 expression. On the other hand, KCs might play an important role in mediating liver injuries and inflammatory disorders in the liver by changing the TLR2 signal transduction pathway. But compared to the sham group, the levels of portal vein TNF-α and ALT were still higher in blockade group, indicating that besides activation of KCs there are other factors regulating the expression of TLR2. Whether KCs themselves or cytokines secreted by KCs regulate the expression of TLR2 in ischemic lobes remains unclear.

KCs are major contributors to cytokine production in hepatic I/R injury[15]. Although many factors, including reactive oxygen species, Ca^{++} overload, adhesive molecules, nitrogen monoxide, *etc*, contribute to the pathogenesis of hepatic I/R injury, all these factors exert their role after the activation of KCs and the resulting inflammatory cascade[3]. Further study on inflammatory reaction controlled by TLRs and KCs may resolve the enigma of hepatic I/R injury.

ACKNOWLEDGMENTS

Authors thank Professor Du-Jun Ye, Pathophysiology Department, Tongji Medical College, Huazhong University of Science and Technology, for his helpful discussions. An excellent technical assistance of Dr. Yun Yang is acknowledged.

REFERENCES

1 **Fondevila C,** Busuttil RW, Kupiec-Weglinski JW. Hepatic ischemia/reperfusion injury-a fresh look. *Exp Mol Pathol* 2003; **74**: 86
2 **Jaeschke H.** Mechanisms of reperfusion injury after warm ischemia of liver. *J Hepatobiliary Pancreat Surg* 1998; **5**: 402
3 Teoh NC, Farrell GC. Hepatic ischemia reperfusion injury: Pathogenic mechanisms and basis for hepatoprotection. *J Gastroenterol Hepatol* 2003; **18**: 891
4 **Enomoto N,** Ikejima K, Yamashina S, Hirose M, Shimizu H, Kitamura T, Takei Y, Sato And N, Thurman RG. Kupffer cell sensitization by alcohol involves increased permeability to gut-derived endotoxin. *Alcohol Clin Exp Res* 2001; **25**: 51S
5 **Lukkari TA,** Jarvelainen HA, Oinonen T, Kettunen E, Lindros KO. Short-term ethanol exposure increases the expression of Kupffer cell CD14 receptor and lipopolysaccharide binding protein in rat liver. *Alcohol Alcohol* 1999; **34**: 311
6 **Kojima Y,** Suzuki S, Tsuchiya Y, Konno H, Baba S, Nakamura S. Regulation of pro-inflammatory and anti-inflammatory cytokine responses by Kupffer cells in endotoxin-enhanced reperfusion injury after total hepatic ischemia. *Transpl Int* 2003; **16**: 231
7 **Colletti LM,** Remick DG, Burtch GD, Kunkel SL, Strieter RM, Campbell DA Jr. Role of tumor necrosis factor-alpha in the pathophysiologic alterations after hepatic ischemia/reperfusion injury in the rat. *J Clin Invest* 1990; **85**: 1936
8 **Frantz S,** Kelly RA, Bourcier T. Role of TLR-2 in the activation of nuclear factor kappaB by oxidative stress in cardiac myocytes. *J Biol Chem* 2001; **276**: 5197
9 **Takeuchi O,** Akira S. Toll-like receptors; their physiological role and signal transduction system. *Int Immunopharmacol* 2001; **1**: 625
10 **Zhang JX,** Wu HS, Wang L, Zhang JH, Wang H, Zheng QC. TLR2 mRNA upregulation in ischemic lobes in mouse partial hepatic ischemia/reperfusion injury model. *J HUST* 2004; **24**: 144-146
11 **Wu HS,** Zhang JX, Wang L, Tian Y, Wang H, Rotstein O. Toll-like receptor 4 involvement in hepatic ischemia/reperfusion injury in mice. *Hepatobiliary Pancreat Dis Int* 2004; **3**: 250
12 **Lee CM,** Yeoh GC, Olynyk JK. Differential effects of gadolinium chloride on Kupffer cells *in vivo* and *in vitro*. *Int J Biochem Cell Biol* 2004; **36**: 481
13 **Gloor B,** Todd KE, Lane JS, Lewis MP, Reber HA. Hepatic Kupffer cell blockade reduces mortality of acute hemorrhagic pancreatitis in mice. *J Gastrointest Surg* 1998; **2**: 430
14 **Ramprasad MP,** Terpstra V, Kondratenko N, Quehenberger O, Steinberg D. Cell surface expression of mouse macrosialin and human CD68 and their role as macrophage receptors for oxidized low density lipoprotein. *Proc Natl Acad Sci USA* 1996; **93**: 14833
15 **Schumann J,** Wolf D, Pahl A, Brune K, Papadopoulos T, van Rooijen N, Tiegs G. Importance of Kupffer Cells for T-Cell-Dependent Liver Injury in Mice. *Am J Pathol* 2000; **157**: 1671
16 **Rivera CA,** Bradford BU, Hunt KJ, Adachi Y, Schrum LW, Koop DR, Burchardt ER, Rippe RA, Thurman RG. Attenuation of CCl4-induced hepatic fibrosis by GdCl3 treatment or dietary glycine. *Am J Physiol Gastrointest Liver Physiol* 2001; **281**: G200
17 **Yang RB,** Mark MR, Gray A, Huang A, Xie MH, Zhang M, Goddard A, Wood WI, Gurney AL, Godowski PJ. Toll-like receptor-2 mediates lipopolysaccharide-induced cellular signalling. *Nature* 1998; **395**: 284
18 **Matzinger P.** The danger model: a renewed sense of self. *Science* 2002; **296**: 301

Science Editor Wang XL and Guo SY **Language Editor** Elsevier HK

PO Box 2345, Beijing 100023, China
www.wjgnet.com
wjg@wjgnet.com

ELSEVIER

World J Gastroenterol 2005;11(28):4427-4430
World Journal of Gastroenterology ISSN 1007-9327

• *BRIEF REPORTS* •

Effect of *c-fos* antisense probe on prostaglandin E_2-induced upregulation of vascular endothelial growth factor mRNA in human liver cancer cells

Yong-Qi Li, Kai-Shan Tao, Ning Ren, Yi-Hu Wang

Yong-Qi Li, Ning Ren, Yi-Hu Wang, Comprehensive Diagnostic and Therapeutic Center, Xijing Hospital, the Fourth Military Medical University, Xi'an 710033, Shaanxi Province, China
Kai-Shan Tao, Department of Hepatobiliary Surgery, Xijing Hospital, the Fourth Military Medical University, Xi'an 710033, Shaanxi Province, China
Correspondence to: Dr. Yong-Qi Li, Comprehensive Diagnostic and Therapeutic Center, Xijing Hospital, the Fourth Military Medical University, Xi'an 710033, Shaanxi Province, China. yongqil33@yahoo.com.cn
Telephone: +86-29-83375151 Fax: +86-29-82516966
Received: 2005-03-01 Accepted: 2005-05-13

Abstract

AIM: To examine the effect of prostaglandin E_2 (PGE_2) on the expression of vascular endothelial growth factor (VEGF) mRNA in the human hepatocellular carcinoma (HCC) HepG2 cells and the possible involvement of c-fos protein in this process.

METHODS: Human HCC HepG2 cells were divided into three groups treated respectively with PGE_2, a combination of PGE_2 and *c-fos* antisense oligodeoxynucleotide (ASO), and PGE_2 plus *c-fos* sense oligodeoxynucleotide (SO). The expression of VEGF mRNA in HepG2 cells after different treatments was detected by reverse transcriptase-polymerase chain reaction (RT-PCR). The relative expression level of VEGF mRNA in HepG2 cells in each group was measured.

RESULTS: Administration of PGE_2 resulted in an increased expression of *c-fos* and VEGF mRNA in HepG2 cells. The relative expression level of *c-fos* mRNA reached the peak at 3 h (68.4±4.7%) after PGE_2 treatment, which was significantly higher than that at 0 h (20.6±1.7%, $P<0.01$). Whereas, the highest expression level of VEGF mRNA was observed at 6 h (100.5±6.1%) after PGE_2 treatment, which was significantly higher than that at 0 h (33.2±2.4%, $P<0.01$). *C-fos* ASO significantly reduced PGE_2-induced VEGF mRNA expression in HepG2 cells.

CONCLUSION: PGE_2 increases the expression and secretion of VEGF in HCC cells by activating the transcription factor *c-fos*, promotes the angiogenesis of HCC and plays an important role in the pathogenesis of liver cancer.

Key words: Hepatocellular carcinoma; Prostaglandin E_2; *c-fos*; Vascular endothelial growth factor; Angiogenesis

Li YQ, Tao KS, Ren N, Wang YH. Effect of *c-fos* antisense probe on prostaglandin E_2-induced upregulation of vascular endothelial growth factor mRNA in human liver cancer cells. *World J Gastroenterol* 2005; 11(28): 4427-4430
http://www.wjgnet.com/1007-9327/11/4427.asp

INTRODUCTION

PGE_2 is produced in various kinds of cancer cells and seems to be particularly important for carcinogenesis[1-3]. PGE2 activates multiple G-protein-linked receptor subtypes (EP1-EP4) in an autocrine or paracrine fashion, which may lead to tumor growth promotion via growth factors and oncogenes[4-6]. However, the mechanism of PGE_2 in promoting tumor growth still remains unclear. VEGF is a regulator of pathological angiogenesis and plays an important role in tumor growth. Studies have revealed that VEGF can be produced by liver cancer cells in a paracrine manner, thus promoting the angiogenesis of liver cancer[7,8]. Studies also indicate that many tumor growth factors stimulate the production of VEGF in tumor cells[3,9]. This study was undertaken to estimate if PGE_2 could affect the expression of VEGF in HCC HepG2 cells and the possible involvement of the oncogene *c-fos* in this process.

MATERIALS AND METHODS

Cell culture and PGE_2 administration

HepG2 cells were cultured in RPMI-1640 medium (Gibco) containing 10 mL/L fetal bovine serum, 100 kU/L penicillin and 0.1 g/L streptomycin at 37 ℃ in 50 mL/L CO_2/950 mL/L air for 4-6 d and then put into fresh 35 mm dishes. Twenty-four hours later, PGE_2 (Sigma) was added into each dish in a final concentration of 1 μmol/L. The dose of PGE_2 in the present study was chosen based on the previous reports and our preliminary experiments. The cells were then cultured for 0, 1, 3, 6, 12, and 24 h, respectively (n = 4/each time point) and collected for RNA extraction.

C-fos ASO administration

C-fos ASO (5'-GAACATCATCGTGGC-3') was synthesized according to reported human *c-fos* mRNA sequence (GenBank Accession No. M16287). C-*fos* SO (5'-GCCA-CGATGATGTTC-3') was also synthesized as a control. Both ASO and SO were modified phosphorothioate

oligodeoxynucleotide.

HepG2 cells were cultured as mentioned above and divided into: (1) control group in which 10 μL physical saline was added, (2) PGE_2-treated groups in which 1 μmol/L of PGE_2 was added, (3) SO-treated group in which 10 μL (50 μg) *c-fos* SO was added followed by addition of 1 μmol/L of PGE_2 after 30 min, (4) ASO-treated group in which 10 μL (50 mg) *c-fos* ASO was added followed by addition of 1 μmol/L of PGE_2 after 30 min. The cells were cultured for 6 h and then collected for RNA extraction.

Primer design and synthesis

Specific primers for human *c-fos* and VEGF were synthesized according to their reported mRNA sequences. The primer pair of *c-fos* were: sense: 5'- TGC TGA AGG AGA AGG AAA AA -3'; antisense: 5'- TGC ATA GAA GGA CCC AGA TA -3' (GenBank Accession No. M16287). The primer pair of VEGF were: sense: 5'-ACC CAT GGC AGA AGG AGG AG -3' antisense 5'-ACG CGA GTC TGT GTT TTT GC-3' (GenBank Accession No. M32977). The primers (sense: 5'- GGC ATC CAC GAA ACT ACC TT-3' antisense 5'-CGT CAT ACT CCT GCT TGC TG -3') for human β-actin (GenBank Accession No. M10277) were also synthesized as internal control in the PCR reaction. The length of PCR product for *c-fos*, VEGF and β-action was 344 bp, 433 bp and 274 bp, respectively.

RNA extraction

Total cellular RNA was extracted from $HepG_2$ cells using TRIzol reagent (Invitrogen) according to the manufacturer's instructions. The purity and integrity of the RNA samples were assessed by $A_{260/280}$ spectrophotometric measurement.

RT-PCR

After measurement of the concentration, cDNA was reversely transcribed in a 50 μL mixture containing 2 μg total RNA, 10 μL 5× RT buffer, 5 μL 10 mmol/L dNTPs, 0.5 μL RNase inhibitor (4×10^5 U/L, Invitrogen) 0.5 μL oligo $(dT)_{12\text{-}18}$ (500 g/L, Invitrogen) 1 μL SuperScript II reverse transcriptase (2×10^4 U/L, Invitrogen), 0.5 μL 0.1 mol/L DTT at 42 ℃ for 60 min followed by enzyme denaturation at 70 ℃ for 10 min. Thirty cycles of PCR were carried out in 25 μL reaction mixture containing 0.1 μg synthesized cDNA, 2.5 μL 10× PCR buffer, 2.5 μL dNTPs (2 mmol/L), 2.5 μL $MgCl_2$ (2.5 mmol/L), 1 μL of each primer (20 μmol/L), 2.5 u of Taq DNA polymerase (Takara) using a PTC-100 programmed thermal controller (MJ Research), each consisting of denaturation at 94 ℃ for 1 min, annealing at 56 ℃ for 30 s, extension at 72 ℃ for 1 min. Then, 10 μL of each PCR product was separated by electrophoresis on a 30 g/L agarose gel and visualized by ethidium bromide staining.

Statistical analysis

For each template, PCR amplification was performed 2-3 times. The electrophoresis results were observed through a gel imaging system (UVP) and the density of each positive band was analyzed by Labworks software. The relative expression level of *c-fos* and VEGF mRNA was expressed as a ratio of densitometric measurements (*c-fos*/β-actin or VEGF/β-actin). The data were expressed as mean±SE, and analyzed by analysis of variance and Dunnets test using SPSS10.1 software.

RESULTS

Effect of PGE_2 on expression of c-fos and VEGF mRNA in HepG2 cells

Addition of PGE_2 to the HepG2 cells resulted in a time-dependent increase in the expression of *c-fos* and VEGF mRNA (Figure 1A). Compared to the expression level at 0 h (20.6±1.7%), the expression of *c-fos* mRNA induced by PGE_2 treatment reached the highest level at 1 h (62.3±4.3%, $P<0.01$) and 3 h (68.4±4.7%, $P<0.01$), and slightly higher level at 6 h (55.3±3.8%, $P<0.05$; Figure 1B). The expression level of VEGF mRNA significantly increased at 3 h after PGE_2 administration (87.6±6.4%, $P<0.01$) when compared to the expression level at 0 h (33.2±2.4%). Its expression level reached a maximum at 6 h (100.5±6.1%, $P<0.01$). At 24 h, the expression level returned to its level at 0 h (35.2±2.8%, $P>0.05$; Figure 1B). The expression level of β-actin mRNA remained unchanged at each time-point, indicating the equal amount of the template used in PCR.

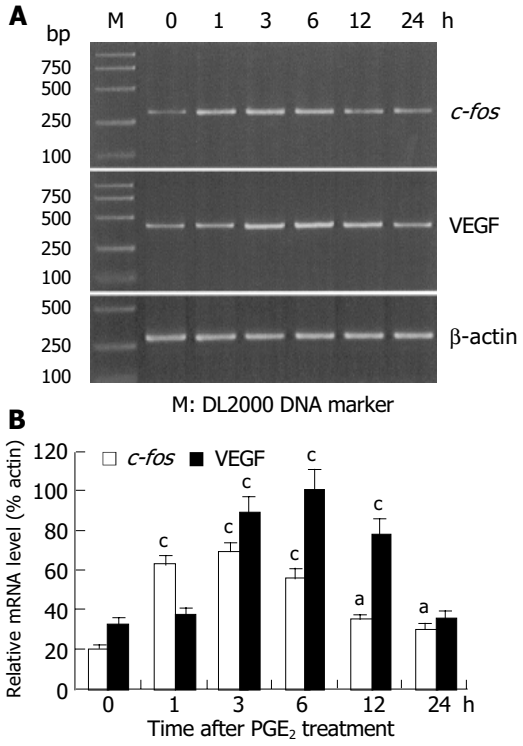

Figure 1 RT-PCR results (**A**) and histographs (**B**) showing effect of PGE_2 on expression of *c-fos* and VEGF mRNA in HepG2 cells. $^aP<0.05$, $^cP<0.05$ *vs* 0 h.

Effect of c-fos ASO on PGE_2-induced upregulation of VEGF mRNA in HepG2 cells

Since the maximal expression level of VEGF mRNA was at 6 h after PGE_2 treatment, this time-point was selected to observe the effect of *c-fos* ASO. The results showed that the expression level of VEGF mRNA significantly decreased in *c-fos* ASO-treated group (39.6±3.2%) when compared to that in PGE_2-treated group (98.6±6.4%, $P<0.01$, Figure 2A

and B). In contrast, no such change in *c-fos* SO-treated group was observed (95.2±6.3%, $P>0.05$).

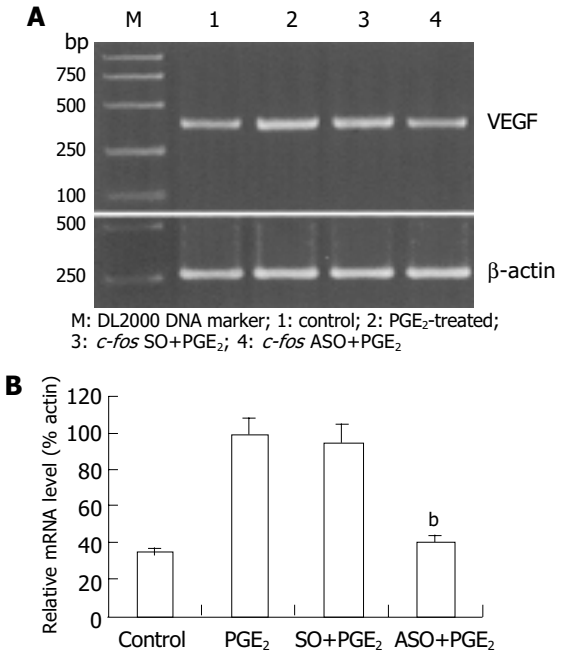

Figure 2 RT-PCR results (**A**) and histographs (**B**) showing effect of *c-fos* ASO on PGE_2-induced VEGF mRNA expression in HepG2 cells. $^bP<0.01$ *vs* PGE_2 group.

DISCUSSION

At present, the exact pathological function and mechanism of PGE_2 in tumors are not fully known. Previous studies indicate that PGE_2 can be produced by tumor cells and plays an important role in tumor immune inhibition[10-12]. Some studies revealed that the PGE_2 level in patients with cancer is higher than that in normal people, and that tumor tissues also contain higher concentration of PGE_2 than normal tissues[13]. Animal experiments indicate that PGE_2 produced by tumor cells, can promote the growth and development of tumors through its immune inhibitory function[10]. Further studies have proved that PGE_2 promotes the growth of liver cancer through its receptor EP3[14]. In the present study, we observed that PGE_2 could stimulate the expression of VEGF mRNA in HepG2 cells in a time-dependent manner, suggesting that PGE_2 may promote the angiogenesis of HCC by increasing the secretion of VEGF from liver cancer cells. This might be one of the mechanisms of PGE_2 in facilitating the growth of liver cancer.

It is well known that the oncogene *c-fos* can function as a third intracellular messenger. Its product Fos protein can form a homo-dimer itself or hetero-dimer with c-Jun protein and then binds to the AP-1 site in the target gene, thus promoting the transcription of target gene. It has been reported that the promoter region for the VEGF gene contains several AP-1 binding motifs[15] and the expression of VEGF gene is controlled by transcription factors AP-1 and AP-2[16-18]. In the present study, we observed that PGE_2 increased the expression of *c-fos* mRNA, the maximal level was at 1 and 3 h after PGE_2 administration, earlier than the PGE_2-induced highest expression of VEGF mRNA. Furthermore, *c-fos* ASO significantly reversed PGE_2-induced VEGF mRNA expression. These results indicate that Fos protein is involved in the PGE_2-induced VEGF expression in HepG2 cells.

The intracellular signaling pathway coupled to PGE_2 is complicated. As a third intracellular messenger, *c-fos* is just located in the downstream of the signaling pathway. Many other molecules should also be involved in the modulation of VEGF expression by PGE_2. In addition, several PGE_2 receptors are present in HCC[6,19]. Which receptors mediate the role of PGE_2 in tumor growth needs to be investigated.

In conclusion, PGE_2 stimulates VEGF induction in HepG2 cells by activating the transcription factor Fos protein.

ACKNOWLEDGMENT

The authors thank Dr. SX Wu, Department of Anatomy, Faculty of Basic Medicine, Fourth Military Medical University for his technical assistance and help with preparation of the manuscript.

REFERENCES

1 **Bishop-Bailey D,** Calatayud S, Warner TD, Hla T, Mitchell JA. Prostaglandins and the regulation of tumor growth. *J Environ Pathol Toxicol Oncol* 2002; **21**: 93-101
2 **Ito H,** Duxbury M, Benoit E, Clancy TE, Zinner MJ, Ashley SW, Whang EE. Prostaglandin E2 enhances pancreatic cancer invasiveness through an Ets-1-dependent induction of matrix metalloproteinase-2. *Cancer Res* 2004; **64**: 7439-7446
3 **Leung WK,** To KF, Go MY, Chan KK, Chan FK, Ng EK, Chung SC, Sung JJ. Cyclooxygenase-2 upregulates vascular endothelial growth factor expression and angiogenesis in human gastric carcinoma. *Int J Oncol* 2003; **23**: 1317-1322
4 **Ushio A,** Takikawa Y, Lin SD, Miyamoto Y, Suzuki K. Induction of Bcl-xL is a possible mechanism of anti-apoptotic effect by prostaglandin E2 EP4-receptor agonist in human hepatocellular carcinoma HepG2 cells. *Hepatol Res* 2004; **29**: 173-179
5 **Yamaki T,** Endoh K, Miyahara M, Nagamine I, Thi Thu Huong N, Sakurai H, Pokorny J, Yano T. Prostaglandin E2 activates Src signaling in lung adenocarcinoma cell *via* EP3. *Cancer Lett* 2004; **214**: 115-120
6 **Amano H,** Hayashi I, Endo H, Kitasato H, Yamashina S, Maruyama T, Kobayashi M, Satoh K, Narita M, Sugimoto Y, Murata T, Yoshimura H, Narumiya S, Majima M. Host prostaglandin E(2)-EP3 signaling regulates tumor-associated angiogenesis and tumor growth. *J Exp Med* 2003; **197**: 221-232
7 **Imura S,** Miyake H, Izumi K, Tashiro S, Uehara H. Correlation of vascular endothelial cell proliferation with microvessel density and expression of vascular endothelial growth factor and basic fibroblast growth factor in hepatocellular carcinoma. *J Med Invest* 2004; **51**: 202-209
8 **Qin LX,** Tang ZY. Recent progress in predictive biomarkers for metastatic recurrence of human hepatocellular carcinoma: a review of the literature. *J Cancer Res Clin Oncol* 2004; **13**: 497-513
9 **Casibang M,** Purdom S, Jakowlew S, Neckers L, Zia F, Ben-Av P, Hla T, You L, Jablons DM, Moody TW. Prostaglandin E2 and vasoactive intestinal peptide increase vascular endothelial cell growth factor mRNAs in lung cancer cells. *Lung Cancer* 2001; **31**: 203-212
10 **Harris SG,** Padilla J, Koumas L, Ray D, Phipps RP. Prostaglandins as modulators of immunity. *Trends Immunol* 2002; **23**: 144-150
11 **Rocca B,** FitzGerald GA. Cyclooxygenases and prostaglandins: shaping up the immune response. *Int Immunopharmacol* 2002;

2: 603-630

12 **Kaur K,** Harris SG, Padilla J, Graf BA, Phipps RP. Prostaglandin E2 as a modulator of lymphocyte mediated inflammatory and humoral responses. *Adv Exp Med Biol* 1999; **469**: 409-412

13 **Majima M,** Amano H, Hayashi I. Prostanoid receptor signaling relevant to tumor growth and angiogenesis. *Trends Pharmacol Sci* 2003; **24**: 524-529

14 **Hashimoto N,** Watanabe T, Ikeda Y, Yamada H, Taniguchi S, Mitsui H, Kurokawa K. Prostaglandins induce prolixferation of rat hepatocytes through a prostaglandin E2 receptor EP3 subtype. *Am J Physiol* 1997; **272**(3 Pt 1): G597-604

15 **Tischer E,** Mitchell R, Hartman T, Silva M, Gospodarowicz D, Fiddes JC, Abraham JA. The human gene for vascular endothelial growth factor. Multiple protein forms are encoded through alternative exon splicing. *J Bio Chem* 1991; **266**: 11947-11954

16 **Clifford SC,** Czapla K, Richards FM, O'Donoghue DJ, Maher ER. Hepatocyte growth factor-stimulated renal tubular mitogenesis: effects on expression of c-myc, c-fos, c-met, VEGF and the VHL tumour-suppressor and related genes. *Br J Cancer* 1998; **77**: 1420-1428

17 **Ryuto M,** Ono M, Izumi H, Yoshida S, Weich HA, Kohno K, Kuwano M. Induction of vascular endothelial growth factor by tumor necrosis factor alpha in human glioma cells. Possible roles of SP-1. *J Biol Chem* 1996; **271**: 28220-28228

18 **Ben-Av P,** Crofford LJ, Wilder RL, Hla T. Induction of vascular endothelial growth factor expression in synovial fibroblasts by prostaglandin E and interleukin-1: a potential mechanism for inflammatory angiogenesis. *FEBS Lett* 1995; **372**: 83-87

19 **Bhattacharya M,** Peri K, Ribeiro-da-Silva A, Almazan G, Shichi H, Hou X, Varma DR, Chemtob S. Location of functional prostaglandin E2 receptors EP3 and EP4 in the nuclear envelope. *J Biol Chem* 1999; **274**: 15719-15724

Science Editor Wang XL and Guo SY **Language Editor** Elsevier HK

PO Box 2345, Beijing 100023, China
www.wjgnet.com
wjg@wjgnet.com

ELSEVIER

World J Gastroenterol 2005;11(28):4431-4434
World Journal of Gastroenterology ISSN 1007-9327

• *BRIEF REPORTS* •

Risk factors for primary liver carcinoma in Chinese population

Rui-Hong Luo, Zhi-Xin Zhao, Xu-Yu Zhou, Zhi-Liang Gao, Ji-Lu Yao

Rui-Hong Luo, Zhi-Xin Zhao, Zhi-Liang Gao, Ji-Lu Yao, Department of Infectious Diseases, The Third Affiliated Hospital of Sun Yat-Sen University, Guangzhou 510630, Guangdong Province, China
Xu-Yu Zhou, Medical Information Institute, Sun Yat-Sen University, Guangzhou 510089, Guangdong Province, China
Correspondence to: Dr. Rui-Hong Luo, Department of Infectious Diseases, The Third Affiliated Hospital of Sun Yat-Sen University, Guangzhou 510630, Guangdong Province, China. ruihongluo2002@yahoo.com.cn
Telephone: +86-20-85263061
Received: 2004-10-09 Accepted: 2004-11-24

Abstract

AIM: To evaluate the risk factors for primary liver carcinoma (PLC) in Chinese population.

METHODS: Chinese Biomedical Literature Database, China Hospital Knowledge Database and MEDLINE were searched. All the related literatures were screened, and the risk factors for PLC in Chinese population were studied. Heterogeneity was evaluated by odds ratio (OR) *q* test. Combined OR and its 95% confidence interval (95%CI) were calculated, the association between the investigated risk factors and PLC was determined. Validity and bias of the findings were evaluated by sensitivity analysis and funnel plot analysis respectively.

RESULTS: Fifty-five of one hundred and ninety identified studies were accepted according to the inclusive criteria. Ten factors related to PLC were demonstrated by sensitive analysis and funnel plot analysis. They were cirrhosis (OR = 11.97, *P* = 0.000), HBV infection (OR = 11.34, *P* = 0.000), HCV infection (OR = 4.28, *P* = 0.000), family history of liver cancer (OR = 3.49, *P* = 0.000), unstable emotion (OR = 2.20, *P* = 0.000), depressed characters (OR = 3.07, *P* = 0.000), aflatoxin (OR = 1.80, *P* = 0.000), alcoholic (OR = 1.88, *P* = 0.000), intake of musty food (OR = 1.87, *P* = 0.000) and drinking contaminated water from pond (OR = 1.77, *P* = 0.003).

CONCLUSION: The main risk factors for PLC in China are liver diseases, family history of liver carcinoma, poor psychic status, aflatoxin, and some unhealthy behaviors.

Key words: Primary carcinoma; Liver; Meta-analysis; Risk factor

Luo RH, Zhao ZX, Zhou XY, Gao ZL, Yao JL. Risk factors for primary liver carcinoma in Chinese population. *World J Gastroenterol* 2005; 11(28): 4431-4434
http://www.wjgnet.com/1007-9327/11/4431.asp

INTRODUCTION

Primary liver carcinoma (PLC) affects more than 500 000 people globally with 110 000 deaths annually. More than one-half of them were Chinese[1]. The incidence rate is 14.58-46 per 100 000 people. In Qidong, Jiangsu Province and Fusui, Guangxi Zhuang Autonomous Region, the morbidity is higher than that in any other areas of China.

It is known that persistent hepatitis B virus (HBV) and HCV infection and aflatoxins are the main causes of PLC[1]. However, most of the investigations were case-control studies. The real risk factors for PLC may be far more than the known causes. The results from different investigated areas are variable. Cohort study on risk factors for PLC in Chinese people is still not available. A meta-analysis confined to case-control studies published from January 1966 to December 2003 was carried out.

MATERIALS AND METHODS

Search strategy

The databases including Chinese Biomedical Literature Database (1979-December 2003), China Hospital Knowledge Database (1994-December 2003) and MEDLINE (1966-December 2003) were searched. The following keywords were used: liver cancer, liver carcinoma, primary liver cancer, primary liver carcinoma, malignant liver tumors, primary liver tumors, hepatocellular carcinoma, hepatocellular cancer, risk factor, cause, etiology, case-control study. In the search of MEDLINE, the keywords of Chinese population, Chinese and China were added. Further studies were identified through scanning reference lists of relevant articles, reviews, and textbooks. Articles published in both English and Chinese were accepted. To eliminate irrelevant studies, the title and abstract of the articles were screened at first, and then the whole texts of selected paper were examined for further screening based the inclusive criteria.

Inclusion and exclusion criteria

Inclusion criteria in the meta-analysis included case-control studies investigating the risk factors for PLC in Chinese population, the data from the articles including the background of population and time investigated, the articles that reported original data or statistical results of odd ratio (OR) and its 95% confidence interval (95%CI), the studies based on similar diagnostic criteria of PLC.

Exclusion criteria in the meta-analysis were poor methodological quality[2], the republished studies, and no sufficient data and/or results in the article.

Data selection and study appraisal

Data used in this study included year of publication, number of case and control, characteristics of patients and control

(gender, age, native place, and living place), suspected risk factor and its definition of exposure, diagnostic criterion of PLC, and outcomes (OR value and its 95%CI of each factor should be provided, if the article did not report the results in the form of OR, we calculated OR and its 95%CI based on the given data).

Two researchers extracted the data from each study independently and any disagreements were discussed for consensus. Quality of the study was assessed by the guideline of Lichtenstein[2].

Statistical analysis

OR q test for heterogeneity was used to examine gross statistical heterogeneity among included studies. If K studies were included, OR_i ($i = 1, 2,\ldots, K$) was OR of the investigated factors in each study, OR_{ui} and OR_{li} were the upper and lower limit of its 95%CI respectively. V_i was variance calculated by the formula of $V_i = [\ln(OR_i/OR_{li})/1.96]^2$ or $V_i = [\ln(OR_{ui}/OR_i)/1.96]^2$. Weight ($W_i$) was calculated by $W_i = 1/V_i$. Supposed $y_i = \ln(OR_i)$ and $y_w = (\Sigma W_i y_i)/(\Sigma W_i)$. The heterogeneity among included studies was tested by $q = \Sigma [W_i(y_i - y_w)^2]$. If the q value was low ($P>0.05$), the results of the included studies were considered as significant homogeneity, otherwise significant heterogeneity existed among studies[3,4].

The association between investigated factors and PLC was presented as OR and its 95%CI. If the studies had no significant heterogeneity demonstrated by OR q test, fixed-effect model was used to calculate the combined OR and its 95%CI. Otherwise, random-effect model was used. Combined OR value greater than one indicated a risk factor for PLC. The significance of the combined OR was tested by $\chi^2 = (\Sigma W_i y_i)^2/(\Sigma W_i)$ with $g = 1$[3,4], and the significant level was $P = 0.05$.

Sensitivity analysis was performed through fixed-effect model and random-effect model. Coherence of the results from two models indicated a valid outcome[4].

Funnel plot analysis was used to assess the potential bias, and its symmetry was tested through linear regression model. Intercept 95%CI of linear regression function spanning 0 and its significant level greater than 0.1 indicated symmetric funnel plot[4].

RESULTS

Description of studies

Fifty-five of 190 identified studies were included in meta-analysis after the quality assessment of each study. They were published in Chinese in 1984-2002. The investigated people were from 24 cities located in 13 different provinces of China.

The investigated factors included liver diseases, family history, psychic status, past history of exposure to poison and style of living. The factors for liver diseases were from 26 studies of HBV infection, 15 of HCV infection, 9 of liver cirrhosis, and 20 of hepatitis history. There were 25 studies on family history of liver carcinoma. Psychological factors for PLC included 10 for negative living events, 6 for unstable emotions, and 6 for depressed characters. The past history of exposure to poison was from five studies of pesticide and four of aflatoxin. The living style included nine factors: drinking (22 studies), smoking (15 studies), intake of musty food (3 studies), intake of pickle (5 studies), intake of bean product (4 studies), tea (4 studies), drinking water from pond (8 studies), drinking water from river (2 studies), and drinking water from well (5 studies).

Heterogeneity of studies

OR q test was carried out in included studies (Table 1). No significant heterogeneity existed among the studies on HCV infection, unstable emotion, past history of exposure to aflatoxin, and intake of musty food ($P>0.05$). The remaining factors in the studies all had significant heterogeneity ($P<0.05$).

Association of outcomes

Association between the factors and PLC was shown by combined OR and its 95%CI. If heterogeneity was significant, OR was combined with random-effect model, otherwise, fixed-effect model was used (Table 2). The OR and its 95%CI of five factors including past history of exposure to pesticide, intake of bean products, tea, drinking water from river and well had no statistical significance ($P>0.05$). According to the value of OR, the strength of association in descending turn was liver cirrhosis, HBV infection, history of hepatitis, HCV infection, family history of liver carcinoma, depressed character, negative living events, unstable emotion, alcoholic, intake of musty food, aflatoxin, drinking water from pond, intake of pickle, and smoking, with their OR value greater than one, 95%CI beyond one. There was a statistical significance ($P<0.05$).

Sensitive analysis

The combined OR and its 95%CI of each factor were calculated by both fixed-effect model and random-effect model, and coherence of the results was assessed. The factors of exposure to pesticide and drinking water from well showed conflicting results from two models (combined OR and its 95%CI of fixed-effect model were 1.69 (1.24 and 2.29) and 0.74 (0.58 and 0.96) respectively). Other factors showed similar results from two models.

Funnel plot

Since only two studies were involved in the factor of drinking water from river, funnel plot analysis was insignificant. According to the linear regression models of funnel plots, four factors including history of hepatitis, negative living events, smoking, and intake of pickle existed as asymmetric funnel plots with their intercept 95%CI beyond 0 and $P<0.1$. Other factors showed symmetry funnel plots with their intercept 95%CI spanning 0 and $P>0.1$ in their linear regression models.

DISCUSSION

A considerable number of chemical agents have been proved to be directly carcinogenic for liver malignant tumor in animal experiments, and also most likely in human beings[5]. But still no evidence is presented as yet. It was reported that the risk factors for PLC include hepatitis viruses, liver

Table 1 Heterogeneity of investigated factors

Factors	Included studies	*q*	*P*
Liver diseases			
HBV infection	26	74.72	0.000[b]
HCV infection	15	10.68	0.711
Liver cirrhosis	9	23.61	0.003[b]
History of hepatitis	20	104.13	0.000[b]
Family history			
Family history of PLC	25	96.95	0.000[b]
Psychological factors			
Negative living events	10	25.54	0.002[b]
Unstable emotion	6	3.46	0.630
Depressed character	6	12.69	0.027[a]
Past history of exposure to poison			
Pesticide	5	16.99	0.002[b]
Aflatoxin	4	3.47	0.325
Living style			
Alcoholic	22	82.13	0.000[b]
Smoking	15	24.58	0.039[a]
Intake of musty food	3	3.72	0.156
Intake of pickle	5	23.73	0.000[b]
Intake of bean products	4	18.56	0.000[b]
Tea	4	16.03	0.001[b]
Drinking water from pond	8	649.10	0.000[b]
Drinking water from river	2	9.05	0.003[b]
Drinking water from well	5	10.44	0.034[a]

The values of *q* shown are statistical values of OR *q* test. [a]$P<0.05$ *vs* significant difference. [b]$P<0.01$ *vs* very significant difference.

Table 2 Summary of the association between factors and PLC

Factors	Total case / control	Combined OR	95%CI	χ^2 (g = 1)	*P*
Liver diseases					
HBV infection	3 390 / 4 604	11.34	8.72-14.75	327.60	0.000[b]
HCV infection	1 737 / 2 534	4.28	3.30-5.56	119.93	0.000[b]
Liver cirrhosis	1 689 / 2 609	11.97	6.19-23.19	54.46	0.000[b]
History of hepatitis	3 625 / 4 903	5.71	4.11-7.92	108.12	0.000[b]
Family history					
Family history of PLC	3 681 / 4 932	3.49	2.68-4.53	87.24	0.000[b]
Psychological factors					
Negative living events	1 688 / 2 096	2.65	1.69-4.15	17.90	0.000[b]
Unstable emotion	1 502 / 2 086	2.20	1.74-2.77	44.48	0.000[b]
Depressed character	1 355 / 1 777	3.07	2.10-4.47	33.99	0.000[b]
Past history of exposure to poison					
Pesticide	755 / 969	1.55	0.82-2.93	1.84	0.175
Aflatoxin	327 / 327	1.80	1.44-2.25	26.90	0.000[b]
Living style					
Alcoholic	3 207 / 3 983	1.88	1.53-2.32	35.60	0.000[b]
Smoking	2 408 / 3 347	1.24	1.09-1.41	10.90	0.001[b]
Intake of musty food	623 / 723	1.87	1.42-2.47	19.74	0.000[b]
Intake of pickle	1 233 / 1 602	1.69	1.34-2.13	47.56	0.000[b]
Intake of bean products	814 / 1 158	0.74	0.29-1.90	0.13	0.718
Tea	656 / 870	0.69	0.31-1.51	0.88	0.348
Drinking water from pond	1 561 / 1 614	1.77	1.09-2.87	8.65	0.003[b]
Drinking water from river	379 / 437	1.41	0.38-5.19	0.27	0.603
Drinking water from well	636 / 856	0.79	0.45-1.36	7.99	0.392

The values of χ^2 shown are statistical values of significant test of combined OR. [b]$P<0.01$ *vs* significant difference.

diseases, mycotoxins or phytotoxins, nutrition, social drugs, metabolic diseases, chemical agents, inorganic substances, medication, and ionizing radiation. However, in 10–15% of patients, there is no risk factor for the development of PLC[5]. This study investigated the association between possible risk factors and PLC in Chinese population by meta-analysis of case-control studies published in the past 37 years, and demonstrated the risk factors for PLC in Chinese population.

This study analyzed 19 suspected risk factors for PLC. The combined outcomes showed that liver diseases were the most important factors for PLC with much a greater OR value than any other factor. Both liver cirrhosis and HBV infection were strongly associated with PLC, with their OR being 11.97 and 11.34 respectively ($P<0.05$). The association between HCV infection and PLC was moderate, with its OR being 4.28 ($P<0.05$). Though history of hepatitis was significantly associated with PLC, its funnel plot was asymmetric. Therefore this outcome might have bias, possibly due to the published bias, and heterogeneity from

the different definitions of history of liver diseases in the included studies. Family history of PLC was another risk factor for PLC, with its OR being 3.61 ($P<0.05$), suggesting that people with family history of PLC have a higher risk. Poor psychological status can strengthen the risk for PLC. In this meta-analysis, the factors for unstable emotion and depressed character were significantly associated with PLC, with their OR being 2.20 and 3.07, respectively ($P<0.05$). The funnel plot of negative living events was asymmetric though its combined OR was significant. The reason may be the published bias, and the conclusion on negative living events could not be made. In regard to exposure to poison, two factors including exposure to aflatoxin or pesticide were investigated. It was demonstrated that aflatoxin played an important role in PLC[5]. In this meta-analysis, the outcome showed that aflatoxin was also a risk factor for PLC in Chinese population, with its OR being 1.80 ($P<0.005$), but it seems to be trivial when compared to the factors for liver diseases, family history of PLC and poor psychological status. The results indicated that there was no significant association between exposure to pesticide and PLC, with its OR being 1.55 ($P>0.05$). Furthermore, this result was unreliable because it was conflicting in sensitivity analysis. Hence, it is not clear whether exposure to pesticide is a risk factor for PLC. The living habits of drinking, intake of musty food and drinking water from pond were all significantly associated with PLC (OR was 1.88, 1.87, and 1.77 respectively, $P<0.05$), suggesting that they may enhance the risk for PLC. Though the factors of both smoking and intake of pickle had a significant combined OR (1.24 and 1.69 respectively, $P<0.05$), it was unable to draw conclusions because of the bias demonstrated by their asymmetric funnel plots ($P<0.1$). Drinking water from river was not significantly associated with PLC (OR = 1.41, $P>0.05$) and its bias was difficult to analyze by funnel plot due to its limited number of the included studies. Thus it is unknown whether it is a risk factor. The ORs of intake of bean products, tea and drinking water from well were all less than 1 (OR being 0.74, 0.69, and 0.79 respectively, $P>0.05$). These, results could not demonstrate that they are protective factors for PLC. Furthermore, the result of drinking water from well was unreliable because the results were conflicting in sensitivity analysis.

Meta-analysis is a tool, but bias in meta-analysis can cause invalid results. In this study, case-control studies were included in meta-analysis. Considering the design of the included studies, validity of their results was inferior to that of prospective studies. Thus, the significance of conclusion from this meta-analysis is limited due to the design of the included studies. Since lack of qualified cohort studies on the risk factor for PLC in Chinese population, the result of this meta-analysis is valuable for further research. Test of heterogeneity is a formal statistical analysis for examining if the observed variation in study results is compatible with the variation expected by chance[4]. When heterogeneity is statistically significant ($P<0.05$), the observed different results should be explained individually. Nineteen factors in the included studies were involved in this investigation, fifteen of which had significant heterogeneity. The various risk factors for PLC were possibly interactive. When an investigated factor is involved in the included studies, the difference between other risk factors and their interaction is not easy to control among studies, thus leading to the heterogeneity. Furthermore, different studies are usually undertaken in different ways, but it is hard to attribute heterogeneity to any single factor[4]. Since the differences in the included studies are of practical significance, random-effect model is used for the factor with significant heterogeneity to make a more conservative estimation of the combined result. In the current study, some original articles were unable to be used because of their deficient data. It is difficult to estimate the effect of these missing data on the combined results. Sensitivity analysis can test the reliability of the outcomes by assessing coherence of the combined results from fixed-effect model and random-effect model. In this study, most factors passed sensitivity analysis successfully (17/19), thus proving the reliability of the results in this meta-analysis. Publication bias is associated with funnel plot asymmetry. However, the reasons for asymmetric funnel plot may include publication bias and others such as selection biases, poor methodology of smaller studies, true heterogeneity and chance[4]. Since the funnel plots of history of hepatitis, negative living events, smoking, and intake of pickle were found asymmetric, conclusions about these factors should not be drawn due to the bias.

In conclusion, the main risk factors for PLC in Chinese population are related to liver diseases, family history of liver carcinoma, poor psychological status, aflatoxin, and bad living style. Liver diseases are most important in all these factors. Control of HBV infection, HCV infection, and liver cirrhosis is the essential measure for the prevention of PLC. In addition, balanced psychological status, avoidance of musty food or food polluted by aflatoxin-contaminated food, and no alcoholic can reduce the risk for PLC.

REFERENCES

1 **Hall AJ,** Wild CP. Liver cancer in low and middle income countries. *BMJ* 2003; **326**: 994-995
2 **Lichtenstein MJ,** Mulrow CD, Elwood PC. Guidelines for reading case-control studies. *J Chron Dis* 1987; **40**: 893-903
3 **Me HY,** Shi LY. Meta-analysis of the risk factors on lung cancer in Chinese people. *Zhonghua Liuxingbingxue Zazhi* 2003; **24**: 45-48
4 **Zhou XY,** Fang JQ, Yu CH, Xu ZL, Lu Y. Meta analysis In: Lu Y, Fang JQ. Advanced medical statistics. *Singapore World Scientific Publishing Co Pte Ltd* 2003: 233-318
5 **Erwin Kuntz,** Hans-Dieter Kuntz. Malignant liver tumours In: Erwin Kuntz, Hans-Dieter Kuntz, eds. Hepatology: principles and practice. *New York: Springer-Verlag Berlin Heidelberg* 2002: 699-730

Science Editor Wang XL and Guo SY **Language Editor** Elsevier HK

PO Box 2345, Beijing 100023, China
www.wjgnet.com
wjg@wjgnet.com

ELSEVIER

World J Gastroenterol 2005;11(28):4435-4438
World Journal of Gastroenterology ISSN 1007-9327

• *BRIEF REPORTS* •

Effects of sulfasalazine on biopsy mucosal pathologies and histological grading of patients with active ulcerative colitis

Ying-Qiang Zhong, Hua-Rong Huang, Zhao-Hua Zhu, Qi-Kui Chen, Jun Zhan, Lian-Chun Xing

Ying-Qiang Zhong, Zhao-Hua Zhu, Qi-Kui Chen, Jun Zhan, Department of Gastroenterology, the Second Affiliated Hospital, Sun Yat-Sen University, Guangzhou 510120, Guangdong Province, China
Hua-Rong Huang, Department of Pediatrics, the Second Affiliated Hospital, Sun Yat-Sen University, Guangzhou 510120, Guangdong Province, China
Lian-Chun Xing, Department of Pathology, the Second Affiliated Hospital, Sun Yat-Sen University, Guangzhou 510120, Guangdong Province, China
Correspondence to: Ying-Qiang Zhong, Department of Gastroenterology, the Second Affiliated Hospital, Sun Yat-Sen University, Guangzhou 510120, Guangdong Province, China. zhongyingqiang@21cn.com
Telephone: +86-20-81332598
Received: 2004-07-19 Accepted: 2004-09-19

Abstract

AIM: To investigate the mechanisms of sulfasalazine (SASP) in the treatment of ulcerative colitis (UC).

METHODS: Changes of pathological signs and histological grading of 106 patients with active UC were observed before and after the treatment with SASP, 1 g, thrice daily for 6 wk.

RESULTS: The effect of SASP on the vasculitis in lamina propria was 48.2% and 17.4% in the mild active UC ($P<0.001$) and 68% and 26.7% in the moderate active UC ($P<0.001$) before and after treatment. Fibroid necrosis of vessel wall was found in one case of mild UC and two cases of moderate UC before treatment and was not found after treatment. No thrombosis was found in mild UC before and after treatment, while thrombosis was found in one case of moderate UC before treatment. The effect on mucosal glandular abnormality was 30.4% and 13.0% in mild UC ($P<0.05$), and 42% and 40% in moderate UC ($P>0.05$) before and after treatment. The rate of eosinophil infiltration was 98.2% and 80.4% in mild UC ($P<0.01$), and 100% and 91.1% in moderate UC ($P<0.05$) before and after treatment. The effect on crypt abscess was 21.4% and 4.4% in mild UC ($P<0.05$), and 48% and 13.3% in moderate UC ($P<0.001$) before and after treatment. The effect on mucosal pathohistological grading was 2.00±0.84 and 0.91±0.46 in mild UC ($P<0.001$), and 2.49±0.84 and 1.31±0.75 in moderate UC ($P<0.001$) before and after treatment.

CONCLUSION: SASP can improve small vessel lesions and crypt abscesses and reduce neutrophilic and eosinophilic leukocyte infiltration in inflammatory mucosa of UC.

Key words: Ulcerative colitis; Biopsy mucosae; Sulfasalazine; Pathology

Zhong YQ, Huang HR, Zhu ZH, Chen QK, Zhan J, Xing LC. Effects of sulfasalazine on biopsy mucosal pathologies and histological grading of patients with active ulcerative colitis. *World J Gastroenterol* 2005; 11(28): 4435-4438
http://www.wjgnet.com/1007-9327/11/4435.asp

INTRODUCTION

Ulcerative colitis (UC) is an inflammatory bowel disease mainly characterized by inflammatory changes in mucosa and submucosa of the rectum and colon. The continuous inflammatory lesions commonly involve rectum and extend to the proximal colon and even to pancolitis. The main clinical manifestations are chronic relapsing diarrhea, mucopurulent hematochezia and abdominal pain.

Though sulfasalazine (SASP) has been used to treat active UC for more than 60 years, its mechanisms have not been completely clarified[1]. The purpose of the present study was to investigate the mechanisms of SASP in treatment of active UC.

MATERIALS AND METHODS

Patients[2]

Following patients were enrolled in the study: patients aged 14-69 years with chronic or relapsing diarrhea, mucopurulent hematochezia, abdominal pain and systemic symptoms, and extraintestinal presentations of their joints, skin, eyes, mouth, liver, and gall bladder, as well as those with inflammatory lesions of rectum and colon. Patients with bacillary or amoebic dysentery, fungous or tuberculous colitis, ischemic bowel disease, radiation colitis, Crohn's disease and large bowel cancer and those who did not complete the course of treatment due to drug allergy or quitted the study were excluded.

Objects of study

A total of 106 patients (50 males and 56 females) with active UC were enrolled in the study[2]. The ratio of male to female was 0.98:1. Their age was 20-66 years (41.6±11.4 years). Fifty-six cases (22 males and 34 females) had mild UC, and their age was 22-66 years (41.5±10.6 years). Fifty cases (28 males and 22 females) had moderate UC, and their age was 20-65 years (42.8±12.1 years). There were no significant

differences in their age, ratio of male to female and clinical types between the two groups ($P>0.05$). Forty-six of fifty-six cases of mild UC and 45 of 50 cases of moderate UC were followed up.

Treatment

The patients received 1 g SASP thrice daily for 6 wk. Endoscopy was carried out before and after treatment. Biopsy specimens were taken at the same sites before and after treatment.

Grouping

Patients were divided into two groups according to the criteria of mild and moderate UC[2].

Endoscopy and mucosal biopsy

The colon and rectum were examined with electronic colonoscope and 3-5 biopsy specimens were taken from the most obvious inflammatory lesions on the left side of colon or rectum. The specimens were fixed in 40 g/L formaldehyde and embedded in paraffin wax, then cut into continuous sections and stained with hematoxylin and eosin. Pathologic morphometry was analyzed by one pathologist with double blind method. The final morphologic results were obtained from the average of three observations under a high power microscope.

Observed pathological items[3-6]

The following pathlogical items were observed: small vessel lesions in lamina propria such as vasculitis, fibroid necrosis of vessel wall, thrombosis and focal hemorrhage; mucosal gland lesions including glandular abnormality, epithelial cell regeneration, atypical hyperplasia, goblet cell depletion (GCD) and Paneth cell metaplasia (PCM); inflammatory cell infiltration in mucosal epithelium such as lymphocyte hyperplasia, lymphoid follicular formation, eosinophils (Eos) and plasmacytes; cellular stromal lesions including granulation tissue formation, fiber tissue hyperplasia and pseudo-polyp; crypt abscess.

Pathohistological grading criteria[7,8]

Grade 0: no neutrophilic leukocyte infiltration in lamina propria; grade I: a small number of neutrophilic leukocytes (<10/HPF) in lamina propria with minimal infiltration of crypts; grade II: prominent neutrophilic leukocytes (10-50/HPF) in lamina propria with infiltration of more than 50% of crypts; grade III: a large number of neutrophilic leukocytes (>50/HPF) in lamina propria with crypt abscesses; grade IV: significant acute inflammation with ulcerations in lamina propria.

Statistical analysis

Results were expressed as mean±SD. The data of two groups were analyzed using independent and paired t test. The counted data were expressed as rate or ratio, and analyzed by χ^2 test. All data were analyzed with SPSS10.0 software.

RESULTS

Effects of SASP on small vessel lesions in lamina propria

No significant changes were found in all specimens before and after SASP treatment ($P>0.05$). The effect of SASP on vasculitis in lamina propria was 48.2% and 17.4% in mild active UC ($P<0.001$), and 68% and 26.7% in moderate active UC ($P<0.001$) before and after treatment. Fibroid necrosis of vessel wall was found in one case of mild UC and two cases of moderate UC before treatment but was not found after treatment. Thrombosis was not found in mild UC before and after treatment, but was found in one case of moderate UC before treatment and not found after treatment (Table 1).

Effect of SASP on mucosal gland lesions

The effect of SASP on mucosal glandular abnormality was 30.4% and 13.0% in mild UC ($P<0.05$), and 42% and 40% in moderate UC ($P>0.05$) before and after treatment. No significant effect of SASP on epithelial cell regeneration, atypical hyperplasia, GCD, and PCM was observed before and after treatment ($P>0.05$, Table 2).

Effects of SASP on inflammatory cell infiltration

The rate of Eos infiltration was 98.2% and 80.4% in mild UC ($P<0.01$), and 100% and 91.1% in moderate UC ($P<0.05$)

Table 1 Effect of SASP on small vessel lesions in lamina propria (*n*%)

	n	Focal hemorrhage	Vessel inflammation	Fibroid necrosis	Thrombosis
Before treatment (mild)	56	41 (73.2)	27 (48.2)	1 (1.8)	0
After treatment (mild)	46	25 (54.3)	8 (17.4)	0	0
Before treatment (moderate)	50	32 (64.0)	34 (68.0)	2 (4.0)	1 (2.0)
After treatment (moderate)	45	22 (48.9)	12 (26.7)	0	0

Table 2 Effect of SASP on mucosal gland lesions (*n*%)

	n	Glandular abnormality	Epithelial cell regeneration	Atypical hyperplasia	GCD	PCM
Before treatment (mild)	56	17 (30.4)	19 (34.0)	8 (14.3)	3 (5.4)	0 (0)
After treatment (mild)	46	6 (13.0)	13 (28.3)	2 (4.4)	2 (4.4)	1 (2.2)
Before treatment (moderate)	50	21 (42.0)	15 (30.0)	15 (30.0)	12 (24)	2 (4.0)
After treatment (moderate)	45	18 (40.0)	7 (15.6)	8 (17.8)	6 (13.3)	0 (0)

Table 3 Effects of SASP on inflammatory cell infiltration (*n*%)

	n	Lymphocyte hyperplasia	Lymphoid follicle	Eos infiltration	Plasmacyte infiltration
Before treatment (mild)	56	42 (75.0)	44 (78.6)	55 (98.2)	50 (89.3)
After treatment (mild)	46	30 (65.2)	32 (69.6)	37 (80.4)	37 (80.4)
Before treatment (moderate)	50	37 (74.0)	35 (70.0)	50 (100)	46 (92)
After treatment (moderate)	45	32 (71.1)	26 (57.8)	41 (91.1)	39 (86.7)

before and after treatment. No significant effects of SASP on lymphocyte hyperplasia, lymphoid follicular formation and plasmacyte infiltration were observed before and after treatment ($P>0.05$, Table 3).

Effect of SASP on cellular stromal lesions

No significant effect of SASP on granulation tissue formation, fiber tissue hyperplasia and pseudo-polyp was found before and after treatment ($P>0.05$).

Effect of SASP on crypt abscess

The effect of SASP on crypt abscess was 21.4% and 4.4% in mild UC ($P<0.05$), and 48% and 13.3% in moderate UC ($P<0.001$) before and after treatment.

Effect of SASP on mucosal pathohistological grading

The effect of SASP on mucosal pathohistological grading was 2.00±0.84 and 0.91±0.46 in mild UC ($P<0.001$), and 2.49±0.84 and 1.31±0.75 in moderate UC ($P<0.001$) before and after treatment (Table 4).

Table 4 Effect of SASP on mucosal pathohistological grade (mean±SD)

	n	Mild	*n*	Moderate
Before treatment	46	2.00±0.84	45	2.49±0.84
After treatment	46	0.91±0.46	45	1.31±0.75

DISCUSSION

The common drugs used in treatment of patients with active UC are still SASP and glucocorticoids. Sangfelt *et al*.[9], used prednisolone enema to treat active UC and showed that the release quantity of neutrophil myeloperoxidase (MPO), eosinophil cationic protein (ECP) and eosinophil peroxidase (EPO) in enema liquid is correlated with their clinical, endoscopic and histological activities before treatment. When the patients respond to the treatment, their MPO markedly decreases, but ECP and EPO do not decrease. The results suggest that glucocorticoids can reduce mucosal neutrophil infiltration, but cannot improve Eos infiltration. The increase of MPO is correlated with neutrophil-activated peptide-interleukin 8 and tumor necrosis factor-α[10].

The mechanism of SASP against active UC is that it depresses the production of leukotrienes (LTs), prostaglandin and free radicals[1,11]. SASP plays a role in the treatment of active UC by interfering with synthesis of inflammatory media[12]. SASP can depress immune responses of immune cells and prevent relapse of UC. But the mechanisms have not been completely clarified[1]. Wright *et al*.[13], used 20 mg/100 mL sucralfate once or twice daily to treat distal active UC for 4 wk and showed that it can improve the clinical, endoscopic and histological scores.

The present study using oral SASP to treat active UC for 6 wk showed that it could improve small vessel inflammation and crypt abscess in lamina propria of inflammatory mucosa, decrease neutrophil and Eos infiltration in mucosal epithelium, and decline the histological grading after treatment. There was no fibroid necrosis of vessel wall and thrombosis in all specimens after treatment. Significant effect of SASP on mucosal glandular abnormality, lymphocyte hyperplasia and lymphoid follicular formation, plasmacytes infiltration and cellular stromal lesions was not observed.

The insufficient mucosal blood supply and submucosal vessel lesions are also the pathogenic factors for active UC. SASP could improve mucosal small vessel lesions, crypt abscess, mucopurulent hematochezia and mucosal inflammation in patients with active UC, thus improving and promoting the healing of inflammatory mucosa.

One cause of inflammatory lesions include all kinds of hydrolase and cationic protein released from neutrophil granules of damaged local tissues, which play an important role in the course of inflammation of type III hypersensitivity[14]. The activated neutrophils produce active oxygen and several active molecules that promote occurrence and development of inflammation[15]. SASP could decrease neutrophil infiltration and histological grading, thus decreasing the production of inflammatory factors and improving inflammation.

In this study, SASP obviously decreased mucosal Eos infiltration. Mucosal Eos infiltration is associated with chronic intestine inflammation[16]. Eos collected from the inflammatory mucosa is attracted by immune complex and Eos chemokine releases from mast cells. Eos could synthesize prostaglandins E and E_2, which restrain the synthesis of histamine, neutralize hypersusceptibility and inflammatory reactants. Eos accompanying degranulation phenomena result from allergic reaction by main degranulation way[17]. The number of Eos not only reflects the degree of inflammation[18], but also is an important index of prognosis[19]. There are more acidophil granules in Eos's cytoplasm, containing four toxic cationic proteins: alkalescent protein, ECP, neurotoxin and peroxidase, all of which have toxic effect on normal cells[14]. Raab *et al*.[20], also confirmed that there are more Eos infiltrating lamina propria of active UC, and ECP obviously increases. The activation or degranulation of Eos is correlated with mucosal inflammatory responses. The changes in intestinal mucosa resulted from Eos infiltration in the inflammatory mucosa that are activated and cause mucosal lesions during degranulation and release

of ECP[21].

In conclusion, SASP can effectively treat patients with active UC and improve small vessel lesions, crypt abscesses, and decrease neutrophil and Eos infiltration.

REFERENCES

1 **Hu PJ.** Ulcerative colitis. In: Ye RG: Internal medicine, 5nd ed. Beijing: *People Healthy Publishing House* 2000: 428-434
2 The digestive academy of Chinese medical academy. Suggestion of diagnosis and treatment regulation of inflammatory bowel disease. *Zhonghua Xiaohua Zazhi* 2001; **21**: 236-239
3 **Gong EC,** Liu CL, Shi XY. Pathological diagnosis and the differential diagnosis of inflammatory bowel disease. *Zhonghua Xiaohua Zazhi* 2001; **21**: 233
4 **Ou YQ,** Zhang GY, Li SH. Diagnostic study of chronic non-special ulcerative colitis: in 66 cases. *Zhonghua Xiaohua Zazhi* 1987; **7**: 142-144
5 **Xia B,** Zhou Y, Luo N, Chen DJ, Zhou ZY. Biopsy and diagnosis of inflammatory bowel disease. *Zhonghua Xiaohua Neijing Zazhi* 1996; **13**: 276-278
6 **Qu HS,** Lv YM, Sun YK, Zheng J. Clinical pathological analysis of 35patients with chronic non-special ulcerative colitis. *Beijing Yixueyuan Xuebao* 1981; **13**: 121-124
7 **Truelove SC,** Richards WC. Biopsy studies in ulcerative colitis. *Br Med J* 1956; **6**: 1315-1318
8 **Pullan RD,** Rhodes J, Ganesh S, Mani V, Morris JS, Willian GT, Newcombe RG, Russell MA, Feyerabend C, Thomos GA. Tansdermal nicotine for active ulcerative colitis. *N Engl J Med* 1994; **330**: 811-815
9 **Sangfelt P,** Carlson M, Thorn M, Loof L, Raab Y. Neutrophil and eosinophil granule proteins as markers of response to local prednisolone treatment in distal ulcerative colitis and proctitis. *Am J Gastroenterol* 2001; **96**: 1085-1090
10 **Raab Y,** Gerdin B, Ahlstedt S, Hallgren R. Neutrophil mucosal involvement is accompanied by enhanced local production of interleukin-8 in ulcerative colitis. *Gut* 1993; **34**: 1203-1206
11 **Li DG,** Liu YL, Liu HB. The abstract of academic conference of chronic non-infective intestinal disease in China. *Zhonghua Xiaohua Zazhi* 1993; **13**: 351-353
12 **Zheng JJ.** Ulcerative colitis. In: Zheng JJ, Inflammatory bowel disease, 1nd ed. *Shanghai: Shanghai Publishing House of Literature of Science and Technology* 1998: 24-43
13 **Wright JP,** Winter TA, Candy S, Marks IS. Sucralfate and methylprednisolone enemas in active ulcerative colitis: a prospective, single-blind study. *Dig Dig Sci* 1999; **44**: 1899-1901
14 **Li BQ.** Immune system, immune organ and immune cell. In: Wu MY, Liu GZ, Medical immunology, 3nd ed. *Hefei: Publishing House of Chinese University of Science and Technology* 1999: 45-46
15 **Oshitani N,** SawaY, Hara J, Adachi K, Nakamura S, Matsumoto T, Arakawa T, Kuroki T. Functional and phenotypical activa-tion of leucocytes in inflamed human colonic mucosa. *J Gastroenterol Hepatol* 1997; **12**: 809-814
16 **Bischoff SC,** Wedemeyer J, Herrmann A, Meier PN, Trantwein C, Cetin Y, Maschek H, Stolte M, Gebel M, Manns MP. Quantitative assessment of intestinal eosinophils and mast cells in inflammatory bowel disease. *Histopathology* 1996; **28**: 1-13
17 **Wang ZM,** Xu YJ, Shi P. Observation on eosinophilic degranulation in chronic ulcerative colitis. *Zhongguo Gangchangbing Zazhi* 1994; **14**: 6-7
18 **Zhong YQ,** Huang HR, Zeng ZY, Xing LC. Application of eosinophils grading for the assessment of severity of patients with active ulcerative colitis. *Zhonghua Xiaohua Zazhi* 2004; **24**: 559-560
19 **Deng ZH,** Xu DY. Laboratory items of assessment of activity and treatment effect of chronic ulcerative colitis. *Zhonghua Xiaohua Zazhi* 1992; **12**: 292-293
20 **Raab Y,** Fredens K, Gerdin B, Hallgren R. Eosinophil activation in ulcerative colitis: studies on mucosal release and localization of eosinophil granule constituents. *Dig Dig Sci* 1998; **43**: 1061-1070
21 **Makiyama K,** Kanzaki S, Yamasaki K, Zea-Itiarte W, Tsuji Y. Activation of eosinophils in the pathophysiology of ulcerative colitis. *J Gastroenterol* 1995; **30**(Suppl 8): 64-69

Science Editor Wang XL and Guo SY **Language Editor** Elsevier HK

PO Box 2345, Beijing 100023, China
www.wjgnet.com
wjg@wjgnet.com

ELSEVIER

World J Gastroenterol 2005;11(28):4439-4442
World Journal of Gastroenterology ISSN 1007-9327

• *BRIEF REPORTS* •

Liposome transfected to plasmid-encoding endostatin gene combined with radiotherapy inhibits liver cancer growth in nude mice

Ai-Qing Zheng, Xian-Rang Song, Jin-Ming Yu, Ling Wei, Xing-Wu Wang

Ai-Qing Zheng, Tianjin Medical University, Tianjin 300070, China
Ai-Qing Zheng, Xian-Rang Song, Ling Wei, Xing-Wu Wang, Cancer Research Center, Shandong Cancer Hospital, Jinan 250117, Shandong Province, China
Jin-Ming Yu, Department of Radiation Oncology, Shandong Cancer Hospital, Jinan 250117, Shandong Province, China
Correspondence to: Dr. Ai-Qing Zheng, Cancer Research Center, Shandong Cancer Hospital, Jinan 250117, Shandong Province, China. aiqingzheng@yahoo.com.cn
Telephone: +86-531-7984777-82423
Received: 2004-09-23 Accepted: 2004-10-04

Abstract

AIM: To evaluate whether intratumoral injection of liposome-endostatin complexes could enhance the antitumor efficacy of radiation therapy in human liver carcinoma (BEL7402) model.

METHODS: Recombinant plasmid pcDNA3.End was transfected into human liver carcinoma cell line (BEL7402) with lipofectamine to produce conditioned medium. Then BEL7402 cells and human umbilical vein endothelial cells (HUVECs) were treated with the conditioned medium. Cell cycle and apoptosis were analyzed by flow cytometer and endothelial cell proliferation rates were determined by MTT assay. The antitumor efficacy of endostatin gene combined with ionizing radiation in mouse xenograft liver tumor was observed.

RESULTS: Endostatin significantly suppressed the S phase fraction and increased the apoptotic index in HUVECs. In contrast, endostatin treatment had no effect on BEL7402 cell apoptosis (2.1±0.3% *vs* 8.9±1.3%, $t = 8.83$, $P = 0.009<0.01$) or cell cycle distribution (17.2±2.3% *vs* 9.8±1.2%, $t = 4.94$, $P = 0.016<0.05$). The MTT assay showed that endostatin significantly inhibited the proliferation of HUVECs by 46.4%. The combination of local endostatin gene therapy with radiation therapy significantly inhibited the growth of human liver carcinoma BEL7402 xenografts, the inhibition rate of tumor size was 69.8% on d 28 compared to the untreated group. The tumor volume in the pcDNA3.End combined with radiation therapy group (249±83 mm^3) was significantly different from that in the untreated group (823±148 mm^3, $t = 5.86$, $P = 0.009<0.01$) or in the pcDNA3 group (717±94 mm^3, $t = 6.46$, $P = 0.003<0.01$). Endostatin or the radiation alone also inhibited the growth of liver tumor *in vivo*, but their inhibition effects were weaker than those of endostatin combined with radiation, the inhibition rates on d 28 were 44.7% and 40.1%, respectively.

CONCLUSION: Endostatin not only significantly suppresses tumor growth but also enhances the antitumor efficacy of radiation therapy in human carcinoma xenograft.

Key words: Endostatin; Human liver carcinoma; Radiotherapy; Gene therapy

Zheng AQ, Song XR, Yu JM, Wei L, Wang XW. Liposome transfected to plasmid-encoding endostatin gene combined with radiotherapy inhibits liver cancer growth in nude mice. *World J Gastroenterol* 2005; 11(28): 4439-4442
http://www.wjgnet.com/1007-9327/11/4439.asp

INTRODUCTION

Tumors are dependent on angiogenesis for sustained growth[1]. Endostatin, an endogenous antiangiogenic agent, is a M_r 20 000 COOH-terminal fragment of collagen XVIII. It is a potent inhibitor of angiogenesis *in vitro*, and has significant antitumor effects in a variety of preclinical tumor models[2,3]. Endostatin specifically inhibits endothelial cell proliferation without direct effects on tumor cell or non-neoplastic cell growth[4-7], whose overexpression can lead to primary tumor regression and growth inhibition[8].

Most therapeutic investigations of endostatin utilized the purified protein, but the protein purification process is difficult and may denature endostatin. For maintaining therapeutically effective serum levels the protein must be repeatedly used because it has a short half-life *in vivo*. One possible approach to overcome this problem may be the utilization of gene therapy strategy. Studies using viral vectors to deliver endostatin gene have demonstrated its efficacy in treatment of mouse tumor models[9-11].

Although antiangiogenic therapies have shown significant antitumor effects in preclinical investigations, angiogenesis inhibitors cannot achieve tumor cures on their own. Antiangiogenic strategies in combination with conventional anticancer approaches may achieve better results. The involvement of antiangiogenic agents during the course of radiotherapy have been shown to produce significant therapeutic effects[12-15].

In this study, we investigated whether intratumoral injection of liposome-endostatin complexes could enhance the treatment efficacy of ionizing radiation in a human liver carcinoma (BEL7402) model.

MATERIALS AND METHODS

Plasmid and cell lines

The plasmid pcDNA3.End containing a synthetic rat insulin leader sequence and the full-length mouse endostatin cDNA was kindly provided by Dr. Wang Jianli (Shandong Medical University, Jinan, China). The synthetic rat insulin leader was cloned in front of the endostatin gene. Human liver carcinoma cell line BEL7402 and human umbilical vein endothelial cell line (HUVEC) were kept in our laboratory. HUVECs and BEL7402 cells were maintained in DMEM (Gibco) containing 10% FBS.

In vitro transfection and production of conditioned endostatin medium

BEL7402 cells were grown in 6-well plates at the density of 2×10^5 cells/well to 50-80% confluence, then transfected with 10 μL of lipofectamine (Invitrogen) mixed with 4 μg of plasmid (pcDNA3.End or pcDNA3) as described by the Invitrogen protocol. After 24 h transfection, the cells were extensively rinsed with PBS and incubated in serum-free DMEM for another 24 h. The conditioned media were collected, centrifuged and cell debris was cleared off. Endostatin in the culture media was measured with a murine endostatin enzyme immunoassay kit (Chemicon Inc.). The conditioned media were concentrated 20-fold with Amicon membranes (Amicon Inc.), and endostatin protein levels were determined by immunoassay before being stored at -80 ℃ for further use.

Cell cycle assay

BEL7402 cells and HUVECs were plated in 6-well plates at the density of 2×10^5 cells/well and allowed to attach overnight. The cells were treated with conditioned medium containing certain concentration of endostatin and 10% FBS after removal of the medium. Forty-eight hours later, the cells were trypsinized, counted and fixed in 50% ethanol overnight, then treated with PBS (containing 1 g/L RNase) for 30 min. Samples were washed with PBS twice and resuspended in PBS at a concentration of 1×10^6 cells/mL. The cells were stained with PI in darkness for 30 min and cell cycle distribution was analyzed with a flow cytometer (Becton-Dickinson FACS Calibur).

Apoptosis assay

BEL7402 cells and HUVECs were cultured in 6-well plates at the density of 2×10^5 cells/well and incubated for 24 h. The medium was replaced with 2 mL of conditioned medium containing certain concentration of endostatin and 10% FBS. After being incubated for 48 h, the cells were trypsinized, counted, washed twice with cold PBS and then resuspended in 1× binding buffer at a concentration of 1×10^6 cells/mL. Five microliters of annexin V-FITC and five microliters of PI were added. The cells were gently vortexed and incubated for 15 min at RT in the dark, and then 400 μL of 1× binding buffer was added. Apoptosis was analyzed with a flow cytometer.

Endothelial cell proliferation assay

HUVECs were incubated in 96-well dishes at the density of 10^4 cells/well and allowed to attach overnight. The medium was then replaced with 20 μL of conditioned medium and incubated for 30 min. Eighty microliters of DMEM containing with 10% FBS and 1 μg/L bFGF (Sigma) were then added. After the cells were incubated for 48 h, 20 μL MTT solution (5 g/L) was added. Then, 4 h later, 100 μL 100 g/L SDS was added. After being vortexed gently for 10 min, the number of cells was quantified by colorimetric MTT assay.

In vivo treatment of tumor cells by liposome-DNA complex injection combined with radiation therapy

Female nude mice aged 4-6 wk were obtained from Animal Center of Shandong Medical University and fed with a standard rodent diet. To establish xenografts, animals were subcutaneously injected into the right flank with 1×10^6 BEL7402 cells suspended in 200 μL 0.9% saline. Seven days after the injection of tumor cells, the mice were randomly divided into five treatment groups: untreated, empty vector (Lip-pcDNA3), Lip-pcDNA3.End, pcDNA3.End combined with radiation, and radiation. Six mice were enrolled in each group. To deliver the gene therapy, each mouse in groups 2, 3, and 4 received three intratumoral injections of liposome-DNA complex which consisted of 40 μL lipofectamine and 20 μg of DNA (1 g/L) and 40 μL 0.9% saline on d 7, 14, and 21 after the injection of tumor cells. Irradiations were performed using a 6 MV Varian 2100 C linear accelerator, operating a single dose of 10 Gy 7 d after injection of tumor cells. Before irradiation, the mice were confined in plastic containers. The animals' tumor-bearing sites extended through openings in the containers allowing the tumors to be irradiated locally. Tumors were measured every 3-4 d. Tumor response to treatment was determined by growth delay assay. The tumor volume was calculated by the formula: tumor volume = $ab^2\times0.52$, where a is the length, and b is the width.

RESULTS

In vitro endostatin quantification

Unconcentrated media (100 μL) collected from BEL7402 cells transfected with pcDNA3.End and pcDNA3 were measured with a murine endostatin enzyme immunoassay kit. The experiment showed that BEL7402 cells transfected with pcDNA3.End efficiently secreted endostatin protein into the culture media. Endostatin levels were 486.2±56.5 mg/L in conditioned media from BEL7402 cells transfected with pcDNA3.End, and 6.8±2.6 mg/L in conditioned media from BEL7402 cells transfected with pcDNA3. There were significant differences in endostatin levels between the two groups ($t = 14.68$, $P = 0.005<0.01$, Figure 1).

Endostatin-affected HUVEC cell cycle and apoptosis

After being treated with conditioned medium, compared to conditioned medium from BEL7402 cells transfected with pcDNA3, conditioned medium from BEL7402 cells transfected with pcDNA3.End significantly suppressed the S phase fraction (17.2±2.3% *vs* 9.8±1.2%, $t = 4.94$, $P = 0.016<0.05$) and increased the apoptotic index (2.1±0.3% *vs* 8.9±1.3%, $t = 8.83$, $P = 0.009<0.01$) in HUVECs. In contrast, after being treated with the two-conditioned media respectively,

there were no differences in BEL7402 cell apoptosis or cell cycle distribution, suggesting that endostatin treatment had no effect on BEL7402 tumor cell apoptosis or cell cycle distribution.

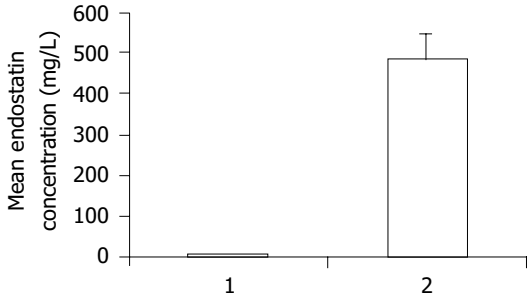

Figure 1 Mean concentration of endostatin protein in supernatant. 1: Secretion of endostatin by BEL-7402 cells transfected with pcDNA3; 2: secretion of endostatin by BEL-7402 cells transfected with pcDNA3.End.

Endostatin-inhibited endothelial cell proliferation

After 24 h incubation with conditioned media, endostatin-inhibited HUVECs proliferation by 46.4±9.7%, while the conditioned media derived from cultures of BEL7402 cells transfected with pcDNA3 control vector did not affect endothelial cell proliferation, the inhibition rate was 8.7±0.5% (t = 6.72, P = 0.02<0.05, Figure 2).

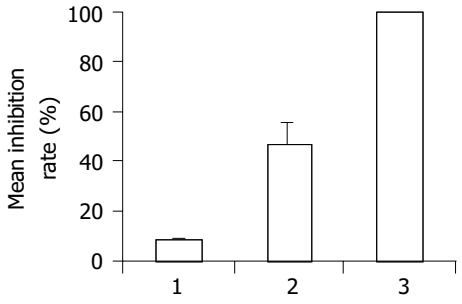

Figure 2 HUVEC proliferation rates inhibited by endostatin. 1: Proliferation rate inhibited by conditioned media derived from cultures of BEL7402 cells transfected with pcDNA3; 2: proliferation rate inhibited by conditioned media derived from cultures of BEL7402 cells transfected with pcDNA3.End; 3: control group.

Endostatin gene therapy combined with radiation-inhibited tumor growth in nude mice

As shown in Figure 3, tumors treated with Lip-pcDNA3. End combined with radiation group grew very slowly in nude mice, the inhibition rate of tumor size was 69.8% on d 28 compared to untreated group. The tumor volume of the pcDNA3.End combined with radiation group (249±83 mm^3) was significantly different from that of the untreated group (823±148 mm^3, t = 5.86, P = 0.009<0.01) or the pcDNA3 group (717±94 mm^3, t = 6.46, P = 0.003<0.01). Tumors of the pcDNA3.End group and radiation group also grew slower than those of the untreated group or the pcDNA3 group, but the inhibitory effects on tumor growth were slightly weaker than those of the pcDNA3.

End combined with radiation group, the inhibitory rates on d 28 were 44.7% and 40.1%, respectively. The tumor volume of the pcDNA3.End group (492±97 mm^3) or the radiation group (455±124 mm^3) was significantly different from that of the untreated group (the pcDNA3.End group, t = 3.14, P = 0.039<0.05 and the radiation group, t = 3.30, P = 0.03<0.05) or the pcDNA3 group (the pcDNA3.End group, t = 2.89, P = 0.045<0.05 and the radiation group, t = 2.92, P = 0.047<0.05).

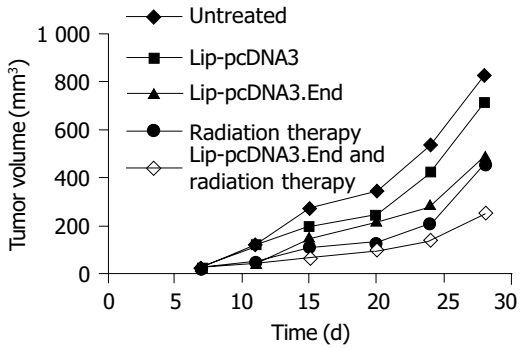

Figure 3 Tumor growth after intratumoral injections of liposome-plasmid complexes or irradiation or both.

DISCUSSION

Radiotherapy is one of the most important treatment modalities for solid tumors. Today, 45-50% of all cancer patients can be cured, and nearly 70% of those who are cured have received radiation either alone or in combination with other modalities, but a large number of patients have no response to radiotherapy treated with curative intent ultimately fail, not only because of metastasis of the disease, but also because of relapse at the local treatment site. One reason responsible for radiotherapy failure may be the tumor vasculature. Numerous studies have shown that tumor cells stop growing when the diameter of tumor exceeds 1-2 mm if new blood vessels supplying the tumor fail to generate[16]. Hence, the combined radiotherapy with antiangiogenic agents has aroused great concerns[17,18].

Angiogenesis is a complex process with multiple, sequential, and interdependent steps. Tumor cells promote new vessel formation by releasing endothelial cell growth factors that support endothelial cell proliferation, migration, and survival. Tumor angiogenesis is the consequence of enhanced expression of proangiogenic factors relative to antiangiogenic factors in the tumor microenvironment.

The combination of radiation treatment with endostatin may improve radiotherapy outcome by enhancing antitumor efficacy, reducing the total radiation dose, improving local tumor control rate, alleviating radiation damage. These considerations, along with the extensive clinical use of radiotherapy, make thorough investigation of strategies combining conventional treatment modality with endostatin. It was reported that combined endostatin gene therapy with radiotherapy can improve tumor response[19-22].

We chose liposome to transfect BEL7402 cells with endostatin gene due to its high transfection efficiency. In

our pre-experiment, we chose lipofectamine to transfect BEL7402 cells with pcDNA3.GFP, the transfection rate was 73.5%. ELISA analysis of conditioned media from BEL7402 cells transfected with pcDNA3.End showed that the level of endostatin protein was 486.2±56.5 mg/L, suggesting that BEL7402 cells transfected with pcDNA3.End plasmids secrete endostatin proteins into the culture media. The conditioned medium significantly suppressed the S phase fraction and increased the apoptotic index in HUVECs. However, it had no effect on BEL7402 cell apoptosis or cell cycle distribution. *In vivo*, endostatin significantly enhanced the treatment efficacy of ionizing radiation. The antitumor inhibition rate of combined endostatin gene therapy with radiation in BEL7402 human liver tumor model was 69.8%, which was significantly different from the untreated group ($t = 5.86$, $P = 0.009<0.01$) or the empty vector group ($t = 6.46$, $P = 0.003<0.01$) on d 28. Tumors of the radiation group and the pcDNA3.End group grew slower than those of the untreated group or the pcDNA3 group. These results indicate that intratumoral injection of liposome-endostatin complex significantly enhances the antitumor efficacy of radiation therapy.

In summary, gene therapy can deliver antiangiogenic polypeptide endostatin. Cationic liposomes transfected to endostatin gene can not only suppress endothelial cell proliferation, but also enhance the treatment efficacy of ionizing radiation.

REFERENCES

1 **Folkman J.** Angiogenesis in cancer, vascular, rheumatoid and other disease. *Nat Med* 1995; **1**: 27-31

2 **Perletti G,** Concari P, Giardini R, Marras E, Piccinini F, Folkman J, Chen L. Antitumor activity of endostatin against carcinogen-induced rat primary mammary tumors. *Cancer Res* 2000; **60**: 1793-1796

3 **Chen QR,** Kumar D, Stass SA, Mixson AJ. Liposomes complexed to plasmids encoding angiostatin and endostatin inhibit breast cancer in nude mice. *Cancer Res* 1999; **59**: 3308-3312

4 **Du Z,** Hou S. The anti-angiogenic activity of human endostatin inhibits bladder cancer growth and its mechanism. *J Urol* 2003; **170**: 2000-2003

5 **Wang X,** Liu F, Li X, Li JS, Xu GX. Anti-tumor effect of human endostatin mediated by retroviral gene transfer in nude mice. *Chin Med J* 2002; **115**: 1664-1169

6 **Boehle AS,** Kurdow R, Schulze M, Kliche U, Sipos B, Soondrum K, Ebrahimnejad A, Dohrmann P, Kalthoff H, Henne-Bruns D, Neumaier M. Human endostatin inhibits growth of human non-small-cell lung cancer in a murine xenotransplant model. *Int J Cancer* 2001; **94**: 420-428

7 **Felbor U,** Dreier L, Bryant RAR, Ploegh HL, Olsen BR, Mothes W. Secreted cathepsin L generates endostatin from collagen X VIII. *EMBO J* 2000; **19**: 1187-1194

8 **Herbst RS,** Lee AT, Tran HT, Abbruzzese JL. Clinical studies of angiogenesis inhibitors: the University of Texas MD Anderson Center Trial of Human Endostatin. *Curr Oncol Rep* 2001; **3**: 131-140

9 **Sauter BV,** Martinet O, Zhang WJ, Mandeli J, Woo SLC. Adenovirus-mediated gene transfer of endostatin *in vivo* results in high level of transgene expression and inhibition of tumor growth and metastases. *Proc Natl Acad Sci USA* 2000; **97**: 4802-4807

10 **Ding XQ,** Chen Y, Li L, Liu RY, Huang JL, Lai K, Wu XJ, Ke ML, Huang WL. Inhibition of tongue cancer development in nude mice transfected with adenovirus carrying human endostatin gene. *Aizheng* 2003; **22**: 1152-1157

11 **Chen W,** Fu J, Liu Q, Ruan C, Xiao SD. Retroviral endostatin gene transfer inhibits human colon cancer cell growth *in vivo*. *Chin Med J* 2003; **116**: 1582-1584

12 **Gorski DH,** Mauceri HJ, Salloum RM, Gately S, Hellman S, Beckett MA, Sukhatme VP, Soff GA, Kufe DW, Weichselbaum RR. Potentiation of the antitumor effect of ionizing radiation by brief concomitant exposures to angiostatin. *Cancer Res* 1998; **58**: 5686-5689

13 **Wachsberger P,** Burd R, Dicker AP. Tumor response to ionizing radiation combined with antiangiogenesis or vascular targeting agents: exploring mechanisms of interaction. *Clin Cancer Res* 2003; **9**: 1957-1971

14 **Griscelli F,** Li H, Cheong C, Opolon P, Bennaceur-Griscelli A, Vassal G, Soria J, Soria C, Lu H, Perricaudet M, Yeh P. Combined effects of radiotherapy and angiostatin gene therapy in glioma tumor model. *Proc Natl Acad Sci USA* 2000; **97**: 6698-6703

15 **Harari PM,** Huang SM. Head and neck cancer as a clinical model for molecular targeting of therapy: combining EGFR blockade with radiation. *Int J Radiat Oncol Biol Phys* 2001; **49**: 427-433

16 **Hahnfeldt P,** Panigrahy D, Folkman J, Hlatky L. Tumor development under angiogenic signaling: a dynamical theory of tumor growth, treatment response, and postvascular dormancy. *Cancer Res* 1999; **59**: 4770-4775

17 **Rofstad EK,** Henriksen K, Galappathi K, Mathiesen B. Antiangiogenic treatment with thrombospondin-1 enhances primary tumor radiation response and prevents growth of dormant pulmonary micrometastases after curative radiation therapy in human melanoma xenografts. *Cancer Res* 2003; **63**: 4055-4061

18 **Lund EL,** Bastholm L, Kristjansen PEG. Therapeutic synergy of TNP-470 and ionizing radiation: effects on tumor growth, vessel morphology, and angiogenesis in human glioblastoma multiforme xenografts. *Clin Cancer Res* 2000; **6**: 971-978

19 **Siemann DW,** Shi W. Targeting the tumor blood vessel network to enhance the efficacy of radiation therapy. *Semin Radiat Oncol* 2003; **13**: 53-61

20 **Herbst RS,** O'Reilly MS. The rationale and potential of combining novel biologic therapies with radiotherapy: focus on non-small cell lung cancer. *Semin Oncol* 2003; **30** (4 Suppl 9): 113-123

21 **Shi W,** Teschendorf C, Muzyczka N, Siemann DW. Gene therapy delivery of endostatin enhances the treatment efficacy of radiation. *Radiother Oncol* 2003; **66**: 1-9

22 **Greenberger JS.** Antitumor interaction of short course endostatin and ionizing radiation. *Cancer J* 2000; **6**: 279-281

Science Editor Wang XL **Language Editor** Elsevier HK

PO Box 2345, Beijing 100023, China
www.wjgnet.com
wjg@wjgnet.com

ELSEVIER

World J Gastroenterol 2005;11(28):4443-4444
World Journal of Gastroenterology ISSN 1007-9327

• *CASE REPORT* •

Small bowel non-Hodgkin's lymphoma remaining in complete remission by surgical resection and adjuvant rituximab therapy

Kenichi Nomura, Koichi Tomikashi, Yosuke Matsumoto, Naohisa Yoshida, Takashi Okuda, Chohei Sakakura, Shoji Mitsufuji, Shigeo Horiike, Hisakazu Yamagishi, Takeshi Okanoue, Masafumi Taniwaki

Kenichi Nomura, Yosuke Matsumoto, Shigeo Horiike, Molecular Hematology and Oncology, Kyoto Prefectural University of Medicine, Graduate School of Medical Science, Kyoto, Japan
Koichi Tomikashi, Naohisa Yoshida, Takashi Okuda, Shoji Mitsufuji, Takeshi Okanoue, Molecular Gastroenterology and Hepatology, Kyoto Prefectural University of Medicine, Graduate School of Medical Science, Kyoto, Japan
Chohei Sakakura, Hisakazu Yamagishi, Department of Surgery, Kyoto Prefectural University of Medicine, Graduate School of Medical Science, Kyoto, Japan
Masafumi Taniwaki, Clinical Molecular Genetics and Laboratory Medicine, Kyoto Prefectural University of Medicine, Graduate School of Medical Science, Kyoto, Japan
Correspondence to: Kenichi Nomura, MD, PhD, Molecular Hematology and Oncology, Kyoto Prefectural University of Medicine, Graduate School of Medical Science, Kawaramachi-Hirokoji, Kamigyo-ku, Kyoto 602-0841, Japan. nomuken@sun.kpu-m.ac.jp
Telephone: +81-75-251-5521 Fax: +81-75-251-0710
Received: 2004-06-15 Accepted: 2004-07-17

Abstract

A 44-year-old man was referred to our hospital with intermittent abdominal pain. Because distention of fluid- and gas-filled loops of small intestine was proved by X-ray, the patient was diagnosed as having small bowel obstruction. A laparotomy revealed a segmental stenosis in the jejunum, which showed diffuse thickening of the intestinal wall. Some mesenteric lymph nodes were swollen. Pathological examination was defined. We diagnosed diffuse large B-cell lymphoma based on the pathological findings of diffuse transmural infiltration of large lymphoid cells and flow-cytometric analyses. Rituximab was administered as adjuvant therapy at weekly doses of 375 mg/m^2. Four cycles were performed every 6 mo and he remained CR. Rituximab may be effective as adjuvant therapy.

Key words: Intermittent abdominal pain; Rituximab

Nomura K, Tomikashi K, Matsumoto Y, Yoshida N, Okuda T, Sakakura C, Mitsufuji S, Horiike S, Yamagishi H, Okanoue T, Taniwaki M. Small bowel non-Hodgkin's lymphoma remaining in complete remission by surgical resection and adjuvant rituximab therapy. *World J Gastroenterol* 2005; 11(28): 4443-4444
http://www.wjgnet.com/1007-9327/11/4443.asp

INTRODUCTION

Primary gastrointestinal lymphoma (PGL) accounts for 4-20% of all non-Hodgkin's lymphomas (NHL)[1,2]. The location most frequently involved has been the ileocecal region, followed by small bowel, accounting for 20-40% of PGL[1]. Small bowel lymphoma tends to be annular in the distal ileum, not proximal[2]. Jejunum obstruction in a patient with NHL has been exceptionally described.

Regarding treatment, it has been established that the primary surgical treatment had the most favorable influence on failure-free survival in localized diseases and hence the resection may be appropriate as the primary treatment[3]. On the other hand, the effectiveness of adjuvant therapy for localized NHL remains to be unclear, because some cases could be cured only by surgical resection.

In this study, we have described the primary jejunal NHL with small bowel obstruction, which remained in complete remission by surgical resection followed by rituximab administration.

CASE REPORT

A 44-year-old man was admitted to our hospital in May 2002 because of intermittent abdominal pain. Small bowel series and computed tomography (CT) of the abdomen showed stenosis at jejunum and dilatation of small bowel (Figures 1 and 2), indicating small bowel obstruction. However, the cause of obstruction remained unclear in spite of several workups. Laparotomy disclosed a 3 cm long jejunal segment stenosis at 110 cm from the ligament of Treitz and some mesenteric lymph nodes were swollen.

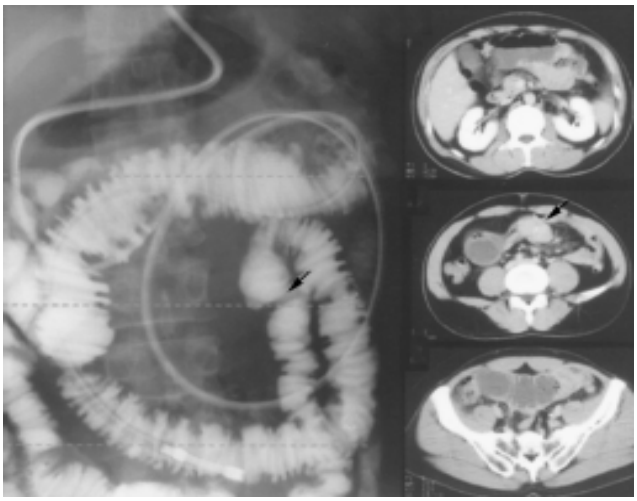

Figure 1 Small bowel series and CT showed both the distention of fluid- and gas-filled loops of small intestine and segmental stenosis indicated by arrow.

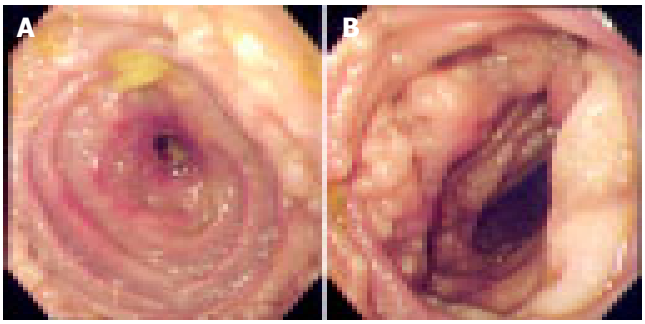

Figure 2 Resected jejunum show. **A**: Resected jejunum showed diffuse thickening of the intestinal wall (oral side); **B**: multiple hyperplastic follicles (anal side).

The resected specimens showed diffuse thickening of the intestinal wall, histopathological analysis of which showed that large lymphoid cells aggregated diffusely. Mesenteric lymph nodes were also involved. Flow-cytometric studies showed that the tumor cells expressed HLA-DR (84.8%), s-IgA (46.6%), γ (69.8%), CD10 (44.7%), CD19 (68.1%), and CD20 (62.4%) with a high-intensity signal. Results for CD5 were negative (26.2%) with a low-intensity signal. Postoperative workup did not demonstrate the evidence of systemic involvement. Thus, the patient was diagnosed having primary jejunal diffuse large B-cell lymphoma at stage II_1. Rituximab was administered as adjuvant therapy at weekly doses of 375 mg/m^2. Four courses were performed every 6 mo and the patient is in complete remission with a follow-up time of 24 mo with no significant adverse effects.

DISCUSSION

We experienced a rare case of primary jejunal NHL as radiological workup including CT and angiography provided no evidence for final diagnosis, we performed laparotomy and segmental intestinal resection. The recognition of the possibility of jejunal obstruction due to NHL may facilitate early diagnosis. Yamamoto *et al*., have recently developed double-balloon endoscopy. This method enables us to survey all intestines with ease[4]. In future, this method may become the routine mode of study for small bowel obstruction.

Regarding treatment, we performed segmental resection of jejunum and rituximab therapy as adjuvant treatment. The efficacy and toxicity of adjuvant therapy for localized NHL remained unclear because excess chemotherapy may provoke secondary malignancies. On the other hand, a new anti-CD20 mAb, rituximab, is effective in the treatment of B-cell lymphoma with slight adverse effects[5,6]. Thus we treated the patient under study with rituximab as adjuvant therapy. He tolerated this adjuvant therapy well, with slight nausea. Rituximab may be effective as adjuvant therapy for PGL. The efficacy and toxicity should be examined in large series.

REFERENCES

1 **Lee J,** Kim WS, Kim K, Ko YH, Kim JJ, Kim YH, Chun HK, Lee WY, Park JO, Jung CW, Im YH, Lee MH, Kang WK, Park K. Intestinal lymphoma: exploration of the prognostic factors and the optimal treatment. *Leuk Lymphoma* 2004; **45**: 339-344
2 **Domizio P,** Owen RA, Shepherd NA, Talbot IC, Norton AJ. Primary lymphoma of the small intestine. A clinicopathological study of 119 cases. *Am J Surg Pathol* 1993; **17**: 429-442
3 **Samel S,** Wagner J, Hofheinz R, Sturm J, Post S. Malignant intestinal non-Hodgkin's lymphoma from the surgical point of view. *Onkologie* 2002; **25**: 268-271
4 **Yamamoto H,** Sugano K. A new method of enteroscopy--the double-balloon method. *Can J Gastroenterol* 2003; **17**: 273-274
5 **Maloney DG,** Grillo-Lopez AJ, Bodkin DJ, White CA, Liles TM, Royston I, Varns C, Rosenberg J, Levy R. IDEC-C2B8: results of a phase I multiple-dose trial in patients with relapsed non-Hodgkin's lymphoma. *J Clin Oncol* 1997; **15**: 3266-3274
6 **Maloney DG,** Grillo-Lopez AJ, White CA, Bodkin D, Schilder RJ, Neidhart JA, Janakiraman N, Foon KA, Liles TM, Dallaire BK, Wey K, Royston I, Davis T, Levy R. IDEC-C2B8 (Rituximab) anti-CD20 monoclonal antibody therapy in patients with relapsed low-grade non-Hodgkin's lymphoma. *Blood* 1997; **90**: 2188-2195

Science Editor Zhu LH and Guo SY **Language Editor** Elsevier HK

PO Box 2345, Beijing 100023, China
www.wjgnet.com
wjg@wjgnet.com

ELSEVIER

World J Gastroenterol 2005;11(28):4445-4446
World Journal of Gastroenterology ISSN 1007-9327

• *CASE REPORT* •

Ovarian carcinoma in two patients with chronic liver disease

Mehlika Isildak, Gulay Sain Guven, Murat Kekilli, Yavuz Beyazit, Mustafa Erman

Mehlika Isildak, Murat Kekilli, Yavuz Beyazit, Gülay Sain Guven, Mustafa Erman, Department of Internal Medicine, Faculty of Medicine, Hacettepe University, Sihhiye, Ankara 06100, Turkey
Gülay Sain Guven, Department of Internal Medicine, Section of General Internal Medicine, Faculty of Medicine, Hacettepe University, Sihhiye, Ankara 06100, Turkey
Mustafa Erman, Department of Internal Medicine, Section of Medical Oncology, Faculty of Medicine, Hacettepe University, Sihhiye, Ankara 06100, Turkey
Correspondence to: Dr. Gülay Sain Guven, Department of Internal Medicine, Section of General Internal Medicine, Faculty of Medicine, Hacettepe University, Sihhiye, Ankara 06100, Turkey. gsain@tr.net
Telephone: +90-312-305-3029 Fax: +90-312-305-2302
Received: 2004-07-23 Accepted: 2004-12-01

Abstract

Ascites is a common and debilitating complication of cirrhosis. However, patients with chronic liver disease are not spared from other causes of ascites and physicians should be careful not to miss an underlying malignancy. Ovarian cancer is an insidious disease, which is difficult to diagnose and it ranks first in mortality among all gynecological cancers. Here, we present two cases of patients with chronic liver disease that developed ascites not simply because of cirrhosis but as a manifestation of ovarian cancer. We would like to emphasize that the causes of ascites, other than the liver itself, should not be overlooked in patients with chronic liver disease.

Key words: Ovarian carcinoma; Ascites; Chronic liver disease

Isildak M, Guven GS, Kekilli M, Beyazit Y, Erman M. Ovarian carcinoma in two patients with chronic liver disease. *World J Gastroenterol* 2005; 11(28): 4445-4446
http://www.wjgnet.com/1007-9327/11/4445.asp

INTRODUCTION

Ascites is the most common complication of viral, alcoholic or metabolic liver cirrhosis. Approximately half of the cirrhotic patients are expected to develop ascites within 10 years after the diagnosis[1]. Development of ascites is an important prognostic sign in the usual course of chronic liver disease since it shortens the 5-year survival rate of a cirrhotic patient[2-4].

Ascites may develop in 75% of all patients with liver disease. The remaining 25% is due to malignancy (10%), cardiac failure (3%), pancreatitis (1%), tuberculosis (2%) and other uncommon causes[5]. However, it is important to comprehend that cirrhotic patients are not spared from these non-cirrhotic causes. Herein we present two patients with chronic liver disease who were diagnosed to have ovarian cancer after a thorough investigation of their ascites.

CASE REPORT

Case 1

A 45-year-old woman with chronic liver disease was seen at the outpatient clinic, because of her recent complaints. She complained of abdominal swelling, in the previous 2 mo. She had abdominal pain radiating to her back, which was aggravated after meals. Famotidine was of no use in relieving the pain. She also complained of weight loss as much as 5 kg in 20 d. The patient had been followed up for chronic hepatitis B infection for 8 years. The diagnosis was confirmed with a liver biopsy, which showed cirrhosis at developmental stage. She underwent esophageal variceal band ligation and transjugular intrahepatic portosystemic shunt (TIPSS) for the management of chronic ascites before 5 years. TIPSS was performed once again before 3 years. She received medical treatment while awaiting liver transplantation. She had no evident family history.

Physical examination revealed that she had massive ascites and was admitted to our hospital for further investigation. Ultrasonographic examination of the abdomen had no remarkable finding except ascites and parenchymal changes in the liver. Hepatic and portal venous systems were normal since the portosystemic shunt functioned well. Diagnostic paracentesis was performed and biochemical analysis was as follows: LDH: 318 U/L (concomitant serum LDH was 337 U/L), albumin: 2.4 g/dL (serum albumin: 2.9 g/dL). Cytological investigation of the ascites showed malignant cells. Abdominal computed tomography (CT) revealed peritoneal carcinomatosis and solid mass lesions of both the ovaries. CT of the thorax showed metastatic nodules on the pleural surface. Serum CA 125 level was 9 853 U/mL.

The patient underwent total abdominal hysterectomy, bilateral salpingo-oopherectomy, omentectomy, and pelvic–paraaortic lymph node dissection. Tumor debulking surgery and histopathological examination of the specimens reported that she had ovarian serous papillary adenocarcinoma (stage III). Paclitaxel–carboplatin therapy was started. Unfortunately, during the first course of chemotherapy she developed acute pneumonia and empyema, which rapidly progressed to septic shock leading to her death.

Case 2

A 40-year-old woman was admitted to hospital because of ascites. She was also suffering from loss of weight and appetite

in the last 10 d. She was known to have had chronic hepatitis B and D. She received interferon treatment for 6 mo, followed by another course of pegylated interferon 2 years later. She had no significant complication of chronic liver disease.

Biochemical analysis of ascites showed an LDH level of 564 U/L and serum-ascites albumin gradient was 0.7. Computed tomography of the abdomen showed massive ascites, omental cake sign and mass lesions of 4-5 cm in both adnexal regions. Serum CA 125 level was 3 028 U/mL. She underwent total abdominal hysterectomy, bilateral oophorectomy, lymph node dissection and tumor debulking surgery. Pathological diagnosis of the tumor was poorly differentiated adenocarcinoma, which was positive for CA 125 and CK7, thus confirming an ovarian origin. Serum CA 125 value of the patient decreased to 25.9 U/mL after the operation.

DISCUSSION

Ovarian carcinoma is difficult to diagnose and it is usually discovered only in its advanced stages. It therefore has the highest mortality among all gynecological malignancies. Cachexia with pelvic mass, ascites and elevated CA125 levels generally lead to its correct diagnosis, but usually there are no pathognomonic radiological or laboratory findings. Therefore, a laparatomy is usually necessary for its final diagnosis.

In the majority of ovarian cancer cases, the etiology is unknown. A small percentage of cases may be attributed to hereditary disorders. Close follow-up with annual transvaginal ultrasound examination and measurement of CA125 levels is advocated for patients with high at genetic risk. Prophylactic oophorectomy after completion of fertility may be a reasonable option for BRCA mutation carriers and might be effective in preventing both ovarian or breast cancers. However, such an approach has not been evaluated[6]. Multiple pregnancies or the use of oral contraceptives might have a protective effect as they can reduce ovulation and related hormonal effect[7].

The 5-year survival rate for advanced disease is about 30%. In a study reviewing the general practice records of patients with epithelial ovarian cancer, the most frequent symptoms are abdominal pain, change in bowel habits, abdominal swelling, vaginal bleeding, weight loss, and backache[8]. The same study revealed that the most significant independent variable for survival is the stage of the disease at surgery[8].

Ascites is an important clinical finding in ovarian cancer. Any patient who presents with ascites should undergo a thorough investigation of ascites influencing cytological analysis and measurement of amylase level. Though an elevated CA125 level should raise a suspicion of ovarian cancer, its interpretation in patients with any serosal involvement may not be easy, since any type of pleural, peritoneal or pericardial irritation can lead to elevated serum level of this high molecular weight glycoprotein[9].

CA125 level greater than 35 U/mL has been reported in 35-75% of cirrhotic patients, most commonly in those with ascites. Studies have shown that cirrhotic patients with ascites have different mean serum CA125 levels of 291 and 572 U/mL, respectively[10-12]. All these data show that CA125 is not a strong diagnostic tool for ovarian cancer in patients with preexisting cirrhotic ascites.

Though it is not possible to define a strict dividing line between "expected" and "alarming" ascites during the course of chronic liver disease, some clues may help physicians to find other underlying causes. We believe that the two cases in our study contribute to this. The first patient had a rapid development of ascites despite a functional TIPSS. The other patient did not have overt signs of cirrhotic changes of the liver, the reason why ascites occurred is not clear. In both cases, the presence of an exudative rather than transudative peritoneal fluid is another underlying cause other than cirrhosis[13]. As mentioned above, an elevated CA125 level is not a specific diagnostic marker for ovarian cancer as it may be elevated in a cirrhotic patient, due to peritoneal irritation. Thus, extremely high CA125 levels merit further investigation.

We conclude that the development of ascites in patients with chronic liver disease should never be considered as "normal" and a search for other causes should be considered. Prompt diagnosis and surgical intervention may be life-saving in such cases.

REFERENCES

1 **Moore KP,** Wong F, Gines P, Bernardi M, Ochs A, Salerno F, Angeli P, Porayko M, Moreau R, Garcia-Tsao G, Jimenez W, Planas R, Arroyo V. The management of ascites in cirrhosis: Report on the consensus conference of the international ascites club. *Hepatology* 2003; **38**: 258-266

2 **Saunders JB,** Walters JRF, Davies P, Paton A. A 20-year prospective study of cirrhosis. *Br Med J* 1981; **282**: 263-266

3 **Llach J,** Gines P, Arroyo V, Rimola A, Tito L, Badalamenti S, Jimenez W, Gaya J, Rivera F, Rodes J. Prognostic value of arterial pressure, endogenous vasoactive systems and renal function in cirrhotic patients admitted to hospital for the treatment of ascites. *Gastroenterology* 1988; **94**: 482-487

4 **Salerno F,** Borroni G, Moser P, Badalamenti S, Cassara L, Maggi A, Fusini M, Cesana B. Survival and prognostic factors of cirrhotic patients with ascites: a study of 134 outpatients. *Am J Gastroenterol* 1993; **88**: 514-519

5 **Reynolds TB.** Ascites. *Clin Liver Dis* 2000; **4**: 151-168

6 **Anderiesz C,** Quinn MA. Screening for ovarian cancer. *Med J Aust* 2003; **178**: 655-656

7 **Molpus KL,** Jones HW 3rd. Gynecological Cancers In: L Goldman, Ausiello D, eds. Cecil Textbook of Medicine. Philadelphia: *WB Saunders* 2004: 1238-1241

8 **Kirwan JM,** Tincello DG, Herod JJ, Frost O, Kingston RE. Effect of delays in primary care referral on survival of women with epithelial ovarian cancer: retrospective audit. *Br Med J* 2002; **324**: 148-151

9 **Sevinc A,** Camci C, Turk HM, Buyukberber S. How to interpret serum CA 125 levels in patients with serosal involvement? A clinical dilemma. *Oncology* 2003; **65**: 1-6

10 **Bergmann JF,** Bidart JM, George M, Beaugrand M, Levy VG, Bohuon C. Elevation of CA 125 in patients with benign and malignant ascites. *Cancer* 1987; **59**: 213-217

11 **Eerdekens MW,** Nouwen EJ, Pollet DE, Briers TW, DeBroe ME. Placental alkaline phosphatase and cancer antigen 125 in sera of patients with bening and malignant diseases. *Clin Chem* 1985; **31**: 687-690

12 **Collazos J,** Genolla J, Ruibal A. CA 125 serum levels in patients with nonneoplastic liver diseases. A clinical and laboratory study. *Scand J Clin Lab Invest* 1992; **52**: 201-206

13 **Runyon BA,** Montano AA, Akriviadis EA, Antillon MR, Irving MA, McHutchinson JG. The serum–ascites albumin gradient is superior to the exudate-transudate concept in the differential diagnosis of ascites. *Ann Intern Med* 1992; **117**: 215-220

Science Editor Wang XL **Language Editor** Elsevier HK

PO Box 2345, Beijing 100023, China
www.wjgnet.com
wjg@wjgnet.com

ELSEVIER

World J Gastroenterol 2005;11(28):4447-4449
World Journal of Gastroenterology ISSN 1007-9327

• *CASE REPORT* •

Acute pancreatitis caused by leptospirosis: Report of two cases

Ekrem Kaya, Adem Dervisoglu, Cafer Eroglu, Cafer Polat, Mustafa Sunbul, Kayhan Ozkan

Ekrem Kaya, Department of Surgery, Uludag University, Bursa, Turkey
Adem Dervisoglu, Cafer Eroglu, Department of Surgery, Ondokuz Mayis University, Samsun, Turkey
Cafer Polat, Mustafa Sunbul, Department of Infectious Disease, Ondokuz Mayis University, Samsun, Turkey
Kayhan Ozkan, Department of Surgery, Ondokuz Mayis University, Samsun, Turkey
Correspondence to: Ekrem Kaya, MD, Department of Surgery, HPB Unit, Uludag University School of Medicine, Gorukle-Bursa 16059, Turkey. ekremkaya@uludag.edu.tr
Telephone: +90-224-4428598 Fax: +90-224-4428398
Received: 2004-07-31 Accepted: 2004-11-04

Abstract

Two cases of acute pancreatitis with leptospirosis are reported in this article. Case 1: A 68-year-old woman, presented initially with abdominal pain, nausea, vomiting, and jaundice. She was in poor general condition, and had acute abdominal signs and symptoms on physical examination. Emergency laparotomy was performed, acute pancreatitis and leptospirosis were diagnosed on the basis of surgical findings and serological tests. The patient died on postoperative d 6. Case 2: A 62-year-old man, presented with fever, jaundice, nausea, vomiting, and malaise. Acute pancreatitis associated with leptospirosis was diagnosed, according to abdominal CT scanning and serological tests. The patient recovered fully with antibiotic treatment and nutritional support within 19 d.

Key words: Acute pancreatitis; Leptospirosis; Infection

Kaya E, Dervisoglu A, Eroglu C, Polat C, Sunbul M, Ozkan K. Acute pancreatitis caused by leptospirosis: Report of two cases. *World J Gastroenterol* 2005; 11(28): 4447-4449
http://www.wjgnet.com/1007-9327/11/4447.asp

INTRODUCTION

Leptospirosis is a spirochetal bacterial infection and causes clinical illness in animals and humans. This zoonosis is common in some other parts of the world but rather rare in Turkey[1,2]. This disease is predominantly seen in farmers, trappers, veterinarians, and rice-field workers. Leptospirosis mainly affects liver and kidney. Rarely, other organs such as lung, heart, gallbladder, brain, and ophthalmic tissues are involved, mainly due to vasculitis[3,4]. Hyperamylasemia can be present in leptospirosis infection due to renal impairment[5-7]. Therefore, the diagnosis of acute pancreatitis is controversial in this disease.

Pancreatitis is a rare complication of leptospirosis and only a few cases have been reported in literature[1,5,8,9]. We report two cases here.

CASE REPORT

Case 1

A 68-year-old woman was referred to Ondokuz Mayis University hospital for abdominal pain, nausea, vomiting, and jaundice with 1-d history. She had no history of contact with jaundiced persons, blood transfusions and drug abuse. She was operated on 3 years ago for hip fracture and occasionally she took some analgesics. On physical examination, she was in poor general condition with dehydration and her scleras were icteric. Her pulse rate was 120/min, blood pressure 14.6/10.6 kPa and she was tachypneic. Urine output was normal. There was a marked tenderness in her whole abdomen with guarding and rebound tenderness. No other abnormalities were noted. Laboratory investigations on admission revealed Hb: 13 g/dL, Htc: 39.7, WBC: 9 000/mm^3, platelet count: 120 000/mm^3 (*n*: 150×10^3-300×10^3), BUN: 60 mg/dL (*n*: 5-24), creatinine (Cr): 2.7 mg/dL (*n*: 0.4-1.4), lactate dehydrogenase (LDH): 2 321 U/L (*n*: 95-500), total/direct bilirubin: 6.5/4.7 mg/dL, Ca: 7.8 mg/dL (8-10), amylase: 630 U/L (28-100), lipase: 642 U/L (*n*: 0-190), aspartate transaminase (AST): 2 500 U/L (*n*: 8-46), alanine transaminase (ALT): 1 900 U/L (*n*: 7-46), serum C-reactive protein (CRP): 192 mg/L (*n*: 0-5), PaO_2: 7.71 kPa, base excess (BE): -5 mmol/L, with negative viral hepatitis markers. The Ranson score was 8. Abdominal ultrasonographic examination revealed acute calculus cholecystitis and abdominal fluid collection. Biliary dilatation was not observed in ultrasonographic examination.

The patient was operated on with the diagnosis of surgical acute abdomen. On exploration, 500 mL sero-hemorrhagic fluid was found in the abdominal cavity, and gallbladder and pancreas were found to be markedly edematous. Areas of fatty necrosis were seen on peripancreatic tissues. Cholecystectomy and common bile duct exploration were done. Pre-operative cholangiogram was normal. Histopathologic diagnosis of the gallbladder was acute cholecystitis. Leptospires were seen in blood, intra-abdominal fluid and bile on dark-field microscopy. Leptospira microagglutination test was positive (at 1:100 *Leptospira samaranga Patoc I*). Penicillin G, 3 million units four times per day was given to the patient intravenously. Total parenteral nutrition was also started for artificial nutrition. The patient recovered after operation and oral intake was started on postoperative d 5. Although liver function tests and laboratory values returned to normal within 5 d, others included Hb: 11 g/dL, platelet count: 170 000/mm^3, BUN: 43 mg/dL, Cr: 0.8 mg/dL, total/direct bilirubin: 1.9/1.56 mg/dL, AST: 47 U/L, ALT:

168 U/L. Six days after the operation the patient died due to a suddenly developed cardiopulmonary arrest.

Case 2

A 62-year-old man was admitted to Ondokuz Mayis University hospital with fever, marked jaundice, nausea, and vomiting. The patient had also 2 wk' history of malaise, fever, and dizziness before hospital admission. On examination, the patient was icteric and there was conjunctival hyperemia. His temperature was 39 ℃ and blood pressure was 19.9/11.9 kPa. Urine output was 30 mL/h. The remainder of the physical examination was normal. Laboratory investigations on admission showed Hb: 8.6 g/dL, Htc: 27.8, WBC: 23 000/mm^3, platelet count: 53 000/mm^3, glucose 140 mg/dL, total/direct bilirubin: 48/44 mg/dL, AST: 70 U/L, ALT: 85 U/L, alkaline phosphatase: 516 U/L (*n*: 95-280), γ-glutamic transpeptidase: 104 U/L (*n*: 7-49), BUN: 120 mg/dL, Cr: 17 mg/dL, LDH: 1 638 U/L, total protein 4.8 g/dL (*n*: 6-8.5), albumin: 2.2 g/dL (*n*: 3.5-5), amylase 980 U/L, pancreatic amylase: 830 U/L (*n*: 13-53), lipase: 797 U/L, Ca: 7.5 mg/dL, CRP: 68, negative viral hepatitis markers. The Ranson score was 6. Leptospira microagglutination test was positive (at 1/800, *L icterohemorrhagica*). Leptospires were seen in blood on dark-field microscopy. Abdominal CT examination revealed bilateral pleural effusion, intra-abdominal minimal fluid collection, pancreatic edema and peripancreatic tissues heterogeneity (Figure 1A).

A diagnosis of leptospirosis with acute pancreatitis was made. The patient had renal failure in acute non-oliguric form. Hemodialysis was performed at the beginning of the treatment. Intravenous fluid resuscitation and ampicillin-sulbactam treatment were given. Nasojejunal feeding tube was inserted endoscopically for adequate caloric intake. Four days after the treatment, body temperature decreased to 37.5 ℃, amylase levels decreased to normal value 150 U/L and platelet count increased to 150 000/mm^3. Bilirubin levels, liver function tests, and creatinine level slowly returned to normal within 2 wk (laboratory tests at the discharge time revealed WBC: 9 000/mm^3, Hb: 90 g/L, total/direct bilirubin: 2/1.8 mg/dL, BUN: 30 mg/dL, Cr: 1.2 mg/dL, AST: 24 U/L, ALT: 45 U/L, LDH: 380 U/L). Oral intake was started on d 19 of admission and the patient was discharged. Abdominal CT findings at the discharge time revealed minimal edema in the pancreas (Figure 1B). The patient was examined 2 mo later and he was in a completely healthy condition.

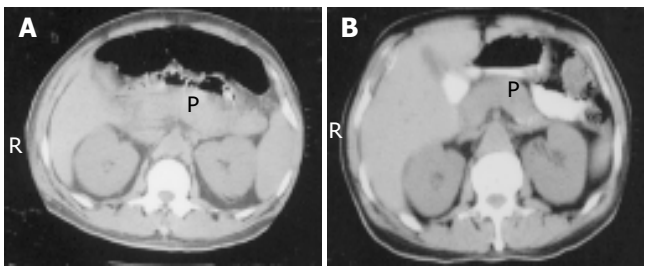

Figure 1 Abdominal CT scan of case 2. **A:** Pancreatic edema, heterogeneity and minimal intra-abdominal fluid collection; **B:** minimal edema in the pancreas after treatment. P: pancreas.

DISCUSSION

Leptospirosis is a spirochetal zoonosis that causes clinical illness in humans as well as in animals. The source of infection in humans is usually either direct or indirect contact with the urine of infected animals. These bacteria infect humans by entering through abraded skin, mucous membrane, conjunctivae. Direct transmission between humans is rare[3,4]. Leptospirosis is a common disease in rice-field workers due to prevalence of wild rats[4,8]. Both of our patients were from rural area of the middle Black Sea region of Turkey and have worked in rice fields. Rice field with stagnant water and humid condition is an ideal environment for leptospira.

Leptospirosis is characterized by the development of vasculitis, endothelial damage, and inflammatory infiltration. This disease mostly affects tissues of the liver and kidney. Other tissues such as the pancreas can be affected due to vasculitis[4].

This disease occurs as two clinically recognizable syndromes: the anicteric leptospirosis (80-90% of all cases) and the remainder icteric leptospirosis[3,4]. Icteric leptospirosis is known as Weil's disease, which is characterized by hemorrhage, renal failure, and jaundice. Icteric leptospirosis is a much more severe disease than anicteric form. The clinical course is often rapidly progressing. Our cases seemed to be icteric leptospirosis. Serological tests confirmed on blood samples as *L icterohemorrhagica* and *L samaranga Patoc*. First of these is responsible for icteric form of the disease. *L samaranga Patoc* sero-type is not the cause of Weil's disease but cross-reaction is possible between the serotypes of leptospirosis.

Thrombocytopenia is a common finding in leptospirosis, occurring in 40-85% of this disease. But the exact reason for thrombocytopenia is unknown. Vasculitis, increased peripheral destruction and decreased thrombocyte production have been considered as potential causes of thrombocytopenia[4,10]. Thrombocytopenia was also present in the two cases reported here which were remedied by our treatment.

Oliguric and non-oliguric acute renal failure may be observed in icteric leptospirosis[7], as also seen in our cases. It was reported that oliguria was a significant predictor of death in leptospirosis[4]. Urine output was normal in case 1 but case 2 was oliguric. Renal insult was treated with intravenous fluid replacement and other supportive treatment including antibiotic and hemodialysis in case 2.

Jaundice occurring in leptospirosis is not commonly associated with hepatocellular necrosis and impaired liver function. There are moderate rises in transaminase levels, and minor elevation of alkaline phosphatase level usually occurs[3,4]. Hepatic dysfunction occurs but resolves, and it is rarely the cause of death. The serum bilirubin level is usually <20 mg/dL but can be as high as 60-80 mg/dL. The bilirubin level of case 2 was close to this value (48 mg/dL). In case 1, transaminase levels were very high (more than 2 000 U/dL). The elevation of transaminases that is more than threefold of the normal value is not usual. Some sporadic cases with very high transaminase level were reported in the medical literature[11]. Furthermore, hepatocyte degeneration and liver cell necrosis have been reported in biliary pancreatitis[12,13]. So, elevated transaminases levels as high as that in case I may be seen in leptospirotic hepatitis. Pancreatic and bile tree involvement can be additional factors

for liver cell necrosis. Acute cholecystitis was pathologically confirmed and leptospires were seen in bile in case 1. Therefore, we believe that hepatobiliary and pancreatic involvement could be possible in this case.

For the diagnosis of acute pancreatitis, a simultaneous determination of both amylase and lipase is recommended for the evaluation of patient with abdominal pain. The serum amylase test is available in nearly all laboratories and at all hours. Elevation of lipase level with serum amylase is important for the diagnosis of acute pancreatitis. Elevation of pancreatic izoamylase level also supports the diagnosis[14]. Hyperamylasemia also can be seen in leptospirosis due to renal function alterations or other unknown reasons[5,6]. The serum amylase and lipase levels were elevated more than threefold of normal level in both cases. Pancreatic izoamylase level was also elevated at diagnostic level in case 2.

CT scan is a gold standard in diagnosis of acute pancreatitis, as shown by many authors who use it. This diagnostic test has 100% specificity and over 90% sensitivity for this disease[15-17]. We also routinely use CT for both diagnosis and follow-up of the treatment as in case 2. Because abdominal CT scan was not available in the emergency condition in our hospital, we could not use it in case 1. However, the pathologic findings of acute pancreatitis were clearly observed at laparotomy in this case. So, there is no diagnostic dilemma for both of two presented cases.

The treatment of acute pancreatitis in leptospirosis includes antibiotic treatment against leptospira and supportive treatments for acute pancreatitis (including intravenous fluid resuscitation and nutrition). We preferred the nutritional support (parenterally or enterally but mostly enterally) in severe acute pancreatitis. This regime was successful in case 2. Case 1 also completely recovered after d 5 and she could feed orally. We believe that the reason of mortality was pulmonary embolism in case 1.

In conclusion, pancreatitis may be seen in leptospirosis infection. Leptospirosis should also be considered in the differential diagnosis of hyperamylasemia, pancreatitis, and obstructive jaundice in endemic areas. Early diagnosis and appropriate treatment is essential for life saving.

REFERENCES

1 **Leblebicioglu H,** Sencan I, Sunbul M, Altintop L, Günaydin M. Weil's disease: Report of 12 cases. *Scand J Infect Dis* 1996; **28**: 637-639

2 **Casella G,** Scatena L. Mild pancreatitis in leptospirosis infection (letter to the Ed.). *Am J Gastroenterol* 2000; **95**: 1843-1844

3 **Farr RW.** Leptospirosis. State-of-the-art article. *CID* 1995; **21**: 1-6

4 **Levett PN.** Leptospirosis. *Clin Microbiol Rev* 2001; **14**: 296-326

5 **Edwards CN,** Evarard COR. Hyperamylasemia and pancreatitis in leptospirosis. *Am J Gastroenterol* 1991; **86**: 1665–1668

6 **Kameya S,** Hayakawa T, Kemaye A, Wtarabe T. Hyperamylasemia in patients at an intensive care unit. *J Clin Gastroenterol* 1986; **8**: 438-442

7 **Cengiz K,** Sahan C, Sunbul M, Leblebicioglu H, Cuner E. Acute renal failure in leptospirosis in the black- sea region in Turkey. *Int Urol Nephrol* 2002; **33**: 133–136

8 **Sunbul M,** Esen S, Leblebicioglu H, Hokelek M, Pekbay A, Eroglu C. Rattus acting as reservoir of leptospira interrogans in the middle black sea region of Turkey, as evidenced by PCR and presence of serum antibodies to leptospira strain. *Scand J Infect Dis* 2001; **33**: 896-898

9 **O'Brien MM,** Vincent JM, Person DA, Cook A. Leptospirosis and pancreatitis: a report of ten cases. *Pediatr Infect Dis J* 1999; **18**: 399-400

10 **Turgut M,** Sunbul M, Bayýrlý D, Bilge A, Leblebicioglu H, Haznedaroglu I. Trombocytopenia complicating the clinical course of leptospiral infection. *J Int Med Res* 2002; **30**: 535-540

11 **Kuntz E,** Kuntz HD. Hepatology. 1 st ed. *Hiedelberg: Springer Verlag, Berlin* 2000: 425

12 **Tenner S,** Dubner H, Steinberg W. Predicting gallstone pancreatitis with laboratory parameter meta-analysis. *Am J Gastroenterol* 1994; **89**: 1863–1866

13 **Isogai M,** Yamagýchi A, Hori A, Nakano S. Hepatic histopathological changes in biliary pancreatitis. *Am J Gastroenterol* 1995; **90**: 449–454

14 **Frank B,** Gottlieb K. Amylase normal, lipase elevated : Is it pancreatitis? *Am J Gastroenterol* 1999; **94**: 463-469

15 **Clavien PA,** Hauser H, Meyer P, Rohner A. Value of contrast-enhanced computerized tomography in the early diagnosis and prognosis of acute pancreatitis. *Am J Surg* 1988; **155**: 457-463

16 **Moossa AR.** Diagnostic tests and procedures in acute pancreatitis. *N Engl J Med* 1984; **311**: 639-643

17 **Lott JA.** The value of clinical laboratory studies in acute pancreatitis. *Arch pathol Lab Med* 1991; **115**: 325-326

Science Editor Zhu LH **Language Editor** Elsevier HK

PO Box 2345, Beijing 100023, China
www.wjgnet.com
wjg@wjgnet.com

ELSEVIER

World J Gastroenterol 2005;11(28):4450
World Journal of Gastroenterology ISSN 1007-9327

Acknowledgments to Reviewers of *World Journal of Gastroenterology*

Many reviewers have contributed their expertise and time to the peer review, a critical process to ensure the quality of *World Journal of Gastroenterology*. The editors and authors of the articles submitted to the journal are grateful to the following reviewers for evaluating the articles (including those were published and those were rejected in this issue) during the last editing period of time.

Takafumi Ando, M.D.
Nagoya University Graduate School of Medicine, Therapeutic Medicine, 65 Tsurumai-cho, Showa-ku, Nagoya 466-8550, Japan

Zong-Jie Cui, Professor
Institute of Cell Biology, Beijing Normal University, Beijing 100875, China

Er-Dan Dong, Professor
Department of Life Science, Division of Basic Research in Clinic Medicine, National Natural Science Foundation of China, 83 Shuanqing Road, Haidian District, Beijng 100085, China

Sheung-Tat Fan, Professor
Department of Surgery, The University of Hong Kong, Queen Mary Hospital, 102 Pokfulam Road, Hong Kong, China

Xue-Gong Fan, Professor
Xiangya Hospital, Changsha 410008, China

Joachim Labenz, Associate Professor
Jung-Stilling Hospital, Wichernstr. 40, Siegen 57074, Germany

Ansgar W Lohse, Professor
Department of Medicine, Hamburg University, Martinistr. 52, Hamburg 20246, Germany

Giovanni Maconi, M.D.
Department of Gastroenterlogy, 'L.Sacco' University Hospital, Via G.B.Grassi, 74, Milan 20157, Italy

James Neuberger, Professor
Liver Unit, Queen Elizabeth Hospital, Birmingham B15 2TH, United Kingdom

Bo-Rong Pan, Professor
Departmant of Oncology, Xijing Hospital,Fourth Military Medical University, No.1,F.8,Bldg 10,97 Changying East Road, Xi'an 710032, Shaanxi Province, China

Heitor Rosa, Professor
Department of Gastroenterology and Hepatology, Federal University School of Medicine, Rua 126 n.21, Goiania - GO 74093-080, Brazil

Jose Sahel, Professor
Hepato-gastroenterology, Hospital sainti Marevenite, I270 Boolevard AE Sainti Margrenise, Marseille 13009, France

Tilman Sauerbruch, M.D.
Department of Internal Medicine I, University of Bonn, Sigmund-Freud-Strasse 25, 53105 Bonn, Germany

Rudi Schmid, M.D.
211 Woodland Road, Kentfield, California 94904, United States

Tadashi Shimoyama, M.D.
Hirosaki University, 5 Zaifu-cho, Hirosaki 036-8562, Japan

Yoshio Shirai, Associate Professor
Division of Digestive and General Surgery, Niigata University Graduate School of Medical and Dental Sciences, 1-757 Asahimachi-dori, Niigata City 951-8510, Japan

Manfred Stolte, Professor
Institute of Pathology, Klinikum Bayreuth, Preuschwitzer Str. 101, Bayreuth 95445, Germany

Simon D Taylor-Robinson, M.D.
Department of Medicine A, Imperial College London, Hammersmith Hospital, Du Cane Road, London W12 0HS, United Kingdom

Frank Ivor Tovey, M.D.
Department of Surgery, University College London, 5 Crossborough Hill, Basingstoke RG21 4AG, United Kingdom

Hong-Yang Wan, M.D.
International Co-operation Laboratory on Signal Transduction Eastern Hepatobiliaty Surgery Institute, SMMU, 225 Changhai Road, Shanghai 200438, China

Jia-Yu Xu, Professor
Shanghai Second Medical University, Rui Jin Hospital, 197 Rui Jin Er Road, Shanghai 200025, China

Michael Zenilman, Professor and Chairman
Department of Surgery, SUNY Downstate Medical Center, 450 Clarkson Avenue, Brooklyn NY, United States

Jian-Zhong Zhang, Professor
Department of Pathology and Laboratory Medicine, Beijing 306 Hospital, 9 North Anxiang Road, PO Box 9720, Beijing 100101, China

Zhi-Rong Zhang, Professor
West China School of Pharmacy, Sichuan University, 17 South Renmin Road, Chengdu 610041, Sichuan Povince, China